The architecture, growth and tectono-stratigraphic significance of rift-oblique lineaments on the NE Atlantic Margin

MOY, DAVID,JOHN

How to cite:

MOY, DAVID,JOHN (2010) *The architecture, growth and tectono-stratigraphic significance of rift-oblique lineaments on the NE Atlantic Margin*, Durham theses, Durham University. Available at Durham E-Theses Online: http://etheses.dur.ac.uk/178/

THE ARCHITECTURE, GROWTH AND TECTONO-STRATIGRAPHIC SIGNIFICANCE OF RIFT-OBLIQUE LINEAMENTS ON THE NE ATLANTIC MARGIN

David J. Moy

A thesis submitted for the degree of
Doctor of Philosophy

Department of Earth Sciences
University of Durham

2010

DECLARATION

No part of this thesis has previously been submitted for a degree at this or any other university. The work described in this thesis is entirely that of the author, except where reference is made to previously published or unpublished work.

David J. Moy

University of Durham

Department of Earth Sciences

March 2010

ABSTRACT

Fault domain boundaries are characteristic features of segmented rift systems and have been recreated in analogue models. Two end member conceptual models of fault domain boundaries currently exist. 1) Accommodation zones, which are broad regions of overlapping normal faults and which trend oblique to the rift axis. 2) Transfer zones, which are discrete sub-vertical fault systems that directly link en-echelon normal fault domains. These structures are commonly believed to segment natural rift systems on a variety of scales and impact directly upon the stratigraphic and magmatic evolution of a basin.

The NE Atlantic Margin is a volcanic passive margin which has undergone a series of rift events culminating with continental breakup in the Early Cenozoic. From potential field, seismic reflection, seismic refraction and ocean bottom seismometer datasets, a series of rift-oblique lineaments (loosely referred to as 'transfer zones') have been identified which are commonly inferred to compartmentalise and laterally offset structural highs and depocentres developed within the Mesozoic – Cenozoic rift basins. A range of hypotheses are proposed to explain the origin of these lineaments, including fault domain boundaries, basin-wide strike-slip faults and other, non-tectonic origins. Using well-calibrated 2D and 3D seismic data, this study critically assesses the structural, stratigraphic and magmatic evidence for the rift-oblique lineaments in the Faroe-Shetland Basin and Vøring Basin, both located upon the NE Atlantic Margin.

Results from the Faroe-Shetland Basin show structures previously attributed to basin-wide strike-slip deformation can be more simply explained as igneous intrusions, hydrothermal vent complexes, gas chimneys and/or faults that transfer extensional strain between en-echelon rift segments (i.e. fault domain boundaries). There is little evidence to suggest that activity along a series of discrete, basin-wide lineaments controlled Paleocene sedimentation in the basin.

In the northern Vøring Basin, a previously identified fault domain boundary (the Rym Accommodation Zone) is analysed to understand if, and how strain is transferred between two adjacent fault domains. The results of this study highlight major differences between the offset rift segments in view of the style of rifting, timing, the loci of faulting, the relative uplift and subsidence histories as well as the impact of variations in the deep crustal structure. Analyses reveal that strain is not fully transferred across the fault domain boundary, with significant variation in beta factors calculated for each rift segment. The structural style within the Rym Accommodation Zone is complex, with the rotation of normal fault orientations, major relay ramp formation and rift perpendicular normal oblique faulting observed, elements that are not present in most existing conceptual models of accommodation zones. The results also imply that transfer zones may be an integral part of a larger accommodation zone rather than an opposite end member as previously believed.

In the final aspect of the study, a second rift-oblique lineament is analysed in the northern Vøring Basin: the Gleipne Lineament. Results highlight the close structural relationship between the Gleipne Lineament and underlying basement structure, with the lineament acting as a conduit for sediment to enter the Vøring Basin during phases of rifting. Under periods of minimal upper crustal deformation, the lineament exerted a lesser control upon basinal sedimentation. The Rym Accommodation Zone in contrast did not source sediment into the Vøring Basin, instead, it compartmentalised the basin during rifting which increased the complexity of the predicted basin fill. Increased Late Paleocene intrusive and extrusive igneous deposits are observed along the strike of both lineaments but are not directly linked to active tectonic deformation.

In conclusion, rift-oblique lineaments are unlikely to be basin-wide features and each appears to be unique in its structural style and geological origin. In turn, this means that different lineaments are likely to have different impacts upon the stratigraphical and magmatic development of a basin. Previous inferences that basin-wide lineaments have controlled sediment entry and transport within rift basins on the NE Atlantic Margin need to be substantiated on a case-by-case basis. The results of this study are further considered and discussed to predict the nature of rift-segmenting structures in the sub-basalt region of the Faroe-Shetland Basin, which is poorly resolved by current 2D and 3D seismic imaging.

ACKNOWLEDGEMENTS

First, and most importantly, I would like to thank my primary supervisor Dr. Jonathan Imber. Without Jonny's continual guidance and support this project would certainly not have been possible. Jonny inspired me from day one with his enthusiasm and continuing interest in my research through frequent discussions at all stages of the Ph.D. Helping to overcome problems that arose, encouraging the presentation and publication of the research, and offering sound advice and commentary certainly improved the quality of the final thesis. My other supervisors at the University of Durham, Dr. Mark Allen and Prof. Robert Holdsworth are also thanked for their comments and constructive thoughts, as are other members of the Reactivation Research Group and Department of Earth Sciences to whom I have presented my results. In particular, Richard Walker has been very supportive of the research, drawing analogies from his own onshore study of the Faroe Islands. To have as good a friend as Rich, with whom I have shared various ideas and had frequent discussions surrounding the nature of the 'transfer zones', has proved invaluable.

The National Environmental Research Council (NERC) with Statoil U.K. Ltd as the industrial CASE partner (NER/S/C/2006/14276) are thanked for providing financial support in relation to the Ph.D. My project supervisors at Statoil U.K. Ltd, Dr. David Ellis and Dr. Joseph Gallagher (and other members of the Faroes Exploration team) are thanked for their continued support of the research which has led to fruitful discussions regarding the nature and influence of the rift-oblique lineaments within the Faroe-Shetland Basin. StatoilHydro, in particular members of the Vøring Basin regional and licence exploration teams, are particularly thanked for their support of the study, financial assistance and the timely provision of seismic and well datasets when the project refocused due to the initial results of the research. Prof. A. Doré and Dr. R. England are also thanked for their constructive reviews of my first publication which was a direct result of this research.

Dave Stevenson and Gary Wilkinson are thanked for their continual efforts in maintaining the IT equipment and provision of support in the department. Landmark Graphics Corporation through the Strategic University Alliance Agreement (2006.COM-032168) is acknowledged for providing seismic processing/interpretation software and technical support. My former colleagues at Senergy Ltd who develop the ODM3^{TM} software are also thanked for granting free use of their software. Similarly, I also express thanks to Badley Geoscience for the provision of TrapTester software in the department.

A variety of companies and organisations are now thanked for the supplying of multiple datasets, the analyses of which were of critical importance for the research. Heri Ziska at Jarðfeingi (Faroese Earth and Energy Directorate), the British Geological Survey (BGS) and the Sindri Group are thanked for allowing the access, use and display of potential field data across the Faroese region prior to the public release of the data. Statoil U.K. Ltd and StatoilHydro are thanked for the provision of well and seismic data, as are PGS Geophysical, WesternGeco, TGSNopec, Fugro-Geoteam and the Norwegian Petroleum Directorate (NPD) who consented to the use and display of their valuable seismic datasets. Dr. Jonathan Imber, NERC, Statoil U.K. Ltd and ExxonMobil are also thanked for financial assistance provided for the attendance and presentation of my research at ten national and international conferences. These proved particularly valuable due to productive discussions with other delegates and earned me a variety of awards.

Finally, I would like to thank my family. My parents Brian and Gillian, grandparents Albert and Ellen Moy, my brother Adam and other members of my family who have always supported me with my studies. Yet it is my fiancée, Nicola Dolan, to whom I voice my utmost gratitude for her patience and understanding during the many weekends and evenings which I would rather have spent with her instead.

CONTENTS

FIGURE LIST

Chapter 1: Introduction

Chapter 2: Dataset and methodology

Chapter 3: Significance of rift-oblique lineaments in the Faroe-Shetland Basin

Chapter 4: Tectonic evolution of a fault domain boundary

Chapter 5: Stratigraphic and magmatic evolution of segmented rift systems

Chapter 6: Discussion, conclusions and further work

TABLE LIST

Chapter 1: Introduction

Chapter 6: Discussion, conclusions and further work

Chapter One

1 INTRODUCTION

Accommodation zones and transfer zones (fault domain boundaries; Schlische & Withjack 2009) are found in a variety of segmented rift systems from around the world. These include the East African rift system (Rosendahl 1987; Ebinger 1989a; Morley *et al.* 1990; Nelson *et al.* 1992), Gulf of Suez (Coffield & Schamel 1989; Moustafa 1996; McClay & Khalil 1998; Moustafa 2002; Younes & McClay 2002), the Basin and Range (Mack & Seager 1995; Axen 1998; Beratan 1998; Duebendorfer *et al.* 1998; Faulds & Varga 1998; Rowley 1998) and a variety of passive margins (e.g. Lister *et al.* 1986) including northwest Australia (Hopper *et al.* 1992; Keep & Harrowfield 2005), the U.S. Atlantic Margin (Behn & Lin 2000), South American Atlantic Margin (Franke *et al.* 2007), east Greenland (Karson & Brooks 1999) and NW Europe (Doré *et al.* 1999). The structures which have been recognised in these and other natural rift systems have also been reproduced using analogue modelling techniques (McClay & White 1995; Acocella *et al.* 1999a; McClay *et al.* 2002; Corti *et al.* 2003; McClay *et al.* 2004; Acocella *et al.* 2005; Schlische & Withjack 2009). Within analogue models, the conditions to recreate basin-scale segmenting structures commonly utilise a modification of the base plate to form a basement heterogeneity which has often been inferred as a cause for the development of rift-segmenting structures (e.g. Ebinger 1989b; Moustafa 1997; Henry 1998; Ebinger *et al.* 2000).

The structural style associated with each of the segmented rift systems varies greatly between each of the basins (Fig. 1.01). Although this variation could be attributed to a variety of strain kinematics which formed each individual basin (e.g. McClay & White 1995) a series of generic concepts have been identified from the models. The structural configuration of the basin can differ within each adjacent rift segment across the fault domain boundary, primarily with alternations in the polarity of half-graben asymmetry and/or apparent lateral offsets of rift-bounding structures or intrabasinal highs (e.g. McClay & White 1995; McClay & Khalil 1998; McClay *et al.* 2002). Yet this marked variation in rift structure along strike is not always observed (e.g. Ebinger 1989a; Fig. 1.01) and the structural geometry can differ greatly between individual rift settings. The tectonic nature of the fault domain boundary can also vary dramatically which has led to two end member models of fault domain boundaries proposed; a 'hard-linked' (Walsh & Watterson 1991) transfer zone (Gibbs 1984) formed of rift-oblique faulting or a 'soft linked' accommodation zone in which basin forming normal faults tip out along strike (Faulds & Varga 1998). Despite the appearance of the rift segmentation, the fault domain boundary is further defined on the basis of conserving and transferring strain between the adjacent rift segments (Faulds & Varga 1998). The style of sedimentation in natural rift systems is also considered to be influenced by fault domain boundaries, in particular as pathways for sediment to enter basins during rifting (Nelson *et al.* 1992; Gawthorpe & Hurst 1993; Beratan 1998; Kornsawan & Morley 2002; Younes & McClay 2002; Khalil & McClay 2009). Similarly, enhanced igneous activity has been associated with fault domain boundaries particularly within the East African Rift System (Ebinger *et al.* 1989; Ebinger *et al.* 1993; Ebinger & Casey 2001), upon volcanic passive margins (Ritchie *et al.* 1999; Jolley & Bell 2002a; Kimbell *et al.* 2005; Franke *et al.* 2007) and other rift systems (Rowley 1998; Acocella *et al.* 1999b; Corti *et al.* 2003 and references therein). Therefore, further improvements in the understanding of these structures are of scientific importance to provide an enhanced understanding of natural rift systems and the relative impact fault domain boundaries have upon basin evolution and dynamics in both space and time.

The NE Atlantic Margin formed during Early Cenozoic continental break-up between NW Europe and Greenland following a protracted phase of crustal stretching. The rifts have a NE-SW orientation, but regional potential field datasets highlight a series of

NW-SE trending lineaments or ‘transfer zones’ along the length of the margin (Fig. 1.02). The origin and significance of these lineaments is however unclear, but a timely geological investigation of these lineaments is expected to yield an improved understanding of the nature, growth and tectono-stratigraphic significance of the lineaments. Although the term ‘transfer zone’ has commonly been used for the NW-SE oriented features upon the margin (e.g. Rumph *et al.* 1993; Doré *et al.* 1997b; Kimbell *et al.* 2005; Ellis *et al.* 2009), the term ‘lineament’ or ‘rift-oblique lineament’ has been used herein to distinguish structural trends that have been identified primarily using potential field datasets from specific geological features identified through analysis of well-calibrated 2D and 3D seismic reflection data (Moy & Imber 2009).

The NE Atlantic Margin is a volcanic passive margin, part of the North Atlantic Igneous Province (NAIP), within which some of the most voluminous lavas on Earth were deposited in the Paleocene and Eocene, covering a region of 1.6 x 10^6 km^2 (Eldholm & Grue 1994). Associated with these lavas are other sets of intrusive and extrusive volcanic material in the form of sill and dyke complexes, and the formation of hyaloclastite lava deltas where subaerial lava flows interact with an aqueous environment such as a lake or marine system (Smallwood *et al.* 1999; Planke *et al.* 2000; Bell & Butcher 2002; Eldholm *et al.* 2002; Jolley & Bell 2002a; b; Smallwood & Maresh 2002; Praeg *et al.* 2005). Recently, new interest from the hydrocarbon industry exploring in these frontier basins which are blanketed by volcanics has seen an upsurge in scientific research focused on understanding the problems associated with these flood volcanic provinces (e.g. the Rosebank discovery by Chevron Corporation in 2004). One of these is the ‘sub-basalt imaging problem’ which occurs due to the attenuation of the seismic wavelet at the sediment-volcanic interface (Planke & Eldholm 1994) leading to a significant drop in the resolution of seismic reflection data from intra- and sub-basalt horizons. In these frontier areas such as the Faroe-Shetland Basin and Vøring Basin (Fig. 1.03), major petroleum plays are considered to be present in the sub- and intra-volcanic stratigraphy making this a major hydrocarbon exploration issue. In areas both beneath and away from the volcanic succession, rift-oblique lineaments have been inferred to exist however the nature of these lineaments remains enigmatic with few published examples as to the structural geometry and evolution published. The rift-oblique lineaments have often been cited to link with heterogeneities in the Precambrian basement of the margin. Fichler *et al.* (1999) inferred the lineaments to be linked with major Precambrian shear zones of a similar orientation onshore Scandinavia. Similarly, lineaments have been tied to lateral variations in the deep crustal structure of the NE Atlantic Margin as typified by the so-called Lower Crustal Body (LCB) offshore Norway, a high density, high velocity body located at the base of the crust. Identified using seismic refraction datasets (Mjelde *et al.* 2001) the interpreted origin and nature of this body varies with magmatic underplating (e.g. Mjelde *et al.* 2002), serpentinised mantle (e.g. Ren *et al.* 1998) and high-grade eclogitic remains of the Caledonian orogen (e.g. Gernigon *et al.* 2003) hypotheses all proposed. Nevertheless, the interpretation of rift-oblique lineaments upon the NE Atlantic Margin has been correlated to this lateral variation in the crustal heterogeneity as observed in other rift basins. The rift-oblique lineaments are also inferred as pathways for sediments to enter the basin due to the preferential orientation of the lineaments (Fjellanger *et al.* 2005; Lien 2005; Jolley & Morton 2007), and have also been associated with variations in the concentration of volcanic material along basin strike (Planke *et al.* 2000; Tsikalas *et al.* 2001; Ren *et al.* 2003) which implies them to be very important features in developing a fuller understanding of the NE Atlantic Margin geological history.

The identification of such a problem, poses the following questions:

- What is the tectonic nature of the rift-oblique lineaments? Are they fault domain boundaries as have been recognised in other rift systems (Faulds & Varga 1998) and if so, what styles of deformation do they display? Could the lineaments have an alternative structural origin to that of fault domain boundaries, such as major wrench faults or do the lineaments have a non-tectonic origin, such as sedimentary and volcanic features?
- How does the tectonic significance of the rift-oblique lineaments differ through time, in particular during the different stages of basin formation? Many previous studies have focussed upon rift-segmenting structures during rift formation, but what is the structural nature and influence of the lineament on basin evolution prior to, during and following the cessation of rifting?
- Does the nature of each individual rift-oblique lineament vary? Can one model of a rift-oblique lineament be used to explain the nature of all rift-oblique lineaments within a basin? If not, why is this not possible, what are the controls upon the formation of the lineament and what varying degrees of structural deformation can be attributed to the rift-oblique lineaments?
- Can the rift-oblique lineaments be associated with along strike variations in the crustal structure, either correlated with basement shear zones or a deeper crustal heterogeneity? If so, does the tectonic influence of the rift-oblique lineament vary with the tectonic origin?
- How do the rift-oblique lineaments impact sedimentation within evolving rift basins? Do the rift-oblique lineaments act as sediment entry points and/or do they compartmentalise the basin along strike?
- What influence do the rift-oblique lineaments have on the emplacement of intrusive and extrusive volcanic material in the basin prior to continental break-up?

- Can an understanding of the rift-oblique lineaments on the NE Atlantic Margin enhance hydrocarbon prospectivity upon segmented passive margins worldwide? Can improved knowledge of the lineaments lead to development of new hydrocarbon plays not previously considered?

This thesis synthesises the results of a 3 year investigation into the architecture, growth and tectono-stratigraphic significance of rift-oblique lineaments on the NE Atlantic Margin using well-calibrated 2D and 3D seismic reflection data from the Faroe-Shetland and Vøring Basins on the NE Atlantic Margin. From the analysis of these datasets, a suite of tectono-stratigraphic and volcanic evolutionary models are formed of the rift-oblique lineaments and subsequently applied to a frontier sub-basalt region of the Faroe-Shetland Basin to provide an improved understanding of sedimentary rift basins immediately prior to continental breakup and volcanic passive margin formation.

The Ph.D. research has been funded by the National Environment Research Council (NERC) through a CASE studentship with Statoil U.K. Ltd as the industry partner (NER/S/C/2006/14276).

Before the main aims of the project are presented, an overview of the evolution of the NE Atlantic Margin is given and previous research into rift-oblique lineaments upon the NE Atlantic Margin is introduced. From this, a series of testable hypotheses are defined and a brief summary given as to the nature of these features within other sedimentary basins worldwide.

1.1 Tectono-stratigraphic evolution of the NE Atlantic Margin

The NE Atlantic Margin extends up to 2600 km from southern Ireland to Mid-Norway and is up to 800 km wide (Fig. 1.02) between the inner shelf and the continent-ocean boundary (Ceramicola *et al.* 2005). Prior to the formation of the Atlantic Ocean in the Early Eocene (c. 55 Ma; Eldholm *et al.* 2002), several phases of episodic extension occurred, and is suggested to have involved a stepwise displacement of successive rift axes northwest towards the present day continental margin (Doré *et al.* 1999; Fig. 1.02). This is believed to occur due to a strengthening of previously rifted lithosphere (e.g. van Wijk & Cloetingh 2002). This c. 400 My period of variable extension has been described in detail by a number of workers (e.g. Doré & Gage 1987; Ziegler 1988; Doré *et al.* 1999; Roberts *et al.* 1999; Shannon & Spencer 1999).

The region is characterised by a dominant NE-SW lineament set with a more diffuse NW-SE 'transfer zone' trend mainly observable through fault terminations and offsets (Doré *et al.* 1997b). Little is known regarding the Caledonian Orogen and closure of the Iapetus Ocean and older geological history of the NE Atlantic Margin despite a good understanding of the processes exposed onshore (Coward 1990). The configuration of the NE Atlantic Margin is however considered to be influenced by the NE-SW trending basement grain (Kimbell *et al.* 2005). The Caledonian megacycle which lasted from the Cambrian to the Early Devonian (Ziegler 1988) is also believed to have formed compressional transfer zones which may relate to the NW-SE trend that seemingly segments the margin (Doré *et al.* 1997b). Alternatively, the basement control of the margin has also been proposed to have been controlled by Precambrian shear zones (Grønlie & Roberts 1989; Séranne 1992; Doré *et al.* 1997b) as has been recognised in fracture patterns of outcrops both onshore Scotland and Norway (Watson 1984; Romer & Bax 1992; Fichler *et al.* 1999; Beacom *et al.* 2001). A third, N-S trend is also found unique to offshore Norway, the Porcupine and the Northern Rockall Basins, related to Late Jurassic E-W oriented rifting which affected these areas (Doré *et al.* 1997b; Morewood *et al.* 2005; Readman *et al.* 2005).

In response to the Caledonian Orogeny, a number of wholly continental 'Old Red Sandstone' basins were formed due to the gravitational collapse and negative inversion of reverse faults (orogenic collapse; Roberts *et al.* 1999). These include the Munster Basin in southern Ireland, the Orcadian Basin in Scotland, the East Greenland Basin and the Hornelen Basin in Western Norway (Friend *et al.* 2000). Each of the basins contain predominantly alluvial and fluvial sequences comprising of stacked braided channel systems (Meadows *et al.* 1987; Mudge & Rashid 1987). Ages of active tectonism vary along the length of the collapse axis, with basins in the south and east experiencing an earlier Devonian growth phase compared to those in the north-western sector of the Old Red Sandstone Basin province where formation commenced in the Middle Devonian (Roberts *et al.* 1999). The variation in timing of orogenic collapse has been proposed as being controlled by the Lower Crustal Body (LCB; Ebbing *et al.* 2006). The nature of the LCB is unclear but the deep crustal structure is believed to have influenced the later segmentation of the NE Atlantic Margin.

Continued relaxation of the former Caledonian orogen led to renewed rifting during the Permo-Triassic (Kirton & Hitchen 1987), where deposition was controlled by northwest dipping faults forming asymmetrical half graben basins (Booth *et al.* 1993; Dean *et al.* 1999). These include the Slyne – Erris basins, offshore Ireland, the Solan and West Shetland basins, north of Scotland and the Trøndelag Platform – Halten Terrace region, offshore Norway (Shannon 1991; Herries *et al.* 1999; Brekke 2000). The sedimentary fill is typically composed of continental clastics deposited in arid to semi-arid conditions, in the form of alluvial and fluvial deposits (Booth *et al.* 1993). Playa and lake deposits of salt and anhydrite are also found, predominantly offshore Norway (Roberts *et al.* 1999).

An Early Jurassic marine incursion followed the Permo-Triassic rift events, but the Lower and Middle Jurassic has been removed by a major unconformity across much of the NE Atlantic Margin (Booth *et al.* 1993). Renewed east-west oriented rifting in the Late

Jurassic is very well documented in the North Sea (e.g. Doré 1991), Halten Terrace (Brekke 2000), East Greenland (Surlyk 1991) and the Porcupine Basin (Tate *et al.* 1993). It is however unclear whether rifting occurred within the Faroe-Shetland Basin at this time (Earle *et al.* 1989). The rift event has been proposed to last into the Early Cretaceous by various authors (e.g. Badley *et al.* 1984). However a clear distinction has been made subsequently between the Late Jurassic rifting and either Early Cretaceous (Hauterivian) rifting in a NW-SE extension direction (Lundin & Doré 1997) or Early Cretaceous thermal subsidence (Færseth & Lien 2002). Combined with anoxic marine conditions, the deposition of organic rich Kimmeridgian mudstones has made this interval the key source rock for hydrocarbon generation on the NW European continental shelf before returning to oxic conditions in the Early Cretaceous.

Due to the lack of wells penetrating down to and low resolution of seismic data imaging at Upper Jurassic levels in the Faroe-Shetland and Rockall Basins, to understand the Upper Cretaceous evolution analogues have been drawn from the Lofoten, Vøring and Møre Basins as the geological histories are considered to be very similar (e.g. Doré *et al.* 1999). Also, there are increased amounts of well data in the region penetrating the entire Cretaceous succession and the resolution of seismic data is generally superior. Yet even here there is disagreement between workers as to the timing of event activity. There is evidence of a modest mid-Cretaceous extension stage offshore Norway (Surlyk 1990; Lundin & Doré 1997; Doré *et al.* 1999; Whitham *et al.* 1999; Tsikalas *et al.* 2001) but it was major Late Cretaceous extension that formed many of the structural highs and depocentres within the Vøring and Møre Basins of the NE Atlantic Margin that are recognised today (Grunnaleite & Gabrielsen 1995; Ren *et al.* 1998; Doré *et al.* 1999; Gabrielsen *et al.* 1999; Brekke 2000; Skogseid *et al.* 2000; Ren *et al.* 2003; Gernigon *et al.* 2004; Roberts *et al.* 2009). This was initiated in Middle Campanian time, and is believed to have continued at varying magnitudes until continental break-up in the Early Eocene (Færseth & Lien 2002). The Upper Cretaceous succession is dominantly mud-prone; however marine fan and turbidite siliciclastics are found in the outer regions of the margin (Kittilsen *et al.* 1999; Fjellanger *et al.* 2005). Various authors have proposed that Greenland may have acted as a sedimentary source for the marine fans in the outer reaches of both the Faroe-Shetland and Vøring basins (Hitchen & Ritchie 1987; Doré *et al.* 1999; Larsen *et al.* 1999; Skogseid *et al.* 2000; Fjellanger *et al.* 2005; Jolley *et al.* 2005; Jolley & Morton 2007).

Within the Faroe-Shetland Basin there is disagreement as to whether there was a Paleocene rift event. Dean *et al.* (1999) associated this rift with a significant shift in the axes of depocentres to the northwest region of the basin from the south-eastern region which underwent earlier Cretaceous rifting in the basin. However, Mudge & Rashid (1987) had earlier proposed that Paleocene deposition was controlled by post-rift thermal subsidence rather than fault controlled subsidence due to rifting. There is no evidence of a Paleocene rift in the Rockall-Porcupine region either (Hall & White 1994; Clift & Turner 1998), however Paleocene extension is evident in the northern Vøring Basin despite regional uplift at the time (Gernigon *et al.* 2003; Ren *et al.* 2003). Lundin & Doré (1997) postulated that Paleocene rifting occurred away from the Cretaceous rift axes towards the line of continental break-up, possibly within the Hatton Basin offshore Ireland or below the Paleocene/Eocene basalts in the Faroe-Shetland and Møre Basins. Lithosphere extension models (Skogseid 1994; Roberts *et al.* 1997; Skogseid *et al.* 2000; Kusznir *et al.* 2005) have also recognised that the magnitude of extension increased significantly towards the continent-ocean boundary; hence evidence for a Paleocene rift may be hidden below the volcanic succession. The cause of uplift of the NE Atlantic Margin basins also of Paleocene age remains poorly explained. Champion *et al.* (2008) proposed the uplift to be related to transient mantle convective uplift. Equally, the Paleocene uplift has also been related to the effects of the Iceland Plume (Clift *et al.* 1998; Smallwood *et al.* 1999; Maclennan & Lovell 2002). Nevertheless, whichever process or set of processes caused this relative uplift, it led to the shallowing of basins, erosion and reworking of Upper Cretaceous sands and increased siliciclastic input from the basin margins at the time (Naylor *et al.* 1999; Gernigon *et al.* 2003).

Prior to continental break-up during the Early Cenozoic, voluminous amounts of igneous material were emplaced within the Atlantic Margin basins forming a range of volcanic features. These include seaward-dipping reflector sequences, abnormally thick oceanic crust, underplating of the crust, intrusives into the continental crust and extrusives over the sedimentary basins (Eldholm 1990; Skogseid *et al.* 1992; Skogseid 1994; Kiørboe 1999; Planke *et al.* 2000; Bell & Butcher 2002; Jolley & Bell 2002a; b; Mjelde *et al.* 2002; Thomson 2005a; b). Widespread magmatism in the form of continental flood basalts, sill complexes and central volcanoes have all been ascribed to the inception of the Iceland Plume arriving at the base of the lithosphere during the Early Paleocene (Eldholm & Grue 1994; Skogseid *et al.* 2000; Eldholm *et al.* 2002). This process erupted up to 5-10 x 10^6 km^3 of melt (White & McKenzie 1989), resulting in the north Atlantic being characterised as a large igneous province (LIP). The plume has also been considered as a primary control of basin stratigraphy (White & Lovell 1997). Through geochemical analyses of isotopes from direct sampling of outcrop and well data (Ritchie *et al.* 1999; Jolley & Bell 2002a), intrusive and extrusive activity in the region has been proposed to have occurred over an interval of 30 My with sills in the Faroe-Shetland Basin dated at up to 81 Ma (Gibb & Kanaris-Sotiriou 1988) in comparison to the youngest extrusives ~50 Ma (Jones *et al.* 1986). Two major phases of volcanic emplacement can be distinguished, the first between 62 – 60 Ma and second between 58 – 56 Ma (Raum *et al.* 2005). Modelling of gravity and magnetic anomaly data suggest the extrusives that blanket the margin are up to 7 km thick in the location of the Faroe Islands (White *et al.* 2003). Unfortunately, the intrusive and extrusive igneous material makes seismic imaging of the older and deeper crustal structure difficult due to the attenuation and scattering effects of the seismic wavefield (Planke & Eldholm 1994; Smallwood *et al.* 2001). This places a severe hindrance upon the understanding of the margin prior to continental break-up despite attempts to image below the basalt cover through long offset seismic surveys (Fliedner & White 2001) and reprocessing of commercial data (Gallagher & Dromgoole 2007; 2008).

The presence of a whole mantle plume (presently below Iceland) remains unproven (Anderson 2000; Foulger *et al.* 2001; Foulger 2002), with Early Cenozoic igneous activity alternatively attributed to elevated upper mantle temperatures (Anderson 2000). Another topic of current debate linked to the Cenozoic volcanic activity is the origin and nature of the LCB at the base of the crust. It has often been attributed to magmatic underplating of the crust in the Paleocene (Skogseid *et al.* 1992; Mjelde *et al.* 2001; van Wijk *et al.* 2001; Fernandez *et al.* 2004; Mjelde *et al.* 2005) but alternative hypotheses suggest it may form part of the ancient Caledonian root as a series of ultrahigh pressure metamorphic rocks (Gernigon *et al.* 2003; Gernigon *et al.* 2004; Ebbing *et al.* 2006). More recently, Raum *et al.* (2006) developed a mixed mode model of an eclogitic LCB acting as a barrier to magma flow during magmatic underplating of the crust.

The Iceland plume has frequently been applied to explain the continental break-up at c. 55 Ma (Eldholm *et al.* 2002) through thermal weakening of the lithosphere (e.g. Skogseid *et al.* 2000). Alternatively, Lundin & Doré (2005) suggest continental break-up was more likely a result of a long-lived extensional history which persisted until crustal separation was finally achieved exploiting the Caledonian suture zone. Following continental separation, the NE Atlantic Margin has experienced thermal subsidence punctuated by episodes of compression which has been studied in detail by numerous authors (e.g. Boldreel & Andersen 1993; 1998; Boldreel *et al.* 1998; Andersen *et al.* 2002; Ritchie *et al.* 2003; Johnson *et al.* 2005; Løseth & Henriksen 2005; Stoker *et al.* 2005c; Doré *et al.* 2008). However, due to a lack of well ties to seismic picks within the Neogene succession, caution has to be exercised in view of exact timings of events. Despite this, broad timings have been ascertained, with Praeg *et al.* (2005) and Stoker *et al.* (2005c) recognising regional Eocene – Oligocene rapid differential subsidence, compressive doming in the Early to Middle Miocene and tilting of the margin (onshore and shallow shelf uplift with accelerated offshore subsidence) in the Early Pliocene. Comparatively, on a more local scale, Lundin & Doré (2002) identified a compressional/transpressional phase during the Late Eocene – Oligocene, both in the Faroe-Shetland Basin and upon the Norwegian continental margin. The compressional effects on the NE Atlantic Margin are recorded by a series of N-NNE trending domes and arches offshore Norway (Doré *et al.* 2002; Doré *et al.* 2008), and anticlines in various orientations to the west of Shetlands (Ritchie *et al.* 2008). The extent of compressional structures differ greatly along the length of the margin, with Cenozoic domes abundant in the Faroe-Shetland and Vøring Basins (Boldreel & Andersen 1993; Doré & Lundin 1996; Ritchie *et al.* 2003; Davies *et al.* 2004; Johnson *et al.* 2005) but lacking in the Møre Basin and Lofoten Margin (Doré *et al.* 1999; Løseth & Henriksen 2005).

A number of authors have attempted to relate episodes of Cenozoic deformation with specific processes linked to the development of the adjacent oceanic crust (e.g. changes in sea floor spreading geometries, mantle drag and ridge push forces; Boldreel & Andersen 1993; Lundin & Doré 2002; Mosar *et al.* 2002); however the imprecision of timing of the events has delayed a resolution for the driving mechanisms. Other causes include the closure of the Tethys Ocean (Ziegler *et al.* 1995), intra-plate stresses (Vagnes *et al.* 1998; Stoker *et al.* 2005a) and the effect of the mantle plume (Brodie & White 1994; Clift *et al.* 1998). A summary is given by Doré *et al.* (2008) of the various processes and these authors also propose a new hypothesis relating NE Atlantic Margin uplift to growth of the Iceland plateau.

Many authors (e.g. Ritchie *et al.* 2003) have suggested the reactivation of preferentially-oriented pre-existing structures has significantly influenced the formation of Cenozoic folds along the margin. These in turn have continued to grow due to differential sedimentary loading and compaction (Lundin & Doré 2002; Mosar *et al.* 2002). Examples of reactivated structures include inversion and buttressing against normal faults at depth originally formed during Jurassic and Cretaceous rift events (Doré & Lundin 1996; Davies *et al.* 2004) and the NW-SE trending lineaments in strike-slip reactivation (Johnson *et al.* 2005). Mjelde *et al.* (2005) and Ebbing *et al.* (2006) suggested that a more prominent control on the location of Cenozoic domes on the Norwegian continental margin may tie to the deep crustal structure and the distribution of the LCB.

1.2 Rift oblique lineaments ('transfer zones')

The NE Atlantic Margin is segmented by a series of NW-SE striking lineaments that extend oceanwards across the continental shelf but rarely couple into oceanic fracture zones (e.g. Andersen & Boldreel 1995; Doré & Lundin 1996; Brekke *et al.* 1999; Brekke 2000; Mogensen *et al.* 2000; Doré *et al.* 2002; Lundin & Doré 2002; Ritchie *et al.* 2003; Løseth & Henriksen 2005). A common inference is that these lineaments accommodate strike-slip movements upon the passive margin (Doré *et al.* 1997b; Mogensen *et al.* 2000; Tsikalas *et al.* 2001; Ritchie *et al.* 2003; Imber *et al.* 2005; Stoker *et al.* 2005b; Tsikalas *et al.* 2008; Ellis *et al.* 2009). In contrast, Mosar *et al.* (2002) and Kimbell *et al.* (2005) concluded independently that the oceanic fractures zones and corresponding continental 'transfer zones' do not require strike-slip movements along them and the offsets along the continent-ocean boundary are believed to have formed due to the irregular geometry of the final continental break-up. The origin of the rift-oblique lineament trend is not clear and remains enigmatic; some authors have interpreted them as having a Proterozoic origin as shear zones (e.g. Knott *et al.* 1993; Brekke *et al.* 1999; Fichler *et al.* 1999), formed during the Caledonian Orogeny as compressional transfer zones (e.g. Rumph *et al.* 1993; Doré *et al.* 1997b), under extensional collapse of the orogen in the Devonian as major fault detachments (e.g. Ebbing *et al.* 2006) or due to variations in the relief and thickness of the deep crustal structure (e.g. Mjelde *et al.* 2003b). These origins are considered important but in understanding the nature and influence of these features in the Mesozoic – Cenozoic succession the origin is not directly considered. A summary is given below as to history and enigmatic tectono-stratigraphic and magmatic nature of the rift-oblique lineaments within the Faroe-Shetland and Vøring Basins which are selected for study upon the NE Atlantic Margin (Fig. 1.03).

1.2.1 Faroe-Shetland Basin

The Faroe-Shetland Basin is located between the West Shetland Platform and the Faroe Islands (Doré *et al.* 1999) to the north of the United Kingdom (Fig. 1.04). The basin contains a series of NE-SW trending sub-basins and structural highs which have formed as a response to successive rift events (Fig. 1.05) occurring during the Devono-Carboniferous (McClay *et al.* 1986; Coward & Enfield 1987; Nichols 2005), Permo-Triassic (Morton *et al.* 1987; Nelson & Lamy 1987; Herries *et al.* 1999), Cretaceous (Mudge & Rashid 1987; Turner & Scrutton 1993; Dean *et al.* 1999; Grant *et al.* 1999; England *et al.* 2005) and Paleocene (Hitchen & Ritchie 1987; Mitchell *et al.* 1993; Turner & Scrutton 1993; Dean *et al.* 1999; Smallwood & Gill 2002). Evidence of a Jurassic rift event is found in the Faroe Bank Channel Basin to the SSW of the Faroe Islands (Keser Neish & Ziska 2005) with only limited evidence within the main basin itself (Dean *et al.* 1999). A number of compressional episodes during the Late Paleocene through Miocene (Boldreel & Andersen 1993; Dean *et al.* 1999; Smallwood *et al.* 2001) have also led to a further complication of the basin morphology with the growth of abundant anticlines (Ritchie *et al.* 2003; Johnson *et al.* 2005; Ritchie *et al.* 2008).

Extensive magmatism around 61-56 Ma (Naylor *et al.* 1999) was expressed through the development of igneous centres (Ritchie *et al.* 1999), continental flood basalts (Kiørboe 1999; Ritchie *et al.* 1999; Ellis *et al.* 2002; White *et al.* 2003), igneous underplating (Clift 1999; England *et al.* 2005) and the intrusion of dyke and sill complexes (Mudge & Rashid 1987; Gibb & Kanaris-Sotiriou 1988; Bell & Butcher 2002; Davies *et al.* 2002; Smallwood & Maresh 2002) within both the Faroe-Shetland Basin and presently subaerially-exposed Faroe Islands (Fig. 1.04). These flood basalt units are believed to rest upon Cenozoic, Mesozoic and possibly older sedimentary rocks (White *et al.* 2003), which in turn were deposited on basement that is believed to be similar to the Proterozoic Lewisian Complex exposed in NW Scotland (England *et al.* 2005). The result of this is that the south-eastern margin has been studied much more extensively than the central and north-western regions due to thick (up to 7km) extruded subaerial basalt flows and shallow marine hyaloclastites affecting the seismic imaging (Smallwood *et al.* 2001).

The rift-oblique lineaments of the Faroe-Shetland Basin, which are inferred to offset discrete structural highs and depocentres along strike were first recognised by Duindam & van Hoorn (1987) but elaborated on by Rumph *et al.* (1993) who identified 15 NW-SE trending lineaments from regional gravity and magnetic data (Fig. 1.06). Evidence of the ‘transfer zones’ was also provided in examples of seismic reflection data displaying 1 – 2 km zones across which major offsets of horizons were interpreted and folding of the strata occurred (Fig. 1.06). They were also interpreted in seismic reflection data by sub-vertical offsets of Mesozoic and Cenozoic horizons across deep seated listric faults by

Lamers & Carmichael (1999). However, despite the recognition of the ‘transfer zone’ trend, at present, only seven lineaments are commonly recognised within the basin and form an integral part of tectonic element maps of the basin (Ellis *et al.* 2009). Similarly, these lineaments are believed to exert a structural control upon the evolution of the Faroe Islands (Rumph *et al.* 1993; Sørensen 2003; Ellis *et al.* 2009).

The interpreted structure of the lineaments varies greatly across the basin but is poorly defined. The north-eastern limit to the Faroe-Shetland Basin is governed by the Magnus Lineament, the position of which is well resolved by the change in modelled sedimentary thickness across it (Kimbell *et al.* 2005). Combined with the Marflo Lineament to the NE, these two lineaments create a zone of lateral offset with the Møre Basin to the east. The south-western limit to the Faroe-Shetland Basin is defined by the Judd Lineament which also marks the transition from a relatively thick sedimentary succession in the northeast from a thinner and more variable sequence to the southwest (Kimbell *et al.* 2005). The Judd Lineament has been inferred as a strike-slip fault system which is seismically resolvable away from the basalt cover (Hitchen & Ritchie 1987; Kirton & Hitchen 1987) and is believed to continue to the southwest of the Faroe Islands, west of Suðuroy as a normal fault which was later inverted (D. Ellis, Statoil U.K. Ltd, pers. comm.). Other lineaments within the basin have also been proposed to accommodate major dextral strike-slip movements on the basis of field work conducted in the Faroe Islands (Ellis *et al.* 2009). Dean *et al.* (1999) also recognised a Paleocene antiform which was interpreted as a transpressional popup structure located along the strike of the Clair Lineament. Ritchie *et al.* (2003) recognised changes in orientations of Cenozoic fold strikes across the Magnus and Erlend lineaments which led the authors to postulate Quaternary sinistral strike-slip movements along the lineaments; this has since been retracted however (Ritchie *et al.* 2008). Other tectonic activity that has been associated with the lineaments include the formation of Cenozoic aged, NW plunging anticlines (Grant *et al.* 1999) which have been linked to undefined Paleocene tectonic movements (Kimbell *et al.* 2005).

The deep structure of the Faroe-Shetland Basin also appears to have been influenced by the rift-oblique lineaments. Analysis of deep seismic reflection lines across the Faroe-Shetland Basin, England *et al.* (2005) documented a change in the Moho depth across the Westray Lineament. The deep crustal nature and influence of the Westray Lineament was also further validated by Raum *et al.* (2005) using seismic refraction datasets who noted the lineament marks a transition from a thick (24km) crust with 2-3km of sediments in the west to a thinner (18km) crust with up to 5km of sedimentary rocks to the east.

The rift-oblique lineaments have also been commonly inferred to control the stratigraphical and volcanic fill of the basin. For example, a marked reduction in the relief of the Faroe-Shetland escarpment (formed at the palaeo-shoreline between Paleocene lava units and the marine environment) has been tentatively suggested as being controlled by the Clair Lineament (Kiørboe 1999; Sørensen 2003). The Magnus and Erlend lineaments may have also exerted a control upon the magmatic evolution of the basin, with the Paleocene Erlend volcanic centres located between the two lineaments aligned in a similar NW-SE orientation (Rumph *et al.* 1993).

The NW-SE lineaments have also been considered as analogous structures to Mesozoic features in Kangerlussuaq, southeast Greenland. Here, a 900 m thick Cretaceous-Eocene sedimentary succession rests upon Archaean basement gneiss and is topped by up to 6 km of Paleogene flood basalts (Larsen *et al.* 1996; Larsen *et al.* 1999; Jolley & Whitham 2004). In the Christian IV Gletscher, a major NW-SE oriented normal fault focussed sediment transport south-eastwards towards the Faroe-Shetland Basin (Larsen & Whitham 2005).

This analogy has led many authors to suggest the lineaments form key sedimentary entry points to the basin (Grant *et al.* 1999; Lamers & Carmichael 1999; Jolley & Morton 2007; Fig. 1.06). Sediment is thought to have been transported during lowstands along the lineaments throughout the Late Cretaceous and Paleogene prior to continental separation (Whitham *et al.* 2004; Jolley *et al.* 2005; Larsen & Whitham 2005). However, Frei *et al.* (2005) concluded from detrital zircon studies that the Greenland sourced sediments are more likely to be found beneath the lava pile in the undrilled central and western regions of the basin, rather than to the south and east. Onshore evidence of these Greenland sourced sediments are exposed within the Faroe Islands Basalt Group (Passey & Bell 2007) and a control on their deposition has been tied to the tectonic movements of the rift-oblique lineaments ('transfer zones'; Ellis *et al.* 2009). In the southern region of the basin, the rift-oblique lineaments have acted as pathways for Cretaceous and Paleocene sediment to enter the basin from the Shetland Platform as well as function as barriers to sediment distribution within the basin (Hitchen & Ritchie 1987; Mitchell *et al.* 1993; Lamers & Carmichael 1999; Naylor *et al.* 1999). The only one model has been published which has attempted to link tectonic movements along the lineaments with sedimentation in the Faroe-Shetland Basin was proposed by Ellis *et al.* (2009; Fig. 1.07). Yet, the precise mode of deformation along the lineaments and influence upon sedimentation remains poorly defined, despite the inferred importance of the lineaments and increasing availability of high-resolution 3D seismic datasets.

Tectonic movements upon the rift-oblique lineaments have also been inferred to continue into the Neogene. The Pleistocene Miller Slide (Wilson *et al.* 2004) is located in close proximity to the Erlend Lineament suggesting a link between the two features.

Similarly, the Holocene Afen Slide (Wilson *et al.* 2004) is spatially coincident with the Victory Lineament to the southwest.

1.2.1.1 Rationale for study area selection

The Faroe-Shetland Basin was selected for use in this study of rift-oblique lineaments on the NE Atlantic Margin for several reasons. The tectonic nature and significance of the lineaments in the basin is highly enigmatic and poorly constrained despite first recognition of the features over 20 years ago. Much research has focussed upon the Faroe-Shetland Basin due to the availability of well, seismic and potential field datasets over vast regions of the basin but no previous studies upon the rift-oblique lineaments has been completed. Rarely are the rift-oblique lineaments considered within other studies which in part is probably due to the questions which surround their influence in the basin at the various stages of its evolution. To better understand the rift-oblique lineaments in the sub-basalt frontier region of the Faroe-Shetland Basin, the southern region of the basin external to the area of Paleocene flood basalts was selected for study. It is felt that an analysis of the lineaments in this region of the basin would represent the predicted nature of the lineaments in the sub-basalt stratigraphy of the northern Faroe-Shetland Basin and is expected to be a suitable analogue. It is also the southern Faroe-Shetland Basin in which the majority of available geological and geophysical datasets are located. These datasets sample and image the upper crust which the rift-oblique lineaments are commonly inferred to influence and therefore this area was deemed suitable for the study.

1.2.2 Vøring Basin

Upon the Norwegian continental margin, three main phases of extension have been recognised; the Carboniferous – Permian, Middle Jurassic – Early Cretaceous and Late

Cretaceous – Early Paleocene (Bukovics & Ziegler 1985; Ziegler 1988; Doré *et al.* 1997a; Walker *et al.* 1997; Swiecicki *et al.* 1998; Brekke *et al.* 1999; Doré *et al.* 1999; Spencer *et al.* 1999; Brekke 2000; Reemst & Cloetingh 2000) with the locus of strain migrating progressively westward towards the zone of future crustal separation (Figs 1.08 and 1.09). Compressional events post-dating continental break-up since the Early Eocene (Ziegler *et al.* 1995; Doré & Lundin 1996; Lundin & Doré 2002; Doré *et al.* 2008) have also exerted an influence on the present day morphology of the margin.

The along margin segmentation has previously been defined on the basis of offsets in the continent-ocean boundary (Tsikalas *et al.* 2002) and cross-margin structural features or lineaments recognised in regional potential field data (Doré *et al.* 1997b; Kimbell *et al.* 2005; Tsikalas *et al.* 2005b), seismic refraction datasets (Mjelde *et al.* 2003b; Mjelde *et al.* 2005) and seismic reflection datasets (Brekke 2000; Ren *et al.* 2003; Tsikalas *et al.* 2008); this implies that the lineaments structural features are of a crustal scale (Fig. 1.10). The rift-oblique lineaments have been tentatively tied to similar trending shear zones and detachment faults onshore Scandinavia (Fichler *et al.* 1999; Ebbing *et al.* 2006) and have even been linked to features upon the east Greenland conjugate margin (Tsikalas *et al.* 2002).

The Vøring Basin is bounded to the north by the Bivrost Lineament and south by the Jan Mayen Lineament, separating the Vøring Basin from the Lofoten Margin and Møre Basin respectively (Fig. 1.08). In addition to these, three other lineaments in the Vøring Basin have been proposed, the Gleipne and Surt Lineaments (Blystad *et al.* 1995; Doré *et al.* 1997b; Tsikalas *et al.* 2002; Gernigon *et al.* 2003) as well as Lineament L inferred by Mjelde *et al.* (2005). The lineaments that traverse the Norwegian Continental Margin all have differing lithospheric, crustal, magmatic and stratigraphical signatures which imply the origins of the lineaments may also differ. Therefore, a summary of each of the five lineaments is given to outline the present understanding of the tectono-stratigraphic and magmatic influence within the Vøring Basin.

The Bivrost Lineament is a major boundary in terms of margin physiography, structure and break-up magmatism (Eldholm & Grue 1994; Blystad *et al.* 1995; Mjelde *et al.* 2001; Tsikalas *et al.* 2002; Mjelde *et al.* 2003a; Tsikalas *et al.* 2008). This includes the lateral offset and segmentation of highs via a c. 20 km apparent sinistral offset between the Vøring Basin and Lofoten Margin (Tsikalas *et al.* 2005a). Alternatively, an apparent dextral offset has been proposed (Blystad *et al.* 1995; Doré *et al.* 1999). A shift in fault trends across the lineament, basin bounding fault terminations against the feature and a region of obliquely intersecting oceanic magnetic anomalies with the continental slope and shelf are all found in the vicinity of the Bivrost Lineament (Tsikalas *et al.* 2005a) implying that this is a major tectonic boundary. It is also believed to have formed in the Late Jurassic – Cretaceous (Eldholm *et al.* 2002), exerting a control on the distribution and volume of break-up magmatism (inferred by a reduction in thickness and volume of the LCB from the Vøring Basin to the Lofoten Margin; Eldholm & Grue 1994; Mjelde *et al.* 2001; Mjelde *et al.* 2003b). Similarly, at upper crustal levels, a reduction in the frequency of sill intrusions is evidenced to the north of the lineament upon the Lofoten Margin (Berndt *et al.* 2001). Crustal profiling also reveals that crustal densities, velocities and magnetic susceptibilities differ across the Bivrost Lineament (Blystad *et al.* 1995) leading to the conclusion that this is a major Mesozoic and possibly older tectonic boundary between the Vøring and Lofoten Margins (Ebbing *et al.* 2006). Its origin is unknown but has been proposed as a reactivated extension of the Proterozoic shear zones exposed onshore (Mokhtari & Pegrum 1992; Fichler *et al.* 1999; Olesen *et al.* 2002).

The Jan Mayen Lineament is at least of equal scale to the Bivrost Lineament, similarly offsetting large positive gravity and magnetic anomalies (Mjelde *et al.* 2005).

Eldholm *et al.* (2002) has also inferred a sinistral offset of structural highs and depocentres across the structure. Nonetheless, in complete contrast to the Bivrost Lineament, the Jan Mayen Lineament is only weakly expressed by changes in petrophysical parameters or crustal configuration and has a corresponding oceanic fracture zone to the northwest (Ebbing *et al.* 2006). Its upper crustal configuration has been defined by Eldholm *et al.* (2002) as having formed in the Late Jurassic – Early Cretaceous above a weak Palaeozoic or older basement structure. Raum *et al.* (2006) proposed that this basement structure was a Caledonian zone of weakness that channelled crustal intrusive activity within the Vøring Basin. Major anticlinal structures have also been found to trend en-echelon to the Jan Mayen lineament such as the Ormen Lange Dome, Helland Hansen Arch and Modgunn Arch implying a possible weakness in the basement configuration which was prone to later reactivation (Brekke 2000; Lundin & Doré 2002; Løseth & Henriksen 2005). Fichler *et al.* (1999) has also suggested a Precambrian origin to the lineament, but this is very tentative.

Similar to the Faroe-Shetland Basin, Evans *et al.* (2002) recognised that the Storregga slide complex located above the Jan Mayen Lineament may have been caused by tectonic movements along the Jan Mayen Lineament during Plio-Pleistocene times. A similar conclusion was reached for the Bivrost Lineament, with a close spatial alignment between the Traenadjupet slide and Bivrost Lineament (Haflidason *et al.* 2004).

The Gleipne and Surt lineaments have been termed ‘second order’ tectonic features due to no notable changes in the petrophysical nature of the crust across them. They can however be correlated with changes in the crustal geometry (e.g. the volume of the LCB; Ebbing *et al.* 2006). They are also of a smaller physical size and are mappable on multichannel seismic data as well as potential field data which has led to them being defined as rift-related accommodation zones (Rosendahl 1987; Ren *et al.* 2003), representing Late Cretaceous – Early Cenozoic adjustment features between offset rift segments which also constrained the emplacement of magma during the latest stage of Paleocene rifting (Gernigon *et al.* 2003; Mjelde *et al.* 2005). Notably however, the oceanic fracture zones associated with these lineaments (Tsikalas *et al.* 2002) have more recently been proven not to exist due to improvements in the accuracy of previously acquired potential field data (Ebbing *et al.* 2006; Olesen *et al.* 2007). Seismic refraction datasets have also been used to recognise changes across the Surt and Gleipne Lineaments such as changes in the depths to crystalline basement and the LCB (Fig. 1.10; Mjelde *et al.* 2003b).

Lineament L (Fig. 1.08; Mjelde *et al.* 2003b; Mjelde *et al.* 2005) was defined from seismic refraction datasets as the boundary of the LCB but similarly to the previous lineaments has also been tied to a long lived Precambrian feature (Ebbing *et al.* 2006). This implies that the lineaments defined on the basis of the deep crustal structure not only control the distribution of the LCB, but potentially have an important control on passive margin geodynamics and heavily influence the basin evolution.

1.2.2.1 Rationale for study area location

The outer Vøring Basin was selected for the study of rift-oblique lineaments on the NE Atlantic Margin as it could also be considered as an analogue for the rift-oblique lineaments in the sub-basalt succession of the Faroe-Shetland Basin. The study area includes the Gleipne and Surt Lineaments which due to their recognition in potential field and seismic reflection data, are considered akin to the rift-oblique lineaments of the Faroe-Shetland Basin. These two ‘second order’ lineaments are not on the scale of the Bivrost and Jan Mayen Lineaments, nor are they defined on the basis of the lower crustal structure (e.g. Lineament L). The lineaments are also located upon the NE Atlantic Margin in a basin which has a very similar geological history and therefore may mirror the tectonic events which occurred in the Faroe-Shetland Basin. Equally, the two lineaments are located within the Cretaceous – Paleocene rifted region of the basin, located in close proximity to the continent-ocean boundary. The equivalent region in the Faroe-Shetland Basin is expected to be overlain by the Paleocene lava flows on the basis of the outstepping rift model proposed by Doré *et al.* (1999). Therefore the lineaments of the outer Vøring Basin may be better analogues than the southern Faroe-Shetland Basin counterparts which are analysed in a region apparently not influenced by Paleocene rifting. Similarly, the Vøring Basin does not contain the voluminous amounts of subaerially erupted volcanic material allowing for increased resolution of the 2D and 3D seismic data in the region. It does however contain abundant sill and dyke complexes which can also be analysed in view of the influence of the two lineaments. Exploration well data is also available in the region providing a control on sedimentation styles and timing within the basin. Despite the nature of the deeper crustal features of the Vøring Basin still being debated, there is better control upon its characteristics than is currently understood in the Faroe-Shetland Basin. This means the deep crustal structure and the influence of crustal heterogeneities can also be considered when analysing the rift-oblique lineaments of the outer Vøring Basin.

1.3 Testable hypotheses

From the review of the available literature of rift-oblique lineaments on the NE Atlantic Margin, a range of hypotheses are introduced and briefly described as to the potential structural style of these lineaments within segmented rift systems (Table 1.01). Each of these hypotheses influences sedimentation and volcanic activity in rift basins differently, which can be tested using well-calibrated 2D and 3D seismic data. 3D seismic is considered as being critically important in understanding the rift-oblique lineaments as they have only previously been identified and analysed in 2D seismic data as well as within regional-scale potential field data which may have led to incorrect interpretations being made. The apparent NW-SE fabric may have also resulted from the subjective interpretation of coincidentally aligned, but geologically unrelated structural elements within the rift basin; 3D seismic data will be able to test this linkage.

1.3.1 Fault domain boundaries

All normal fault systems must terminate laterally along strike. Most of these systems terminate in either transfer or accommodation zones (fault domain boundaries) as has been recognised in other rift basins around the world. It is important to distinguish that these are features which are developed as an integral part of the rift system. A nomenclature issue within the available literature is highlighted due to the use of both terms to describe a variety of structural styles and processes which has led to much complication and a poor understanding of their importance in segmented rift systems. The preferred definitions for use in this study are given by Faulds & Varga (1998) which includes a review and history of nomenclature used for rift segmentation, culminating in clear definitions for end member models of fault domain boundaries, a transfer zone and an accommodation zone as described here.

1.3.1.1 Accommodation zone

An accommodation zone is defined as a belt of overlapping fault terminations and can separate either systems of uniformly dipping normal faults or adjacent domains of oppositely dipping normal faults. They can trend parallel, perpendicular or oblique to the extension direction (Faulds & Varga 1998; Fig. 1.11). McClay *et al.* (2002) furthered this classification by defining accommodation zones as either high-relief features which trend perpendicular to the rift axis or low relief features which are oblique. A key criterion of identifying an accommodation zone is that extensional strain is transmitted and conserved between the adjacent rift segments via a series of relay ramps (Faulds & Varga 1998).

Furthermore, accommodation zones are developed as a direct result of rifting and do not extend beyond the region of active rifting (McClay & White 1995). 3D seismic data can also be used to recognise depositional sequences (Mitchum *et al.* 1977a) which thicken in proximity to the accommodation zones, and may also be more sand prone due to sediment entering the rift and increased proximity to the source region (e.g. Gawthorpe & Hurst 1993; Younes & McClay 2002).

Due to the acoustic impedance contrast formed at the sediment-igneous interface (Planke & Eldholm 1994) igneous material is visible upon seismic reflection datasets. Variation in the concentration of intrusive and extrusive volcanic material may be expected to occur in close proximity to accommodation zones (Corti *et al.* 2003) and this can similarly be tested.

Physical modelling has often been utilised to understand the orientation, geometry and kinematics of structures which form in fault domain boundaries. McClay & White (1995) modelled both orthogonal and oblique rift systems through a series of sandpack analogue models. In each of the experiments, accommodation zones were formed consisting of interlocking conjugate extensional faults which led to the switching of half graben polarity and the offsetting of rift depocentres along the basin strike.

The influence of basement heterogeneity has often been linked to the formation of accommodation zones (e.g. Ebinger 1989a; Moustafa 1996; Younes & McClay 2002) and has since been recreated by modifying the base plate configuration within analogue models. McClay *et al.* (2004) recognised that basement offsets in analogue models generated intra-basinal accommodation zones that remain active throughout the duration of rifting. Similarly, these accommodation zones strongly influenced the ability of faults to propagate along strike due to the interlocking nature of the conjugate fault systems within them. Yet recent modelling of homogeneous sand and clay packs by Schlische & Withjack

(2009) recognised that the orientation of fault domain boundaries is not systematically related to the extension direction or pre-existing zones of weakness. Instead, the authors proposed that accommodation zones developed because early-formed faults perturb the stress field causing nearby faults to dip in the same direction. As extension continued, opposite-dipping faults from adjacent fault domains propagate along strike and interfere with each another forming an accommodation zone.

Examples of accommodation zones have been identified in a variety of basins around the world, both onshore and offshore. Onshore examples include the East African Rift (Rosendahl 1987; Morley *et al.* 1990), the Gulf of Suez (Younes & McClay 2002) and Basin and Range province (Axen 1998). Offshore examples are becoming more widely recognised due to the advent of 3D seismic technology which allows for an improved analysis of the geological structure compared to 2D seismic data. Examples of offshore accommodation zones are identified in the southern North Sea (McClay *et al.* 2004), the NE Atlantic Margin (Ren *et al.* 2003), the Gulf of Thailand (Kornsawan & Morley 2002) and the Lake Baikal Rift, Siberia (Scholz & Hutchinson 2000).

1.3.1.2 Transfer zone

A transfer zone is defined as a discrete zone of strike-slip and oblique-slip faulting that generally trend parallel to the extension direction and facilitate the transfer of strain between extended domains generally arranged in an en-echelon pattern (Gibbs 1984; Faulds & Varga 1998; Fig. 1.12). Similar to the accommodation zone hypothesis, a transfer zone is an integral part of the rift system and does not continue outside of the rift boundaries (Fig. 1.12). Strain is also expected to be conserved and transferred between the rift segments by means of the rift perpendicular faulting which can be calculated from an analysis of mapped faults in 3D seismic data. The impact transfer zones have on sedimentation is poorly defined, although fieldwork in the Basin and Range has suggested sediment transported along the rift axis may feed point-sourced fan systems across transfer faults (Beratan 1998). Volcanic activity is also expected to increase in the vicinity of the transfer zone due to faults acting as pathways for transport of magma, with possible lateral offsets of previously emplaced igneous features due to normal-oblique and lateral movements along the transfer zone (e.g. Duebendorfer *et al.* 1998).

Transfer zones are less well recognised in 3D seismic datasets than their accommodation zone counterparts. The best exposed areas in which to study these features are located in the hyper-extended Basin and Range Province, USA, where transfer zones including the Las Vegas Shear Zone (Duebendorfer *et al.* 1998) and Tascotal Mesa Fault (Henry 1998) are present. However, the issue with all field-based research is that often only a two-dimensional view of the outcrop is available for a problem which is inherently three-dimensional. Therefore, many of the transfer zone models proposed by Faulds & Varga (1998) are largely conceptual but are considered the best available at present based on results of analogue modelling of fault domain boundaries (Schlische & Withjack 2009).

Despite multiple attempts to physically model transfer zones, only Acocella *et al.* (2005) has successfully recreated these structures in analogue models. The results highlighted that the primary control on the formation of transfer zones was the percentage difference of extension rates between the adjacent rift segments. If the extension rate between the rift segments differed by > 21% ± 3, transfer faults striking sub-parallel to the extension direction were more likely to form than relay ramps. Many other authors have attempted to form transfer zones (e.g. McClay & White 1995; Acocella *et al.* 1999a; McClay *et al.* 2002; McClay *et al.* 2004; Schlische & Withjack 2009) but only successfully recreated accommodation zones.

Despite the rift-oblique lineaments being referred to commonly as ‘transfer zones’ on the NE Atlantic Margin, it is considered that there is no direct relationship between the terminology used in the literature and the definition used in this study. It is recognised however that the use of poorly defined terminology may have caused confusion between the various authors researching the margin, which has led to problems in the expression and dissemination of information between the individuals involved.

1.3.2 Strike-slip faulting

A common inference for the rift-oblique lineaments is that they have accommodated varying amounts of movement at different times of strike-slip reactivation (e.g. Lundin & Doré 1997; Johnson *et al.* 2005; Kimbell *et al.* 2005; Stoker *et al.* 2005b; Ellis *et al.* 2009). This is therefore a hypothesis which requires further testing within the seismic datasets. Harding (1990) set out a series of guidelines for the identification of strike-slip faulting using subsurface structural data which entails the identification of structures consistent with strike-slip (or transpressional/transtensional) deformation and then refuting possible alternative interpretations that involve predominantly dip-slip deformation. The structural criteria consistent with strike-slip faulting are (1) a through-going, steeply dipping master fault at depth, (2) changes in relative separation sense and/or fault dip direction along the strike of the master fault, (3) offset of the top basement, (4) positive or negative flower structures above the master fault, (5) coeval extensional and contractional structures within a single across-fault profile and (6) coeval en-echelon faults and/or folds on either side of the master fault (Christie-Blick & Biddle 1985; Harding 1990; Fig. 1.13).

Associated with strike-slip faulting, are other forms of deformation due to bends and stepovers within the master fault system (or principal displacement zone; PDZ; Fig. 1.14). Where strike-slip faults become curved they form either releasing or restraining bends, and in these areas, zones of extension (e.g. pull apart basins; negative flower structures) or compression (e.g. popup structures; positive flower structures) respectively may develop. If the strike-slip fault is segmented with significant offset of the individual fault segments, the stepovers are formed. These are termed either releasing stepovers or restraining stepovers and commonly are zones of extension and compression respectively (Woodcock & Fischer 1986; Fig. 1.14). Transfer zones (Faulds & Varga 1998) also accommodate significant strike-slip faulting however these are deemed separate to strike-slip faulting described here. Transfer zones are formed intrinsic to the rift evolution and movements along the faults are controlled by movements in the adjacent rift segments. The definition of strike-slip faulting used here does not require synchronous normal fault movements within the offset segments across the master fault, nor does the fault have to be located solely within the rift zone.

1.3.3 Deep crustal structure

A further complication associated with the NE Atlantic Margin is the poorly defined and debated deep crustal structure of the margin, particularly within the Vøring Basin (Mjelde *et al.* 2003b; e.g. Gernigon *et al.* 2004; Ebbing *et al.* 2006). Each of the competing hypotheses for the nature of the LCB will impact heavily upon the style and timing of deformation within the upper crust (Gernigon *et al.* 2004; Fig. 1.15). Firstly, if the LCB is related to magmatic underplating, replacement of mantle at the base of the crust by hotter, more buoyant material would lead to uplift of the margin. This would occur in areas which were rifted (and therefore have sufficient Moho relief) and is expected to occur during the Paleocene – Eocene at which time the plume impinged upon the base of the lithosphere (Skogseid *et al.* 2000). Erosion and depositional variations in the Paleocene would ultimately reflect the areas with increased and reduced magmatic underplating respectively (e.g. White & Lovell 1997). The magmatic underplating would also be the most likely source for igneous intrusives (Berndt *et al.* 2000) to be emplaced into the upper crust and therefore increased amounts of sills and dykes would also be expected to occur within the extended regions (Gernigon *et al.* 2006). However, if the LCB is formed due to magmatic underplating, it is expected that during the initial period of rifting in the Late Cretaceous, the rift would not be impacted by the younger magmatic underplating. Therefore, if rift segmenting structures had developed prior to magmatic underplating, the LCB can not be considered as a control on the along strike segmentation of the NE Atlantic Margin.

Secondly, if the LCB is related to serpentinisation of the mantle (Boillot *et al.* 1989) simple shear low-angle faulting is required to display large offsets during which time upper crustal unroofing is expected to develop, ultimately leading to the development of metamorphic core complexes (Wernicke 1985). Beta factors calculated from fault heaves are expected to be very large (e.g. > 5; Reston *et al.* 2001). If these parameters are recognised upon the NE Atlantic Margin, along strike variation in the structural style and beta factors would instead control the location of the LCB rather than the LCB controlling the location (and segmentation) of rifting. Increased concentrations of volcanic material would also be intruded where the upper crust is thinnest and therefore an increased density of sills and dykes would be located in the rifted areas. Sedimentation in the basin would be very complex due to the synchronous interaction between extension and uplift (and therefore erosion), but notable variations may be expected to occur between adjacent fault domains.

Finally, if the LCB is a high-grade metamorphic root associated with the Caledonian orogeny (a long-lived basement feature) the variation in upper crustal deformation may be controlled by the relief and thickness of the basement at depth (Gernigon *et al.* 2004). Variation in the relief of the basement will control long lived depocentres and structural highs for extended periods of time, which may be enhanced due to regional processes controlling subsidence and uplift of the basin. The basement will be modified during periods of rifting assuming the faults couple through and offset the basement. If the faults do not, instead detaching within a stratigraphically-higher sequence, the basement thickness and relief will only be modified by processes associated with whole lithosphere-scale stretching (e.g. pure shear lithosphere thinning), which has been proposed to occur upon the NE Atlantic Margin as depth-dependent stretching prior to continental breakup (Kusznir *et al.* 2005). Therefore, the only way in which the LCB can influence rift segmentation would be if it was a pre-existing crustal heterogeneity formed prior to rifting upon the NE Atlantic Margin. In areas where the basement was thickest, fewer sill intrusions may be expected due to a potentially thinner overlying sedimentary sequence. Sedimentation (through thickness and facies variations) in the basin would also reflect the variation in basement relief before, during and after rifting occurs.

Thus, depending upon the nature of the LCB, a crustal heterogeneity could explain the formation of rift-oblique lineaments upon the NE Atlantic Margin (if a basement feature), but in contrast could be controlled by the upper crustal extension (if serpentinised mantle). A magmatic underplating model for the LCB would only exert a control upon upper crustal rift segmentation if the segmentation developed synchronously or after the impingement of the Iceland plume at the base of the lithosphere.

1.3.4 Non-tectonic origins

With a significant improvement in seismic technology since the rift-oblique lineaments were first recognised upon the NE Atlantic Margin within 2D seismic reflection datasets, major strides have been made to the understanding of volcanic passive margins and rift basin evolution and dynamics. Therefore, when these lineaments were first recognised in geophysical datasets, at the time they were generally considered to be tectonic features. However, with the advent of 3D seismic data alternative processes have now been recognised, described and understood in basins both upon the NE Atlantic margin and elsewhere. These can be mapped with increased accuracy utilising 3D seismic data which allows for an improved interpretation rather than those made from the analysis of a single line or suite of 2D seismic data. A synopsis of other testable hypotheses is therefore given which, although are not of a tectonic origin, may have the apparent characteristics of a structural feature.

1.3.4.1 Sandstone injectites

Sedimentary features which are comparable to the 1-2 km wide seismic ‘transfer zone’ examples of Rumph *et al.* (1993) have recently been recognised within the Faroe-Shetland Basin (Fig. 1.16). These features are described as kilometre-scale sandstone intrusions formed in a deep water clastic system resulting from the remobilisation and injection of sand during the early stages of burial (Davies *et al.* 2006; Shoulders *et al.* 2007). The bodies form sub-vertical conical bodies with up to 300 m in positive relief. The age of the features is Late Miocene and sourced from overpressured Paleocene strata through a dominantly mud-prone Eocene – Oligocene succession which previously acted as a seal. Although the age of these features is much younger than the tectonic events which occurred in the basin, the distortion of reflectors with apparent offset across sub-vertical features may have led to the misinterpretation as a strike-slip principal displacement zone (PDZ). To test this hypothesis using well-calibrated 3D seismic data, these features would need to display the features described above, but are unlikely to form basin-scale features as inferred by the rift-oblique lineaments. They may only be expected to align along distinct rift-oblique structural trends if they formed during periods of rifting and could be correlated with active faulting in the basin at the time. Similarly, although they are of a sedimentary origin, they would not control basin-scale variations in stratigraphical fill and emplacement of igneous material unlike accommodation and transfer zones, as well as major strike-slip fault systems.

1.3.4.2 Volcanic intrusives

A suite of studies have focussed upon the NE Atlantic Margin over recent years due to the intrusive and extrusive volcanics imaged within seismic datasets (e.g. Kiørboe 1999; Planke *et al.* 2000; Bell & Butcher 2002; Thomson 2005a; b; Hansen 2006; Hansen & Cartwright 2006; Thomson 2007) appearing as high amplitude reflections due to the density contrast between the igneous and sedimentary rocks. On seismic data of older vintage those reflections associated with igneous material were not as readily identifiable as they are at present. Also the issue of using 2D seismic to understand a 3D problem also limited a full analysis of the problem which subsequently led to errors in geological interpretations (Chapter 2). This is particularly so with sills which intrude along sedimentary horizons and if on sufficient scale, may be misinterpreted as the original sedimentary reflectors. Inaccurate interpretations between offset sills (inferred as the same horizon) may lead to the inference of faults which are not actually present. The sub-vertical nature of igneous dykes which are difficult to image on conventional seismic data also adds to the complexity in understanding the evolution of the volcanic margin, presenting features which too may be interpreted as having a structural origin due to distortions of the seismic data (e.g. Thomson 2005a; b; Fig. 1.17). More recently, products directly related to the intrusion of igneous material into sedimentary sequences have been recognised. Hydrothermal vent complexes (Planke *et al.* 2005; Hansen 2006) are sourced from sill tips and lead to sub-vertical chimneys of remobilised sediment and volatiles expelled from the intrusion (Fig. 1.17). Equally, the sills can have an apparent tectonic effect locally affecting uplift and subsidence patterns through the growth and formation of forced folds (Hansen & Cartwright 2006). Therefore, products associated with volcanic activity would be local in extent and not basinal, but may be constrained by faulting if the volcanic material was emplaced synchronously with faulting or influenced by pre-existing structures (e.g. Thomson 2007). They would also have a minimal impact on sedimentation in the basin in comparison to major tectonic features such as fault domain boundaries and/or strike-slip faulting.

1.3.4.3 Resolution and display of the seismic dataset

The final hypothesis is that the interpretation of rift-oblique lineaments is an artefact associated with the condensed display of the seismic data and/or seismic processing. Improvements made in seismic data acquisition and processing sequences resulting in the enhanced resolution of seismic data as well as the increasing availability of 3D seismic data available has led to substantially increased accuracy of seismic interpretation. However, inaccuracies still exist but can be minimised if the interpreter understands the limitations of the dataset available. Geophysical processing artefacts have plagued the geological interpreter for many years with costly mistakes made on the basis of inferred geological structures (e.g. syncline bow-ties). It is therefore apparent that the latest 3D seismic data may reveal that these 'transfer zones' do not actually exist and are an artefact of the processing sequence. Alternatively, as seismic data is conventionally displayed at high vertical exaggeration, when displayed at true 1:1 scale, the features may have a very different style to that originally portrayed.

1.4 Project aims

The main aims of this thesis are to:

I. To constrain the geometry, kinematics and structural evolution of rift-oblique lineaments on the NE Atlantic continental margin using well-calibrated 3D seismic reflection datasets from the Faroe-Shetland Basin.

II. To develop a series of testable structural models explaining the geometry and kinematics of rift-oblique lineaments, and the interactions with structural highs/depocentres within the northern Vøring Basin.

III. To develop tectono-stratigraphic and volcanic models defining the impact of these lineaments on the evolution of the northern Vøring Basin with a view to understanding sedimentary pathways in segmented rift systems.

IV. To apply the developed structural and stratigraphical models to the sub-basalt region of the Faroe-Shetland Basin using potential field data, exploration 2D/3D seismic and recently acquired well data in order to better understand the role of rift-oblique lineaments in the tectono-stratigraphic evolution of the Faroe-Shetland Basin.

1.5 Thesis outline

This thesis is organised into five major chapters which are supplemented by several appendices containing supporting material.

Chapter 2 provides an overview of the geological and geophysical basis of the datasets available to this study and the methodologies and software used in the analysis and integration of various data types.

In **Chapter 3**, analyses are made of the rift-oblique lineaments in the Faroe-Shetland Basin using well-constrained 3D seismic data of regional extent. The chapter critically analyses the nature and tectonic significance of the rift-oblique lineaments in the Faroe-Shetland Basin concluding that the previously-published examples can be more simply explained as igneous intrusions, hydrothermal vent complexes, gas chimneys and/or faults that transfer extensional strain between en-echelon rift segments.

In **Chapter 4**, a strain analysis is performed across a fault domain boundary (the Rym Accommodation Zone) of the northern Vøring Basin, offshore Norway. The Rym Accommodation Zone separates two rift segments with contrasting rift styles, timing, loci of faulting, relative uplift and subsidence histories and deep crustal structure. The nature of the fault domain boundary is also analysed which displays features which are a departure from current conceptual models for accommodation zones.

In **Chapter 5**, a tectono-stratigraphic and magmatic analysis of the Rym Accommodation Zone and the rift-oblique Gleipne Lineament in the northern Vøring Basin is presented. This provides a model for the interaction between sedimentation and Late Cretaceous – Paleocene rifting as well as the distribution of both extrusive and intrusive volcanic material in relation to each of the rift segmenting structures.

In **Chapter 6**, the models formed in the previous two chapters are applied to a frontier region of the Faroe-Shetland Basin using regional potential field data as well as regional mapping of well-calibrated seismic data. A discussion is made as to the applicability of the models to the Faroe-Shetland Basin and the implications this has on our understanding of the basin evolution and dynamics as well as the impact upon hydrocarbon exploration in the region.

Conclusions are drawn together from each of the preceding chapters into a bullet-point list of new insights and advancements made in the understanding of rift-oblique lineaments on the NE Atlantic Margin in light of this work. Some recommendations for future expansion of this field of research are also stipulated.

It is important to note that the principal research chapters of this thesis (3, 4 and 5) have been prepared as scientific papers for publication in three different scientific journals. The present status of each publication is summarised as follows:

Chapter 3 has been published as: MOY, D. J. and IMBER, J. 2009. A critical analysis of the structure and tectonic significance of rift-oblique lineaments ('transfer zones') in the Mesozoic-Cenozoic succession of the Faroe-Shetland Basin, NE Atlantic Margin. *Journal of the Geological Society*, **166**, 831-844.

Chapter 4 is to be shortened and submitted to Tectonics as: MOY, D. J. and IMBER, J. Structurally complex fault domain boundaries (accommodation and transfer zones): an example from the northern Vøring Basin, offshore Norway.

Chapter 5 is to be shortened and submitted to American Association of Petroleum Geologists Bulletin as: MOY, D. J. and IMBER, J. The stratigraphic and magmatic evolution of segmented rift systems: an example from the northern Vøring Basin, offshore Norway.

Although each article is jointly authored with Dr. Jonathan Imber they are the work of the lead author, David J. Moy. Project supervisors provided editorial support in accordance with a normal thesis chapter. A reprint of Moy and Imber (2009) is available in Appendix E.

A series of appendices containing supporting material which is critical to the scientific case but is generally not published within scientific journals are provided. These include, but not limited to, seismic survey acquisition parameters, overviews of seismic processing sequences, well-seismic ties, time-depth tables and other scientific research deemed surplus to the research scope of each chapter. The appendices also include appropriate evaluation of the data quality, limitations and uncertainties where felt necessary. Where an appendix figure or series of appendices are relevant to the scientific case, these have been referred to as (Appendix A, B, C etc…) in the main text body of the thesis. A contents page is provided at the start of each appendix that the reader is recommended to consult, to identify and locate the relevant supplementary information. Appendix B (Chapter 3) is split into sections associated with each analysed lineament. This allows for all of the relevant supplementary material to be grouped together and be considered as a whole. This is in contrast to the other appendices which are ordered as referred to in the text.

An additional CD is also appended containing an electronic copy of the thesis, appendices, an electronic reprint of the Moy and Imber (2009) publication as well as PowerPoint and poster presentations which were given at various stages of the research at a range of national and international conferences. Due to a large quantity of statistics which are difficult to reproduce in the printed form, the CD also includes the time-depth tables for wells used in this study and a series of Microsoft Excel 2003 (.xls) spreadsheets used for the fault analyses completed in Chapter 4. A listing of the CD contents is given in Appendix F.

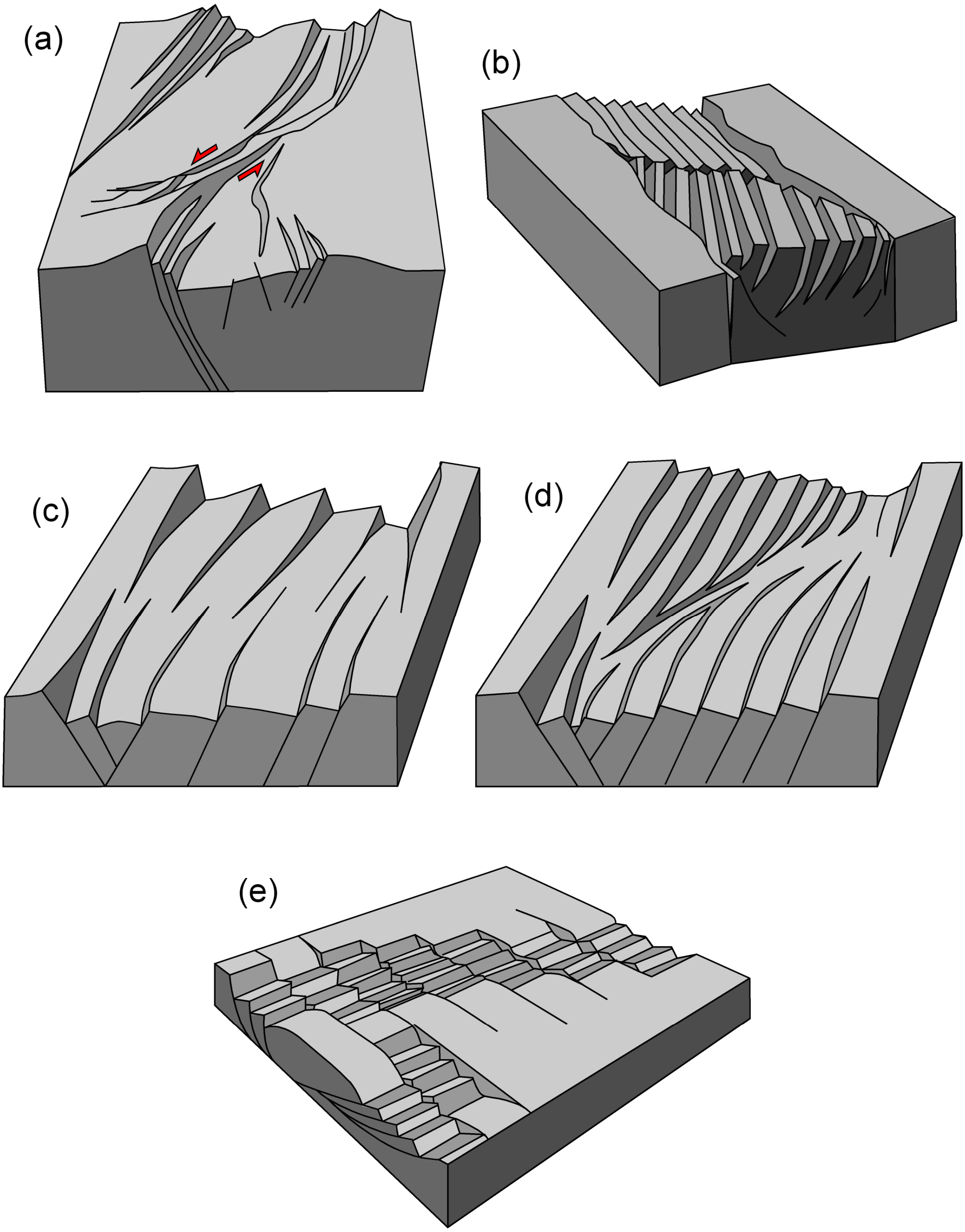

Figure 1.01: Variety of tectonic styles exhibited in segmented rift systems after (a) Ebinger (1989a), (b) McClay & White (1995), (c & d) McClay *et al.* (2002) and (e) Lister *et al.* (1986). The general consensus of models is that segmentation occurs on a basin-wide scale yet there is notable variation between the recognised structural styles. Segmentation structures form perpendicular or oblique to the basin bounding faults. Deformation styles also vary with either discrete basin segmenting fault systems or broad zones of overlapping normal faults present.

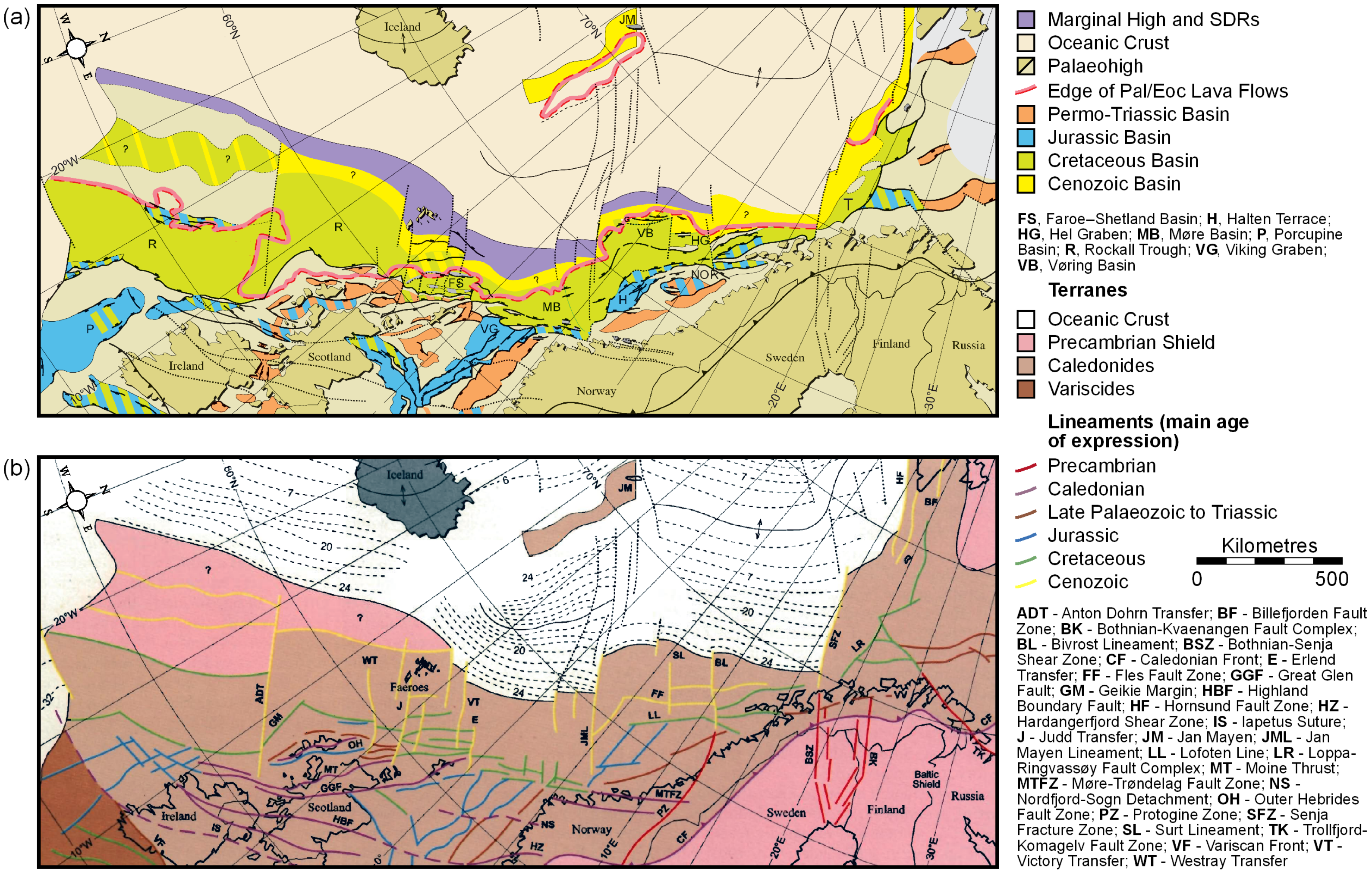

Figure 1.02: (a) Tectonic elements map of the NE Atlantic Margin. Basins are coloured according to the principal extension events responsible for their formation. (b) Basement terranes and lineaments coloured according to their main observed age of expression (after Doré *et al.* 1999; Keep & Harrowfield 2005).

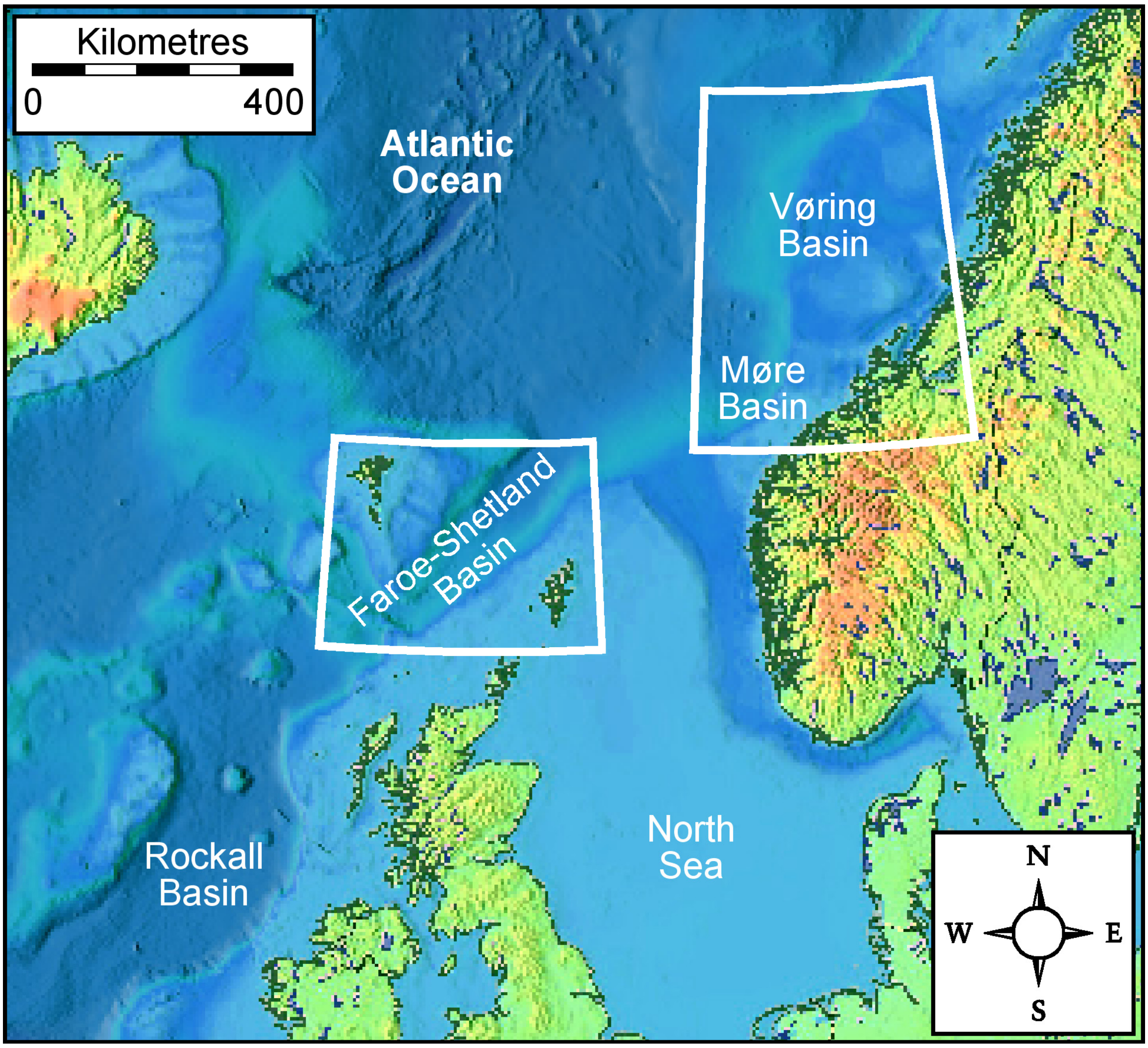

Figure 1.03: North Atlantic bathymetry map with study area locations. Blue shading are marine regions (darker = deepest regions), green regions are land (yellow/orange areas of highest elevation). Bathymetry data courtesy of USGS CMG InfoBank Atlas.

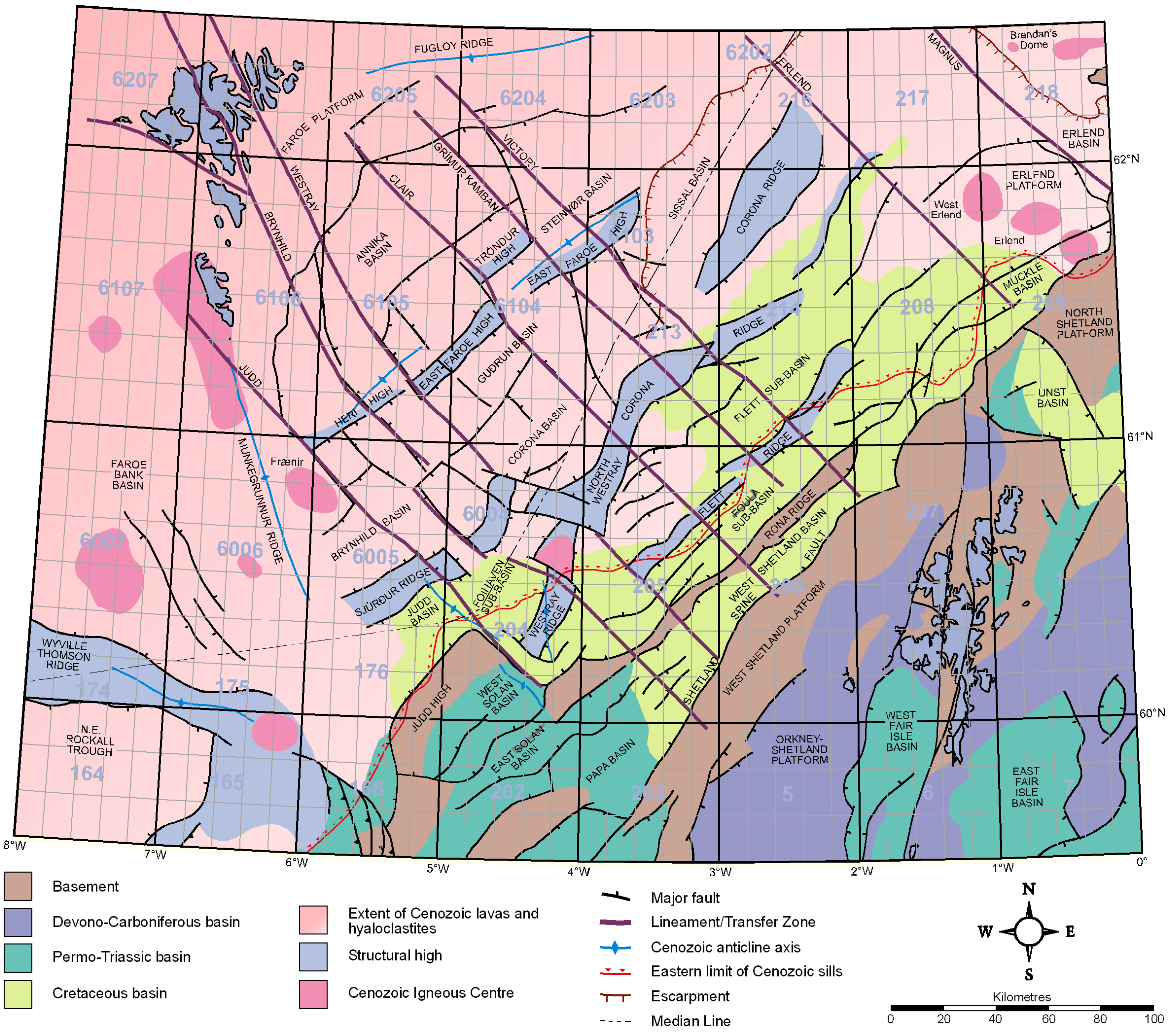

Figure 1.04: Faroe-Shetland Basin tectonic elements map modified after Ellis *et al.* (2009).

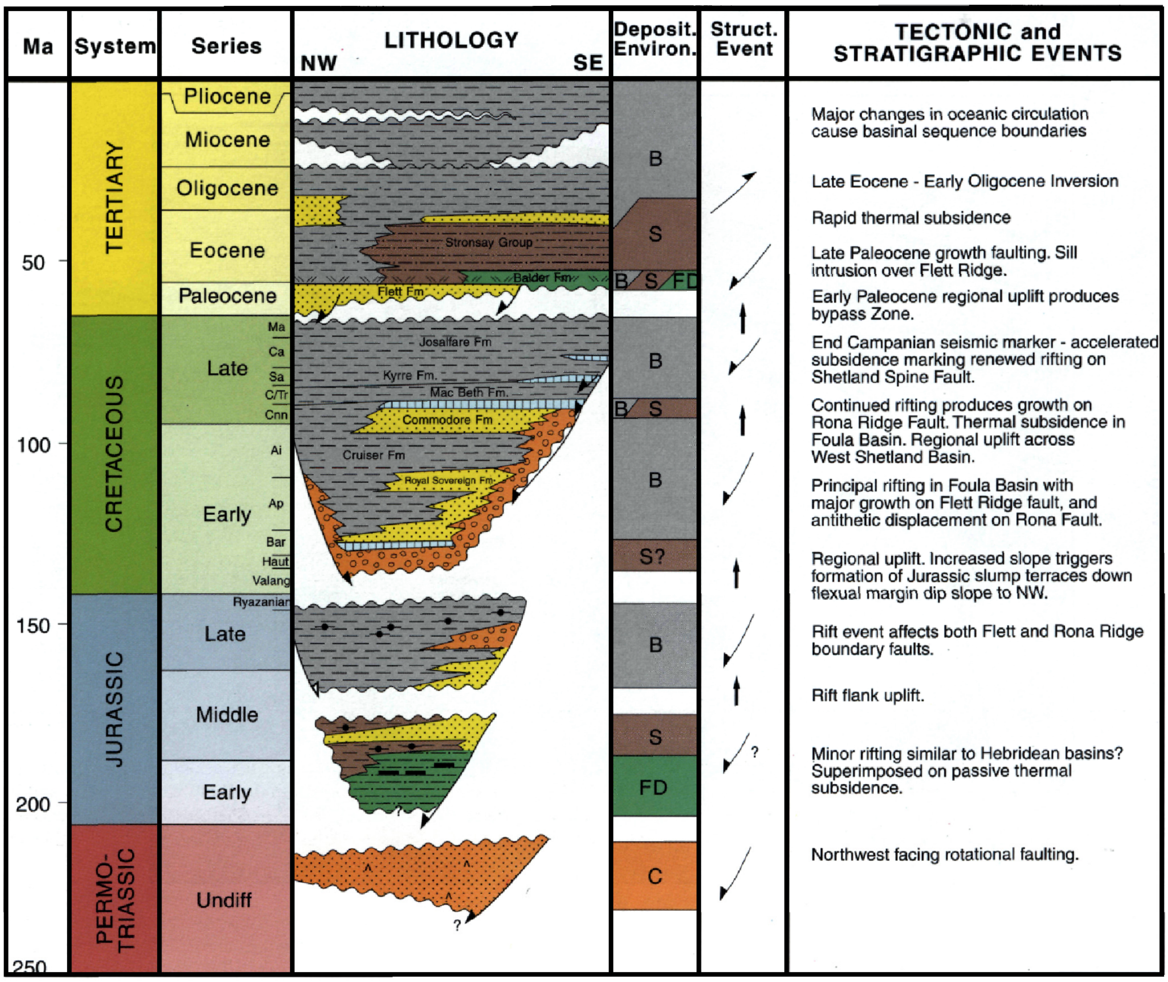

FD - Fluvio-Deltaic; **S** - Shallow Marine
C - Continental; **B** - Outer Shelf - Bathyal

Figure 1.05: Tectono-stratigraphic summary of the southern region of the Faroe-Shetland Basin (after Grant *et al.* 1999).

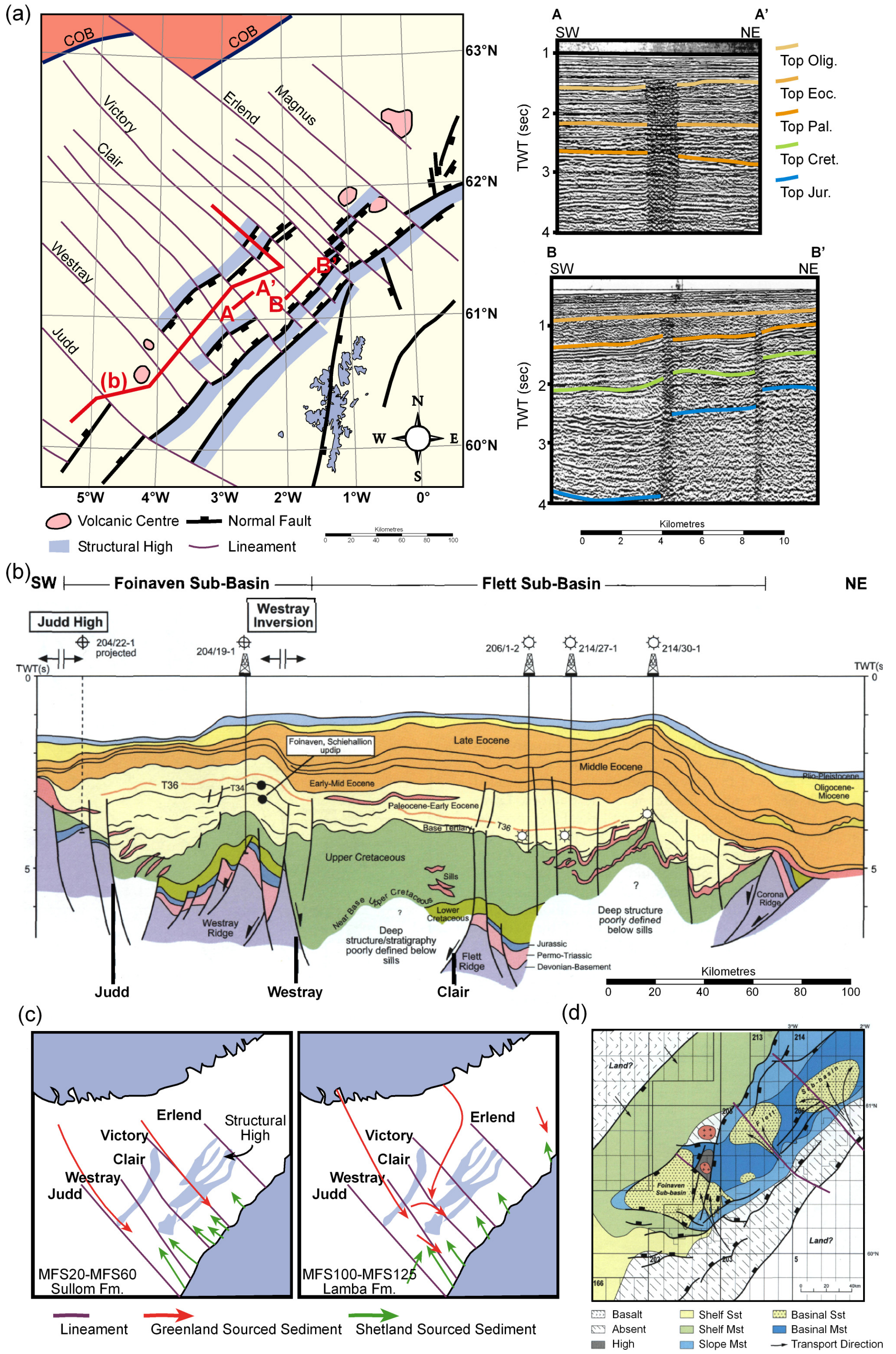

Figure 1.06: Rift-oblique lineaments of (a) Rumph *et al.* (1993) in map and cross sectional view. (b) Geo-section illustrating the faulting associated with the Judd, Westray and Clair Lineaments after Lamers & Carmichael (1999) and maps displaying the inferred control of the lineaments upon sediments entering the basin from (c) Greenland (Jolley & Morton 2007) and (d) the Shetland Platform (Lamers & Carmichael 1999).

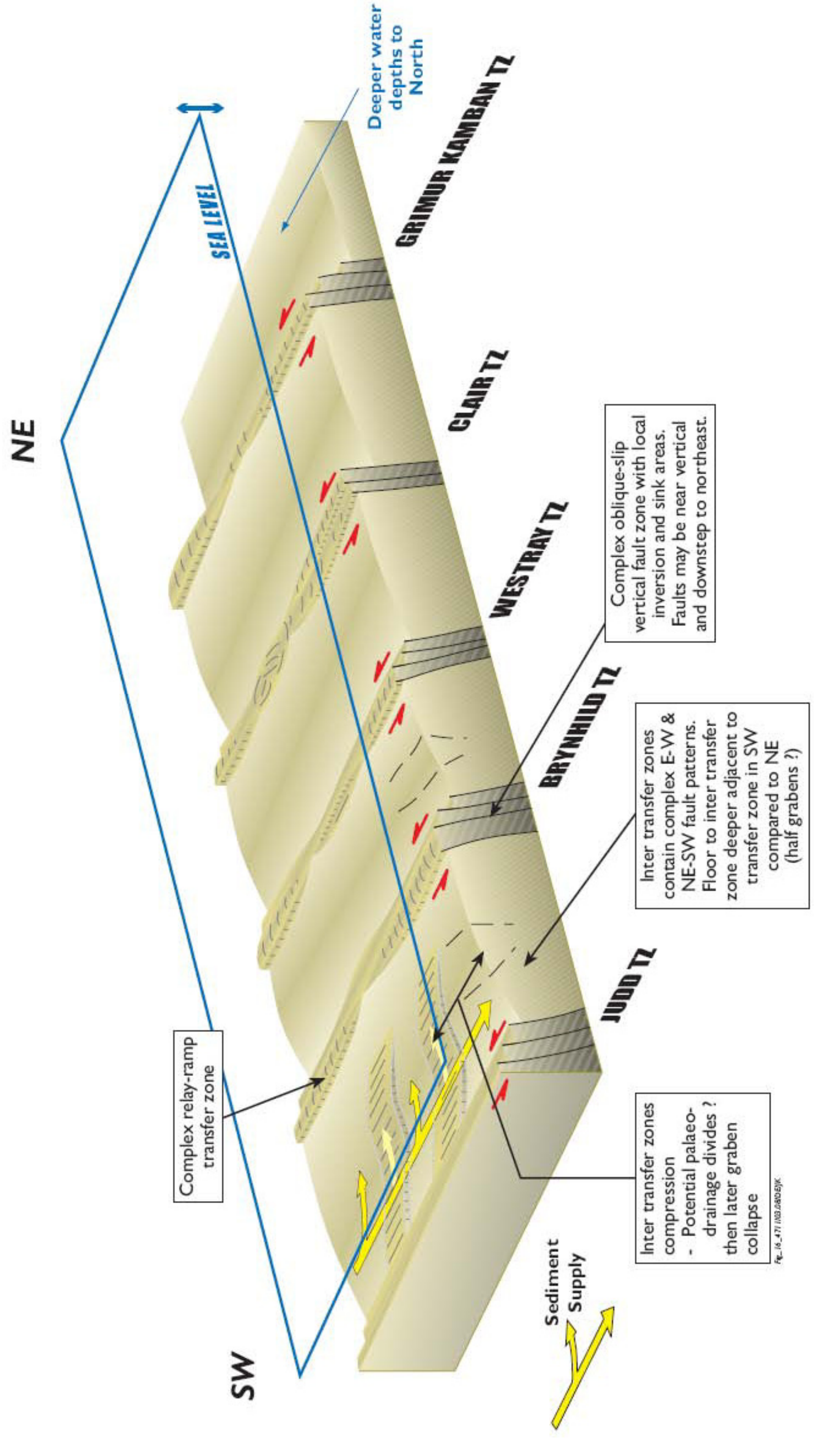

Figure 1.07: Conceptual model for the influence of rift-oblique lineaments on Paleocene sedimentation in the Faroe-Shetland Basin (Ellis *et al.* 2009). Note how the strike-slip movements along the 'transfer zones' lead to an along-strike segmentation of the basin. This forms a series of localised depocentres into which sediment into which sediment sourced along the lineaments is deposited.

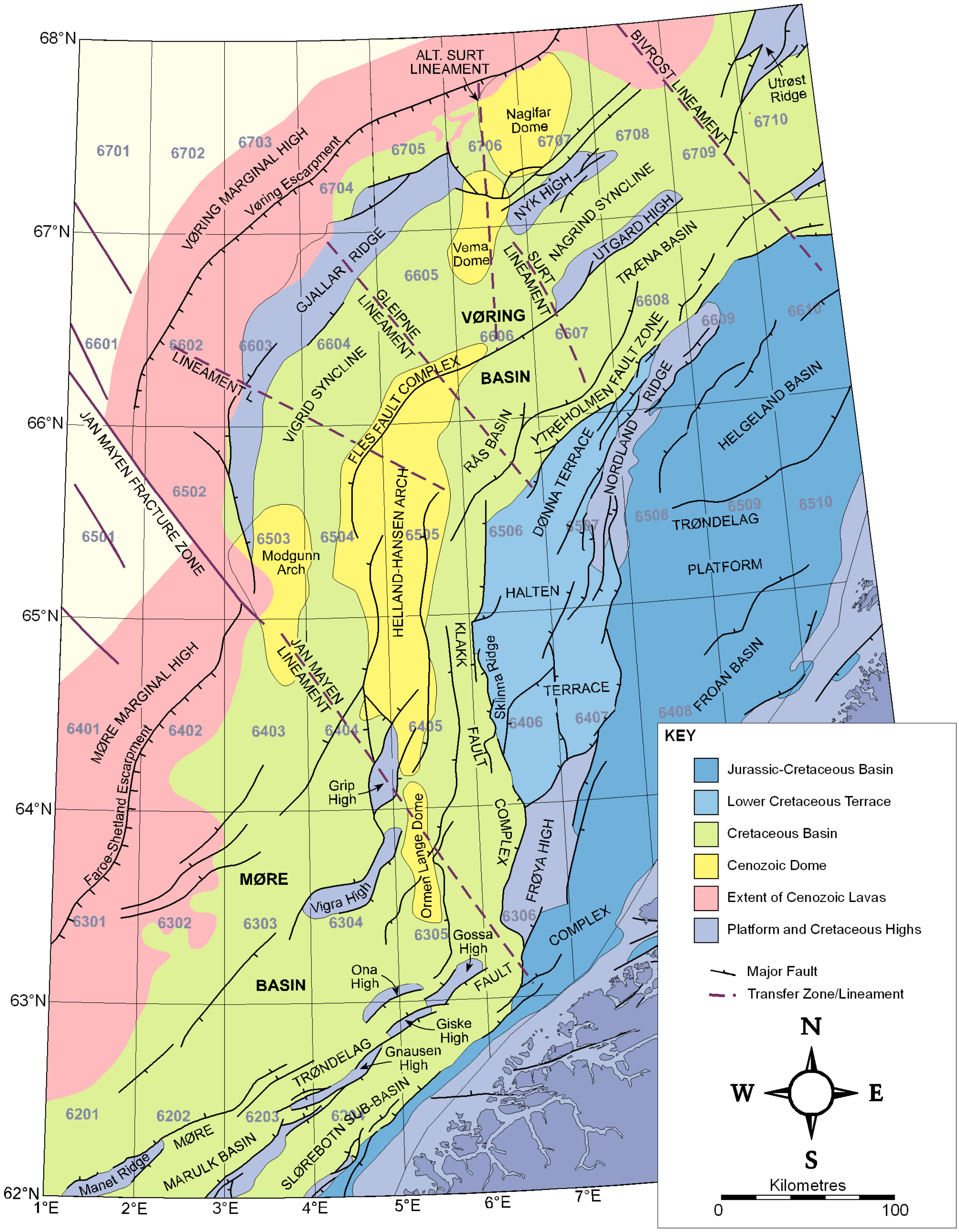

Figure 1.08: Norwegian continental margin tectonic elements map modified after Blystad *et al.*(1995) and Mjelde *et al.* (2005).

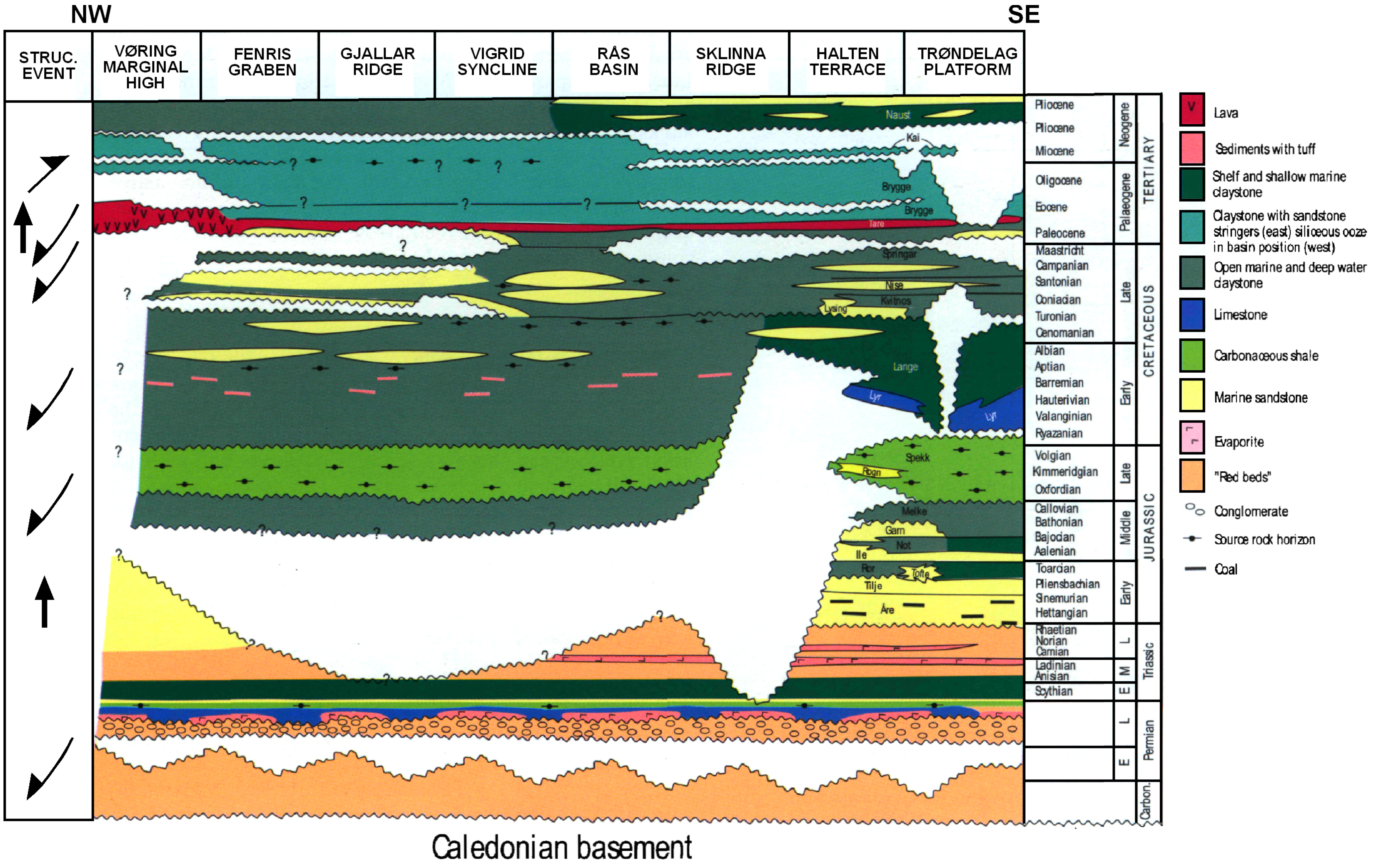

Figure 1.09: Tectono-stratigraphic evolution of the Vøring Basin (modified after Brekke *et al.* 1999; Doré *et al.* 1999).

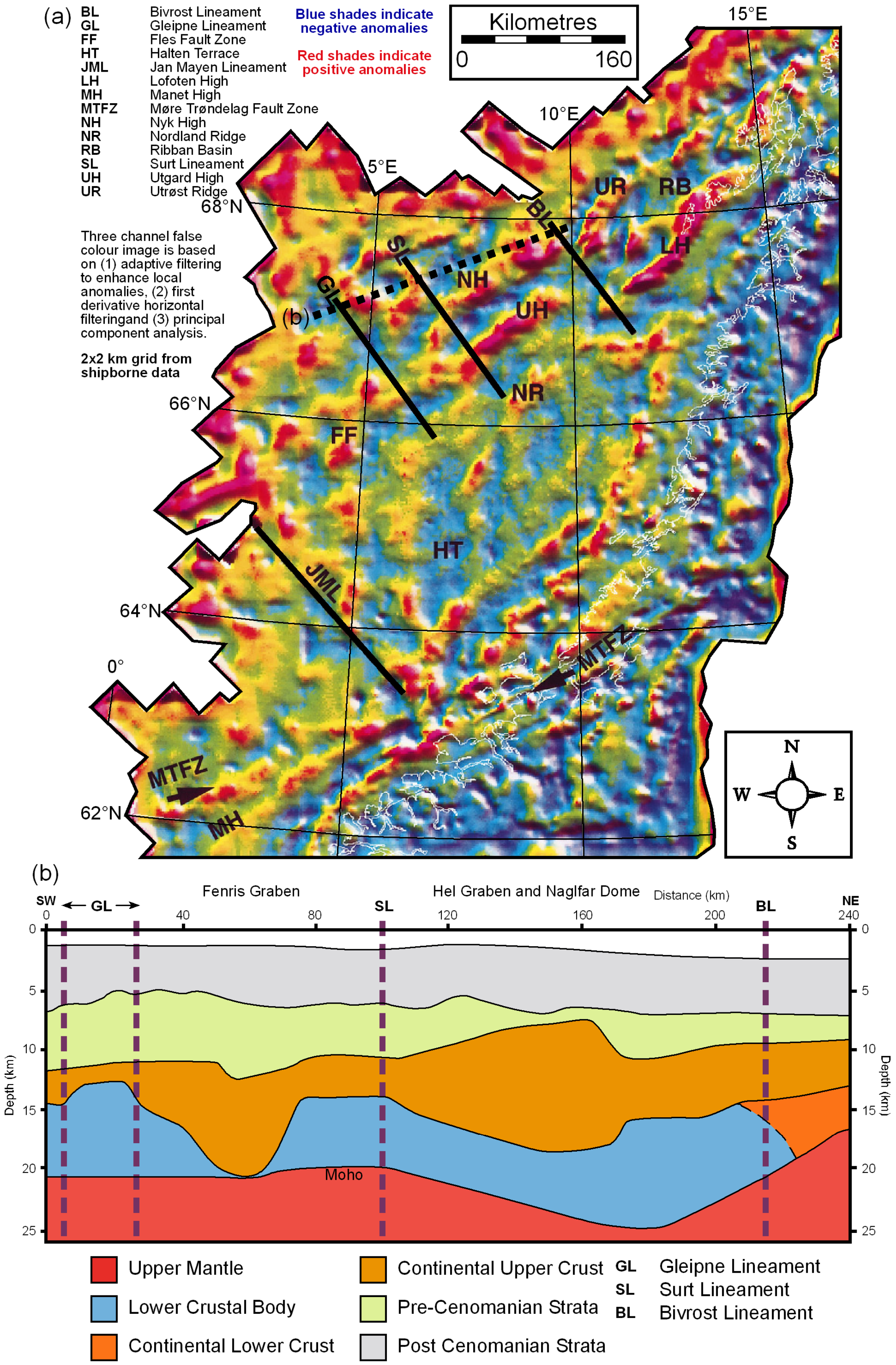

Figure 1.10: (a) Gravity anomaly map of the Norwegian Continental with location of rift-oblique lineaments identifiable within the dataset (after Doré *et al.* 1997b; Fichler *et al.* 1999). (b) Seismic refraction line across the lineaments of the outer Vøring Basin highlighting the changes in crustal configuration across the margin (Mjelde *et al.* 2003b).

Origin, Nature and Influence of Rift-Oblique Lineaments in Rift Basins

Deeper crustal structure	Strike-slip deformation	Fault domain boundaries (intrinsic to rift development)	Non-tectonic origin
Basement structure • Rift-oblique lineaments may be solely located within basement. • Yet, the nature, thickness, geometry and depth of basement varies greatly and each of these variables can influence the upper crustal evolution of rift basins. • Ancient zones of weakness are commonly cited as a direct influence on the development of fault domain boundaries. Basin structure • Fault systems formed under earlier periods of tectonic deformation (e.g. rift basin formation). • Formed within the underlying sedimentary succession. • May influence the later episodes of rift formation by direct reactivation of the fault structures or previous modification of the lithosphere structure.	Wrench faulting • Discrete zones of wrench faulting which segment natural rift systems. • Potentially active prior, during and after rift basin formation. • May extend outside the limits of the rift system and are directly related to the development of the basin. • Variety of deformational styles along the strike of fault system (Woodcock and Fischer 1986) resulting in areas of compression (restraining bends; pop-up structures & positive flower structures) and extension (releasing bends; mini-basins & negative flower structures). • Sedimentation patterns vary along the strike of the deformation linked to the style of deformation. • Further complicated by possible transtensional and transpressional effects.	Accommodation zones • Soft linked form of rift segmentation. • Characterised by a broad zone of overlapping normal faults. • Strain is transferred directly between the fault tips through a series of *relay ramps*. • Regions where sediment is most likely to enter the rift. • Onshore examples: East African Rift and Gulf of Suez. • Key Reference: Faulds and Varga 1998 Transfer zones • Hard linked segmentation of two offset rift segments. • Typically a discrete sub-vertical structure of oblique and strike-slip faulting. • Trend sub-parallel to the extension direction. • Movements along transfer zone are governed by the motion of the adjacent rift segments. • Strain is transferred directly between the rift segments by discrete rift-oblique transfer faults. • Sediment is likely to flow across transfer zones. • Onshore example: Basin and Range Province, USA. • Key reference: Faulds and Varga 1998. Transverse zones • Broad zone of complex deformation. • Contain a series of oblique-slip faults which form at high angles to the rift axis. • Other styles of deformation include dip-slip and strike-slip faults, folding, jointing and areas which have undergone varying degrees of torque/rotation. • Onshore example: Basin and Range Province, USA. • Key reference: Rowley 1998.	Volcanic features • Volcanic rift basins contain a variety of features associated with enhanced igneous activity on both local and regional scales. • Features include dyke and sill complexes, laccolithic intrusions, seabed fissures and dyke-fed volcanoes. Sedimentary features • Localised remobilisation of overpressured water-rich sediment has led to the intrusion of sands into the overlying sedimentary overburden. • The intrusion of igneous sills into a sedimentary sequence can lead to the formation of discrete hydrothermal vent complexes.

Table 1.01: Hypotheses for the origin, nature and influence of rift-oblique lineaments in rift basins.

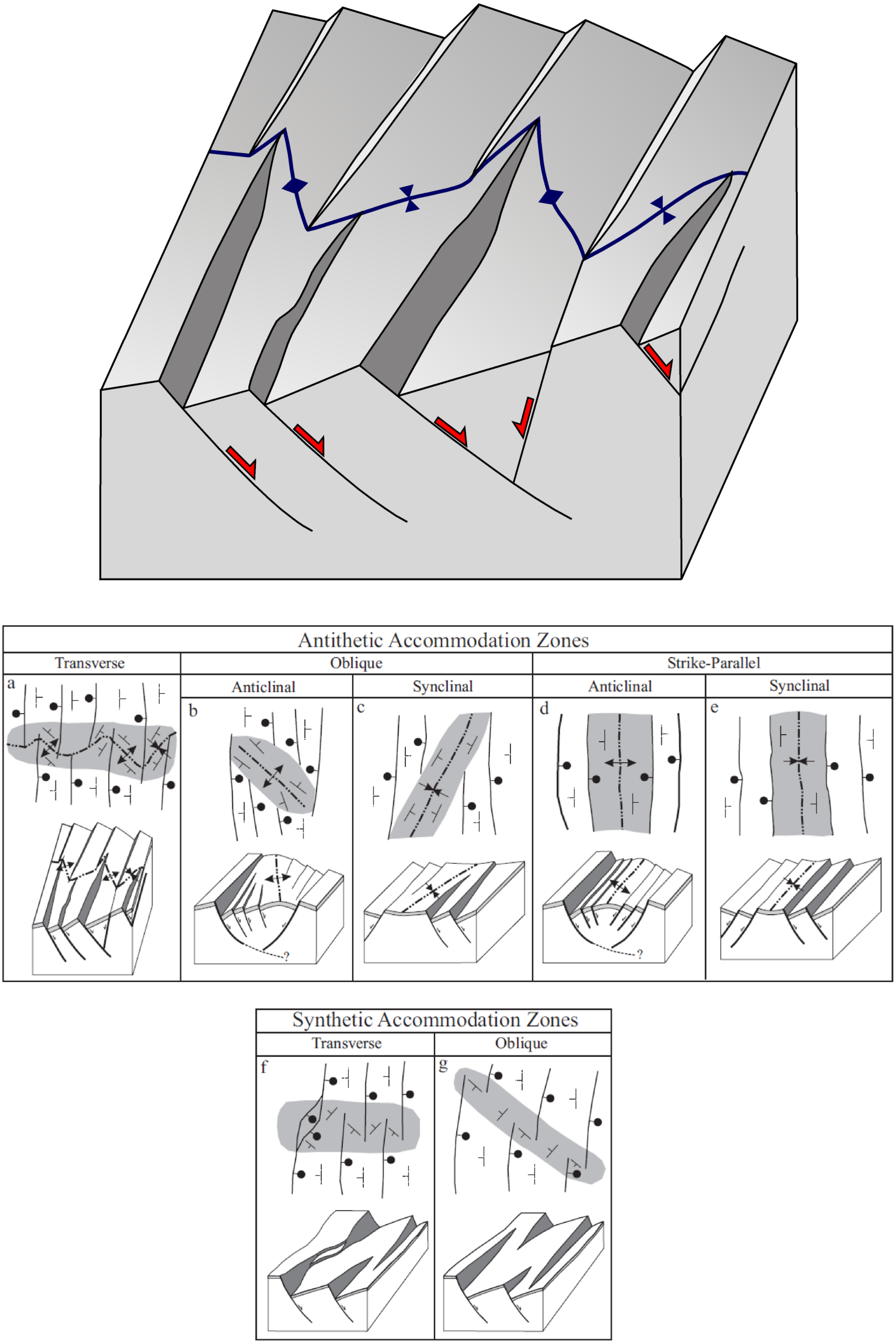

Figure 1.11: Conceptual models of an accommodation zone (Faulds & Varga 1998).

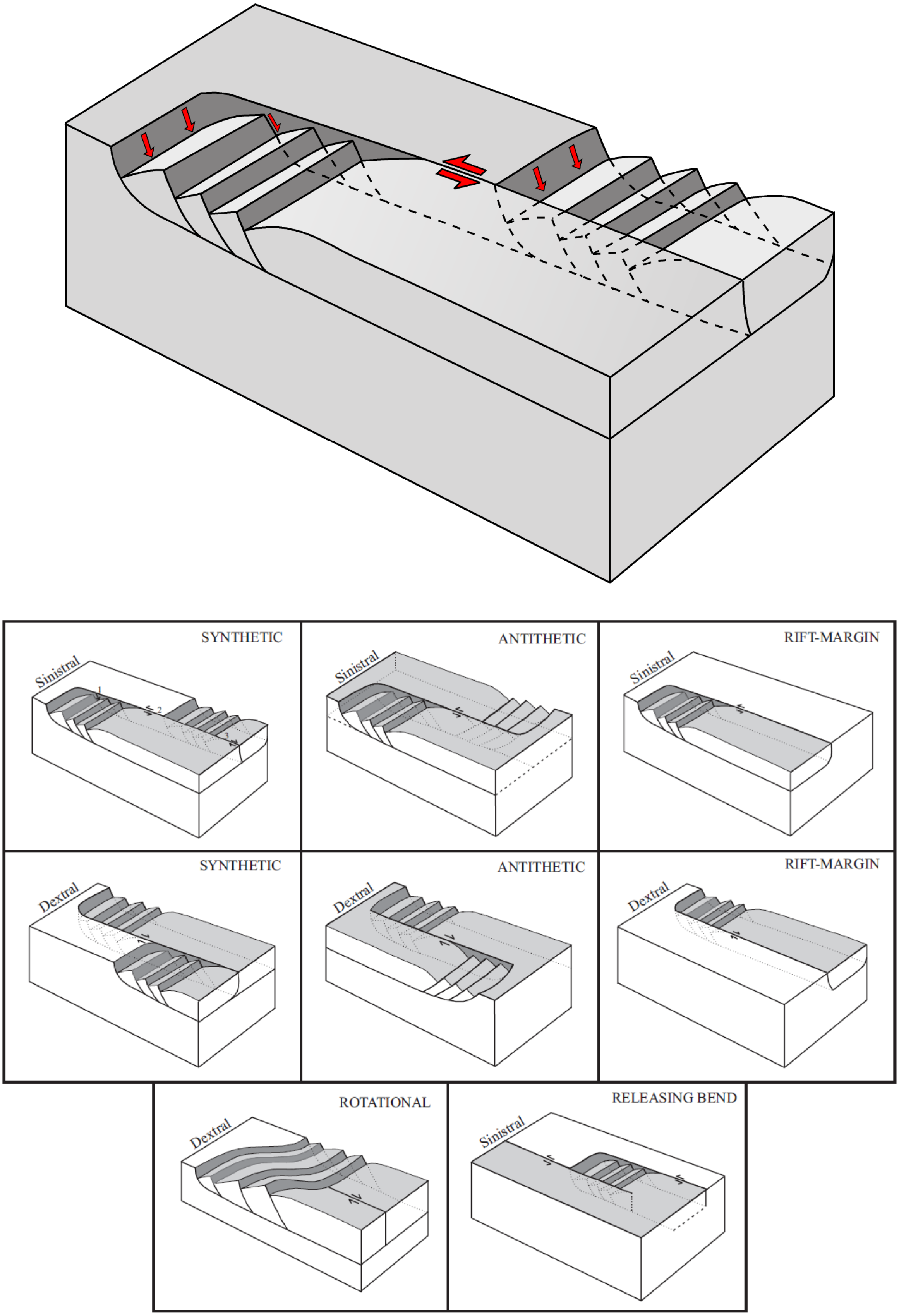

Figure 1.12: Conceptual models of a transfer zone (Faulds & Varga 1998).

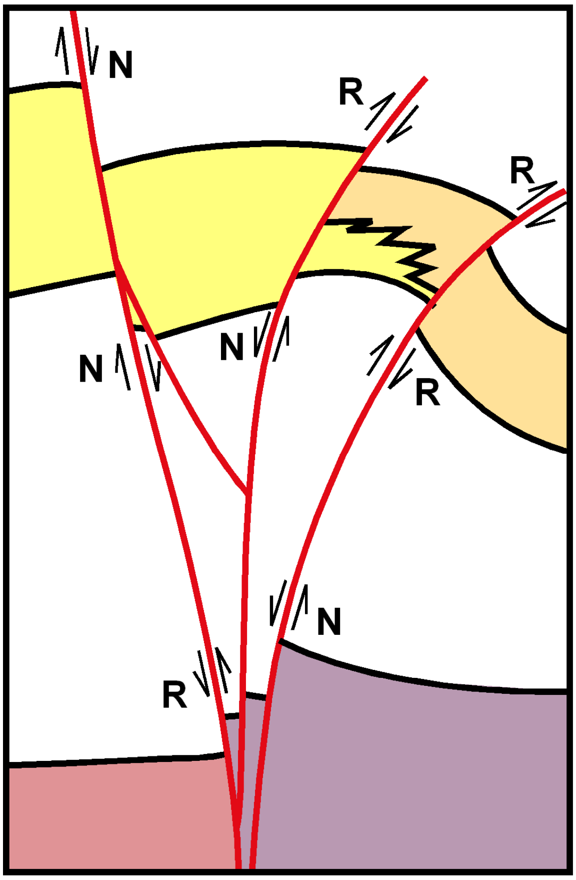

🟥🟪 Crystalline Basement

🟨🟧 Time-stratigraphic unit with variable sedimentary facies

N **Normal fault offset**

R **Reverse fault offset**

MAJOR CHARACTERISTICS
Basement involved.
PDZ sub-vertical at depth.
Upwards diverging and rejoining splays.

JUXTAPOSED ROCKS
Contrasting basement type.
Abrupt variations in thickness and facies in a single stratigraphic unit.

SEPARATION IN ONE PROFILE
Normal and reverse separation faults in the same profile.
Variable magnitude and sense of separation for different horizons offset by the same fault.

SUCCESSIVE PROFILES
Inconsistent dip direction on a single fault.
Variable magnitude and sense of separation for a given horizon on a single fault.
Variable proportions of normal and reverse separation faults.

Figure 1.13: The major characteristics of an idealised strike-slip fault in cross section (modified after Christie-Blick & Biddle 1985; Allen & Allen 1990).

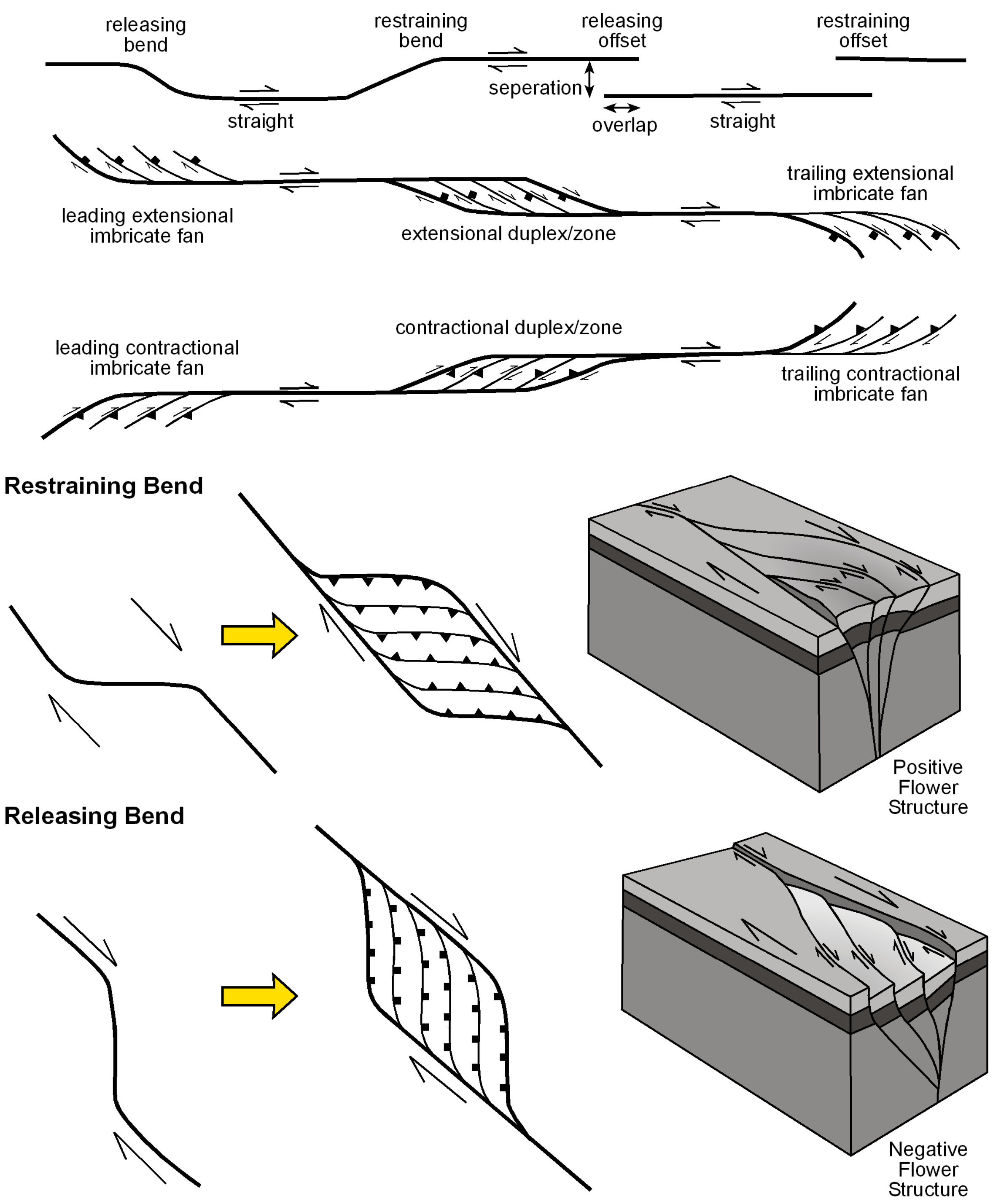

Figure 1.14: Deformation associated with strike-slip faulting (modified after Woodcock & Fischer 1986).

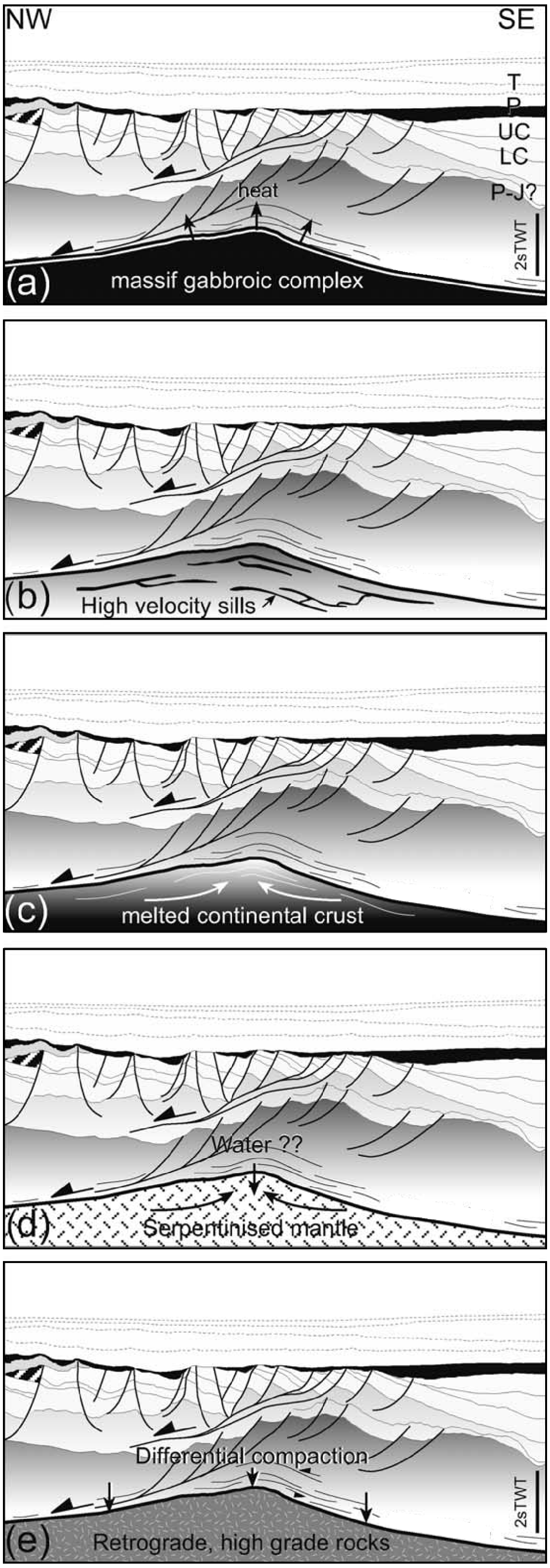

Figure 1.15: Hypotheses for the nature of the Lower Crustal Body (LCB) in the northern Vøring Basin. The various models are (a) magmatic underplating of the crust during continental breakup, (b) igneous intrusions of the lower crust, (c) melting of the continental crust, (d) serpentinisation of the mantle and (e) metamorphic basement rocks. **T** Tertiary; **P** Paleocene; **UC** Upper Cretaceous; **LC** Lower Cretaceous; **P-J** Paleozoic – Jurassic (Gernigon *et al.* 2004).

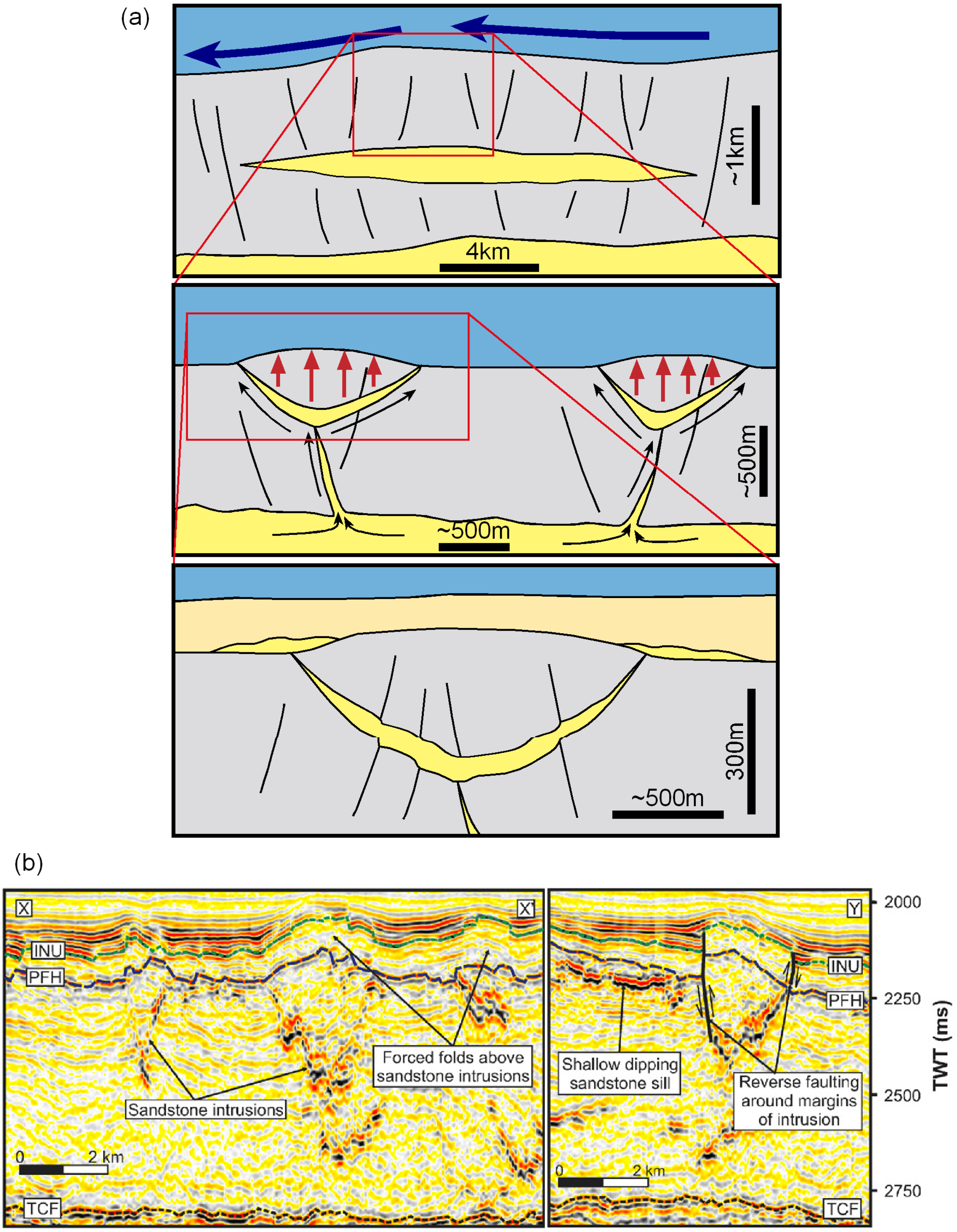

Figure 1.16: (a) Formation and evolutionary model of Late Miocene sandstone injectites in the Faroe-Shetland Basin (Shoulders & Cartwright 2004). They have an unusual seismic character (b) associated with bright amplitudes at the base with localised folding due to the volume change at depth (Shoulders *et al.* 2007). **TCF** Top Caledonian Fan; **PFH** Polygonal Fault Horizon; **INU** Intra Neogene Unconformity.

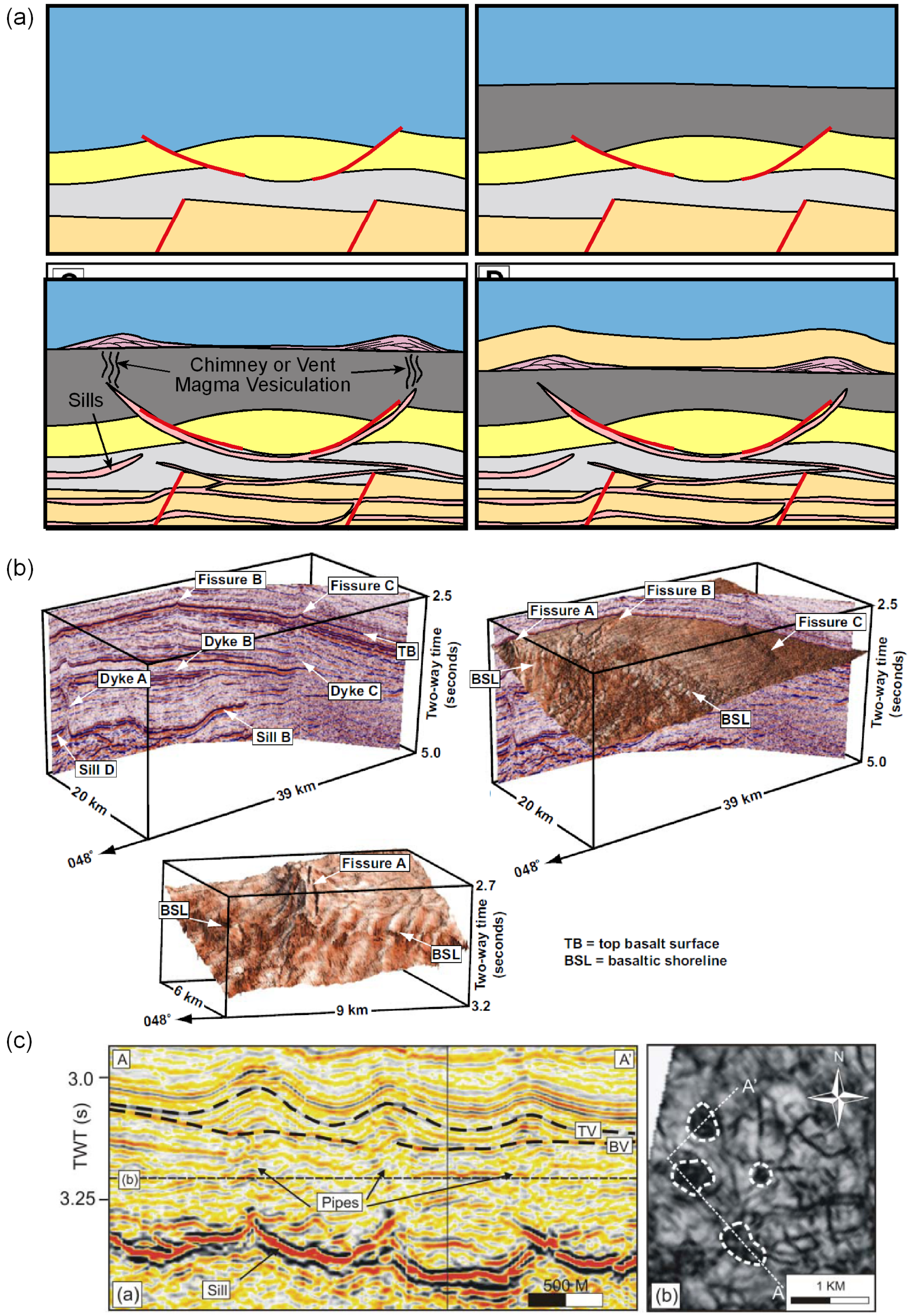

Figure 1.17: (a) Paleogene submarine dyke fed volcano evolution (Davies *et al.* 2002) with 3D seismic data highlighting the interaction between sills, dykes and volcanic fissures on the NE Atlantic Margin (Thomson 2007). (c) Chimneys located above sill tips are termed hydrothermal vent complexes (Hansen 2006) of similar form to the aforementioned igneous features, but were not recognised until the 2000's in seismic data due to the advent of 3D seismic data and greater exploration in igneous-affected basins.

Chapter Two

2 DATASET AND METHODOLOGY

The data requirements for the analysis of ancient rift-oblique lineaments located within a predominantly offshore environment requires the integration of multiple geophysical and geological datasets. The following chapter therefore opens with a section which acts as an introduction to these techniques. The datasets used for the analysis are subsequently discussed followed by the methodical approach and the software used to investigate the problem. The main aim of this chapter is to outline the data and methods used in the present study and how they were incorporated to define the growth, nature and tectono-stratigraphic significance of rift-oblique lineaments on the NE Atlantic Margin.

2.1 Physical basis of geophysical and geological datasets

A series of marine, airborne and satellite acquired datasets are used for a better understanding of submarine geological systems on a variety of scales. First hand analysis of the sub-seabed geology is limited, with much of the data acquired from commercial (e.g. hydrocarbon exploration) and scientific (e.g. the Integrated Ocean Drilling Program; IODP) drilling operations. Other data is gathered by remotely-sensed geophysical methods, each of which has distinct advantages and disadvantages; however, the integration of results and interpretations from each of the individual datasets may provide a more comprehensive understanding of the geological evolution of continental margins.

2.1.1 Potential field data

Potential field datasets are often acquired remotely within marine basins by means of ship, aircraft or satellite surveys, the selected method depending upon a range of variables including the research objectives, funding constraints and availability of the necessary technology. Shipborne and airborne surveying are the most commonly used methods as they produce a high resolution dataset compared to satellite surveys which often study the Earth as a whole and are very expensive. Shipborne surveys can be conducted synchronously with seismic surveys however they are more expensive compared to airborne surveys which can be completed within shorter time spans. Basin-scale gravity and magnetic surveys when used together can provide more information about the subsurface, particularly the basement rocks, than either technique on its own. These are often undertaken in a region prior to acquiring seismic data which provides more detailed information about the subsurface.

2.1.1.1 Gravity data

Gravity surveying measures the variation of the Earth's gravitational field due to differences in the density of the sub-surface geology. Gravity surveying has a range of applications which include, but are not limited to, hydrocarbon exploration, regional geological studies, monitoring volcanic hazards and exploration for and volume estimation of mineral deposits. Each rock type is associated with a relatively well-constrained density range which varies depending upon the in-situ conditions at the time (Telford *et al.* 1990). As a general rule of thumb, sedimentary rocks have the lowest density (average ~ 2.1 ± 0.3 kg/m^3) ranging from chalk with an approximate average density of 2.01 kg/m^3 through to dolomite with a density of 2.70 kg/m^3. The variation in density of sedimentary rocks is controlled by at least seven factors; composition, cementation, age and depth of burial, tectonic processes, porosity and pore-fluid type. Igneous rocks are generally denser than sedimentary rocks, with basic rocks denser (e.g. basalt, 2.99 kg/m^3 and gabbro, 3.03 kg/m^3) than acidic rocks (e.g. rhyolite, 2.52 kg/m^3 and granite, 2.64 kg/m^3) due to the difference in silica content. Metamorphic rocks vary considerably depending upon the original lithology and grade of metamorphism, but within sedimentary basins generally range between 2.5 and 3.0 kg/m^3.

Collected gravity data often has to be processed and corrected to a common datum such as sea level (the geoid). A number of corrections are able to be made depending upon the area surveyed. Upon continental margins and ocean basins, an elevation correction has to be applied; either by free-air correction or Bouguer correction. Free-air correction allows for a reduction in the magnitude of gravity with height above the geoid. The Bouguer correction accounts for the low density of sea water which is effectively replaced by an equivalent thickness of rock (with a specified density). When each of these corrections are also corrected for variation in latitude, the free-air and bouguer anomalies are calculated which are commonly used to display corrected gravity data for oceans and continental margins.

2.1.1.2 Geomagnetic data

Geomagnetic methods can be used in a wide range of investigations on a variety of scales from locating basic igneous sills and dykes, identifying boundaries between lithologies with contrasting geological boundaries (e.g. faults) and well as mapping the extent of large-scale geological structures. The magnetic susceptibility of rocks within the Earth's magnetic field ranges greatly and is dominantly controlled by the concentration of ferro- and ferri-magnetic minerals. As a result, basic and ultra basic rocks have the highest magnetic susceptibilities of all rock types. The average susceptibility for sedimentary rocks ranges from 0 – 360 SI units with basic igneous rocks ranging from 550 – 122000 SI units (Reynolds 1997). This induced magnetisation is further complicated by the remnant magnetisation of a rock, where in the absence of an applied field, a measurable intensity of magnetisation is sustained due to permanently magnetised particles. The summation of both induced and remnant magnetisation magnitudes form the resultant magnetisation, which leads to greater degrees of freedom and variation in the rocks magnetisation. The natural remnant magnetisation is acquired by the rock under natural conditions at the time of deposition. Other processes by which a rock can acquire a remnant magnetisation include the cooling and solidification of an igneous rock from above the Curie temperature where the magnetic minerals have the ability to realign prior to returning to a normal temperature (thermal remnant magnetisation). Secondary remnant magnetisations may be acquired later in the rocks history through chemical, viscous or post-depositional processes.

Corrections also need to be made during the processing stage, the most significant correction being for the diurnal variation in the Earths magnetic field from a known datum taken at a point close to the survey location. In ship and airborne surveys, due to it not being possible to frequently return to a base station (where a datum is calculated), surveys are designed so that the track lines intersect allowing for the dataset to be corrected appropriately. Latitude and longitudinal variations in the Earths magnetic field also need to be taken into consideration, particularly on surveys of regional extent. With the processed magnetic anomaly map, both qualitative (e.g. tectonic element maps) and quantitative (e.g. depth to magnetic body estimations) interpretations of the dataset can be made.

2.1.2 Seismic reflection data

Seismic reflection surveying is the most widely used geophysical technique and has been used since the 1930's. Its predominant applications are for hydrocarbon exploration and research of the upper crustal structure of the Earth with depths of penetration in the order of several kilometres. There is a vast amount of technical literature available upon seismic reflection surveying as a very large amount of research and development has been undertaken within the hydrocarbon industry. The basic synopsis of the seismic reflection technique is to measure the time taken for a seismic wave to travel from a source (e.g. air or water gun) down to a horizon (the boundary between two lithologies of contrasting densities and velocities creating an acoustic impedance contrast) where it is then reflected back to the surface, detected by a receiver (e.g. a hydrophone). The time it takes for this to happen is known as the two way travel time (TWTT). From this data, an important processing sequence is undertaken to produce the final time-migrated seismic section. The processing sequence is often the same but the contractor's choice of parameters can alter the final product dramatically. A typical processing sequence would be (I. Stimpson, Keele University, Pers. Comm.):

1) *Gain correction* – increases the amplitudes that are reduced due to absorption and geometrical spreading of the energy from the point source as a function of time.

2) *Editing* – removes incorrect data to improve the signal-to-noise ratio such as erroneous traces due to misfires of air guns.

3) *Statics corrections* – removes the near surface effects to improve signal to noise ratio. Example surface effects are an irregular topography and a weathering layer of variable thickness and velocity in land based surveys, and the need to compensate for a delay between the air gun firing and start of recording in marine surveys.

4) *Signature deconvolution* – removes the source wavelet effect to increase the resolution of the seismic dataset such as the removal of bubble pulses from airgun sources in marine surveys.

5) *Predictive deconvolution* – reduces the energy from multiples to increase the signal to noise ratio. Multiples are predictable in seismic data and by using a convolution filter to predict the response of a trace, multiples are removed and reflections are enhanced.

6) *Frequency filtering* – also known as a velocity filter (frequency domain) or dip filter (time domain), this removes noise from the seismic data (which is generally of

steeper dips than reflections on a common mid-point gather) and therefore increases the signal to noise ratio.

7) *Velocity analysis, dip and normal move out and stacking* – corrects data for a non-zero offset and adds the results together the results to cancel out the effects of noise. This also reduces the geometric distortion of the data and increases the signal to noise ratio.

8) *Predictive deconvolution* – the earlier predictive deconvolution uses a large gap between a known trace and a predicted trace to reduce the overall multiple energy. At this stage of the processing sequence, a short gap is generally applied to give the sharpest possible reflections.

9) *Migration* – the purpose of the migration process is to place a given seismic event in its correct geometrical position on the time section. The basis of the migration method is Huygens' secondary source principle. This states that any point on a wavefront can act as a secondary source producing circular wavefronts in three dimensions. The process of migration is to collapse the secondary wavefronts to their points of origin.

10) *Improving the display of the processed seismic dataset* – a band pass filter is applied to remove any remaining noise that was created by the earlier steps yet a compromise has to be made between noise rejection and a loss of seismic resolution. The data is then scaled to a suitable level for display.

The seismic reflection technique is used to gain important details regarding the subsurface geology, not only the geometry of the structures but also the physical properties of the materials present, at a much higher resolution to what potential field data is capable. The most important problem associated with seismic reflection surveying is the conversion from two way travel time to depth which is predominantly controlled by the seismic velocity, a parameter which is not simple to define.

Two dimensional (2D) seismic acquisition is formed as a loose grid of dip lines (also know as inlines) perpendicular to the basin strike previously defined from potential field data and strike lines (also known as crosslines) which are shot along strike to tie the inlines. Three dimensional (3D) surveys were first undertaken in 1975 and provide many more advantages to the conventional 2D seismic acquisition. In 2D seismic, adjacent lines are separated by hundreds of metres to kilometres. In 3D seismic data, inline spacing is comparable to crossline spacing (often ~25 m), hence the final processed data consists of a 3D cube rather than a series of 2D sections. 3D seismic data has numerous advantages in view of the resolution of the seismic data. Imaging is improved because previously 'out-of-plane' reflections are now useful data rather than noise as previously out of plane reflections can be successfully migrated; a 2D section is a response to a 3D wavefield. Reflectors also tie better between inlines and crosslines and seismic lines can be viewed in any orientation, with the added benefit of producing horizontal 'time slices' of the seismic cube at different TWTT. For the interpreter of the 3D seismic data, much more confidence can be taken from the mapping of structures and sequences which are inherently three-dimensional. In 2D data, aliasing of geological features can, and almost certainly will occur due to the large spatial separation of the lines (Cartwright & Huuse 2005). 3D seismic data is a critical component in the analysis of rift-oblique lineaments in rift basins as these features would be difficult to distinguish on 2D seismic reflection lines predominantly oriented parallel to the extension direction.

A significant drawback with 3D seismic data is that acquisition and processing are much more expensive and as such 3D is only employed to study particular localised areas of interest in more detail. Seismic reflection surveying also has a variety of other problems associated with it, in particular the vertical and horizontal resolution varies based upon four factors; quality of the acquired raw data (the correct equipment must be used and operated properly), the appropriate frequency range system for the objective of the survey, level of understanding of the source response characteristics and the nature of the vertically stacked sequence of subsurface reflectors. Steeply dipping (> 45°) horizons and sub-vertical features are often poorly imaged within seismic datasets due to the high angles between the feature and downward directed seismic wave.

Seismic interpretation is associated with a range of pitfalls but these are minimised when the final product is of a sufficient quality. The acquisition and processing stages of seismic reflection surveying have notably improved over time which means seismic data of an earlier vintage is likely to be less well processed than more modern datasets. Care does need to be taken when analysing seismic data in the time domain as the apparent dip on a seismic reflector is produced by velocity variation within a layer. As velocity increases and decreases within the horizon, so the travel time through the material decreases or increases respectively even though the reflector is horizontal. A second aspect are bulges and cusps in an otherwise planar reflector which are caused by anomalous velocities above the reflector. A pull up occurs when the overlying velocity is faster (e.g. an overlying salt dome), conversely, a push down when the overlying velocity is lower (e.g. hydrocarbon saturated rock is of a lower velocity to water saturated rock). Seismic interpretation is just that, an interpretation of the Earth's geological evolution, but if the above considerations are taken into account, seismic interpretation can be a useful aid in understanding the upper crustal evolution of the Earth

2.1.3 Well data

Well data is the only direct way of sampling subsurface geology but is expensive compared to the aforementioned geophysical methods. Data predominantly remains confidential until publically released, as this key data point is of particular value to hydrocarbon companies into which a considerable amount of time and money has been expended during both the well planning and drilling process. A variety of datasets are obtained from wellbores which includes rock chippings, well cuttings and cores as well as geophysical wireline well logs. As a rule of thumb, chippings are used during the drilling phase and interpretation of core samples and geophysical well logs is completed post drilling of the wells.

Rock chippings are often used by the mud logging geologist upon a drilling rig. These are fragments of rock returned to the surface within the drilling mud which both acts to lubricate and cool the drill bit. These rock chippings can be used to understand the lithology at each stage of the drilling process, with an interpretation made as to which stratigraphic interval each sample belongs. Apart from the lithology, relatively little information can be gained from the rock chippings in contrast to core samples. These are taken prior to casing being emplaced around the interior of the well to prevent collapse of the side walls. These are often pre-selected intervals of particular interest to the hydrocarbon company or scientific research team. A selected interval which can be hundreds of metres in vertical extent is extracted from the well and then analysed directly as would be completed at a surface outcrop. Often only a few inches wide, this limited but important information can lead to improved interpretations of sedimentological systems, depositional environments and give a better understanding of small-scale fault and fracture orientations which are not visible on seismic reflection data. Cuttings are irregular samples of the geology whilst drilling which leaves a very imprecise record of the formations encountered. Yet a third method of collecting data from the well is by geophysical wireline well logs, each of which provides a continuous recording of a geophysical parameter along a borehole. For example, the resistivity log is a continuous plot of a formations resistivity from the bottom of the well to the top and may represent over 4 km of readings. Many different modern geophysical well logs exist but there are several common well measurements taken. These include mechanical measurements (calliper; measuring the hole diameter), spontaneous measurements (gamma ray, temperature and self potential) and induced measurements (resistivity, induction, sonic, density, photoelectric and neutron). From the variations in these measurements, petrophysicists can make interpretations as to the subsurface geology and identify stratigraphical sequences (Rider 1991). These logs with an interpretation are often displayed in the form of a composite log, an industry standard display of the common logging results with an associated geological interpretation. A composite log when combined with the investigation and result summaries provided within the final well report can give the geologist crucial information which can refine geological models of the area, yet predictions often need to be made of the subsurface geology for other regions away from this key data point.

Wells also need to be ‘tied’ to the seismic data to provide a known data point from which subsurface interpretations can be made. This allows for actual rather than relative timings to be specified for ancient geological processes (e.g. timing of fault movements and syn-kinematic sedimentation). This procedure of correlating seismic data with borehole logs often has to be converted from the depth domain (the well data) into the time domain (the seismic data). An established method of correlation is to use the sonic (from which a measurement of the seismic velocity can be calculated) and density geophysical logs which when multiplied derive a log of acoustic impedance. This vertical reflectivity series when convolved with an artificial wavelet produces a synthetic seismogram that can be compared directly with the observed seismogram of the seismic data. An added advantage with direct correlation with borehole logs is that an actual measurement of depth against which a seismic section can be constrained.

2.2 Datasets

A variety of datasets were made available from numerous organisations for this study. The databases were selected on the basis of the resolution and spatial distribution for analysis of the rift-oblique lineaments and are considered to be the best available at present. Each type of data has been separated by geographical location, within either the Faroe-Shetland Basin or the Vøring Basin database.

2.2.1 Potential field data

2.2.1.1 Faroe-Shetland Basin

Potential field data were sourced from Chacksfield & Kimbell (2005) which is the latest compilation of both gravity and magnetic data that has been produced for the Faroese region. Gravity data includes released data from hydrocarbon exploration and results of surveys by Kort og Matrikelstyrelsen (KMS; the Danish National Survey and Cadastre) and was processed to generate derived fields including Bouguer and free air gravity anomalies (Appendix A.01). A low resolution magnetic compilation was made based upon previously released data collected from significantly inferior marine surveys to more modern airborne surveys. The magnetic dataset has a very sparse coverage which fails to recognise known magnetic anomalies (e.g. the Westray igneous centre). In areas of the Faroe-Shetland Basin in which the magnetic dataset was not processed by Chacksfield & Kimbell (2005), an extra released survey from Ark Geophysics Ltd of the United Kingdom continental shelf was provided by Statoil U.K. Ltd.

2.2.1.2 Vøring Basin

The potential field data for the Vøring Basin is provided by StatoilHydro under licence from Norges Geologiske Underøkelse (NGU) and is composed of multiple surveys as described by Olesen *et al.* (2007).

2.2.2 Seismic data

All seismic data used in this study is time-migrated and is used under licence from the respective seismic contractors.

2.2.2.1 Faroe-Shetland Basin

2D seismic data were provided by Statoil U.K. Ltd under licence of the respective seismic contractors. The selection was made upon the basis of the inferred resolution of the seismic data. The 2D seismic surveys used in the study have the following prefixes: OF94/95; IS-FST; GDC; NWZ96RE06; ST0514; ST0513; ST0510; iSimm; CV05; SF94; SFE-95; RM; GA95; WS94; BP83 and R-8413. The coverage of the Faroe-Shetland Basin of these data is considered excellent allowing for a full analysis of the basin (Fig. 2.01a). The processing parameters of the seismic data are unknown but are expected to have followed the standard processing sequence; however, differences between surveys were observed probably due to different acquisition methods and processing parameters used.

3D seismic data was provided courtesy of PGS Geophysical which is of regional extent (Fig. 2.01b). The total coverage is in excess of 22,600 km^2 and is comprised of more than 30 original 3D surveys (including surveys from both the Faroe and UK sectors of the basin). A processing summary of the merging process between four example seismic surveys to form the PGS MegaSurvey as well as a flow chart of the processing sequence is supplied in Appendix A.02-03. A selection of individual 3D seismic datasets were also provided by Statoil U.K. Ltd. However, the PGS MegaSurvey included many of these thus individual surveys were deemed surplus to requirement for the study.

2.2.2.2 Vøring Basin

2D seismic data were provided by StatoilHydro under licence from the respective seismic contractors (Fig. 2.02a). The seismic surveys used in this study have the following prefixes and owned by the following companies: NGI-98 (TGSNopec); GVN-92 (WesternGeco); VB-86/87/89/90 (Norwegian Petroleum Directorate – NPD); MNR-04/07 and GVF00RE 08 (Fugro-Geoteam). The 2D seismic data was used to compliment the 3D seismic surveys of limited coverage in the northern Vøring Basin. A summary of the processing parameters used for the VB, MNR and GVF00RE08 surveys are given in Appendix A.04-06 and are believed to be typical of the other 2D seismic reflection seismic datasets acquired in the region.

3D seismic data was provided by StatoilHydro under licence from the respective seismic contractors. Two main seismic surveys were provided which were formed from the merging of three seismic surveys acquired above the Gjallar Ridge and two above the Nyk High (Fig. 2.02b). The seismic surveys used in this study have the following prefixes and owned by the following companies:

- *Gjallar Ridge*: GRE-02 (TGSNopec); SG9604 (WesternGeco) and ST0410 (PGS Geophysical)
- *Nyk High*: ST9603R99 (WesternGeco) and BPN9601 (PGS Geophysical).

Standard acquisition and processing techniques were used in the development of the final time-migrated seismic datasets. A typical methodology used was demonstrated in the acquisition and processing of BPN9601, a summary is hereby given. The survey employed a 2 boat configuration towing 6 streamers, 4 km in length, with average source strength of 2620 cubic inches. The source was ‘flip-flopped’ to give an effective shot interval of 50 m while collecting 12 lines of data per sail-line. The cross line interval was 37.5m. The final bin size was 12.5 m x 12.5 m in the final processed dataset with zero phasing of the data completed from wavelet extraction from an offset well by means of proprietary 2D seismic data in what was considered at the time to be of very high quality and interpretability. Signal to noise ratio is high and residual multiple energy is not considered a problem.

2.2.3 Well data

All well data used in this study was provided by Statoil U.K. Ltd and StatoilHydro in the form of digital geophysical well logs, composite logs and final well reports. The wells were tied to the seismic data based upon synthetics produced from the sonic and density geophysical logs by Statoil U.K. Ltd and StatoilHydro in the Faroe-Shetland and Vøring Basins respectively.

2.2.3.1 Faroe-Shetland Basin

A total of 212 wells were available for the study, the majority (204) of which were exploration wells drilled offshore in the UK sector of the Faroe-Shetland Basin, most of which are publically released (Fig. 2.03). The remaining five offshore hydrocarbon exploration wells drilled in the Faroes sector were made available for the study by Statoil U.K. Ltd but only three are presently released (6004/12-1, 6004/16-1z and 6005/15-1); two of which remain confidential (6104/21-1 and 6004/17-1). Three released onshore wells located upon the Faroe Islands (Vestmanna, Glyvursnes and Lopra) were also available for the study but were not required.

2.2.3.2 Vøring Basin

Three exploration wells were made available for the study by StatoilHydro located in the northern Vøring Basin. The results of these wells (6704/12-1, 6706/11-1 and 6707/10-1; Fig. 2.04) are released and have been published by a variety of authors (e.g. Ren *et al.* 2003; Fjellanger *et al.* 2005; Lien 2005).

2.3 Methodology and software

2.3.1 Potential field data management and interpretation

Potential field data was managed and interpreted within a digital environment. Modern potential field datasets are in the form of geographically referenced images which allows them to be integrated into the ESRI ArcGIS software environment. Geographical Information Systems (GIS) are computer based systems that are used to capture, store, analyse, manage and present geographical information. It allows the integration of multiple datasets of different forms and from assorted sources all inherently linked to each other by their geographical location into a single project. For example, in a project containing potential field data of a submarine basin, land masses of defined area, location of well points and seismic lines may be overlain above a geo-referenced Bouguer anomaly image. It is of particular use in the hydrocarbon industry as 100% of offshore data contains a geographical component.

Using tools within ArcGIS 9.2, a qualitative fault interpretation of the various datasets can be made to locate structural highs and lows, and infer the location of faults due to the abrupt changes between adjacent areas in the potential field data. Not only can faults be interpreted on the basis of potential field data, but the magnetic data also highlights the basic igneous material in the basin, in particular areas affected by dykes. Interpreting these geological features accurately within a geographically constrained environment fails to allow these inaccuracies to arise which can occur during manual transfer to non-spatial software programs (e.g. drafting software).

2.3.2 Seismic data interpretation and management

2.3.2.1 Overview of Landmark OpenWorks® software

Landmark OpenWorks® is a specialist piece of software that manages all aspects of geotechnical data and can be used for the interpretation of geological data by the majority of subsurface disciplines (e.g. geologists, geophysicists, engineers and petrophysicists). The software was predominantly used for the interpretation and manipulation of seismic reflection datasets available for the study which could be analysed with the incorporated well data. The specific packages used within the OpenWorks® software were SeisWorks 2003.12.2 and GeoProbe 3.1.1.

SeisWorks software allows for the direct interpretation of geological horizons and faults to be made from the digital seismic data. The display is split between two windows; firstly, a cross sectional view of the seismic line and secondly, a shot point map view of the seismic survey. Interpreting a horizon on the seismic cross section, the horizon is also displayed in the map window with a colour scale attributed the TWTT of the mapped horizon (Z) spatially located on the 2D map (X,Y). Interpretation of inlines and crosslines of a 2D survey, once fully interpreted, can be used as data points to form a three dimensional surface which is interpolated in areas where the seismic data is not present. On a 3D seismic survey, accuracy is increased in the spatial mapping of subsurface horizons due to the reduced line spacing and 3D migration. An interpreted grid of regularly spaced seismic lines is made with each line needing to be accurately tied with each other. A secondary piece of software can then be used (Zap!) which extends the interpretation onto adjacent lines and crosslines based on the reflectors phase, amplitude or other variables.

GeoProbe is a volume visualisation and interpretation software package that renders 3D seismic data in a 3D environment. Unlike SeisWorks, GeoProbe software allows the interpreter to view, analyse and understand 3D problems which were previously interpreted in 2D segments. Similarly to SeisWorks, the interpreter can map horizons, faults and any other geological bodies within the seismic cube with greater accuracy but resolve the complexities through the 3D visualisation of geological features. All variations of geotechnical data can be used in the 3D environment which is only spatially limited by the size of the seismic volume.

2.3.2.2 Seismic stratigraphy

Seismic stratigraphy was developed to understand the nature of the sediments and sedimentology from seismic data analysis. The development of seismic stratigraphy stemmed from research conducted in the hydrocarbon industry in the 1970's, the results of which were published by Payton (1977) as a volume containing multiple papers to which the reader is referred for a more detailed summary than what is given here. The reflection amplitudes on any given seismic lines are controlled by the acoustic impedance contrast formed between two lithologies (of differing densities and velocities). Thus, an interpretation can be made on the basis of amplitude and regional knowledge as to predicted lithology, and in turn the environment and mode of deposition. High amplitudes on seismic data imply a rapidly alternating environment such as deep marine deposition of turbidite sequences. Where low amplitudes are present, the lithologies are inferred to be relatively homogeneous formed within unchanging environments such as marine chalk deposition. Reflector continuity is similarly indicative of depositional environment with continuous reflections characteristic of uniform conditions (e.g. deep marine) and discontinuous characteristic of environments with rapid lateral facies change (e.g. fluvial). Vertical reflection spacing, like lateral continuity, indicates the rate of alternating depositional environment. Reflection configuration also can signify lateral variations in deposition with parallel and sub-parallel configuration (both even and wavy; Mitchum *et* *al.* 1977b) suggesting event depositional rates on an uniformly subsiding shelf or stable plain, and a divergent reflection configuration representing lateral variations in the deposition rate and/or progressive tilting of the depositional surface (e.g. caused by fault block rotation).

A key assumption of sequence stratigraphy is that seismic reflectors represent specific time markers. A depositional sequence is defined as genetically related sediments normally comprising as a succession of concordant strata that exhibit discordance with the under- and overlying sequences (i.e. they are bounded by unconformities or their correlative conformities; Mitchum *et al.* 1977a). Reflector termination is the main criterion for determining a sequence boundary at both the base (e.g. lapout, onlap and downlap) and top of a sequence (e.g. toplap and erosional truncation). After seismic sequences are defined, environment and lithofacies within the sequences are interpreted from the seismic data (and any additional well information). Seismic facies are determined as groups of reflectors that have parameters such as amplitude, frequency and continuity which differ from adjacent groups of reflectors. Grouping these parameters into mappable seismic facies allows their interpretation in terms of firstly the depositional environment and if possible the lithology. I.e. if an interpreted clastic environment has sufficiently high energy, the lithology is considered to be sand prone in contrast to a low energy environment which is predicted to be mud prone (Vail *et al.* 1977).

2.3.2.3 Seismic geomorphology

From the mapped three dimensional horizons, a range of analyses are available within the software package which reveals features that are often not recognised in time-structure maps. These are summarised below and are discussed in greater detail by Posamentier *et al.* (2007):

- *Amplitude extraction*: This extracts the amplitudes from the seismic response that correspond to time values that have been stored in a horizon. The result of this analysis is the identification of weak and strong amplitude responses of the horizon in space at a particular point in time. These relate to the contrasting lithologies and fluid content of varying densities and velocities and in turn the modes of deposition can be inferred.
- *Dip*: A dip map displays the magnitude of the time gradient. It is constructed by comparing each sample of the horizon with the adjacent samples in orthogonal directions. A plane is then fit through the three points with a magnitude of dip measured in ms per unit distance x 1000. The formula used is:

  $$\text{Dip} = \sqrt{\left[\left(\frac{dt}{dx}\right)^2 + \left(\frac{dt}{dy}\right)^2\right]} \quad \text{x } 1000$$

  where *dt/dx* is the dip in the x direction, *dt/dy* is the dip in the y direction, with x and y in real world coordinates.
- *Azimuth*: The azimuth displays the direction of maximum dip and likewise to the dip map is constructed by comparing each sample of the horizon with the two adjacent samples in orthogonal directions. The formula used is:

  Azimuth = arctan [(dt/dy)/(dt/dx)

  where *dt/dx* is the dip in the x direction, *dt/dy* is the dip in the y direction. An azimuth value of 0° is aligned with true north.
- *Dip Azimuth*: This map combines dip and azimuth values to show both aspects of dip and azimuth synchronously in a single display. The dip azimuth map generalises the azimuth into four quadrants of an azimuth map (represented by colours; red - north, yellow - east, green - south and blue - west), with variation of colour brightness representing variations in dip.

- *Edge detection*: This process highlights discontinuities in an image and exaggerates sharp dip changes such as reef edges, faults or steep horizon dip. In particular it detects differences in dip across a horizon, but using a different algorithm from that used in formation of a dip map. Edge detection involves the mathematical comparison of horizon points (A-D & F-K) around a single sample horizon point (E). The algorithm compares sets of samples on either side of each sample point in a 3 x 3 mask (three samples on either side of a point in both directions) across a horizon. This technique is illustrated below:

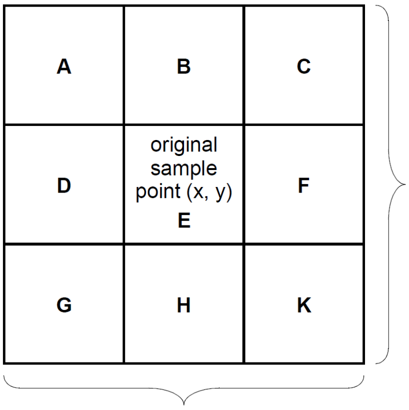

difference between these rows = y coordinate of edge detection plane at the sample

difference between these columns = x coordinate of the edge detection plane at the sample

The equations for calculating the x, y at the sample horizon point (E) are:

$x = (C + 2F + K) - (A + 2D + G)$

$y = (A + 2B + C) - (G + 2H + K)$

$\text{edge} = \sqrt{(x^2 + y^2)}$

2.3.2.4 *Seismic attribute volumes*

3D seismic data volumes are able to be processed by techniques which highlight features within the seismic data itself. They are used much in the same way a 3D mapped horizon is as described above but is unencumbered by the interpreter or automatic picker bias from the original horizon interpretation. Two techniques are used in this study; firstly, the semblance-based coherency algorithm within Landmark OpenWorks® accessed via the

GeoProbe software package and secondly the chaos (for stratigraphical analyses) and variance (for structural analyses) algorithms within Schlumberger Petrel 2005 software. These processing tools highlight lateral variations in the seismic response caused by changes in structure, stratigraphy, lithology, porosity and the presence of hydrocarbons (i.e. processing highlights the areas of discontinuity to the conventional seismic display of continuous reflectors). A more complete overview of the semblance based coherency algorithm is given by Marfurt *et al.* (1998).

The chaos algorithm within Schlumberger Petrel 2005 software is a measure of the lack of organisation in the dip and azimuth within a seismic volume. This is predominantly used for seismic facies analysis of the seismic signal. Example areas which a chaos algorithm would be expected to highlight include areas affected by gas migration paths (e.g. hydrocarbon chimneys), salt body intrusions (e.g. salt diapirs) and areas of chaotic reflection continuity (e.g. remobilised shale). In contrast, variance is predominantly used for a structural analysis of the seismic volume as it analyses the variance in the seismic signal which is particularly useful for edge detection (e.g. discontinuities at faults). The processing result can be adjusted by using different parameters in view of the number of traces used to define horizontal variance in a volume and the amount of vertical smoothing which aids in reducing noise (but conversely reduce the resolution of detected edges). From the calculated variance volume, a second algorithm can be applied known as the 'ant tracking' algorithm. This follows an analogy of ants finding the shortest path between the nest and the food source by communicating using pheromones, a chemical substance which attracts other ants. The shortest path will be marked by increased pheromones to the longer routes and so the next ant is more likely to choose the shortest route. Applying this concept to a seismic volume, a large number of 'ants' are initially distributed; where deployed upon a fault, the ant should be able to trace the fault surface leaving a strongly marked trail of 'pheromone'. This would be in contrast to other surfaces which are unfaulted where only weakly marked zones would exist. From this ant tracked seismic volume, the algorithm automatically extracts fault patches which can then be used for fault modelling. A more detailed overview of the ant tracking algorithm and process is given in Appendix A.07.

2.3.3 Fault modelling and analysis

Badleys TrapTester 5.4 software can be used for seismic interpretation and fault modelling through to advanced analysis for fault seal potential and flow simulation in reservoir models. Seismic, well, horizon and fault data can be imported from other software including Landmark OpenWorks® into TrapTester which has a range 3D visualisation and modelling tools. From this, structural analysis fault seal tools are accessed, predictions can be made for fracture characteristics and with in-situ stress and pore pressure data, the likelihood of fault reactivations can be quantified. A series of fault statistics are also available including orientation, length/throw diagrams and frequency plots, which are able to be exported in a format which can be manipulated using conventional spreadsheet software (e.g. Microsoft Excel).

An overview is given of the process to create a structural framework model as is completed in this study. Precise and more detailed information regarding the formation of a coherent fault model is given by Needham *et al.* (1996). The first step is to model the raw fault segments into independent fault surfaces and to create lines of intersection (known as branch lines) between the fault surfaces. A quality control check must be made on correlated fault segments of an individual fault to identify and correct irregularities in the modelled fault surface. To fix these problems, three options are available. Firstly, a modification of the modelling parameters is the fastest option but means any anomalous data remains in the project. Secondly, the fault polygons can be edited relatively quickly but can be time consuming in complex datasets. Finally, an edit of the raw horizon and fault data is the most thorough method of quality control as it removes all the anomalous data from the project but is very time consuming. Correlating unassigned fault segments is completed using interpreted horizon surfaces as well as raw 3D seismic data to map individual faults along strike. Many fault networks contain at least some linked faults and these linkages need to be formed within the fault model. An important feature regarding interlinking faults is that the fault displacement along a single fault will jump at the branch lines but the summations of displacements are conserved upon all the linking fault segments (e.g. Needham *et al.* 1996). Once this is complete, fault-horizon intersections are modelled within TrapTester with the horizon extrapolated to the fault forming a series of fault polygons. The quality of fault polygons is dependent upon the raw horizon and fault data and as such, abrupt irregularities in the fault polygon geometry are likely to reflect anomalies in the data. Once a quality control check has been made and modifications to the horizon and/or fault raw data have been made, fault polygons and a horizon surface are modelled based upon a range of parameters which can be defined for each horizon. This process culminates in a structural fault model which is applicable for a series of horizons, from which a series of fault statistics (e.g. fault heaves) can be extracted and utilised.

2.3.4 Well data interpretation and management

Oilfield Data Manager 3.5 (ODM3^{TM}) is a windows based software program designed to store, manage and interpret geological well data. A range of different data types and sources including drilling reports, wireline log data and geological interpretations of numerous wells can be managed in a single database, instantly accessed in customisable 2D section and map views, as well as a 3D interface. Direct links between ODM3^{TM} and the Landmark OpenWorks$^{®}$ database also allows for the direct access, modification and update of well data within the seismic projects on-the-fly. Due to the multitude of well data used in the study, this software is utilised to interpret chrono-, sequence and litho-stratigraphic boundaries for each of the wells where required and for the construction of well correlation panels.

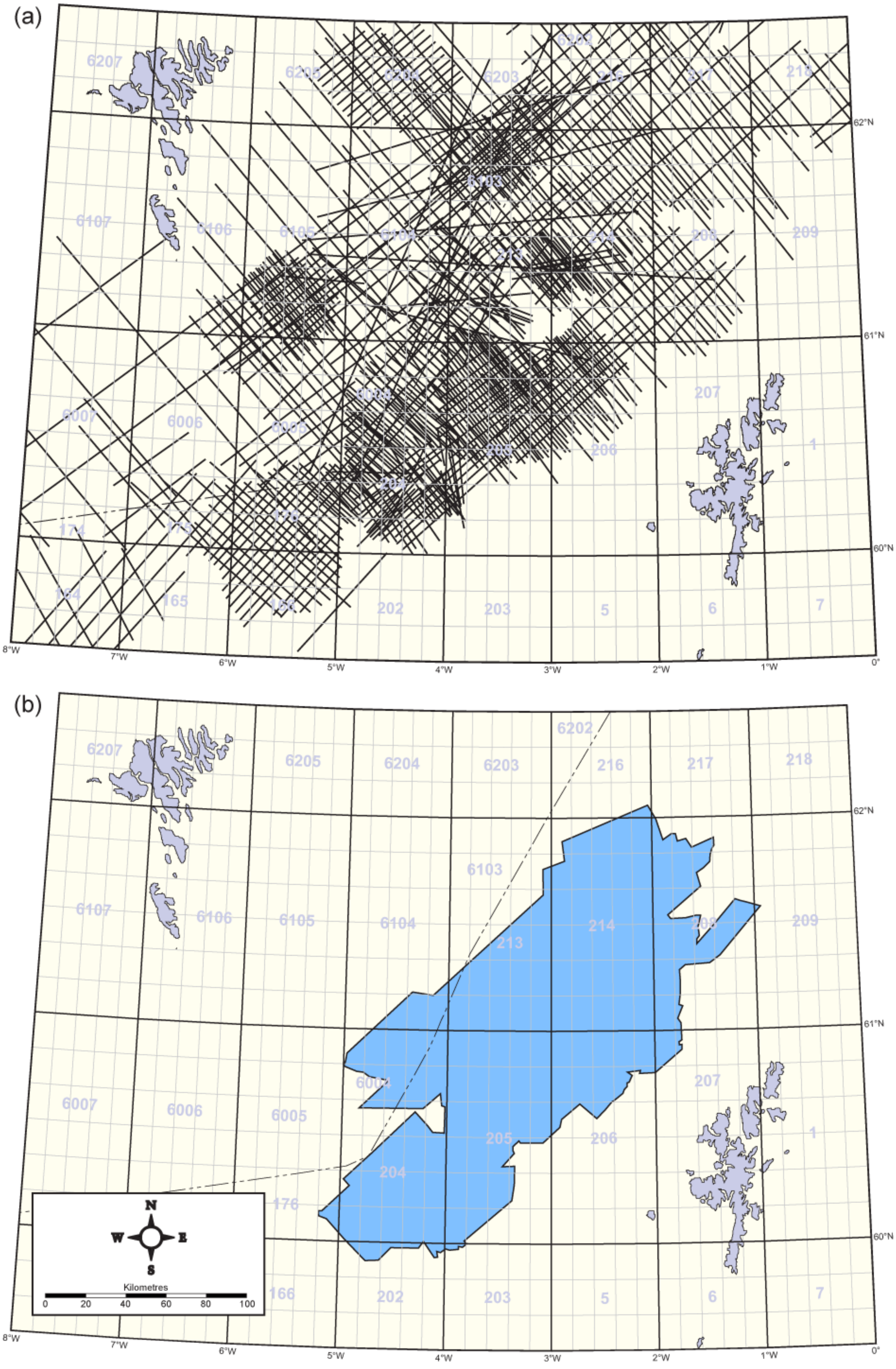

Figure 2.01: Faroe-Shetland Basin (a) 2D and (b) 3D seismic database.

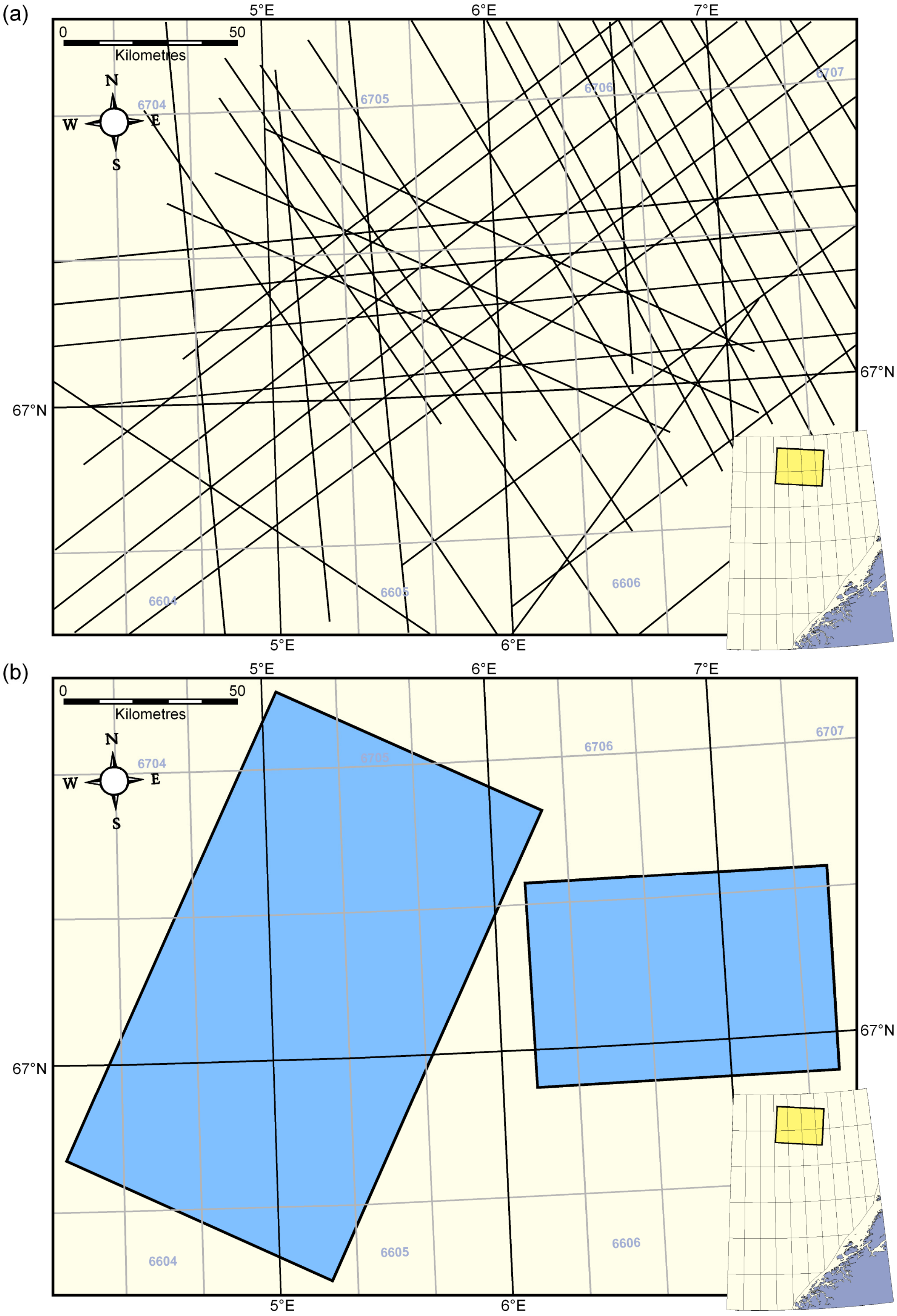

Figure 2.02: Vøring Basin (a) 2D and (b) 3D seismic database. Inset map with location relative to Norway.

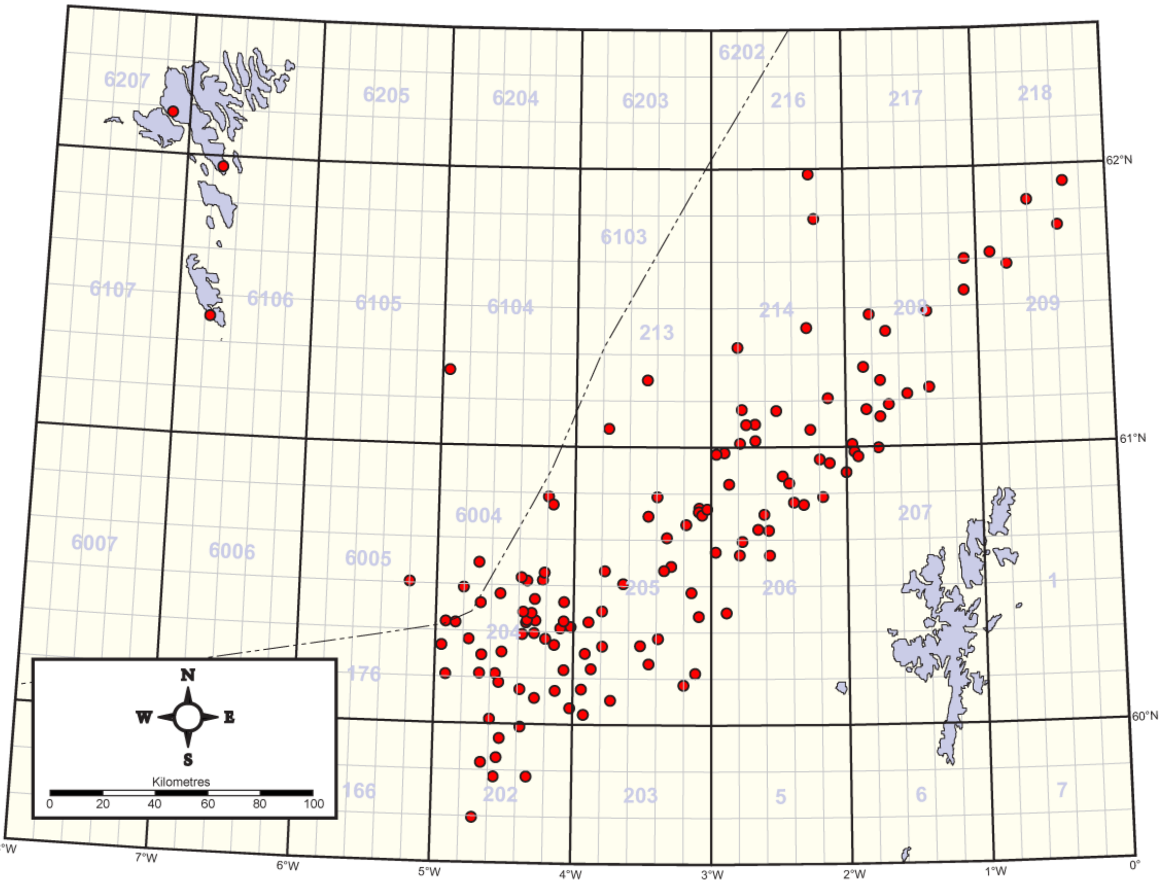

Figure 2.03: Faroe-Shetland Basin well database.

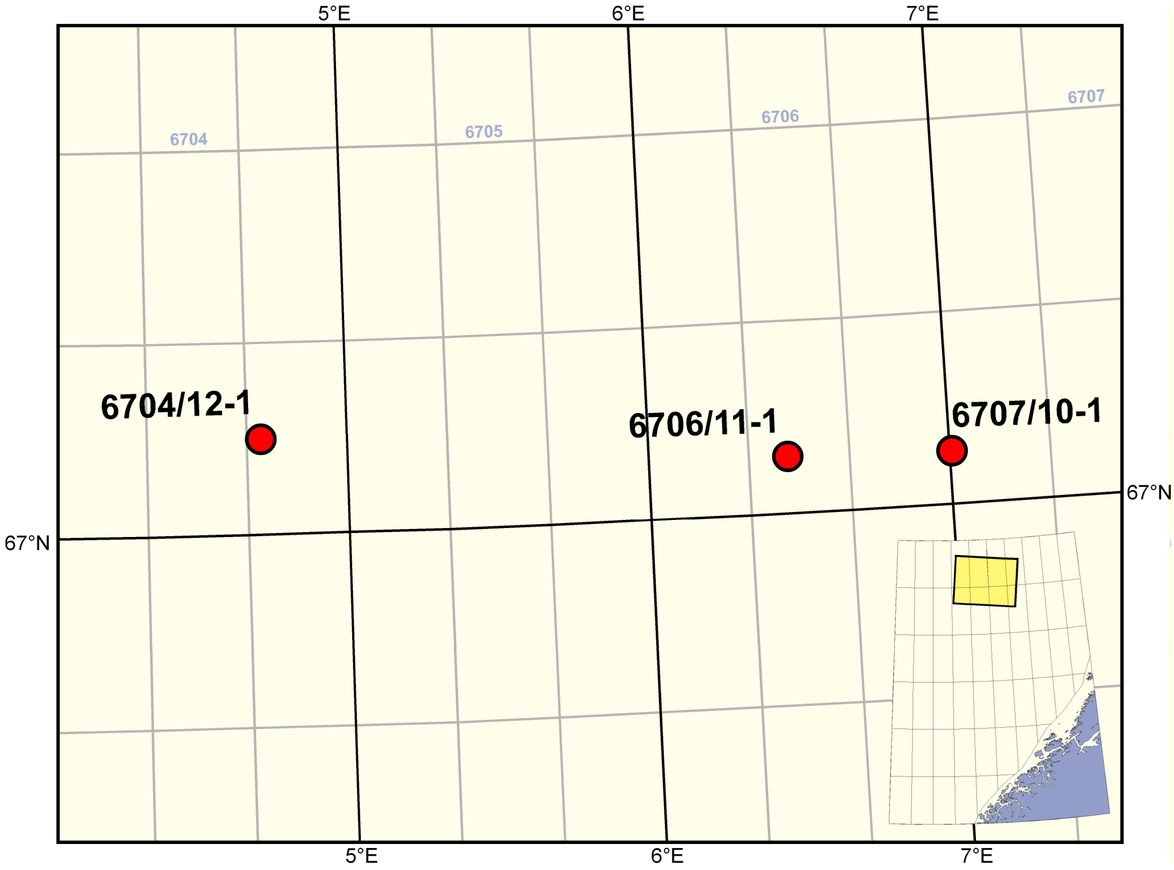

Figure 2.04: Vøring Basin well database. Inset map with location relative to Norway.

Chapter Three

3 SIGNIFICANCE OF RIFT-OBLIQUE LINEAMENTS IN THE FAROE-SHETLAND BASIN

3.1 Abstract

NW-SE trending rift-oblique lineaments ("transfer zones") occur along the length of the NE Atlantic Margin. Previous authors have suggested these lineaments played an important role in providing conduits and/or barriers to sedimentation during the Cretaceous and Paleocene; it has also been suggested they were active as discrete, basin-wide strike-slip faults. This study uses a well-calibrated 3D seismic survey of regional extent to critically assess the structural and stratigraphic evidence for three rift-oblique lineaments in the UK sector of the Faroe-Shetland Basin (Victory, Clair and Judd Lineaments). Structures previously attributed to basin-wide strike-slip deformation can be more simply explained as igneous intrusions, hydrothermal vent complexes, gas chimneys and/or faults that transfer extensional strain between en-echelon rift segments. There is little evidence to suggest that activity along discrete, basin-wide lineaments controlled Paleocene sedimentation within the Faroe-Shetland Basin. Rather, sediment transport and deposition at this time are likely to have been controlled by along- and across-strike variations in the magnitude of thermal subsidence, which in turn reflect the three-dimensional nature of the underlying Mesozoic rift architecture.

3.2 Introduction

Rift basins and passive margins are commonly inferred to be segmented by lineaments that are oriented sub-perpendicular to the basin trend. In onshore extensional provinces, such as the East African Rift, Gulf of Suez and the Basin and Range (Morley *et al.* 1990; Stewart 1998; Younes & McClay 2002), field mapping and analysis of satellite and aerial images have been used to identify and ground-truth these rift-oblique trends.

Here, these lineaments are often associated with marked changes in structural geometry along the strike of the basin. Such changes include alternations in the polarity of half-graben asymmetry and/or apparent lateral offsets of rift-bounding structures or intrabasinal highs (e.g. Morley *et al.* 1990). In many cases, these lineaments appear to compartmentalise the basin on a variety of scales, which in turn influences the stratigraphic evolution of the rift zone (e.g. Younes & McClay 2002).

Potential field data have been widely used to identify rift-oblique trends in offshore basins such as the NE Atlantic volcanic passive margin and the NW Shelf of Australia (e.g. Doré *et al.* 1997b; Keep & Harrowfield 2005). These lineaments are commonly inferred to be associated with abrupt changes in crustal structure (e.g. Mjelde *et al.* 2003b) and/or have controlled sediment transport and deposition within the basin (e.g. Jolley & Morton 2007). Thus, better understanding of these rift-oblique trends is important both in terms of assessing their apparently fundamental control on rift architectures, and their implications for hydrocarbon exploration in extensional basins. Nevertheless, there is surprisingly little published information available on the structural expression of such lineaments in offshore regions, primarily due to the low resolution of regional potential field datasets and/or the limited availability of well-calibrated seismic reflection datasets. In many cases, these lineaments are simply represented on regional maps as straight lines crossing the continental margin (e.g. Jolley & Morton 2007, p. 554, fig. 1).

The NE Atlantic volcanic passive margin is an important target for hydrocarbon exploration and therefore benefits from extensive coverage by a range of geological and geophysical datasets, including wells and gravity, magnetic and seismic reflection surveys. The dominant trend of the major rift basins ranges from NE-SW to N-S, but highly oblique NW-SE trending lineaments have been long been recognised from analysis of potential field data (Rumph *et al.* 1993; Doré *et al.* 1997b; Kimbell *et al.* 2005). These lineaments appear to extend across the continental shelf, but rarely align with the oceanic fracture zones that develop following continental breakup c. 54 Ma. The origin of these proposed margin-scale lineaments remains unclear and a variety of hypotheses have been proposed: reactivation of Precambrian shear zones, such as those exposed in NW Scotland and Norway (e.g. Watson 1984; Knott *et al.* 1993; Fichler *et al.* 1999); structural inheritance from compressional fault systems that originated during the Caledonian Orogeny (Doré *et al.* 1997b); or due to Mesozoic rift processes accommodating oblique extension (Rumph *et al.* 1993; Ren *et al.* 2003).

The three-dimensional (3D) structure and kinematic significance of these lineaments also remain poorly understood. The aim of this study is to critically assess the structural and stratigraphic evidence for three regional-scale lineaments that have been inferred within a major rift basin on the NE Atlantic Margin: the Faroe-Shetland Basin (FSB; Fig. 3.01). Previous studies have attempted to address this problem through analysis of regional potential field data and correlation of structures and stratigraphic markers using 2D seismic datasets of variable resolution. In contrast, this study will use well-calibrated 2D *and* 3D seismic data to constrain the geometry, growth and tectonic significance of these enigmatic lineaments.

Rift-oblique lineaments within the Faroe-Shetland Basin – and other similar features elsewhere on the NE Atlantic Margin – have previously been referred to as “transfer zones” (e.g. Doré *et al.* 1997b; Ellis *et al.* 2009). However, to avoid confusion, we use the term “lineament” (or “rift-oblique lineament”) to distinguish structural trends that have been identified primarily using potential field datasets from specific geological features identified through analysis of well-calibrated 2D and 3D seismic reflection data (see below).

3.3 Tectonic framework of the Faroe-Shetland Basin

The FSB comprises a series of NE-SW trending sub-basins (Fig. 3.01) that formed during a sequence of Devono-Carboniferous, Permo-Triassic, Cretaceous and Paleocene rift events following the end of the Caledonian Orogeny (c. 390Ma; Coward (1990)). The sub-basins are separated by horst blocks (locally referred to as “highs” or “ridges”) that are cored by metamorphic basement rocks. This basement can be correlated with the Precambrian gneisses of the Lewisian Complex exposed onshore in NW Scotland (Ritchie & Darbyshire 1984; Hitchen & Ritchie 1987). Many authors (e.g. Duindam & van Hoorn 1987; Mudge & Rashid 1987; Earle *et al.* 1989; Dean *et al.* 1999; Sørensen 2003) have given full accounts of the basin evolution, so only a summary is given here.

Collapse of the Caledonian Orogen in the Devonian led to the formation of several ‘Old Red Sandstone’ basins in the proto North Atlantic region (Roberts *et al.* 1999). Renewed rifting during the Permo-Triassic was associated with the development of strongly asymmetrical half graben basins in a semi-arid environment (Herries *et al.* 1999). Fluvial and alluvial environments gave way to marine conditions in the Early Jurassic, with a regional unconformity removing much of the Middle Jurassic succession (Booth *et al.* 1993). Jurassic extension in NW Europe (Doré *et al.* 1999) was characterised by the formation of mainly N-S trending rifts, including the North Sea and Porcupine Basins and parts of the Halten Terrace. However, the distinct lack of N-S trending structures within the FSB implies that Late Jurassic rifting probably did not occur here.

Early Cretaceous rifting has been inferred from the observation that packages of coarse grained, Lower Cretaceous clastic sediments thicken towards the hanging walls of mainly NE-SW trending normal faults within the FSB (Booth *et al.* 1993). Minor rifting in the Middle Cretaceous (Dean *et al.* 1999) continued into the Late Cretaceous against a backdrop of rising eustatic sea levels, leading to dominantly marine conditions and the deposition of a regressive, highly mud prone sequence (Mudge & Rashid 1987; Turner & Scrutton 1993). The dominant NE-SW trend of the FSB had been established by the end of the Cretaceous, by which time rifting had ceased and basin flank uplift gave rise to deposition of a regressive Paleocene succession (Smallwood & Gill 2002).

Paleocene rifting in the southwest part of the Faroe-Shetland basin has been inferred by Dean *et al.* (1999) on the basis that some Cretaceous normal faults appear to have been reactivated during the Paleocene. Nevertheless, Dean *et al.* (1999) acknowledged that these “rift” faults could be attributed to minor deformation during post-rift thermal subsidence (Duindam & van Hoorn 1987). Alternatively, fault initiation and/or reactivation at this time may have been associated with differential compaction of sediments over structural highs (e.g. Færseth & Lien 2002). Current models for the development of the NE Atlantic Margin imply a progressive northwestward migration in the locus of active rifting, towards the eventual zone of continental break-up (Lundin & Doré 1997). Thus, evidence for a Paleocene rift event may exist beneath - and be largely obscured by - the thick Paleogene lava pile in the northwest part of the present day FSB (Fig. 3.01).

Continental break-up (Eldholm & Grue 1994) was associated with widespread basin uplift and magmatism across the NE Atlantic region, in the form of continental flood basalts, sill and dyke complexes, igneous centres, magmatic underplating and the deposition of regional tuff horizons (White & McKenzie 1989; Naylor *et al.* 1999; Lundin & Doré 2005). Following continental break-up in the Early Eocene (c. 54 Ma) the tectonic evolution of the FSB has been dominated by thermal subsidence and the growth of large-scale Cenozoic anticlines (Davies *et al.* 2004; Stoker *et al.* 2005c; Ritchie *et al.* 2008). These folds have been attributed to a variety of mechanisms including ridge push, sedimentary draping and reactivation of basement structures (Doré *et al.* 2008 and references therein).

Despite the uncertainties surrounding the precise nature and timing of individual deformation events, the consensus is that the Faroe-Shetland Basin developed due to multiple rift episodes prior to continental break-up. Nevertheless, several previous authors have proposed that NW-SE trending rift-oblique lineaments played an important role during basin evolution, and may have influenced the quality and distribution of reservoir sands. The following section summarises previous work on these lineaments and proposes a number of testable hypotheses to explain their origin and development.

3.4 Rift-oblique lineaments ('transfer zones') within the Faroe-Shetland Basin

Rift-oblique lineaments were initially recognised within the FSB by Duindam & van Hoorn (1987) and further discussed by Rumph *et al.* (1993), who inferred 15 orthogonal-to-basin strike lineaments from interpretations of regional gravity and magnetic datasets. Today, up to seven lineaments are generally recognised, although the reason for this reduction in number has not been clearly explained in the subsequent literature. Nevertheless, these remaining seven lineaments appear to form a key component of the tectonic architecture of the (Fig. 3.01; cf. Jolley & Morton 2007; Ellis *et al.* 2009).

Various authors have argued that the distribution of Paleocene age sediments in the southeastern part of the basin was strongly influenced by rift-oblique lineaments (Mitchell *et al.* 1993; Grant *et al.* 1999; Lamers & Carmichael 1999; Naylor *et al.* 1999), implying that the lineaments had significant structural and geomorphological expressions at the Earth's surface during and after rifting (cf. Gawthorpe & Leeder 2000). More recently, with hydrocarbon exploration interest turning towards the Faroese sector in the NW part of the basin, it has been proposed that rift-oblique lineaments played an important role in the transport of sediments sourced in the Kangerlussuaq region of Greenland (Larsen *et al.* 1999; Larsen & Whitham 2005), through the Faroe Islands (Passey & Bell 2007; Ellis *et al.* 2009), and into the Faroe-Shetland Basin (Whitham *et al.* 2004; Frei *et al.* 2005; Jolley & Morton 2007). They are believed to have exerted a control upon the Paleocene sediment distribution within this part of the basin, as well as on the distribution and thickness of sub-aerial basalt flows, shallow marine hyaloclastites (White *et al.* 2003; Ellis *et al.* 2009), the locations of dyke swarms (Naylor *et al.* 1999) and igneous centres (Rumph *et al.* 1993; Ritchie *et al.* 1999).

Several previous authors have inferred large scale (basin wide) strike-slip or transpressional deformation along NW-SE trending lineaments within the FSB and elsewhere on the NE Atlantic Margin (e.g. Dean *et al.* 1999; Ellis *et al.* 2009). Other authors (e.g. Doré *et al.* 1997b) have suggested some of these apparent discontinuities (e.g. the Jan Mayen Lineament, offshore Norway) may have originated as shear zones in the basement, and in some instances have accommodated minor strike-slip movements in the Cenozoic. These interpretations were based primarily on the lateral offsets in the continental margin, the presence of en-echelon Cenozoic anticlines within strata that overlie the inferred position of these lineaments, and from the apparent offsets of structural highs within the Atlantic Margin basins (e.g. Fig. 3.01; Dean *et al.* 1999; Brekke 2000; Ritchie *et al.* 2003). The hypothesis that these lineaments accommodated strike-slip movements implies they are likely to be associated with the classic indications of strike-slip faulting, such as the presence of positive and negative flower structures within the Cenozoic overburden (e.g. Harding 1990). These features should be clearly visible and capable of being mapped along strike using modern, high resolution 3D seismic datasets.

Alternatively, segmentation of rift basins by rift-oblique lineaments may be controlled by the development of transfer zones or accommodation zones (sensu Faulds &

Varga 1998). Transfer zones are defined as discrete zones of sub-vertical strike-slip and oblique-slip faulting that trend near-parallel to the extension direction, facilitating the transfer of strain between two en-echelon rift domains (Faulds & Varga 1998). Accommodation zones are defined as regions of overlapping fault terminations where strain is transferred between fault tips through a series of relay structures (i.e. “soft-linkage”) (e.g. Morley *et al.* 1990; Acocella *et al.* 1999a; Moustafa 2002). The key criteria defining transfer and accommodation zones are that extensional strain is conserved along the length of the segmented rift basin (Gibbs 1984; Morley *et al.* 1990), and that transfer and accommodation zones do not extend beyond the region of active rifting (Faulds & Varga 1998, p. 8, fig. 4). Thus, transfer and accommodation zones are second-order features that are inherently related to the rift architecture. They are distinct from the regional-scale strike-slip fault interpretations previously proposed to explain the NW-SE trending lineaments on the NE Atlantic Margin. An alternative hypothesis, therefore, is that the rift-oblique lineaments observed within the FSB may have originated as transfer or accommodation zones during periods of rifting prior to continental breakup.

It is also important to consider other hypotheses that are not directly related to tectonic or structural processes. These include the influence of intrusive igneous rocks on seismic and regional magnetic field data, or the misinterpretation of other geological phenomena (e.g. hydrothermal vent complexes) that may be difficult to identify using sparse 2D seismic data. Equally, the apparent NW-SE fabric may result from the subjective interpretation of coincidentally aligned, but geologically unrelated structural elements within the rift basin. The following sections will test each of these hypotheses against new interpretations of structures that appear to be associated with three previously inferred rift-oblique lineaments in the Faroe-Shetland Basin: the Victory, Clair and Judd Lineaments. Notably, the study areas encompass regions where the lineaments are inferred to cut both sub-basins (Flett, Foula, Foinaven and West Solan Sub-Basins) and structural highs (Judd High and Flett Ridge) within the FSB (Fig. 3.01).

3.5 Dataset and methodology

PGS Geophysical's time-migrated Faroe-Shetland Basin 3D seismic MegaSurvey – in effect, a 3D seismic survey of regional extent – was used to analyse structures within the UK sector (i.e. southeastern part) of the FSB that appear to be associated with these previously inferred lineaments (Appendix A.02 & 03). Well data provided by Statoil U.K. Ltd were used to date, correlate and understand the stratigraphic significance of seismic reflections mapped within the MegaSurvey dataset (Appendix B.01-03, 21-22 & 33-35). Importantly, the locations of the three case studies lie beyond the southern extent of the Paleogene flood basalts (Fig. 3.01), which are known to cause a drop in resolution of seismic data due to the attenuation of high frequency waves at the sediment-igneous interface (Gallagher & Dromgoole 2008).

The reliance on mainly 3D, as opposed to 2D seismic data is critical to this study because exploration 2D seismic lines are most commonly acquired perpendicular to basin strike, making it difficult to recognise structures that are oblique to the basin trend. Additionally, 3D seismic data allow features to be traced and mapped along strike, providing greater confidence in any subsequent geological interpretations. Importantly, the PGS MegaSurvey covers a substantial portion of the UK sector of the FSB. Analysis of the entire dataset revealed little direct structural evidence for most of the previously inferred rift-oblique lineaments (Fig. 3.01), with only three of the aforementioned lineaments having any expression within the Mesozoic-Cenozoic succession.

3.6 Victory Lineament

The Victory Lineament study area is located within the Cretaceous Flett Sub-Basin to the northwest of the Flett Ridge. The area is intruded by igneous bodies which affect seismic imaging at depth (> 4000 ms TWT), particularly within the Cretaceous section.

Dean *et al.* (1999) interpreted the Victory lineament to be a Paleocene transpressional popup structure, which they incorrectly associated with the Clair Lineament, some 50 km to the southwest. This sub-vertical popup structure appears to be characterised by a vertical offset (throw) of > 100 ms at the level of the base Tertiary unconformity, a marked antiformal structure within the intra-Paleocene (Kettla Tuff) interval, and a low amplitude monocline within Early Eocene strata (at around Balder Tuff level). Thus, movement along the popup was inferred to have continued until Early Eocene times, synchronous with deposition of the Balder Tuff (Fig. 3.02a). Various Paleocene seismic reflectors display notable changes in amplitude across the trace of this structure (Appendix B.17), consistent with distinct across-fault changes in seismic facies. These observations are all characteristic of strike-slip (or transpressional) faulting as inferred from seismic data (Harding 1990). However, not all seismic reflections are offset across the structure and there is little direct evidence of faults splaying upwards from the inferred principal displacement zone at depth (Appendix B.19).

New 3D seismic mapping of the intra-Paleocene Kettla Tuff reflector reveals a NW-SE trending antiform oriented parallel to the inferred trace of the Victory Lineament. However, the antiform lies 5 km to the SW of the lineament and is clearly not laterally continuous across the basin, being only c. 5 km in length. Two raised, sub-circular structures immediately to the northeast and southwest of the antiform are also recognised at this level, and appear to be continuous with this structure (Fig. 3.02b).

The apparent absence of seismically imaged faults along the length of the antiform and the small lateral extent of this structure are not consistent with a wrench or transpressional faulting hypothesis. An alternative hypothesis is that the antiform may have originated as a sediment injectite, due to its potentially diapiric character (Fig. 3.02a) and structural relief in map view (Fig. 3.02b). Such features have been recognised from 3D seismic datasets in other parts of the FSB (Davies *et al.* 2006) and in the North Sea (Hurst *et al.* 2003). The timing of sediment or fluid migration would appear to have been during the Paleocene. However, this hypothesis fails to explain the sub-circular structures either side of the central antiform.

Well 214/27-1 (Figs 3.02b and 3.03) penetrates the complete Paleocene sequence, encountering a series of alternating marine mudstones and sandstones, which shallow upwards into shelf facies deposits (Smallwood & Gill 2002). It also penetrates two regionally important seismic marker horizons, the Kettla Tuff (c. 58.5 Ma) and Balder Tuff (c. 55.0 Ma; ages estimated from model 1 of Jolley *et al.* (2002)). A c. 200 m thick dolerite sill was encountered within the Maastrichtian succession just beneath the Late Cretaceous unconformity near the bottom of the well. Unspecified radiometric age dating by Chevron Exploration North Sea Ltd in 1985 collected from a sample of spotted hornfels below the sill, yielded an age of 55.0 ± 0.6 Ma implying that deposition of the Balder Tuff and intrusion of the sill were near contemporaneous.

This sill can be correlated with the high amplitude “Near Top Cretaceous” reflection (Fig. 3.02a), which lies close to the position of the top Cretaceous unconformity. 3D seismic mapping of this and adjacent reflections reveals the presence of a second sill, with similar seismic characteristics, immediately to the NE of the antiformal structure (Appendix B.04-06). Both sills have sub-circular outlines in map view (slightly elongated in a NE-SW direction; Fig. 3.01) and display concave up, ‘saucer shape’ geometries (Fig.

3.04a), which are characteristic of igneous sills mapped elsewhere on the NE Atlantic Margin (e.g. Bell & Butcher 2002). Thus, the two raised circular structures observed at the level of the Kettla Tuff horizon (Fig. 3.04b) can be explained by 'jacking up' (Trude *et al.* 2003) of the Paleocene strata by c. 150m, leading to the development of forced folds with four way dip closure (Hansen & Cartwright 2006) during the emplacement of two sills within the underlying Upper Cretaceous succession.

The intervening NW-SE trending antiform (Figs 3.01a and 3.04b) is located immediately above the sill tips (Appendix B.18). Viewed in seismic sections displayed at near 1:1 scale (i.e. no vertical exaggeration), the region between the sill tips and the crest of the Paleocene antiform is characterised by high amplitude reflections that dip at c. 60° and cross-cut surrounding sub-horizontal reflectors (Fig. 3.05). These observations suggest that the cross-cutting reflectors represent the edge of an intrusive igneous body with a laccolithic style emplacement. We propose that the laccolith was fed by sub-vertical dykes, which in turn were sourced from the tips of the two mapped sills (Fig. 3.06; cf. the "antiformal junction" described by Thomson and Hutton (2004)). The NW-SE trending antiformal structure is therefore interpreted to have formed as a consequence of the localised volume increase during igneous intrusion within the Paleogene section above the steeply dipping sill tips.

The reflections overlying the crest of the antiform and immediately beneath the Balder Tuff marker are characterised by an apparent thickening and a distinct increase in seismic amplitude, across a c. 2 x 3 km wide area (Fig. 3.05). These observations are consistent with the hydrothermal vent complexes described elsewhere on the NE Atlantic Margin by Hansen (2006) and references therein. These complexes are associated with sediment remobilisation towards the surface due to the expulsion of liquids and gases from underlying igneous intrusions. Alternatively, Thomson (2007) has hypothesised that such features may in fact be volcanic fissures, generating local accumulations of pillow lavas or hyaloclastites at the seafloor, which originate from a series of feeder dykes. Nevertheless, both interpretations imply that hydrothermal circulation or igneous extrusion took place immediately prior to deposition of the Balder Tuff. The timing and location of this enhanced hydrothermal and/or extrusive activity are therefore consistent with our preferred explanation for the antiformal structure, and are consistent with the radiometric age date obtained from thermally metamorphosed sediments beneath the dolerite sill encountered in well 214/27-1.

In summary, a previously interpreted Paleocene transpressional popup structure associated with the Victory Lineament is more likely to have originated due to local igneous and/or hydrothermal activity just prior to continental breakup (Appendix B.20). There is no conclusive evidence from the seismic data to support the idea that the Victory Lineament had a significant regional structural expression at any time during the Cenozoic, apart from localised uplift above the igneous intrusions. Nevertheless, the high density of sills within the underlying Cretaceous section makes it impossible to test the hypothesis that a through-going strike-slip (or transpressional) fault exists at depth within the basin, at least using existing 3D seismic datasets (Appendix B.06).

3.7 Clair Lineament

The Clair Lineament is located to the southwest of the Victory Lineament, with the study area encompassing part of the NE-SW trending Flett Ridge and Flett and Foula Sub-Basins (Figs 3.01 and 3.07a). This area was selected in order to understand the possible structural and stratigraphic interaction between the hypothesised Clair Lineament and the two regional depocentres and structural high. Furthermore, Grant *et al.* (1999) have previously recognised a plunging anticline associated with the Clair Lineament in the study area that in a regional sense compartmentalises the FSB along its strike but notably was not formed by ‘discrete transfer faults’.

Four NE-SW trending seismic sections spaced every 5 km across the inferred position of the Clair Lineament are displayed in Figure 3.07a. The sections clearly show a rapid change in structural style along the strike of the lineament. This observation, and the development of antiformal structures at the level of the Top Cretaceous marker are consistent with the presence of a NW-SE trending strike-slip fault in this area (Harding 1990). However, accurate fault and horizon interpretation is difficult due to the poor quality of the seismic imaging. These problems are caused firstly by NE-SW trending Mesozoic normal faults that bound the Flett Ridge (Fig. 3.01) making highly oblique intersections with the seismic lines (Appendix B.25 & 28). Secondly, there is a high density of sills (high amplitude, concave-upward reflections in Figure 3.07; cf. Figs 3.02 and 3.04) within the pre-Cenozoic section in the vicinity of the Clair Lineament (Appendix B.29). Thirdly, a significant (~3 km wide, up to 500 m thick) Late Paleocene aged hydrothermal vent complex has led to an area of increased structural relief at the Top Cretaceous horizon along a section of the inferred Clair Lineament (Appendix B.31). Finally, there are a number of gas discoveries in the area; gas chimneys give rise to local velocity push down effects and can lead to identification of spurious structural features in normal time-migrated seismic data (Appendix B.30).

Analysis of the data at near 1:1 scale (no vertical exaggeration; Fig. 3.07b) shows that the marked Cretaceous antiform visible in Figure 3.07a can be attributed as an artefact of the condensed display. Moreover, there is little evidence of major faulting within the Cenozoic section. It is therefore difficult to demonstrate conclusively that the Clair Lineament had a significant structural and/or geomorphological expression during the Paleogene, apart from possible localised uplift above igneous intrusions in this region.

This conclusion is similar for the Victory Lineament described previously, and also for the intervening Grimur Kamban Lineament shown in Figure 3.01.

3.8 Judd Lineament

The Judd Lineament, originally known as the Faroe Transfer Zone (Mudge & Rashid 1987), is located in the southwest of the FSB (Fig. 3.01). In the UK sector, the lineament has a well defined structural expression as a NW-SE oriented fault system, which is believed to mark the south-western limit to the basin in this area (Duindam & van Hoorn 1987). The Judd Lineament has been inferred to extend north-westward across the Judd Basin, into the Faroese sector of the FSB (Fig. 3.01). However, its structural expression is not well-defined in this region, which lies outside the area of continuous 3D seismic data coverage. In the UK sector, the NW-SE trending faults that make up the Judd Lineament (informally referred to here as the "Judd fault system") juxtapose the basement-cored Judd High in the footwall to the southwest against the Cretaceous Foinaven Sub-Basin in the hanging wall to the northeast. The Judd fault system appears to terminate against, or link with the NE-SW trending faults that define the northern margin of the Rona Ridge, a major basement-cored horst block that separates the Foula Sub-Basin from the West Shetland Basin (Fig. 3.01). The NW-SE trending faults of the Judd fault system have previously been inferred to have either a sinistral (Kirton & Hitchen 1987) or dextral (Hitchen & Ritchie 1987) sense of displacement, a conclusion which is discussed further below.

A time-structure map of the top Precambrian basement seismic marker (Fig. 3.08) displays the gross structure of the study area highlighted in Figure 3.01. The dominant fault trends in this area are NE-SW (040-070°; as exemplified by the faults bounding the Rona Ridge) and NW-SE (120-130°; as exemplified by the faults associated with the Judd Lineament), with a subordinate, approximately E-W (080-100°) trending fault set (Fig.

3.08; Appendix B.54 & 55). The Permo-Triassic West Solan Basin, an asymmetric half graben system with an alluvial and fluvial sedimentary fill (Booth *et al.* 1993), is located on the south-eastern part of the Judd High, adjacent to the Rona Ridge. Previous authors have proposed this rift detaches onto Caledonian thrust planes, which are believed to have been reactivated as low-angle normal faults within the Precambrian basement (Coward & Enfield 1987; Nelson & Lamy 1987).

The NW-SE trending fault system associated with the Judd Lineament has been reinterpreted using the 3D seismic dataset and is seen to comprise three major, en-echelon faults and associated splays, which show large apparent normal offsets that down throw (a minimum of ~ 1000 ms TWT) towards the northeast (Appendix B.57). This new mapping also reveals that the Judd fault system does not continue inboard across, nor does it terminate against the Rona Ridge. Rather, the faults appear to swing round towards a NE-SW trend and merge with the faults on the northern margin of the Rona Ridge, apparently without significant change in displacement (Fig. 3.08). The north-western extent of the Judd fault system lies beyond the limit of the 3D seismic MegaSurvey, but analysis of regional 2D lines suggests that this fault system may link with NE-SW trending faults that define the north-western margin of the Judd High (Fig. 3.01).

Figure 3.09a shows a NE-SW seismic section across the Judd High into the Foinaven Sub-Basin. A thin, discontinuous Cretaceous sequence on the Judd High (i.e., in the footwall of the Judd fault system) is seen to expand to more than 1500 ms thickness within the Foinaven Sub-Basin. This Upper Cretaceous marine sequence has been dated in a number of wells in the basin. However, due to the poor imaging within the Cretaceous section (which is common throughout the FSB because of the dominant mudstone lithology), it is difficult to ascertain whether internal fanning of stratal fills occur against the Judd fault system (Fig. 3.09a). Nevertheless, the most plausible explanation for some, if not all, the observed across-fault thickening is that the Judd fault system – and associated NE-SW trending faults at the northern margin of the Rona Ridge (not shown) – were active and accommodated large basinward throws during deposition of the Upper Cretaceous sequence. The base of this syn-rift package has not been drilled and can only be inferred from regional 2D seismic data which image the deeper structure.

Figure 3.09b shows a NW-SE oriented seismic section across the Judd High and West Solan Basin. Here, there is clear thickening of Permo-Triassic, Lower Jurassic and Upper Cretaceous strata towards the mainly NW-dipping faults. The Upper Cretaceous sequence appears to be thinner within the West Solan Basin than it is in the Foinaven Sub-Basin, implying that the magnitude of Late Cretaceous rifting was greater in the FSB than in the West Solan Basin (Figs 3.09a and 3.09b). Some faults shown on these sections appear to have been continuously active (or reactivated) into the Paleocene and/or Eocene (Figs 3.09a and 3.09b), but along-strike mapping shows that such activity was discontinuous along the length of both the NW-SE Judd and NE-SW Rona Ridge fault systems. Thus, the main phase of rifting in both the West Solan Basin and the south-western part of the FSB is inferred to have ceased by the Paleocene.

To summarise, the Judd and Rona Ridge fault systems both show large apparent normal displacements and (within the limitations of the available data) appear to link rather than cross-cut. These observations suggest that both NE-SW (Rona Ridge) and NW-SE (Judd) fault systems – together with relatively minor faults within the West Solan Basin – were active synchronously during Late Cretaceous rifting. Taken with the generally accepted view that the FSB is an extensional rift basin, the simplest explanation is that the Judd fault system represents a transfer zone (sensu Gibbs 1984; Faulds & Varga 1998) that transfers some of the displacement (extensional strain) from the Rona Ridge fault system outboard by c. 30 km to the NE-SW trending faults on the northern margin of the Judd High (Fig. 3.08). Thus, the Judd Lineament does *not* represent a through-going basin scale strike-slip fault (Ellis *et al.* 2009); rather, it is a second order structure that was active during Late Cretaceous rifting within the FSB (Fig. 3.10). In this model, the bounding faults of Rona Ridge are inferred to have accommodated predominantly normal displacements, whilst the Judd fault system is expected to have accommodated sinistral oblique movements with a down throw towards the northeast (Fig. 3.10; cf. Gibbs 1984, p. 616, fig. 14). Whilst this hypothesis is, in our view, the most parsimonious explanation of the available data, more rigorous testing will not be possible until there is an improvement in seismic resolution below the Paleogene flood basalts and an extension of the 3D seismic coverage into the Faroese sector.

An outstanding issue is to explain why a transfer fault system developed adjacent to the Judd High. One possibility is that this “stepping” of the rift towards the proto-Atlantic Margin may have been caused by strengthening of the lithosphere beneath the West Solan Basin following Late Palaeozoic and Mesozoic rifting (cf. Steckler & Tenbrink 1986). Lundin & Doré (1997) used a similar argument to explain the progressive northwest migration in the locus of active rifting prior to continental breakup in the Norwegian Sea region. Alternatively, Hitchen and Ritchie (1987) have inferred a lateral offset of the Moine Thrust plane along strike from the Judd fault system, which they attributed to activity along a Paleozoic shear zone. We speculate that the location of the Judd fault system may also have been influenced by a pre-existing zone of weakness in the crystalline basement if this – or an older structure comparable to the similarly oriented NW-SE trending Precambrian shear zones exposed within the Lewisian basement of NW Scotland (e.g. Beacom *et al.* 2001) – were to extend north-westwards beneath the FSB (Appendix B.37 & 53). A similar hypothesis has been proposed for the origin of the NW-SE lineaments in the Møre and Vøring Basins offshore Norway by Doré *et al.* (1997b).

3.9 Discussion

Analysis of three previously inferred rift-oblique lineaments ("transfer zones") in the Faroe-Shetland Basin using a well-calibrated regional 3D seismic survey has not found any conclusive evidence to support the hypothesis that the Victory, Clair or Judd Lineaments acted as basin-wide strike-slip faults with significant structural or geomorphological expressions during the Cenozoic. Rather, structures associated with these lineaments appear to be local features that developed due to igneous processes (e.g. sill emplacement and associated hydrothermal activity) or transfer of extensional strain between one rift segment to another. This re-interpretation is partly the result of an improved understanding as to the processes that occur on volcanic margins (e.g. Bell & Butcher 2002; Hansen 2006; Hansen & Cartwright 2006) and partly the result of a more data-driven approach using better quality seismic reflection datasets than have hitherto been available (e.g. Gallagher & Dromgoole 2007). Nevertheless, two important questions remain. The first is to address whether the previously hypothesised control of rift-oblique lineaments ("transfer zones") on sediment transport and deposition within the FSB is compatible with our findings. The second is to consider whether our results are compatible with observations that rift-oblique lineaments are associated with abrupt changes in crustal structure.

3.9.1 Control on sediment transport and deposition within the Faroe-Shetland Basin

Jolley & Morton (2007) have used palynological and heavy mineral analyses of rock samples from boreholes to investigate along-strike variations in sediment source and distribution within the UK sector of the Faroe-Shetland Basin. They identified four distinct geographic populations of flora which varied along the basin trend. Jolley & Morton (2007) suggest that NW-SE trending "transfer zones" may have acted as both barriers and long-range conduits to sediment transport at different times throughout the Paleocene. Our findings suggest that active rifting had largely ceased within the southeastern (UK) part of the FSB at this time, and that there is little evidence to suggest that the basin was compartmentalised by major, through-going NW-SE structures. We speculate that sediment pathways across and depocentres within the southeastern FSB during the Paleocene were mainly controlled by the topographic relief associated with post-rift thermal subsidence following Late Cretaceous rifting. It is clear that the Late Cretaceous rift was segmented, for example by the Judd fault system and probably elsewhere, too – such as at the en-echelon segments observed along the Flett and Corona Ridges (Fig. 3.01). Thus, the spatial distribution of thermal subsidence is likely to have been variable along the strike of the basin and cannot be modelled adequately using a two-dimensional “steers head” representation. Along strike changes (e.g. Mitchell *et al.* 1993; Lamers & Carmichael 1999) in patterns of sediment transport and deposition may largely reflect the along strike variations in thermal subsidence (i.e. accommodation space), which in turn was controlled by the complex, segmented geometry of the underlying Mesozoic rift. Uplift due to “jacking up” of strata above igneous intrusions during the Late Paleocene may have *locally* modified the geometry of these thermally-subsiding sediment depocentres, whilst sediment transport from further afield (e.g. Greenland; Larsen & Whitham 2005; Jolley & Morton 2007) may also have been controlled by the evolving Paleocene rift system within the northwestern (Faroese) part of the FSB (cf. Gawthorpe & Leeder 2000). Thus, we see little requirement to invoke activity along discrete, basin-wide NW-SE “transfer zones” during the Paleocene. A critical test of our revised model would be to map regional changes in thickness and seismic facies within the post-rift Paleocene succession using well-calibrated 3D seismic data. These observations should be integrated with sediment provenance data and a comprehensive study of the underlying Late Cretaceous rift architecture within the southeastern part of the FSB.

3.9.2 Deep crustal structure

Mjelde *et al.* (1998, 2003b) have mapped 5 NW-SE to N-S trending lineaments on the Vøring Margin, offshore Norway, using wide-angle seismic and gravity data. These lineaments are defined by abrupt changes in the thickness of the crystalline basement, variations in Moho depth and by apparent lateral offsets in the locations of high-velocity, lower-crustal bodies, which may have originated as igneous material underplated at the base of the crust during continental breakup and/or as eclogitic roots formed during the Caledonian Orogeny. There is some uncertainty in the precise location and orientation of these lineaments, but structures in the basement and lower crust appear to be critical in defining these features. Upper crustal structures are less significant in this respect (Mjelde *et al.* 2003b). These findings from the Vøring Margin are compatible with our results from the Faroe-Shetland Basin. We have found no basin-scale expressions of the Victory, Clair or Judd Lineaments within the post-rift Cenozoic sequence. However, these observations in no way rule out the possibility that these lineaments, originally identified using potential field data, may be associated with changes in deep crustal structure along the strike of the FSB (e.g. England *et al.* 2005). Such changes would be consistent with the distinct crustal terranes that have been inferred to exist within the Lewisian Complex of NW Scotland (Friend & Kinny 2001) and which are bounded by mainly NW-SE trending shear zones. In addition, variations in deep crustal structure could explain the possible increase in the number of igneous intrusions in the vicinity of the Clair Lineament (Fig. 3.07). A heterogeneous deep crustal structure could even provide a rationale for the observed segmentation of the Late Cretaceous rift along NW-SE transfer zones (sensu Faulds & Varga 1998). Nevertheless, such models remain speculative until future studies precisely resolve the deep crustal structure beneath the Faroe-Shetland Basin.

3.10 Conclusions

Structural and stratigraphic interpretations of a well-calibrated 3D seismic survey from the UK sector of the Faroe-Shetland Basin suggest that three previously inferred NW-SE trending rift-oblique lineaments ("transfer zones") did not have regional structural or geomorphological expressions during the Cenozoic. There is no evidence to suggest that the Victory, Clair, Judd, or any other previously inferred rift-oblique lineaments were active as discrete, basin-wide strike-slip faults at this time. New results show that:

- Structures within the Flett Sub-Basin that are associated with the Victory Lineament (Dean *et al.* 1999) can be related to the effects of igneous intrusion at depth below the Cenozoic strata. Emplacement of two concave up sills (c. 200 m thick) below the base Tertiary unconformity led to uplift of the sedimentary overburden, with laccolithic style emplacement at the junction between two sills. The timing of hydrothermal vent and/or extrusive igneous activity above the sill tips agrees with unpublished radiometric dates of one of the sills.
- Structures within the Flett and Foula Sub-Basins that are associated with the Clair Lineament (Grant *et al.* 1999) can be attributed to the compressed display of low resolution seismic data, and the oblique intersection with NE-SW trending normal faults that bound the Flett Ridge, a NE-SW trending structural high. Imaging problems are exacerbated by velocity push down effects from a gas chimney and the large number of igneous sills in the vicinity of the Clair Lineament.
- The Judd Lineament (Kirton & Hitchen 1987) is defined by a NW-SE trending normal fault system, which we infer to have developed during Cretaceous rifting. This "Judd fault system" probably transferred extensional strain between two en-echelon, NE-SW trending rift segments, the Rona Ridge and the Judd High.

The complex architecture of the underlying Late Cretaceous rift system may have given rise to along-strike variations in thermal subsidence (accommodation space), which was the principal control on sediment transport pathways and depocentres during the Paleocene.

3.11 Acknowledgements

This work forms part of a NERC CASE Studentship with Statoil U.K. Ltd (NER/S/C/2006/14276). PGS Geophysical is gratefully acknowledged for permission to publish images from the Faroe-Shetland Basin Seismic MegaSurvey. Landmark Graphics Corporation through the Strategic University Alliance Agreement (2006-COM-032168) is acknowledged for providing seismic processing/interpretation software and technical support. D. Stevenson and G. Wilkinson provided ongoing technical support within the Department of Earth Sciences. The authors would also like to thank R. England and A. Doré for their constructive reviews of the manuscript. Funding of the colour reproduction costs met by Statoil U.K. Ltd is appreciated.

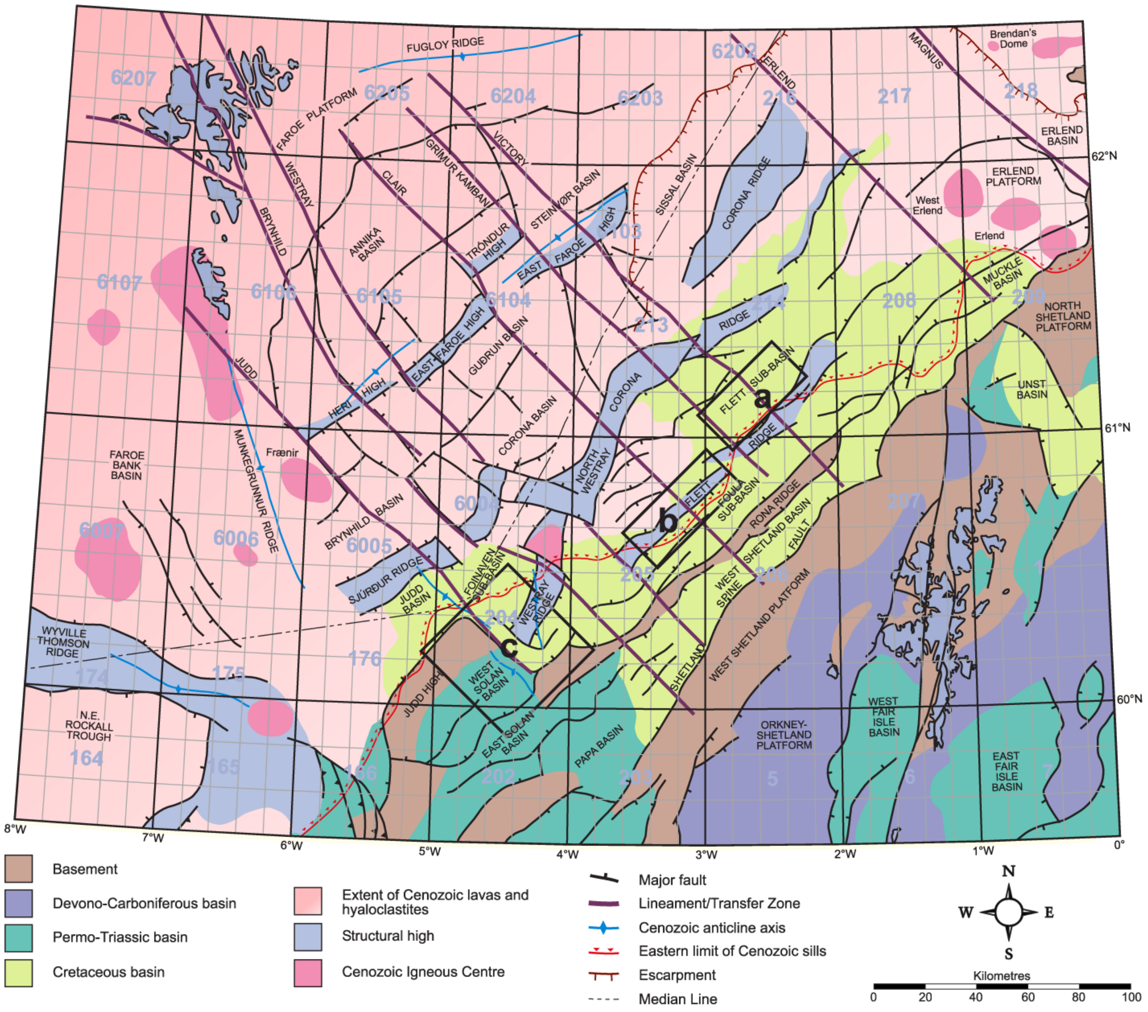

Figure 3.01: Structural elements of the Faroe-Shetland Basin with the location of the three lineament case studies described in this paper (a) Victory Lineament, (b) Clair Lineament and (c) Judd Lineament (after Ellis *et al.* 2009). Map projection is WGS84, UTM 30N.

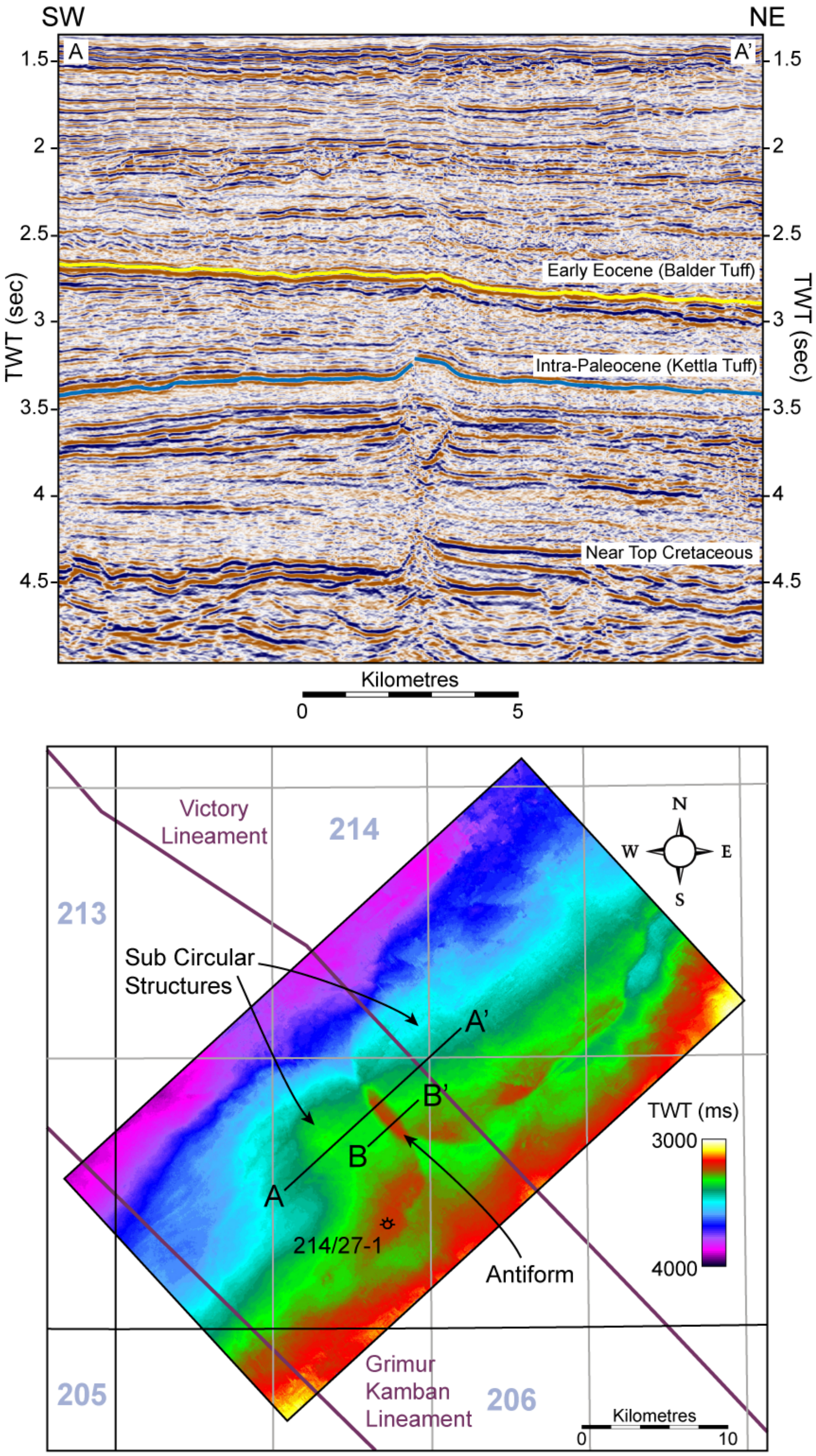

Figure 3.02: The transpressional pop-up structure associated with the Victory Lineament interpreted by Dean *et al*. (1999) (left) and a time-structure map of the top Kettla Tuff horizon (right). MegaSurvey seismic data courtesy of PGS Geophysical.

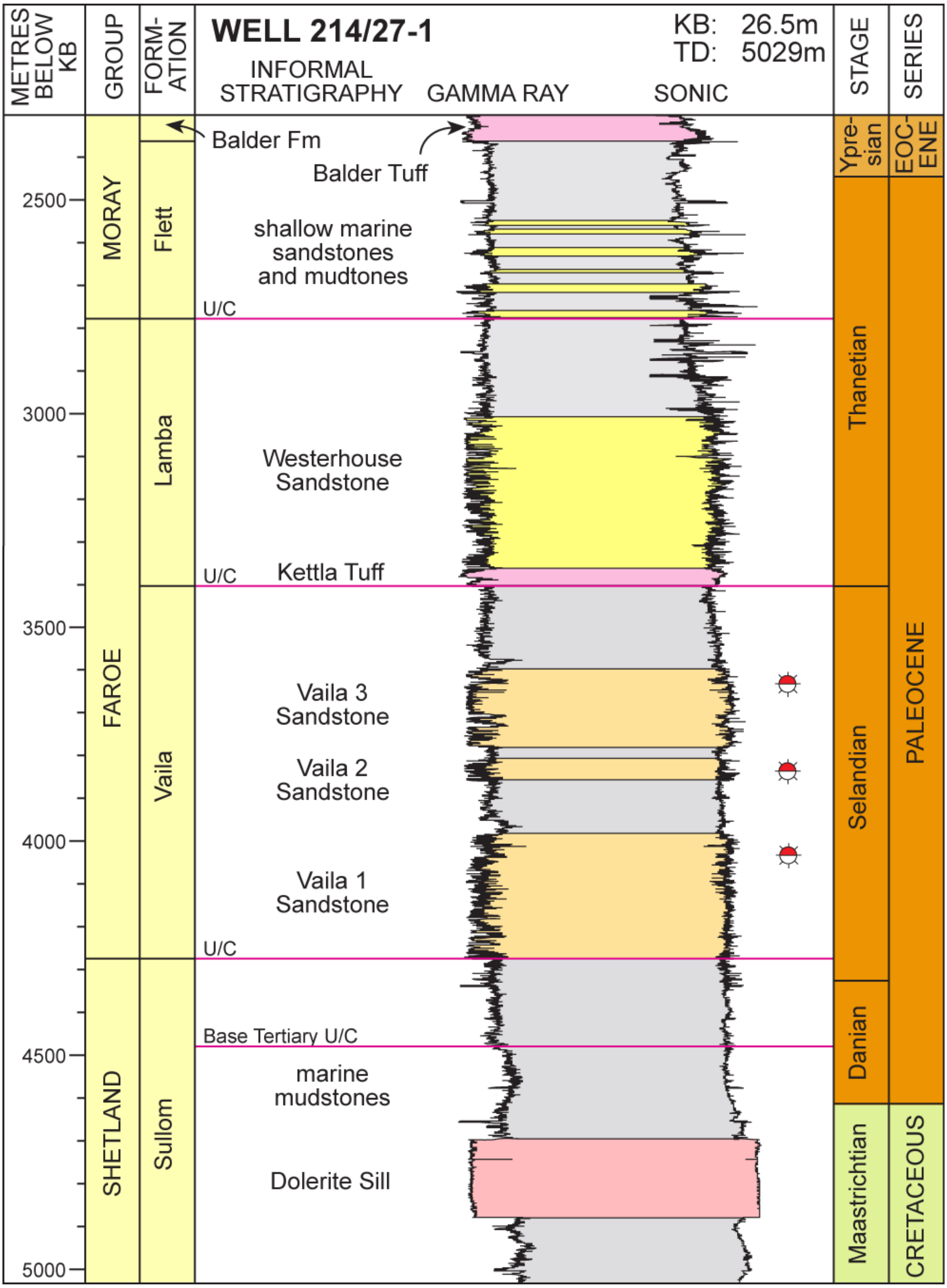

Figure 3.03: Well 214/27-1 displaying the Lower Cenozoic to Maastrichtian stratigraphy and the Eocene aged dolerite sill (after Mudge & Bujak 2001; Gallagher & Dromgoole 2007). **U/C** unconformity; **TD** total depth; **KB** kelly bushing.

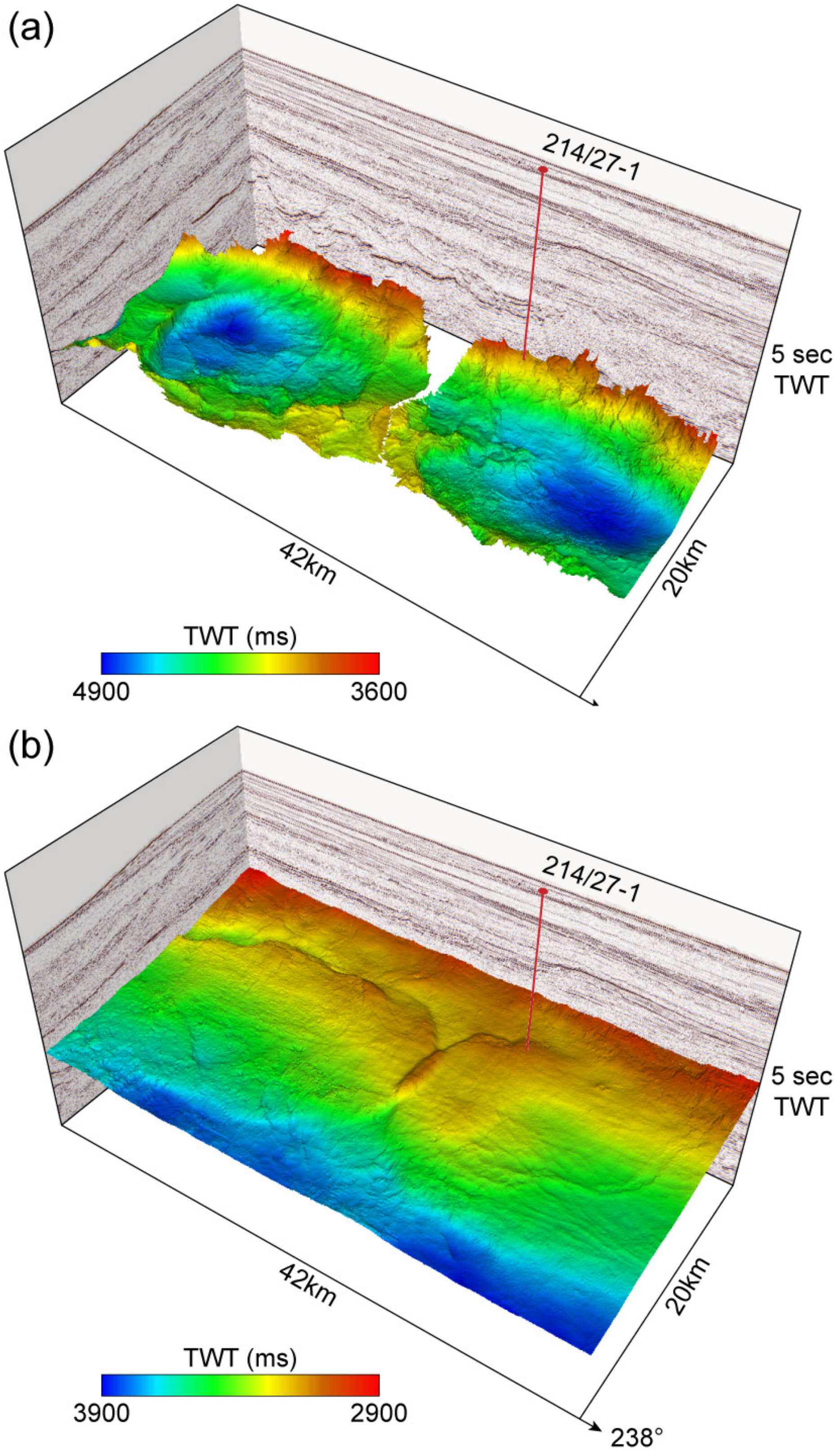

Figure 3.04: (a) The two Eocene sills with concave up ‘saucer shape’ characteristics and (b) the associated uplift of the sedimentary overburden displayed by the Kettla Tuff horizon producing two large, low relief forced folds.

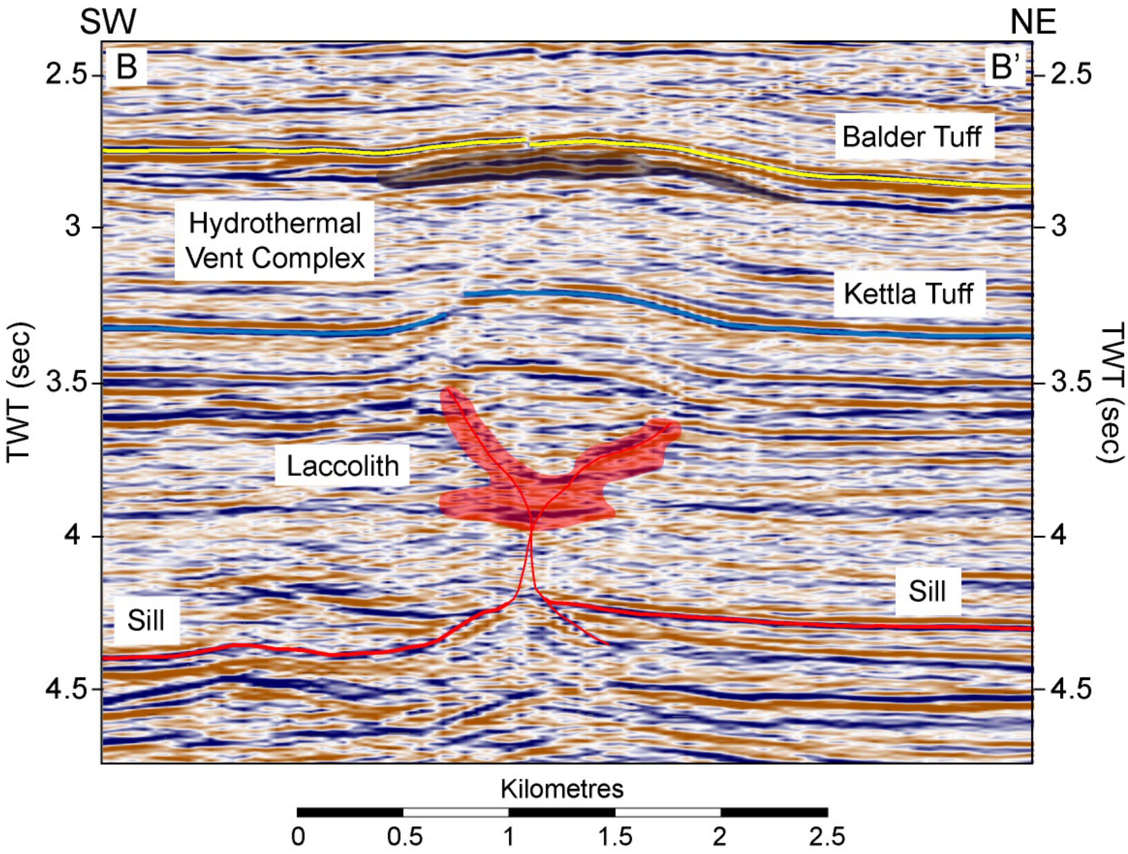

Figure 3.05: Near 1:1 scale display of a laccolithic intrusion within the Paleocene strata (highlighted by red shading). The intrusion is fed by two near sub-vertical dykes extending from the sill tips. Timing of emplacement of the igneous material can be ascertained from the age at which a hydrothermal vent complex (highlighted by dark shading) formed prior to the deposition of the Balder Tuff in the Early Eocene. For line location, refer to Figure 3.02. MegaSurvey seismic data courtesy of PGS Geophysical.

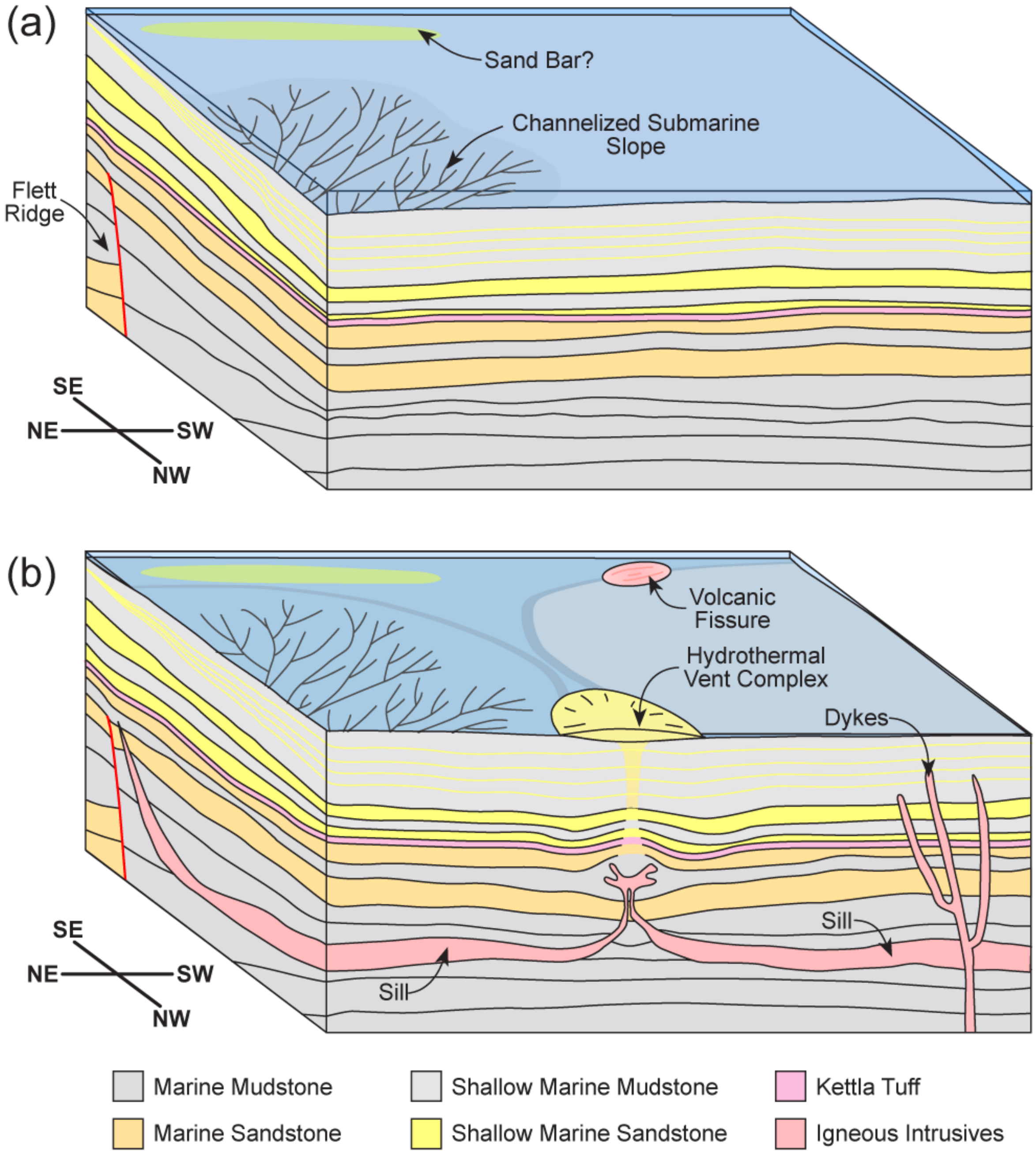

Fig 3.06: Block model summary of the inferred Victory Lineament example of Dean *et al*. (1999) (a) prior to sill emplacement and (b) post sill emplacement. Interpreted hydrothermal vent complexes could be volcanic fissures and visa-versa, see Hansen (2006) and Thomson (2007) for discussion. Palaeogeographical interpretation from Lamers & Carmichael (1999).

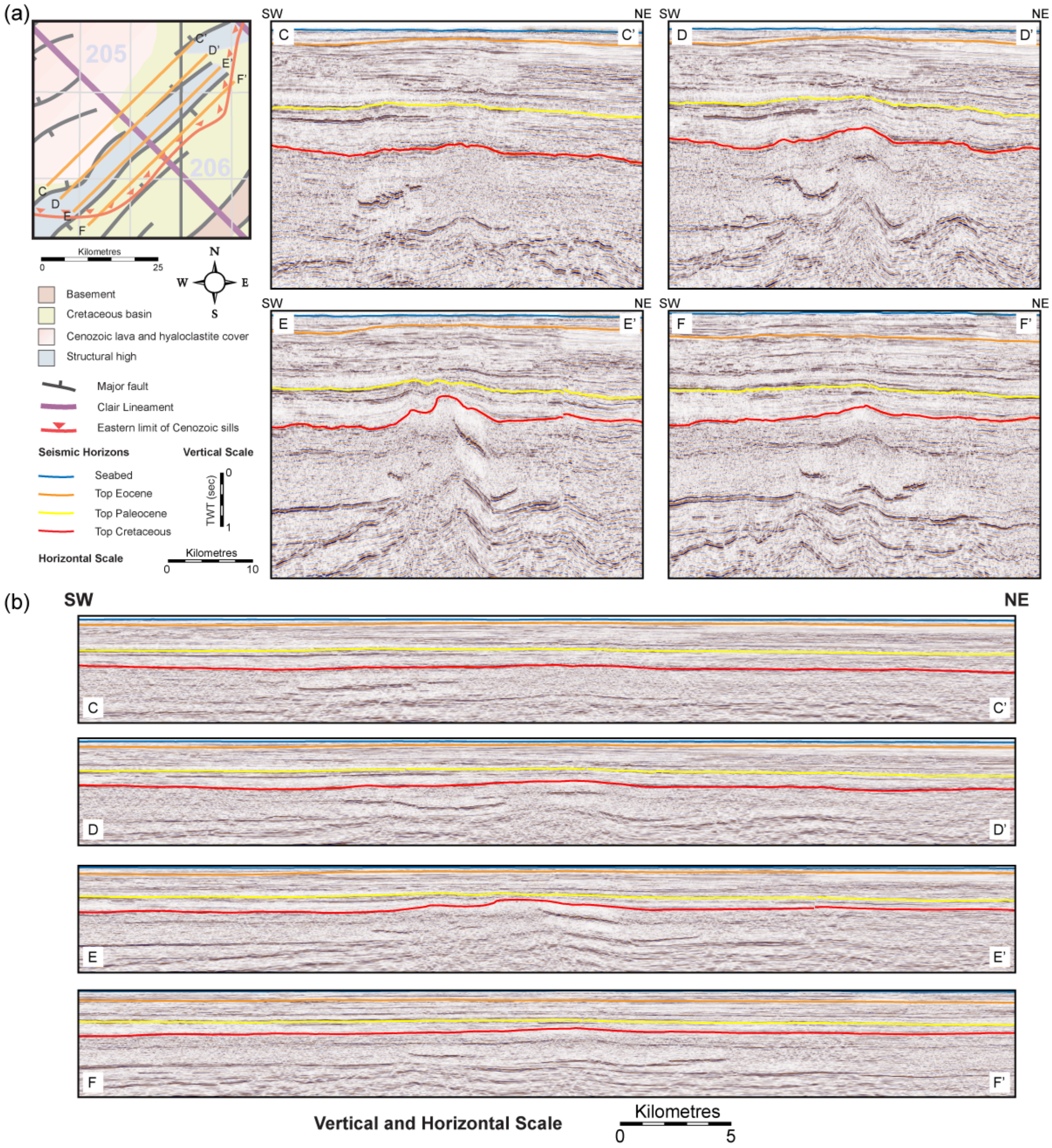

Figure 3.07: Four seismic lines at 5 km spacing across the inferred Clair Lineament displaying (a) a rapid change in structure along strike due to the compressed display of the data. When displaying (b) at near equal horizontal and vertical scale, the apparent effect of the Clair Lineament is negligible with uplift of strata probably caused by the emplacement of sills into the Cretaceous succession. The Clair Lineament is inferred to intersect near the centre of each seismic line. MegaSurvey seismic data courtesy of PGS Geophysical.

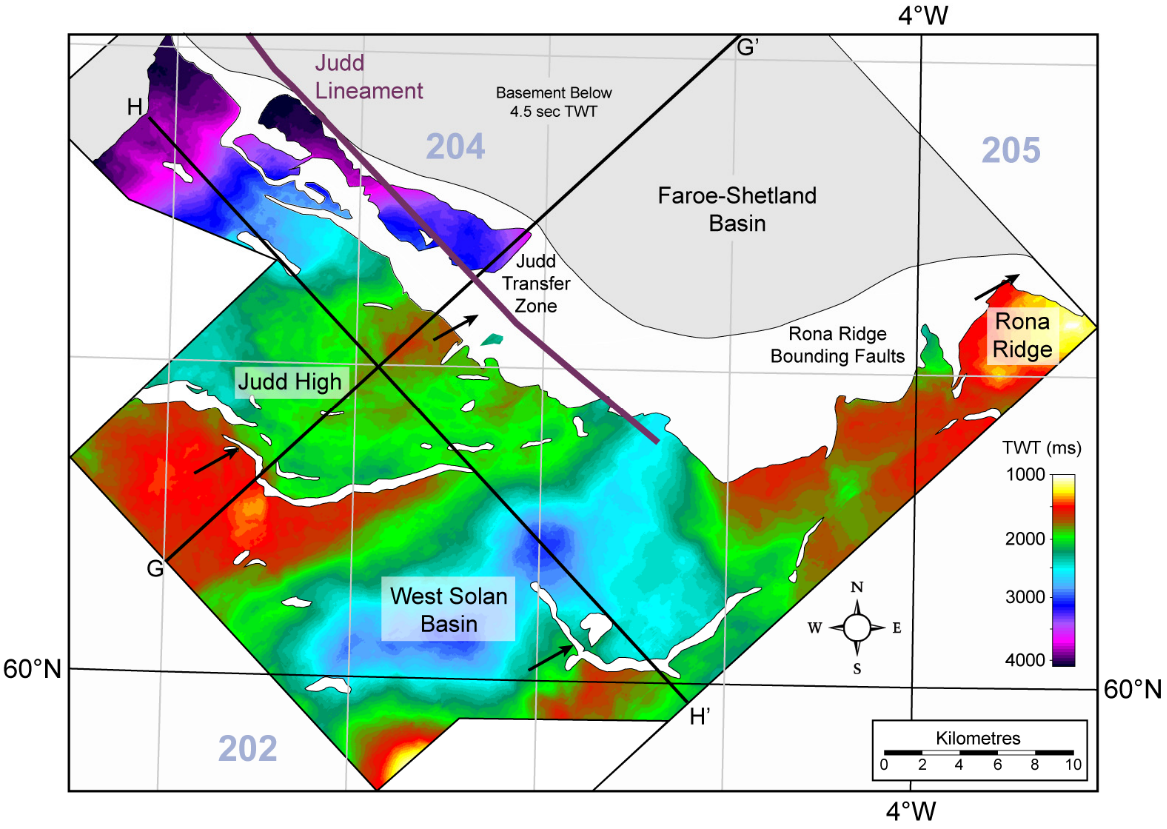

Figure 3.08: Time-structure map of the top Precambrian basement displaying the West Solan and Faroe-Shetland Basins. Fault polygons are displayed in white with black outline and display the dominant fault orientations within the basin (NE-SW, NW-SE and E-W). Arrows highlight the areas of NW-SE faulting referred to in the text. Areas shaded in grey are beyond the resolution limits of the seismic data.

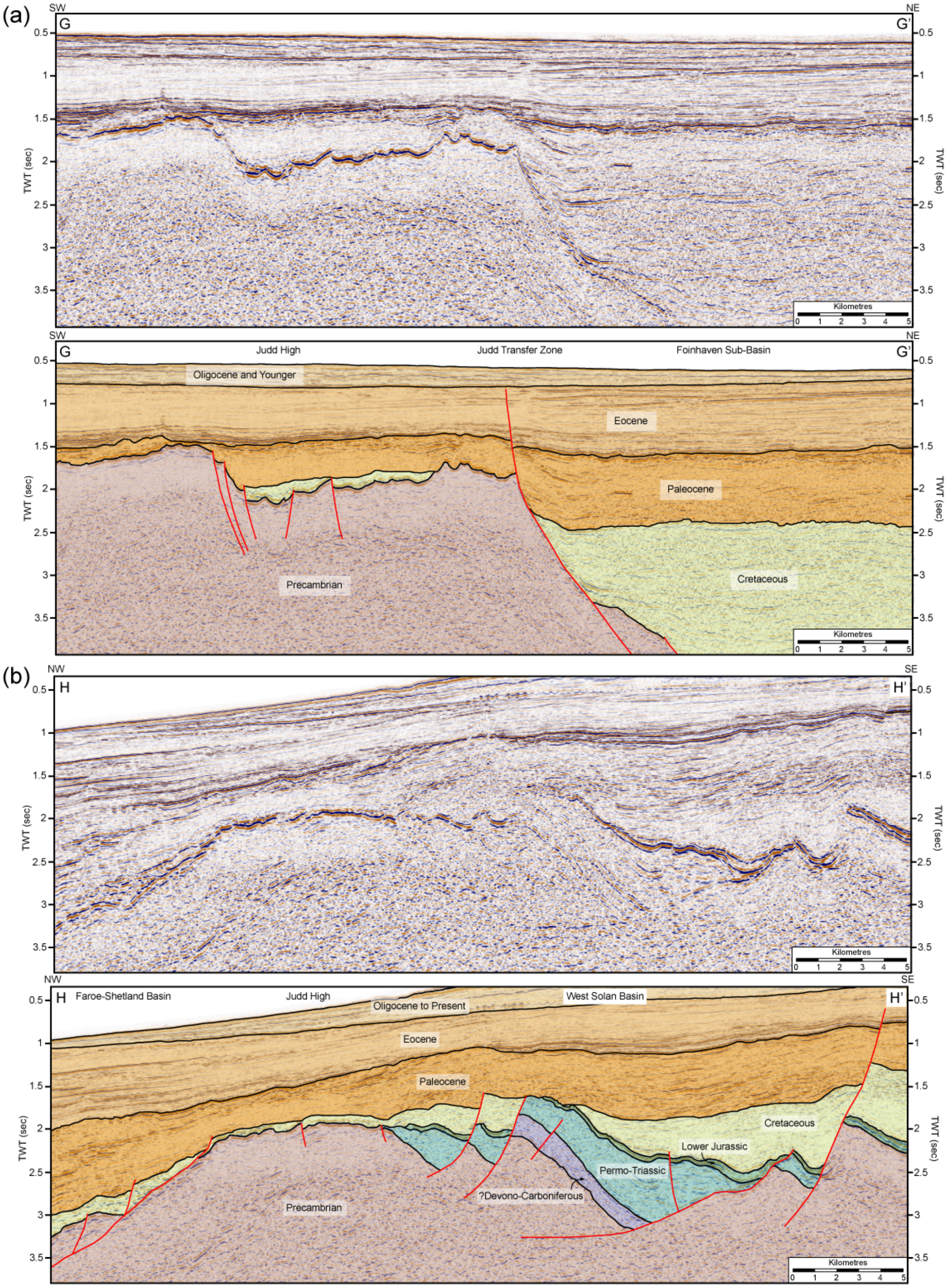

Figure 3.09: Seismic lines displaying the tectonic style across the (a) Judd Transfer Zone and (b) the West Solan Basin. For line location, refer to Figure 3.08. MegaSurvey seismic data courtesy of PGS Geophysical.

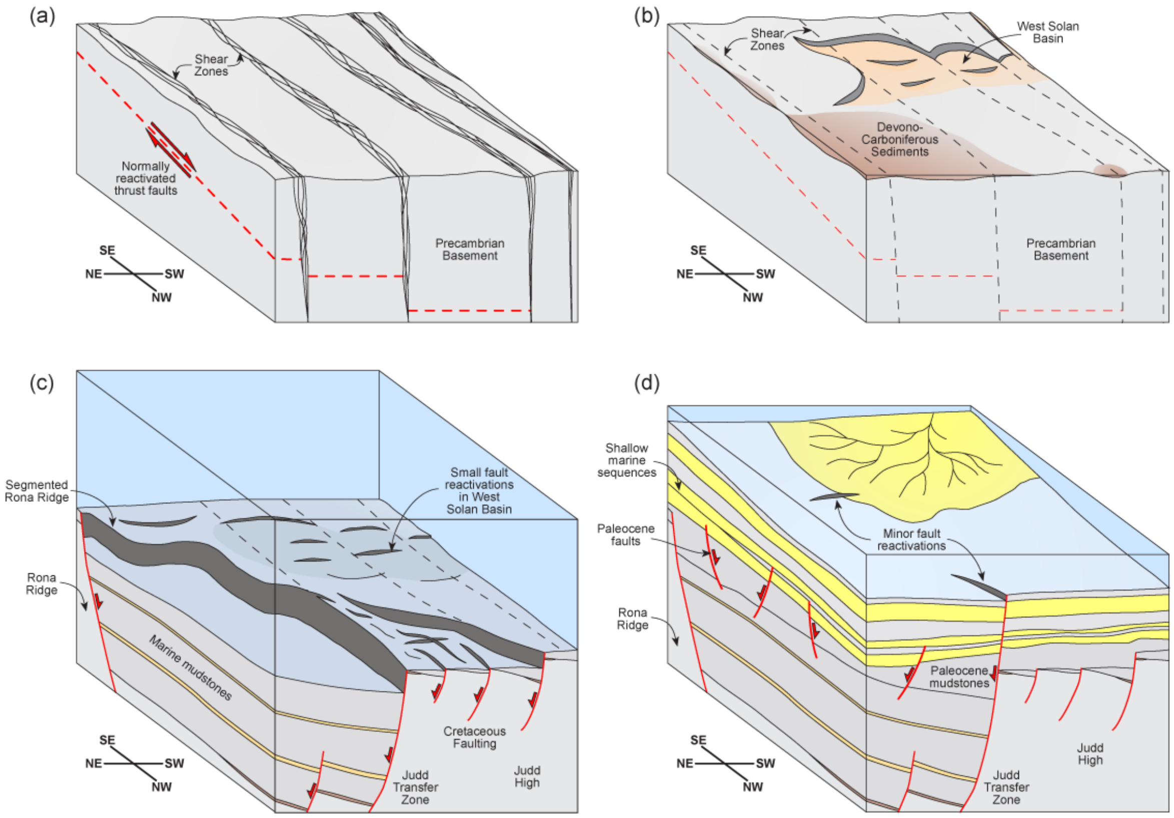

Figure 3.10: Block model summaries at various stages of the evolution in the present day southwest Faroe-Shetland Basin. (a) Proterozoic and Archaean shear zones are reactivated during the Caledonian Orogeny with thrust faults normally reactivated during orogenic collapse. (b) The Permo-Triassic rift of the West Solan Basin is apparently segmented by NW-SE faulting, potentially reactivating inferred NW-SE zones of weakness. (c) Major Late Cretaceous rifting led to the formation of the Rona Ridge and Judd fault systems. (d) Following the cessation of rifting and continental breakup, the Eocene is a period of tectonic quiescence with only minor fault reactivations.

Chapter Four

4 TECTONIC EVOLUTION OF A FAULT DOMAIN BOUNDARY

4.1 Abstract

Fault domain boundaries (accommodation and transfer zones) are common within rift systems around the world, but despite their recognition in onshore and offshore studies, and successful recreation in laboratory based analogue modelling, little is known surrounding their internal structural geometry. Equally, they have been assumed to conserve and transfer strain between adjacent rift segments but little research has focussed on this aspect. Therefore the primary aim of this study is to understand if, and how strain is transferred between two adjacent fault domains. Using high resolution 2D and 3D seismic data, the Rym Accommodation Zone is analysed in the northern Vøring Basin, NE Atlantic Margin, offshore Norway. The results of the study highlight major differences between the offset rift segments in view of the style of rifting, timing, the loci of faulting, the relative uplift and subsidence histories as well as the impact of variations in the deep crustal structure. Analyses reveal that strain is not fully transferred across the fault domain boundary, with significant variation in beta factors calculated for each rift segment. The structural style within the Rym Accommodation Zone also varies with the rotation of normal fault orientations, major relay ramp formation and rift perpendicular normal oblique faulting observed; these features are atypical of conceptual models of accommodation zones that exist at present. The results also imply that transfer zones may be an integral part of a larger accommodation zone rather than an opposite end member as previously believed.

4.2 Introduction

Accommodation zones and transfer zones (fault domain boundaries; Schlische & Withjack 2009) have been recognised in a range of segmented rift systems from around the world (e.g. Morley *et al.* 1990; Axen 1998; Henry 1998; Younes & McClay 2002; Khalil & McClay 2009). These features are commonly inferred to have formed as adjustment features between two en echelon rift segments of uniformly and oppositely dipping faults (e.g. McClay *et al.* 2002), and have been proposed to accommodate the transfer of strain between each fault domain (Faulds & Varga 1998). However, little work has focussed on the fundamental details whether, and if so how, strain is directly transferred across fault domain boundaries despite their recognition in both onshore and offshore study areas.

Faulds & Varga (1998) reviewed all previous research into fault domain boundaries which resulted in the definition of two, mutually exclusive end member models; the 'hard linked' transfer zone and 'soft-linked' accommodation zone (c.f. Walsh & Watterson 1991), currently considered as the most accurate representations of the fault domain boundaries from analogue modelling results (Schlische & Withjack 2009). Fault domain boundary studies have been conducted in a range of onshore regions including but not limited to the Basin and Range Province, USA (e.g. Henry 1998; Faulds *et al.* 2002), the East African Rift (e.g. Rosendahl 1987; Morley *et al.* 1990; Nelson *et al.* 1992) and the Gulf of Suez (Moustafa 1996; 2002; Younes & McClay 2002). A key problem with field based mapping is that often only limited exposure is available to investigate an inherently three dimensional problem.

Analogue modelling successfully recreates accommodation zones although the internal structure of these rift-oblique zones is not resolvable. For example, McClay & White (1995) modelled a maximum 15 cm wide rift using sand of 275 μm average width, which when applied to a 150 km wide rift, will only resolve features a minimum of ~ 275 m in width at the granular scale. Similarly, Schlische & Withjack (2009) modelled fault domain boundaries within sand boxes and clay packs with increased amount of extension over greater distances, yet the scales are such that 1 cm within the model still represents only 1 km distance within natural rift systems. Equally, analogue models infer a homogeneous pre-rift succession which results in generally symmetrical rift systems which are rare within natural continental rifts (Morley 1999). One aspect of particular revalence to the study of fault domain boundaries is the influence of pre-existing crustal heterogeneities which have been inferred to control the location of the rift segmenting features as has been recognised in numerous rift basins (e.g. Cordell 1978; Milani & Davison 1988; Ebinger 1989a; b; Mack & Seager 1995; Moustafa 1996). These accommodation and transfer zones have subsequently been recreated in analogue models above a change in the base plate configuration across which extension rates vary (e.g. Acocella *et al.* 2005), but despite this apparent basement control, little work has focussed upon the precise influence of these pre-rift structures within each fault domain.

High resolution 3D seismic data has led to the further recognition and study of accommodation zones (e.g. Scholz & Hutchinson 2000; McClay *et al.* 2004). 3D seismic data does not have the limitations imposed that an onshore study does, equally, the resolution is greater than currently available through sandbox and clay pack analogue models. Unfortunately, previous studies utilising 3D seismic data have commonly described the broad geometry of these features but failed to analyse in detail the controls upon their formation and by which aspect of extensional tectonics (e.g. structural geometry, location and kinematics of faulting and variation of structural styles along strike) these accommodation zones are defined apart from an inferred en-echelon offset between rift segments.

The definition of a fault domain boundary may not solely be based upon the polarity of faulting or discontinuity of fault segments as inferred by the conceptual models (Faulds & Varga 1998). Instead fault domain boundaries could also be defined on the basis of the other aforementioned dynamic aspects of rift systems. Transverse zones (c.f. Rowley 1998) are fault domain boundaries up to 25 km in width which commonly contain a series of oblique slip faults which form at high angles to the rift axis. Other transverse zones can contain a variety of deformational styles including dip-slip and strike-slip faults, folds, joints and areas which have undergone varying degrees of rotation. These zones are inferred to have formed due to differing extensional style, amounts and rates of extension within the adjacent rift domains. Therefore, questions need to be posed, including whether a rift domain boundary can separate rift segments of contrasting structural styles of faulting (e.g. half graben formation vs. a series of horst and grabens). Alternatively, can they be defined on differences in the fault dip angles, possibly due to the presence of a localised detachment horizon within one of the adjacent rift segments? Equally, can the uplift and subsidence histories of each rift segment vary and the fault domain boundary separate areas of differential rift kinematics and erosion? The controls upon these processes may in turn be influenced by differences in deep crustal structure within each rift segment. Thus, the variation in rift segment processes could be linked to the same basement heterogeneities which control the original location of the fault domain boundary.

Within analogue models, major large scale relay ramp structures are inferred to be present within accommodation zones. McClay *et al.* (2004) developed relay ramps in sand pack analogue models which were the equivalent of ~ 10 km wide in a 150 km wide orthogonal rift having undergone 20% extension. An even larger relay ramp ~ 100 km wide has also been recognised in an onshore study of northeast Greenland (Peacock *et al.* 2000). However, are the relay ramps which formed within analogue models or interpreted from limited outcrop exposure in onshore studies realistic in natural examples? Breached relay ramps are common within rift basins (e.g. Trudgill & Cartwright 1994) so is it realistic to expect major relay ramps between major faults in a basin wide zone, or is the internal structural geometry of the fault domain boundaries much more complex than presently believed? A further aspect which requires attention is whether transfer zones which are predominantly recognised in onshore studies are an integral part of a much larger relay ramp or accommodation zone? An obvious scale discrepancy exists between basin scale transfer faults (Faulds & Varga 1998) with the breaching relay faults between two overlapping normal faults (Peacock & Sanderson 1994). Similarly the inferred movements upon each fault set differs greatly with dominantly lateral movements interpreted upon transfer faults (e.g. Henry 1998) and normal oblique movements inferred upon the breaching faults of relay ramps (Crider & Peacock 2004, fig 5c, p697). Or are these transfer zones independent discrete zones of oblique and strike-slip faulting which do exist in their own right but can not be modelled within laboratory based investigations at present?

Directly related to the definition of the fault domain boundary is by which methods strain is transferred between the adjacent rift segments. It is assumed at present the overall strain is conserved across accommodation zones, transferred by a series of relay ramps onto a separate set of overlapping faults within the adjacent fault domain (Faulds & Varga 1998). Within a transfer zone, strain is transferred directly between fault domains via a through going transfer fault (Gibbs 1984). Within a transverse zone which contains multiple structural styles, strain may be transferred through a variety of methods such as faulted and unfaulted relay ramps, folding and transfer faulting. However, as each of these structural processes interact, it could be expected either increased or reduced amounts of strain may be transferred. Similarly, the deformation style within the adjacent rift segments will also influence whether strain can be transferred via the fault domain boundary. If strain is of a greater magnitude in one domain, how is strain expected to be transferred directly across the fault domain boundary? This can be influenced by the methods used for strain calculations but also any differential uplift and subsidence effects occurring within each individual domain will also impact upon any calculations. If this is the case, only within idealised end member models would strain be expected to be wholly transferred between rift domains. The results of this study are therefore expected to impact directly upon the already complicated use of transfer and accommodation zone terminology within segmented rift systems (see Faulds & Varga 1998) and may prompt a further review of our present knowledge and understanding of fault domain boundaries.

Utilising 2D and 3D seismic data, this study investigates a fault domain boundary in the Vøring Basin, offshore Norway. It allows a high resolution spatial and temporal analysis of the two adjacent rift-related fault segments as well as the internal deformation within the Rym Accommodation Zone (Ren *et al.* 2003). A limitation of the study area is that the full extent of the accommodation zone is not at present known, and is expected to continue into the east Greenland conjugate margin which is poorly understood with little seismic data acquired upon that margin. However, this analysis is inherently different to previous studies utilising 3D seismic data within failed rift systems (e.g. the North Sea; McClay *et al.* 2004) and onshore field-based studies which are currently experiencing lithospheric thinning (e.g. the east African rift; Ebinger *et al.* 2000; Ebinger & Casey 2001). These study areas fail to characterise the full evolution of a fault domain boundary from the initial rift conception through to the rift culmination stage resulting in continental breakup which is of critical importance in understanding how fault domain boundaries evolve. Therefore, an analysis of strain through space and time is achievable with 3D seismic data. In particular, the question whether fault domain boundaries conserve strain between adjacent rift segments can be addressed.

4.3 Geological setting

The Norwegian continental margin was formed by episodic rifting that initiated after the closure of the Iapetus Ocean during the Silurian – Early Devonian forming the Caledonian Orogen (Bukovics & Ziegler 1985). Extensional events are recognised during the Early – Middle Devonian, Carboniferous, Late Permian – Early Triassic, Late Jurassic – Early Cretaceous and Late Cretaceous – Paleocene times (Ziegler 1988; Blystad *et al.* 1995; Lundin & Doré 1997; Swiecicki *et al.* 1998; Doré *et al.* 1999; Gabrielsen *et al.* 1999; Roberts *et al.* 1999; Brekke 2000; Reemst & Cloetingh 2000; Mosar *et al.* 2002). The succession of outward stepping to the NW rift events (Doré *et al.* 1999; Reemst & Cloetingh 2000; van Wijk & Cloetingh 2002; van Wijk *et al.* 2004) culminated in continental breakup between Greenland and Norway in the Early Eocene c. 55 Ma (Eldholm *et al.* 2002) and was associated with major magmatic activity on the Vøring Marginal High and within the Vøring Basin (White & McKenzie 1989; Skogseid *et al.* 1992; Eldholm & Grue 1994; Mjelde *et al.* 2001). Within the North Atlantic passive margins that formed as a result of continental breakup, a series of Cenozoic aged domes are observed, the origins of which remain enigmatic (Lundin & Doré 2002; Doré *et al.* 2008). The present day margin geometry (Fig. 4.01) reflects these extensional and later compressional events by the formation of two dominant sets of fault orientations, N-S and NE-SW, further complicated by NW-SE to N-S trending lineaments which have been inferred to cause along strike segmentation of the basin (e.g. Bukovics & Ziegler 1985; Doré *et al.* 1997b; Brekke 2000).

The Vøring Basin is located upon the Norwegian Continental Shelf between 63° - 68° north, and 2° - 10° east (Fig. 4.01). The basin is bounded to the north by the Bivrost

Lineament and by the Jan Mayen Lineament to the south. These lineaments separate the Vøring Basin from the Lofoten Margin to the north and the Møre Basin to the south. The eastern limit of the basin is defined by the fault complexes along the edge of the Trøndelag Platform and to the west by the Vøring Marginal High and the poorly-understood continent-ocean boundary (e.g. Mjelde *et al.* 2007; Olesen *et al.* 2007). The basin is typified by a series of rifted structural highs separated by major Cretaceous synclines with estimated depths in the order of 11 km (Walker *et al.* 1997).

Rift oblique lineaments have been identified primarily by changes in the structure and petrophysical nature of the basement and lower crust on the Norwegian margin inferred from ocean-bottom seismometer experiments and seismic refraction datasets (Mjelde *et al.* 2003b; Mjelde *et al.* 2005). They have also been identified on regional potential field datasets (Doré *et al.* 1997b) and in multichannel seismic data (Ren *et al.* 2003; Tsikalas *et al.* 2008). These features are observed along the length of the margin, associated with the termination and offsetting of structural highs and depocentres, changes in fault orientation and may have acted as lateral barriers to fault propagation (Tsikalas *et al.* 2001; Mjelde *et al.* 2003b). The fact that the Jan Mayen and Bivrost Lineaments define the northern and southern limits of the Vøring Basin implies these features are tectonically significant. However, the Jan Mayen Lineament does not correspond with changes in the petrophysical nature of the crust nor crustal configuration and has been more recently inferred as a broad accommodation zone (c.f. McClay *et al.* 2002; Gomez *et al.* 2004). This is in contrast to the Bivrost Lineament, defined as a pronounced boundary with major changes in crustal structure and associated sinistral (Tsikalas *et al.* 2008) or dextral (Doré *et al.* 1999; Brekke 2000) strike-slip movements between the Vøring and Lofoten Margins. These different processes have tentatively been suggested as a reason as to why the Jan Mayen Lineament has an associated fracture zone within the adjacent oceanic crust whereas the Bivrost Lineament does not (Ebbing *et al.* 2006).

Apart from the aforementioned Jan Mayen Lineament and Bivrost Lineament, the Vøring Basin is proposed to be segmented by two other lineaments, the Gleipne and Surt Lineaments proposed by Fichler *et al.* (1999) and Blystad *et al.* (1995) respectively, the latter of which is the subject of focus for this study. A new lineament was more recently defined by Mjelde *et al.* (2005), lineament L, at the south-western limit of the so-called Lower Crustal Body (LCB) which lies beneath the northern Vøring Basin.

The LCB is a high velocity, high density body at the base of the crust detected by ocean-bottom seismometer experiments (e.g. Mjelde *et al.* 2002) the nature of which has been the focus for intense discussion and debate. Magmatic underplating (Skogseid *et al.* 1992; Mjelde *et al.* 1997; 2001; 2002; Raum *et al.* 2002; Torne *et al.* 2003), serpentinisation of the mantle and metamorphic core complex formation (Ren *et al.* 1998; Osmundsen & Ebbing 2008) or retrograde and high grade metamorphic rocks associated with the Caledonian orogenic root (Gernigon *et al.* 2003; 2004; Ebbing *et al.* 2006; Gernigon *et al.* 2006; Fjeldskaar *et al.* 2009) have all been proposed as possible origins for the LCB. Each of these hypotheses are inferred to have a differing influence upon the upper crustal evolution of the Norwegian margin and impact upon volcanic margin rift models (e.g. Bjørnseth *et al.* 1997; Roberts *et al.* 1997; Mjelde *et al.* 2007; Osmundsen & Ebbing 2008). For example, uplift in the latest Cretaceous – Paleocene has been inferred to occur along the margin due to magmatic underplating (e.g. Skogseid *et al.* 1992). However, other uplift related processes cannot be ruled out which occur on local and regional scales such as faulting (pure or simple shear of the crust; McKenzie 1978; Wernicke 1985), elastic/isostatic response to faulting, footwall collapse, local sediment loading and compaction as well as changes in eustatic sea level leading to erosion of structural highs (Gabrielsen *et al.* 2005). Equally, the influence of older rift systems upon later basin subsidence and uplift (which are recognised upon the inboard region of the margin; Fig. 4.01) have been inferred to exist beneath the outer Vøring Basin (Brekke 2000) but little evidence has been cited for this (e.g. Færseth & Lien 2002). However, Oligo-Miocene domes which are frequently observed within the Vøring Basin (Fig. 4.01) have at least in part been inferred as being related to inversion and buttressing against pre-existing deeper crustal structures at depth (Doré *et al.* 2008). The dominant north-south orientation of the domes in the Vøring Basin (Fig. 4.01) implies this may be influenced by the commonly north-south oriented Jurassic rifts as expressed elsewhere on the NW European Continental Shelf (e.g. Doré & Gage 1987; Doré 1991; Doré *et al.* 2008).

Many of the rift-oblique lineaments on the continental shelf were previously believed to be associated with oceanic fracture zones but newly compiled aeromagnetic data demonstrates the oceanic counterparts do not exist (Tsikalas *et al.* 2002; Ebbing *et al.* 2006; Olesen *et al.* 2007). The origin of the lineaments is difficult to trace but have commonly been correlated to Precambrian structures with a similar orientation onshore Scandinavia (Blystad *et al.* 1995; Doré *et al.* 1997b; Fichler *et al.* 1999; Eldholm *et al.* 2002; Ebbing *et al.* 2006). These features are not unique to the NE Atlantic Margin (e.g. Rumph *et al.* 1993; Doré *et al.* 1997b; McGrane *et al.* 2001; Kimbell *et al.* 2005; Wilson *et al.* 2006; Moy & Imber 2009; Chapter 3) and are commonly displayed on a variety of passive margins worldwide (e.g. Lister *et al.* 1991; Harrowfield & Keep 2005; Fournier *et al.* 2007; Franke *et al.* 2007); however, the structure and importance of these features is not well constrained despite their inferred significance prior to passive margin formation.

4.3.1 The northern Vøring Basin

The outer Vøring Basin is characterised by NW-SE oriented extension during the Late Cretaceous – Paleocene resulting in a c. 150 km wide rift zone (Morton *et al.* 2005).

A definitive age for the timing of rifting in the outer Vøring Basin is difficult with wide ranging interpretations being made. Færseth & Lien (2002) and Gernigon *et al.* (2003) infer a Campanian – Paleocene rift episode however other authors have suggested rifting commenced during the Cenomanian (Bjørnseth *et al.* 1997; Brekke 2000), Maastrichtian (Lundin & Doré 1997; Ren *et al.* 1998; Skogseid *et al.* 2000) or even Paleocene (Roberts *et al.* 1997; Walker *et al.* 1997). The range of interpretations for rift initiation has been caused by a lack of released well data in the northern Vøring Basin at the time of publication which resulted in the tying of the available 2D seismic data across vast distances and fault systems to wells located more inboard upon the margin. This issue is still currently experienced in offshore Norway, with the base Cretaceous horizon not constrained by well data to the west of the Halten and Dønna Terraces, where two prominent unconformities are mapped (J. Bjørgan Kristensen, StatoilHydro, pers. comm.). This limitation of the dataset is considered very important for the purposes of this study, but is minimised by using the available well data in the region as well as high-resolution 3D seismic data to conduct the investigation. This is further constrained by regional 2D seismic data which allows for the 3D analysis to be set within a wider regional context.

The stratigraphical fill of the basin varies greatly through time (Chapter 5). The Nise Sandstone Member is easily identifiable due it being expressed as a high-amplitude, parallel package on seismic data. This unit was deposited as an up to 1 km thick marine fan sandstone package in the Campanian (Kittilsen *et al.* 1999). The Maastrichtian is also a marine basin slope and floor fan sequence which gives way to a shallow marine environment in the Paleocene prior to continental breakup.

The area affected by Late Cretaceous – Paleocene rifting is located at the north-western edge of the non-faulted, NE-SW trending Cretaceous – Paleocene Någrind and Vigrid Synclines (Fig. 4.02a; Blystad *et al.* 1995). The Nyk High and Gjallar Ridge are located at the edge of the synclines respectively and are prominent structural highs in a NE-SW orientation. The Gjallar Ridge consists of deeply-eroded rotated fault blocks with a westward dip, mainly involving the pre-Cenozoic sequences (Blystad *et al.* 1995). Formed during the Late Cretaceous, some authors have inferred rifting continued into the Early Paleocene (e.g. Corfield *et al.* 2004), by which time erosion of the syn-rift strata is evident. This erosion and removal of inferred syn-rift strata is a notable limitation of the dataset for the calculation of strain within the adjacent rift segments. This will lead to a possible underestimation of fault heaves/throws but is considered an important discussion point surrounding the evolution of fault domain boundaries. The Nyk High is defined at Upper Cretaceous levels, extending ~ 75 km along strike, 15 - 20 km wide; with steep north-westerly dipping faults present with a thin Cenozoic cover sequence (Blystad *et al.* 1995). The structure is believed to have formed synchronously with the Gjallar Ridge. The Nyk High and Gjallar Ridge are separated from the Hel and Fenris Grabens respectively to the northwest by major NE-SW trending, north-westerly dipping set of normal faults. The Hel Graben is believed to contain ~ 4 km of Late Cretaceous – Paleocene syn-rift sediments (Walker *et al.* 1997). The Fenris Graben is largely covered by Paleocene – Eocene volcanic units (Planke *et al.* 2000) but is expected to contain similar age strata. However, as with the Vigrid and Någrind Synclines, a lack of faulting is recorded in direct comparison to the faulted, yet structurally higher Gjallar Ridge and Nyk High.

The Gjallar Ridge and Nyk High terminate, respectively to the northeast and southwest at the Rym Accommodation Zone (RAZ; Fig. 4.02a). Previously identified as the Rym Fault Zone, it contains north-westerly dipping faults with a NE-SW trend in the southern region of the zone which rotate clockwise through to more north-south trends (Blystad *et al.* 1995; Brekke 2000). Ren *et al.* (2003) reaffirmed this interpretation, recognising the faults of the Nyk High upon entering the RAZ altered dramatically from the dominant NE-SW orientation through to east-west and NNE-SSW orientations.

The fault zone was initially considered part of the NW-SE trending Surt Lineament, with the change in fault orientations linked to a structural feature in the basement which was identifiable as a low in gravimetric data (Blystad *et al.* 1995; Doré *et al.* 1997b; Fig. 4.01). To the south of the RAZ, the Surt Lineament was inferred to act as a tectonic hinge due to thickening of Upper Cretaceous reflectors from south to north across the feature between the Vigrid and Någrind Synclines (Blystad *et al.* 1995; Brekke 2000). However a more recent interpretation of gravity, magnetic and seismic data by Ren *et al.* (2003) did not support the existence of a deep crustal lineament extending across the outer Vøring Basin. This led the authors to separate the RAZ, which can be mapped using seismic data, from the Surt Lineament for which no evidence could be cited for its existence. This conclusion is similar to a set of rift-oblique lineaments recognised from potential field data analysed elsewhere upon the NE Atlantic Margin, in the Faroe-Shetland Basin (Moy & Imber 2009; Chapter 3). The results of that study concluded a lack of seismic evidence for the presence and influence of the lineaments within the upper crustal structure of the basin, although a deep seated basement origin could not be ruled out.

Mjelde *et al.* (2003b; 2005) using seismic refraction datasets modified the orientation of the Surt Lineament to a north-south orientation on the basis of changes across the lineament in the upper and lower crustal structure (Fig 4.01; Alt. Surt Lineament). Mogensen *et al.* (2000) suggested the Surt Lineament is a NNW-SSE oriented feature based upon the interpretation of multi-channel seismic data. This has subsequently led to a range of orientations for the lineament in the literature, however it appears the north-south orientation is now preferred (e.g. Ebbing *et al.* 2006), but it remains unclear whether one or more lineaments exist in the region. A deep crustal link has also been proposed between the Surt Lineament and growth of the Cenozoic Vema Dome along the north-south version (Mjelde *et al.* 2005; Fig. 4.01). Both versions of the Surt Lineament are believed to have influenced the magmatic intrusion of the crust, with an associated reduction across the feature to the northeast in both the upper and lower crustal levels (Mjelde *et al.* 1998; Brekke 2000; Mjelde *et al.* 2003b; Mjelde *et al.* 2005).

Ren *et al.* (2003) defined the RAZ as an accommodation zone from a stratigraphic and structural analysis of regional 2D seismic data using the terminology of Rosendahl (1987) based upon the East African Rift. Accommodation zones were described by Rosendahl (1987) as areas of fault dip-reversal in normal fault systems and recognised that the geometry of accommodation zones was largely dependent on the extent of overlap between the normal fault systems. The confusing terms of ‘low’ and ‘high’ relief accommodation zones were used in the study despite each of the accommodation zones being elevated relative to the adjacent depocentres in the study (Faulds & Varga 1998). The primary difference between the types of accommodation zone was the polarity of the overlapping fault systems, dipping either towards (low relief) or away (high relief) from each other (Rosendahl 1987, fig 6, p469-470). However, despite the confusing use of terminology, the models of Rosendahl (1987) are considered integral in the definition of an accommodation zone in this study (Faulds & Varga 1998). Ren *et al.* (2003) correctly utilised these terms in specific areas between the rift segments, which when considered as a whole system, resulted in the definition of a rift wide accommodation zone. Curiously, Ren *et al.* (2003) and other authors (Mogensen *et al.* 2000; Imber *et al.* 2005) have inferred the RAZ to accommodate Cenozoic strike-slip movements which are not typically attributable to accommodation zones (Faulds & Varga 1998). Often indications of the stress rotation within accommodation zones are displayed upon conceptual models (e.g.

Nelson *et al.* 1992, fig 6, p1165) but there is little evidence of strike-slip activity associated within accommodation zones from field based observations in the Basin and Range province (Faulds & Varga 1998). Therefore, with strike-slip movements inferred within the accommodation zone (Blystad *et al.* 1995; Ren *et al.* 2003), this brings into question the accommodation zone interpretation, and whether the faults upon which the movements acted upon are akin to breaching relay-ramp style faults or transfer fault structures.

This study aims to address the differences between the RAZ and the NW-SE Surt Lineament utilising a regional 2D seismic dataset which is tied to well data points. This is critical in defining the bounding limits of the Late Cretaceous – Paleocene rifted region as fault domain boundaries do not extend beyond the rift limits (Faulds & Varga 1998) and therefore would need to be either included or excluded from the strain analysis. Equally, the study needs to constrain the influence of pre-existing crustal structure prior to the Late Cretaceous – Paleocene rift phase which can be assessed from the results of previous deep crustal studies upon the Norwegian continental margin as well as from recently acquired deep seismic reflection lines in the region. This will give an improved understanding as to the impact of variations in the deep crustal structure has upon the formation of fault domain boundaries and in turn the adjacent rift segments. From this, high resolution 3D seismic data, when correlated with well data points located within each of the rift segments and within the fault domain boundary, allows for the spatial mapping of structural features and their associated deformational styles, as well as the temporal evolution of the fault domains. Strain variations in space and time can then be constrained and used to provide insights into how strain is transferred across fault domain boundaries within widely segmented rift systems; these observations may be directly applicable to other rift basins and passive margins worldwide.

4.4 Dataset and methodology

4.4.1 Seismic Data

A suite of 2D seismic data was used to understand the large scale geometry and evolution of the northern Vøring Basin (Fig. 4.02b). The lines were selected from a variety of surveys primarily for their coverage and data quality, having been time processed by their respective owners; NGI-98 (TGSNopec); GVN-92 (WesternGeco); VB-86, VB-87, VB-89, VB-90 (reprocessed in 1994 by Fugro Multi Client Services for the Norwegian Petroleum Directorate) and GVF2000R, MNR04, MNR07 (Fugro Multi Client Services). These lines allow for a more complete imaging and regional understanding of the Hel and Fenris Grabens, Någrind and Vigrid Synclines, the Surt Lineament and the Vøring Escarpment close to the Continent-Ocean transition (Mjelde *et al.* 2007). Contoured time-structure maps were also created from interpretation of the 2D seismic data; the parameters used are detailed in Appendix C.01.

Two 3D seismic datasets were used in the study. The Gjallar Ridge 3D time migrated seismic survey is composed of three individual seismic datasets which have been merged into a single dataset covering an area ~ 6000 km^2 with 25 m line spacing above the Vigrid Syncline, Gjallar Ridge and Fenris Graben (Fig. 4.02). The three seismic surveys used within the dataset are GRE02 (shot by TGSNopec) in the southeast, SG9604 (shot for Saga Petroleum by WesternGeco) in the west and ST0410 (shot for Statoil by PGS Geophysical) to the northeast. The seismic data are of excellent quality, imaging the Late Cretaceous to Neogene (Santonian to Pleistocene) succession clearly except in the close vicinity of, and below high amplitude volcanic units. These features attenuate and scatter the seismic wavelet, absorbing the higher frequencies and reducing the resolution of the sub-igneous reflections (e.g. Planke & Eldholm 1994; Gallagher & Dromgoole 2007).

A second 3D time migrated seismic dataset was made available by StatoilHydro to analyse the structural evolution of the Någrind Syncline, Nyk High, Vema Dome and the Hel Graben (Fig. 4.02). The dataset covers an area of ~ 3200 km^2 with 25 m line spacing and has been formed from the merging of two 3D seismic surveys shot by WesternGeco and PGS Geophysical for Statoil and BP respectively (ST9603R99 above the Vema Dome to the west and BPN9601 above the Nyk High to the east). Seismic resolution differs dramatically between the two surveys due to remobilisation of low density Oligo-Miocene siliceous ooze-related diapirs and sills (Hjelstuen *et al.* 1997; Hovland *et al.* 1998; Berndt *et al.* 2000) which scatter and absorb the seismic energy giving rise to poor imaging of the deeper succession. Seismic data over the Nyk High are good, successfully imaging the Late Cretaceous through to recent (Campanian to Pliocene) succession. However, an analysis of resolvable fault throws (Fig. 4.03) highlights that the Nyk High 3D seismic dataset is of a lesser effective resolution to that shot over the Gjallar Ridge. Within the dataset, poor processing of the data has led to remnant geophysical artefacts within the final seismic volume, illustrated in Appendix C.02.

4.4.2 Well data

Cretaceous seismic picks were provided by StatoilHydro which have been tied back to three exploration wells in the study area by means of a checkshot survey and formation of synthetic seismic traces in each of the wells (Appendix C.03-05); 6704/12-1 on the Gjallar Ridge, 6706/11-1 drilled upon the Vema Dome in the RAZ and 6707/10-1 on the southernmost footwall of the Nyk High (Fig. 4.02). These wells have also been used as a guide for depth conversion of the seismic data in respect to individual geological areas. From velocity calculations for the Campanian – Maastrichtian interval in each of the wells, 1 sec TWT correlates with 1600 m vertical depth in the Gjallar Ridge, 1300 m in the Nyk High and 1100 m in the southern RAZ (Appendix C.06). Within the adjacent regions, velocities have been assumed to be 3000 ms^{-1} due to the amount of volcanic material highlighted by high amplitude reflectors interpreted as sills (Berndt *et al.* 2000; Appendix C.06).

4.4.3 Horizon interpretation

Mapping has been focussed upon maximum flooding surfaces which are dated by Henriksen *et al.* (2005). Four seismic marker horizons were used in the study: KCaMFS115 (top Middle Campanian horizon marking the top of the Nise Sandstone Member within the initial rift sequence); KCaMFS118 (top Campanian near the base of the main syn-rift megasequence); Top Cretaceous (a major erosional unconformity marking the cessation of the main phase of rifting) and Top Paleocene (unconformity formed following the third and final phase of rifting). Each of these horizons can be mapped across the each of the seismic datasets in the vicinity of the RAZ except for the KCaMFS115 and KCaMFS118 horizons which are locally eroded by the Top Cretaceous Unconformity in the transition between the Late Cretaceous Nyk High and the Oligo-Miocene Vema Dome.

Other horizons mapped in the north of the Gjallar 3D seismic dataset were: KCoMFS100 (top of the Coniacian and tied to wells inboard of the Vigrid Syncline by 2D seismic data); KCaMFS113 (top of the Santonian and tied to well 6704/12-1); KMaMFS123 (top of the Early Maastrichtian within the main syn-rift sequence); KMaUnc (a local erosional unconformity within the Late Maastrichtian); a selection of intra-Paleocene horizons and unconformities; top Eocene; intra-Oligocene; top Oligocene (base of the Miocene siliceous ooze); Opal A-CT; top Ooze; near top Miocene; base Quaternary and the seabed which have been illustrated upon the interpreted cross sections. These were not interpreted elsewhere as they were thin or absent within the other 2D and 3D seismic surveys. Horizons interpreted within the seismic survey over the Nyk High and Vema

Dome and illustrated upon example cross sections are: KCoMFS97 (for the purpose of this study is the near top Coniacian horizon, but is the top Middle Coniacian and is the top of the Lysing Sandstone Member); KMaMFS122 & KMaMFS123 (intra and top Early Maastrichtian horizons respectively within the main syn-rift sequence); top Eocene; top Oligocene; a suite of intra-Miocene horizons; base Quaternary and the seabed. Uncertainty remains as to the exact age of Cretaceous horizons mapped particularly in the Fenris and Hel Grabens, due to major normal fault systems and Paleocene intrusives between these and the drilled structural highs, resulting in possible interpretation mispicks in the order of tens of milliseconds in the Fenris Graben, or hundreds of milliseconds in the Hel Graben. Improvements are made in interpretation uncertainty within 3D seismic data over 2D seismic data as horizons can be mapped along relay ramps rather than jump correlated across major faults into the grabens. However, this is still difficult to complete in a tectonically complex region with little well control. An added difficulty within the Gjallar Ridge is correlating away from well 6704/12-1 drilled upon a greatly rotated fault block resulting in differing ages assigned to each of the reflectors (M. Seger, A/S Norske Shell, Pers. Comm.).

4.4.4 Fault analysis

A cumulative heave analysis was conducted upon the Gjallar Ridge, Nyk High and across the fault system of the southern RAZ. Heaves were calculated between the hangingwall and footwall intersections of the pre-rift sequence as despite erosion of the syn-rift strata in areas, this would not affect the calculations as to how much extension had been accommodated across each fault system. The only time when heaves would be underestimated is if the pre-rift sequence was eroded in close proximity to the fault, however the seismic lines selected for the analysis had experienced little or no erosion of the pre-rift succession (Appendix C.07).

Fault interpretations were made in Landmark Seisworks software every 10 inlines or 250 m across the northern region of the imaged Gjallar Ridge into the RAZ. Fault interpretation was also conducted along crosslines to aid the identification of transfer faults, a critically important feature to identify within the 3D seismic dataset. Similarly, every 10 lines or 250 m were interpreted across the Nyk High and Vema Dome in a NNW-SSE orientation, oblique to the various structural trends observed in this area (Fig. 4.02). The fault sticks, raw horizon grids and 3D seismic data were then imported into Badleys TrapTester^{TM} Software. Fault correlations were performed in TrapTester with reference to the 3D seismic data and coupled with the horizon grids and dip maps (Appendix C.08) to create Late Cretaceous to Paleocene structural models of the faulted highs (Appendix C.09-11).

An analysis of fault heaves perpendicular to the dominant strike of the fault populations allows for an assessment of strain variation (and therefore stretching factors) along strike. Upon the Gjallar Ridge, fixed length sample lines were in a NW-SE (310°) orientation. However due to the rotation of faults from dominant NE-SW orientation in the Nyk High to more E-W and NW-SE faults to the west, two sets of sample lines were used, NW-SE (330° across the Nyk High) and NNE-SSW (010° across the Oligo-Miocene Vema Dome). Sample lines have 1 km spacing. More detailed information for this process is given in Appendix C.12-13.

Key horizons for fault analyses were selected based upon their close temporal relation to key rift events in the region: offsets across KCaMFS115 would quantify the amount of Campanian and earlier rifting; KCaMFS118 would form a marker horizon for the major Maastrichtian rifting; the top Cretaceous would act as a marker horizon for any faulting associated with Paleocene rifting (or thermal subsidence in the region of the Gjallar Ridge). To remove the possible effect of fault reactivations under post-rift conditions the top Paleocene horizon was used which marks the cessation of rifting in this region. Using the fault heaves, extensional strain can be quantified and mapped through time across the survey area. Fault heaves calculated from the latter rift events and those due to post-rift thermal subsidence or differential compaction effects which can be seen to reactivate the pre-existing normal faults, were subtracted from the earlier rift event analyses allowing for accurate strain factors to be ascertained for each of the main rift events that affected the region. A series of assumptions are made when conducting a strain analysis within a rift system. The first underlying assumption is that no previous extension or compressional events have occurred in the region prior to the oldest age which is quantified. This is obviously not the case upon the Norwegian continental margin, and is unclear whether the faults are reactivating pre-existing features at depth. Secondly, strain analyses are possible using multiple methods. For ease, and to avoid errors associated with the depth conversion of seismic data, fault heaves have been selected for the analysis. However, if faults are backward rotated since their formation, any sort of strain calculation will have a large degree of error involved. Thirdly, all calculated strain is assumed to be accommodated by seismically resolvable faulting rather than through sub-seismic scale faulting, folding or rotation of horizons, nor is strain calculated upon spatially aliased faults. Fourthly, the strain analysis does not account for whole lithosphere extension which may be depth-dependent and variable through time (Kusznir *et al.* 2005). Finally, the strain analysis is only performed across the entire rift segment in areas of 3D seismic data coverage and well control as this would otherwise increase the error in any calculation greatly. An important limitation for the strain analysis of the rift segments was the impact of erosion removing evidence of the later rift events. If this occurs, the removal of fault heaves from the earlier rift events is not possible resulting in an overestimation of strain for the earlier rift stages, and an underestimation for the later rift events. Other limitations include the resolution of the seismic data, amount of well control and interpreter error which although are important factors, have been attempted to be minimised using the techniques outlined above.

4.5 Tectonic elements of the northern Vøring Basin

4.5.1 Gjallar Ridge and Nyk High fault domains

The en-echelon arrangement of the Gjallar Ridge and Nyk High results in structurally high regions being set against structurally low regions (Fig. 4.04). The relative amounts of relief between the two segments vary through time due to different timings and styles of deformation, as well as the relative vertical movements experienced in each element of the rift segment. For example, the Gjallar Ridge is directly adjacent to the Hel Graben, the Nyk High to the Vigrid Syncline and between each of these the Hel Graben is adjacent to the Vigrid Syncline (Fig. 4.02). The transition zone between each of these rift elements for the purposes of this study form the Rym Accommodation Zone, and as such the RAZ is divided into the northern, southern and central regions respectively. The transition between the Vigrid and Någrind Synclines has previously been defined by the Surt Lineament (Blystad *et al.* 1995). The region between the Fenris and Hel Grabens is a possible north-westerly continuation of the RAZ. However this structure is not currently resolvable due to the outbuilding of basalt flows associated with the Vøring Marginal High and the consequent problems with seismic imaging (Fig. 4.02; Skogseid *et al.* 1992).

The two rift segments superficially display very similar structural styles (Fig. 4.05). Each of the two structural highs is formed upon the north-westerly flank of the Vigrid and Någrind Synclines respectively. Similarly, the Gjallar Ridge and Nyk High are separated from the Fenris and Hel Graben respectively by major northwest dipping normal faults with throws greater than 1 sec TWT. The Vigrid and Någrind Synclines display a very similar unfaulted structure, yet the southern continuation of the Oligo-Miocene Vema Dome has led to the Vigrid Syncline to appear as an anticlinal fold in Figure 4.05. Cretaceous and Paleocene sediment thickness is greatest towards the centre of the synclines implying the synclines were continuing to develop during this time, relative subsidence apparently ceasing prior to the deposition of sediment during the Eocene. The Late Cretaceous strata thin upon the northwest flanks of each syncline, particularly so in the Vigrid Syncline. Truncation of the Maastrichtian sequence is witnessed prior to the deposition of the Paleocene sequence forming the top Cretaceous unconformity; this is particularly evident above the Gjallar Ridge (Fig. 4.05c & d).

Within the Gjallar Ridge, the Maastrichtian sediment is thicker than on the north-westernmost flank of the Vigrid Syncline, apparently caused by increased accommodation space formed through active normal faulting at the time. Faults predominantly dip to the northwest at angles ~ 20°. The Nyk High has a thicker Maastrichtian sequence which, unlike the Gjallar Ridge, is up to 1 sec TWT thick on the northwest flank of the Någrind Syncline. Variation in the thickness of the Maastrichtian sequence within the Nyk High ties directly with the horsts and graben structures which are formed between the more steeply dipping faults (~ 50 - 60°) observed here than upon the Gjallar Ridge. In contrast to the Gjallar Ridge, these faults do not tip out at the top Cretaceous unconformity, but appear to continue into the Paleocene and later Cenozoic cover sequence. Variations in the thickness of the Paleocene sequence similarly relate to the gross tectonic structure leading to the inference that this too was a period of rifting. This rift event is not recognised upon the Gjallar Ridge, although any evidence of an Early Paleocene rift event *may* have been subsequently eroded. Therefore, it can be conclusively recognised that the RAZ as a fault domain boundary can separate rift systems with very different structural styles and kinematics. Little can be ascertained regarding the Fenris Graben to the northwest of the

Gjallar Ridge due to a significant drop in the resolution of the seismic data beneath the Paleocene volcanic inner flows and Vøring Marginal High. Although by direct analogy it may be similar to the Hel Graben (e.g. the similarities between the Vigrid and Någrind Synclines) the thickness of Late Cretaceous and Paleocene stratigraphical fill may vary significantly between the Fenris Graben and Hel Graben. This is particularly well displayed on the results of the regional mapping of the Cretaceous horizons (Fig. 4.04) as the Fenris Graben is of structurally greater relief than the major Hel Graben depocentre to the northeast.

4.5.2 Hel Graben

The Hel Graben is located to the northwest and northeast of the Nyk High and RAZ respectively (Fig. 4.02). During the Late Cretaceous, the Hel Graben increased in structural prominence forming a depocentre into which over 1.7 sec TWT of Maastrichtian sediment was deposited (Figs 4.05 and 4.06). Due to intensive intrusive igneous activity during the Paleocene and earliest Eocene (Hansen 2006), much of the deeper structure (Campanian and older) of the Hel Graben is poorly defined on regional 2D seismic datasets (Figs 4.05a and 4.05b). Despite this, the interpreted sills have been utilised to aid in the picking of key horizons after making the assumption that sills have intruded laterally along bedding planes and migrated steeply up dip cross cutting the horizons via non-imaged fault planes (e.g. Thomson 2007). In the shallow section, this assumption appears to be valid particularly within the Maastrichtian section where the dip of sub-sill horizons can be mapped and shown to be parallel to the overlying intrusives (Fig. 4.06d). The Hel Graben has further been partially inverted to form the broadly N-S trending Naglfar Dome, inferred to be Early Miocene in age by the observed thinning of the strata across it.

The base of the KCaMFS115 sequence is particularly difficult to map upon the regional 2D seismic lines and has not been interpreted in Figure 4.06. This displays the difficulty in assessing where the Nise Sandstone Member is of greatest thickness. However the overlying KCaMFS118 sequence broadly thickens into the Hel Graben suggesting this was the primary depocentre at the time. In the northwest of the Hel Graben, shallowly northwest dipping normal faults (~ 15°) within the Campanian sequences are speculatively interpreted based upon the offsetting and climbing of igneous sills in this area (Fig. 4.06d). Mapping of the KCaMFS118 package in this area is very speculative but may display thickening of the sequence adjacent to the faults. These two features of the rotated fault blocks in the Hel Graben are similar to the characteristics displayed by the Gjallar Ridge (note the onlap of the Maastrichtian sequence against the ridge to the southeast; Fig. 4.06c); this may therefore be an along strike continuation of the Gjallar Ridge in the Hel Graben.

The increased thickness of Late Cretaceous strata to the southeast of the inferred Gjallar Ridge is similar to the structure of the Någrind Syncline (Fig. 4.05). Despite faulting at the south-eastern boundary of the Hel Graben, this does not appear to be the primary control on the depocentre in the Late Cretaceous, with the greatest thickness of Late Campanian and Maastrichtian strata positioned away from the flanks and directed towards the centre of the syncline (graben). This central zone of the syncline fails to display any evidence of normal faulting and is similar to the gross structure displayed to the Någrind Syncline to the south (Fig. 4.05d). An alternative hypothesis therefore is that this succession accumulated due to post-rift thermal subsidence across an earlier Campanian and/or Jurassic rift which is not well imaged, implied by the 'steers head' (McKenzie 1978) geometry of the Maastrichtian sequence. This is despite Maastrichtian rifting upon the Nyk High and relatively minor faulting above the inferred Gjallar Ridge at depth to the northwest. There is little evidence of major reactivation of the Campanian faults with subtle thickening of the Maastrichtian sequence in the fault hangingwalls in close proximity to the RAZ (Fig. 4.06c). Along strike the faults reverse polarity (Fig. 4.06d) and appear to detach upon but fail to reactivate the Campanian faults at depth.

The Hel Graben remained a depocentre during the Paleocene where up to 700 ms TWT of sediments were deposited thinning to ~ 150 ms TWT at the margins. Reactivation of the generally east-west trending Maastrichtian age faults in the north of the Hel Graben (Figs 4.02a and 4.06d) occurs with notable thickness changes of the sediment across the faults, but apart from these, there is remarkably little faulting elsewhere. Minor small-scale faults are present towards the crest of the Naglfar Dome but their frequency and failure to detach at great depths suggests they are not directly related to rifting in the Vøring Basin. During this time igneous material (e.g. Planke *et al.* 2000) was emplaced within the Hel Graben as a suite of intrusive sills and dykes, and towards the eventual continental boundary (Fig. 4.02a) as a lava delta formed of submarine hyaloclastites and sub-aerial flows. This influences the resolution of the seismic dataset making interpretation of the earlier sequences difficult, but the interpreted horizons are expected to continue beneath these up to 700 ms TWT thick extrusives (Fig. 4.06).

Previous authors (e.g. Brekke *et al.* 1999; Mjelde *et al.* 2007) have inferred the Vøring Escarpment to be faulted due to the steep dip which is directly comparable to that of the Paleocene faults. There is no evidence from this study to suggest that the escarpment is faulted as there is no Paleocene syn-tectonic thickening and believe this gradient change represents the slope section of the outbuilding flows as illustrated by Planke *et al.* (2000). The visible high gradient of the escarpment may be an artefact due to the difference in velocities between the adjacent volcanic and sedimentary rocks within time-migrated seismic datasets (L. Gernigon, NGU, pers. comm.).

4.5.3 Rym Accommodation Zone

The transition from the Gjallar Ridge and Nyk High into the RAZ varies dramatically along the strike of the feature, as does the nature of the zone itself (Fig 4.07). At the north-eastern edge of the Gjallar Ridge, a northeast dipping normal fault has formed along the boundary of the northern RAZ. Due to the Paleocene age inner flows (Planke *et al.* 2000), it is unclear whether other similar faults are formed within the northern RAZ, but on the basis of tying regional mapping between the Gjallar Ridge and the Hel Graben, a second fault is inferred (dashed in Figure 4.07c). Paleocene sills may also give support for the interpretation of a second north-easterly dipping fault as the sills stop abruptly in an area which the faults down dip projection is inferred. It has to be stressed that this second fault is speculative as mapping of the top Campanian sequence which it apparently offsets is particularly difficult. However, both faults appear to have been active during the Maastrichtian with associated thickness changes observed from upon the Gjallar Ridge 'footwall', into the Hel Graben and northern RAZ 'hangingwall'.

Along strike to the southeast within the central RAZ there is little or no evidence of the aforementioned northeast dipping faults. A fault could be interpreted but this is a tentative interpretation (Fig. 4.07d). This may be an along strike continuation of a NW-SE trending fault (Fig. 4.07c) within the Maastrichtian sequence but can not be corroborated at depth due to the thick sills in the area. Instead, a gentle ramp structure dipping (~ 5°) to the northeast is observed. The ramp structure between the Vigrid Syncline and Hel Graben in the central RAZ was of increased prominence during the Campanian (Fig. 4.04) implying it was predominantly active at the time. Figure 4.07d confirms this as the Late Campanian sequence thins and onlaps onto KCaMFS115 horizon. Although the Maastrichtian sequence is heavily intruded by sills at its base, the sequence similarly thins above the ramp, akin to the tectonic hinge described for the Surt Lineament by Blystad *et* *al.* (1995) and Brekke (2000). During the Paleocene, the ramp is less prominent (Fig. 4.04c) yet thinning and downlap of the sequence onto the top Cretaceous unconformity is recognised onto the ramp structure suggesting the Hel Graben was uplifted later in the Cenozoic (Fig. 4.07d). Therefore the RAZ displays characteristics which are both common to the transfer zone fault domain boundary (rift-oblique faulting) as well as a major ramp structure which is readily identifiable within accommodation zones.

4.5.4 Surt Lineament

The Surt Lineament is located between the largely unfaulted Vigrid and Någrind Synclines, therefore any change in sediment thickness across the inferred lineament is expected to be passive and not fault controlled. Blystad *et al.* (1995) and Brekke (2000) inferred a major tectonic hinge across the NW-SE extension of the lineament. Analysis of the seismic data available to this study suggests there is very little evidence within the upper crust to support the existence of the Surt Lineament with the only notable variation in stratigraphical thickness of the Late Campanian sequence, up to 1.5 sec TWT thick within the Någrind Syncline, reducing to 0.5 sec TWT across the Surt Lineament into the Vigrid Syncline (Fig. 4.08). This change may be related to differential subsidence of the two adjacent synclines within each rift segment, resulting in a ramp like structure as seen in the central RAZ at the same time. Therefore, a tentative link may be inferred between the methods of passive development of the Hel Graben and Någrind Syncline (e.g. thermal subsidence above an earlier subsiding rift). But, the authors agree with Ren *et al.* (2003) that the NW-SE Surt Lineament is a separate feature to the NW-SE trending RAZ, and is to be considered external to the main Late Cretaceous – Paleocene rift zone, yet the ramp-like structure between the adjoining rift segments may have formed at least in part by the same processes and potentially have the same origin. The finding that variations in the concentration of Paleocene-aged upper crustal sill intrusions vary across the lineament

(Brekke 2000) does also appear valid (note the amount of high amplitude reflectors in the Vigrid Syncline compared to the Någrind Syncline; Figs 4.05 and 4.08) but this can not be linked directly to the development of the Campanian ramp structure. Instead this may be related to a deep crustal control.

The north-south oriented Surt Lineament was originally defined on the basis of deep crustal structure (Mjelde *et al.* 2003b; 2005) and is therefore not expected to be identifiable within seismic reflection data. There is no notable change in the stratigraphical thickness of the sedimentary fill of the Vigrid Syncline except for a thickening of Oligocene strata within a sub-syncline (Fig. 4.08), however this is considered a negligible feature from which a lineament could not be identified. Therefore, the north-south Surt Lineament is considered to be a deeper crustal feature which may not have been directly reactivated during Late Cretaceous – Paleocene rifting in this area.

4.6 Influence of deeper crustal structure on Late Cretaceous – Paleocene tectonics

Two deep crustal features have been identified from this study which may impact upon the upper crustal deformation within each rift segment. Variations between each rift segment may influence the formation of the accommodation zone.

4.6.1 Late Jurassic rift system

Recent 2D seismic data acquired by Fugro Multi Client Services in cooperation with TGSNopec successfully images the deeper structure of the Vøring Basin, the interpretation of which reveals a previously un-proven but inferred (Færseth & Lien 2002; Skilbrei & Olesen 2005) Late Jurassic rift underlying the outer Vøring Basin (Fig. 4.09). The age of rifting is inferred as no wells have penetrated such a deep succession in this area of the basin but has been based upon recognised rift events which have affected the Norwegian continental margin and the trend of the major fault systems (Doré 1991).

Evidence for rifting is through the divergence of stratigraphically older reflectors towards normal faults at depth (Figs 4.09b and 4.09c), evidence of deposition during active extension. This is visible in at least two areas beneath the Late Cretaceous-Paleocene Nyk High and the Oligo-Miocene Vema Dome. The top of the syn-rift sequence is difficult to identify as much depends upon whether the Lower Cretaceous sequence infills a sediment starved Late Jurassic rift or whether rifting continued until this time (see Færseth & Lien 2002). The interpretations presented implies the presence of a Jurassic syn-rift sequence which links chronologically with other Late Jurassic rift systems in NW Europe (e.g. the North Sea and Porcupine Basins; Tate 1993; Roberts *et al.* 1999) in which rifting had concluded by the Early Cretaceous. Yet both interpretations of the deeper rift structure (Figs 4.09b and 4.09c) indicates the Lower Cretaceous sequence to thicken into the easternmost fault system which may be evidence of Neocomian aged NW-SE extension as proposed by Lundin & Doré (1997).

It is unknown whether an underlying Permo-Triassic rift is developed below the Upper Jurassic rift sequence as recognised inboard of the Vøring Basin upon the Halten Terrace and Trøndelag Platform (Fig. 4.01; Blystad *et al.* 1995; Mosar 2000). Parallel reflections are recognised within the inferred pre-rift unit with a high amplitude unconformity at its top, but to avoid speculation the term pre-Jurassic rift sequence has been used. A sill could cause the bright reflectivity, but there is a distinct lack of igneous material within this area (Fig. 4.09). Following the cessation of rifting, a phase of post-rift thermal subsidence is interpreted within the basin. The associated stratal unit, which is up to 3.5 sec TWT thick, displays parallel reflections in a generally low reflectivity sequence in contrast to a moderate Middle Cretaceous rift event with a predicted syn-rift stratal fill as proposed by Lundin and Doré (1997). The Late Cretaceous – Paleocene phase of rifting (as described previously) in the Nyk High does not appear to reactivate the Late Jurassic rift faults. Instead the faults sole out within the Lower-Middle Cretaceous sequence which is an important observation to fully understand the influence of the deeper crustal structure. Deterioration of the seismic data in this area cannot accurately rule out the linkage of the two fault sets, however they are of opposing polarities and the regionally imaged reflectors do not appear to be offset (Fig. 4.09).

Erosion of the Paleocene strata in the vicinity of the Nyk High is illustrated in Figure 4.10. The erosion or non-deposition of Paleocene sediment upon the horsts and at the north-western edge of the Någrind Syncline evident and is probably attributed to dominantly submarine and minor sub-aerial erosion. Within the transition zone between the Nyk High and southern RAZ, a ~ 30 km wide zone exists where Paleocene sediment is very thin (< 50 ms TWT) or absent, notably trending in a N-NNE orientation. This region directly overlies the Jurassic rift system at depth which could be interpreted as having been reactivated under compression in the earliest Cenozoic (an inversion harpoon structure could be interpreted within the Jurassic syn-rift sequence; Fig. 4.09b). Erosion of the overlying Upper Cretaceous and Paleocene strata is estimated to have removed ~ 1 sec TWT of sediment over a region ~ 40 km wide based upon horizon reconstruction. This is comparable with the region which has been eroded or not deposited in Figure 4.10 and may be equivalent to the palaeo-Vema Dome suggested by Hjelstuen *et al.* (1997) of Paleocene age. In this interpretation, it is unclear whether reverse fault reactivation occurred under compression, although buttressing against the bounding faults would cause a similar uplift effect as previously hypothesised by Fichler *et al.* (1999) and Lundin & Doré (2002).

An interpretation of a thinner Late Jurassic syn-rift sequence causes the previously interpreted harpoon structure to be part of the overlying Lower Cretaceous sequence (Fig. 4.09c). If rifting had ceased by the Early Cretaceous, the harpoon could be interpreted as a stratigraphical rather than structural feature, with sediment sourced from the west (Greenland?), infilling a sediment starved Late Jurassic rift (Færseth & Lien 2002). This alternative interpretation however would fail to provide a direct link between the overlying Paleocene erosion and underlying Jurassic rift geometry.

The Vema Dome to the west appears to be the result of Oligo-Miocene compression resulting in the buttressing of the Upper Jurassic strata at depth. Mapping and correlation of the Jurassic faults between seismic lines is difficult to the north. However, based on the N-NNE trend of the Vema Dome (Fig. 4.02a) and the N-NNE zone of Paleocene erosion and/or non-deposition (Fig. 4.10), as well as from the results of other regional studies (e.g. Doré *et al.* 1999) the Jurassic faults are believed to strike in a broad north-south orientation. Similarly, based on 2D regional mapping of the Vøring Basin, a NNE-SSW structural high is recognised at top Cretaceous and top Paleocene levels in the Hel Graben (Figs 4.04c and 4.04d). This too is believed to have formed as an along strike continuation of the uplift and erosion witnessed between the Nyk High and southern RAZ, adding further support for an important uplift event at this time, which particularly affected the Nyk High rift segment. This pre-existing crustal heterogeneity does not align with the NW-SE oriented RAZ but its effects are noticed within both the southern RAZ and the Hel Graben. Equally, it is in the southern RAZ that the faults rotate from the NE-SW trend of the Nyk High clockwise into rift-oblique trends (Ren *et al.* 2003) which may be related to the influence of the Jurassic structure at depth (Fig 4.02a). A significant other alignment with this deep crustal rift structure is the N-S oriented Surt Lineament (Mjelde *et al.* 2003b; 2005) which may be highlighting changes in the deep crustal structure associated with Jurassic rifting.

A mechanism for the mid-Cenozoic uplift is unknown (see Doré *et al.* 2008 and references therein), nor as to the reason why specific faults could be reactivated at different times (Fig. 4.09b). Similarly, a reason for why the Jurassic faults would invert is required. The Jurassic rift resulted in extensive crustal thinning (Skogseid *et al.* 1992) which would then be expected to cool and result in significant strengthening of the lithosphere (van Wijk & Cloetingh 2002). Thus, why would inversion focus in a region of thicker mantle lithosphere and thinner crust which is presumably stronger than non-stretched crust? If the interpretation that the harpoon structure is a stratigraphical feature, this would at least remove the requirement for Paleocene inversion of the Jurassic rift faults (Fig. 4.09c). An alternative explanation to the compressional hypothesis for the Paleocene rift-oblique uplift could be related to a lateral flow of convecting material sourced from the Iceland Plume at the base of the lithosphere. This has been recognised to occur elsewhere upon the NE Atlantic Margin in the Paleocene and resulted in up to 500 m of transient vertical uplift across a region > 80 km wide (Champion *et al.* 2008).

4.6.2 Lower Crustal Body

Ebbing *et al.* (2006) used OBS data available from a range of studies to determine the depth and thickness of the LCB (Fig. 4.11). The three principal hypotheses for the origin of the high density, high velocity body are magmatic underplating, serpentinisation of the mantle and a basement remnant of the Caledonian root (Gernigon *et al.* 2004). If the LCB originated from magmatic underplating of the margin it would have to be Paleocene in age due to the impingement of the Iceland plume at the base of the crust at the time (e.g. Skogseid *et al.* 2000). This proposed emplacement of magmatic material would post date the Late Cretaceous rifting and therefore would not provide any control upon the formation of Late Cretaceous fault domain boundaries. The magma would preferentially infill the relief formed at the base of the crust due to crustal thinning and in turn would structurally uplift those regions due to the replacement of mantle lithosphere by hot, buoyant material sourced from the plume. Although this does appear to occur for the

Gjallar Ridge, there is no apparent influence on the LCB relief caused by crustal thinning in the region of the Nyk High, despite this area being structurally higher than the surrounding region (Fig. 4.05d). Similarly, at top Paleocene levels (Fig. 4.04d), the Gjallar Ridge along with the Hel Graben would be expected to form prominent structural highs to the lower relief Nyk High which is not the case.

A serpentinised mantle hypothesis for the origin of the LCB (e.g. Ren *et al.* 1998) is doubtful as major simple shear upper crustal extension (Wernicke 1985) is not evident implying it is unlikely that seawater could penetrate to the base of the crust and form serpentinite (Boillot *et al.* 1989).

In the study area, the LCB is shallowest towards the centre of the Gjallar Ridge (2.5 – 5 km) and remains of relatively constant depth (5 – 7.5 km) along a NE-SW strike. This parallels the geometry of the Late Cretaceous Gjallar Ridge (Fig. 4.12a), both to the southwest of the RAZ but also to the northeast within the Hel Graben where an interpreted lateral continuation of the Gjallar Ridge may exist (Fig. 4.06). Similarly the relief of the Gjallar Ridge to the southwest mirrors the relative variation in the relief of the LCB (Fig. 4.04; Kjennerud & Vergara 2005; Chapter 5). This link between the relief of the Late Cretaceous structural elements with the depth to the LCB is further recognised at the north-western margin of the Vigrid Syncline where Maastrichtian strata is thin or absent directly above an area of high LCB relief (Fig. 4.05c). Only where Maastrichtian faulting is present within the Gjallar Ridge are thick sedimentary deposits observed, implying that the Gjallar Ridge would have been at or near sea level if Maastrichtian rifting had not occurred. Within the Nyk High, the depth to the LCB is considerably greater when compared to the Gjallar Ridge, deepening significantly towards the Någrind Syncline. This corresponds with an increased thickness of Campanian and Maastrichtian strata upon this rift segment (Fig. 4.05d) which is related to the greater bathymetrical relief at the time and formation of a basin floor marine fan systems in contrast to the slope fan deposits of the Gjallar Ridge (Kittilsen *et al.* 1999; Fjellanger *et al.* 2005; Kjennerud & Vergara 2005; Chapter 5). Notably, the depth to the LCB increases in the vicinity of the Fenris Graben and along strike to the southwest above the Gleipne Lineament (and associated saddle upon the ridge; Gernigon *et al.* 2003) which was tectonically active during the Late Cretaceous (Chapter 5). Each of these relationships suggests the LCB to have been present and forms a key influence upon the northern Vøring Basin during the Late Cretaceous. Yet, there seems to be little direct influence of the LCB depth upon the formation of the RAZ with no notable variation in relief recognised in this region. However, this may not be the primary control upon the formation of the RAZ. Instead the differences in the LCB relief within the two adjacent rift segments as highlighted by the contour spacing may have led to the formation of the fault domain boundary (e.g. Acocella *et al.* 2005; Fig. 4.11). The contours are much closer upon the Gjallar Ridge rift segment than within the Nyk High rift segment, implying the LCB may have in part formed the RAZ due to relative changes in the deep crustal structure either side of the fault domain boundary. In regards to the NW-SE Surt Lineament, a notable increase in the depth of the LCB is clearly recognised which implies the lineament may have a structural expression in the basement as originally inferred by Blystad *et al.* (1995). These relationships between the deep crustal structure and Late Cretaceous tectonic elements would therefore have to assume an older origin than Paleocene magmatic underplating for the LCB which a long-lived basement origin for the LCB (e.g. the remnants of the Caledonian Orogenic root) is the most parsimonious explanation for the LCB.

There is no apparent connection between LCB thickness and the geometry of the overlying Late Cretaceous – Paleocene rift. Faults do not appear to link through to basement at depth (rather detaching on Lower-Middle Cretaceous shales; Fig. 4.09) and are therefore not expected to directly influence the thickness of the LCB through upper crustal thinning. On the contrary, the relief of the LCB is expected to exert a control upon the upper crustal faulting. As the LCB is shallower beneath the Gjallar Ridge, the faults would be expected to detach within a shallower (Lower-Middle Cretaceous) level than beneath the Nyk High where the depth to the top of the LCB (and Lower-Middle Cretaceous levels) is much greater. A further link between upper and lower crustal structure is the inferred dip of the LCB, which is expected to be steeper in the Gjallar Ridge than in the Nyk High (note the spacing of contours). These observations may therefore provide a rationale to explain the contrasting symmetry and difference in fault dips observed within each fault domain.

Magmatic underplating of the crust cannot be fully ruled out and mixed mode models of basement and magmatic material have been proposed (e.g. Raum *et al.* 2006). However, recent modelling of seismic data by Fjeldskaar *et al.* (2009) has concluded that the LCB is not related to magmatic underplating or even to significant sill intrusion which further enhances the conclusions of Gernigon *et al.* (2006). The only major pure shear rifting witnessed in this region of the basin is during the Late Jurassic (Fig. 4.09). This (and any other earlier rift events) would ultimately control the thickness of the LCB if it is formed of a basement root, which is only expected to be tilted by the later dominant depth-dependent rift process (Roberts *et al.* 1997). Although deep seismic lines fail to image the top LCB in the region of the Nyk High and Vema Dome (Fig. 4.09), decreasing thickness of the LCB to the east ties well with the apparent crustal thinning associated with Late Jurassic rifting, and notably this occurs across the north-south oriented Surt Lineament. Depth-dependent stretching as well as the previous major rift events (e.g. Late Jurassic) are therefore inferred to be the main processes of lithosphere thinning which culminated in the formation of the North Atlantic during the Early Cenozoic (Kusznir *et al.* 2005).

4.7 Structural evolution of the Gjallar Ridge

Figure 4.12a displays the gross NE-SW trending structure of the Gjallar Ridge as mapped at the top Cretaceous unconformity. It is structurally highest towards the centre of the ridge (~ 3000 ms) near to where well 6704/12-1 was drilled upon the crest of a rotated fault block and reduces gradually to the southeast over an irregular structural relief, broadly related to the geometry of the fault blocks at depth. The faults display a complex pattern of varying trends which link and overlap in a variety of locations but generally follow a NE-SW orientation. The fault interpretation in Figure 4.12a relates to faults imaged at depth within the Cretaceous succession. These do not offset the top Cretaceous Unconformity but have been added to demonstrate the complex anastomosing fault pattern which characterises the structural high.

Three structural interpretations of the Gjallar Ridge (Fig. 4.13) display the nature of the high and how it varies along strike from the southwest to the northeast in proximity to the RAZ. A series of faults dip dominantly towards the northwest producing a succession of rotated half grabens. Faults dip at very low angles ~ 20 - 30° at the top of the fault reducing to ~ 10° within the interpreted Lower – Middle Cretaceous pre-rift sequence, but this may be due to increasing interval velocities on time-migrated seismic data (Appendix C.06). The faults are believed to have formed at these shallow dips and not later backward rotated as the estimated dips of the faulted horizons (~ 12°) are directly comparable with the dips of horizons in the Nyk High (~ 10°; Fig. 4.05d). It is unclear at which depth the faults sole out upon the seismic data, whether detaching within Lower – Middle Cretaceous shales at ~ 6 km depth as inferred by Gernigon *et al.* (2003) and Gomez *et al.* (2004), detaching at mid-crustal levels proposed by Ren *et al.* (1998) or cross cut the entire crust detaching in the upper mantle (Walker *et al.* 1997; Mjelde *et al.* 2007). Due to the apparent low angle, this would require a major simple shear of the crust (e.g.

Osmundsen & Ebbing 2008) but on the basis of deep seismic lines across the basin (e.g. Fig. 4.09), the faults are expected to sole out within the Lower – Middle Cretaceous sequence as proposed by Gernigon *et al.* (2003). Therefore, it appears that the fault domains are not hard-linked through to basement and the RAZ is a rift segmentation feature formed and contained within the Late Cretaceous – Paleocene rift sequence.

The Gjallar Ridge is defined as the region between the bounding faults which are inferred to display Late Cretaceous normal movements by the recognition of syn-rift sequences that are not evident in the Vigrid Syncline to the southeast, and the Fenris Graben to the northwest where a major fault system with a throw of 1 – 1.5 sec TWT is located (Fig. 4.13), considerably larger than elsewhere upon the Gjallar Ridge. Normal movements along the faults appear to have been initiated within the Gjallar Ridge during the Santonian with subtle fanning of reflectors into the bounding faults of each package (Fig. 4.13d) but the interpretation is speculative in regards to the age of this sequence particularly within the Fenris Graben which remains undrilled. It is interpreted that the Santonian sequence is notably thicker in the Fenris Graben (up to 500 ms) in contrast to the Gjallar Ridge (up to 300 ms) implying the Gjallar Ridge was structurally higher in relief and the focus for deposition was within the Fenris Graben to the northwest at this time (Fig. 4.13f).

Minor rifting continued during the deposition of the KCaMFS115 sequence. The Santonian age faults continued to be active during this period with discordant fanning reflectors observed within the Campanian sequence fault hangingwalls. Once again, the sequence is thinner upon the Gjallar Ridge in contrast to the Fenris Graben (Fig. 4.13f) implying the Gjallar Ridge was of greater relief than the Fenris Graben. This minor rift period is believed to have ceased prior to deposition of the Campanian package bounded at the base by the KCaMFS115 and the top by KCaMFS118 horizons. This sequence does not display the thickening of the previous sequences and is of a relatively constant thickness across the Gjallar Ridge and into the Fenris Graben implying a period of tectonic quiescence.

The major rift event that affected the region occurred during the Maastrichtian with thick syn-rift deposits evident within the Gjallar Ridge (up to 800 ms thick) and in the Fenris Graben (> 1000 ms thick). Many of the previously active faults during the Santonian and Campanian were reactivated but new faults (predominantly to the northwest) also formed due to apparently accommodating the increased extension at this time (Fig. 4.13). Thickness of the sequence varies greatly across the Gjallar Ridge increasing from southeast to northwest, associated with the increasing magnitudes of fault offset. Figure 4.14 highlights the increasing extensional heaves upon faults in the north-westerly region of the Gjallar Ridge compared with those in the SE. Multiple unconformities are evident within the Maastrichtian syn-rift sequence in the fault hangingwalls and correlate both above and across footwall crests, some of which are associated with the erosion of the sequence, implying the Gjallar Ridge was at or near sea level towards the end of the Cretaceous and Early Cenozoic, a brief period of lower eustatic sea levels (Haq *et al.* 1988). The tips of major faults terminate against the Late KMaUnc erosional unconformity (e.g. Figs 4.13d and 4.13e) suggesting extension may have reduced during the latest Maastrichtian along the strike of the Gjallar Ridge.

As mentioned previously, the structurally lower Fenris Graben contains the greatest thickness of Maastrichtian strata and is therefore expected to contain the most complete Maastrichtian syn-rift sequence in the region. This is due to major erosion in the earliest Cenozoic across the Gjallar Ridge, eroding footwall crests with an estimated 950 m of Upper Cretaceous sediments removed upon the Gjallar Ridge and 630 m from the Fenris Graben (calculated from structural restorations of 2D seismic data; Ren *et al.* 1998).

The structural relief of the Gjallar Ridge compared to the Fenris Graben throughout the Late Cretaceous is constantly highlighted due to the increased thickness of preserved sediment in each of the respective regions area despite very similar amounts of erosion occurring. This variation of relative relief at upper crustal levels links closely with the relief of the LCB (Fig. 4.11a). The relief of the LCB reduces notably from the Gjallar Ridge (7.5 – 10 km depth) into the Fenris Graben (10 – 15 km depth). This would therefore further support the presence of the LCB in the Late Cretaceous controlling the primary rift depocentres, *prior* to the previously inferred magmatic underplating of the crust in the Paleocene. Preserved Maastrichtian sediments thin along the strike of the Gjallar Ridge towards the RAZ which suggests the Gjallar Ridge was structurally highest towards the northeast in the Early Cenozoic. It is unclear as to how much material was eroded within the Fenris Graben, if any, as the unconformity trends parallel to the stratigraphy, but major erosion is evidenced at the north-western edge of the Vigrid Syncline with eroded Santonian deposits subcropping the top Cretaceous unconformity (Fig. 4.13).

The Gjallar Ridge remained a structural high in the Cenozoic with evidence of onlapping Paleocene horizons to the northwest and southeast, with only the latest Paleocene sediments preserved upon the high (Chapter 5). Rifting at this time could be interpreted as having ceased with only minor fault movements evident. Yet, as a large amount of Early Paleocene strata is missing, evidence for Early – Middle Paleocene rifting may have been removed as well. Within the Fenris Graben, fanning of reflectors is observed within the hangingwall of the Gjallar Ridge bounding fault (Fig. 4.13) which although not dated, could conceivably be Early Paleocene in age.

4.7.1 Gjallar Ridge and the northern Rym Accommodation Zone

The transition from the Gjallar Ridge to the RAZ is a similarly sharp transition (Fig. 4.12a) with a reduction in relief of the top Cretaceous unconformity from ~ 3200 ms upon the high to ~ 4100 ms within the RAZ across a distance of ~ 10 km, resulting in a gradient of ~ 8°. This rapid increase in the dip of the Late Paleocene horizons tie to a NW-SE trending fault (Figs 4.07 and 4.15) which can be mapped to bound the north-eastern edge of the Gjallar Ridge. The normal fault dips to the northeast at ~ 50°. The fault can be mapped for up to 40 km along the north-eastern edge of the Gjallar Ridge and is inferred to have been active during the Late Maastrichtian through changes in the thickness of the syn-rift sequence. Increased truncation of the Late Cretaceous sequence in the hangingwall of this rift-oblique fault (Fig. 4.15) compared to upon the Gjallar Ridge is unusual in view of the present day structural configuration. This enhanced hangingwall erosion can be accounted for via three methods. Firstly, relative uplift and erosion of the Gjallar Ridge may have been of differing magnitudes along its strike, with enhanced erosion of the ridge to the northeast than to the southwest (a possible tilting effect). Synchronous downthrown fault movements in the Late Maastrichtian – Early Paleocene would not be preserved due to the erosion of the Gjallar Ridge above the regional base level, with Late Paleocene shallow marine sediment directly resting upon the preserved Upper Cretaceous strata (Fig. 4.16). Alternatively, submarine erosion (Chapter 5) is inferred to have occurred during the Paleocene within the Nyk High and Hel Graben, the currents may have also eroded the strata within the fault hangingwall. A third hypothesis is that differential erosion has occurred due to differing lithologies outcropping at the surface. Any of these methods are able to produce the erosional truncation observed in Figure 4.15, but whichever cause for the erosion, the hangingwall of the rift-oblique fault is required to have been downthrown during the Early Paleocene. Thickening of the Late Paleocene sequence across the fault from upon the Gjallar Ridge into the northern RAZ is associated with this increase in accommodation space formed by the Early Paleocene reactivations of the NW-SE fault, which also implies the northern RAZ to be a depocentre at this time (Fig. 4.04d), not due to strike-slip movements within the northern RAZ as previously inferred (Ren *et al.* 2003).

Elsewhere, the rift-oblique fault can be imaged to offset Late Paleocene horizons suggesting sections of the fault may have been active since the Maastrichtian until continental break-up. Tentative calculations inferred from the offset of perpendicular faults across this NW-SE fault suggest normal left-lateral movements in the order of a few hundred metres laterally have occurred (Fig. 4.17). A further more detailed study is required to analyse the offsets along the fault as dextral movements are also observed along the same fault which may mean fault identification is incorrect. Furthermore, differential extension upon each the low angle normal faults in the footwall and hangingwall may result in different amounts of lateral movements along the rift-oblique fault with the varying senses of lateral offset inferred.

4.8 Structural evolution of the Nyk High

The gross structural style of the region around the Nyk High is best viewed using the KCaMFS115 horizon which has been affected by the multiple Late Cretaceous - Paleocene rift events (Fig. 4.12b). The Nyk High trends NE-SW and is formed of a series of horsts and grabens. The horsts and grabens form prominent highs (~ 3000 ms TWT) and lows (~ 4100 ms TWT) across the Nyk High, both sets of structures not varying greatly in width (~ 5 km) along strike. The transition from the Nyk High to the Någrind Syncline is marked by a bounding normal fault system down to the northwest (Fig 4.18). A similarly northwest dipping normal fault system with throws > 1 sec TWT offset the Nyk High from the Hel Graben to the north. The transition from the Late Cretaceous Nyk High to the RAZ is complex and no distinct boundary can be defined in contrast to the faulted boundary of the Gjallar Ridge. Within the southern RAZ, faults rapidly change in orientation from NE-SW towards dominantly E-W and NW-SE orientations. It is unclear as to whether the faults link from the Nyk High with those in the southern RAZ due to the erosion of Cretaceous deposits (Figs 4.09 and 4.10) as well as limitations in seismic imaging due to remobilised Miocene ooze (Appendix C.02). The southern RAZ is further complicated by the compressional deformation associated with the Vema Dome in the Oligo-Miocene (Doré *et al.* 2008) and the positive uplift (up to 2700 ms TWT) associated with this (Fig. 4.09).

The Nyk High is characterised by 50 – 60° dipping synthetic and antithetic planar faults (dipping northwest and southeast respectively) and has formed a suite of horst and graben structures in contrast with the low angle faults and half grabens of the Gjallar Ridge (Fig. 4.18). The antithetic faults are often recognised to link to the dominant synthetic faults, the detachment horizon for which can not be ascertained from the 3D seismic data due to limited vertical extent but is inferred as being Early – Middle Cretaceous in age (Fig. 4.09). The greatest vertical extent of the Nyk High is located on the flank of the Någrind Syncline with a reduction in relief across the horsts and grabens towards the northwest. The width of deformation in the Nyk High also varies greatly along strike, increasing towards the southwest (~ 11 km, Fig. 4.18d; ~ 13 km, Fig. 4.18e; ~ 17.5 km, Fig. 4.18f). This is contrary to the Gjallar Ridge which narrows towards the RAZ (Fig. 4.13), as is the fact that distribution of extension is more evenly spread across all faults in contrast to the increasing offsets across faults to the northwest on the Gjallar Ridge (Fig. 4.14). This interpretation may be complicated by the effect of erosion and the removal of Upper Cretaceous syn-kinematic sequences from the Gjallar Ridge but focussing this analysis on horizons which have been less prone to erosion (e.g. Santonian and Campanian), this interpretation holds true (Appendix C.07). The bounding fault system between each of the structural highs and their respective grabens to the northwest displays the greatest offset within each of the study areas implying the Gjallar Ridge and Nyk High were at the margin of the main rift system, despite a distinct lack of faulting in the Hel Graben (Fig. 4.06).

There is little evidence for Santonian rifting in the region of the Nyk High as has been mapped in the Gjallar Ridge. This may be due to the reduced resolution of the dataset (Fig. 4.03) or there was no rifting in the vicinity of the Nyk High at this time. The sequence is of a relatively constant thickness along the strike of the Nyk High and within the Någrind Syncline to the southeast. The first evidence of rifting is during deposition of the Campanian Nise Sandstone Member bounded at its top by KCaMFS115 with normal faults offsetting this horizon with throws of a few tens of ms, tipping out in the overlying Late Campanian sequence. Minor thickening of horizons in the hangingwalls of faults are only recognised in a few areas (e.g. in the grabens of Figures 4.18e and 4.18f). Other thickness variations of the sequence are controlled by the major marine fan deposition in the Middle Campanian with a major depocentre for sediment developing in the region of the Nyk High and Någrind Syncline at the time (note the high reflectivity sequence in Figure 4.05b; Fjellanger *et al.* 2005). Rifting may have continued until the end of the Campanian but this is unclear as the dominantly mud prone (Fjellanger *et al.* 2005) Late Campanian sequence (KCaMFS118) appears to deform in a ductile manner rather than by seismically imaged faults (there are notable thickness changes of the horizon but faults often do not extend through the sequence, possibly associated with the seismic resolution).

The dominant rift event which affected the Nyk High was Maastrichtian in age with major deposition of divergent fanning reflectors into the normal faults within the grabens (> 1 sec TWT thick). Sediment was also deposited upon the horsts, as well as within the Någrind Syncline to the southeast (Fig. 4.05) and Hel Graben to the northwest

(Fig. 4.06). It is unknown as to the total thickness of sediment deposited upon the Nyk High horsts as a marked erosional unconformity (top Cretaceous unconformity) has removed much of the syn-rift sequence within the grabens. It is difficult to explain this as being associated with sub-aerial exposure since the structurally highest point in the region at the time (northwest edge of the Någrind Syncline) fails to display evidence of any such erosion. Instead, sidewall erosion of the horst structures (e.g. the north-westerly edge of the horsts; Fig. 4.18) forming a northwest dipping unconformity may be associated with submarine erosion by bottom water currents (Chapter 5). This may be linked to the shallowing of the Nyk High due to falling eustatic sea levels or relative uplift of the structure (e.g. rift flank uplift). The amount of preserved Maastrichtian sediments varies greatly along strike with ~ 1.2 sec TWT preserved in the northeast (Fig. 4.18d) with little or none preserved in the southwest (Fig. 4.18f). In this location, Paleocene sediments directly overlie Campanian strata upon the horsts with ≤ 20 ms TWT of Maastrichtian sediments preserved within the grabens and in the north-western edge of the Någrind Syncline, due to the buttressing and uplift above the Jurassic rift system at the time (Figs 4.09 and 4.10).

In contrast with the Gjallar Ridge, major normal faulting is observed to occur within the Nyk High during the Paleocene offsetting the top Cretaceous unconformity. It is unknown whether this is a continuation of the Late Cretaceous rift event or whether there was a break/change in extension when reactivating the Late Cretaceous faults. Additional faults also formed splaying predominantly from the south-eastern bounding faults of the Nyk High (e.g. Fig. 4.18e). Thickness changes are observed across the faults with thickening primarily against either of the two bounding faults of the graben in the northeast and southwest (Figs 4.18d and 4.18f). However, towards the centre of the Nyk High in the study area sediment thickens towards the centre of the grabens than into the bounding faults (Fig. 4.18e), which may be attributed to focussed flow of marine currents leading to submarine erosion (Chapter 5). The rifting is believed to have continued until the end of the Paleocene when fault movements ceased, marking the cessation of rifting in the Nyk High fault domain.

4.8.1 Nyk High and the southern Rym Accommodation Zone

As noted previously, a rotation in fault trends occurs from NE-SW within the Nyk High to E-W and NW-SE as the faults enter the southern RAZ. The zone of deformation continues to widen to the west (> 30 km, Figs 4.19d and 4.19e) but eventually narrows to ~ 20 km (Fig. 4.19f) as faults decrease in displacement along strike (Fig. 4.12b). Faults dip at 50 – 60° with both synthetic and antithetic faults observed, the antithetic faults regularly detaching upon the northerly dipping synthetic faults as also observed in the Nyk High. The previous asymmetry of the Nyk High is replaced by a more symmetrical style of fault deformation (compare Figure 4.18d with Figure 4.19f). Despite this, the northern edge of the Någrind and Vigrid Synclines remains the structurally highest points in the area despite the positive structural growth of the Oligo-Miocene Vema Dome affecting much of the area. Strain is similarly taken up equally upon all of the faults, although the total amount of extension is actually greater in the southern RAZ than in the Nyk High (Fig. 4.14).

Previously observed evidence of minor Campanian rifting in the Nyk High continues along strike and is identifiable within the eastern region of the southern RAZ demonstrated by steepening dips at depth and inferred fanning of the truncated KCaMFS118 sequence (Fig. 4.19d). However, evidence for Campanian rifting does not continue to the west with observed thickness changes believed to be caused by inflation of the sequence by Paleocene sills (Fig. 4.19f). The first phase of rifting in this area occurred during the Maastrichtian with an increasing thickness of preserved sediment from east (<

300 ms TWT, Fig. 4.19d) to west (< 600 ms TWT, Fig. 4.19f) due to erosional truncation of the sequence in proximity to the Nyk High. The Paleocene sequence similarly thickens away from the Nyk High to the west as major rifting continued into the Paleocene with thickness changes and fanning observed in the fault hangingwalls (compare Figure 4.19d with 4.19e and 4.19f). This implies that the eastern region of the RAZ was structurally higher and eroding (truncation of the Late Cretaceous stratigraphy) during the Paleocene due to the north-south oriented uplift compared to the west which continued to act as a fault controlled depocentre for the reworked sediment (Fig. 4.10).

4.9 Strain analysis

Strain analyses of the en-echelon fault domains allows two other variables not previously considered within the qualitative description of the fault domains; these are how strain varies along strike into the fault domain boundary and also how it varies through time. The results are directly comparable quantitatively between the Gjallar Ridge and Nyk High fault domains, to fully address if and how strain is conserved across the fault domain boundary.

Results of the upper crustal extension analysis (Fig. 4.20; Appendix C.08-13) calculated from fault heaves across the Gjallar Ridge and Nyk High display a variety of trends. The data display a generally wide scattering of the points but is deemed acceptable in an area of poor well control and complex faulting, and which is further complicated by the widespread erosion of syn-rift strata. The Gjallar Ridge was analysed in view of Campanian, Maastrichtian and Paleocene extension, as was the Nyk High but with the addition of post-Paleocene extension which is assumed to have been caused by minor reactivations of the faults under post-rift thermal subsidence. Post-Paleocene extensions is a minor occurrence upon the Gjallar Ridge and would be expected to be accounted for in the Paleocene extension calculation.

Beta factors are generally larger for the Gjallar Ridge with a maximum of 1.3 during Maastrichtian rifting in comparison to the Nyk High with a maximum of 1.1 for the duration of the same rift event. Total upper crustal stretching also varies between the two structural highs with up to 1.4 in the Gjallar Ridge and 1.14 in the Nyk High. This is due to using fault heaves for calculations which are heavily dependent upon fault dips. As the Gjallar Ridge faults dip in the order of ~ 20° compared to the more steeply dipping faults of the Nyk High (50 – 60°), increased beta factors are obtained, yet these calculations are deemed reasonable as the Late Cretaceous strata of the Gjallar Ridge dip at similar amounts to the Nyk High, which implies the faults of the Gjallar Ridge have not undergone subsequent post-rift rotation and formed at the low angles observed.

Upon the Gjallar Ridge, Campanian rifting may also include an element of Santonian rifting which is believed to be very small and was not mapped widely across the study area (Fig. 4.13). Beta factors for the Campanian rifting range from 1.01 to 1.24 varying along strike of the structural high. These generally increase from the west to the east before rapidly reducing across the NW-SE bounding fault of the Gjallar Ridge with very little extension within the RAZ (Fig. 4.17). The major Maastrichtian rifting of the Gjallar Ridge produced increased beta factors between 1.1 and 1.3 averaging between 15 – 20% extension at this time. Similarly to the Campanian rifting, beta factors reduce to ~ 1 in the vicinity of the NW-SE bounding fault, once again implying little or no extension within the northern RAZ. Paleocene extension is negligible with many calculated beta factors close to 1 confirming no preserved evidence of major rifting occurring on the Gjallar Ridge at the time.

The Nyk High and its transition into the southern RAZ displays a much more diverse set of beta factors compared to the Gjallar Ridge. Campanian beta factors reach a maximum of 1.14 towards the centre of the study area close to the inferred trend of the

Jurassic rift fault at depth (Fig. 4.09). The calculated beta factors reduce along strike to 1 and ~1.02 in the west and east respectively. Caution as to the exact amount of Campanian extension has to be exercised in the region of the inferred maximum as these may be influenced by the later Maastrichtian and Paleocene rift events, the evidence of which may have been eroded away during the Paleocene uplift event, resulting in an overestimation of beta factors. It is therefore expected that Campanian rifting is more likely to tend towards lower beta factors than those displayed, reducing from the Nyk High into the southern RAZ where no Campanian extension is interpreted (Fig. 4.19).

Maastrichtian rifting was focussed within the Nyk High displaying maximum beta factors 1.1, reducing along strike in the southern RAZ. Calculations display a major decrease in beta factors within the zone of Cenozoic erosion but increasing again with a calculated 6% extension within the southern RAZ. Similarly to the Campanian rifting, it is generally expected that Maastrichtian rifting gradually decreased from east to west rather than what is observed and calculated here, but has been subsequently modified by the erosion of the Maastrichtian sequence in the Early Cenozoic resulting in an underestimation of the beta factor.

The Paleocene rifting which characterises this area displays a very different trend to the Late Cretaceous rift events. Within the Nyk High, beta factors are calculated at ~ 1.04 reducing to no observed extension in the zone affected by Cenozoic erosion. To the west, extension is at its greatest within the southern RAZ with beta factors of up to 1.14 inferring the focus for the rifting shifted from the Nyk High to the southern RAZ at this time. No major notable erosion of the Nyk High apart from possible submarine erosion can explain the low beta factor, but an alternative hypothesis may be that the major extensional stress reoriented to more a more north-south trend yet this is unlikely based upon recent plate tectonic reconstructions (Gaina *et al.* 2009). Post-Paleocene extension is generally minor, tending to produce beta factors < 1.04 and implying rifting had generally ceased by the Eocene.

The upper crustal beta factors calculated from this study are in general agreement with those calculated by previous authors from structural restorations of the northern Vøring Basin. Walker *et al.* (1997) and Ren *et al.* (1998) calculated beta factors between 1.5-1.6 across the Gjallar Ridge and Fenris Graben. Although these are larger than the total maximum extension calculated in this study (~1.4; Fig. 4.20a) this is expected to vary due to differences between interpreted horizons upon 2D seismic datasets compared to the well-calibrated 3D seismic datasets used in this study. Kusznir *et al.* (2005) calculated upper crustal extension to be in the order of 10% across the Nyk High which is directly comparable with the total maximum extension calculated from this study (~1.14; Fig. 4.20b). Similarly, relatively low beta factors were calculated by Roberts *et al.* (1997) of 1.2 for the Gjallar Ridge, Nyk High and southern RAZ. Kusznir *et al.* (2005) concluded that a major element of depth-dependent stretching has to occur to explain the observed post continental breakup thermal subsidence of the margin .

4.10 Summary

4.10.1 Late Jurassic

The Late Jurassic rift which affected the inboard region of the Norwegian continental margin (e.g. Doré *et al.* 1999; Fig. 4.01) is believed to underlie the outer Vøring Basin, as revealed within recent regional 2D seismic data (Fig. 4.09). The rift structure is expected to trend in a N-NNE orientation as exemplified elsewhere along the Norwegian continental margin, the North Sea rift system and Porcupine Basin offshore Ireland (Roberts *et al.* 1999; Brekke 2000; Naylor & Shannon 2005). Limited data makes it unclear as to whether the rift system is present elsewhere, however the major normal faults (heaves in the order of up to 5 km) in the vicinity of the Nyk High suggests extension may occur across the entire Vøring Basin, reducing in scale to the west. It remains unclear as to whether rifting continued into the Early Cretaceous (Lundin & Doré 1997) or whether a passive infill of the rift bathymetry occurred (Færseth & Lien 2002).

4.10.2 Santonian - Campanian

Earliest evidence of Late Cretaceous rifting in the Vøring Basin occurred in the Santonian in the vicinity of the Gjallar Ridge. NE-SW trending normal faults formed attributed to inferred NW-SE extension in the region (Fig. 4.21). Minor rifting continued into the Campanian in this area (Fig. 4.22a), possibly tipping out in the vicinity of the northern RAZ. A north-western extension of the Gjallar Ridge may be present within the Hel Graben but this is highly speculative (Fig. 4.06). The Nyk High also experienced minor Campanian rifting which similarly did not appear to extend along strike into the southern RAZ at its south-western end. Interpretations of deep seismic lines suggest that the faults do not detach in basement nor reactivate the Late Jurassic rift architecture, rather detaching within the mud-prone Lower – Middle Cretaceous post-rift sequence. Within the RAZ, a prominent ramp structure formed between the Vigrid Syncline and structurally lower Hel Graben.

4.10.3 Maastrichtian

Major rifting occurred during the Maastrichtian and reactivated the Campanian rift faults (Fig. 4.22b). The Gjallar Ridge remained a structural high in relation to the Fenris Graben which also experienced major rifting. At the north-eastern limit of the Gjallar Ridge, a NW-SE normal oblique fault formed offsetting the Gjallar Ridge from the northern RAZ and Hel Graben. Maastrichtian rifting is evident within the Hel Graben but does not appear to be on such a scale as exhibited upon the Gjallar Ridge. Normal fault movements also occurred within the Nyk High which propagated along strike, rotating into dominantly east-west trends within the southern RAZ. Within the central RAZ the ramp became of increased structural prominence acting as a hinge between the Vigrid Syncline and passively subsiding Hel Graben.

4.10.4 Paleocene

During the Early Paleocene (Fig. 4.22c), the Gjallar Ridge was actively eroded due to its structural prominence. Fault movements continued to occur along the bounding fault of the Fenris Graben as well as inferred normal oblique movements along the NW-SE trending fault between the Gjallar Ridge and northern RAZ. However, any major Paleocene faulting which occurred upon the Gjallar Ridge was eroded prior to the Late Paleocene. This is in direct contrast to the Nyk High where Paleocene normal fault movements are recognised and little evidence of subaerial erosion has occurred. Apparent uplift in the Middle – Late Paleocene (Fig. 4.22d) led to a north-south trending structural high at the south-western edge of the Nyk High (Fig. 4.21) and into the Hel Graben. Major erosion along this trend occurred; with Eocene sediments resting upon the Late Cretaceous unconformity implying erosion occurred throughout the Paleocene until continental breakup. An explanation for the lack of observed upper crustal extension in the northern Vøring Basin may be evidence of Paleocene depth-dependant stretching as proposed by Kusznir *et al.* (2005) in which upper crustal faulting gives way to pure shear extension of the lithospheric mantle directly prior to continental breakup. Beta factors in the region are greatest within the southern RAZ (maximum of 1.14) yet these alone are not sufficient for continental breakup to occur.

4.11 Discussion

4.11.1 Strain transfer between fault domains

From the results of this study, fault domain boundaries appear not to solely separate rift segments with opposing polarities of faults (Faulds & Varga 1998). Within each of the rift segments, the tectonic deformational style can vary dramatically, as recognised with the Nyk High characterised by 50 – 60° normal faults creating a series of grabens and horst structures in contrast to the ~ 20° low angle faults of the Gjallar Ridge forming a series of asymmetric half grabens. Kinematically, the faults of each rift segment were initiated and active at different times, with the Gjallar Ridge experiencing Santonian – Maastrichtian/Paleocene rifting and the Nyk High, Campanian – Paleocene rifting. Furthermore, the spatial distribution of strain across each of the rift segments contrasts greatly, with the Gjallar Ridge faults preferentially accommodating extension upon faults away from the rift margins whereas upon the Nyk High, strain is distributed more evenly. Similarly, the uplift and subsidence histories can vary significantly across the fault domain boundary. Major erosion of the Gjallar Ridge in the Late Maastrichtian – Early Paleocene has eroded any evidence of Paleocene rifting which may or may not have occurred, yet the only erosion upon the Nyk High is expected to be submarine rather than subaerial. Each of the observed differences between the adjacent rift segments may be influenced by the pre-existing deep crustal structure within each rift segment which is only simply modelled in laboratory analogue models (e.g. McClay *et al.* 2002; Younes & McClay 2002; McClay *et al.* 2004). This influence of a deep crustal heterogeneity is seen within the northern Vøring Basin where the LCB largely parallels the relief of the Late Cretaceous upper crustal deformation. Although the Late Cretaceous – Paleocene rifting is not expected to directly control its relief due to the faults detaching within a mid-Cretaceous horizon (e.g. Fig. 4.09), this pre-existing basement structure passively influenced the rift relief, and as such, changes in the vertical uplift and subsidence vary on either side of the fault domain boundary.

Each of these dissimilarities fundamentally impacts whether strain is transferred, and conserved between adjacent rift segments. The calculated beta factors within this study vary greatly between each fault domain for each stage of rifting (Fig. 4.20). The total amount of strain also varies greatly between each fault domain with beta factors of up to 1.4 in the Gjallar Ridge compared to a maximum of 1.14 in the Nyk High. A limitation of the study is that the full expanse of the rift zone is not considered for the study which is expected to include the region beneath the basalt as well as the conjugate Greenland margin. But the two fault domains within each rift segment are located at the south-eastern rifted margin and are therefore considered equivalent fault domains. Also, there is relatively little faulting within the Hel Graben (Fig. 4.06) to potentially accommodate the extra extension required for the fault domain boundary to conserve strain between each rift segment. A tentative interpretation of an along strike continuation of the Gjallar Ridge in the Hel Graben is made which may accommodate some of the extension, but equally another fault domain may exist beneath the Vøring Marginal High in the Fenris Graben or upon the inferred conjugate rift segment offshore Greenland. Therefore, fault domain boundaries in nature do not necessarily appear to conserve strain between the adjacent fault domains, which is a result of the different upper crustal deformation and pre-existing crustal heterogeneities that *may* actually lead to the initial formation of the fault domain boundary.

4.11.2 Structural configuration of fault domain boundaries

Previously, accommodation zones have been associated with the formation of major relay ramps between a series of overlapping fault tips, in stark contrast to transfer zones in which a rift-oblique fault forms between the offset rift segments (Faulds & Varga

1998). A third, but little referenced form of fault domain boundary is a transverse zone (e.g. Rowley 1998) in which a wide range of deformational styles are present. However, it would be inconceivable to believe that natural examples of fault domain boundaries would be as simple as the conceptual models (e.g. Faulds & Varga 1998). Therefore accommodation zones and transfer zones (and in effect transverse zones) can not be considered as separate, end-member models. Each type of fault domain boundary may contain deformation which would be more suitably attributed to an alternative fault domain boundary.

Within this study, a range of deformation has been observed to occur in specific regions of the fault domain boundary. Within the southern RAZ, faults rotate from the dominant NE-SW trend of the Nyk High rotating into east-west and NW-SE trends as observed in analogue modelling and onshore studies of rifts (e.g. Corti *et al.* 2003 and references therein). Maastrichtian faults decrease in displacement along strike after entering the southern RAZ (Fig. 4.20), a process typical of an accommodation zone (c.f. Faulds & Varga 1998). Equally, the ramp which has formed between the Vigrid Syncline and Hel Graben in the central RAZ (Fig. 4.07) is also a key attribute of an accommodation zone. Yet it is the NW-SE normal oblique faulting in the northern RAZ bounding the north-eastern edge of the Gjallar Ridge (Figs 4.07 and 4.15) which is not typically associated with an accommodation zone, instead more often considered inherent to a transfer zone. Strain analyses of the Gjallar Ridge does highlight a rapid drop in beta factors in proximity to the NW-SE fault which would be expected to occur if a transfer zone was present (Faulds & Varga 1998). However, the amount of lateral and normal offset along the fault is only in the order of a few hundred metres. This is small in contrast to the larger offsets recognised elsewhere along the NE Atlantic Margin (e.g. Moy &

Imber 2009; Chapter 3) and in other rift provinces (e.g. Henry 1998), as these faults appear to be trivial in comparison to the fault domain boundary (Fig. 4.17).

An alternative explanation for the NW-SE fault(s) is provided by McClay *et al.* (2004) who witnessed the rotation and elongation of fault tips into an accommodation zone within analogue models. These rotated faults form highly oblique to the rift trend and could cut other faults, leading to them being misinterpreted as transfer faults on a local scale. The origin of the NW-SE fault(s) in the northern RAZ could therefore be an extension of one of more major faults in the Fenris Graben not recognised beneath the lavas, rotating clockwise into the RAZ (e.g. Acocella *et al.* 1999a). This fault or set of faults would be analogous to the breaching of a relay ramp between two normal faults but on a much larger scale and would explain why little lateral or vertical offset is observed. The only known analogue models which have successfully recreated transfer faults was by Acocella *et al.* (2005). Results highlighted that transfer faults formed part of an accommodation zone but only when significant stretching occurs (> 39% extension) and the rift achieves differential extension of > 21% between each rift segment. The results of this study highlight that upper crustal extension barely reaches the required total extension in the most extended region (i.e. the Gjallar Ridge) but the differential extension across the northern RAZ *may* be sufficient. This hypothesis could also explain the lack of evidence for a through-going fault between the Vigrid Syncline and Hel Graben as the fault tips out to the southeast.

Using the breaching of a relay ramp analogy between two normal faults (e.g. Peacock & Sanderson 1994), if rifting was of an increased magnitude, the NW-SE fault is hypothesised to fully breach the ramp formed between the Vigrid Syncline and Hel Graben (Fig. 4.23). The fault would still apparently reduce in offset along strike to the southeast, but as it links through to the south-western edge of the Nyk High, it may be incorrectly termed a transfer fault (and thus a transfer zone), along which oblique slip movements are interpreted to occur. The difference between a transfer zone (Faulds & Varga 1998) and a breached relay ramp would be particularly difficult ascertain from field based studies of fault domain boundaries, particularly those of limited scale. Notably, it is field based studies (e.g. Duebendorfer *et al.* 1998) in which transfer zones are principally recognised. It is therefore hypothesised that transfer zones could be integral to a much larger accommodation zone type fault domain boundary, with movements along the rift-oblique fault(s), controlled by the relative movements between the adjacent rift segments, which in turn can be varied and complex (e.g. Acocella *et al.* 2005). In particular this would be controlled by the differential uplift and subsidence of the adjacent fault domains as observed in this study. Evidently, the proposal for this region to be defined as an accommodation zone proposed by Ren *et al.* (2003) seems best suited for this structure compared to the relay ramp terminology as it is assumed to also be present upon the conjugate east Greenland passive margin to the northwest.

4.11.3 Paleocene evolution of the northern Vøring Basin

Evidence of Paleocene extension in the Vøring Basin varies between the two studied rift segments. Upon the Nyk High, beta factors of ~ 1.04 are calculated, but upon the Gjallar Ridge Paleocene extension is negligible (Fig. 4.20). This may be due to erosion of the Gjallar Ridge during the Late Maastrichtian – Middle Paleocene, with all evidence of Paleocene rifting having been removed. The only observable fanning of Paleocene strata occurs in the hangingwall of the bounding fault between the Gjallar Ridge and structurally lower Fenris Graben (Fig. 4.13). Yet, it is upon the generally east-west and NW-SE trending faults in the southern RAZ where Paleocene beta factors are greatest (~ 1.12; Fig. 4.20). The faults of the southern RAZ are interpreted to have formed during the Maastrichtian, as a westerly propagation along strike from the Nyk High (Fig. 4.22b) and as such fault displacements generally decrease towards the Vigrid Syncline. Rotation of the fault tips with reduction in fault offset into accommodation zones are frequently cited (e.g. McClay & White 1995; Corti *et al.* 2003; McClay *et al.* 2004; Schlische & Withjack 2009). This is believed to occur due to the local scale variations in the stresses between each of the extensional rift segments (Acocella *et al.* 1999a; Fournier *et al.* 2007, fig 4, p 9).

A hypothesis as to the cause of the predominant reactivation of east-west striking faults in the Paleocene could be linked to a rotation in the stress vector to a north-south orientation, leading to reactivation of the Nyk High faults under dextral transtension (e.g. Allen *et al.* 1997). A mechanism for a change in stress orientation is not clear, although other east-west (inferred north-south extension) Paleocene faults have been recognised elsewhere along the NE Atlantic Margin, but their origin also remains enigmatic (e.g. Dean *et al.* 1999; Lamers & Carmichael 1999; Ellis *et al.* 2009). Yet, these examples are on a lesser scale to those of the southern RAZ. The proposed north-south orientation does not correlate well with the relative plate motion vector of 165 – 168° calculated by Tsikalas *et al.* (2002) which is of a similar orientation to the recent plate tectonic breakup models in the region (Gaina *et al.* 2009). Imber *et al.* (2005) also did not recognise any evidence of dextral reactivation of the Nyk High faults which would have to occur, instead preferring a minor sinistral component of movement. Mogensen *et al.* (2000) previously proposed Late Cretaceous – Paleocene north-south extension reactivated the NNW-SSE oriented Surt Lineament in sinistral strike-slip, suggesting the east-west faults in the RAZ were transfer faults linking the NW-SE and NE-SW fault systems. However, evidence of the required major strike-slip movements (e.g. Harding 1990) along the RAZ are not observed.

An interesting observation is that the east-west trending normal faulting in the southern RAZ appears to have occurred syn-tectonically with the broadly N-S oriented uplift in the Paleocene. A hypothesis to explain synchronous north-south extension and inferred east-west compression could be related to a localised domain of transtension above a N-S oriented Jurassic fault system. However to explain the uplift and extension effects observed, a NE-SW extension vector would be required (De Paola *et al.* 2005) which once again seems highly unlikely prior to NW-SE oriented continental breakup (Gaina *et al.* 2009). Similarly, upper crustal extension is evident upon the NE-SW trending faults of the Nyk High during the Paleocene (Fig 4.20), and extension may have also occurred upon the NE-SW trending faults Gjallar Ridge. Each of these observations would further question the likelihood of a NE-SW oriented extension event at this time.

A second hypothesis to explain synchronous extension and uplift may be related to a combination of interacting processes. Firstly, assuming there is no Paleocene aged compression (and therefore no need to interpret a harpoon structure within the Jurassic syn-rift sequence; Fig. 4.09c), an alternative source for the Paleocene uplift in the region may be caused by uniform stretching of a heterogeneous lithosphere of varying crustal thickness. Assuming a constant lithosphere thickness of 125 km, if the thickness of the crust is less than 17 km, this will result in uplift rather than subsidence during rifting (Dewey 1982). The Late Jurassic rift event (Fig. 4.09) is expected to have modified the relative amounts of crustal thickness in the Vøring Basin. Therefore, pure shear extension of the lithosphere in the Late Cretaceous – Paleocene may have resulted in varying areas of basinal uplift and subsidence in the Vøring Basin (Fig. 4.09). However, for this to occur in the Paleocene would require a regional pure shear extension of the lithosphere (i.e. evidence of upper crustal faulting) which is not widely recognised in this study, with depth-dependent stretching considered the principal method of lithosphere thinning at the time (see below).

Instead, the Paleocene uplift may relate to transient uplift effects attributed to the Iceland plume (e.g. Champion *et al.* 2008). This uplift effect is expected to be regional in extent as observed elsewhere upon the NE Atlantic Margin. A similar effect in the northern Vøring Basin may also be highlighted within the top Paleocene time-structure map in Figure 4.04d. Here a N-NNE trending, up to 50 km wide high is recognised within the southern RAZ, narrowing both to the north in the Hel Graben and south into the Någrind Syncline. Notably, the uplift is greatest (and widest) in the southern RAZ, a conclusion supported by the zone of Paleocene erosion in this area (Fig. 4.10). As this area is expected to have formed the structurally highest point along this N-NNE trend at this time, possibly further accentuated by the isostatic response due to erosional unloading, this may provide an explanation for the increased Paleocene fault heaves. The generally east-west trending normal faults may have reactivated under extension due to being elevated and becoming gravitationally unstable, leading to fault reactivation and increased fault offsets in this area.

This uplift and extension process may be further complicated by NW-SE oriented depth-dependent stretching which occurred during the Paleocene (Roberts *et al.* 1997; Kusznir *et al.* 2005). With an underlying Jurassic rift event, considerable thinning of the crust is expected to occur (Skogseid *et al.* 1992), resulting in the thinning of the crust and an increased component of mantle lithosphere. Therefore, the amount of depth-dependent stretching may vary across the margin due to the relative amounts of mantle lithosphere and the obliquity of the stretching to Jurassic rift trend. In turn, the relative influence of the Iceland plume and amount of transient uplift may also vary along the strike of the margin. The combination between depth-dependent stretching, the relative thickness of the mantle lithosphere due to Late Jurassic rifting and the convective effect of mantle plume material at the base of the crust may explain the formation of this N-S oriented, localised zone of uplift.

The proposed hypotheses may therefore influence the structural and stratigraphical interpretation of the Late Jurassic rift structure and the impact on Paleocene uplift. In particular, it will allow us to interpret whether a harpoon structure due to Paleocene compression is likely to have formed within the Late Jurassic syn-rift sequence (Fig. 4.09b). A transtensional origin for the structure seems unlikely, and there is relatively little evidence supporting an inferred E-W oriented Paleocene compressional event in the Vøring Basin (Doré *et al.* 2008). Yet, a harpoon structure is also interpreted to have formed beneath the younger Oligo-Miocene Vema Dome. Could the harpoon structure have therefore formed during this younger Cenozoic compressional event? Evidence implying this is not the case is presented in Appendix C.14. Clear thinning of the Oligo-Miocene sequence occurs above the Vema Dome, but above the harpoon structure to the east (Fig. 4.09b), the time-thickness of the sediments is at its greatest. If the harpoon had formed in the Oligo-Miocene a thinning of the strata should be observed due to uplift of the overlying stratigraphy. Therefore, on the basis of the reasons outlined above and our current regional understanding of the Norwegian continental margin, the favoured interpretation of the syn-rift sequence is presented in Figure 4.09c which implies the harpoon structure to be a Lower Cretaceous stratigraphical feature infilling the rift bathymetry (Færseth & Lien 2002). Thus, the most likely explanation for the enhanced fault offsets in the southern RAZ and broadly N-S oriented uplift in the region is due to a complex interaction between Paleocene depth-dependent stretching, a heterogeneous lithosphere structure and the effect of convecting material at the base of the lithosphere.

However, this hypothesis needs to be investigated further to explain whether the observations made in this study can be correlated with these interacting processes at depth.

Results of this study support the interpretation of an ancient crustal root as the origin for the LCB inboard of the continent-ocean boundary for similar reasons that Gernigon *et al.* (2006) detail. This is based on the apparent link between the geometry of the predominant Late Cretaceous rift elements and depth to the top of the LCB (Fig. 4.11). Various authors have inferred uplift along the margin during the Paleocene due to magmatic underplating caused by the replacement of dense mantle by significantly less dense enriched material sourced from the Iceland plume (e.g. Skogseid *et al.* 1992). This has been proposed as the reason why the faulted Nyk High and Gjallar Ridge appear elevated compared to their adjacent graben and syncline. However, this does not explain why sill injection is greatest in those areas which were not as uplifted and exposed to erosion (e.g. the Hel Graben; Fig. 4.07), compared to the structural highs which are inferred to be the primary focus of underplating and uplift yet do not display increased volumes of igneous intrusives (Fig. 4.06). Instead, the prominence of structural highs in the Paleocene may actually reside in a combination of factors including the relief of the LCB; plume related regional uplift; extension of a heterogeneous lithosphere; fault block rotation along low-angle faults; rift flank uplift between the highs and their associated grabens as well as being located upon the flanks of two thermally subsiding major synclines, all of these processes are preferred processes in varying amounts to magmatic underplating and localised uplift in regions of upper crustal thinning.

The continental break-up model proposed by Gernigon *et al.* (2006, fig 8, p270) appears to be the most accurate model published to-date relating the lack of upper crustal faulting in the Paleocene to depth-dependent stretching of the lithosphere, as well as interpreting the LCB as a basement feature; this is in broad agreement with the results of this study. However, it must be noted that as the RAZ appears to separate two contrasting structural provinces with different rift sets of styles and kinematics, any rift models need to account for the tectonic variation along strike of the Norwegian continental margin, possibly linked to the inherited structural heterogeneity at depth. This also implies that the RAZ and other similar fault domain boundaries are an important feature influencing continental break-up along the NE Atlantic Margin.

4.12 Conclusions

- The Gjallar Ridge is a structural high formed under Campanian – Maastrichtian rifting (evidence of Paleocene rifting is not preserved) and is characterised by a suite of northwest dipping low angle normal faults (20 – 30°) forming a series of asymmetric half grabens.
- The Nyk High differs in structural style and kinematics to the Gjallar Ridge with evidence of Maastrichtian – Paleocene rifting forming a series of NE-SW trending horsts and grabens. Faults dip at steeper angles ~ 50 – 60° to the northwest and southeast.
- The two rift segments are separated by the NW-SE oriented Rym Accommodation Zone which formed under Late Cretaceous – Paleocene rifting prior to continental breakup. Although fault domain boundaries are considered to conserve and transfer strain between adjacent rift segments, the Rym Accommodation Zone appears to unsuccessfully complete this, instead separating segments with contrasting structural styles, kinematics, loci of extension accommodating faults and deeper crustal structure.
- The Rym Accommodation Zone displays a varied structural style between the adjacent tectonic elements of each rift domain. Within the fault domain boundary a rotation of regional NE-SW fault orientations into generally east-west trends

occurs, a major ‘relay ramp’ has formed and rift perpendicular normal oblique faulting is evident in contrast to pre-existing conceptual models of accommodation zones.

- Previous end member models of transfer zones are hypothesised as being integral to a larger accommodation zone. A through going rift-oblique fault is inferred as being a larger equivalent to a cross fault of a breached relay ramp formed between two normal faults.
- Enhanced Paleocene upper crustal extension in the southern RAZ is proposed to have formed due to transient uplift and the gravitational collapse of the fault domain. Synchronous uplift and extension may have been further complicated due to the effect of the Late Jurassic rift system modifying the pre-existing lithosphere structure and effect of later NW-SE oriented depth-dependent stretching in the Paleocene.
- Results from this study concur that the Lower Crustal Body (sensu Gernigon *et al.* 2004) most likely of a basement origin based upon structural relationships between the depth of the Lower Crustal Body and the Late Cretaceous rift related features. It is in part considered the reason for the enhanced relief of faulted Gjallar Ridge and Nyk High along with plume related regional uplift, fault block rotation, rift flank uplift location upon the flanks of two thermally subsiding major synclines, not through the result of magmatic underplating as has previously been inferred.
- The Rym Accommodation Zone is expected to be an important feature controlling continental break-up. It separates two rift segments which display a disparity between the style and the kinematics associated with rifting. Therefore, any subsequent rift and continental break-up models need to recognise the along strike variation of the Norwegian Margin.

4.13 Acknowledgements

This work forms part of a NERC CASE Studentship with Statoil U.K. Ltd (NER/S/C/2006/14276). PGS Geophysical, TGSNopec, WesternGeco, Fugro Multi Client Services and the Norwegian Petroleum Directorate are gratefully acknowledged for permission to publish interpretations from the respective seismic datasets. Landmark Graphics Corporation through the Strategic University Alliance Agreement (2006-COM-032168) is acknowledged for providing seismic processing/interpretation software and technical support. Badleys Geoscience is also acknowledged for continual provision, training and technical support for TrapTester software. D. Stevenson and G. Wilkinson provided ongoing technical support within the Department of Earth Sciences.

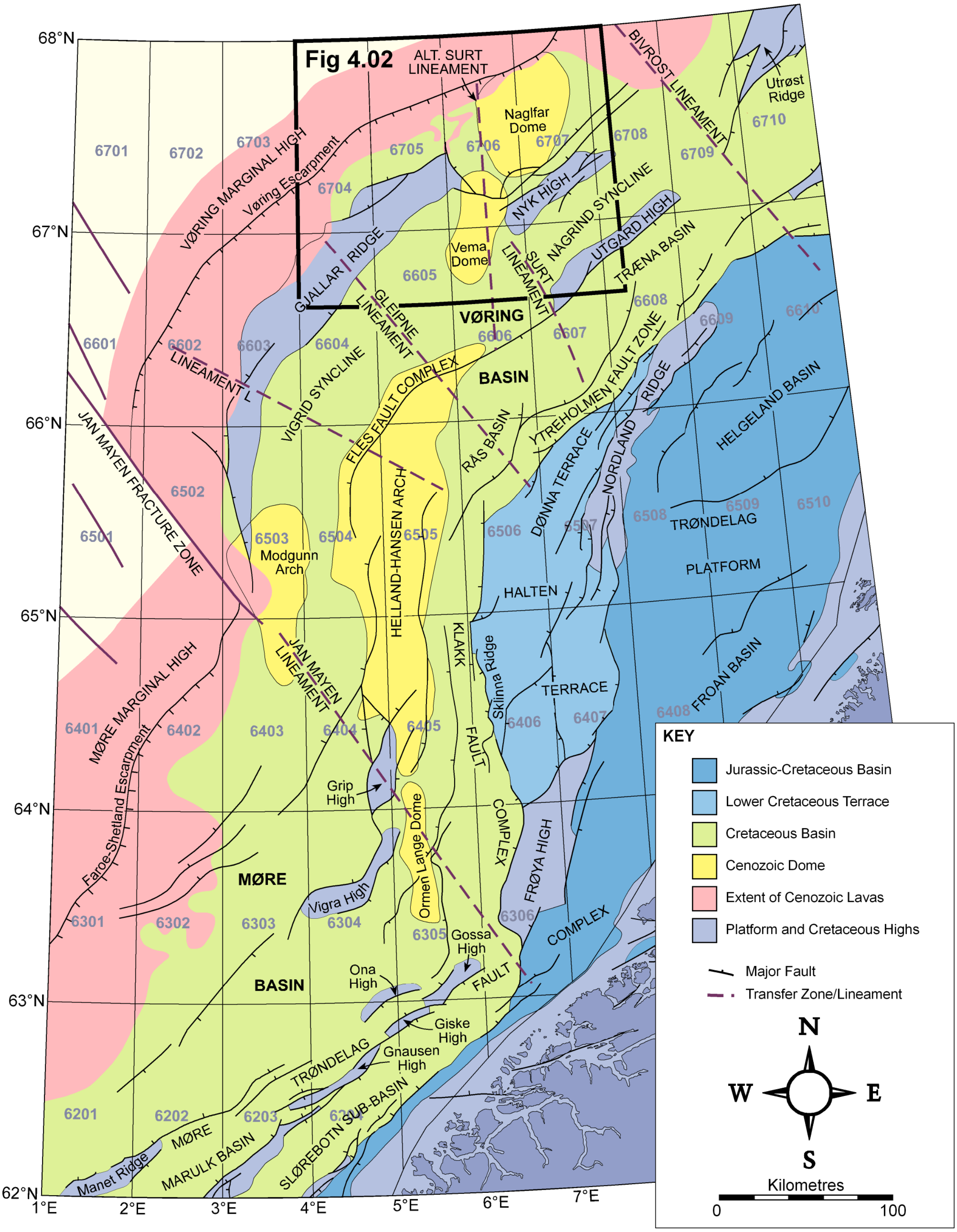

Figure 4.01: Tectonic elements map of the Norwegian continental shelf displaying the gross N-S and NE-SW structural trends form during successive rift events. Numerous NW-SE rift oblique lineaments ('transfer zones') are recognised along the margin recognised from various geophysical datasets. Modified after Blystad *et al.* (1995), Ren *et al.* (2003) and Mjelde *et al.* (2005). Map projection is WGS84, UTM 31N.

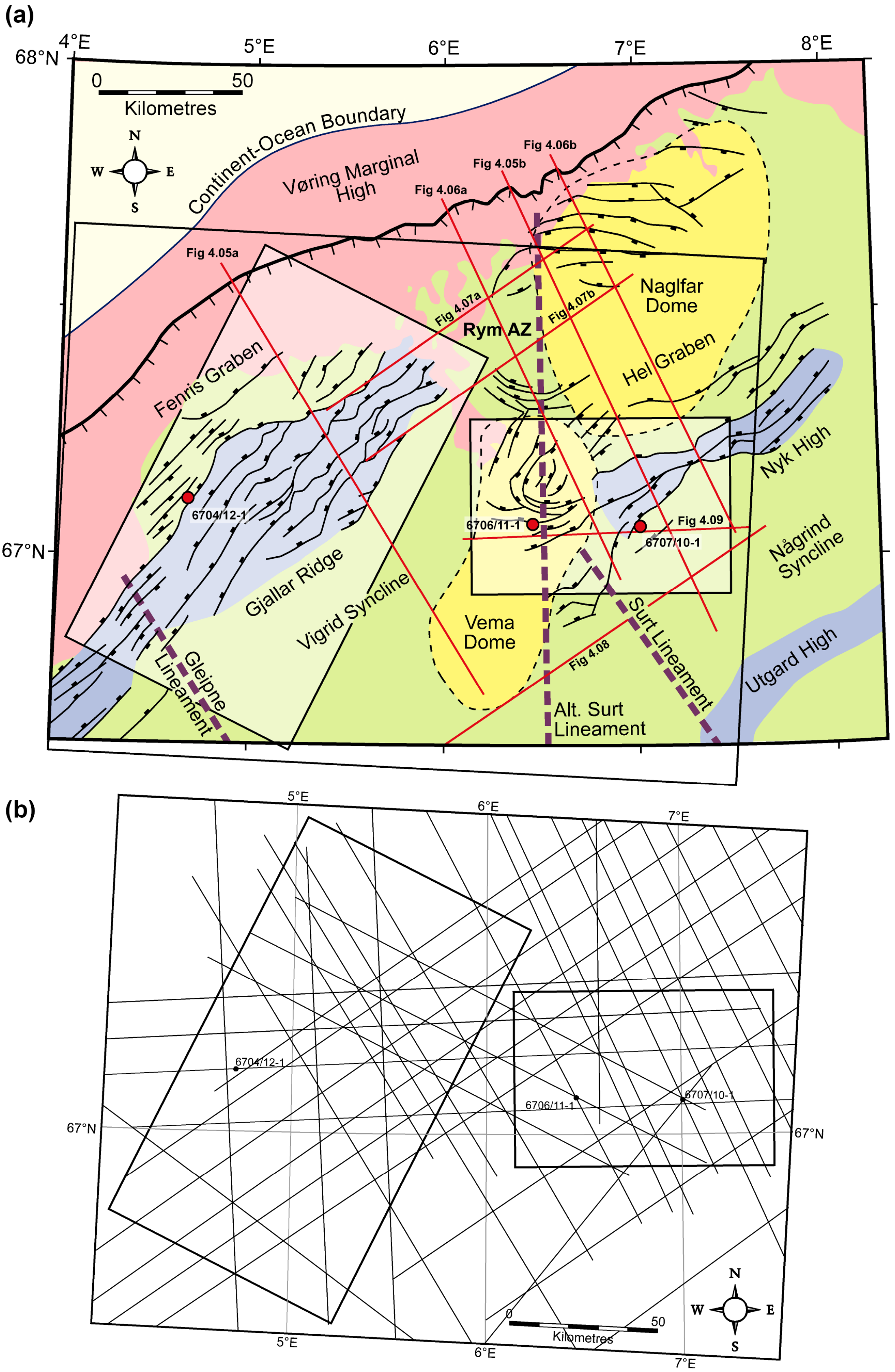

Figure 4.02: (a) Structural features of the northern Vøring Basin seemingly offset towards the end of the Surt Lineament by the Rym Accommodation Zone (modified after Ren *et al.* (2003) and Mjelde *et al.* (2005)) and (b) the location of the 2D and 3D seismic data used within the current study.

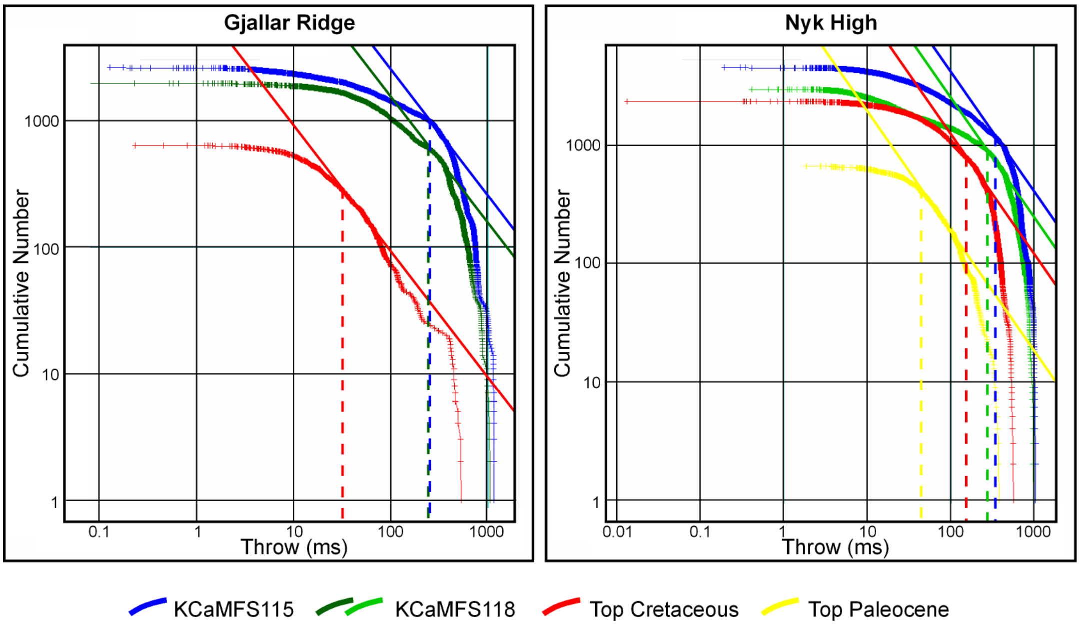

Horizon	**Minimum effective resolution (Gjallar Ridge)**	**Minimum effective resolution (Nyk High)**
KCaMFS115	115 ms	125 ms
KCaMFS118	114 ms	118 ms
Top Cretaceous	32 ms	107 ms
Top Paleocene	N/A	45 ms

Figure 4.03: Seismic resolution of faults in the Gjallar Ridge and Nyk High seismic surveys using the cumulative frequency method after Pickering *et al.* (1995).

(a) **KCaMFS115** (b) **KCaMFS118**

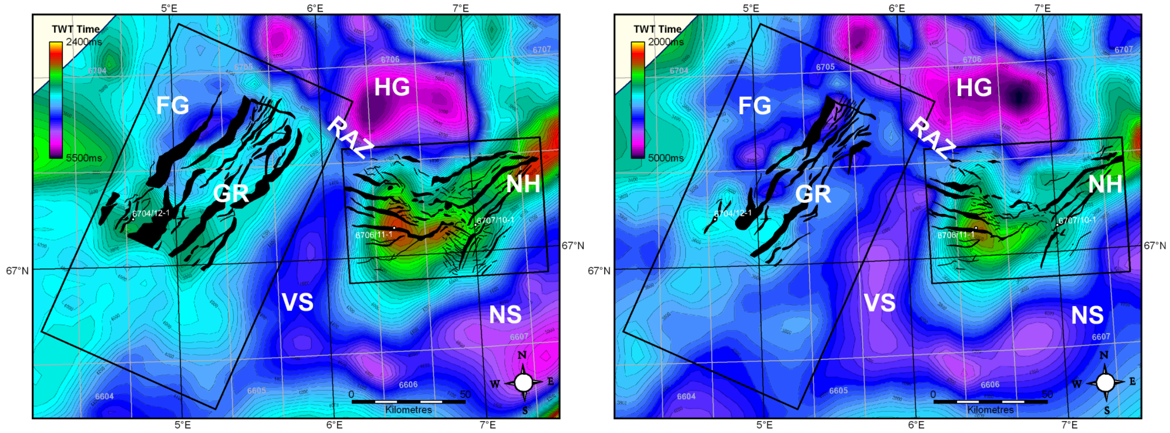

(c) **Top Cretaceous** (d) **Top Paleocene**

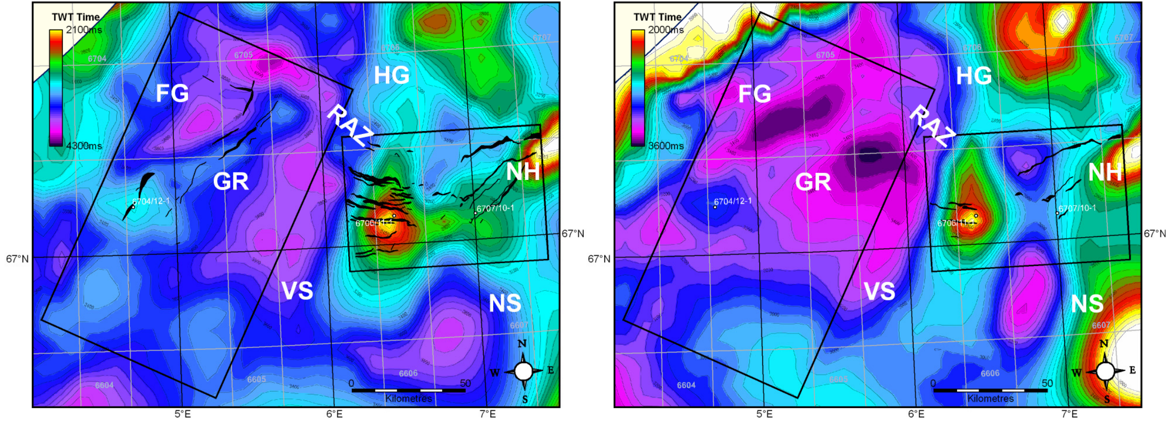

Figure 4.04: Series of TWT structure maps of the (a) KCaMFS115 (Top Middle Campanian), (b) KCaMFS118 (top Campanian), (c) top Cretaceous and (d) top Paleocene horizons in the northern Vøring Basin interpreted from the 2D and 3D seismic datasets available for the study. Fault polygons within the structure maps are those used in the later strain analyses. **GR** Gjallar Ridge; **NH** Nyk High; **HG** Hel Graben; **FG** Fenris Graben; **NS** Någrind Syncline; **VS** Vigrid Syncline; **RAZ** Rym Accommodation Zone.

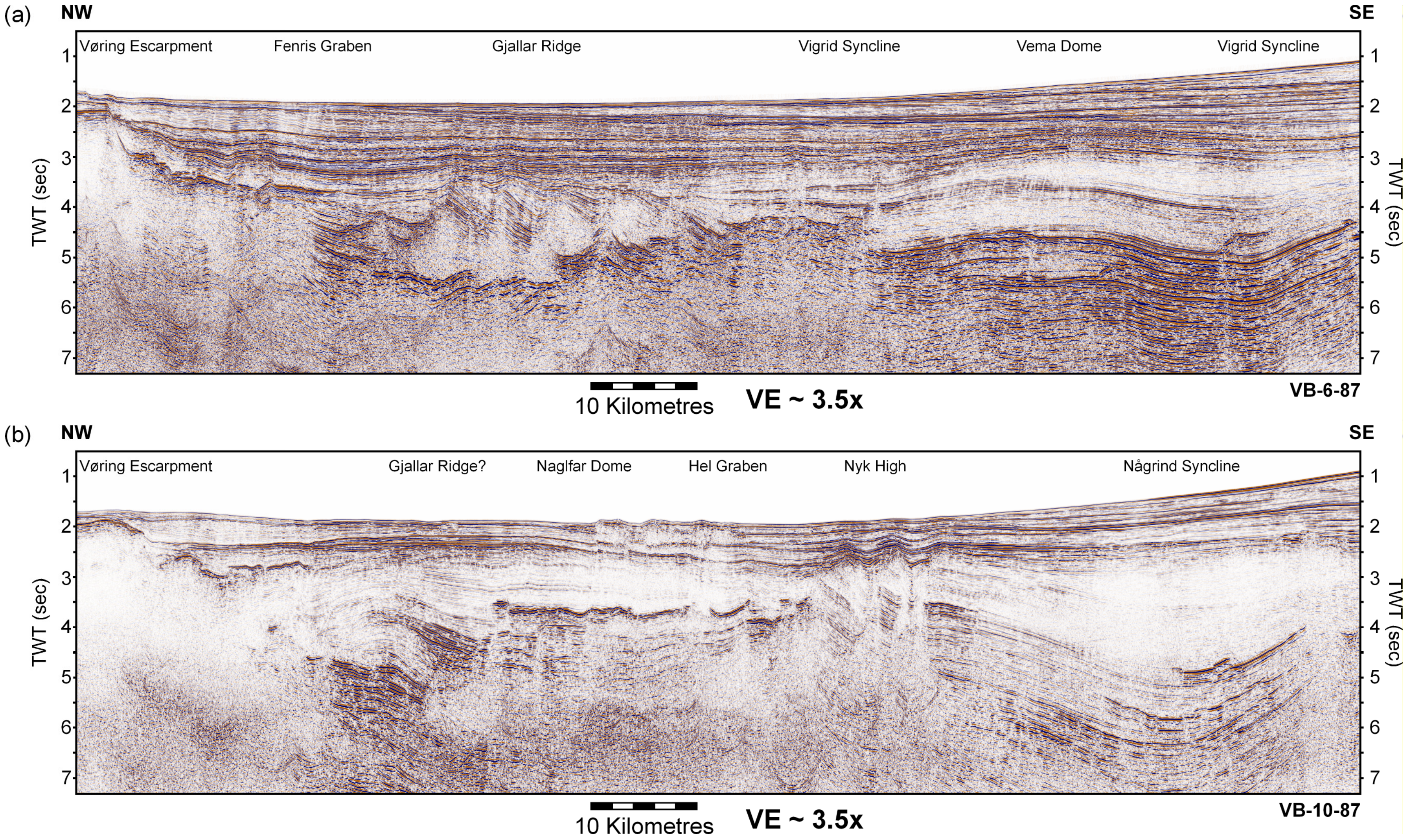

Figure 4.05a & b: Regional seismic lines across the (a) Vigrid Syncline, Gjallar Ridge and Fenris Graben, and (b) Någrind Syncline, Nyk High and Hel Graben. Seismic data courtesy of the NPD. For line locations, see Figure 4.02a.

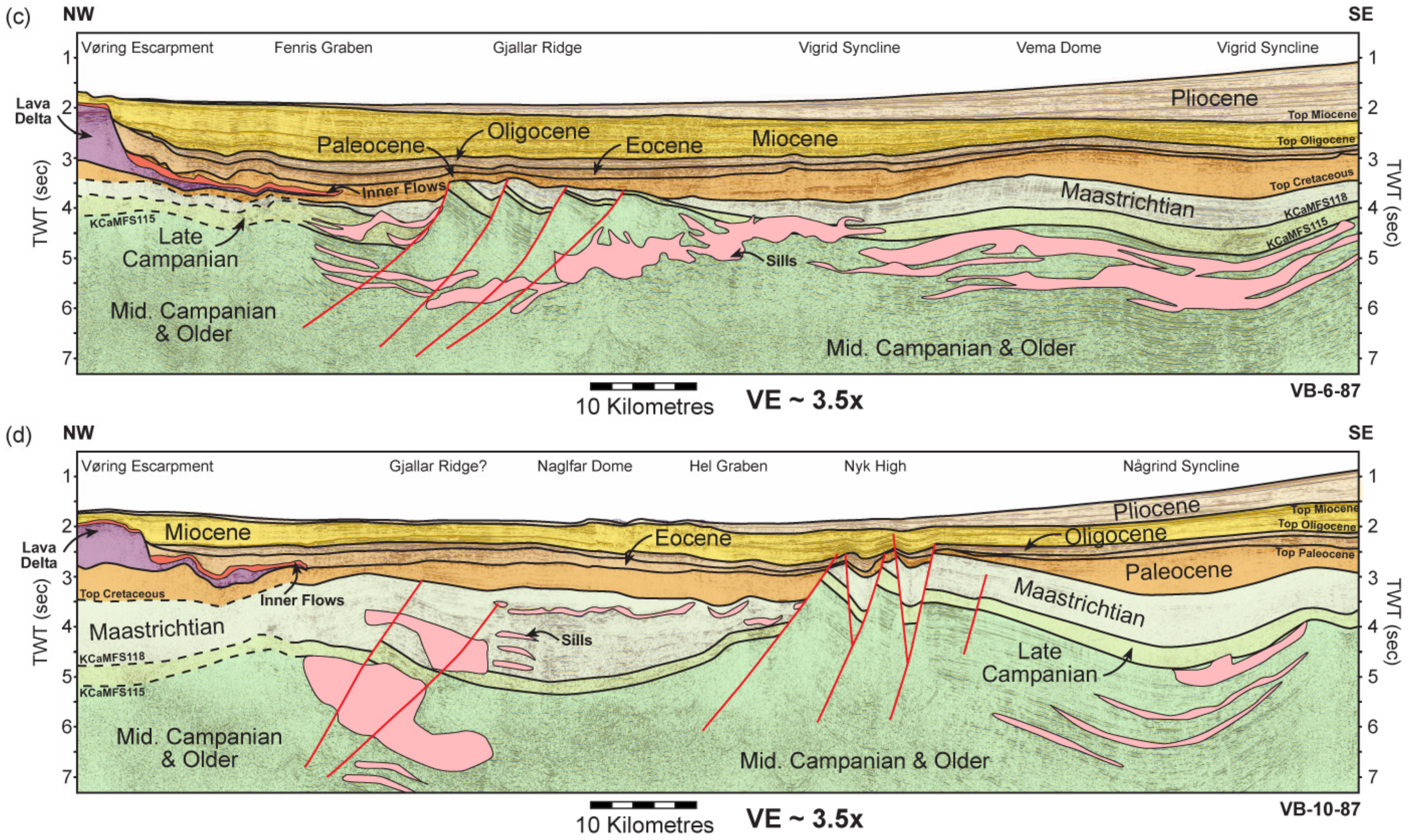

Figure 4.05c & d: Interpreted regional seismic lines across the (c) Vigrid Syncline, Gjallar Ridge and Fenris Graben, and (d) Någrind Syncline, Nyk High and Hel Graben. Seismic data courtesy of the NPD. For line locations, see Figure 4.02a.

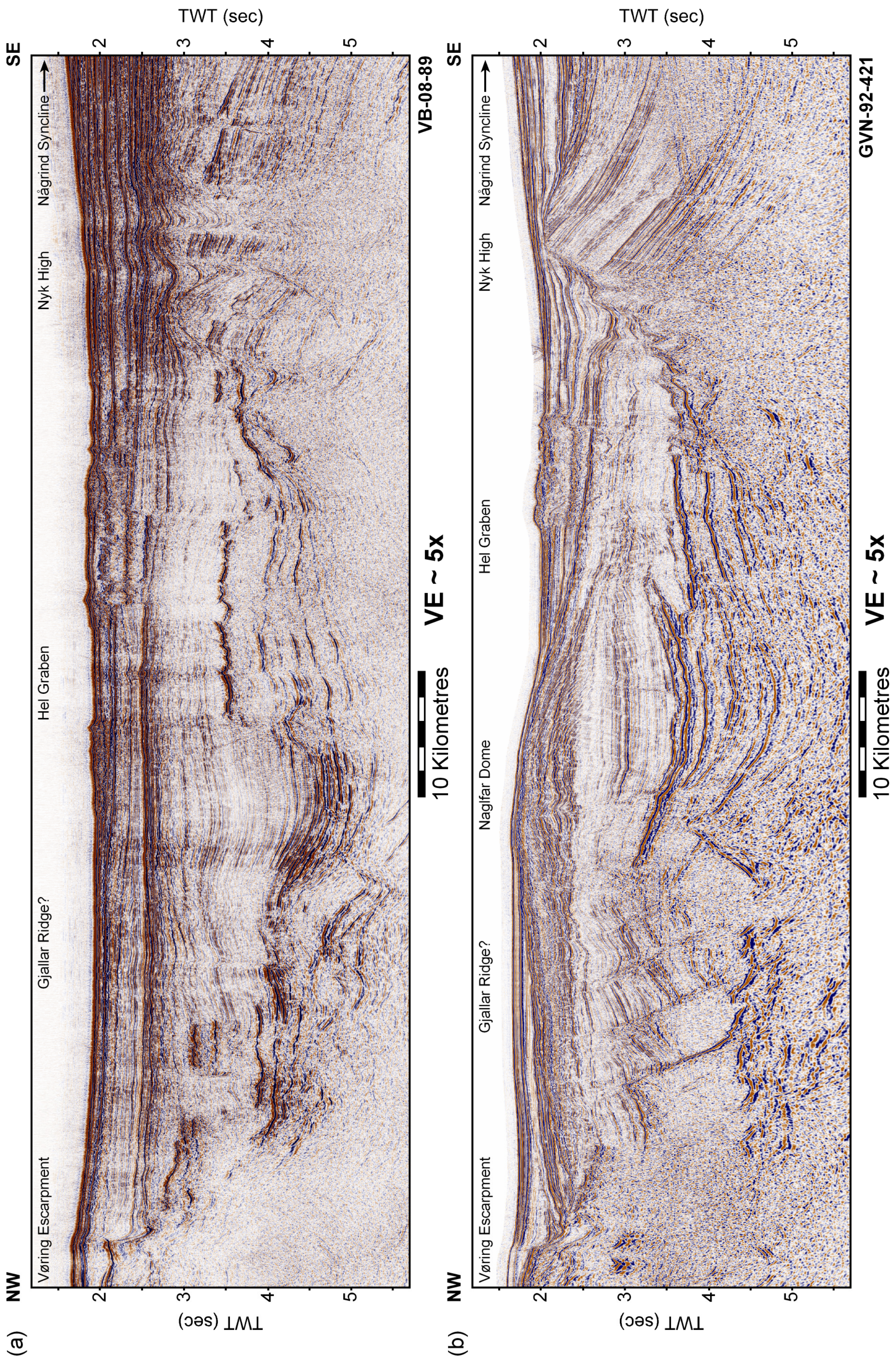

Figure 4.06a & b: Two seismic lines of the Hel Graben (a) along the strike of the Rym Accommodation Zone (courtesy of the NPD) and (b) from the Nyk High across east-west trending Maastrichtian-Paleocene normal faults to the north (courtesy of WesternGeco). For line locations, see Figure 4.02a.

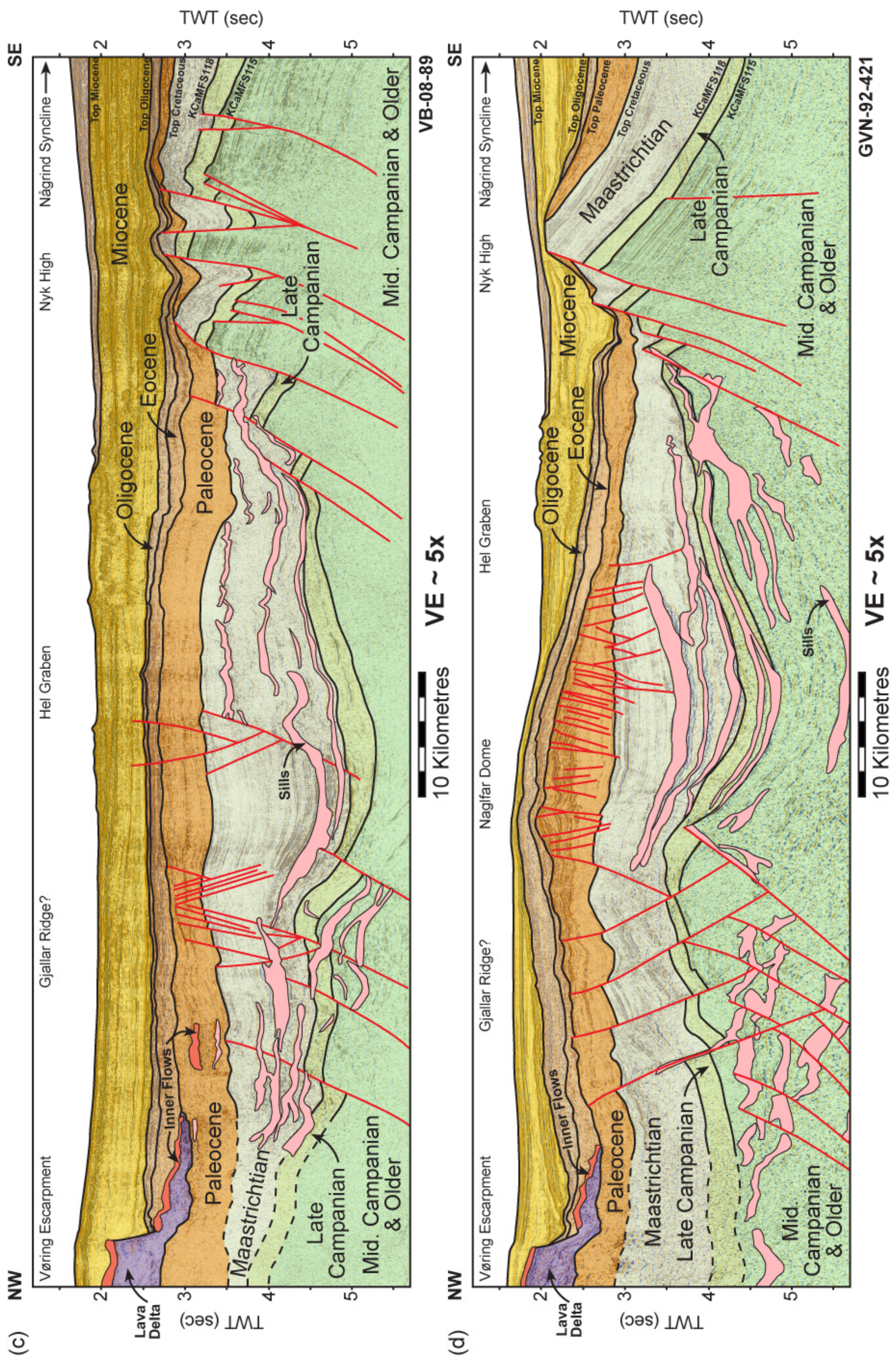

Figure 4.06c & d: Two seismic line interpretations of the Hel Graben (c) along the strike of the Rym Accommodation Zone (courtesy of the NPD) and (d) from the Nyk High across east-west trending Maastrichtian-Paleocene normal faults to the north (courtesy of WesternGeco). The Hel Graben is a major Late Cretaceous – Paleocene depocentre despite a lack of rift related faulting, with a possible along strike continuation of the Gjallar Ridge interpreted at depth. For line locations, see Figure 4.02a.

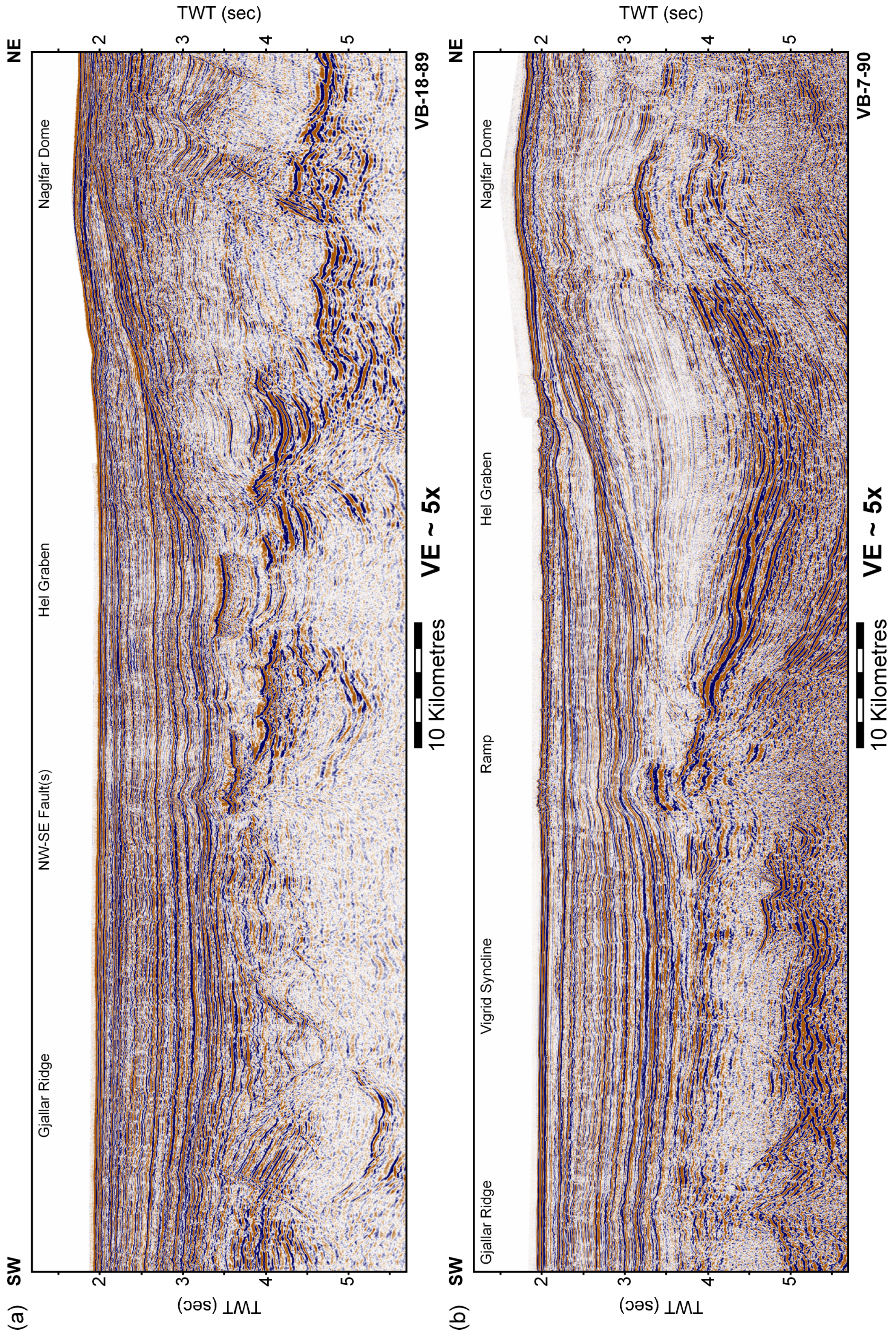

Figure 4.07a & b: Two seismic lines of the (a) northern and (b) central Rym Accommodation Zone. For line locations, see Figure 4.02a.

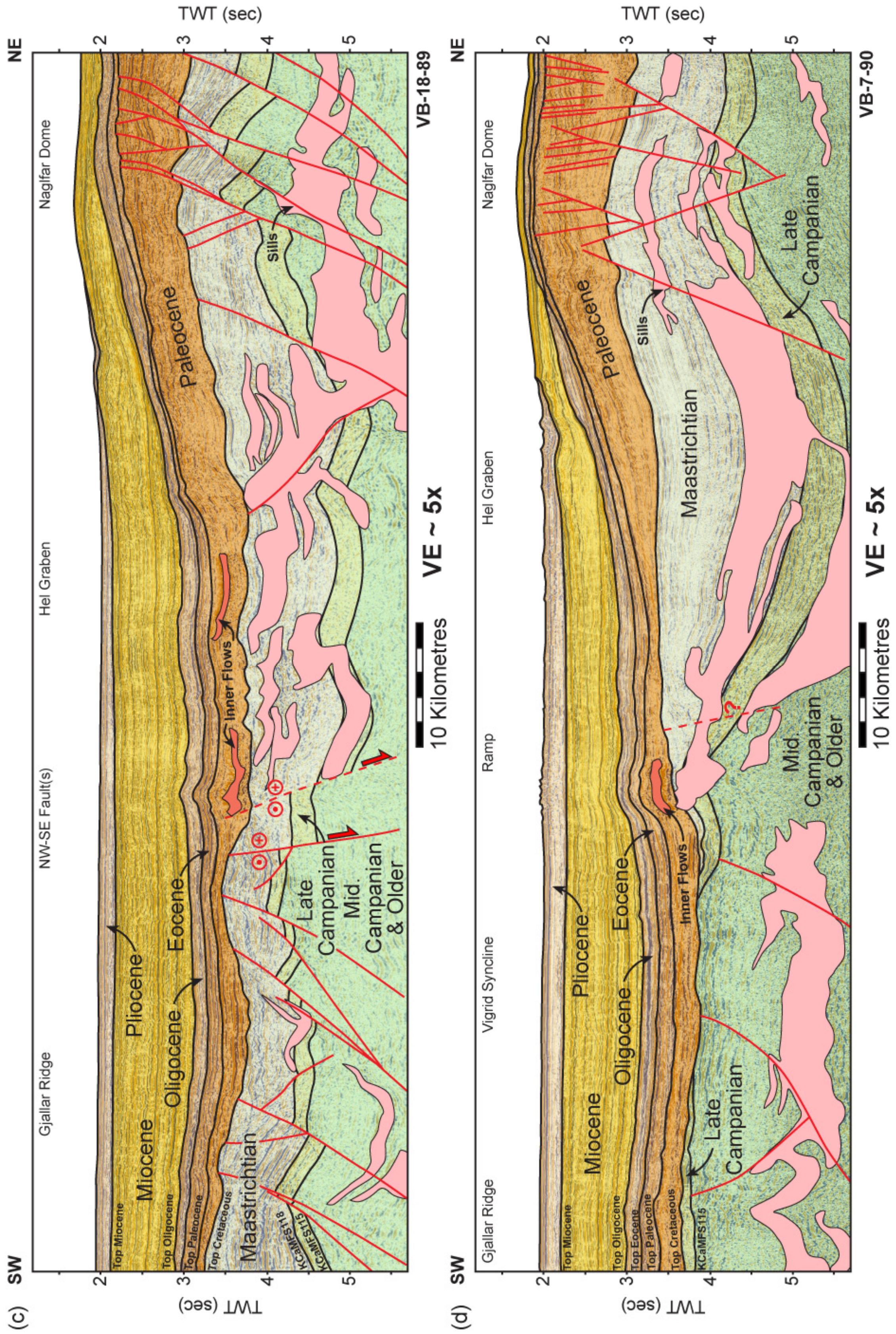

Figure 4.07c & d: The along strike geometry of the Rym Accommodation Zone varies from being (c) fault controlled in the northwest with (d) little evidence of these faults present to the south. In this case, a major ramp (or 'hinge') formed between the Vigrid Syncline and the lower Hel Graben to the northeast. For line locations, see Figure 4.02a.

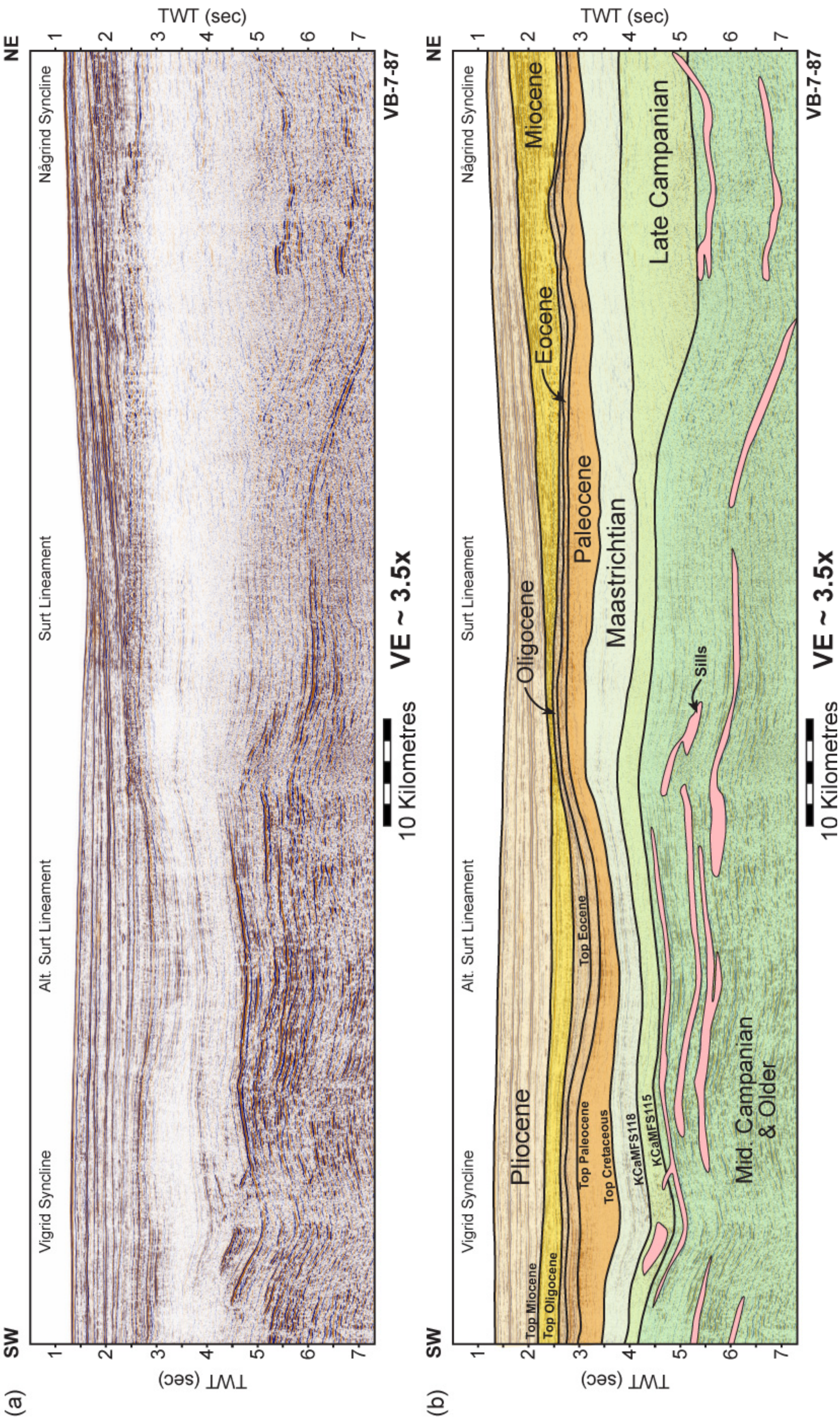

Figure 4.08: (a) Seismic line and (b) interpreted section along the strike of the Vigrid and Någrind Synclines across the inferred location of the Surt Lineaments. Seismic data courtesy of the NPD. For line location, see Figure 4.02a.

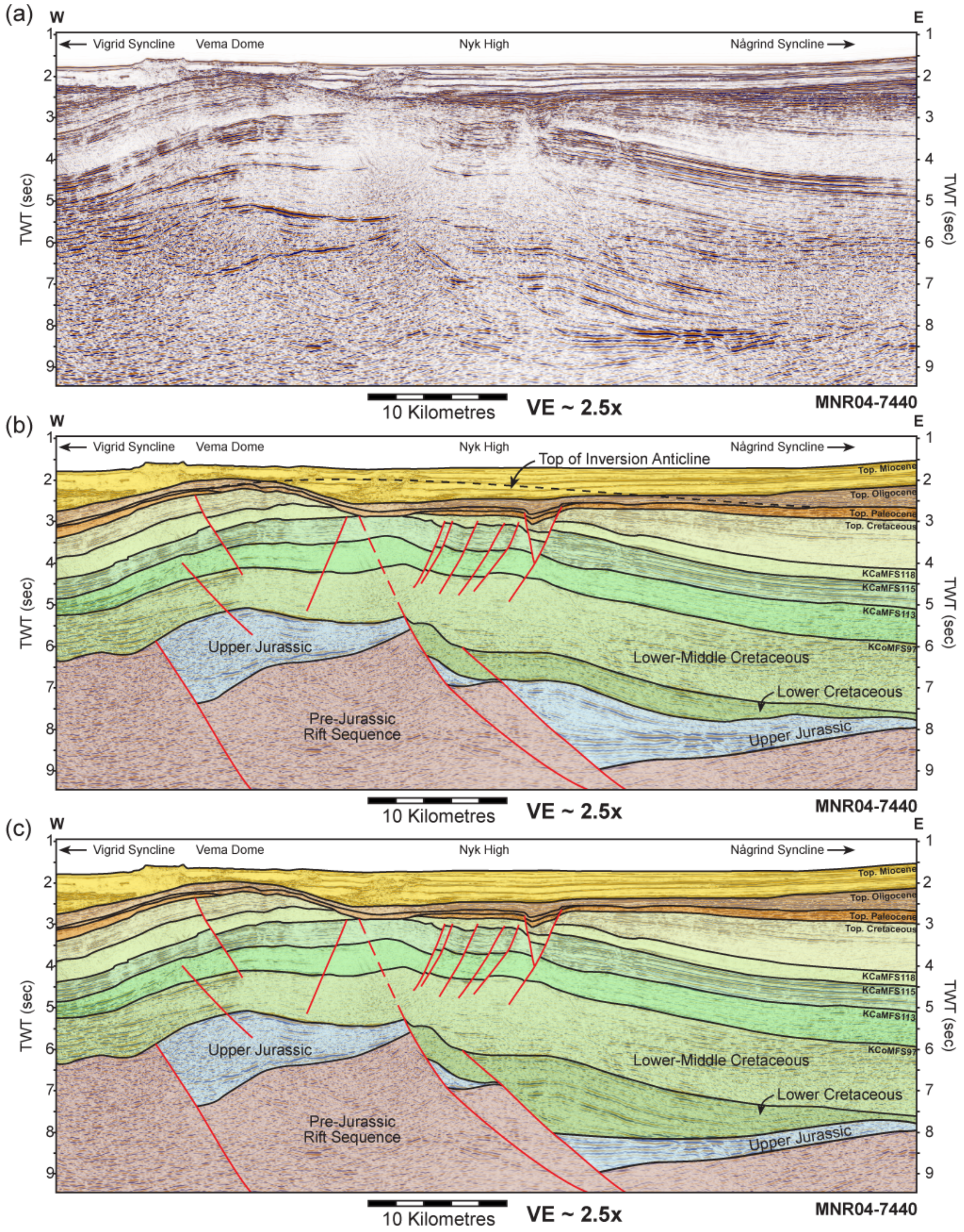

Figure 4.09: (a) Deep seismic line (courtesy of Fugro Multi Client Services) across the Vema Dome, Nyk High and Någrind Syncline. Late Cretaceous – Paleocene rift faults do not appear to reactivate eastward dipping normal faults interpreted as part of an underlying Late Jurassic rift. Two interpretations are provided of the Late Jurassic rift structure. (b) An inversion harpoon formed due to buttressing against the deep Jurassic faults in the Paleocene and Oligo-Miocene leading to uplift and erosion of the overlying strata. Alternatively (c) the harpoon is interpreted as a depositional feature formed due to an infilling of the rift bathymetry in the Early Cretaceous. For line location, see Figure 4.02a.

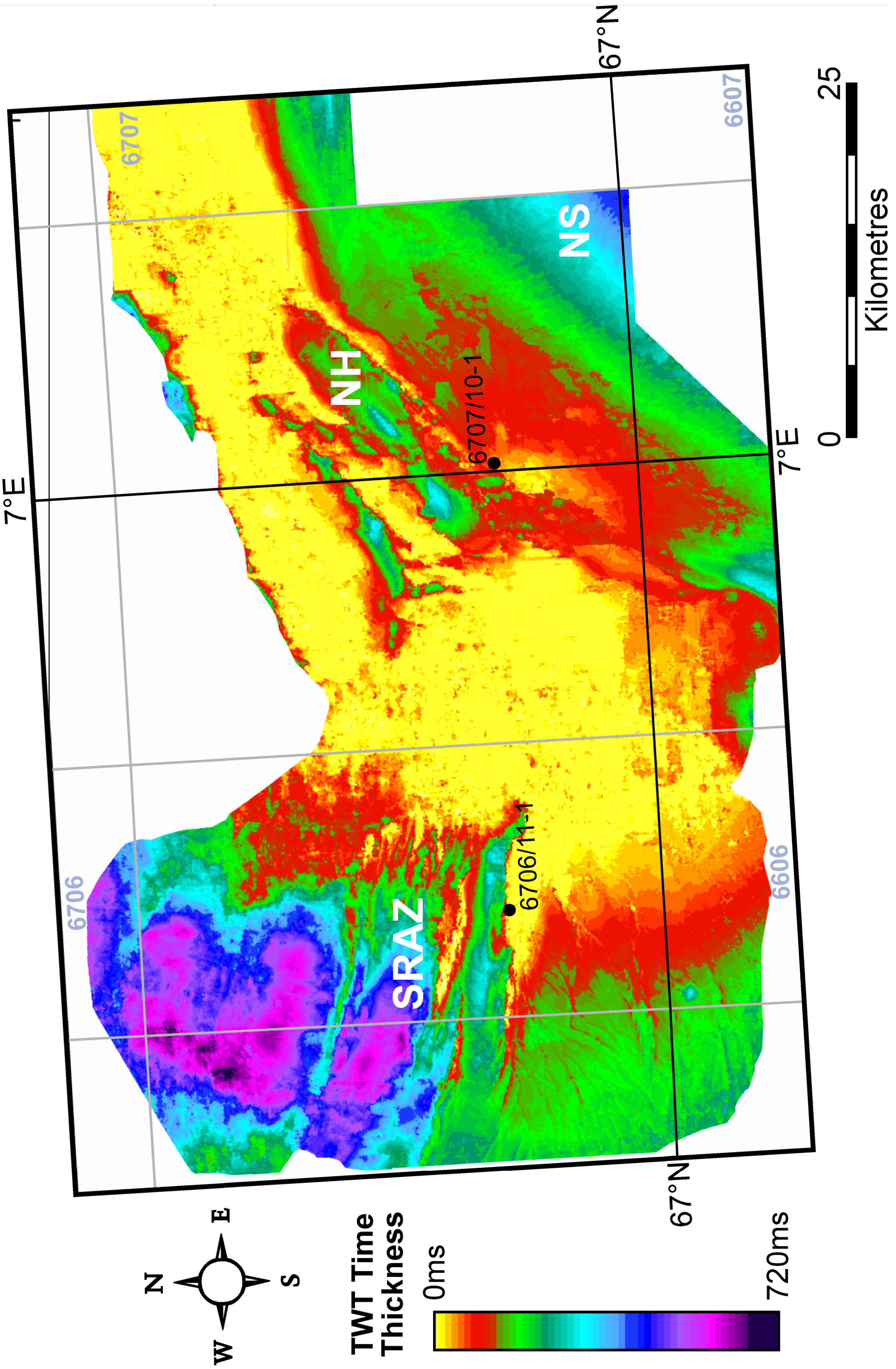

Figure 4.10: Paleocene sediments thin dramatically along a north-south trend between the south-western limit of the Nyk High and the southern Rym Accommodation Zone. Depocentres for the eroded sediment lie to the west and east in syn-tectonic half grabens and the Någrind Syncline respectively. **NH** Nyk High; **SRAZ** Southern Rym Accommodation Zone; **NS** Någrind Syncline.

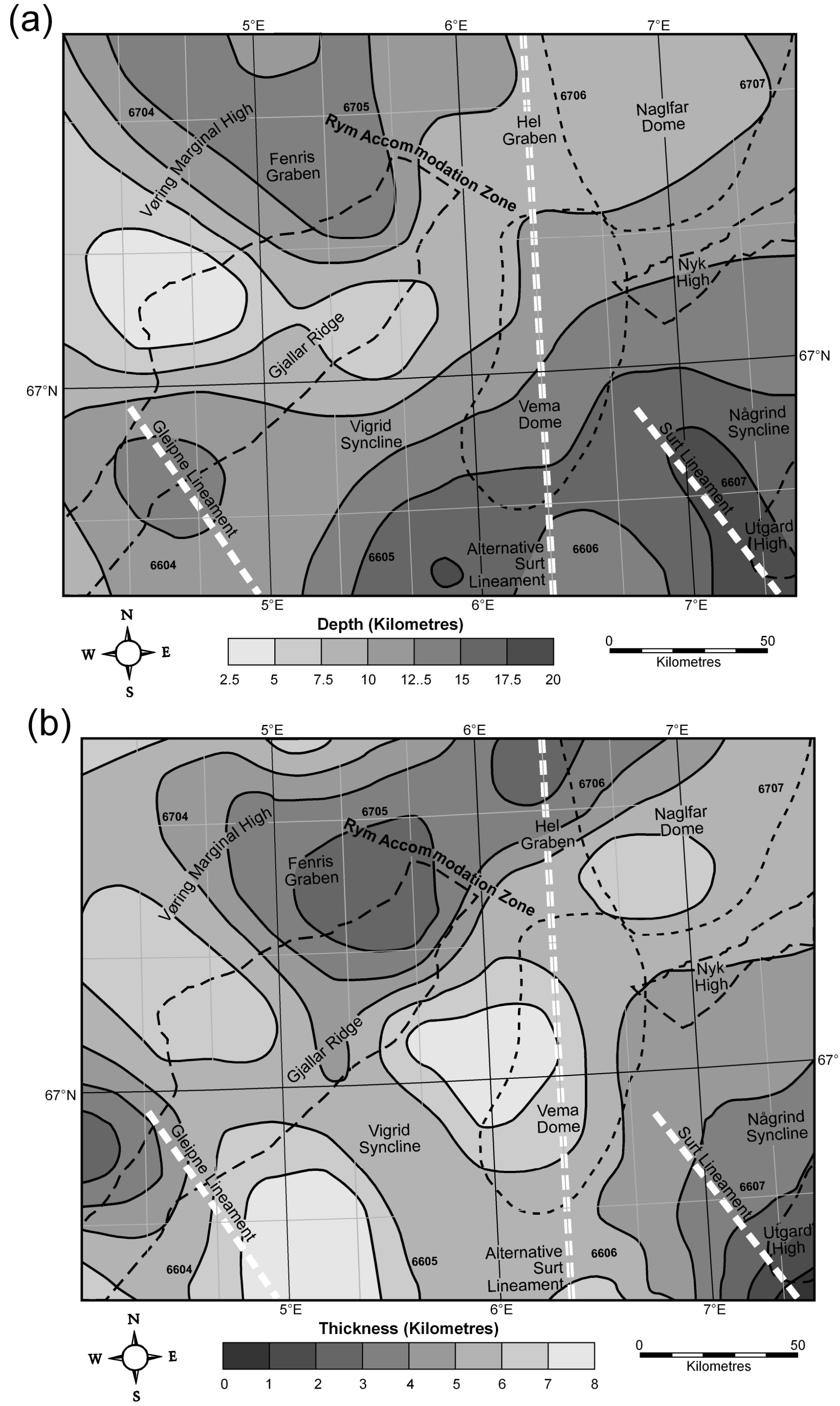

Figure 4.11: (a) Depth to the Lower Crustal Body (LCB) and (b) thickness of LCB after Ebbing *et al.* (2006) in the northern Vøring Basin. The depth to the feature ties well with the Mesozoic – Cenozoic rift features implying the LCB is more likely to be an related to the c. 400 Ma Caledonian Orogen rather than younger Late Cretaceous inferred serpentinisation or Paleocene magmatic underplating. The thickness of the body is also believed to be dominantly controlled by Jurassic rifting and depth-dependent stretching. Dashed lines = outlines of major structural features.

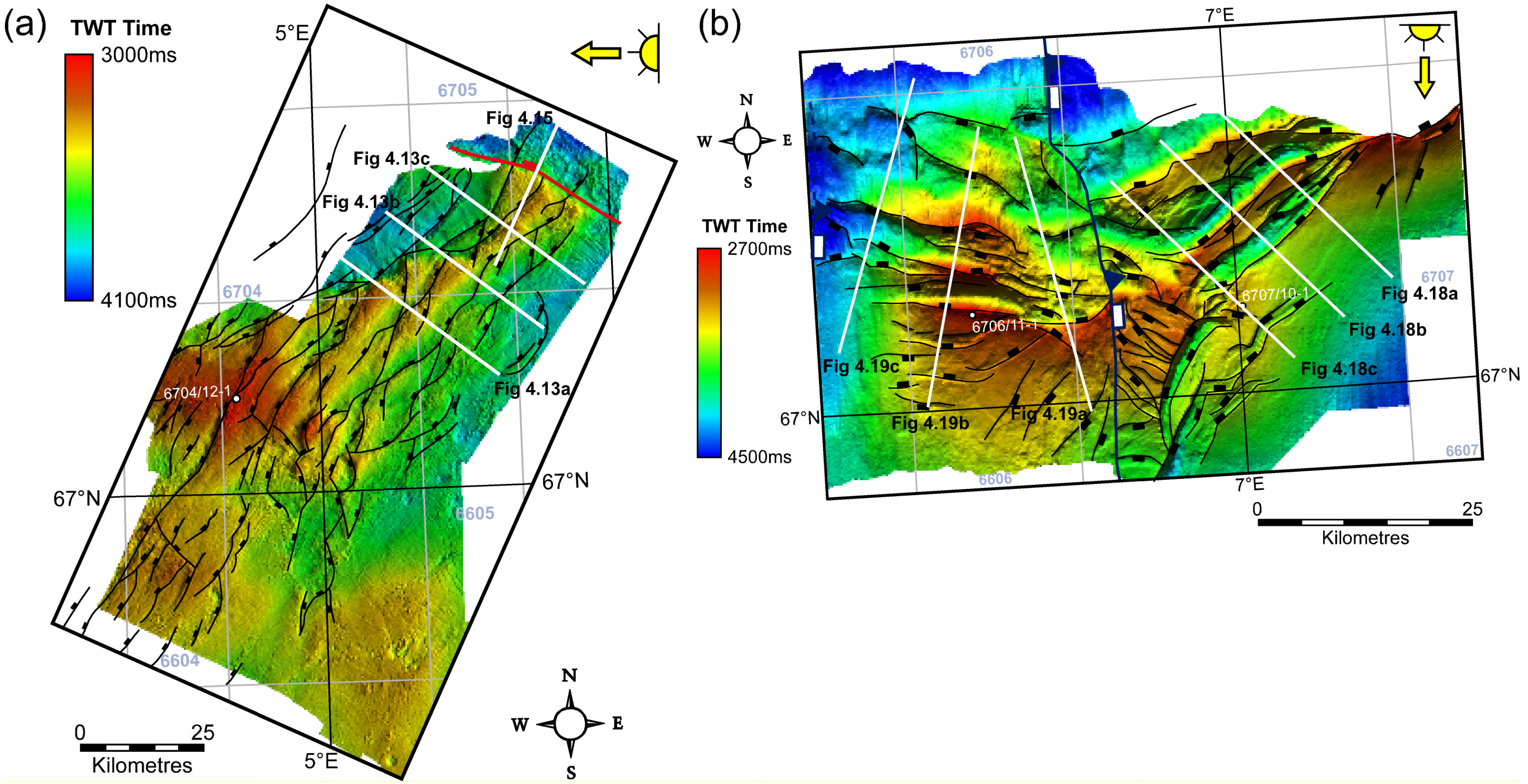

Figure 4.12: Time-structure maps of the principal structural trends in the region of (a) the Gjallar Ridge exhibited at Top Cretaceous level and (b) the Nyk High at KCaMFS115 (Top Nise Sandstone Member) levels. Note the contrasting transitions from the highs into the Rym Accommodation Zone to the northeast and southwest respectively.

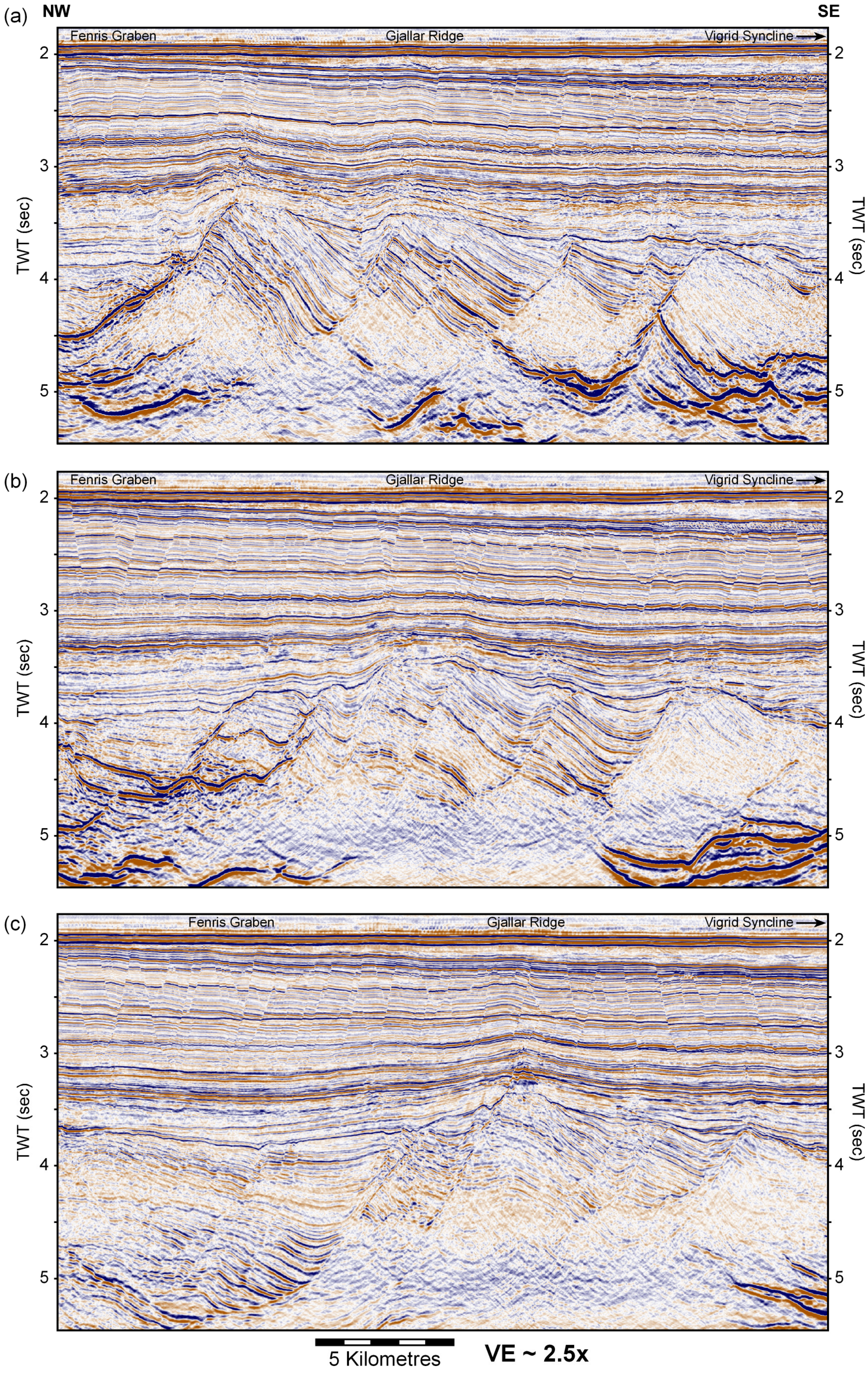

Figure 4.13a, b & c: Seismic lines across the Gjallar Ridge and Fenris Graben. For line locations, see Figure 4.12a. Seismic data courtesy of PGS Geophysical.

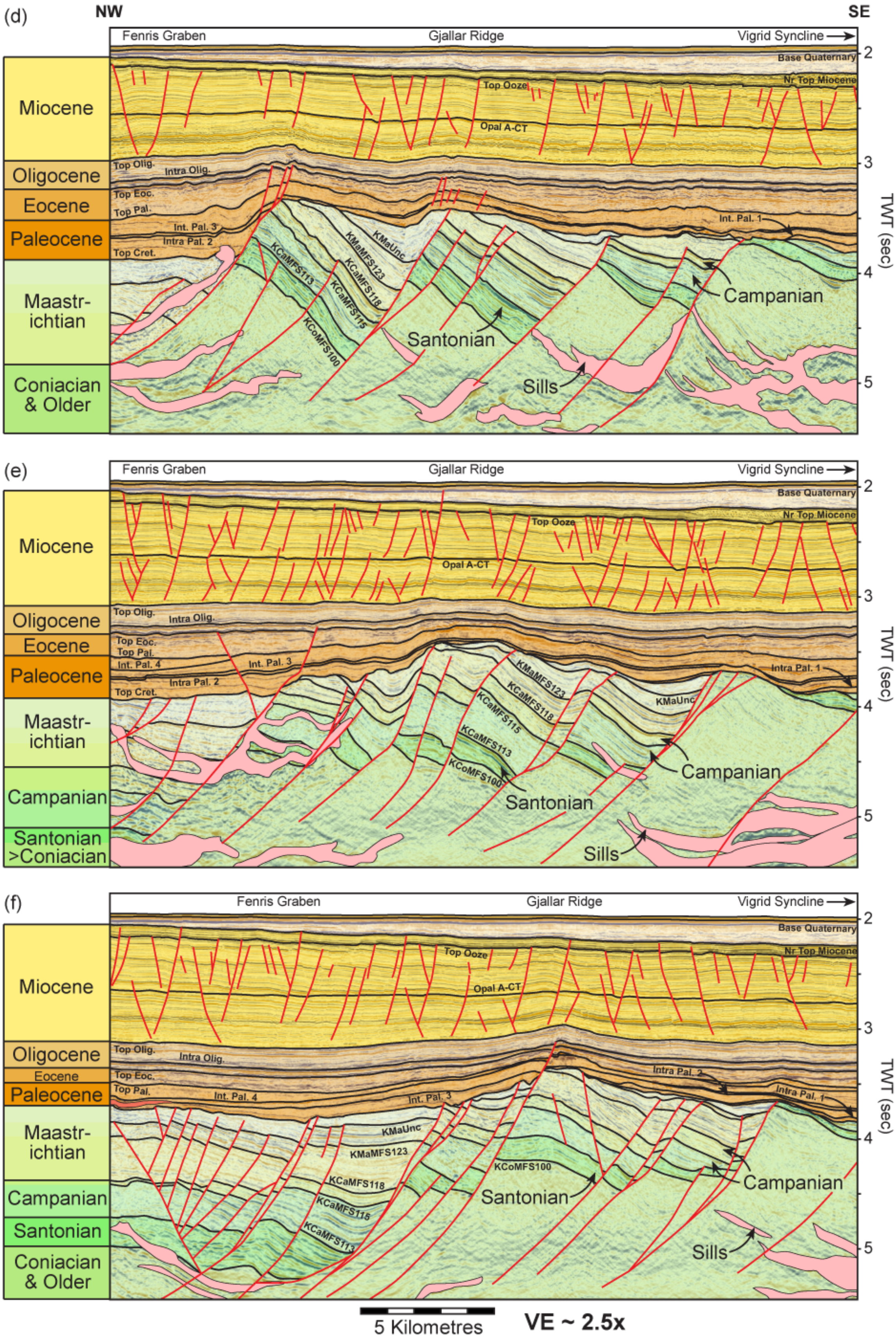

Figure 4.13d, e & f: Interpreted cross sections displaying the along strike variation in the geometry of the Gjallar Ridge and Fenris Graben at the north-western edge of the Vigrid Syncline. For line locations, see Figure 4.12a. Seismic data courtesy of PGS Geophysical.

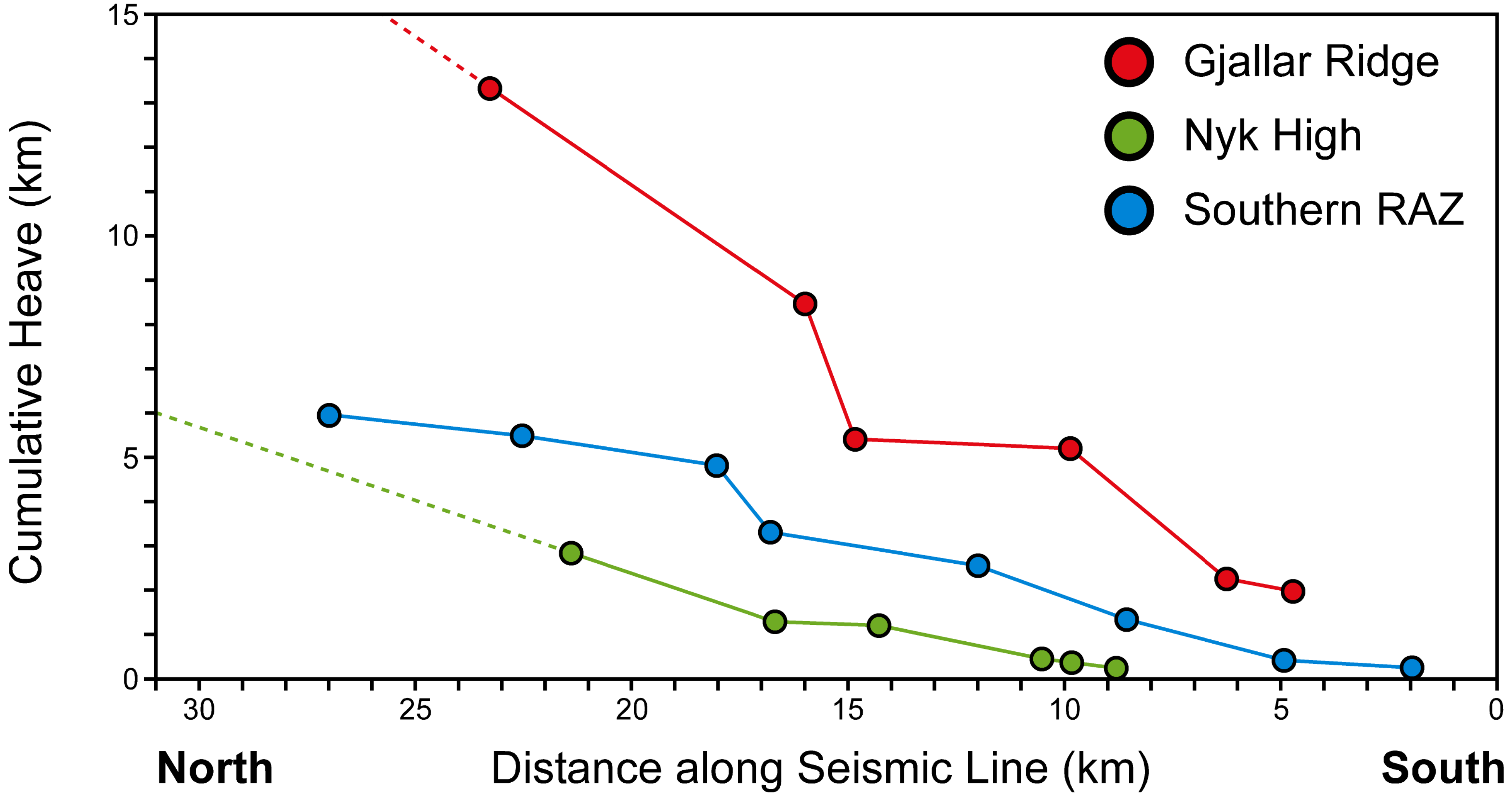

Figure 4.14: Cumulative heave vs. displacement plot for the Gjallar Ridge, Nyk High and southern Rym Accommodation Zone. Fault heaves calculated at the junction between the footwall and hangingwall of the pre-rift sequence which varies locally within the region (**Gjallar Ridge** top pre-rift sequence = KCoMFS100, Fig. 4.13a; **Nyk High** = KCaMFS113, Fig. 4.18b; **Southern RAZ** = KCaMFS118, Fig. 4.19b).

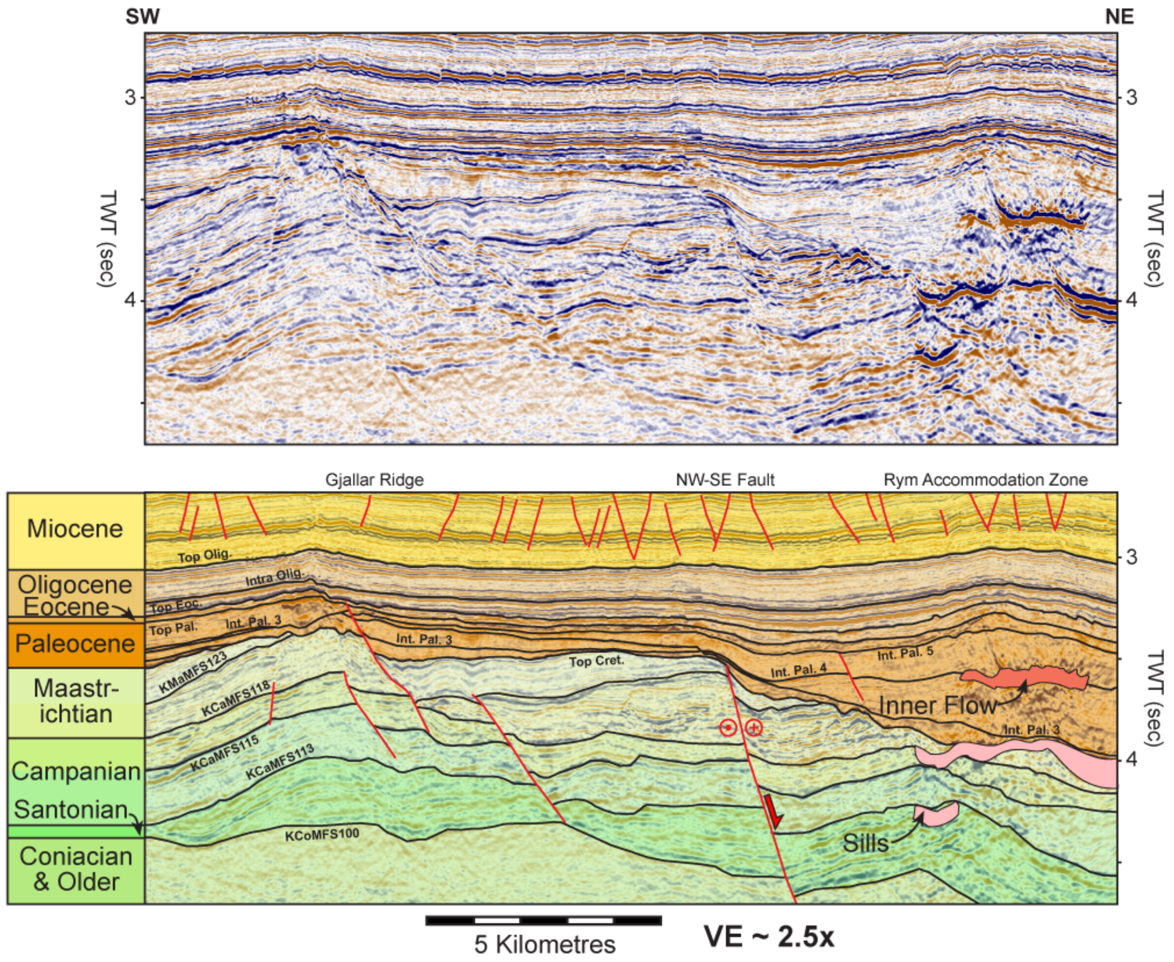

Figure 4.15: The abrupt transition from the Gjallar Ridge into the northern Rym Accommodation Zone is marked by a NW-SE trending normal fault with inferred oblique sinistral movements along it during the Maastrichtian and Paleocene. For line location, see Figure 4.12a. Seismic data courtesy of PGS Geophysical.

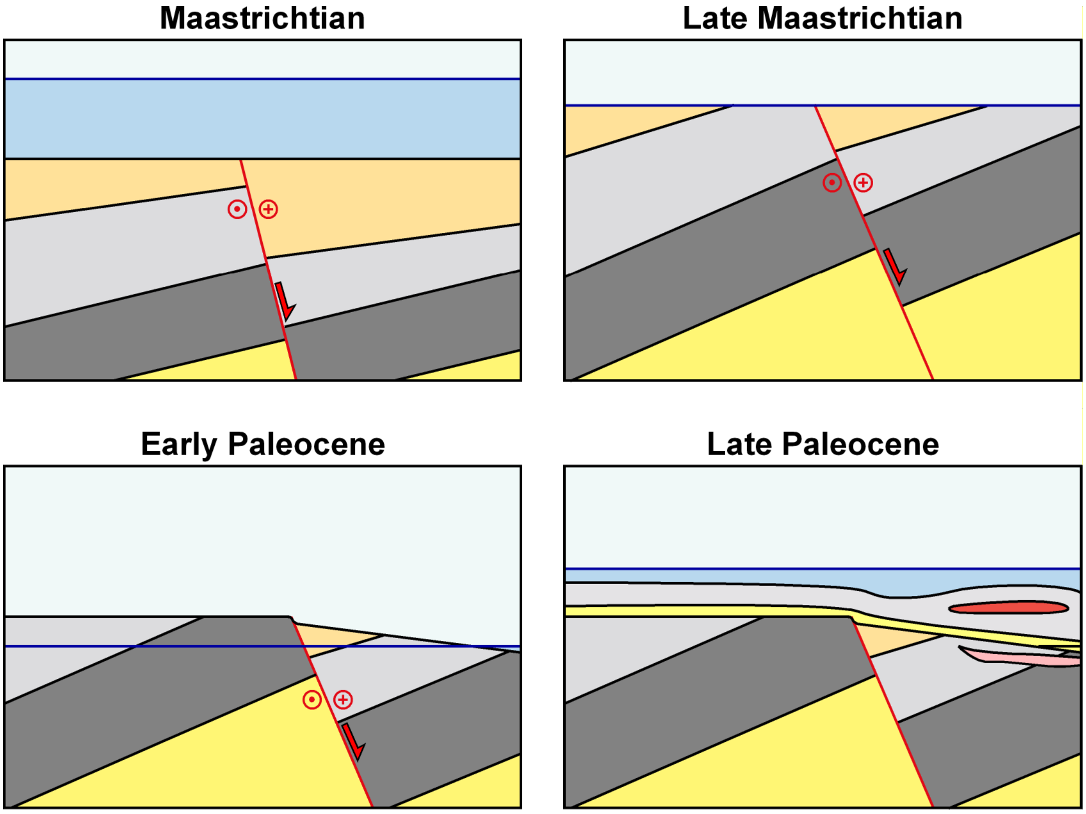

Figure 4.16: Tectonic evolution of the NW-SE fault at the edge of the Gjallar Ridge. A complex interplay between uplift, differential erosion, sedimentation and normal oblique faulting results in complex evolution which is expected to vary along strike. Subsurface geology for illustrative purposes only.

KCaMFS115

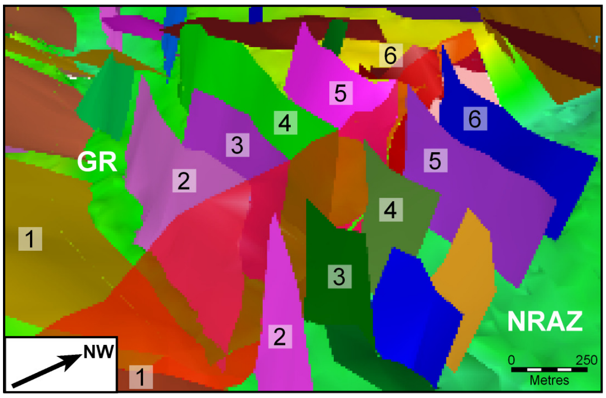

Fault ID	Heave	Throw	Lateral offset	Movement
1	11 m	81 ms	130 m	Dextral
2	198 m	132 ms	48 m	Sinistral
3	109 m	173 ms	58 m	Sinistral
4	353 m	12 ms	157 m	Sinistral
5	64 m	47 ms	98 m	Sinistral
6	46 m	120 ms	111 m	Sinistral

KCaMFS118

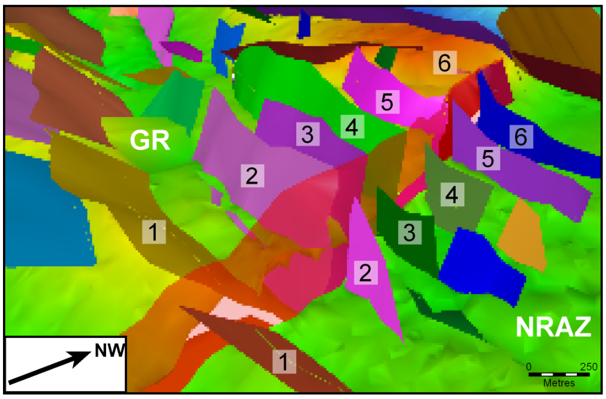

Fault ID	Heave	Throw	Lateral offset	Movement
1	10 m	82 ms	128 m	Dextral
2	126 m	96 ms	101 m	Sinistral
3	106 m	118 ms	54 m	Sinistral
4	201 m	101 ms	151 m	Sinistral
5	63 m	48 ms	97 m	Sinistral
6	42 m	6 ms	103 m	Sinistral

Figure 4.17: Calculated heave, throw and lateral offset for the KCaMFS115 and KCaMFS118 horizons along the NW-SE oblique fault at the north-western edge of the Gjallar Ridge. **GR**, Gjallar Ridge; **NRAZ**, Northern Rym Accommodation Zone.

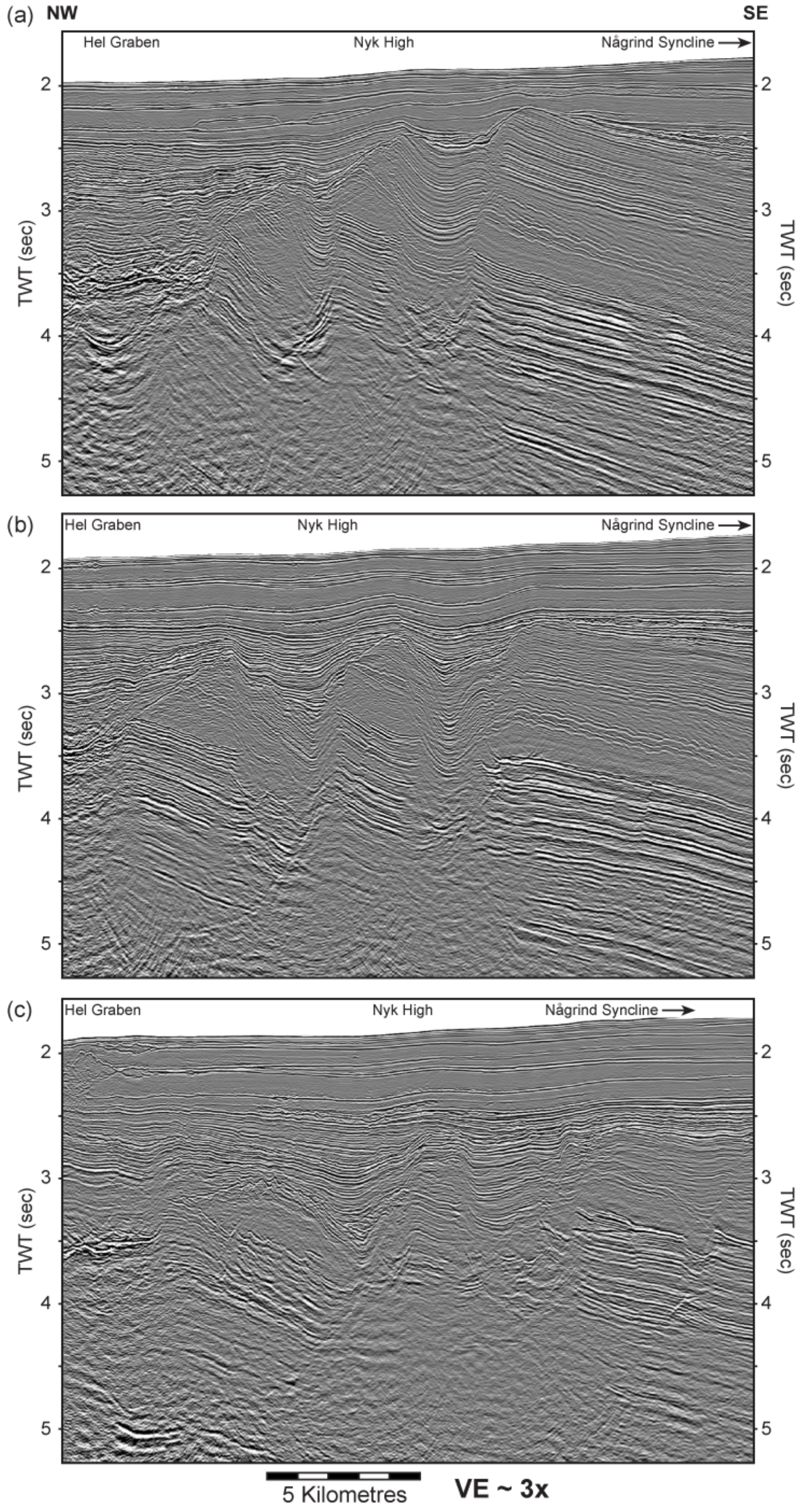

Figure 4.18a, b & c: Seismic lines across the Nyk High and Hel Graben. For line locations, see Figure 4.12b. Seismic data courtesy of PGS Geophysical.

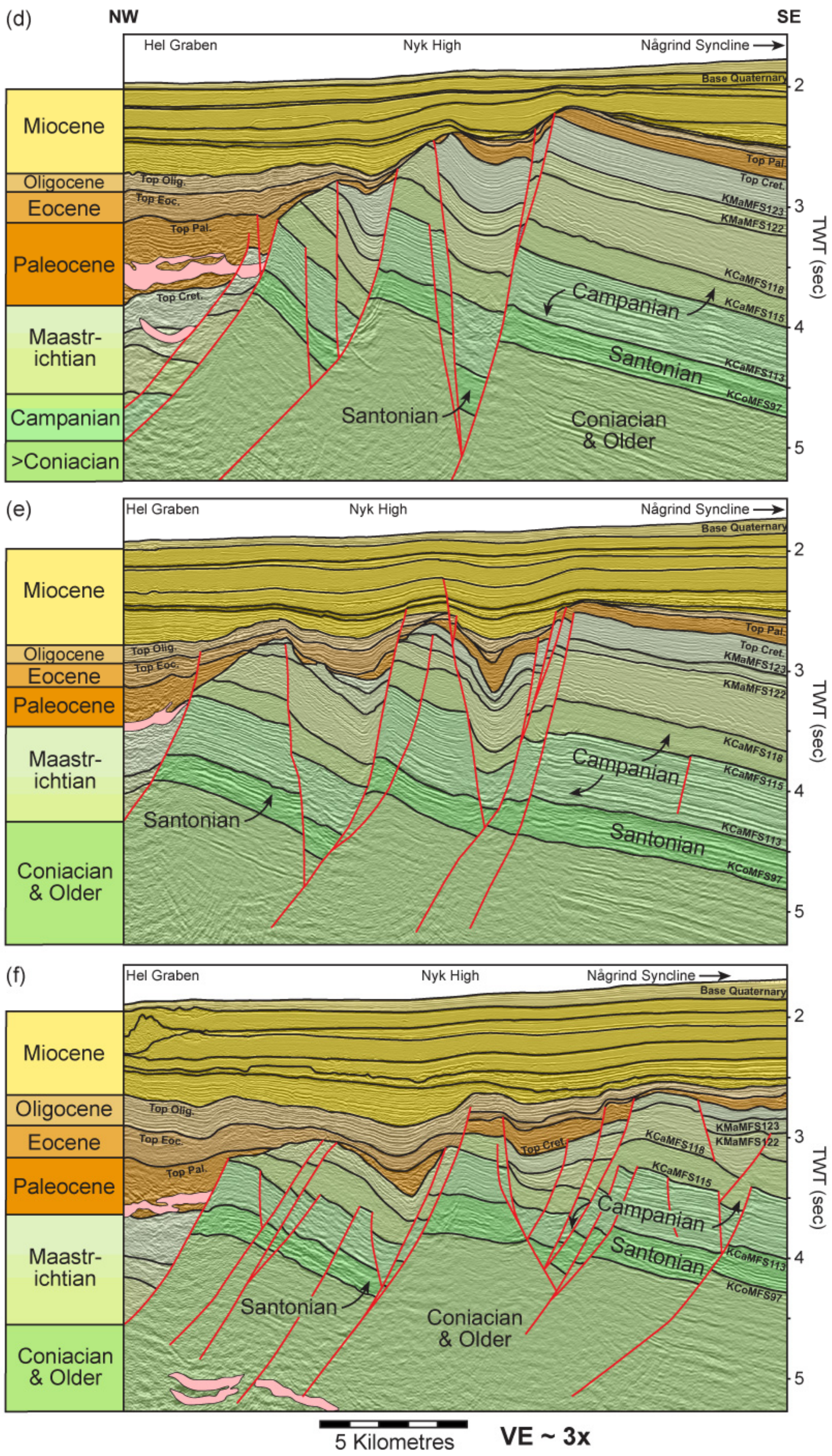

Figure 4.18d, e & f: The structural geometry and kinematics differ to that of the Gjallar Ridge which may tie to the influence of the Lower Crustal Body at depth. A series of horsts and grabens are formed, with the region of deformation widening along strike to the southwest. For line locations, see Figure 4.12b. Seismic data courtesy of PGS Geophysical.

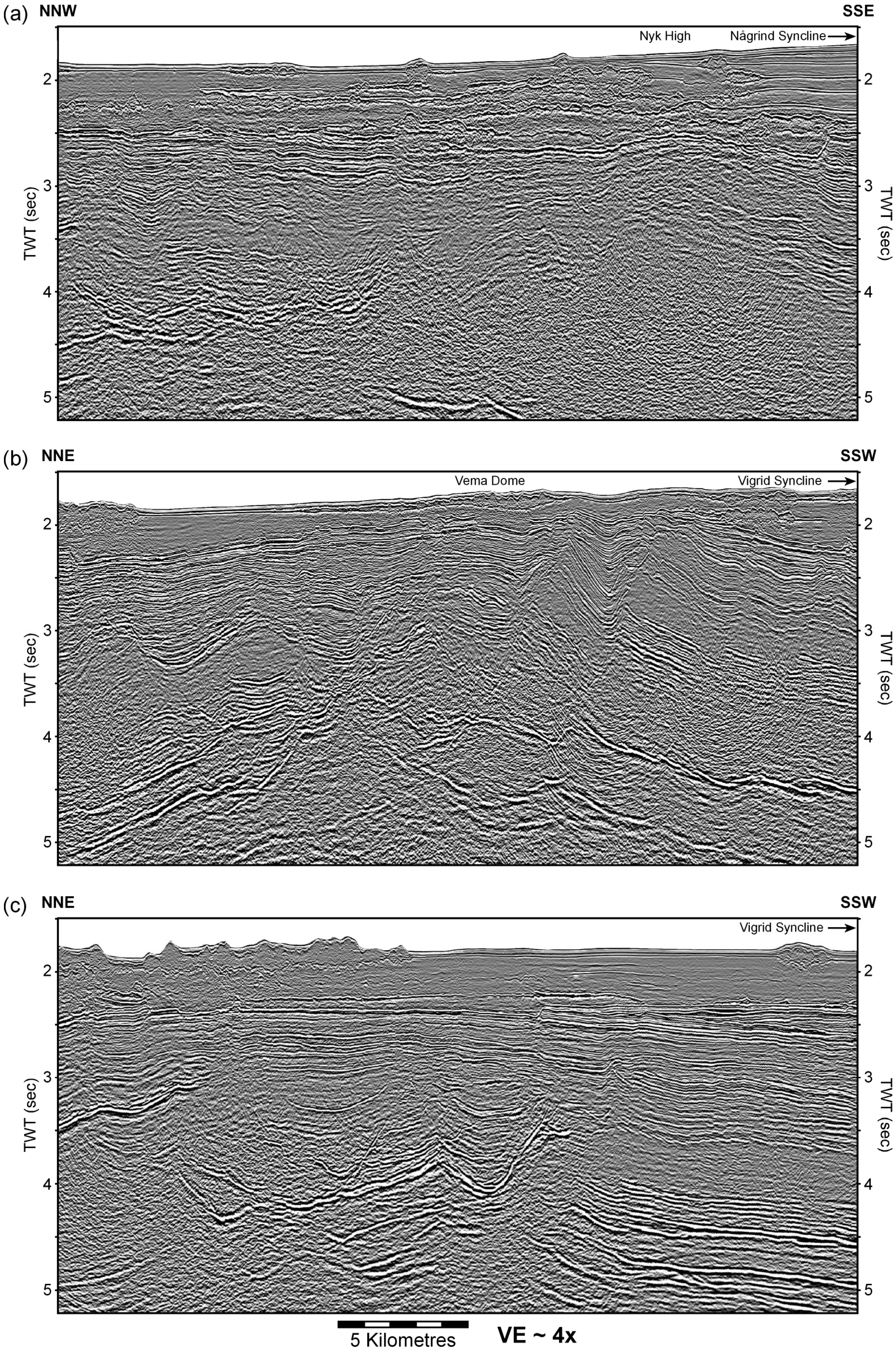

Figure 4.19a, b & c: Seismic lines across the southern Rym Accommodation Zone along strike from the Nyk High. For line locations, see Figure 4.12b. Seismic data courtesy of WesternGeco.

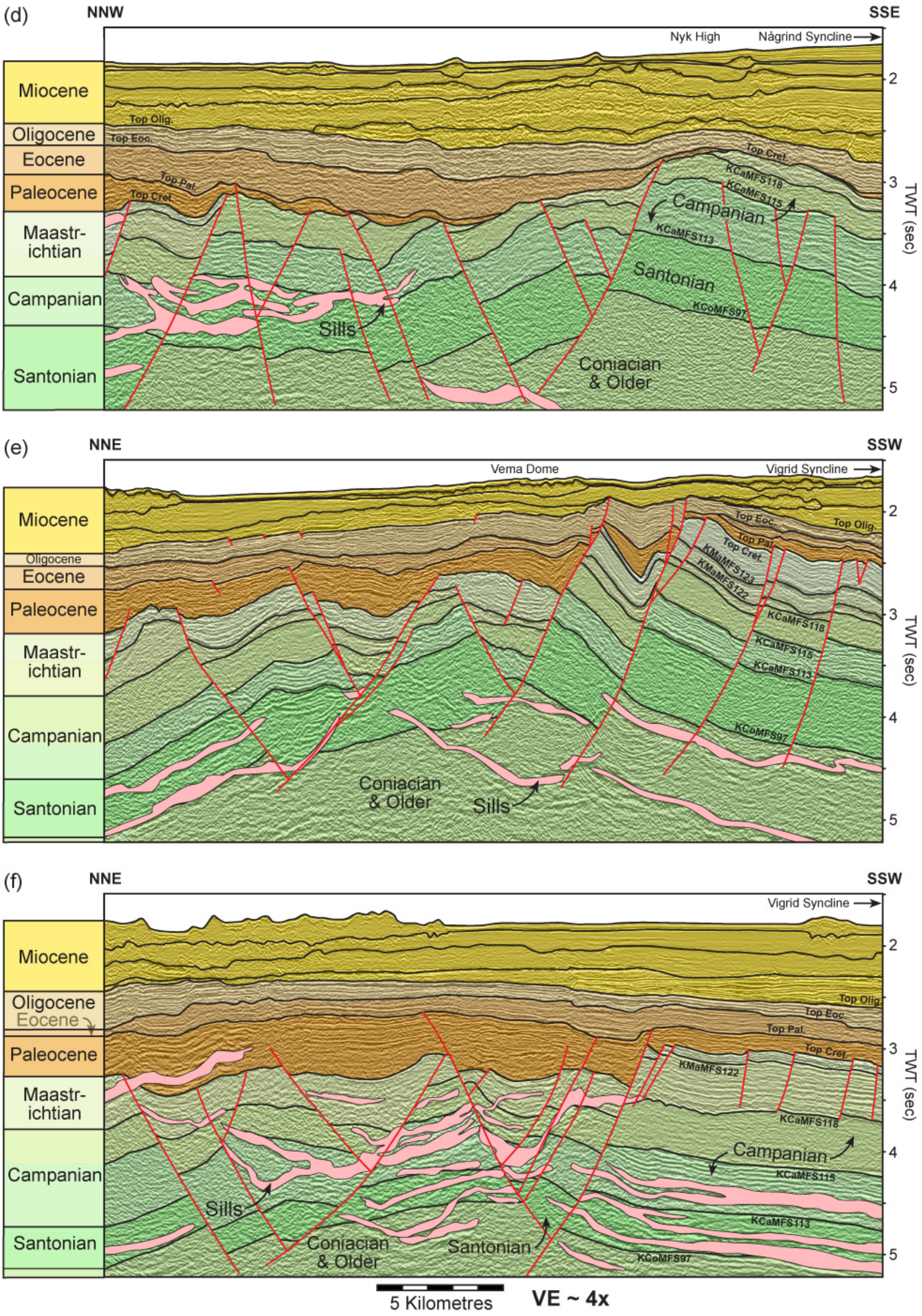

Figure 4.19d, e & f: Structural geometry of dominantly east-west trending faults formed along strike from the Nyk High in the southern Rym Accommodation Zone with evidence for deformation occurring in the Maastrichtian and Paleocene. For line locations, see Figure 4.12b. Seismic data courtesy of WesternGeco.

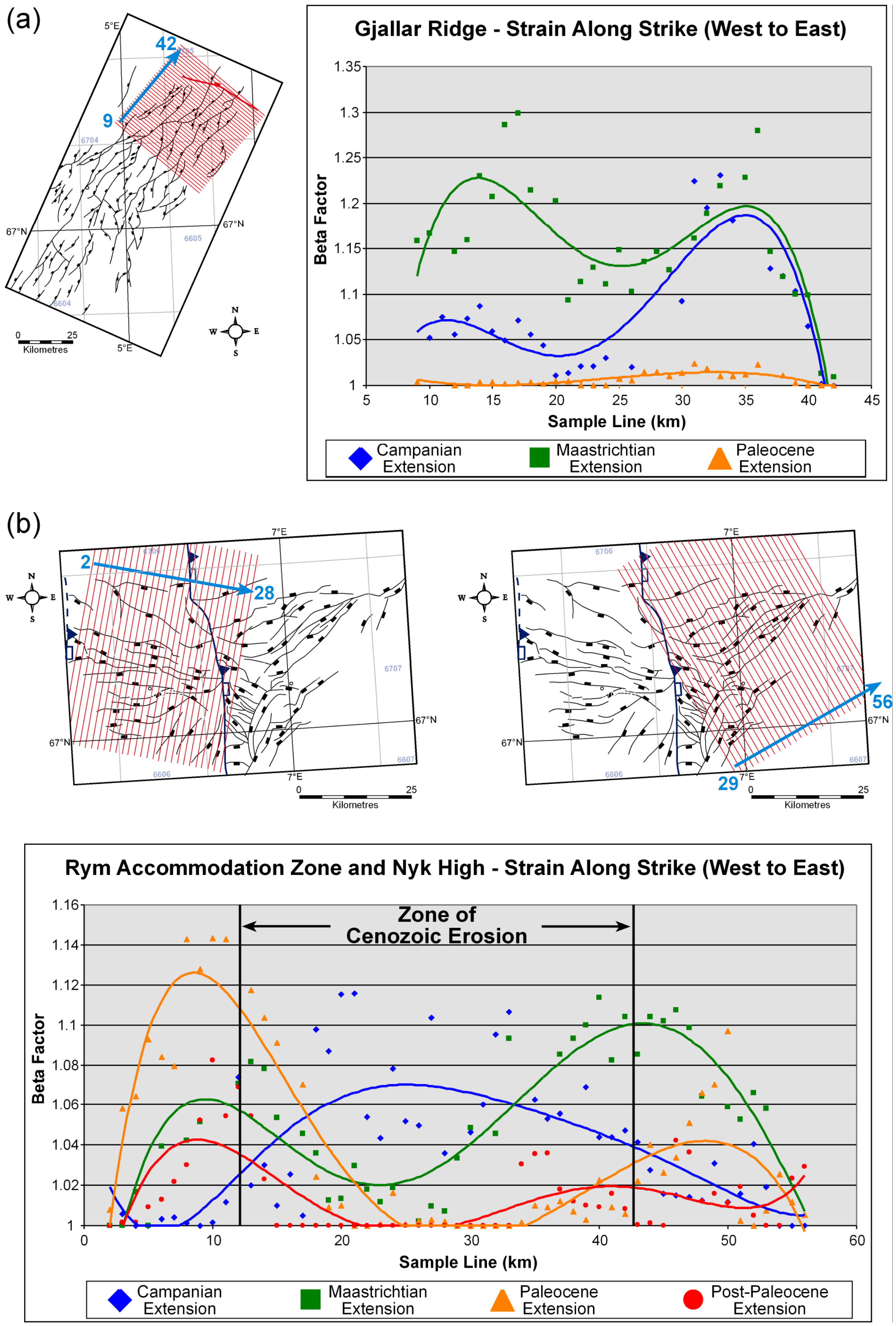

Figure 4.20: Results of an upper crustal strain analysis from fault heaves across (a) the Gjallar Ridge and (b) the Nyk High focussing upon their along strike variation through time in the region of the Rym Accommodation Zone. Rapid reduction occurs in close proximity to NW-SE faulting to the north-western end of the Gjallar Ridge but strain tends to decrease gradually along strike from the Nyk High.

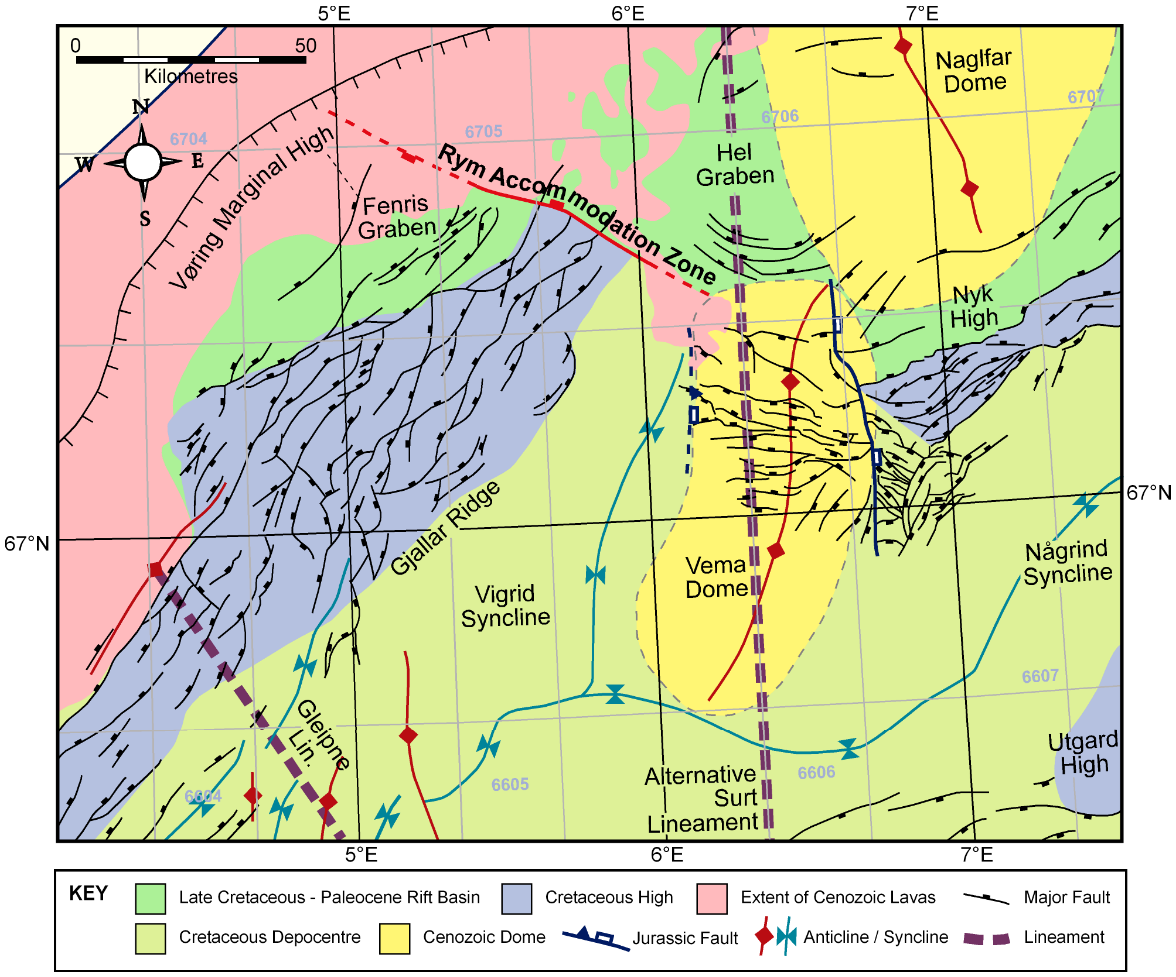

Figure 4.21: New tectonic elements maps from the results of this study displaying the complex interaction between overlying successive rift events (Late Jurassic and Late Cretaceous – Paleocene) and the Cenozoic compressional structures. Rift oblique lineaments identified from various geophysical datasets (modified after Ren *et al.* (2003) and Mjelde *et al.* (2005)) tie well with the recognised features from interpreted multi-channel seismic data analysed within this study.

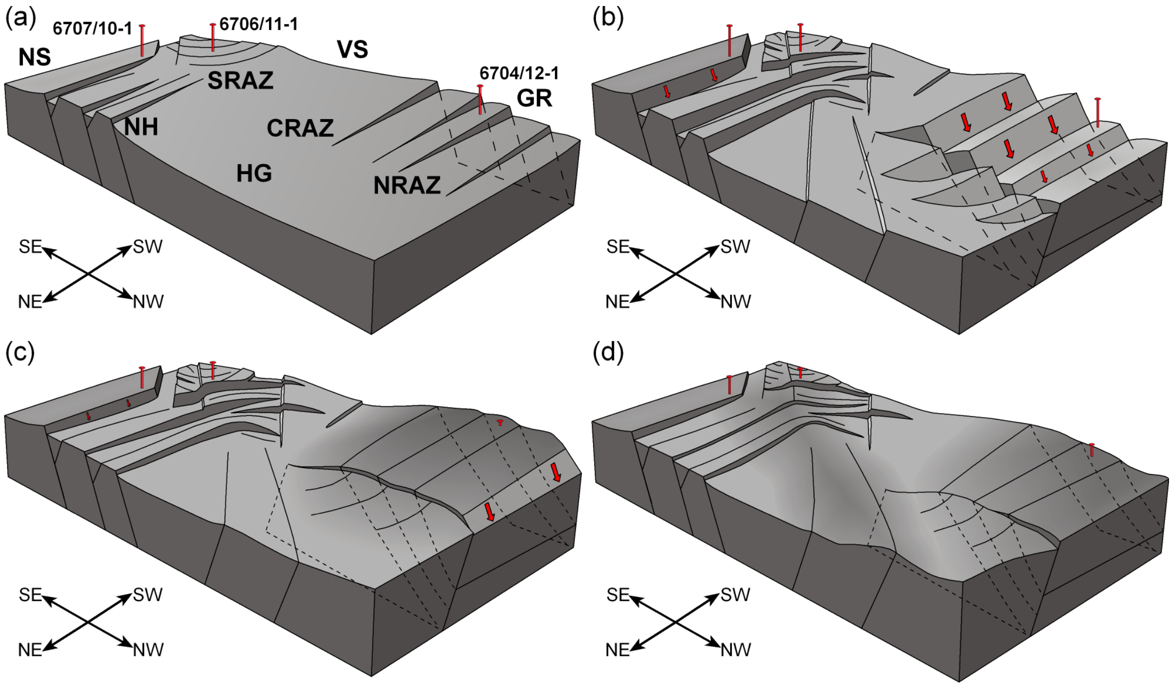

Figure 4.22: Tectonic block models displaying the structural evolution of the northern Vøring Basin which initially started to form due to (a) minor rifting of the Gjallar Ridge and Nyk High during the Campanian. Maastrichtian rifting (b) led to the large scale tectonic development of the Gjallar Ridge and Nyk High and complex faulting in the Rym Accommodation Zone. Regional uplift and erosion of the Gjallar Ridge and Nyk High in the Early Paleocene (c) was synchronous with continued normal faulting along strike from the Nyk High in the Rym Accommodation Zone, an area (d) which experienced concurrent uplift and extension during the Middle-Late Paleocene. **GR** Gjallar Ridge; **NH** Nyk High; **S/C/NRAZ** Southern/Central/Northern Rym Accommodation Zone; **HG** Hel Graben; **VS** Vigrid Syncline; **NS** Någrind Syncline. Each model scale approximately 50 x 100 km.

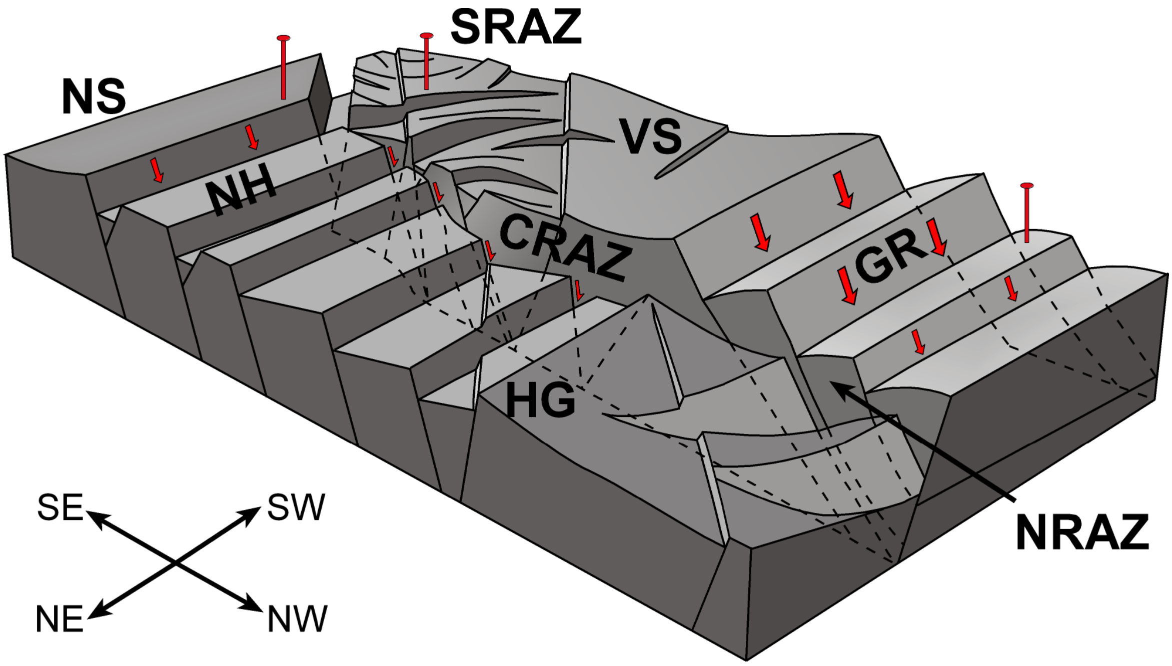

Figure 4.23: A through going 'transfer' fault between the Gjallar Ridge and Nyk High is expected to have evolved in the Rym Accommodation Zone if upper crustal thinning as experienced in the Maastrichtian had continued into the Paleocene. This is due to the increased β factors making it more efficient to fault the ramp rather than increasing the dip, akin to the breaching of a relay ramp. View to the south. **GR** Gjallar Ridge; **NH** Nyk High; **S/C/NRAZ** Southern/Central/Northern Rym Accommodation Zone; **HG** Hel Graben; **VS** Vigrid Syncline; **NS** Någrind Syncline. Model scale approximately 50 x 100 km.

Chapter Five

5 STRATIGRAPHIC AND MAGMATIC EVOLUTION OF SEGMENTED RIFT SYSTEMS

5.1 Abstract

Natural rift systems and passive margins are often inferred to be segmented by discrete structures which influence the stratigraphical and magmatic evolution of the basin and therefore directly influence aspects of the hydrocarbon system. Yet the precise three-dimensional evolution of these structures through time is poorly defined. Using well-calibrated 2D and 3D seismic data, the Vøring Basin offshore Norway is analysed which is segmented by a series of rift-oblique lineaments identified from geophysical datasets. Hypothesised as fault domain boundaries (transfer or accommodation zones), wrench faults or linked to the along-strike variation in the deeper crustal structure, each can control the tectono-stratigraphic and magmatic nature of the rift system differently. The previously defined Rym Accommodation Zone and Gleipne Lineament are the focus for the study which segment the Late Cretaceous – Paleocene rift prior to continental breakup. Results highlight the close structural relationship between the Gleipne Lineament and underlying basement structure, acting as a conduit for sediment to enter the Vøring Basin during phases of rifting. Under periods of minimal upper crustal deformation, the lineament exerts a lesser control upon basinal sedimentation. The Rym Accommodation Zone in contrast does not source sediment into the Vøring Basin, forming upon the south-eastern flank of the rift zone. Instead, the Rym Accommodation Zone compartmentalises the basin during rifting which increases the complexity of the predicted basin fill. Increased Late Paleocene intrusive and extrusive igneous deposits are observed along the strike of both lineaments but are not directly linked to active tectonic deformation.

5.2 Introduction

Rift-oblique lineaments have been recognised from analyses of multiple rift basins and passive margins around the world (Milani & Davison 1988; Morley *et al.* 1990; Nelson *et al.* 1992; Mack & Seager 1995; Doré *et al.* 1997a; Faulds & Varga 1998; Hudson *et al.* 1998; Moustafa 2002). These have commonly been interpreted as fault domain boundaries (c.f. Schlische & Withjack 2009) in the form of accommodation and transfer zones (Faulds & Varga 1998) which segment the rift systems on a variety of scales (e.g. Gawthorpe & Hurst 1993; McClay & White 1995; Ebinger *et al.* 2000; McClay *et al.* 2002). Some rift-oblique lineaments have also been inferred to accommodate major strike-slip movements (e.g. Mogensen *et al.* 2000; Ren *et al.* 2003; Ellis *et al.* 2009). Upper crustal rift segmentation has also been frequently been linked to variations in the basement and deep crustal structure (Ebinger 1989b; Moustafa 1997; Henry 1998; Acocella *et al.* 1999a; Lezzar *et al.* 2002). Not withstanding the deformational style, rift sedimentation is also considered to be influenced by these segmenting structures (Gawthorpe & Hurst 1993; Mack & Seager 1995; Beratan 1998; Young *et al.* 2000; Ellis *et al.* 2009; Khalil & McClay 2009). Similarly, volcanic activity has been tied closely with the segmenting structures as is particularly well recognised in the East African Rift System (Ebinger *et al.* 1989b; Ebinger *et al.* 1993; Bosworth 1994; Ebinger *et al.* 2000; Ebinger & Casey 2001; Abebe *et al.* 2007). Yet the precise structural evolution of these complex 3D structures is poorly defined in natural rift systems, and in particular the precise impact upon the sedimentary and volcanic fill of the basin through time is rarely investigated.

Three dominant fault trends have been recognised from geophysical datasets in the Vøring Basin offshore Norway and elsewhere along the NE Atlantic Margin (e.g. Blystad *et al.* 1995; Doré *et al.* 1997b; Brekke 2000; Mjelde *et al.* 2003b; Kimbell *et al.* 2005) which are oriented NE-SW, N-S and the primary orientation for analysis in this study, the NW-SE rift-oblique 'transfer zone' trend. The two former orientations have been ascribed to the effects of Mesozoic rifting (Doré *et al.* 1997a; Swiecicki *et al.* 1998; Færseth & Lien 2002); however the primary aim of this study is to characterise the tectono-stratigraphic and magmatic nature of the NW-SE rift-oblique trend prior to continental breakup. This is important to better understand the regional evolution of the North Atlantic prior to continental breakup as well as the along strike variation of tectonic deformation on the Norwegian continental margin. In particular, the origin, nature and evolution of segmenting rift structures and the impact these have upon sedimentation and volcanism in the basin are considered, which is of relevance to the hydrocarbon industry due to present day exploration occurring both within the frontier Vøring Basin and elsewhere along the NE Atlantic Margin and conjugate Greenland Margin.

Recent research has focused on the NW-SE lineaments, not only offshore Norway (e.g. Tsikalas *et al.* 2005b; Wilson *et al.* 2006; Tsikalas *et al.* 2008; Chapter 4) but elsewhere along the NE Atlantic Margin (e.g. Kimbell *et al.* 2005; Ellis *et al.* 2009; Moy & Imber 2009; Chapter 3) due to the increasing availability of commercial 2D and 3D seismic data. The lineaments are commonly observed to segment major structural features, resulting in the modification of fault patterns and acting as barriers to fault propagation (Brekke 2000; Tsikalas *et al.* 2001). The lineaments are also considered to be economically important as major hydrocarbon fields have been discovered in close proximity to the trends such as the Paleocene Ormen Lange gas field near to the trend of the Jan Mayen Lineament offshore Norway (Moller *et al.* 2004; Gjelberg *et al.* 2005). The Jan Mayen lineament is considered a major influence on sedimentation patterns (Doré *et al.* 1999; Henriksen *et al.* 2005) and a link between the structural formation of the Ormen

Lange Dome as well as other Cenozoic domes positioned along the length of the Jan Mayen Lineament has been tentatively suggested (Doré *et al.* 2008).

A range of hypotheses for the origin of the rift-oblique lineaments in the Vøring Basin have been proposed as being correlated with heterogeneities within the underlying basement (e.g. Doré *et al.* 1997b; Fichler *et al.* 1999; Skilbrei & Olesen 2005; Ebbing *et al.* 2006). In turn, these hypotheses are inherently linked to the nature and geometry of the deep crustal structure of the margin, and in particular the nature of a high density, high velocity body located at the base of the crust (the Lower Crustal Body; LCB; Mjelde *et al.* 2005; Gernigon *et al.* 2006). Hypotheses for the origin of the LCB range from magmatic underplating to serpentinisation of the mantle as well as high-grade metamorphic rocks associated with the root of the c. 400 Ma Caledonian Orogen (Gernigon *et al.* 2004 and references therein). In Chapter 4, results concluded that the LCB is a long-lived basement feature and is a primary control upon the morphology and evolution of the Norwegian Continental Margin. The origin of the LCB is important for the hydrocarbon industry in view of source rock maturation, timing of migration and basin uplift and subsidence patterns (e.g. Fjeldskaar *et al.* 2009). What is also of critical importance to the hydrocarbon industry is the tectonic nature of the rift-oblique lineaments as, depending upon the style of deformation, each will impact upon the stratigraphical and volcanic fill of the basin, as well as trap types formed in these zones.

Tectonic models of the lineaments offshore Norway generally fall into two schools of thought. Firstly, strike-slip faulting (e.g. Hovland *et al.* 1998; Mogensen *et al.* 2000; Tsikalas *et al.* 2008) as identified in seismic datasets by Harding (1990) or secondly, as fault domain boundaries such as transfer and accommodation zones (e.g. Ren *et al.* 2003; Chapter 4) which although are similar features, conserving and transferring extensional strain between adjacent rift segments, differ dramatically in terms of deformational style

(Faulds & Varga 1998). Fault domain boundaries also form as intrinsic features of the evolving rift system and therefore a key criterion of defining transfer and accommodation zones is that they do not extend beyond the region of active rifting. This is different to strike-slip faults which are not formed through the rifting process and may extend beyond the boundaries of the rift zone. However, these two hypotheses for the rift-oblique lineaments are not mutually exclusive as each rift-oblique lineament upon the Norwegian continental margin has differing crustal characteristics (Ebbing *et al.* 2006) and may have formed by different mechanisms. Therefore it is unlikely that a single model of rift-oblique lineament formation would be applicable to each of the NW-SE oriented lineaments identified upon the NE Atlantic Margin. A third hypothesis for the tectonic nature of the lineaments is that they are inherently related to the deep crustal structure. Variation in the thickness and relief of the deep basement structure may also influence the formation of rift-oblique lineaments forming long-lived structural lows and highs which are expected to be enhanced during periods of basin-scale uplift and subsidence (Gernigon *et al.* 2004), but not linked to major fault activity. The lineament can therefore also extend outside the rift zone as it will not be directly formed due to the rift-related faulting. The use of well-constrained 2D and in particular 3D seismic mapping is critical for a clearer definition of the structural styles based upon the criteria described above.

5.2.1 Influence on basin sedimentation

Previous authors (e.g. Fjellanger *et al.* 2005; Lien 2005) have made inferences that the lineaments acted as conduits for sediment to enter the Vøring Basin from the north and west prior to continental breakup. Little evidence has supported this interpretation of the lineaments which has largely been drawn from their preferential orientation and inferred segmentation of the rift structure. Depending on the style of deformation associated with the lineaments, the predicted stratigraphic fill will vary. Identification of strike-slip related deformation from seismic datasets (Harding 1990) can lead to the inference of complex sedimentation patterns (e.g. May *et al.* 1993). This includes the juxtaposition of sedimentary rocks across faults with abrupt variations in thickness and facies of individual stratigraphical units (Christie-Blick & Biddle 1985). The recognised sedimentation patterns within wrench settings differ greatly to the distribution of sedimentation in and around fault domain boundaries. Accommodation zones are considered as entry points for sediment into rift systems transported along major relay ramps formed between the overlapping normal faults (e.g. Gawthorpe & Hurst 1993; Whitham *et al.* 1999; Younes & McClay 2002; Khalil & McClay 2009). With transfer zones, much less is known regarding the impact of rift-oblique faulting in rift systems, however onshore studies in the Basin and Range have suggested sediments flow along the rift axis and where crossing the transfer zone form point sourced fan systems within the transfer zone hangingwall (Beratan 1998). Similarly, rift-oblique faulting may also increase the compartmentalisation of basin sediments (Faulds & Varga 1998). If the lineaments are tied directly to vertical changes in the basement relief, increased sediment infill is expected to occur along the strike of the lineament during periods of subsidence but notable thinning and possible erosion of the strata would occur during periods of relative uplift. Similarly, the type of sediment entering the rift system may be linked to periods of subsidence and uplift (e.g. Gawthorpe *et al.* 1994). Therefore, whichever the structural origin for the rift-oblique lineaments, they are expected to have a direct influence on styles of sediment distribution in the Vøring Basin under rift conditions.

Using 3D seismic data, amplitude extractions of mapped horizons can help to define depositional processes, and highlight areas of sand and mud prone deposition, for example in marine fan systems (e.g. Fugelli & Olsen 2005). The characteristics of a lithology are often contained within the seismic response of the reflection, and the challenge for seismic analysis is to provide an accurate interpretation of these responses. Each geological characterisation of the 3D seismic data requires a framework for comparison with tectonic history, stratigraphy, depositional system and lithofacies (Vail *et al.* 1977). In this context, regional well data has proved crucial in linking the observed seismic response with directly sampled well data. In combination with the mapping of fault structures identified from seismic data, an integrated tectono-stratigraphic approach can be used to address the problem.

5.2.2 Influence on the emplacement of igneous material in basins

Accommodation and transfer zones have also been recognised to exert an influence on the emplacement of igneous material in rift basins (e.g. Corti *et al.* 2003 and references therein). This takes the form of intruded sills and dykes as well as the formation of volcanoes and extrusive products within the fault domain boundaries. Equally, basic igneous material is a characteristic of pull-apart basins due to their great depths as displayed in a variety of basins around the world (e.g. Harding 1974; Rocchi *et al.* 2003; Schaltegger & Brack 2007). The influence of basement relief and thickness upon the emplacement of igneous bodies is poorly defined, although it may be hypothesised that regions with low basement relief (associated with a thick sedimentary cover sequence) may be more prone to sill intrusion than if the opposite is true. Cartwright & Hansen (2006) inferred the sills in the Vøring Basin to be sourced from the LCB which was suggested to be of a magmatic origin. However the LCB fails to display any high amplitude (sill) reflections within the body itself, but if the LCB is of a basement origin it would suggest the sills do not preferentially intrude the basement (Gernigon *et al.* 2004). Therefore if the LCB is of increased thickness this may block the intrusion of magmatic material into the basin. Variation in the relative concentration of igneous material have previously been illustrated to be linked with the NW-SE lineaments upon the Norwegian

Margin (Brekke 2000; Ren *et al.* 2003; Tsikalas *et al.* 2005b; 2008), however their mode of emplacement and the overriding influence of the tectonic lineaments remains unclear. This forms the final hypothesis, that the NW-SE lineaments exert an influence upon the spatial distribution of both intrusive and extrusive igneous material in the basin by focussing the distribution of igneous material along the length of the rift-oblique lineaments. The style of tectonic deformation may also impact upon the nature of the emplaced igneous material. The nature of the processes for the emplacement of igneous material can be tested in 3D seismic data due to the large acoustic impedance contrasts generated at the sediment-volcanic interface (Planke & Eldholm 1994; Berndt *et al.* 2000) as well as the mapping of the igneous bodies.

The primary aim of this study is to analyse the impact of two rift-oblique lineaments identified from geophysical datasets upon the tectono-stratigraphic and magmatic evolution of the Vøring Basin, offshore Norway immediately prior to passive margin formation. Using 2D and 3D seismic data constrained by three exploration wells, a four dimensional analysis of the tectonics, stratigraphic and magmatic fill of the Vøring Basin is performed. 3D seismic data has allowed for the seismic stratigraphical analysis and mapping of structural and volcanic features which are often poorly constrained from 2D reflection seismic data. In locations where 3D coverage was not available, 2D seismic data was of benefit to improve the context of the results on a regional scale. It is of critical importance to analyse all aspects of the evolving rift system to fully understand the significance of the NW-SE lineaments. This will result in a thorough analysis as to the growth, nature and ultimately the significance of these features during the Late Cretaceous – Paleocene phase of continental extension which culminated in continental breakup in the earliest Eocene. It is believed that the results of this study will impact upon research and hydrocarbon exploration in other segmented volcanic passive margins worldwide including the U.S East Coast Atlantic Margin (e.g. Behn & Lin 2000), East Greenland (e.g. Karson & Brooks 1999), the south Atlantic (e.g. Franke *et al.* 2007) and other basins cited by Coffin & Eldholm (1994).

5.3 Geological evolution

The present day mid-Norwegian continental margin has developed as a result of several successive compressional and extensional events. Closure of the Iapetus Ocean in the Silurian – Early Devonian (Bukovics & Ziegler 1985) led to the formation of the Caledonian Orogen which underwent orogenic collapse during the Early – Middle Devonian, the extended remains of which are expected to constitute the basement rocks which underlie the present day NE Atlantic Margin (Andersen 1998; Osmundsen *et al.* 2002; Ebbing *et al.* 2006). A series of younger rift events have occurred in the region during the Carboniferous, Late Permian – Early Triassic, Late Jurassic – Early Cretaceous and Late Cretaceous – Paleocene (Ziegler 1988; Blystad *et al.* 1995; Lundin & Doré 1997; Doré *et al.* 1999; Roberts *et al.* 1999; Brekke 2000; Færseth & Lien 2002) which culminated in continental breakup between Norway and Greenland during the latest Paleocene – Early Eocene (c. 55 Ma; Eldholm *et al.* 2002; Mjelde *et al.* 2007). Associated with continental breakup was voluminous magmatic activity which was manifest as a sequence of intrusive and extrusive igneous rocks in the Vøring Basin (Skogseid *et al.* 1992; Eldholm & Grue 1994; Planke *et al.* 2000; Skogseid *et al.* 2000). These earlier events, which have been subsequently modified by Cenozoic compressional deformation (see Doré *et al.* 2008 and references therein), have fashioned the Norwegian continental passive margin as observed today (Fig. 5.01).

The northern Vøring Basin is the result of Campanian – Paleocene rifting (25 – 27 Myr in duration; Færseth & Lien 2002) and is characterised by two prominent structural highs; the Gjallar Ridge and Nyk High (Fig. 5.02a). These are formed at the north-western edge of the Vigrid and Någrind Synclines respectively with the Fenris and Hel Grabens located to the northwest. The two rift segments are laterally discontinuous across the Rym Accommodation Zone (RAZ) which is structurally complex with diverse NW-SE and E-W fault trends present in contrast to the dominant NE-SW trend characterised by the Gjallar Ridge and Nyk High faults (Chapter 4). The area is further complicated by the addition of extrusive volcanic material primarily deposited at the Vøring Marginal High and as the 'inner flows' which are mapped within the RAZ and to the northwest of the Gleipne Saddle (Planke *et al.* 2000; Ren *et al.* 2003; Tsikalas *et al.* 2008). The Vema and Naglfar Domes are structurally uplifted areas; these are of Oligo-Miocene age and their influence on the latter stage of basin evolution is not considered in this study.

This study focuses upon two zones of rift segmentation in the northern Vøring Basin, namely the aforementioned Rym Accommodation Zone (RAZ) and Gleipne Lineament (Fig. 5.02a). The NW-SE trending RAZ is located at the northern end of the NW-SE Surt Lineament which was first recognised by Blystad *et al.* (1995). The orientation of the lineament was changed to north-south by Mjelde *et al.* (2003b; 2005) on the basis of results from seismic refraction datasets. In Chapter 4 the north-south version of the lineament was inferred to be linked to Jurassic normal faulting which underlies the outer Vøring Basin with little evidence of the NW-SE Surt Lineament at upper crustal levels. The RAZ was initially defined as an accommodation zone by Ren *et al.* (2003) which was corroborated by the results of Chapter 4 using the terminology of Faulds & Varga (1998). For the purposes of this study, the RAZ is split into distinct regions to allow for a better definition of the structural styles, stratigraphic and magmatic evolution of the zone. The northern RAZ is located along strike from the Gjallar Ridge and Hel Graben, the central RAZ between the Vigrid Syncline and Hel Graben and the southern RAZ located along strike of the southwest termination of the Nyk High.

The Gleipne Lineament was originally defined as a continental extension of the oceanic Gleipne Fracture Zone by Blystad *et al.* (1995) but more recent work shows that this previously interpreted oceanic transform fault was the result of inadequate potential field data acquisition and processing (Tsikalas *et al.* 2002; Ebbing *et al.* 2006; Olesen *et al.* 2007). Although the interpretation of a continental 'Gleipne Lineament' had also been previously inferred by Fichler *et al.* (1999) and Ren *et al.* (2003) it may therefore need to be reassessed. Lundin & Doré (1997) and Gernigon *et al.* (2003) recognised a reduction in the relief at the top Cretaceous level of the Gjallar Ridge in the vicinity of the Gleipne Lineament which was termed the Gleipne Saddle, separating the northern Gjallar Ridge from the southern Gjallar Ridge (Fig 5.02a). The terminology used in this study follows the previous use of the term 'saddle', defined as the area of lower relief at top Cretaceous level located along strike from the Gjallar Ridge, a constituent part of the NW-SE oriented Gleipne Lineament. These two NW-SE features have apparently different structural styles, but the precise impact each structure has on the stratigraphic and volcanic fill of the basin is poorly understood.

5.4 Dataset and methodology

The Gjallar Ridge 3D time migrated seismic survey is composed of three individual seismic datasets which have been merged into a single dataset covering an area ~ 6000 km^2 with 25m line spacing above the Vigrid Syncline, Gjallar Ridge and Fenris Graben (Fig. 5.02b). The three seismic surveys used within the dataset are GRE02 (shot by TGSNopec) in the southeast, SG9604 (shot for Saga Petroleum by WesternGeco) in the west and ST0410 (shot for Statoil by PGS Geophysical) to the northeast. The seismic data are of high resolution, imaging the Late Cretaceous to Neogene (Santonian to Pleistocene) succession clearly as well as high amplitude Cenozoic magmatic intrusive and extrusive units (Appendix C.02). The survey unfortunately does not image the southern Gjallar

Ridge to the southwest of the Gleipne Saddle and therefore the geometry of the structural high is less well-understood in this region.

A second 3D time migrated seismic dataset was made available by StatoilHydro to analyse the structural evolution of the Någrind Syncline, Nyk High, Vema Dome and the Hel Graben (Figs 5.02a and 5.02b). The dataset covers an area of ~ 3200 km^2 with 25 m line spacing and has been formed from the merging of two 3D seismic surveys shot by WesternGeco and PGS Geophysical for Statoil and BP respectively (ST9603R99 above the Vema Dome to the west, BPN9601 above the Nyk High to the east). Seismic data over the Nyk High is good, successfully imaging the Late Cretaceous through to recent (Campanian to Pliocene) succession, but is of a lesser resolution to that shot over the Gjallar Ridge (Chapter 4). A suite of 2D seismic lines were used where there was no coverage of 3D seismic data in the region (Fig. 5.02b). The lines were selected from a variety of surveys primarily for their coverage and data quality, having been time processed by their respective owners; NGI-98 (TGSNopec); GVN-92 (WesternGeco); VB-86, VB-87, VB-89, VB-90 (reprocessed in 1994 by Fugro Multi Client Services for the Norwegian Petroleum Directorate) and GVF2000R, MNR04, MNR07 (Fugro Multi Client Services).

Cretaceous seismic picks were provided by StatoilHydro which have been tied by means of checkshot surveys back to three exploration wells (Appendix C.03-05) in the study area (6704/12-1 on the Gjallar Ridge, 6706/11-1 drilled upon the Vema Dome and 6707/10-1 on the southernmost footwall of the Nyk High; Fig. 5.02). Mapping around the RAZ was focussed upon four seismic marker horizons: KCaMFS115 (top Middle Campanian horizon, the top of the Nise Sandstone Member); KCaMFS118 (top Campanian); Top Cretaceous (a major erosional unconformity) and Top Paleocene (unconformity formed at or near the time of continental breakup). An overview and definition of maximum flooding surfaces is given by Galloway (1989) and these have been dated by Henriksen *et al.* (2005) in the Vøring Basin. Chapter 4 analysed the structure of the RAZ in greater detail than described here, and the reader is advised refer to this for further information.

Other horizons mapped in the Gjallar Ridge 3D seismic dataset were: KCoMFS100 (top of the Coniacian); KCaMFS113 (top of the Santonian); KMaMFS123 (top of the Early Maastrichtian); KMaUnc (a Late Maastrichtian erosional unconformity formed in the hangingwalls of the half grabens); Maastrichtian Fans 1, 2 and 3 (from oldest to youngest, three Late Maastrichtian horizons); a selection of intra-Paleocene horizons and unconformities (from oldest to youngest, IP1, IP2, IP3, IP4 and IP5); top Eocene; intra-Oligocene; top Oligocene (base of the Miocene siliceous ooze); Opal A-CT; top Ooze; near top Miocene; base Quaternary and the seabed which are illustrated upon the interpreted cross sections. Horizons interpreted within the seismic survey above the Nyk High and Vema Dome and illustrated upon example cross sections are: KCoMFS97 (for the purpose of this study is considered to be the equivalent of KCoMFS100 in the Gjallar Ridge seismic survey, but is the top Middle Coniacian equivalent to the top of the Lysing Sandstone Member); KMaMFS122 & KMaMFS123 (intra and top Early Maastrichtian horizons respectively within the main syn-rift sequence); top Eocene; top Oligocene; a suite of intra-Miocene horizons; base Quaternary and the seabed.

Due to a lack of available well data, prediction of lithologies and depositional environments has been made from the analysis of the seismic stratigraphy. The study of seismic stratigraphy originates from the work of Vail *et al.* (1977) with the first analysis phase of the seismic dataset consisting of delineating genetically related units known as depositional sequences Mitchum *et al.* (1997a), defined on the basis of reflection termination mapping. Age determination of the sequences was based upon ties between the seismic data and available well data. Where there was no well control of the depositional sequences, the age was predicted on the basis of relative age to depositional sequences of known age and/or tied to other wells in the region using 2D seismic data. Seismic facies analysis is the analysis of reflection configuration and other seismic parameters (e.g. amplitude, continuity and frequency) within the depositional sequence. This was used to express the gross lithological and depositional features of the sediments (Mitchum *et al.* 1977b). After the distribution and thickness of the seismic facies was mapped, the information was combined with the available well data and results of other regional studies to make an interpretation as to the environmental setting and the predicted lithology.

Other horizon-based analyses of the 3D seismic dataset such as the extraction of amplitudes from mapped depositional sequences also enhanced the interpretation of environments, modes of deposition and interpreted lithology (e.g. Posamentier & Kolla 2003; Fjellanger *et al.* 2005; Martinsen *et al.* 2005; Posamentier *et al.* 2007). Amplitude maps were compiled from the direct extraction of the amplitude response for each of the individually mapped horizons. The amplitude of seismic reflectors is directly related to the velocity and density characteristics between two rocks (the acoustic impedance contrast). The velocity of a rock can be affected by variations in the fluid content (e.g. gas, oil or water) and therefore the amplitude response is at least in part related to this. Similarly, diagenetic variations within sedimentary rocks could give rise to changes in the seismic amplitude response of a depositional sequence (e.g. Davies & Cartwright 2002) yet no evidence of this process (e.g. an Opal A-CT related reaction front) is recognised within the Mesozoic and Early Cenozoic stratigraphy. Equally, local scale variation in diagenetic processes may influence the seismic reflector amplitudes but as the study is on a sub-regional scale, this would exert minimal influence upon the results. The variation in fluid content of the rocks or diagenetic changes are relatively unknown for the pre-breakup stratigraphy in this region and therefore the amplitude variations mapped in this study are assumed to be directly related to the changes in sediment type. In particular, sand or mud prone regions are defined and corroborated by the results of the three exploration wells in the region. The interpretation of these lithologies may be further strengthened if the sedimentary rocks contain hydrocarbon fluids which enhance the amplitude response (e.g. bright spots). Conversely polarity reversals may also occur but these would be identifiable from mapping of depositional sequences within the 3D seismic dataset.

Other limitations of the dataset include the influence of intruded igneous material in the basin in the form of sills and dykes which add additional complexity to the interpretation of depositional sequences due to the reduction of the seismic resolution in these regions. This is caused by the strong amplitude response at the sediment-igneous interface and processes associated with the remobilisation of sediment due to the expulsion of volatile gases and liquids from the sill tips (e.g. Hansen 2006). This is particularly well recognised along the strike of the Gleipne Lineament where voluminous igneous sills impede the seismic imaging of the deeper Cretaceous succession below. Remobilised Miocene siliceous ooze (Hjelstuen *et al.* 1997), over-migration of the seismic data and fault shadowing effects particularly within the Nyk High seismic dataset further reduce the identification and analysis of more deeply-buried depositional sequences (Appendices C.02 & D.01-04). Volcaniclastic deposits which were deposited during the Late Paleocene – Eocene as regional tuff horizons along the NE Atlantic Margin (e.g. the Balder Tuff; Haaland *et al.* 2000), are undrilled in the northern Vøring Basin, are expected to be present. Similarly, the evolution of the south-western continuation of the ‘southern’ Gjallar Ridge is also undefined except for a published line across the ridge (Gernigon *et* *al.* 2003; fig 8d, p204) which limits the full interpretation of the tectono-stratigraphic and magmatic evolution of the Gleipne Saddle and Lineament.

Dip and dip-azimuth maps produced using 3D seismic data display the gross structure of the interpreted horizons and were also utilised to provide further control on interpretations of ambiguous features (such as the nature of the volcanic 'inner flows') in regions of little well control. In combination with the well results from the three exploration wells, regional studies and seismic facies analysis, conceptual evolutionary models were formulated to explain the stratigraphic and magmatic fill of the northern Vøring Basin in the vicinity of the RAZ and Gleipne Lineament.

5.5 Stratigraphy of the northern Vøring Basin

A detailed description of the stratigraphical fill and sedimentology of Mesozoic and Cenozoic deposits in the northern Vøring Basin has been given by other authors (Kittilsen *et al.* 1999; Ren *et al.* 2003; Fjellanger *et al.* 2005; Lien 2005; Lien *et al.* 2006) and therefore only a summary is given here. Zircon analyses of the cores from the wells in the Vøring Basin (Morton *et al.* 2005) confirm that much of the sediment in the basin was sourced from the north and west (East Greenland; Fjellanger *et al.* 2005) and very little, if any, was sourced from the east (Norway). Figure 5.03 displays a well correlation of the three released wells in the northern Vøring Basin, datumed on the top Cretaceous unconformity. Each of the wells has penetrated a succession of Late Cretaceous deep marine fan sandstones and mudstones which vary in thickness across the study area. Well 6706/11-1 drilled the oldest strata in the basin, reaching total depth in the Late Turonian sequence. It drilled the Lysing Sandstone Member which is Early Coniacian in age and marks the top of the Cromer Knoll Group. This is the only marine fan sandstone found within what is a predominantly deep marine mudstone succession. It is not until the Campanian that sands become more voluminous in the basin, with the Lower and Upper

Nise Sandstone Members deposited as aggradational sheet-like fan systems (Kittilsen *et al.* 1999) sourced from the north (Kjennerud & Vergara 2005). The deposits consist mainly of stacked, massive, normally graded sandstones deposited from hyper-concentrated and concentrated density flows passing into turbidity flows (Fjellanger *et al.* 2005). These deposits are up to 1 km thick and were deposited in a deep marine environment; they provide the primary reservoir target for the region. The 'Luva' well (6707/10-1) successfully targeted a direct hydrocarbon indicator in the seismic data which was a gas-water contact in the Late Campanian Upper Nise Sandstone Member (Kittilsen *et al.* 1999). Within the southern RAZ (6706/11-1), the sandstones are similar to the Nyk High Succession but are interbedded with bioturbated mudstones; an outer edge basin floor fan interpretation (Fjellanger *et al.* 2005). The Upper Nise Sandstone Member is up to 700 m thick, but no hydrocarbon reserves were recognised. In sharp contrast is the Gjallar Ridge well (6704/12-1), which drilled a much thinner Nise Sandstone sequence, recording up to 180 m thick sands which were similarly interbedded with mudstones. These have been interpreted as submarine fan slope deposits which imply the Gjallar Ridge was of shallower bathymetrical relief than the basin floor settings of the RAZ and the Nyk High.

The Late Campanian Upper Nise Sandstone Member is capped by a regionally significant mudstone package which does not vary in thickness (~ 350 m) across the area. This sequence provides a primary seal to the excellent reservoirs of the Nise Sandstone Members. A secondary play in the region is the Maastrichtian Springar Sandstone Member which is best identified in well 6704/12-1 where up to 450 m of bioturbated, normally graded sandstones were drilled. Although they are similarly interpreted as deposited from concentrated density flows to turbidity flows in a proximal, submarine slope environment, the sandstones are notably less sandy than the Campanian deposits cored in the Nyk High and RAZ wells (Fjellanger *et al.* 2005). The major Upper Cretaceous unconformity at the top of the sequence has removed an estimated 950 m (calculated by seismic line restoration; Ren *et al.* 1998) of Late Maastrichtian strata. Within well 6707/10-1, the Lower Maastrichtian is characterised by deep marine mud deposition with the onset of basin floor marine sand deposition later (i.e. Late Maastrichtian) than in the Gjallar Ridge to the west, similarly capped by the top Cretaceous unconformity. Within the southern RAZ (6706/11-1), a ~ 140 m thick sequence containing no sands of Maastrichtian age was recorded despite both Lower and Upper Maastrichtian strata be preserved. Each of the three wells has targeted rotated fault block crests, but an explanation for the lack of sand within the southern RAZ is required.

The oldest Cenozoic deposits drilled are of Late Paleocene age (Thanetian; Ren *et al.* 2003), and comprise shallow marine sandstones (wells 6706/11-1 and 6707/10-1) in contrast to mudstones which were encountered above the Gjallar Ridge (6704/12-1). This change from deep marine sedimentation to subaerial erosion has been quantified through backstripping of the wells by Ren *et al.* (2003) who recognised that a shallowing of the region commenced in the Maastrichtian. In Chapter 4 a variety of hypotheses for this shallowing and the formation of the top Cretaceous unconformity were proposed (e.g. eustatic fall in sea level, rift flank uplift, regional uplift or increased subsidence to the northwest of the ridge), the effects of which appear to diminish prior to continental breakup with a return to shallow marine deposition upon the structural highs at the time (e.g. in well 6704/12-1).

5.5.1 Palaeogeographic and bathymetric reconstructions

On a regional scale, the location of the outer Vøring Basin was advantageous to sand deposition due to the proximity of the sediment source and short transport distances across a narrow shelf. The main factors which influenced enhanced sediment deposition during rifting in the outer Vøring Basin were a large hinterland sediment source area, increased supply of sand-grade sediment, interconnected sediment transport pathways and localised depocentres (Fig 5.04; Lien 2005). The substantial thickness of Campanian Nise Sandstones deposited in the Vøring Basin implies a significant uplift of the hinterland source, which has been previously linked early-stage plume activity (Skogseid *et al.* 2000). With greater amounts of rifting, the deposition of sediment became increasingly localised due to the enhanced fault development under rifting (Fig. 5.04). Lien (2005) proposed the development of sub-basins (currently located on the Greenland passive margin) led to the sediment be deposited more proximal to Greenland in the late Campanian. The return to sand deposition (Maastrichtian Springar Sandstones) in the outer Vøring Basin was probably due to a combination of rift-flank uplift and the sedimentation rate overcoming the basin subsidence rate, leading to a bypassing of the Greenland sub-basins. During the later stages of rifting prior to continental breakup, the sediment transport routes became progressively more complex due to smaller, localised depocentres bounded by the evolving half grabens.

Similarly, the interaction between uplift, subsidence and erosion further complicates the sediment pathways in the basin as highlighted by Kjennerud & Vergara (2005) through a suite of palaeobathymetric reconstructions (Fig. 5.05). The palaeobathymetry was estimated by combining relevant information from seismic sequence and facies geometries, sedimentological/seismo-stratigraphic indicators of shallow or zero water depth and micropalaeontological interpretation. During the Early Campanian (Fig. 5.05a), the Nise Sandstones were deposited in water depths of up to 1500 m, sourced from the north and north-east. The Nise Sandstones penetrated in Gjallar Ridge well were not connected with the deposits in the Nyk High and RAZ wells. The original Late Campanian palaeobathymetry (Fig 5.05b) is masked by the effects of Maastrichtian –

Paleocene erosion yet the Någrind and Vigrid Synclines appear to be the most appropriate fairways for sourcing the Maastrichtian Springar Sandstones, whose provenance is from the west and north-east respectively. In the Early Paleocene (Fig 5.05c), as a consequence of basin uplift, the Gjallar Ridge and Nyk High were at or very close to sea level creating locally sourced sediment as well as distally sourced material from the north in a shallow marine environment. The primary depocentres for the region were the Någrind and Vigrid Synclines which were in the order of 500m deep. In the Late Paleocene (Fig. 5.05d), sedimentation from the north was shut off with further localised erosion in the region of the Nyk High and Vema Dome. Notably, the Någrind and Vigrid Synclines ceased to exist at this time, with the primary depocentres switching to the Fenris and Hel Grabens to the north. Notably however, these palaeobathymetric maps do not distinguish key links between the rift-oblique lineaments and entry points for sediment into the Vøring Basin as proposed by Fjellanger *et al.* (2005) and Lien (2005).

5.5.2 Isochrons

A range of sediment time-thickness maps display the major areas of deposition and erosion through time formed from mapping of the 2D and 3D seismic data (Fig. 5.06). The thickness of the Late Campanian sequence is thinnest above the Gjallar Ridge, correlating with the marine slope fan interpretation from the 6704/12-1 well data as opposed to the basin floor setting in wells 6706/11-1 and 6707/10-1 (Fig. 5.03). Despite local variations in the thickness of the sequence, the Nyk High appears to also be of structurally higher relief compared to the deep Hel Graben and Någrind Syncline as also recognised by Kjennerud & Vergara (2005). During the Maastrichtian, the Hel Graben was the primary focus for all deposition in the basin, with up to 2000 ms of sediment thickness recognised. The Fenris Graben and Vigrid and Någrind Synclines are also structural lows in contrast to the relative highs of the Gjallar Ridge and Nyk High. The true thickness of the

Maastrichtian sediments upon the Gjallar Ridge (and southern RAZ; Chapter 4) is misrepresented due to erosional truncation of the sequence as observed on seismic in Figures 5.07 and 5.08. During the Paleocene, apart from the Vigrid and Någrind Synclines, the primary depocentre was in the northern RAZ which ties accurately with the mapped inner flows. In the Hel Graben, two north-south trending, en-echelon structural highs are highlighted marking the north-eastern limit of the RAZ bounding this primary depocentre. Sedimentation in the Paleocene was thinnest upon the Gjallar Ridge and at the transition from the Nyk High into the RAZ due to the relative relief of these features at the time. Paleocene strata are thickest to the northwest along the line of continental breakup due to the outbuilding and formation of the Vøring Marginal High by a suite of volcanic deposits at the time (Planke *et al.* 2000).

5.6 The Rym Accommodation Zone

The tectonic evolution of the northern Vøring Basin has been considered by various authors but in Chapter 4 a new tectonic model was formulated which supported the development of an accommodation zone (Ren *et al.* 2003) in the region. This is in contrast to a previously proposed wrench tectonic model (Mogensen *et al.* 2000). Results from Chapter 4 also highlighted a possible influence of the deeper crustal structure on the Late Cretaceous – Paleocene rifting in the region.

5.6.1 Gjallar Ridge

The Gjallar Ridge (Fig. 5.07) is a Late Cretaceous structural high which displays a gross asymmetry with low angle (~ 20 – 30°; Appendix C.06) normal faults dipping to the northwest. Rifting commenced during the Santonian and continued into the Campanian, with minimal thickening of strata into the faults. During the Maastrichtian, thick syn-rift deposits are recognised in the Gjallar Ridge. The Late Paleocene sequence is very thin, but displays parallel reflectors draped above the relief of the structural high with no evidence of major rift-related faulting present. The only Paleocene fault reactivations that are observed occurred at the boundary between the Gjallar Ridge and the Fenris Graben to the northwest (Appendix D.05). It can therefore be concluded that Late Paleocene rifting did not occur in this region, but a continuation of Maastrichtian rifting into the Early Paleocene cannot be ruled out. A stratigraphical section of the Gjallar Ridge (Fig. 5.07b) is based upon well data (Appendix C.03) and seismic stratigraphical analysis of the sequences to determine the dominant lithologies expected to present. These are broadly coincident with the well results, with both Nise and Springar Sandstones developed across the Gjallar Ridge, becoming more sand rich to the southeast. The Maastrichtian sequence of the Fenris Graben is also expected to be sand prone due to its lower relief and forming a depocentre as opposed to the Gjallar Ridge. The Lower Paleocene sequence may also be more sand prone in the Fenris Graben with the addition of locally eroded material from the Gjallar Ridge and sediment entering the basin from the northwest.

5.6.1.1 Volcanics

Sills in the Vøring Basin have been dated as Late Paleocene and/or latest Paleocene to earliest Eocene in age (Hansen 2006). As faulting predates these intrusions (on the basis of mapping well tied seismic data), the sills are influenced by the faults, intruding along the horizons and climbing up along or ending abruptly against fault planes (c.f. Thomson 2007). There is minor evidence for hydrothermal vent complex formation above the Gjallar Ridge (Skogseid *et al.* 2000; Planke *et al.* 2005). However, clear evidence of this process requires a relatively thick Paleocene cover sequence for major sediment remobilisation to occur. Despite this, it is believed that the sills were the product of both the Early and Late Paleocene intrusion events as described by Hansen (2006).

5.6.2 Northern RAZ

The transition from the Gjallar Ridge into the northern RAZ (Fig. 5.08) is abrupt across a NW-SE trending normal fault dipping ~ 50° (Appendix C.06) to the northeast. This fault formed during the Maastrichtian with notable thickness changes observed and is inferred to be active into the Paleocene but due to the erosion of the Gjallar Ridge, stratigraphical evidence for this late activity is limited. A model to clarify this interpretation is provided in Chapter 4. The stratigraphy is considered very similar to that discussed previously, with the Santonian sequence becoming more sand prone to the northeast on the basis of enhanced reflectivity displayed within the northern RAZ. The Paleocene stratigraphy is generally transparent suggesting a dominant mud prone lithology but may contain tuff deposits related to volcanic activity to the northwest (Hjelstuen *et al.* 1999). The oldest Paleocene sequence within the northern RAZ is expected to be Thanetian in age from mapping of the IP3 horizon (recognised in well 6704/12-1) in this area, but thin subcrops of earlier Paleocene sequences may be present. This indicates that the northern RAZ was an area of little or no deposition and was potentially subaerially exposed during the Danian and Selandian. An alternative hypothesis for the erosion is related to submarine erosion which is discussed below. The earliest Thanetian stratigraphy in this region is expected to be more sand prone than elsewhere due to the observed increase in sediment thickness in the northern RAZ and the proximity to the inferred sediment source (the eroding Gjallar Ridge).

5.6.2.1 Volcanics

A distinct high amplitude reflection is recognised within the latest Paleocene in the northern RAZ which has been mapped previously as the ‘inner flows’ by various authors (e.g. Planke *et al.* 2000; Ren *et al.* 2003). This horizon has also been mapped within the structurally low Fenris Graben (Figs 5.08 and 5.09). At present, it is structurally highest to the southeast although this is an effect of Oligo-Miocene uplift of the strata in this area (Appendix D.06). Along this horizon, 1-2 km wide highs (Fig. 5.09a) are evident which appear unrelated to the Cenozoic tectonism. An amplitude extraction of the horizon shows that it is also not seismically homogenous with varying amounts of bright and dim reflectivity. An analysis of dip variation across the surface displays ~ 5 km wide sub-circular areas to the west appearing to overlap each other, with generally lower dips to the centre and increased dips towards the edge. Equivalent but larger features are partially mapped in the east. Towards the centre of the mapped horizon, the dips are less distinct with both low and high dips recorded respectively, which relates to the irregular top of the horizon as displayed in section view (Fig. 5.08). The interpretation of the processes which formed this horizon and implications for the influence of the accommodation zone upon its deposition is discussed later.

5.6.3 Nyk High

The Nyk High contrasts greatly with the Gjallar Ridge with more steeply dipping faults (~ 50 – 60°; Appendix C.06) dipping to the northwest and southeast (Fig. 5.10), forming a series of horst and graben structures. The initial age of observable rifting was during the Campanian and continued into the Late Campanian where strata appear to preferentially deform by folding. The dominant rift event in the region occurred during the Maastrichtian and continued into the Paleocene with notable offsets of the top Cretaceous unconformity recognised. Shallow marine erosion may explain the curious nature of the Late Cretaceous unconformity erosional styles in the Nyk High. Observations which suggest this process may be occurring include a marked differential erosion of the north-westernmost horst of the Nyk High forming a clear unconformity which truncates the Upper Cretaceous strata to the northwest (Fig. 5.10). Similarly, increasing amounts of accommodation space towards the centre of the grabens away from the Paleocene bounding faults is recognised. In these areas (Fig. 5.10) truncation of the underlying Maastrichtian strata has formed a pronounced unconformity onto which the Paleocene strata are seen to onlap. Sufficient energetic bottom-water currents may have formed against a backdrop of local uplift, growth of the Vøring Marginal High (Eldholm *et al.* 2002) and falling eustatic sea levels, leading to the erosion of the horsts as recorded by Laberg *et al.* (2005) elsewhere along the NE Atlantic Margin in the Cenozoic. Yet this hypothesis remains untested in the northern Vøring Basin (Appendix D.07) and alternative hypotheses are equally valid such as fault scarp degradation or slope failure.

The stratigraphical fill of the Nyk High is broadly similar to the results of well 6707/10-1 with the main sand deposition during the Early – Middle Campanian. The high seismic reflectivity of the Nise Sandstone sequence is caused by variations in the characteristics of the sandstones and interbedded thin mudstone units (Kittilsen *et al.* 1999), which based upon the seismic reflection characteristics implies the sandstones are thick and laterally continuous across the Nyk High. The Upper Campanian sequence is mud-prone, particularly upon the horst structures with low internal reflectivity observed. Mud deposition across the Nyk High continued into the Early Maastrichtian with Springar Sandstones deposited in the Late Maastrichtian (Fig. 5.03). In the grabens, increased reflectivity within the sequences may reflect a higher net:gross or the deeper burial of the lithologies drilled in Well 6707/10-1. The reflectivity of the Maastrichtian sequences decreases to the northwest implying the sediment of the Hel Graben may be more homogeneous, either sand or mud rich. The Paleocene stratigraphy is expected to be sand prone due to local erosional reworking of the Late Maastrichtian Springar Sandstones in the Nyk High by hypothesised marine currents. The thickest deposits formed in the grabens, with a complete Paleocene succession expected both here and in the Hel Graben to the northwest. There is a notable lack of high amplitude sills imaged in the seismic data within the Nyk High.

5.6.4 Southern RAZ

The transition from the Nyk High into the southern RAZ is very complex (see Chapter 4 for discussion; Fig. 5.11). The faults continue to dip at ~ 50 – 60° (Appendix C.06) but rotate into more east-west trends compared to the NE-SW trend of the Nyk High (Fig. 5.02b). Separate Paleocene and Oligo-Miocene uplift events have complicated the gross nature of the southern RAZ but thickening of hangingwall sequences suggest rifting commenced in the Maastrichtian. The Maastrichtian rift system which formed was very different to the tectonically quiescent conditions in the Campanian which promoted large-scale marine fan deposition (Nise Sandstone Members), represented by the high laterally continuous reflectivity of the sequence. It is difficult to ascertain the nature of the older sequences due to fault shadowing effects in the seismic data, reduction in the seismic resolution due to Paleocene sills and the effects of remobilised Miocene siliceous ooze (Appendix C.02). The Coniacian Lysing Sandstone Member, drilled in well 6706/11-1, may also be present but is considered part of a thicker more mud prone succession within which the faults detach (Fjellanger *et al.* 2005; Chapter 4).

The low resolution of the seismic data (Chapter 4) makes it difficult to undertake seismic facies analysis in the southern RAZ but it is expected that the Maastrichtian sediment becomes more sand prone to the north as it is structurally lower and more proximal to the westerly source for the sediment (Morton *et al.* 2005). Increased reflectivity is also observed which may be interpreted as marine fan sandstones interbedded with mudstones to the north in the central RAZ. During the Paleocene, rifting climaxed in the southern RAZ with major offsets of the top Cretaceous unconformity observed (Fig. 5.11). Little erosion of the footwalls implies marine conditions prevailed in the west during this time, away from the zone of Paleocene uplift, acting as a sediment depocentre for the eroded Late Cretaceous material (Chapter 4; Appendix D.08). The Late Paleocene is inferred to be associated with more mud prone deposition due to the cessation of local erosion, a cutting-off of the sand supply from the northwest due to the development of the Vøring Marginal High (Eldholm *et al.* 2002) and a return to mud prone deposition in the Eocene as recorded in wells 6706/11-1 and 6707/10-1.

5.6.5 Summary (Figure 5.12)

5.6.5.1 Late Cretaceous

During the Early – Middle Campanian (Fig. 5.12a), thick basin floor fan sandstones were deposited widely across the Vøring Basin. Faulting (exaggerated in Figure 5.12a) in the Gjallar Ridge and Nyk High provide little influence on deposition of the fan systems. Thickest within the Nyk High and Hel Graben, they are much thinner upon the Gjallar Ridge as this was a tectonically elevated marine slope at the time and as such slope fan deposits are recorded in the 6704/12-1 well. The RAZ exerted no influence on the depositional patterns or pathways with sedimentation outpacing the formation of accommodation space created by the faulting and tilting of the basin floor. The Vigrid and Någrind Synclines were also of low relief with the Nise Sandstones deposited in each of these regions as well (Chapter 4).

During the Maastrichtian (Fig. 5.12b) the Gjallar Ridge remained elevated with slope fan sandstones deposited upon it, but the primary transport direction of the sediment is expected to be axial during rifting, along strike from the southwest to the northeast. Upon crossing the bounding NW-SE fault into the RAZ, it is expected that a series of point sourced fans would form, with localised erosion of the fault scarp (e.g. Beratan 1998). As the rift continued to evolve through time, frequent modification as to the location of point-sourced marine fans and the amount and type of sediment flowing across the rift-oblique fault is predicted to lead to a complex stratigraphical architecture in the fault hangingwall. Between the Vigrid Syncline and Hel Graben, where the NW-SE fault is not present (Chapter 4), fan deposition is likely to result in broad sheet sand complexes above an active ‘relay ramp’ structure (Chapter 4). The hypothesised source for this sediment is the eroding south-eastern edge of the Gjallar Ridge (Fig. 5.07). Sand deposition dominated the low regions such as the grabens of the Nyk High and southern RAZ (Kjennerud & Vergara 2005), with background mud deposition occurring primarily upon the footwalls and in the Någrind Syncline to the south. When the accommodation space in the grabens was filled, only then would sand deposition be expected upon the fault block crests and in the Någrind Syncline. Maastrichtian sands are recorded in well 6707/10-1 implying the accommodation space was filled in the Nyk High however a lack of sand in the Maastrichtian sequence of well 6706/11-1 implies that in the southern RAZ, sediment may not have filled the available accommodation space and flowed beyond the rift margins into the Vigrid/Någrind Syncline to the south. If sands do exist to the south, they may have been transported along a SSW trending Maastrichtian graben to the south of the Nyk High (Figs 5.02b and 5.12c). The origin and controls upon the formation of this graben remains unknown but may be related to a complex zone of extensional tectonics within the Nyk High (S. Markussen, StatoilHydro, pers. comm.). To explain the lack of Maastrichtian sands in well 6706/11-1, this model is based upon the assumption that the majority of sediment was either locally sourced from the eroded Vigrid Syncline flanks (Fig. 5.07) and/or entered the basin from the northwest. A south-easterly derived source for sediment can not be ruled out which would impact upon the predicted stratigraphical fill of the northern Vøring Basin, but heavy mineral analysis of core samples of the outer

Vøring Basin wells has not highlighted major evidence for a Norwegian source in this region (Morton *et al.* 2005).

5.6.5.2 Paleocene

In the Early Paleocene (Fig. 5.12c) the focal area for rifting shifts from the NE-SW faults of the basin to the predominantly east-west faults of the southern RAZ. The basin is expected to be generally shallow marine due to a relative uplift of the basin with sands being sourced both distally (Greenland) and locally eroded regions (Gjallar Ridge, Nyk High and the RAZ; Kjennerud & Vergara 2005). There may also be reworking of the Cretaceous strata through shallow marine processes such as bottom-water currents upon the south-eastern and south-western margins of the Hel Graben. The NW-SE trending fault at the boundary of the Gjallar Ridge continued to be active but as the hangingwall has been eroded, no stratigraphic evidence of fault activity (e.g. syn-tectonic strata) is recognised. Despite this, the fault exerted a control on the topographical extent of the Gjallar Ridge which subsided across the fault to the northeast.

In the latest Paleocene (Fig. 5.12d), uplift between the southern RAZ and Nyk High, and within the Hel Graben to the north reached a maximum. Subaerially exposed and eroded to the south, the uplift may have remained below sea level to the north with no evidence of notable erosion in the 2D seismic data. The Gjallar Ridge was at or near sea level at this time with shallow marine muds present upon the high. There is little or no activity upon the NW-SE trending normal fault between the Gjallar Ridge and northern RAZ, but this continued to form a structural boundary to a prominent bathymetrical low between each of the structural highs in the basin into which Paleocene sedimentation is focussed as exemplified by the ‘inner flows’. These are interpreted as being sourced from the north and flowing rift perpendicular during this period of relative tectonic quiescence, in contrast to the axial flow of sediment during rifting.

In Chapter 4, a hypothesised structural model was proposed of a through going 'transfer fault' if Maastrichtian rifting had continued, breaching the ramp between the Vigrid Syncline and Hel Graben. Figure 5.13 displays a predicted tectono-stratigraphic architecture of the basin had this occurred. Much of the sediment would be sourced from regions along strike which when crossing the active rift-oblique fault, the change in relief would lead to down cutting and erosion of the fault scrap, with point sourcing of marine fans deposited in the hangingwall. This would occur along the length of the fault with a complex stratigraphical fill expected within the RAZ and Hel Graben. Only where continual, long lived sedimentation across the fault arose would one expect to find larger marine fan complexes in the RAZ, but these would be further complicated by the increased amount of rift-related normal faulting within the Hel Graben.

5.7 The Gleipne Lineament/Saddle

Tectonic analysis of the Gleipne Lineament/Saddle in the Vøring Basin is severely hampered by sills which have intruded parallel to interpreted stratigraphical markers of Maastrichtian and older strata (Fig. 5.14). Mapping of the Cretaceous horizons has focussed on the Late Maastrichtian marine fan systems tied to well 6704/12-1 which have been less influenced by the sills and can be mapped with confidence. The older horizons are more difficult to map, but coherent reflections imaged beneath the sills means interpretations of the horizons can be completed on a line by line basis.

5.7.1 Gleipne Saddle

The saddle is clearly recognised within the seismic dataset due to a broad reduction in the relief of the top Cretaceous unconformity (Gernigon *et al.* 2003; fig 7, p 203). The change in relief is gradual from upon the Gjallar Ridge at ~ 3.2 sec TWT reducing to ~ 3.5 sec TWT in the Gleipne Saddle over a distance of 20 km (Fig. 5.14). The reduction in relief increases with greater depth as exemplified by other Late Cretaceous levels; a decrease of 0.8 sec TWT of the KCaMFS118 horizon from upon the Gjallar Ridge into the Gleipne Lineament, 1.5 sec TWT of the KCaMFS113 horizon and 1.9 sec TWT of the KCoMFS100 horizon. This NW-SE oriented synform feature therefore appears to have been a low throughout the Late Cretaceous due to thickening of the Late Cretaceous sequences into the saddle. Faults are not readily identifiable beneath the sills however, the thickening of the packages from the northeast (upon the Gjallar Ridge) into the Gleipne Saddle tie well with periods of rifting and subsidence recognised elsewhere in the basin (e.g. during the Santonian, Campanian and Maastrichtian). Within the Upper Maastrichtian sequence, Late Maastrichtian marine fan depositional sequences were mapped in detail to analyse the sediment distribution at the time, some of which were eroded away by the top Cretaceous angular unconformity. The overlying mud prone Paleocene sequences do not thicken as dramatically into the saddle as exemplified during the Mesozoic rift conditions previously (Fig. 5.14).

5.7.2 Gleipne Lineament

Along the general trend of the broad Gleipne Lineament, the Maastrichtian marine fan deposits display a complex interaction between faulting and sedimentation (Fig. 5.15). A series of low offset normal faults which predominantly dip to the northwest appear to have been active during deposition of the fan sequences. Maastrichtian fans 1 and 2 are thicker to the northwest, reducing into the Vigrid Syncline to the southeast in contrast to Maastrichtian fans 3 and 4 which display the opposite. Localised thickening of the sequences into the normal faults also occurs, suggesting the faults were synchronous with deposition. It is unclear whether the faults are linked to rift faults at depth, but the density of faulting is much greater within the Gleipne Lineament than within the Gjallar Ridge. Fans 3 and 4 onlap onto the top of Fan 2 with no evidence of erosional truncation of their upper surface, suggesting they are more likely to have been distributed exclusively within the Vigrid Syncline and not sourced from Greenland. The mottled seismic reflectivity of the Maastrichtian deposits suggests they may be composed of homogeneous to interbedded sandstones and mudstones, although this may be an effect associated with the intrusion of Paleocene sills linked to changes caused by the remobilisation of sediment, thin igneous intrusives and variation of lithological composition due to thermal metamorphism.

The Paleocene has been split into four depositional sequences based upon stratigraphical relationships and internal reflectivity in the vicinity of the Gleipne Lineament. IP1 sequence is highly transparent implying a homogeneous, probably mud prone stratigraphy with evidence of faults detaching upon its top (Fig. 5.15). The overlying IP2 sequence displays increased reflectivity suggesting interbedded sandstones and mudstones are present. The later Paleocene sequences display relatively transparent but occasional reflectivity in the seismic data implying infrequent sand deposits at the time.

5.7.2.1 Gleipne Lineament in the Vigrid Syncline

Within the Vigrid Syncline, the Maastrichtian marine fan deposits can be seen to thicken towards the southwest, into the Gleipne Lineament (Fig. 5.16) implying that the saddle feature persisted into the syncline away from Gjallar Ridge. The Vigrid Syncline has no evidence of Late Cretaceous – Paleocene rifting suggesting the formation of the Gleipne Lineament may not be related to the faulting as the direct result of regional rift events (Chapter 4). Sill abundance in the Vigrid Syncline led to difficulty interpreting older Cretaceous horizons but the Maastrichtian deposits are expected to be both shale and sand rich due to the increased distance from the inferred westerly source region (e.g. Reading & Richards 1994). The underlying Middle Campanian strata are expected to be sand rich as observed elsewhere across the Vøring Basin on the basis of the well results (Fig. 5.03) and the Vigrid Syncline being a sediment depocentre at the time (Fig. 5.06), but this remains untested by drilling. The Upper Cretaceous unconformity is much less distinct along the Gleipne Lineament with little evidence for truncation of the Maastrichtian sequences. This is interpreted as being due to the region forming a NW-SE oriented syncline at the time, probably close to or below sea level. The first Paleocene sequence displays a series of northeast dipping 'domino' fault blocks vertically limited by the sequence boundaries. A whole series of other minor faults are encompassed within the later Paleocene sequences which appear spatially linked to vent structures originally identified by Skogseid *et al.* (1992) but elaborated on by Planke *et al.* (2005). Faults increase in frequency in the latest Paleocene, coincident with timings of sill intrusion provided by Hansen (2006).

5.7.3 Amplitude analyses

5.7.3.1 Late Cretaceous

Maastrichtian Fan 1 is present upon the Gleipne Saddle and in the Vigrid Syncline, but is also mapped within the hangingwalls of major rotated fault blocks of the Gjallar Ridge (Fig. 5.17). These areas were of the shallowest bathymetrical relief defined on the basis of sediment thicknesses at the time suggesting any sediment deposited and eroded may also drain axially from within the Gjallar Ridge, into the Gleipne Saddle and Lineament. Faults displaying increased curvature in map view (Fig. 5.17a) are highlighted within the sequence, striking generally NE-SW within the saddle to more N-S trends within the Vigrid Syncline, once again dissimilar to the rift related faulting observed in the Gjallar Ridge. Bright (high acoustic impedance contrast) sill material affects the analysis of amplitude extraction maps but brighter amplitudes (sand prone) are highlighted in close proximity to the lineament compared to the dimmer (mud prone) amplitudes recognised to the east. Maastrichtian Fan 2 (Fig. 5.17b) follows a similar depositional pattern to Fan 1, structurally higher to the west and also believed to be sourced from eroding footwall crests of the Gjallar Ridge as well as sediment entering the basin from the northwest. A second high of increased prominence is also visible in the Vigrid Syncline but its origin does not appear to have influenced deposition of the sequence, the origin, growth and timing of which is discussed later. The amplitude map displays a more mud prone, darker sequence than previously, but includes sub-rounded features of brighter material in the Vigrid Syncline which could be interpreted as sand rich marine fan lobes.

By the time Maastrichtian Fan 3 (Fig. 5.17c) is deposited, there is little evidence for a north-westerly source as the sequence can not be mapped above or to the northwest of the Gleipne Saddle (Fig. 5.14). Mapped to exist solely within the Vigrid Syncline, onlapping the south-western edge of the Gleipne Saddle and Gjallar Ridge, an amplitude extraction of the sequence boundary (Mitchum *et al.* 1977a) suggests the areas in close proximity to the Gjallar Ridge and Gleipne Saddle to be more sand prone than to the south and east. The deposition of this sequence is also expected to be contemporaneous with the erosion of the Gjallar Ridge which would act as the sediment source region. On the basis of grain size organisation in marine fan systems (Reading & Richards 1994), sands are expected to be deposited in more proximal areas to the sediment source (i.e. the Gjallar Ridge as observed). Dark, NW-SE trending features (submarine channels?), appear to source low amplitude, mud prone fan systems which appear as rounded lobe type features, upon which channels are identifiable (Fig 5.17c). Using an amplitude extraction of the top Cretaceous unconformity, the youngest Maastrichtian sediments within the Vøring Basin can be analysed (Maastrichtian Fan 4; Fig. 5.17d). Broad regions of sand (light) and mud (dark) rich sediment are recognised which are assumed to be sourced locally and may be prone to reworking in what are expected to be shallow marine conditions at the time due to the continuing relative uplift and exposure of the Gjallar Ridge. These apparently become more mud prone towards the Gleipne Lineament in the south which implies this area to be either deeper and/or of increased distance from the sediment source.

The Maastrichtian Fan sequences are seen to thicken along the strike of the Gleipne Lineament and particularly to the northwest where present (Fig. 5.18). This is particularly well exemplified by the Maastrichtian Fan 2 sequence which also thins away from the Gleipne Lineament to the northeast within the Vigrid Syncline. The younger Maastrichtian Fans 3 and 4 thicken to the south and west and are thinnest in close proximity to the Gjallar Ridge which forms the northerly limit and possible source region for the sequences.

5.7.3.2 Paleocene

The ages of the mapped intra Paleocene sequences are dated relative to IP3 which ties to a Thanetian age unconformity in well 6704/12-1 (Figs 5.03 and 5.19). Earlier sequences may be Danian (considered as a major period of shallowing; Brekke *et al.* 1999) and/or Selandian, but a more accurate dating requires drilling of the strata. IP1 is mapped in the Vigrid Syncline with a minor encroachment upon the Gjallar Ridge in the vicinity of the Gleipne Saddle (Fig. 5.19a). This encroachment may be either a submarine or subaerial channel system for transporting eroded sediment but is undrilled. No other notable Lower Paleocene stratigraphy is recognised elsewhere along strike of the Gjallar Ridge. Possible evidence for the channel hypothesis is an observed bright amplitude response observed close to the inferred channel mouth in the Vigrid Syncline, maybe related to deposition of coarser-grained sand deposits (e.g. Fitzgerald *et al.* 2000). This is against a backdrop of mud rich (weak amplitude response) sedimentation with locally sand rich bar deposits close to the Gjallar Ridge (Fig 5.19a). Minor NW-SE curved faults are recognised in the south-easternmost part of the study area (dipping dominantly to the northeast in section view; Fig. 5.16), but their origin is unclear due to the intrusion of Paleocene sills. They do not have throws on the scale as observed elsewhere on the Gjallar Ridge (Fig. 5.07; Chapter 4), nor are they as laterally continuous, therefore the faults are inferred not to be directly related to rifting.

IP2 can be mapped to encroach upon the Gjallar Ridge from the east close to the northern RAZ (Fig. 5.19b). The sediments are observed above the hangingwalls of the Cretaceous syn-rift sequence (Fig. 5.07) but footwall crests remained at or near sea level during this time. These regions may have acted as areas of sediment transport as little or no sand rich sediment appears to have been deposited in the Vigrid Syncline (Fig. 5.12b). Localised brightening of the sequence is enhanced in areas of concentric circular features, highlighted by dark and light amplitude responses. These have been identified as hydrothermal vent complexes, being crater or dome/eye shaped features (Figs 5.15 and 5.16) of remobilised Mesozoic and Cenozoic sediment above sill tips (Hansen 2006; fig 8, p 795). The associated brightening of these features in amplitude maps may be associated with lithological changes as well as fluid variations in the deposits due to the expulsion of volatile gases and liquids from igneous sills at depth.

By the time of deposition of IP3 (Fig. 5.19c), the Gjallar Ridge and Gleipne Saddle were fully submerged again and hydrothermal vent complex formation was rapidly increasing in intensity (note the increased disturbance of the later Paleocene sequence in the vicinity of the vent structures; Figs 5.15 and 5.16). These appear to form the main control on sediment thickness and seismic facies variation within the Vigrid Syncline, producing sub-circular regions of strong and weak amplitude response. By the end of the Paleocene much of the intrusive sill activity had ended with the return to a dominantly seismically dim, mud prone succession. Radial fault networks about the centre of the vent structures are observed, with other fault networks linking each of the vent complexes highlighted by the amplitude extraction process (Fig. 5.19d). The areas of stronger acoustic impedance contrast may be due to the addition of potential volcanic material (e.g. Thomson 2007) or areas into which preferential deposition of sand and/or volcaniclastic material sourced from volcanic activity along the continental line of breakup may have occurred (Planke *et al.* 2000).

The Paleocene depocentre migrates within the Vigrid Syncline through time (Fig. 5.20). Initially, deposition is focussed close to the Gleipne Lineament in the south, but by the time of deposition of the second intra Paleocene sequence, a prominent syncline had formed between the south-eastern edge of the Gjallar Ridge and a high to the east. This high also coincides with the areas in which hydrothermal vent complexes are recognised in the Vigrid Syncline, continuing to be accentuated during the deposition of the Late Paleocene sequences except for local variations due to the vent formation process. It would therefore appear likely that the high in the Vigrid Syncline (as also observed in Fig. 5.17), is of Middle – Late Paleocene in age, caused by the volume change and uplift of the overlying strata due to the lateral intrusion of sills within the Late Cretaceous sequence forming a series of individual uplifts which amalgamated to form a single forced fold (e.g. Fig. 5.16; Appendix D.09; Hansen & Cartwright 2006; Moy & Imber 2009; Chapter 3).

5.7.4 Summary (Figure 5.21)

The Late Maastrichtian was a period of active rifting in the Gjallar Ridge but the structurally lower Gleipne Saddle fails to display major normal faulting; the importance of this is discussed later. Small scale normal faults appear to be synchronous with the deposition of the Maastrichtian marine fan sequences (Maastrichtian Fan 2; Fig. 5.21a), both upon the saddle and within the Vigrid Syncline to the southeast which displays no evidence of Late Cretaceous rifting (Chapter 4). The lower relief of the Gleipne Saddle and the tie with the older Springar Sandstone Member deposits in well 6706/12-1 upon the Gjallar Ridge suggests the Late Maastrichtian sediments may have been deposited in a deep marine environment. Much of the sediment is expected to have been distally-sourced from regions to the northwest (i.e. Greenland) but some sediment may have had a local source from the Gjallar Ridge and transported along strike into the Gleipne Saddle. A similar process of submarine fan deposition sourced from the Gjallar Ridge and transported towards the Gleipne Lineament has also been observed to occur within the Fenris Graben to the northwest (W. Athmer, TU Delft, pers. comm.). These sediments then flowed along the Gleipne Lineament, filled and bypassed the regions of active faulting, and were deposited as a series of lobes in the Vigrid Syncline to the southeast.

Towards the end of the Maastrichtian, the Gjallar Ridge and Gleipne Saddle became structurally more prominent which may be due to a variety of reasons including Paleocene rift flank uplift with rift-related subsidence to the northwest, plume related regional uplift, rifting of a heterogeneous lithosphere, a fall in eustatic sea levels (Haq *et al.* 1988), fault block rotation along low angle faults, or enhanced growth and subsidence of the adjacent synclines leading to increased relief of the Gjallar Ridge and Nyk High located upon the flanks. However, irrespective of which of these processes caused this relative uplift of the Gjallar Ridge, it led to the gradual decrease through time of sediment entering the basin along the Gleipne Lineament (Fig. 5.21b), reflected by a transition to more mud prone sedimentation in the Vigrid Syncline. Increased proportions of locally-sourced, sediment eroded from the Gjallar Ridge which may be mud prone itself is also expected at this time (Appendix D.10). By the end of the Cretaceous and in the Early Paleocene (Fig. 5.21c), all sediment sourced from the northwest was blocked by the structurally higher Gleipne Saddle and Gjallar Ridge. The blocking of Greenland-sourced sediment may have led to increased accumulations within the Fenris Graben to the northwest. Any sands in the Vigrid Syncline are expected to be wholly sourced from the locally eroding Gjallar Ridge at this time (Hjelstuen *et al.* 1999).

During the Early – Middle Paleocene (Fig. 5.21d) sedimentation was dominantly mud prone with little sedimentary input from the subaerially exposed Gjallar Ridge, probably drained by a broad channel/estuarine system flowing into the Vigrid Syncline in close proximity to the Gleipne Lineament. Alternatively, due to the asymmetry of the Gjallar Ridge (Fig. 5.07), much of the eroded sediment may have been deposited into Fenris Graben. This pattern of sedimentation continued into the Middle Paleocene (Fig. 5.21e) when igneous intrusives in the form of sills began to preferentially intrude within the Vigrid Syncline, leading to uplift of the overlying strata. A NE-SW oriented syncline is formed between the structurally high Gjallar Ridge and sill-influenced region where a forced fold developed. Late Cretaceous and Early Paleocene sediments are remobilised through the formation of hydrothermal vent complexes which start to form localised areas of uplift and subsidence. In the Late Paleocene (Fig. 5.21f), the Gjallar Ridge and Gleipne Saddle were fully encroached by shallow marine mudstone deposits which occurred across the region. Sands sourced from the west were stopped from entering the Vøring Basin at this time due to the extrusive volcanic activity occurring 2-3 Ma prior to continental breakup (Eldholm & Grue 1994; Berndt *et al.* 2001). Similarly, increased sill intrusions led to formation of more vent structures and associated minor fault systems. Much of the evidence for the hydrothermal vent complexes is most prevalent in the Vigrid Syncline, probably due to a thick cover sequence. In the latest Paleocene (Fig. 5.21g), sill intrusions reached a maximum extent with the deposition of volcaniclastics and sands in a mud rich shallow marine environment. Tuffaceous deposits may also be widespread due to volcanic activity along the line of continental breakup (Tsikalas *et al.* 2008) which was deposited over vast distances of the NE Atlantic Margin (e.g. the Balder Tuff; Knox & Morton 1988;

Haaland *et al.* 2000). A second element of this volcanic activity is the inner flows which are preferentially deposited along the Gleipne Lineament in the Fenris Graben (Lundin & Doré 1997; Gernigon *et al.* 2003; Ren *et al.* 2003) with the Gjallar Ridge (and Gleipne Saddle) acting as a barrier (Berndt *et al.* 2001).

5.8 Discussion

5.8.1 Tectonic nature of the Gleipne Lineament/Saddle

It is difficult to assign an accommodation zone model to the Gleipne Lineament and Saddle (c.f. Faulds & Varga 1998) due to the lack of major evidence for overlapping fault tips in the region as previously recognised by Gernigon *et al.* (2003) and Ren *et al.* (2003). Rift perpendicular accommodation zones are also commonly of relatively high relief where compared to the adjoining rift segments (e.g. McClay *et al.* 2002). There is also a distinct lack of NW-SE faulting which would be expected if a transfer zone had formed (Gibbs 1984). This leads to the conclusion that the Gleipne Saddle and Lineament are not elements of a fault domain boundary (Schlische & Withjack 2009), nor does it appear that the Gleipne Lineament is at all related to alternative styles of upper crustal deformation such as major strike-slip movements. An alternative explanation for this structural low is related to the Lower Crustal Body (LCB) which has been interpreted as the result of Cenozoic magmatic underplating (e.g. Skogseid *et al.* 1992; Mjelde *et al.* 2002; Raum *et al.* 2002), serpentinisation of the mantle (e.g. Ren *et al.* 1998) and as continental basement remnants of the Caledonian orogenic root (e.g. Gernigon *et al.* 2004; Ebbing *et al.* 2006; Gernigon *et al.* 2006; Fjeldskaar *et al.* 2009). In Chapter 4, structural evidence supported a long-lived basement origin for the LCB. Across the Gleipne Saddle, there is a marked increase in the depth to the top of the LCB in comparison to the Gjallar Ridge both to the northeast and southwest of the structure (Ebbing *et al.* 2006). This increased depth of the LCB is mirrored by the Late Cretaceous horizons which are similarly observed to increase in depth within the Gleipne Saddle (Fig. 5.14). Thickness variations within the sequences also relate to defined periods of subsidence in the Vøring Basin related to the periods of Santonian, Campanian and Maastrichtian rifting and probably into the Paleocene as well. Within the Vigrid Syncline to the southeast, Mesozoic – Cenozoic sedimentation also increases in depth and thickens along the strike of the Gleipne Lineament, equally relating to a deepening of the LCB relief. The Vigrid Syncline is external to the region affected by Late Cretaceous – Paleocene rifting with no evidence of upper crustal fault activity (Chapter 4). Similarly, the development of the Gleipne Lineament predates magmatic activity within the basin and serpentinisation of the mantle is unlikely due to a lack of faulting along which seawater could penetrate the crust. This further supports the hypothesis that the LCB has a basement origin. Thus, the Gleipne Lineament is directly influenced by the long-lived basement relief and the deep crustal structure is an important control upon basin segmentation in the northern Vøring Basin.

5.8.2 Sediment sources, pathways and distribution

Morton & Grant (1998) and Morton *et al.* (2005) provide evidence from heavy mineral constraints that the outer Vøring Basin sediment is dominantly composed of material sourced and eroded from exposed regions of Greenland, with little if any sediment input from Norway. These sediments have been deposited as marine basin floor deposits which have been drilled and cored not only by the wells in this study, but wells elsewhere in the Vøring Basin including upon the Utgard High (6607/5-2), Helland Hansen Arch (6505/10-1), Halten Terrace (6506/12-4 & 6506/12-1) and Dønna Terrace (6507/2-2). The entry points for the sediment into the basin have long been unclear, but the NW-SE lineaments have often been inferred as potential pathways, not only offshore Norway (Martinsen *et al.* 1999; Fjellanger *et al.* 2005; Lien 2005; Martinsen *et al.* 2005) but elsewhere along the NE Atlantic Margin (e.g. Jolley & Morton 2007; Ellis *et al.* 2009). The results of this study both support and oppose this interpretation but rather than simply the location of the lineament, it is the structural nature of the lineament and kinematics of the basin at the time which are the primary controls on this process. Accommodation zones, formed as an overlapping zone or system of normal faults are commonly invoked as pathways for sediments to enter rift basins (e.g. Morley *et al.* 1990; Younes & McClay 2002). The RAZ however is located upon the south-eastern margin of the c. 150 km wide rift zone, an area from which little or no sediment is apparently sourced (Morton *et al.* 2005). The primary source for sediment to enter the rift is expected to be from the northwest (i.e. east Greenland) and would instead be expected to flow directly into the Hel and Fenris Grabens as well as the Gjallar Ridge and Nyk High. In order to prove this hypothesis, a better understanding of the Greenland conjugate margin is required which exposes rift-related Cretaceous deposits (Surlyk 1990; Kelly *et al.* 1998; Larsen *et al.* 1999; Whitham *et al.* 1999) but very little Upper Cretaceous – Paleocene stratigraphy. Plate reconstructions of the Norwegian margin with the east Greenland conjugate margin (Morton *et al.* 2005) indicate the Gjallar Ridge to be ~ 70 km from the onshore outcrops of the aforementioned Cretaceous strata. This places the northern Vøring Basin much more proximal to east Greenland than Norway which is located some 350 km to the east. Although the offshore structural evolution of the east Greenland continental margin is poorly defined and not well studied in the available literature, the studies onshore east Greenland suggest rift-related sediments are present offshore.

As mentioned previously, the nature, kinematics and relative location of the lineaments within the rift system are the primary controls upon whether the lineaments act as pathways or barriers to sedimentation in the basin. The RAZ under rift conditions is predicted to add further complexity to the preserved stratigraphical fill, solely compartmentalising the Late Cretaceous – Paleocene rift zone and not forming a conduit for sediment to enter the more inboard regions of the Vøring Basin such as the Någrind and Vigrid Synclines respectively. A variety of different structural styles are present within the RAZ. In areas affected by rift-perpendicular faulting (e.g. the northern RAZ), sedimentation styles (and the associated stratigraphical facies variation) may differ sharply on either side of the fault. Transfer of sediment would only occur in one direction, from upon the footwall into the hangingwall and are likely to be processes dominated by point sourced deposition (Fig. 5.12d). Within the central RAZ, where an unfaulted 'relay ramp' dipping down towards the Hel Graben formed, compartmentalisation of the basin also occurs but the variation of stratigraphical fill between each rift segment is expected to be a more gradual transition than across the rift-perpendicular fault. In the southern RAZ where the NE-SW faults of the Nyk High rotate into dominant east-west trends, the direction of sediment transport may vary through time. During the Maastrichtian, sediment may be expected to flow from the southern RAZ into the Nyk High hangingwalls due to the increased fault offsets producing a more prominent depocentre at the time. In the Early Paleocene when fault offsets were greater in the southern RAZ, sediment transport direction may be reversed, yet the southern RAZ still acts to compartmentalise the basin. Therefore whichever style of deformation is present in the RAZ, compartmentalisation of the rift is expected to occur rather than acting as a major pathway for sediment to enter the Vøring Basin (e.g. Fjellanger *et al.* 2005).

During periods of upper crustal tectonic quiescence (as exemplified during the Paleocene in the vicinity of the Gjallar Ridge), the RAZ may compartmentalise the basin on a larger scale than observed previously, due to the differential relief of the adjacent rift segments. Rift perpendicular transportation of both locally- and distally-sourced material can be achieved at this time as exemplified by the inner flows within the northern RAZ.

The Gleipne Lineament supports the hypothesis that sediment enters the basin along NW-SE lineaments in the Vøring Basin although this is apparently unique in the northern Vøring Basin. The lineament is not a fault domain boundary but is rather influenced by the deep crustal structure, forming a long-lived structural low, accentuated during periods of rifting and subsidence. Due to the apparent uplift of Greenland combined with the rift-related subsidence of the basin, thick Late Cretaceous sand deposits are expected to flow into the Fenris Graben, and then across the Gjallar Ridge via the Gleipne Saddle. These sediments were then deposited within a tectonically quiescent rift-flank setting to the southeast, external to the main rift zone (Fig. 5.21a). This would suggest that the Gleipne Saddle acted as a 'sink overflow' for sediment which when the accommodation space was close to being filled, would allow for sediment to flow out of the rift to the SE on to the rift margins (i.e. into the Vigrid Syncline; Fjellanger *et al.* 2005). It is therefore expected that a thick Cretaceous sedimentary sequence is preserved within the Fenris Graben beneath the inner flows and the Vøring Marginal High, as well as offshore Greenland, similar to that interpreted within the Hel Graben to the northeast. During periods of tectonic quiescence (e.g. during the Paleocene), the Gleipne Lineament appears to exert little influence on the stratigraphical fill of the basin although minor thickening of the depositional sequences still occurs despite relative basin uplift at the time.

5.8.3 Along strike variations of igneous activity

The inner flows have been commonly inferred to be of igneous origin (e.g. Eldholm 1989; Skogseid *et al.* 1992; Eldholm & Grue 1994) and have been described in detail by Planke *et al.* (2000) and Berndt *et al.* (2001) who suggested that they were formed as a bottom set for a Gilbert-type lava delta represented by a flow-foot breccia (Thomson 2005a). The lava delta is formed at the edge of the Vøring Marginal High and as the inner flows were deposited structurally lower than the delta top, it seems likely that the flows were deposited in a marine setting (Tsikalas *et al.* 2008). The disturbance in the seismic data above the inner flows (Fig. 5.08) may be attributed to a scattering of the seismic waves due an irregular, brecciated top to the flows (Fig. 5.22a). The inner flows which are deposited in the RAZ remain undrilled to date and so the mode of deposition for the inner flows is still contentious. An understanding of this is required to accurately consider the influence of the RAZ upon the deposition of the unit. An alternative hypothesis is that these are subaerial lava flows (Fig. 5.22b) resting upon continental deposits (e.g. fluvial, aeolian and lacustrine) which may be realistic as this area was exposed to erosion in the Early Paleocene, prior to deposition of the inner flows in the latest Paleocene. But this hypothesis seems unlikely as all wells encountered Late Paleocene marine sediments even on the structurally highest points of the basin. Two alternative hypotheses remain for the inner flows in and around the RAZ based on the observation that the flows are often located directly above high amplitude sills (e.g. Fig. 5.08; Chapter 4, figs 4.06 and 4.07, p195-198). The sills may be localised sources for the inner flows and therefore two hypotheses are tenable. Firstly, the inner flows may be the result of seabed fissures and eruptions (e.g. Thomson 2005b) sourced from the sills, producing pillows lavas on the seabed (Fig. 5.22c). Secondly, they may be shallowly intruded sills into poorly-lithified, possibly water-rich sediments, which too have been sourced from the sills at depth (e.g. Thomson & Hutton 2004; Fig. 5.22d). This latter interpretation would require the inner flows to be younger and intruded rather than extruded as is the case for the three previous hypotheses. This mechanically therefore, would have to be the sole process for deposition of the near continuous mapped inner flows which seems unlikely.

The Late Paleocene inner flows are located in what was the primary depocentre in the basin at the time (Fig. 5.06c). As the flows have been mapped to link with the base of the lava delta (Ren *et al.* 2003) it seems likely that the inner flows are at least in part a direct continuation of the hyaloclastite succession. A dip analysis (Fig. 5.09) of the inner flows in 3D seismic data also highlighted sub-circular features which appear flat towards the centre, but dip more steeply at their edge. Interpreted as piled pillow lava deposits (e.g. Davies *et al.* 2002), the morphology may be explained due to the near instantaneous point (fissure) sourcing of lavas from Late Paleocene sills or dykes upon a marine slope at the time. A reason as to why the igneous material reaches the seabed here is that it was of greatest bathymetrical relief in this location with new injections of igneous material preferentially exploiting pre-existing zones of weakness (Thomson & Hutton 2004). Therefore, the authors support Tsikalas *et al.* (2008) interpretation of a mixed mode origin for the inner flows, predominantly formed of submarine breccia material but supplemented by sea floor eruptions of volcanic material probably sourced from the underlying sill complex. It is therefore of no coincidence that the inner flows are deposited within the RAZ for two reasons. Firstly, due to Early – Middle Paleocene movements upon the NW-SE fault producing a boundary of notable relief, and secondly due to synchronous uplift of the strata in a north-south trend which formed a depositional barrier to the east (Hjelstuen *et al.* 1999; Fig. 5.12d). Therefore, in part, the RAZ has controlled deposition of the volcanic material in the basin but this is due to the pre-existing uplift and subsidence patterns and not by major strike-slip faulting and pull-apart basin formation as previously inferred by Ren *et al.* (2003). Differential compaction above the inner flows (Fig. 5.08) has also led to the RAZ increasing in relief following continental breakup in the Eocene (Appendix D.11).

The inner flows also flow into the remnant topography to the northwest of the Gleipne Saddle. However, the nature of the flows in this location was not analysed due to a lack of coverage by the 3D seismic data. It is also difficult to examine whether there is a link between the intrusive volcanic activity (e.g. emplacement of sills, hydrothermal vent complexes and/or volcanic seabed fissures) and the Gleipne lineament due to a lack of 3D seismic data coverage in the Vigrid Syncline away and directly above the Gleipne Lineament. However, Planke *et al.* (2000) illustrate a notable increase in vent activity around the Gleipne Saddle from an analysis of regional 2D seismic data. It is expected that the effects are more visible in this area however due to a thicker and potentially less lithified cover sequence above the sill intrusions. Detailed mapping of the sill complex is needed to revoke or support the hypothesis, which in turn may be related to the thickness of the LCB at depth (Gernigon *et al.* 2003).

5.8.4 Hydrocarbon prospectivity

The regional source rock is considered to be the organic rich Spekk Formation of Late Jurassic age (equivalent to the Kimmeridge Clay of the North Sea and West of Shetland; Scotchman *et al.* 1998; Swiecicki *et al.* 1998; Langrock & Stein 2004) which is expected to be present in the outer Vøring Basin due to evidence of a deeply-buried Late Jurassic rift (Chapter 4). Furthermore, the Luva (6707/10-1) and more recent Snefrid (6706/12-1), Haklang (6707/10-2S) and Asterix (6705/10-1) thermogenic gas discoveries in Late Cretaceous sandstones prove the presence of a prolific oil and gas (type 2) source rock of regional extent which is likely to be gas mature. The NW-SE lineaments are not expected to be focal areas for the migration of hydrocarbons due to the lack of major deep-seated faulting within the NW-SE lineaments. The primary influences that the NW-SE lineaments have upon the petroleum system are the reservoir provenance and distribution, and the nature of both structural and stratigraphic hydrocarbon traps. During Campanian deposition of the Nise Sandstone Members (which house the Nyk High gas discoveries), both lineaments are expected to have present thick deposits due to the widespread deposition of the sequence. The Gleipne Lineament may have formed an entry point for sediment into the Vøring Basin at the time, but thickness variations across the RAZ are possibly due to it being located at the edge of the basin slope and at the boundary of the Hel Graben depocentre, not due to any major tectonic activity.

The RAZ is expected to impact heavily upon the reservoir development and the trap types in which hydrocarbons may be found but does not act as a source for sediment to enter the basin from the west. During rifting, marine fan deposits are expected to be constantly evolving within an actively extending rift basin. In areas across the NW-SE fault of the northern RAZ, laterally discontinuous sandstone deposits may well be present with inter-fingering of sandstones and mudstones sourced from across the fault in the Gjallar Ridge as well as from the northwest and Hel Graben. This may not be of concern depending on the amount (and quality) of the axially drained sediments but may lead to problems in forming a laterally continuous hydrocarbon column and recovery. The fault hangingwalls and regional depocentres are expected to be more sand prone than upon footwall crests as sediment would preferentially drain into these areas during the Late Cretaceous. The pattern of coarser deposits in the fault hangingwalls is expected to continue into the Paleocene, particularly within the faulted southern RAZ, into which locally eroded and distally sourced sediment is expected to be deposited due to major local erosion of the Gjallar Ridge combined with major normal faulting at the time (Appendix D.08). Possible stratigraphical traps may be present in the central RAZ but are dependent upon a flow of sediment into the Hel Graben across the ramp hinge located in this area. Mud prone and volcaniclastic sediment deposited in the Late Paleocene are expected to provide an excellent seal of regional extent. Structural traps would be formed against the normal faults of the Gjallar Ridge, Nyk High and southern RAZ.

During Maastrichtian rifting, the Gleipne Lineament is expected to transfer both locally sourced and distal sediments into the Vøring Basin and distribute the sediment upon the rift flanks. These stacked marine fan deposits are expected to form potential sandstone reservoirs. Paleocene strata are expected to be mud-prone above the Gleipne Lineament, particularly so within the Vigrid Syncline but may provide an excellent seal to the system except where locally removed due to hydrothermal vent complex formation. The Fenris Graben is expected to contain the best Paleocene sandstone reservoirs as sand prone sediment was continuing to be shed from the structurally higher Gjallar Ridge and Greenland at this time (Lien 2005; fig 10, p330). The addition of volcanic material both helps and hinders petroleum prospectivity in the area. In addition to the possible disturbance of the seal horizons, volcaniclastic and tuff material sourced from active volcanoes along the line of continental breakup may reduce the porosity of possible Paleocene reservoirs. Intrusion of the Late Paleocene sills may further enhance the size of stratigraphical hydrocarbon traps through force folding along the length of the Gleipne Lineament but may also reduce the porosity of sandstone reservoirs due to thermal metamorphism (e.g. McKinley *et al.* 2001).

A major risk in hydrocarbon exploration in the basin and a limitation of the models presented here is demonstrated by Whitham *et al.* (1999) who recognised the erosion of sand deposits did not always result in sandy sequences within the fault hangingwalls onshore Greenland. This could similarly be the case in the northern Vøring Basin and therefore any plays based upon the local reworking of footwall sediment (e.g. the Campanian Nise Sandstones) may heavily influence exploration risk. However, the deposits which developed are expected to have formed as a mixture of both the locally reworked sediment mixed with fresh influxes of coarse grained material from the northwest (as drilled in the wells). Only further analysis of reworked footwall strata by marine fan deposits of similar stratigraphy to the outer Vøring Basin will allow for an improved prediction as to relative sand concentrations related to this process; this would also have a direct impact upon the tectono-stratigraphic models proposed.

Other limitations of the study also directly impact upon the inferred hydrocarbon prospectivity and exploration risk of the northern Vøring Basin. The variation in seismic facies has been primarily interpreted due to variation in stratigraphical fill of the basin which although may be considered as good practice in an area of sparse well control (Vail *et al.* 1977) is susceptible to other processes such as fluid content of the rock, intrusive and extrusive igneous activity as well as any diagenetic variations. Therefore interpreted facies may be at least in part the result of other variations in the rock characteristics and care must be taken when applying these models. Similarly, the models presented are based upon the interpretation of seismic data which, although the best seismic data available has been used for the study, is still heavily influenced by the significant volcanic activity in the region as well as remobilisation of Miocene siliceous ooze. Equally, the 3D seismic data does not image the entire northern Vøring Basin, resulting in the use of 2D seismic data which limits an understanding of the basin evolution in these areas. However, the stratigraphical and volcanic evolution of the two rift segmenting structures presented here fits well with the current understanding of the pre-breakup evolution of the Norwegian continental margin and is in agreement with the available well data in the region. The release of recently drilled well information will further our understanding of this complex segmented rift system, as well as give a better grasp of the stratigraphical and volcanic evolution within segmented volcanic passive margins worldwide.

5.9 Conclusions

- The NW-SE Gleipne Lineament in neither an accommodation of transfer zone nor is there any evidence of strike-slip faulting, but is likely to have formed as a long-lived structural low directly related to the underlying basement structure; the Lower Crustal Body (LCB).
- Sedimentation is focussed along the strike of the Gleipne Lineament from both the north and west and locally eroded region during periods of rifting. The sediment is distributed outside the main rift zone as a series of marine fan deposits. During periods of minimal upper crustal extension, the Gleipne Lineament is much less defined with only subtle thickening of strata recorded along the lineaments strike.
- The Rym Accommodation Zone does not transport sediment from the north and west into the Vøring Basin under rift conditions, but rather compartmentalises the basin. Sediments are predicted to flow along strike across the fault domain boundary which increases the predicted complexity of the stratigraphical fill in the Vøring Basin.
- The Gleipne Lineament and Rym Accommodation Zone exert an indirect effect on Paleocene volcanic activity in the basin due to the influence each feature has on the formation of basinal depocentres and thickness of sedimentary deposits. This in turn promotes extrusive eruptions of sill sourced pillow lavas at the seabed, the ponding of lava breccia flows and the increased prominence of hydrothermal vent complex formation formed above sill tips.
- The two lineaments are considered very important for hydrocarbon exploration due to the impact upon reservoir provenance and distribution both within and external to the rift zone, as well as the stratigraphical and structural hydrocarbon traps they potentially contain.

5.10 Acknowledgements

This work forms part of a NERC CASE Studentship with Statoil U.K. Ltd (NER/S/C/2006/14276). PGS Geophysical, TGSNopec and WesternGeco, are gratefully acknowledged for permission to publish lines and interpretations from the respective seismic datasets. Landmark Graphics Corporation through the Strategic University Alliance Agreement (2006-COM-032168) is acknowledged for providing seismic processing/interpretation software and technical support. D. Stevenson and G. Wilkinson provide ongoing technical support within the Department of Earth Sciences.

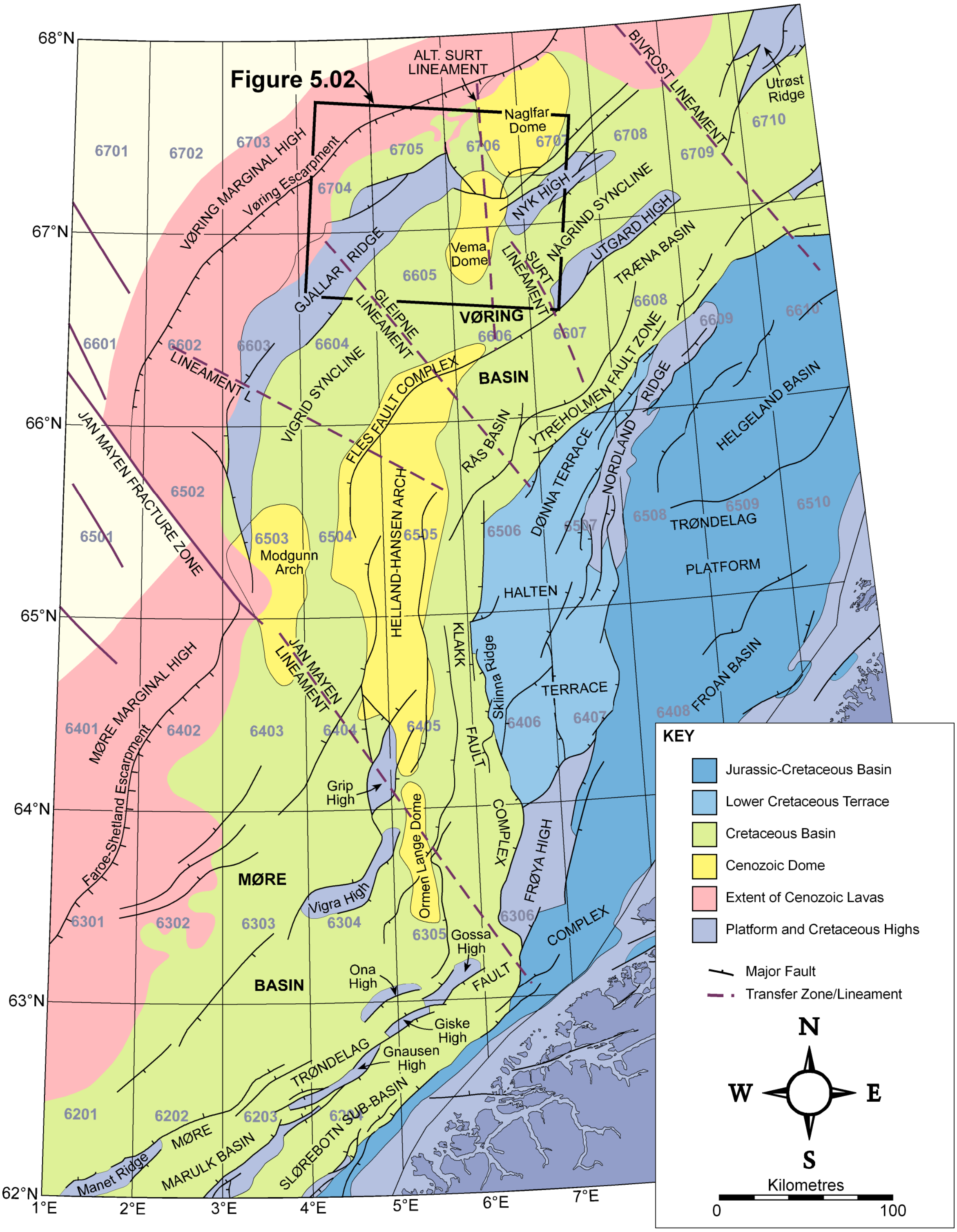

Figure 5.01: Tectonic elements map of the Norwegian continental shelf displaying the gross N-S and NE-SW structural trends formed during successive rift events. Numerous NW-SE rift oblique lineaments ('transfer zones') are recognised along the margin recognised from various geophysical datasets. Modified after Blystad *et al.* (1995), Ren *et al.* (2003) and Mjelde *et al.* (2005). Map projection is WGS84, UTM 31N.

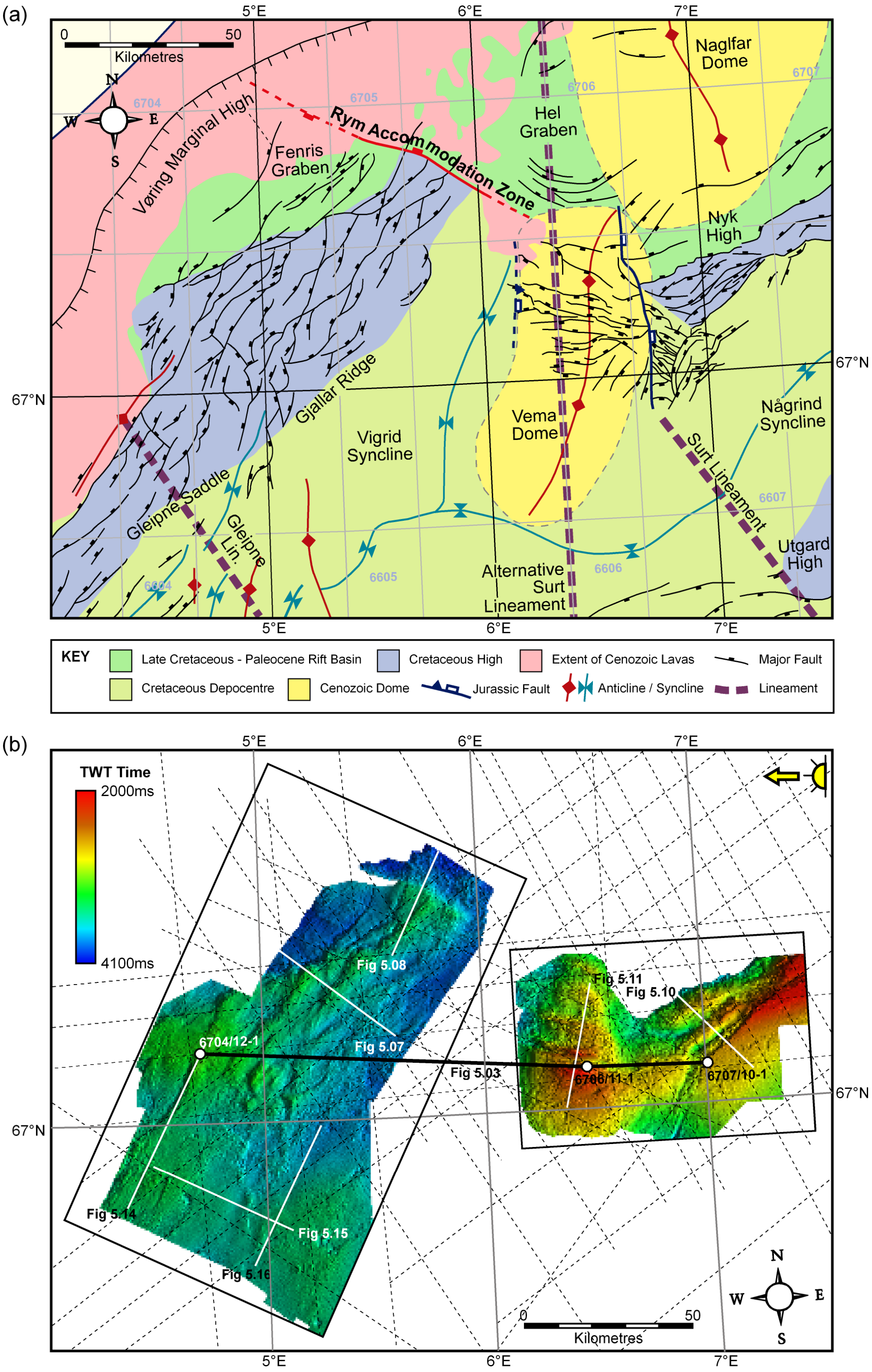

Figure 5.02: (a) The principal tectonic elements of the northern Vøring Basin (after Chapter 4). The Rym Accommodation Zone is located between the offset NE-SW trending Gjallar Ridge and Nyk High. Cenozoic igneous material is mapped to have flowed into the Rym Accommodation Zone (Ren *et al.* 2003). The Gleipne Lineament crosses the Gjallar Ridge to the southwest. (b) Location of the three wells used in the study, and both 2D (dashed lines) and 3D seismic datasets with the top Cretaceous unconformity horizon mapped displaying the gross structural geometry of the structural highs.

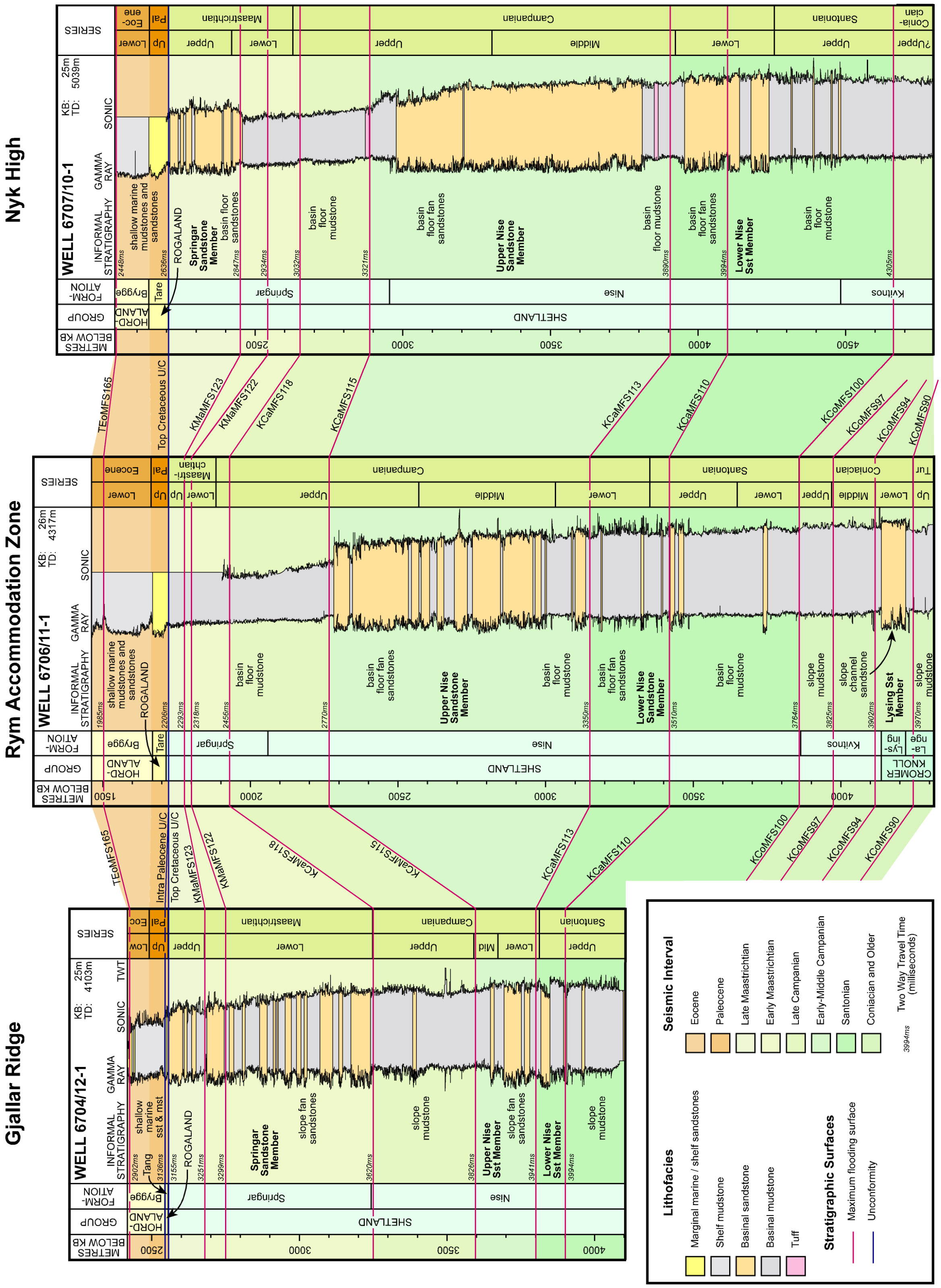

Figure 5.03: Well correlation panel of the three released exploration wells available for the study with correlations of the maximum flooding surfaces within the Late Cretaceous and Paleocene sequences provided by StatoilHydro. For location of wells, see Figure 5.02b.

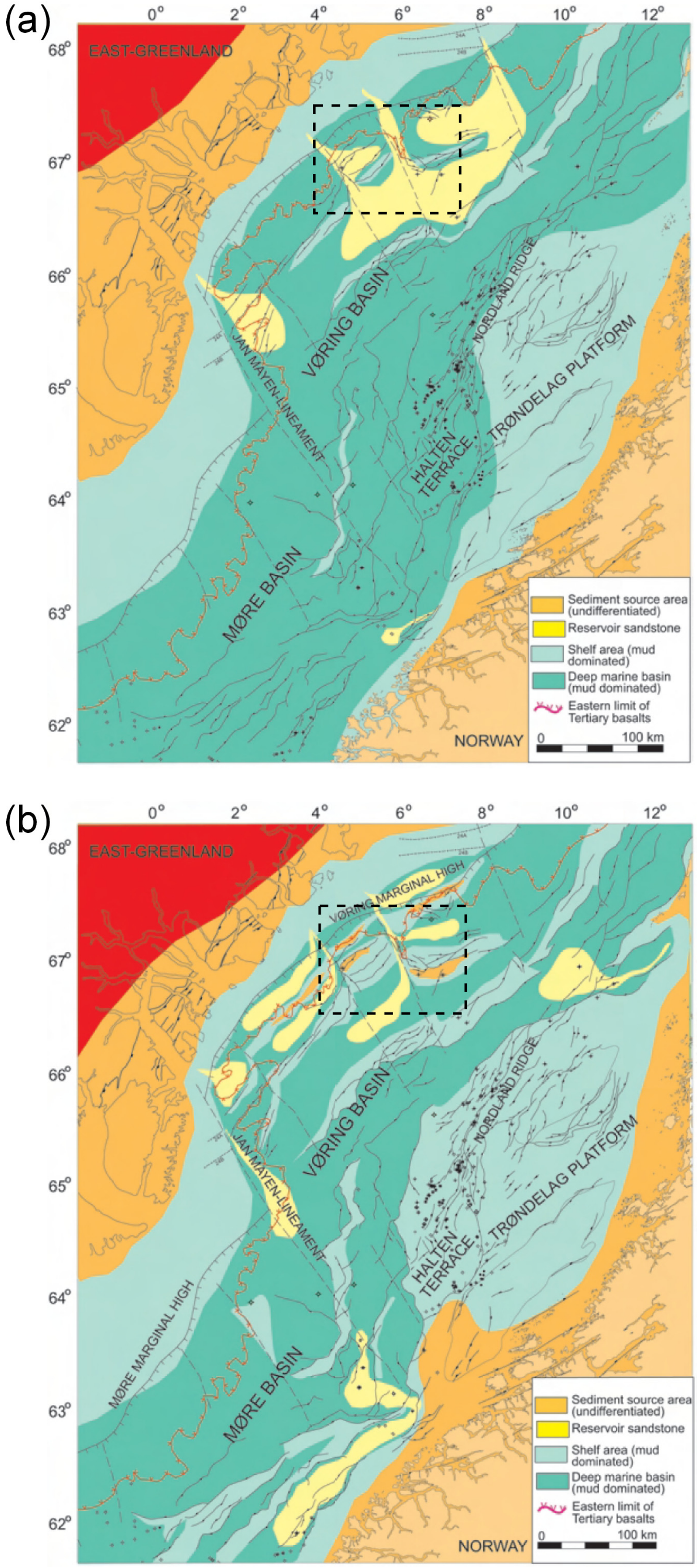

Figure 5.04: Palaeogeographic maps of the (a) Late Cretaceous and (b) Paleocene (Lien 2005). Dashed outline displays the relative location of the study area.

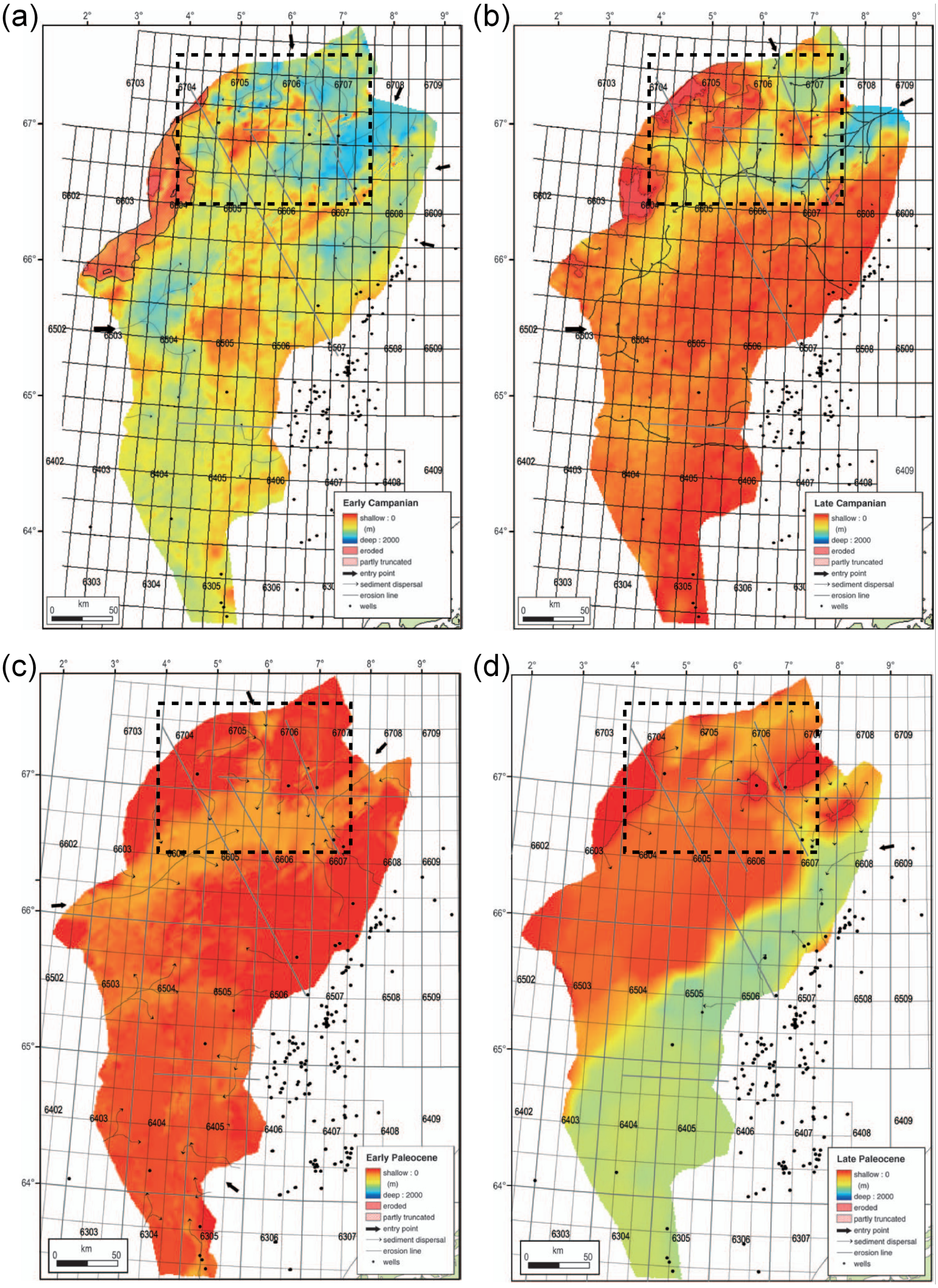

Figure 5.05: Palaeobathymetric reconstructions and sediment dispersal patterns in the Vøring Basin during (a) the Early Campanian, (b) the Late Campanian, (c) Early Paleocene and (d) Late Paleocene (Kjennerud & Vergara 2005). The dashed outline displayed on the maps is the approximate geographical limit of the area analysed in this study.

(a) Late Campanian

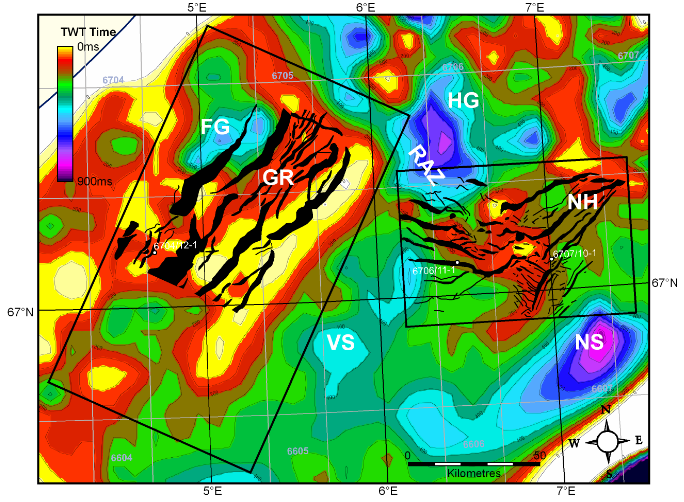

(b) Maastrichtian

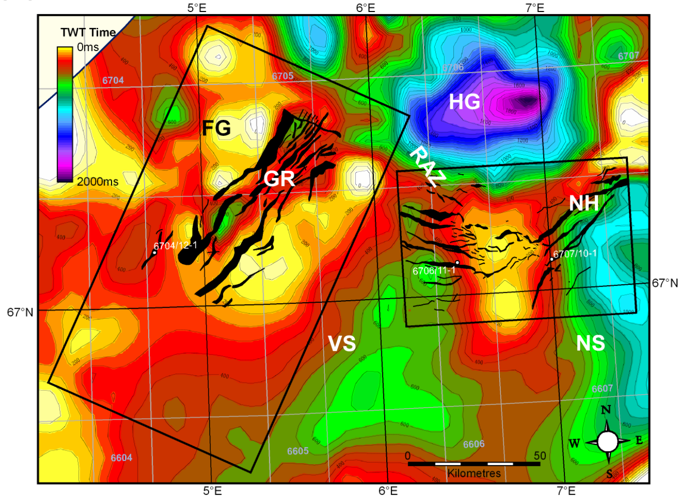

(c) Paleocene

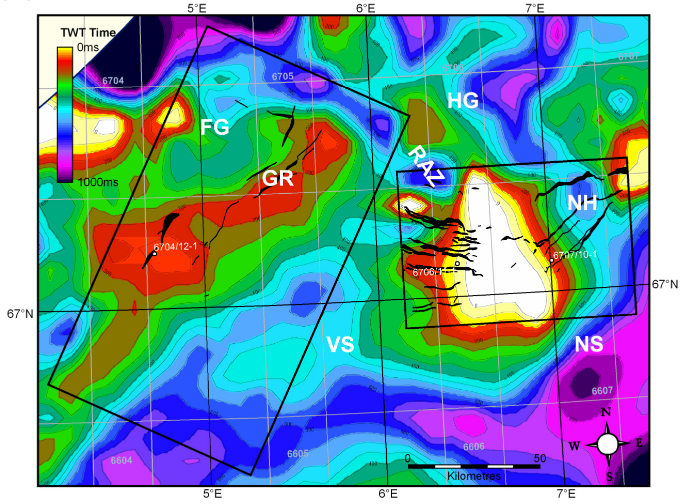

Figure 5.06: Sediment isochrons for the (a) Late Campanian, (b) Maastrichtian and (c) Paleocene calculated from differences between KCaMFS115, KCaMFS118, Top Cretaceous and Top Paleocene horizons from the mapped 2D and 3D seismic datasets. **GR** Gjallar Ridge; **NH** Nyk High; **RAZ** Rym Accommodation Zone; **VS** Vigrid Syncline; **NS** Någrind Syncline; **FG** Fenris Graben; **HG** Hel Graben.

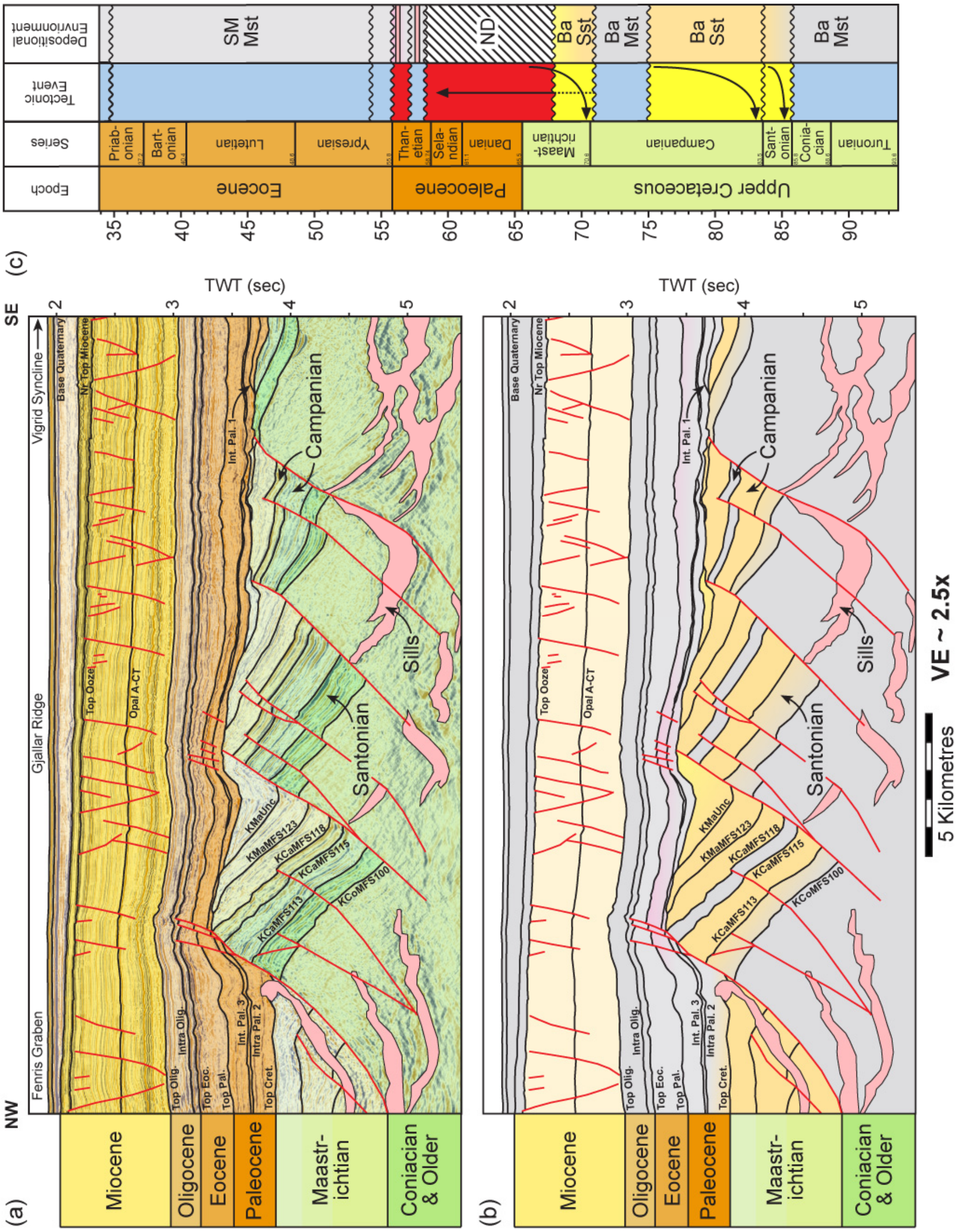

Figure 5.07: The (a) structural geometry of the Fenris Graben, Gjallar Ridge and Vigrid Syncline with (b) the predicted stratigraphical fills for each of the sequences based upon seismic stratigraphical analysis and correlated with results from well data. See Figure 5.03 for key to predicted stratigraphy. (c) A tectono-stratigraphic and volcanic summary is given for the seismic line with periods of rifting in yellow, erosion in red and subsidence in blue. **Ba** Basinal, **SM** Shallow Marine, **ND** Non Deposition of sediments. See Figure 5.02b for line location. Seismic data courtesy of PGS Geophysical.

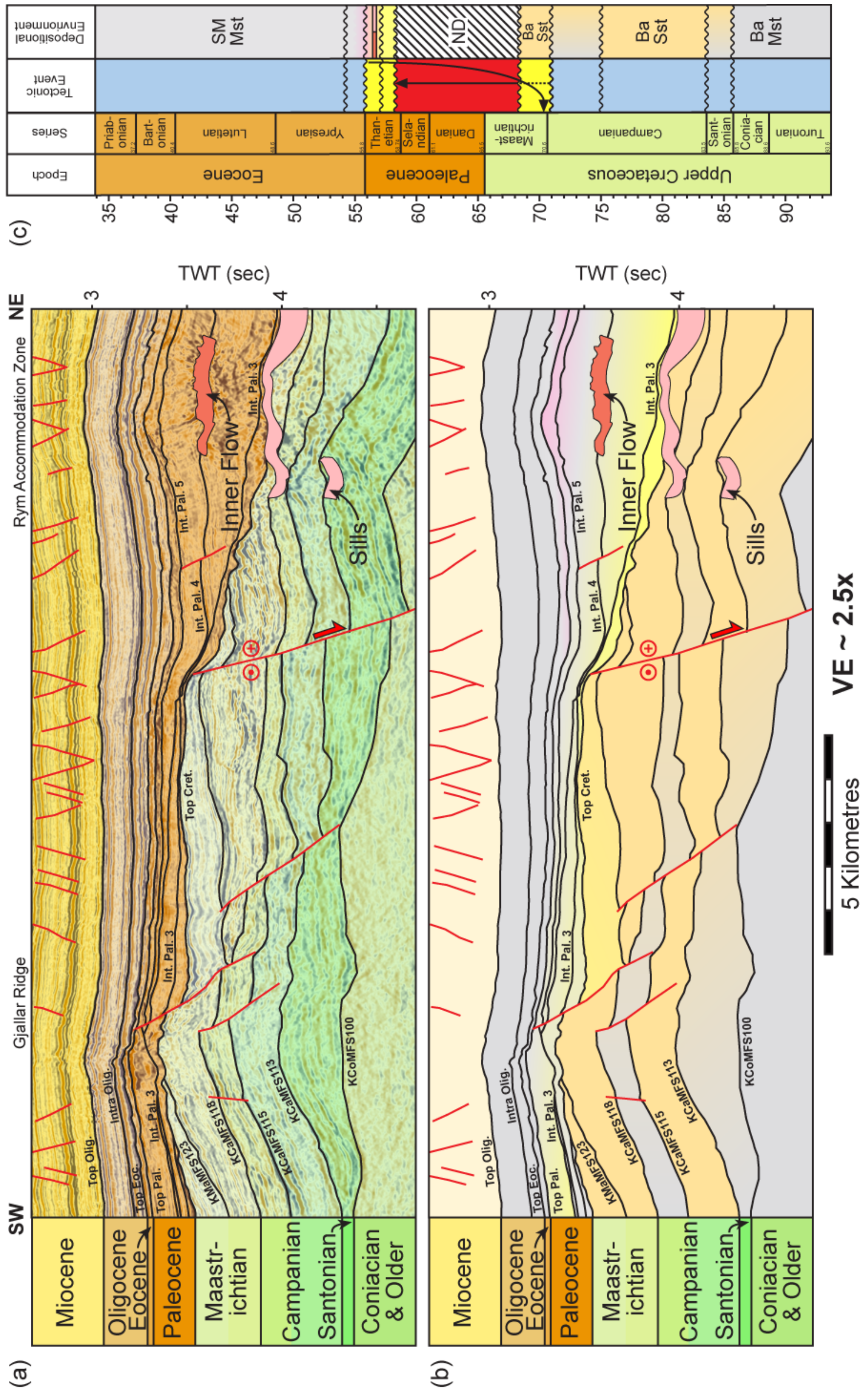

Figure 5.08: The (a) structural geometry of the transition from the Gjallar Ridge into the northern Rym Accommodation Zone, (b) the predicted stratigraphical fill and (c) tectono-stratigraphic and volcanic summary for the illustrated seismic line. See Figure 5.02b for line location. Seismic data courtesy of PGS Geophysical.

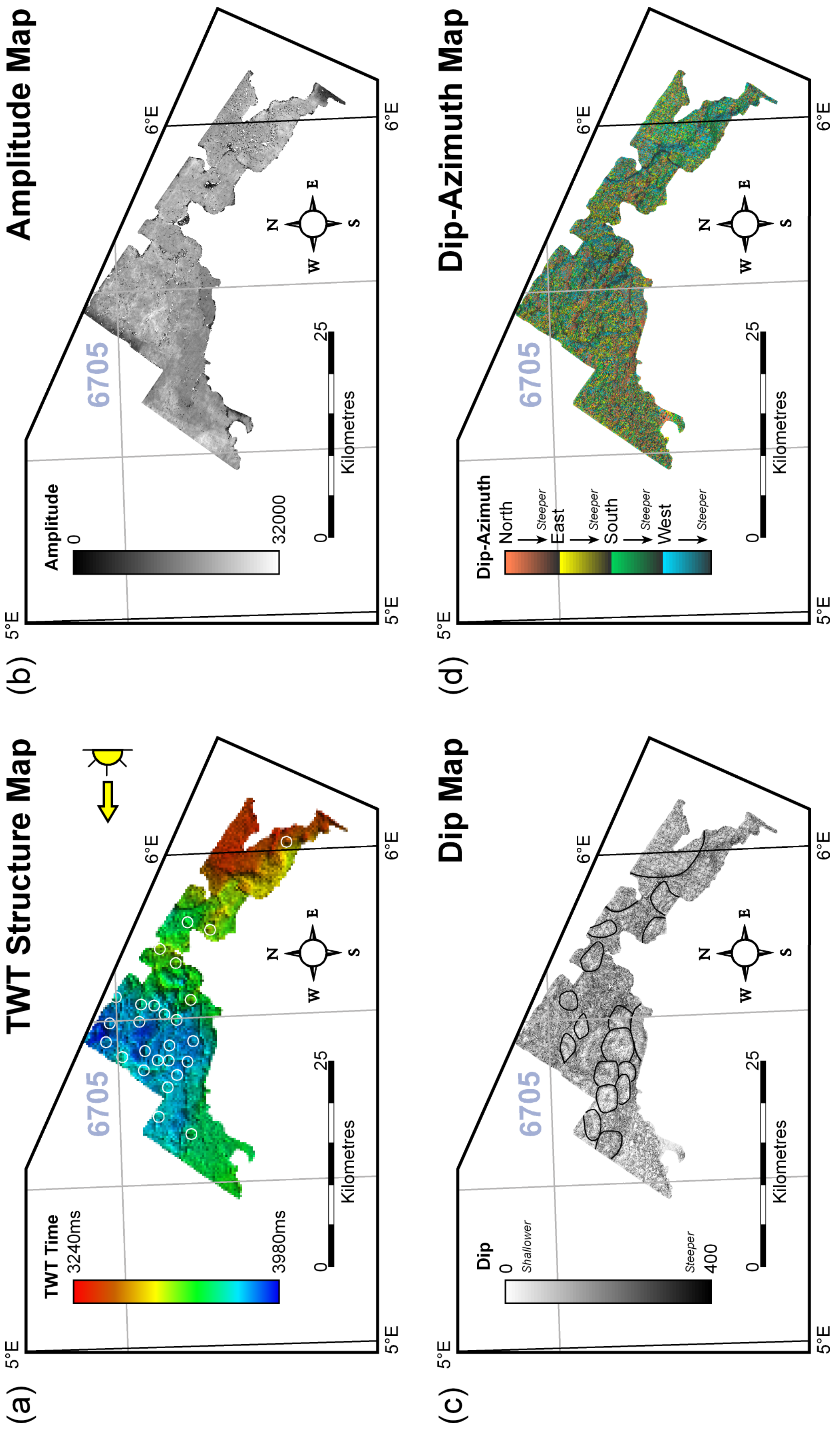

Figure 5.09: Horizon analyses of the mapped inner flows horizon from the Gjallar Ridge seismic survey within the northern Rym Accommodation Zone.

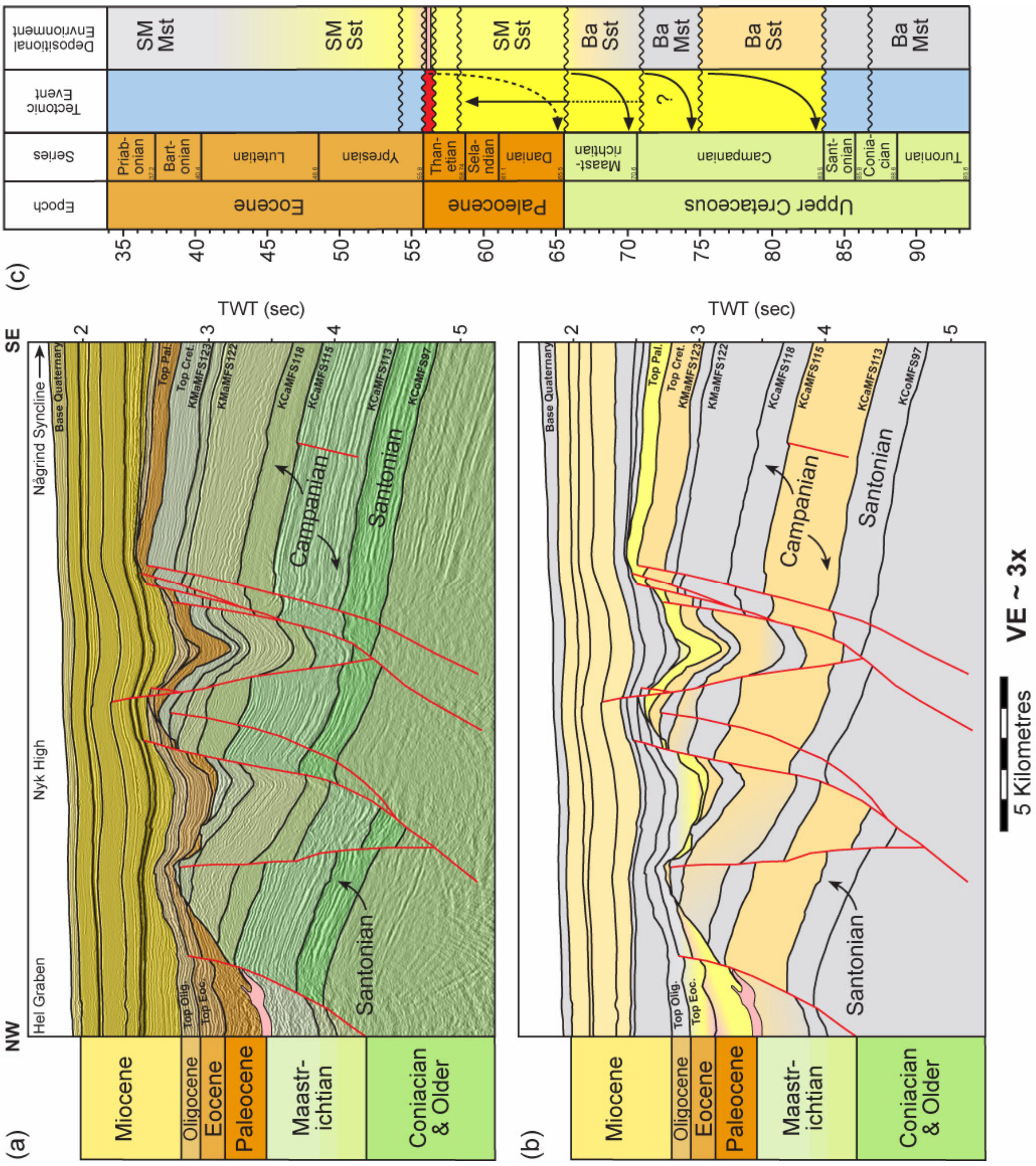

Figure 5.10: The (a) structural geometry of the Hel Graben, Nyk High and Vigrid Syncline, (b) the predicted stratigraphical fill and (c) tectono-stratigraphic and volcanic summary for the illustrated seismic line. See Figure 5.02b for line location. Seismic data courtesy of PGS Geophysical.

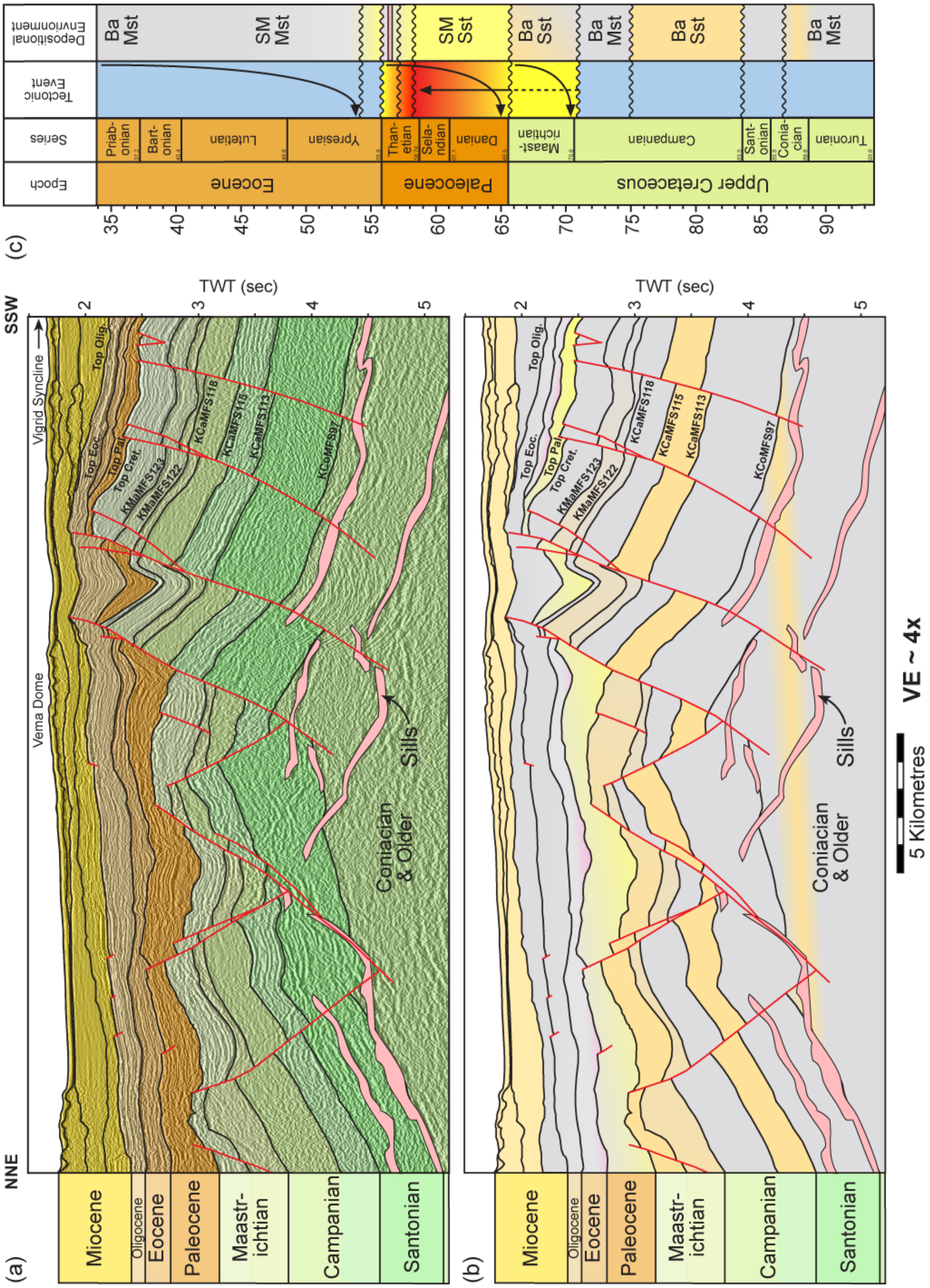

Figure 5.11: The (a) structural geometry of the east-west faults in the southern Rym Accommodation Zone along strike from the Nyk High, (b) the predicted stratigraphical fill and (c) tectono-stratigraphic and volcanic summary for the illustrated seismic line. See Figure 5.02b for line location. Seismic data courtesy of WesternGeco.

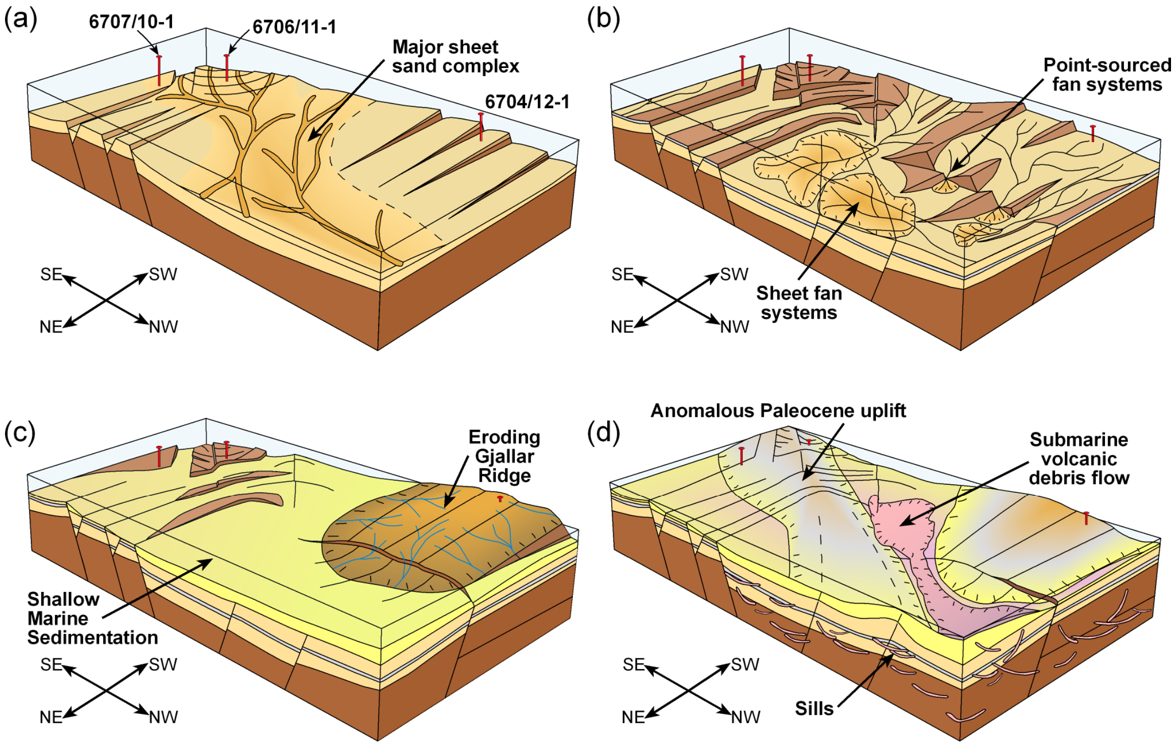

Figure 5.12: Tectono-stratigraphic and volcanic evolutionary block models for the Rym Accommodation Zone during the (a) Campanian, (b) Maastrichtian, (c) Early Paleocene and (d) Late Paleocene. View to the south. Model scale approximately 50 x 100 km.

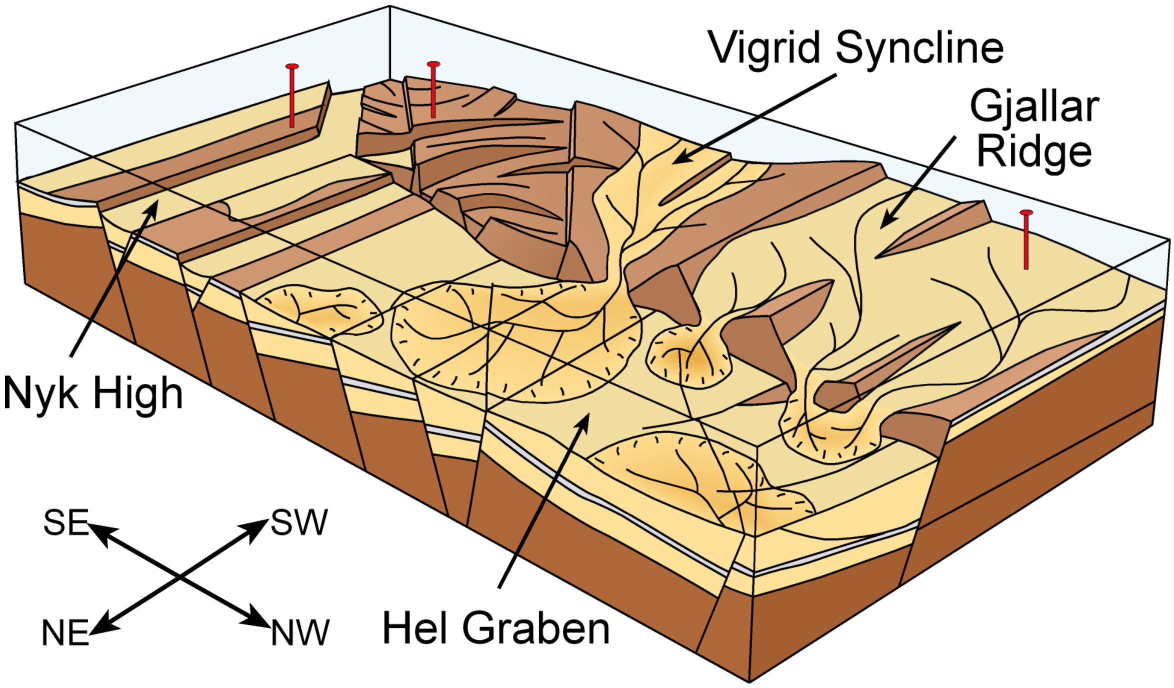

Figure 5.13: Hypothesised tectono-stratigraphic block model for the Rym Accommodation Zone if rifting had continued with the development of a transfer fault system between the Gjallar Ridge and Nyk High. Sediment is likely to flow across the fault scarp rather than along the NW-SE fault against the structural grain. View to the south. Model scale approximately 50 x 100 km.

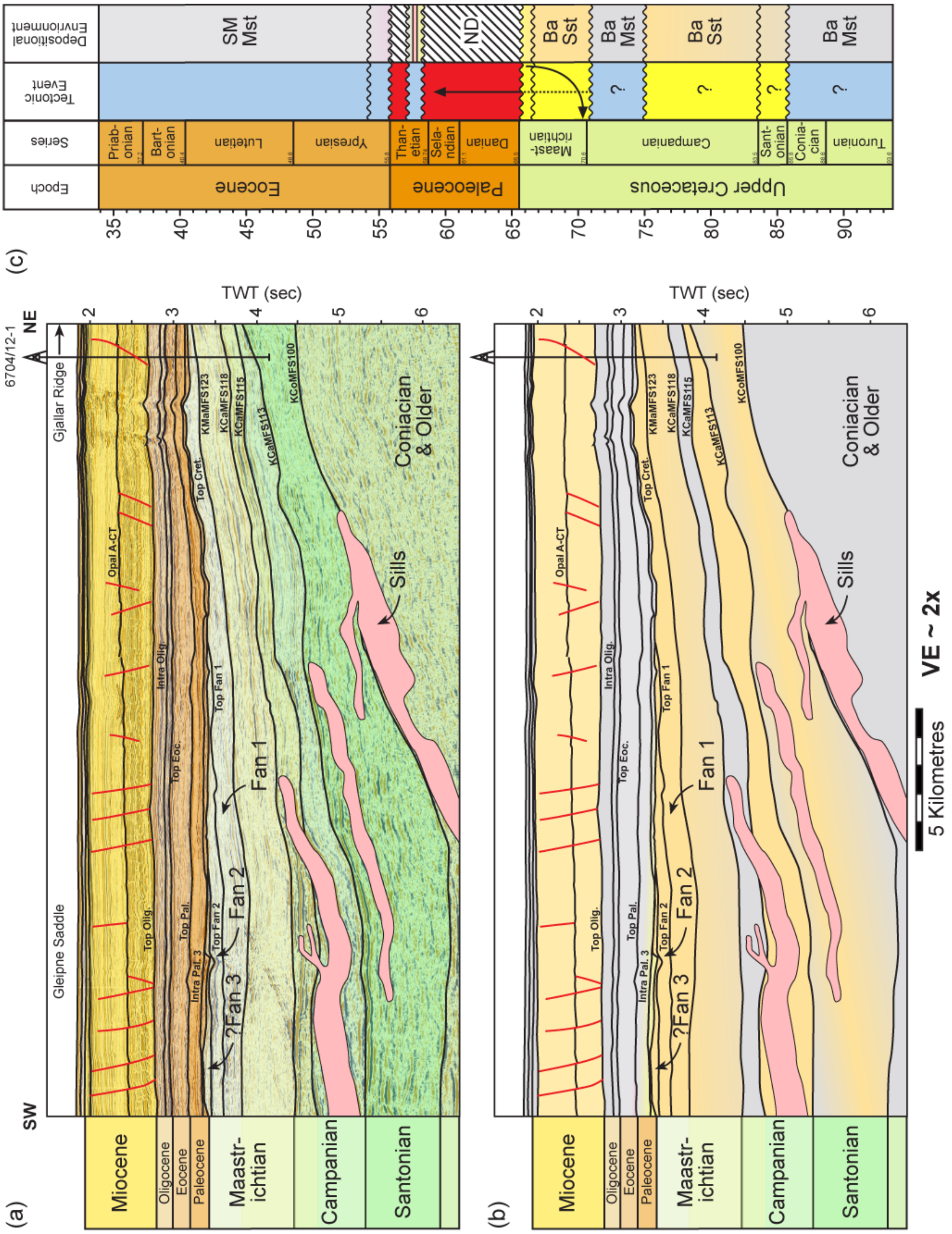

Figure 5.14: The (a) structural geometry of the Gjallar Ridge and the transition into the Gleipne Saddle, (b) the predicted stratigraphical fill and (c) tectono-stratigraphic and volcanic summary for the illustrated seismic line. See Figure 5.02b for line location. Seismic data courtesy of WesternGeco.

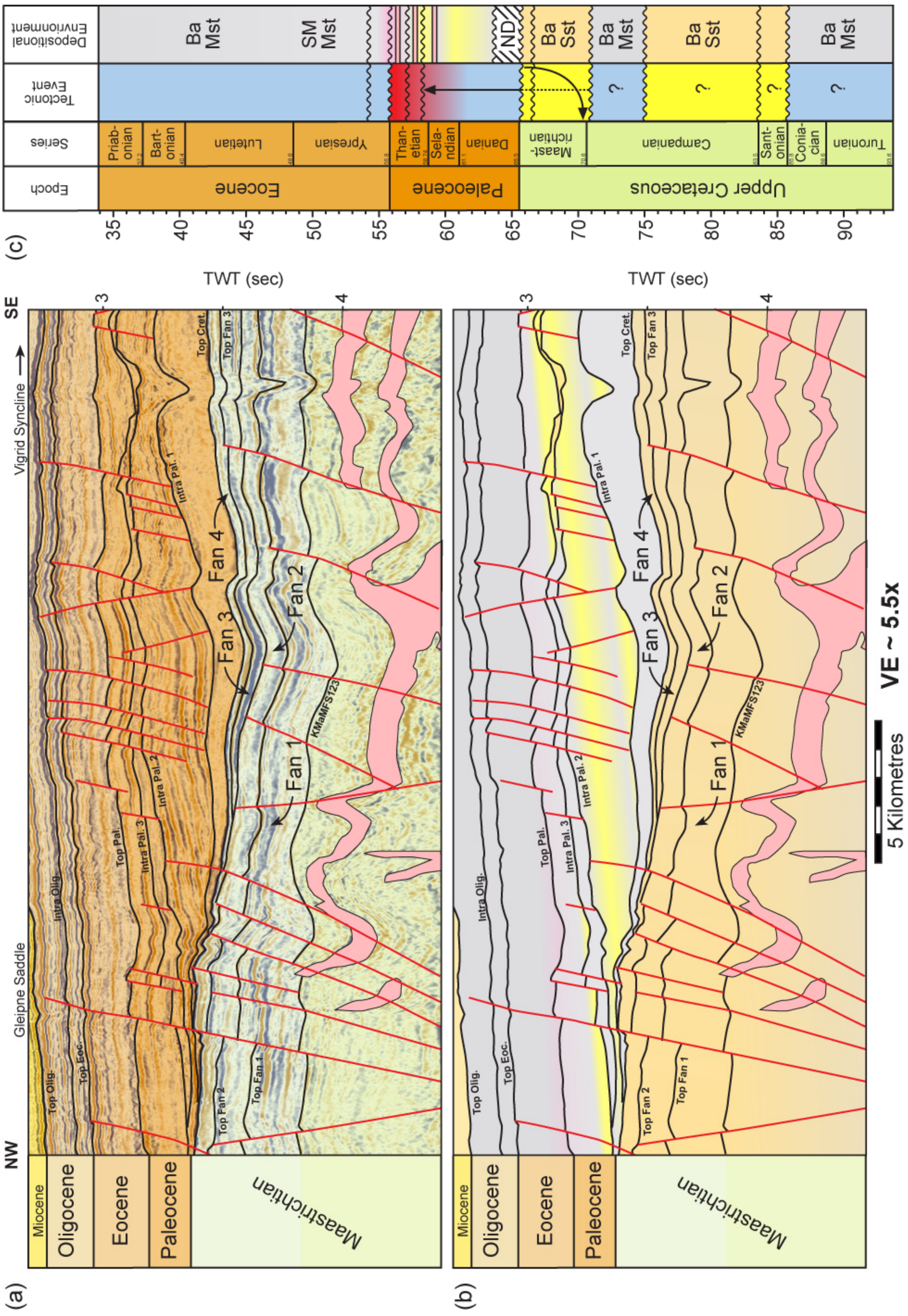

Figure 5.15: The (a) structural geometry along strike of the Gleipne Saddle, (b) the predicted stratigraphical fill and (c) tectono-stratigraphic and volcanic summary for the illustrated seismic line. See Figure 5.02b for line location. Seismic data courtesy of WesternGeco and TGS Nopec.

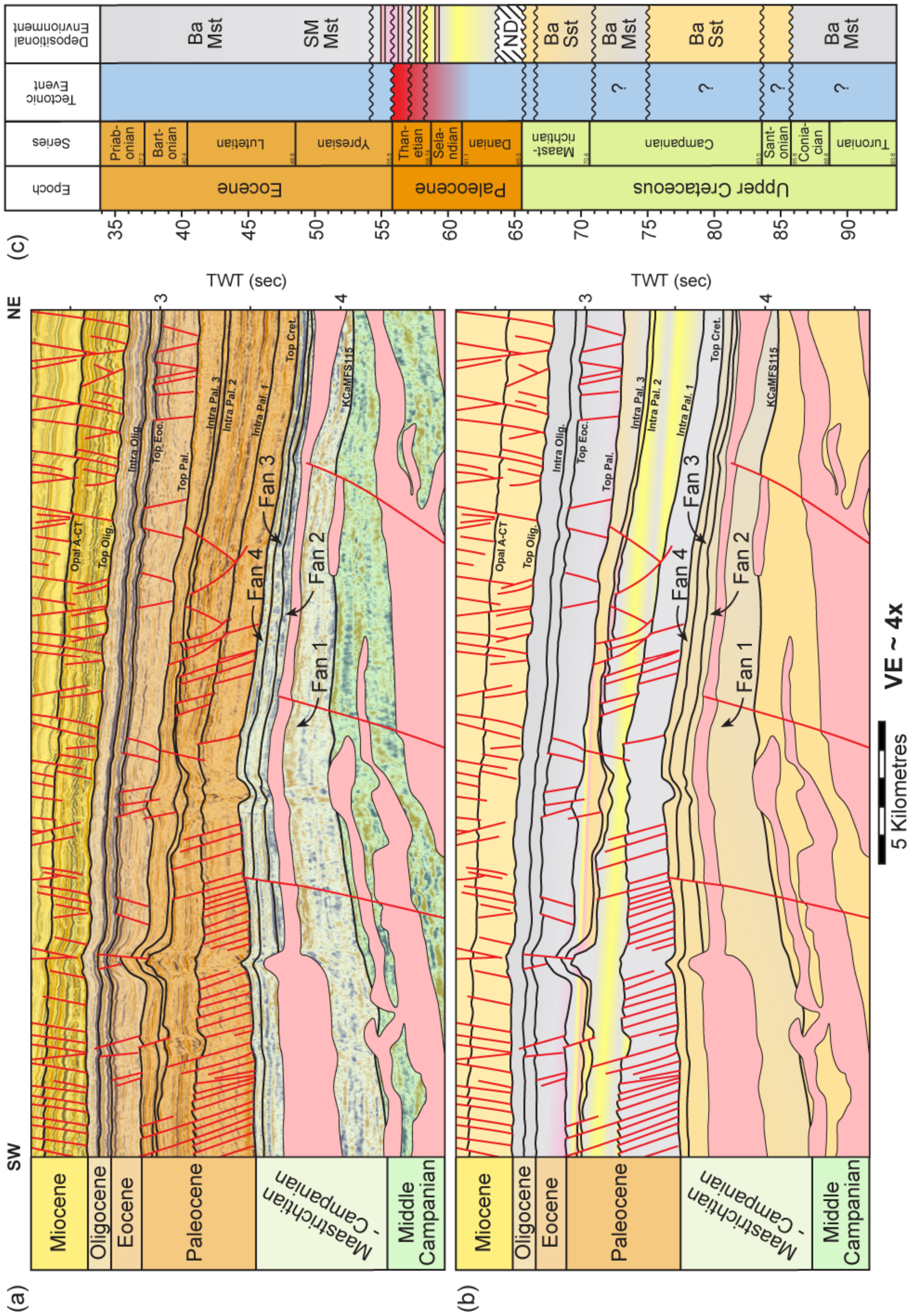

Figure 5.16: The (a) structural geometry along strike of the Vigrid Syncline in the vicinity of the Gleipne Lineament, (b) the predicted stratigraphical fill and (c) tectono-stratigraphic and volcanic summary for the illustrated seismic line. See Figure 5.02 for line location. Seismic data courtesy of TGS Nopec.

(a) Top Maastrichtian Fan 1

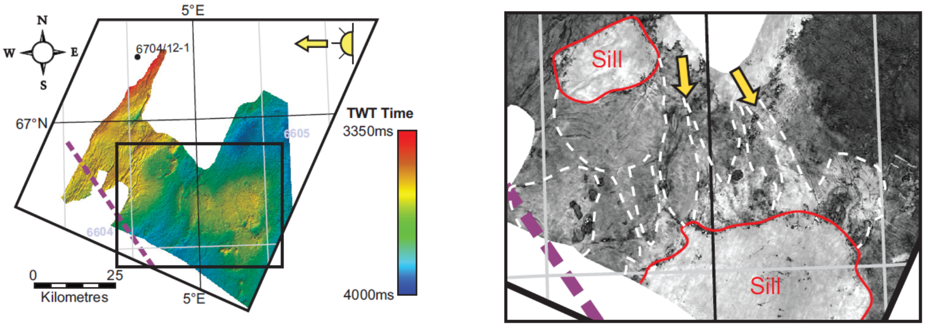

(b) Top Maastrichtian Fan 2

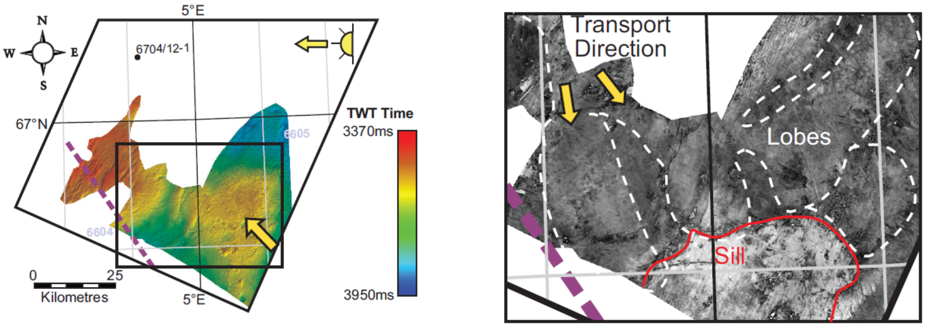

(c) Top Maastrichtian Fan 3

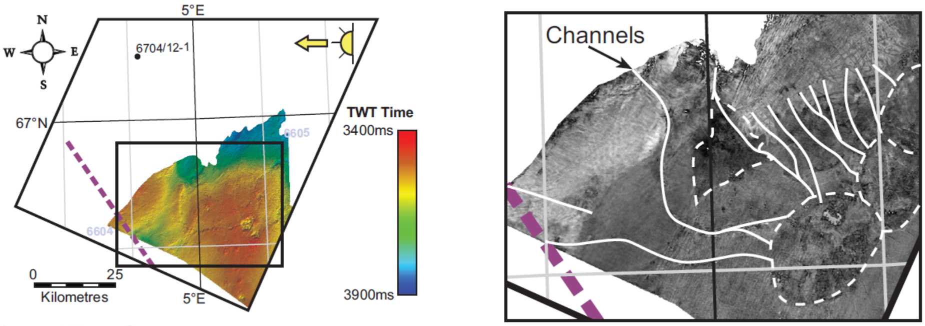

(c) Top Cretaceous

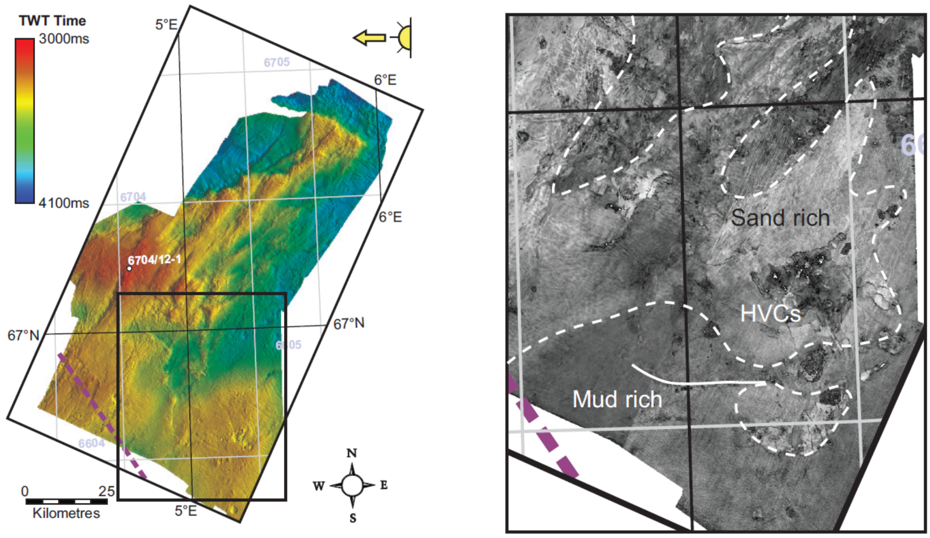

Figure 5.17: TWT structure maps of (left) the successive Maastrichtian marine fan sequences in the vicinity of the Gleipne Lineament. Amplitude extractions (right) of the mapped sequence tops display areas of light (sand rich) and dark (mud rich) reflectivity. Amplitude sample boxes are ~ 50 x 38 km in size except for the Top Cretaceous amplitude extraction which is ~ 50 x 62.5 km.

(a) Maastrichtian Fan 2

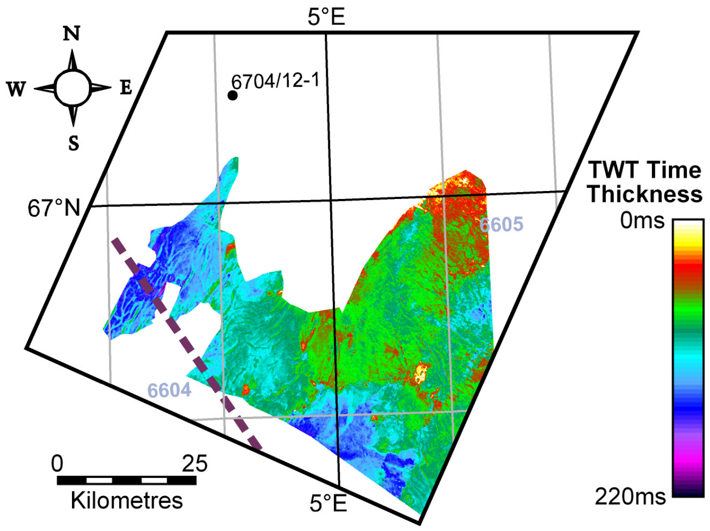

(b) Maastrichtian Fan 3

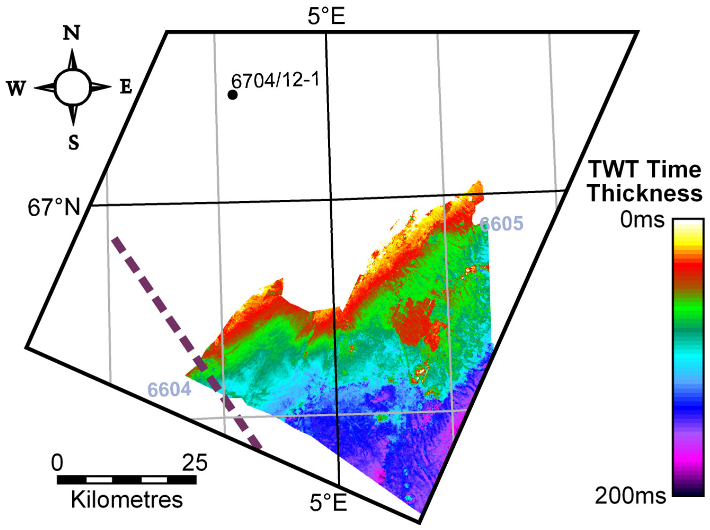

(c) Maastrichtian Fan 4

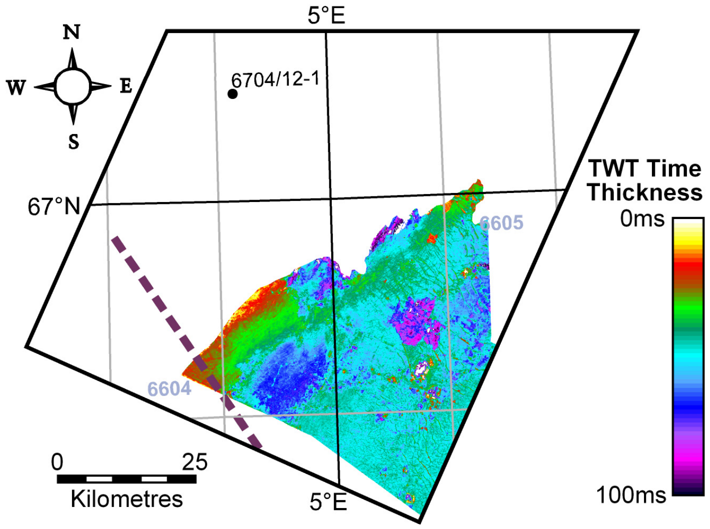

Figure 5.18: Sediment isochron maps of the Maastrichtian marine fan sequences.

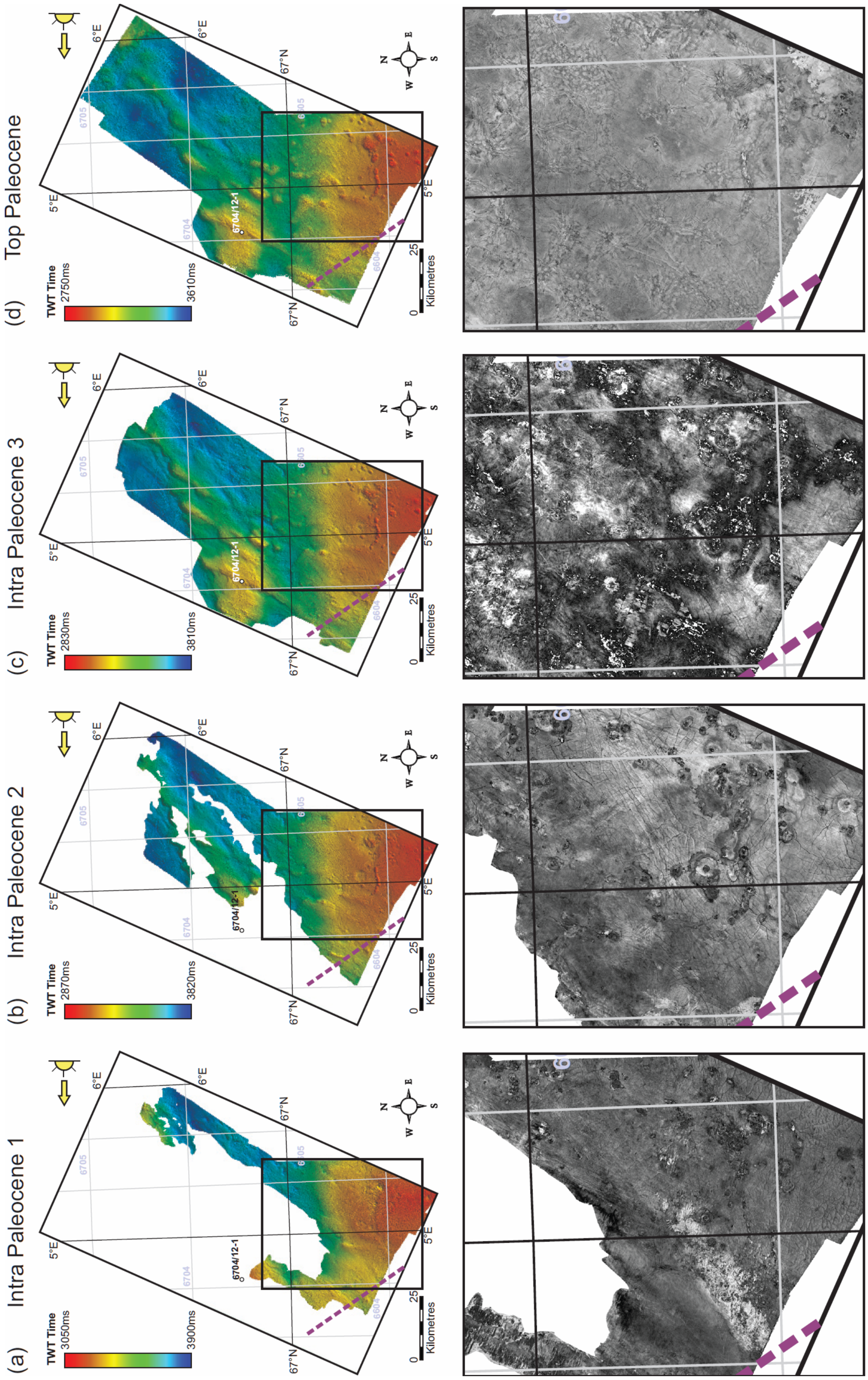

Figure 5.19: TWT structure maps of (top) the successive Paleocene sequences around and above the Gjallar Ridge. Amplitude extractions (bottom) of the mapped sequence tops in the vicinity of the Gleipne Lineament display areas of light (sand rich) and dark (mud rich) reflectivity. Hydrothermal vent activity is also distinct which may be the source for volcaniclastic deposits in and around the feature. Amplitude sample boxes are ~ 50 x 62.5 km in size.

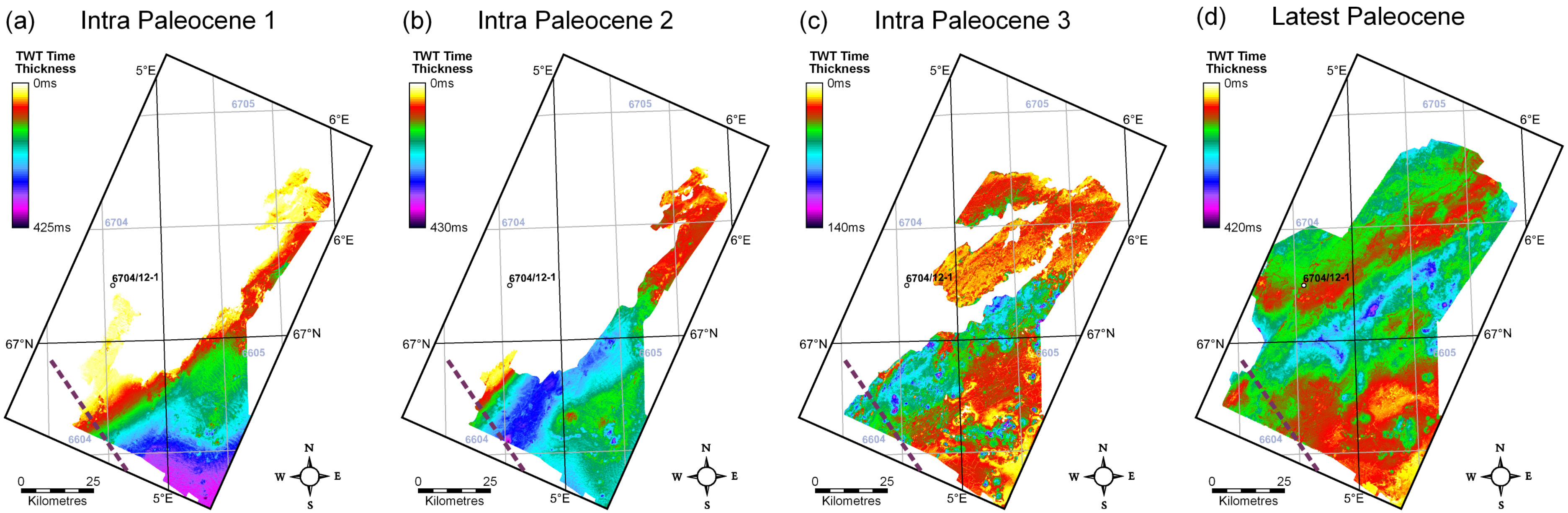

Figure 5.20: Sediment isochron maps of the Paleocene sequences 1, 2, 3 and during the latest Paleocene. Note the migration of the depocentres from the vicinity of the Gleipne Lineament in the early Paleocene to the south-eastern rear of the Gjallar Ridge by the end of the Paleocene.

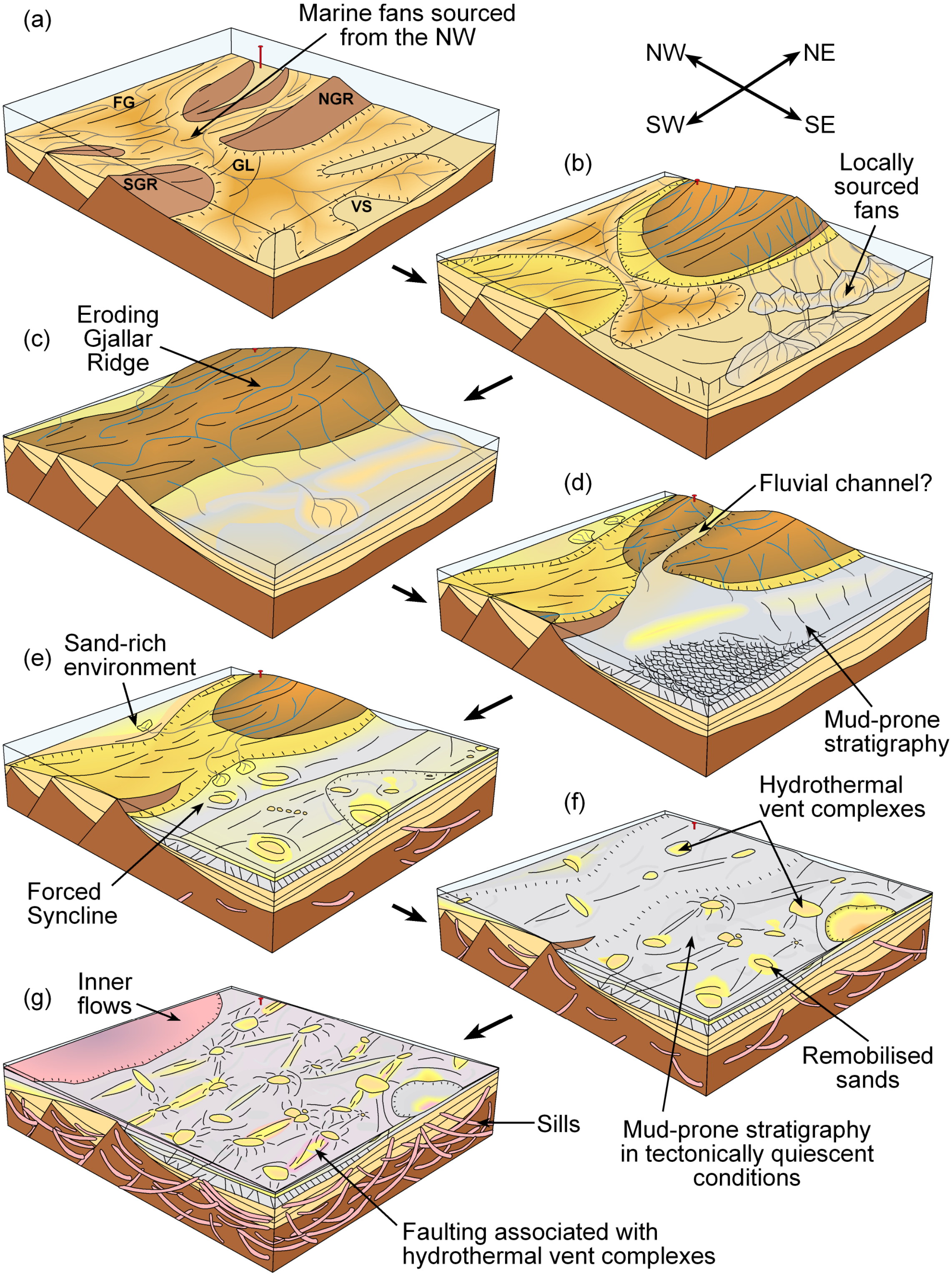

Figure 5.21: Tectono-stratigraphic and magmatic evolutionary block models for the Gleipne Lineament/Saddle during deposition of the (a) Maastrichtian Fan 2 , (b) Maastrichtian Fan 3, (c) Maastrichtian Fan 4, (d) IP1, (e) IP2, (f) IP3 and latest Paleocene sequences. Under rift conditions, the lineament acted as a pathway for sediments from the north and west to enter the Vøring Basin but under post-rift conditions its impact was much less distinguishable. View to the north. **GL** Gleipne Lineament; **N/SGR** Northern/Southern Gjallar Ridge; **FG** Fenris Graben; **VS** Vigrid Syncline. Model scale approximately 60 km x 50 km.

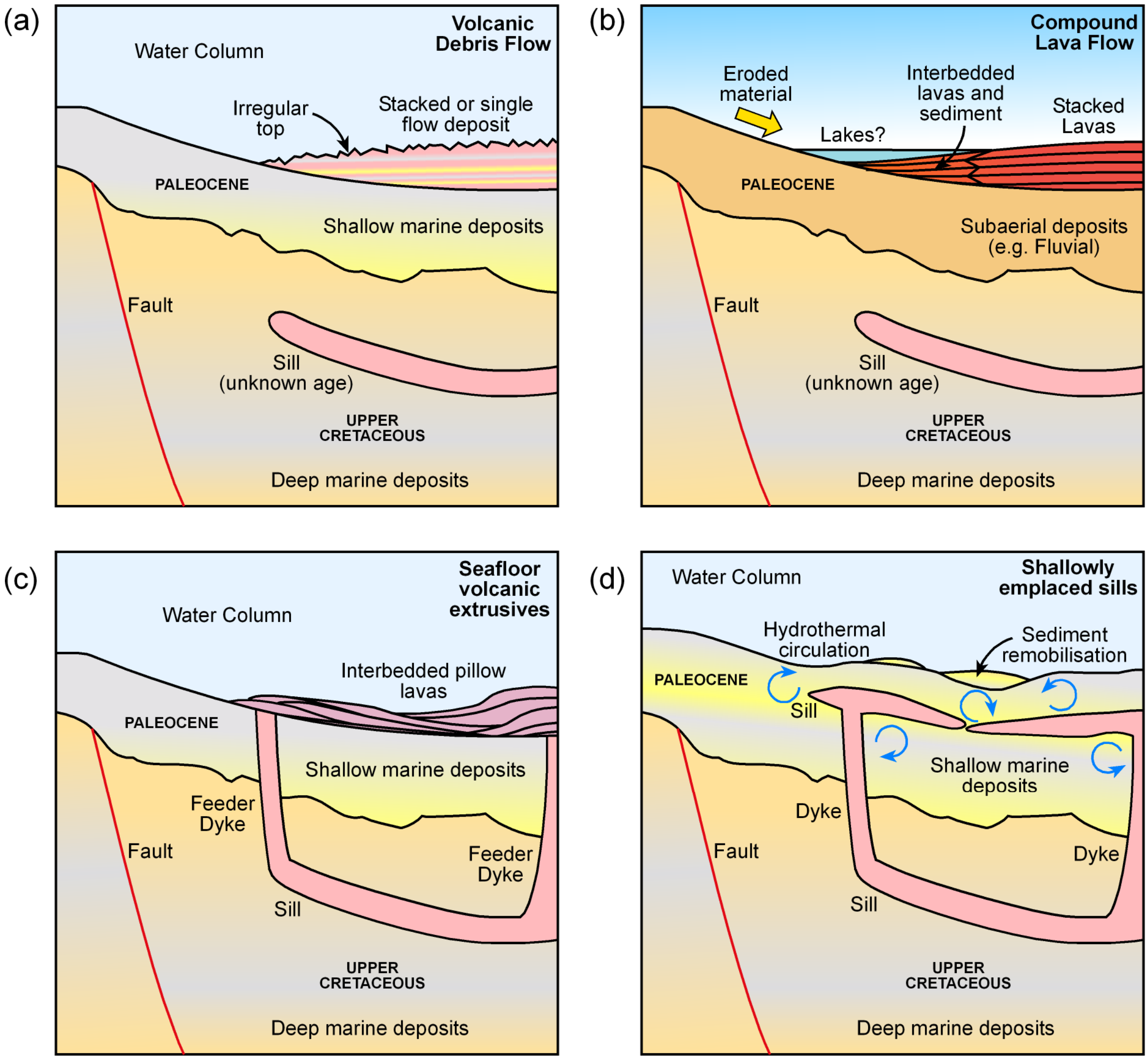

Figure 5.22: Four hypothesised models for the nature of the igneous inner flows within the Rym Accommodation Zone; (a) a subaerial origin, (b) a submarine debris flow, (c) seafloor extrusives sourced from Paleocene sills or (d) shallow sill intrusives within poorly lithified sediments.

Chapter Six

6 DISCUSSION, CONCLUSIONS AND FURTHER WORK

The primary aim of this chapter is to synthesise the results of the previous studies within the thesis and discuss the implications for the evolution of the Faroe-Shetland Basin (FSB). Much of the pre-Eocene structure of the FSB remains unknown, obscured beneath the Paleogene volcanic deposits. Yet on the basis of the results presented in this thesis from the southern FSB and northern Vøring Basin a prediction can be made as to the nature of rift-segmenting structures and general tectono-stratigraphic evolution of the sub-basalt region. To complete this assessment, a multistage process was required involving the production of a new regional tectonic elements map of the FSB using the latest gravity anomaly data and regional 2D seismic data. From this, a new assessment could be made as to the relative tectono-stratigraphic and magmatic influence of the previously inferred rift-oblique lineaments and how likely these features were to exist within the sub-basalt region.

The tectono-stratigraphic models developed in the northern Vøring Basin are considered an appropriate analogue to the sub-basalt region of the FSB for a variety of reasons which are discussed below and detailed in Table 6.01. Therefore the models have been applied directly to the FSB. Two regions in the FSB have been identified from geophysical datasets which may be associated with the two types of rift segmentation observed in the northern Vøring Basin (Chapters 4 and 5). A list of the principal conclusions associated with the research are then presented, as well as some suggestions for further research relating to the rift-oblique lineaments of the NE Atlantic Margin and the analysis of segmentation structures in other rift systems.

6.1 Application of models to the sub-basalt region of the Faroe-Shetland Basin

The results of Chapter 3 highlight that previously inferred seismic examples of rift-oblique lineaments are not necessarily tectonic features but appear predominantly to be the result of processes linked to the intrusion of igneous material into the FSB and the display of vertically exaggerated, low resolution seismic data. Furthermore, faulting oblique to the illustrated seismic sections, gas chimneys and dominantly mud-prone lithologies reduce the seismic data resolution in the basin which could lead to the inference of rift-oblique structures. One major NW-SE oriented fault system (the Judd Transfer Zone) was identified, although its along-strike extent to the northwest remains unclear. To summarise, the study found little evidence supporting the existence of rift-oblique lineaments in the southern FSB away from the Paleocene-Eocene basalt succession.

6.1.1 New Faroe-Shetland Basin tectonic elements map

Given the limited seismic evidence for major basin-scale rift-oblique lineaments, a new tectonic elements map of the FSB was produced (Fig. 6.01) in order to better understand the assumptions which had been made in previously published maps (e.g. Ellis *et al.* 2009) and to question whether the rift-oblique lineaments (Rumph *et al.* 1993) are still identifiable. Equally, the formation of a new tectonic elements map for the basin would result in a robust reassessment of the currently best available potential field data for the FSB.

6.1.1.1 Methodology

The selected dataset for the interpretation of the potential field data was the free air gravity anomaly map provided by Chacksfield & Kimbell (2005) complimented by seabed depth contours. The Bouguer gravity anomaly map from the same report failed to highlight any major contrasts between the structural highs and adjacent depocentres due to the colour scale used, which would have led to increased error in any qualitative fault interpretation. Magnetic data was not used for the production of the new tectonic elements map due to the large susceptibility of magnetic data to igneous material in the basin (Chapter 2). The presence of igneous material in a magnetic survey is highlighted by strong positive anomalies which could be misinterpreted as structural features and override the anomaly response due to variation in basin structure. This is because the average magnetic susceptibility of basic igneous rocks range from 550 – 122,000 SI units in contrast to sedimentary rocks which average a magnetic susceptibility of 0 – 360 SI units (Reynolds 1997). The interpretation of major faults in the FSB was made on the basis of sharp, distinct contrasts between gravity highs and lows. Structural highs were inferred to correspond with gravity highs, depocentres to correspond with gravity lows. From this, dip direction of the interpreted normal faults could be inferred, with structural highs representing the footwalls, structural lows representing the hangingwalls. The interpreted fault systems from the gravity anomaly data were consistent with the configuration of the southern FSB where the basalt cover is absent.

A major assumption in the formation of a new tectonic elements map of the FSB is that the gravity data successfully display variations in the tectonic structure beneath the Paleocene-Eocene volcanic succession. The primary problem is that the volcanic succession is of a relatively high density. Basalt has an average density of 2.99 kg/m^3 (Reynolds 1997) and is therefore expected to affect the final gravity anomaly data significantly. From analysis of density logs collected from the Lopra well drilled onshore the Faroe Islands, densities range between 2.67 – 3.00 kg/m^3 for basaltic lavas and between 2.65 – 2.92 kg/m^3 for hyaloclastites (Christie *et al.* 2006). The average density of sandstones is ~ 2.35 kg/m^3 and shale is ~ 2.40 kg/m^3 (Telford *et al.* 1990). It would therefore be expected that the gravity data may predominantly highlight variations in the volcanic succession. However the crystalline basement structure (which underlies the structural highs and depocentres of the FSB) is expected to be resolvable from the gravity for two reasons. Firstly, the density of metamorphic and igneous basement rocks can range up to 3.02 kg/m^3 for amphibolite grade metamorphic rocks which are comparable with basic igneous rocks (Telford *et al.* 1990). Basement densities have been recorded in wells drilled within the FSB of up to 2.97 kg/m^3 as exemplified in well 204/23-1 which drilled the metamorphic basement of the Judd High (Chapter 3). Secondly, the gravity anomaly data is processed for both short and long wavelengths which will record variations in density in both the shallower and deeper basin structure respectively. Therefore, mapping of the pre-Eocene FSB structure is expected to be possible using the gravity anomaly data. Nevertheless, there is likely to be a major influence of the dense volcanic succession on the dataset which in the extreme could result in basalt-filled depocentres interpreted as basement-cored structural highs.

Following this first stage of structural mapping in the basin, 2D and 3D seismic data were used to constrain the fault interpretations particularly in areas away from the gravity coverage and areas not covered by the Paleocene-Eocene extrusive volcanic deposits. A range of publications were also used to further refine the tectonic elements map of the FSB in areas of sparse seismic coverage, such as the Faroe-Bank Channel Basin to the west of the Munkegrunnur Ridge (Fig. 6.01). Confidence as to the definition of the main tectonic elements (and associated fault trends) in the basin is relatively high. For example, the East Faroe High (EFH) has been mapped by Statoil U.K. Ltd using 3D seismic data, processed using the techniques described by Gallagher & Dromgoole (2007; 2008). The EFH is a Mesozoic horst structure and is located beneath 2.5 km of Paleocene subaerial lava and submarine hyaloclastite deposits (D. Ellis, Statoil U.K. Ltd, pers. comm.). Despite the effect of the volcanic succession, the gravity interpretation of the

EFH matches the size and orientation of the EFH as mapped using the 3D seismic data. This suggests that other tectonic features identified in the map located beneath a similar or reduced thickness volcanic succession are likely to be accurate as well. Unfortunately, the seismic interpretations of the EFH are currently unpublished. Similarly, the gravity anomaly data used in this study remains confidential and therefore these datasets are not presented within this thesis.

6.1.1.2 Results

Within the southern FSB, away from the Paleocene-Eocene volcanic deposits the dominant trend of faulting is NE-SW (Fig. 6.01) which is typical of the NE Atlantic Margin as a whole (Doré *et al.* 1997b). Notably, there is little evidence of the rift-oblique lineaments in the potential field data in this region of the basin, further lending support to the results of Chapter 3. The notable exception is the Judd Transfer Zone located on the south-western margin of the basin where a fault system can be defined but can not be mapped along strike to the northwest. The Grimur Kamban Lineament, although not represented by NW-SE faulting in this area, does appear to segment the FSB the northeastern and southwestern parts of the Flett Ridge. The adjacent fault polarities differ and the Flett Ridge is apparently sinistrally-offset across the lineament. This may be evidence that the Grimur Kamban Lineament, at least within this region of the basin, may be an accommodation zone (Faulds & Varga 1998). The dominant NE-SW trend continues in the sub-basalt region to the northwest of the Corona and Westray Ridges, yet to the northwest of the northern Westray Ridge, a series of E-W and NW-SE trending faults have been interpreted, some of which align along the inferred strike of the Westray Lineament. Further to the northwest, the dominant NE-SW trend gives way to more frequent NW-SE trending faults which appear to segment the interpreted structural highs and depocentres (e.g. Quads 6104 and 6105). Some of the NW-SE trending faults align with the lineaments, particularly the Brynhild, Westray, Clair and Grimur Kamban Lineaments. However, the interpreted faults are not basinal in extent and are believed to tip out along strike to the NW and SE.

6.1.1.3 Implications for the Faroe-Shetland Basin rift-oblique lineaments

From an analysis of the new FSB tectonic elements map (Fig. 6.01) it is apparent that any features which could be associated with the lineaments are not basinal in extent. This is geologically much more realistic than basin wide features which have not been recognised in orthogonal rifting models (e.g. McClay & White 1995) as is commonly inferred for the development of the FSB (e.g. Doré *et al.* 1999). However, sandbox models of rift systems generally oversimplify the pre-existing crustal heterogeneity observed in natural rift systems and therefore basin-wide features can not be ruled out completely (Morley 1999). This may also explain why the lineaments are poorly understood, inferred to be tectonically complex and have varying degrees and styles of deformation along their length. Instead of being single, basin-scale lineaments, they appear to be local scale rift adjustment features formed at varying stages of the basin evolution which although they may align along strike, do not coalesce.

Yet, the basin-scale rift-oblique lineaments can not be disregarded completely. The original rift-oblique lineaments interpreted from regional potential field data was processed using an undefined method (Rumph *et al.* 1993) and therefore it is difficult to ascertain what these lineaments may actually represent, especially if they are not recognised in modern potential field and 3D seismic data. For example, the basin-scale lineaments may be equivalent to the NW-SE trending shear zones as recognised in the Lewisian Basement of NW Scotland (e.g. Beacom *et al.* 2001). Similar basement structures have been identified using potential field data offshore Norway and correlated with basement structures onshore Scandinavia (Fichler *et al.* 1999). Therefore, the basin-scale lineaments may be highlighting Caledonian and/or Precambrian basement trends. The processed gravity and magnetic data may also be highlighting variations in the deep crustal structure of the FSB (e.g. Raum *et al.* 2005). An alternative hypothesis for the basin-scale lineaments is that they are related to igneous processes in the basin such as NW-SE oriented dykes as observed both onshore the Faroe Islands (Mudge & Rashid 1987) and interpreted within the magnetic anomaly dataset directly offshore (Chacksfield & Kimbell 2005). Similarly, the interpreted NW-SE trends could be due to lateral changes in the thickness of the volcanic succession in the basin which varies greatly along strike (White *et al.* 2003; Fig. 6.02). Equally, they could be the result of a broad, widely space data acquisition strategy or an artefact of the techniques and variables used in the processing of the potential field data. Finally, interpreter bias may have also influenced the interpretation of the basin-scale rift-oblique lineaments, which in turn may have been influenced by the geological understanding of the basin at the time. Nevertheless, much of this is speculation and can not be scientifically tested, but for the purposes of this study, the basin-scale rift-oblique lineaments do not appear to significantly influence the upper crustal Mesozoic – Cenozoic evolution of the FSB on a basinal scale.

6.1.1.4 Variation of basalt thickness in the Faroe-Shetland Basin

The lateral variation of the Paleocene-Eocene volcanic succession (White *et al.* 2003; Fig. 6.02) was suggested by Ellis *et al.* (2009) to be controlled by the rift-oblique lineaments of the FSB, with observed thickening of the volcanic succession within the northeast hangingwalls of inferred fault systems associated with the lineaments. The amount of thickening of the volcanic succession across the lineaments can be up to 3 km as exemplified across the Clair Lineament in Quad 6105 (Fig. 6.02). The Grimur Kamban Lineament displays a similar thickening but, in contrast to the Clair Lineament, thickens to the southwest of the lineament by up to 3 km in Quads 6105 and 6205. Similar thickness variations but on a smaller scale also occur across the Victory Lineament (~ 1 km thicker to the northwest; Quad 6204) and Judd Lineament (up to 2 km thicker to the northwest; Quad 6106). Yet notably, there is relatively little, if any variation across the Brynhild and Westray Lineaments. Also the variation in thickness of the volcanic succession does not occur along the entire length of the rift-oblique lineaments. This adds further support that the variation in basalt thickness is predominantly controlled by local features, and *not* basin-scale rift-oblique lineaments.

An alternative hypothesis for the thickening of the volcanic succession along inferred NW-SE features has been provided by fieldwork conducted in the Faroe Islands by R. Walker, University of Durham. The major NW-SE trending fjords which characterise the Faroe Islands structural grain have been interpreted as dip-slip normal faults formed as a result of NE-SW oriented Paleocene extension. Yet, the largest recorded throws of exposed faults in the Faroe Islands are in the order of ~ 70 m (R. Walker, University of Durham, pers. comm.). Even variations in the thickness of Paleocene sedimentary and lava units across the fjords interpreted as a result of tectonic movements along the NW-SE fault systems are in the order of a few hundred metres (Ellis *et al.* 2009). Unless the throws upon the NW-SE faults increase significantly towards the southeast before decreasing again towards the southern FSB, the NE-SW oriented rift event prior to continental breakup fails to explain the much larger variation in thickness of the volcanic successions (of up to 3 km).

As has been concluded from the northern Vøring Basin (Chapters 4 and 5), along strike variations in sediment thickness does not have to be controlled by major NW-SE trending fault systems. Instead, a segmented Late Cretaceous - Paleocene rift with each rift segment having a different tectonic nature and evolution has led to major along strike changes in sediment thickness. Therefore, a third hypothesis is that the evolution of an underlying segmented rift, not major NW-SE trending fault systems, controls the kilometre scale variations in the Paleocene-Eocene volcanic succession of the FSB. This hypothesis is explored and discussed below.

6.1.2 The Vøring Basin as an analogue

For the purposes of this study, the northern Vøring Basin is considered to be an excellent analogue for the development and evolution of the Mesozoic – Cenozoic succession beneath the Paleocene-Eocene volcanic succession in the FSB. The primary reason for this is that each basin is located upon the NE Atlantic Margin, having undergone very similar geological evolutions (see Chapter 1 for a more detailed overview and relevant references). The FSB and Vøring Basin are both formed upon Precambrian aged basement which was previously deformed under compression which led to the Caledonian Orogen. Both basins then underwent distinct periods of rifting in the Devonian, Permo-Triassic, Late Jurassic and Cretaceous – Paleocene, culminating in continental breakup in the Early Eocene. The orientation of the major rift events is also very similar as represented by the major NE-SW fault trends in each of the basins. Similarly, major structural highs and their adjacent depocentres are apparently offset by major NW-SE trending features which are highlighted within regional geophysical datasets and have been previously inferred as key controls on sediment to enter the basin from both the Greenland and Norway basin flanks. Extrusive and intrusive volcanic activity in each of the basins during the Early Cenozoic has also dramatically impacted the evolution of both the FSB and Vøring Basin. For example, thickening of the inner flows in the Vøring Basin is linked to the NW-SE trending Rym Accommodation Zone and the Gleipne Lineament, much in the same way, but on a lesser scale to the variation in basalt thickness in the FSB across the rift-oblique lineaments. Post breakup compression has affected the two basins, with the growth of similar age Cenozoic folds and domes, in a variety of trends. The rift segmentation models which have been formed due to the availability of high resolution 2D and 3D seismic data in the northern Vøring Basin are also considered to be much more applicable to the sub-basalt region of the FSB than any alternative models formed from study of the inboard regions. This is because the outboard location of the models in the northern Vøring Basin is predicted to be more similar to the sub-basalt region of the FSB on the basis of the out-stepping rift model proposed by Doré *et al.* (1999).

As with any analogy, there are problems with using the northern Vøring Basin. For example, relatively little is known regarding the deep crustal structure in the FSB however it is widely considered that magmatic underplating has occurred (e.g. Clift 1999; Smallwood *et al.* 1999). This was similarly the case for the Norwegian passive margin until Gernigon *et al.* (2003) hypothesised that the Lower Crustal Body was a high grade metamorphic basement root of the Caledonian Orogen, which continues to be a focus for debate at present. Therefore, whether magmatic underplating occurs beneath the Faroe-Shetland Basin has to be brought into question. Could evidence for magmatic underplating actually be related to a high grade metamorphic basement root? Recent work by Raum *et al.* (2005) concluded there was little evidence for magmatic underplating beneath the Faroe Islands based upon results from seismic refraction profiling with, White *et al.* (2008) suggesting the intrusion of sills into the crust as an alternative to the magmatic underplating hypothesis. Therefore, it is difficult to gain a full understanding as to how the deep crustal structure of both basins may differ.

As the deep crustal structure has been illustrated to influence the upper crustal structure of the Vøring Basin (Chapters 4 and 5), this may affect the direct application of rift segmentation models in the FSB. Similarly, very little is known regarding the sub-basalt stratigraphical fill of the FSB which may be very different to that of the northern

Vøring Basin. Only one well (6104/21-1; Brugden) has successfully drilled through the Paleocene-Eocene volcanic succession of the FSB. However, the well only penetrated a thin mudstone and sandstone sequence of Paleocene age at the base of the volcanic succession before the drill string became stuck and the hole was abandoned. Nevertheless, this gives some confidence that a similar geological succession is present in the sub-basalt FSB as in northern Vøring Basin, although a widely different stratigraphical fill can not be fully discounted (e.g. Lower Cretaceous carbonates were drilled in well 62/7-1 upon the Goban Spur, offshore Ireland). Yet a major variation from predicted stratigraphical fill from current rift sedimentation models formed for each of the basins (e.g. Larsen & Whitham 2005; Morton *et al.* 2005) is considered unlikely.

This is not the first time that analogies have been drawn from the northern Vøring Basin to other basins located upon the NE Atlantic Margin. Chevron Corporation is currently planning to drill a well using the same analogy as presented here. The company is expecting to find a similar stratigraphical succession beneath the sub-basalt region of the Møre Basin, including deep marine fan systems as proven in northern Vøring Basin located to the north (J. English, Chevron Corporation, pers. comm.). Therefore, on the basis of the rationale outlined above, it is considered that although probably not perfect, the Vøring Basin is the most appropriate analogue to better predict and understand the nature and geological evolution of the Mesozoic – Cenozoic succession in the sub-basalt region of the FSB, and in particular the influence of potential rift segmenting structures.

6.1.3 Rift segmentation in the Faroe-Shetland Basin

The direct application of the rift segmentation models formed in the northern Vøring Basin uses a data driven approach. The two sets of rift segmentation models developed in the northern Vøring Basin (Rym Accommodation Zone and Gleipne Lineament/Saddle) were initially compared to the Bouguer gravity anomaly data of the

Vøring Basin (Fig. 6.03). The Gjallar Ridge and Nyk High correlate with two apparently offset, separate gravity highs which are expected to be related to the structural relief of the features compared to the adjacent synclines and grabens. In the southern RAZ, a N-S oriented high gravity anomaly is recognised, possibly correlating with the region of Paleocene uplift and erosion (Chapter 4). This high gravity anomaly may also relate to the deeper Late Jurassic rift structure at depth which is of a similar orientation and, therefore, what is displayed in the Bouguer gravity data may actually be caused by variation in the deeper crustal structure. From this, the new FSB tectonic elements map (Fig. 6.01) was used to locate areas which could be considered structurally similar to the regions of rift segmentation in the northern Vøring Basin. The free air and Bouguer gravity anomaly data were then analysed again to identify whether the response in the FSB was similar to that in the northern Vøring Basin. Utilising the horizon interpretations of regional 2D, and where available 3D seismic data by Statoil U.K. Ltd, led to further constraining of the potential location of rift segmenting structures. The basalt thickness (White *et al.* 2003) was also utilised to give an understanding of Late Paleocene thickness variations which could be comparable to the time-thickness maps of the Paleocene sequence in the northern Vøring Basin (Chapter 5). Two areas in the sub-basalt region of the FSB were identified from this approach which may have undergone similar style of deformation to the Rym Accommodation Zone and Gleipne Lineament/Saddle in the northern Vøring Basin during the Late Cretaceous – Paleocene.

6.1.3.1 Application of the Rym Accommodation Zone model

The East Faroe High (EFH) is a major NE-SW structural high ~ 150 km in length, primarily located in Quads 6103, 6104 and 6105. Although it has been referred to by a single name, the EFH is commonly displayed as having a marked along strike segmentation (e.g. Ellis *et al.* 2009) as is further highlighted by the new tectonic elements map (Fig. 6.01). The EFH is most prominent in the free air gravity anomaly data with two subtle NE-SW trending features highlighted by the southerly illumination of the data (Fig. 6.04). The Rym Accommodation Zone model is considered to be best applied in a location where the two segments of the EFH appear to be laterally discontinuous along strike, across a ~ 25 km wide NW-SE oriented low free air gravity anomaly. This apparent offset is in the order of 20-30 km in a dextral sense in the region of the previously inferred Clair Lineament (Fig. 6.04). The Bouguer gravity anomaly still highlights this structural trend and apparent segmentation of the EFH, yet due to the colour scale used the structural high is not as clearly defined. However, what is recognised in the Bouguer gravity anomaly data and only to a lesser extent in the free air gravity anomaly data are a series of illuminated NW-SE oriented trends, spaced up to 20 km apart. Notably, they are located to the northwest of the area in which the Rym Accommodation Zone model is applied, and are spatially coincident with the interpreted dykes highlighted in the magnetic data (Chacksfield & Kimbell 2005). Therefore, these NW-SE trending features (which could be interpreted as structural features), are expected to be igneous dykes which are likely to have a contrasting density to the surrounding host rock.

Within the mapped seismic data, the two major northeast and southwest segments of the EFH are separated by a ~ 25 km wide, NW-SE trending region at intra-Paleocene level. On the basis of the interpreted geometrical similarity between this set of structures and those of the northern Vøring Basin, this region is considered as being equivalent to the Rym Accommodation Zone. The north-eastern segment of the EFH is deemed equivalent to the Nyk High with the south-western segment of the EFH equivalent to the Gjallar Ridge. Notably, the width of each EFH segment varies upon either side of the accommodation zone as is also recognised in the northern Vøring Basin. Therefore, different styles and kinematics of tectonic deformation during the Late Cretaceous -

Paleocene may have occurred on either side of the accommodation zone. A ~ 50 km wide N-S structural high is also recognised to the north of the accommodation zone as highlighted in the free air gravity anomaly (the Trondur High; Fig. 6.04) which may be attributable to uplift in the Paleocene as is recognised in the northern Vøring Basin (Chapter 4) and southern FSB (Champion *et al.* 2008). The Paleocene-Eocene volcanic succession thickness also varies across the accommodation zone (Figs 6.02 and 6.04) with an increase in the basalt thickness of up to 1 km to the northeast of the westerly segment of the EFH. In the northern Vøring Basin, the inner flows are present within the accommodation zone and not elsewhere within the rift system, therefore a similar set of processes could cause this thickness increase along the segmented EFH. The basalt further increases in thickness to the northwest suggesting the accommodation zone may be present, and possibly more influential upon the deposition of basalts in this location, however this is unclear due to a lack of sub-basalt seismic mapping in this area. To the southeast, the basalt thickness does not increase into the NW-SE trending accommodation zone, suggesting a south-eastern limit to the zone, once again similar to the Rym Accommodation Zone in the northern Vøring Basin and supporting a local zone of deformation, not basinal in extent.

6.1.3.2 Application of the Gleipne Lineament/Saddle model

The Gleipne Lineament/Saddle model can also applied to the segmented EFH. The location for this inferred style of segmentation is in Quad 6105, to the southwest of where the Rym Accommodation Zone model has been applied (Fig. 6.05). Regional 2D seismic mapping by Statoil U.K. Ltd of the top Cretaceous unconformity highlights a structural low between two structural highs which are considered equivalent to the northern Gjallar Ridge (to the northeast) and the southern Gjallar Ridge (to the southwest). The saddle between the two segments of the EFH is around 25 km wide and aligns well with the previously inferred Westray Lineament. Notably, this saddle does not extend along strike to the NW or SE and appears to be a localised region of low relief between the two adjacent structural highs. In the northern Vøring Basin, the Gleipne Lineament extends into the non-rifted Vigrid Syncline yet its effects are less prominent. Therefore a south-easterly extension of the saddle may exist but may not be mappable as its observed influence may be below the resolution of the seismic data. The basalt thickness is similar to the Gleipne Saddle/Lineament in the northern Vøring Basin with increased thicknesses located to the northwest of the saddle but no apparent local NW-SE oriented thickening of the Paleocene-Eocene volcanic succession above the saddle itself. An unexplained problem with the application of the model in this location is the lack of a pronounced structural high upon the gravity anomaly data for the south-western EFH segment. An explanation for this may be that the high is a younger feature, formed due to compression and uplift in the Cenozoic and therefore this is tectonically different to the southern Gjallar Ridge (Gernigon *et al.* 2003). This structural high may not have existed during the Late Cretaceous and instead may have been a sedimentary depocentre at the time. This would explain the lack of a positive gravity anomaly for this mapped structural high and is a notable problem with applying the Gleipne Lineament model in this location.

6.1.4 Hydrocarbon prospectivity

The main impact each of the rift segmentation models will have on the prospectivity of the FSB is through the reservoir provenance and quality, and the types of traps that may house hydrocarbons. Each segmenting structure appears to exert a unique control upon the local basin architecture and evolution, and therefore the application of the models may not be entirely accurate. However, this method does make a first order attempt to understand a problem which is currently non-resolvable using modern geophysical techniques. Although the hypothesis of structures similar to the northern

Vøring Basin being present beneath the Paleocene-Eocene volcanic succession does appear to be plausible, to explain the along strike segmentation in the FSB other hypotheses including NW-SE normal faults attributed to NE-SW regional extension or major strike-slip faulting along basinal lineaments can not be fully discounted.

If the models are deemed acceptable, segmenting structures in the FSB similar to the Rym Accommodation Zone may provide excellent traps against the highs into which sediments are deposited from regions along strike particularly under syn-rift conditions as well as from the northwest (i.e. Greenland). Areas affected by segmentation akin to the Gleipne Lineament/Saddle may be important areas for sand to enter the basin to the southeast during rifting, with the dominant hydrocarbon trap types being stratigraphical in these regions. These stratigraphical traps may be further enhanced by the uplift effect of intruded igneous material into the sedimentary succession creating major structural 4-way dip closures (Chapter 5). However, the current focus for hydrocarbon exploration in this region is still upon the major structural highs (Fig. 6.01) which remain undrilled. Any commercial drilling of the rift segmenting structures would be considered extremely high risk at present, especially as a working hydrocarbon system is still unproven, the base of the Paleocene-Eocene volcanic succession is still poorly defined and the nature of the Mesozoic – Cenozoic stratigraphy and structural evolution is unknown.

6.2 Conclusions

This study has analysed the rift-oblique lineaments of the Faroe-Shetland and Vøring Basins on the NE Atlantic Margin using a range of data types and techniques. A brief summary of the main conclusions of this thesis are now presented from analyses conducted within each of the basins:

- In the southern Faroe-Shetland Basin, there is little evidence within the Mesozoic – Cenozoic succession of major tectonic activity along NW-SE (rift-oblique) lineaments. Previously published examples are related to processes associated with Paleocene igneous intrusions in the basin and as a result of vertically exaggerated display of low resolution seismic data. One example of a rift-oblique lineament is identified at the south-western margin of the basin, the Judd Transfer Zone, yet the along strike extent of the fault system remains unclear.

- Analysis of the Rym Accommodation Zone within the Late Cretaceous – Paleocene rift axis of the northern Vøring Basin has highlighted that accommodation zones not only separate two laterally offset rift systems, but also rift segments of highly contrasting structural styles, differential fault kinematics, loci of extension and deep crustal structure. The study also highlights that rift-oblique faulting in segmented rift systems may form a constituent part of a larger accommodation zone, which may be incorrectly inferred as a transfer zone in dominantly two-dimensional, spatially limited field based research.
- The rift-oblique lineaments of the northern Vøring Basin are inherently linked to and controlled by the deep crustal structure of the NE Atlantic Margin, supporting a long lived crustal heterogeneity influencing this region.
- Each of the rift-oblique lineaments is unique. Different tectono-stratigraphic models are required to explain the evolution of each identified lineaments. The Rym Accommodation Zone and Gleipne Lineament/Saddle are two unique lineaments formed as a result of different tectonic processes, which impact the stratigraphical development of the northern Vøring Basin greatly in different ways.
- During the syn-rift phase, sediment was routed flow across the Rym Accommodation Zone which compartmentalises the basin. This contrasts with the along strike transport of sediment along the NW-SE oriented Gleipne Lineament/Saddle. During predominantly post-rift conditions, sediments are

expected to flow along the strike of the NW-SE Rym Accommodation Zone with little impact of the Gleipne Lineament/Saddle on the sedimentation at the same time.

- From the analysis of available geophysical and geological data, rift segmenting structures analogous to the northern Vøring Basin are proposed to be present within the Mesozoic – Early Cenozoic succession of the Faroe-Shetland Basin beneath the Paleocene – Eocene volcanic deposits.
- The rift-oblique structures of the northern Vøring Basin and Faroe-Shetland Basin are considered to be important for hydrocarbon exploration in each of the basins. The structures possibly control the deposition of marine source rocks, reservoir and seal sequences and provide both structural and stratigraphical traps which may be enhanced by volcanic activity in the region.
- The rift-oblique lineaments of the NE Atlantic Margin are important in terms of their tectono-stratigraphic and magmatic significance on basin evolution. However, interpretation of basin-wide rift-oblique lineaments from potential field data, without a detailed study of the rift architecture is an *ad-hoc* solution with no firm geological basis.
- From the results of this study, the relative significance of the segmenting features is expected to vary in both space and time during the various stages of basin formation.

6.3 Suggestions for further work

The research undertaken for this thesis has highlighted areas which are of particular interest and should be selected for future study. This would improve our understanding of rift-oblique lineaments upon the NE Atlantic Margin and other segmented passive margins worldwide, as well as provide a further understanding as to the evolution of structures which segment natural rift systems. The recommendations for future research include:

- A greater number of 3D seismic studies of other rift-oblique lineaments upon the NE Atlantic Margin, the conjugate Greenland Margin and other passive margins around the world would lead to a greater number of examples from which to compare the results of this and other studies.
- Integration of gravity, magnetic, seismic refraction datasets, 2D and 3D seismic reflection data and well data is demonstrated here as a powerful suite of integrated datasets for investigation as to the nature, growth and tectono-stratigraphic significance of rift-oblique lineaments on passive margins and rift basins.
- A limitation of this project has been a lack of well data in tectonically complex regions. An integration of 3D seismic data with increased well control could lead to improved relative timings of tectonic movements and a greater degree of certainty for the predicted stratigraphical fill of the basin through time.
- An explanation as to why Paleocene sedimentation in the Faroe-Shetland Basin is apparently compartmentalised is required, as there is a distinct lack of evidence for tectonically active rift-oblique lineaments which has been previously inferred. A further study may therefore test the hypothesis that differential thermal subsidence above an underlying segmented rift system is the primary control on sedimentation in the basin, and may be applicable to other rift basins worldwide.
- Through the use of seismic reflection data, an analysis of the basement structure on the margins of the Faroe-Shetland Basin should be undertaken to identify whether a link can be made between basement features (e.g. shear zones) and the series of Mesozoic – Cenozoic NW-SE trending faults in the region of the Judd High and Rona Ridge. A tentative link has been made between the reactivation of basement

structures and the formation of rift-oblique 'transfer' faults but requires further testing.

- Although the influence of the deep crustal structure and basement heterogeneities upon the upper crustal rift geometry and evolution were not directly investigated in this project, these are considered important to provide an enhanced understanding of the rift-oblique lineaments. Further studies analysing seismic refraction datasets offshore as well as fieldwork focussing on the basement structure onshore may lead to further refining of the inferred link between the upper and lower crustal structure.
- Lithosphere modelling of the interaction between Late Jurassic rifting and depth-dependent stretching, transient mantle uplift and significant upper crustal extension along E-W oriented normal faults in the Paleocene is required. This would aid the understanding of the interaction between complex processes in both space and time and may explain regions of localised Paleocene uplift such as in the southern Rym Accommodation Zone and elsewhere along the NE Atlantic Margin.
- Using structural restoration software (e.g. Midland Valley 2DMove software), the two interpretations of the Late Jurassic rift structure (Fig. 4.09) should be examined to predict whether an inversion/buttressing of the Late Jurassic rift faults is likely to have occurred. This will impact upon the proposed models for the Paleocene uplift observed in the region of the southern Rym Accommodation Zone and Nyk High and the Oligo-Miocene development of the Vema Dome.
- A study focussing upon the kinematics and evolution of the NW-SE fault(s) at the bounding edge of the Gjallar Ridge and northern Rym Accommodation Zone should be carried out. This focussed study should aim to compare the NW-SE fault(s) in the northern Vøring Basin with the results of studies in other segmented

rift basins, particularly in the Basin and Range Province, USA where transfer faults have been primarily identified.

- Increased knowledge as to the tectonic nature of the Greenland conjugate passive margin is required to fully understand the influence of rift-oblique lineaments upon the NE Atlantic Margin as only one side of the rift system has been analysed within this study. This would be particularly beneficial to understand the influence the rift-oblique lineaments have upon the stratigraphical evolution of the Vøring Basin.
- A comparison between the results of this thesis with the onshore field based examples of fault domain boundaries (particularly from the Basin and Range, USA) is required. This will provide a timely reassessment of structures within segmented rift systems. Our understanding of these systems has been aided significantly in recent years with the availability of 3D seismic datasets, critical for the analysis of complex 3D structures through time. Further use of this technology is strongly recommended for analysis of other fault domain boundaries.

Geological History	Faroe-Shetland Basin	Vøring Basin
Jurassic rifting	?	✓
Cretaceous rifting	✓	✓
Paleocene reactivation/rifting	?	✓
Post breakup compression	✓	✓
NW-SE trending lineaments	✓	✓
Geological highs apparently offset by NW-SE lineaments	✓	✓
Paleocene basalt flows thicken near NW-SE lineaments	✓	✓
NW-SE lineaments inferred as entry points for sediment to enter the basin	✓	✓
Complex Cenozoic folding	✓	✓

Table 6.01: Comparison of the key tectonic events and features of the Faroe-Shetland and Vøring Basins.

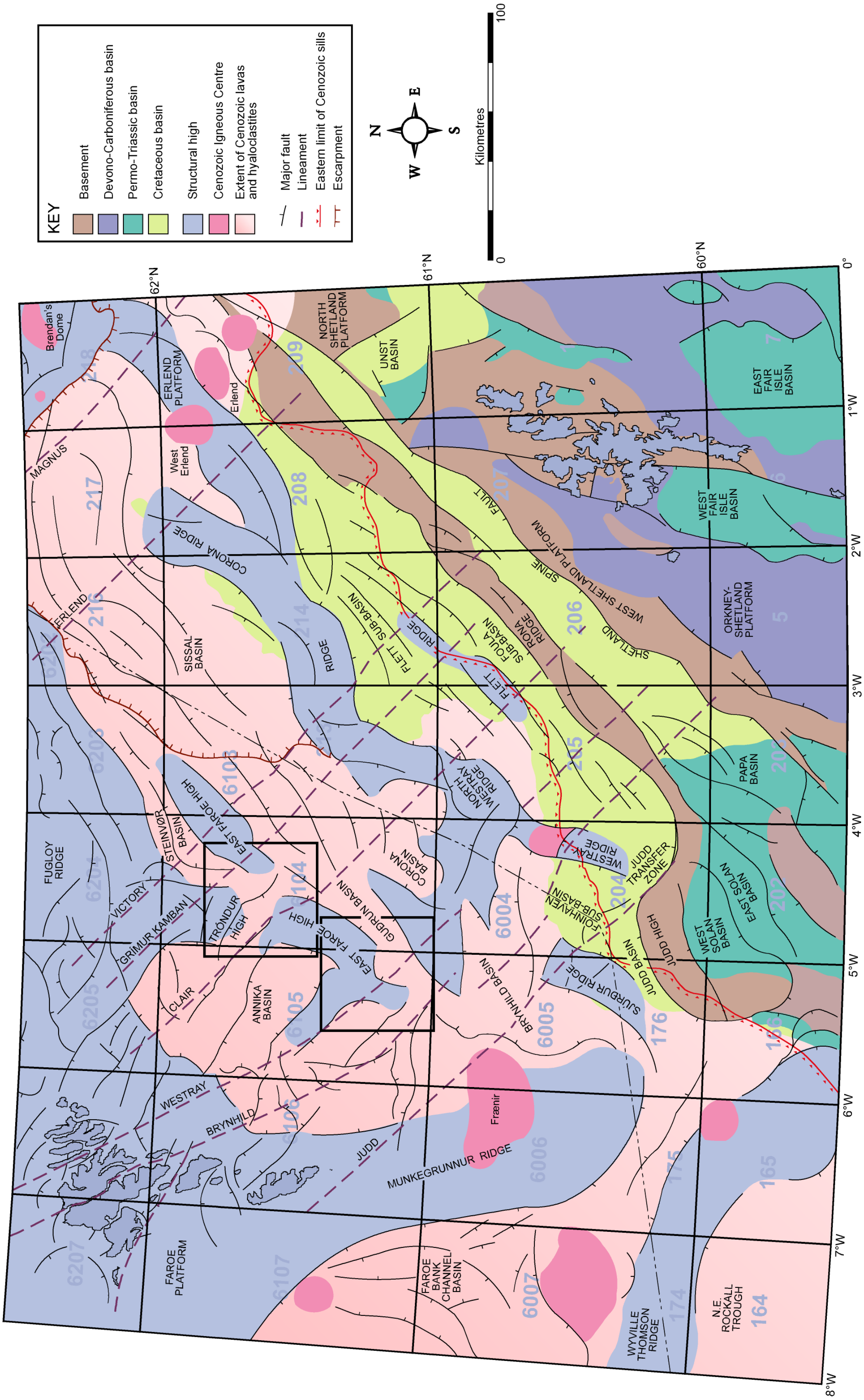

Figure 6.01: New tectonic elements map of the Faroe-Shetland Basin (modified after Duindam & van Hoorn 1987; Shannon & Spencer 1999; Davies *et al.* 2004; Johnson *et al.* 2005; Keser Neish & Ziska 2005; Ellis *et al.* 2009). Previously defined rift-oblique lineaments included for reference *only*.

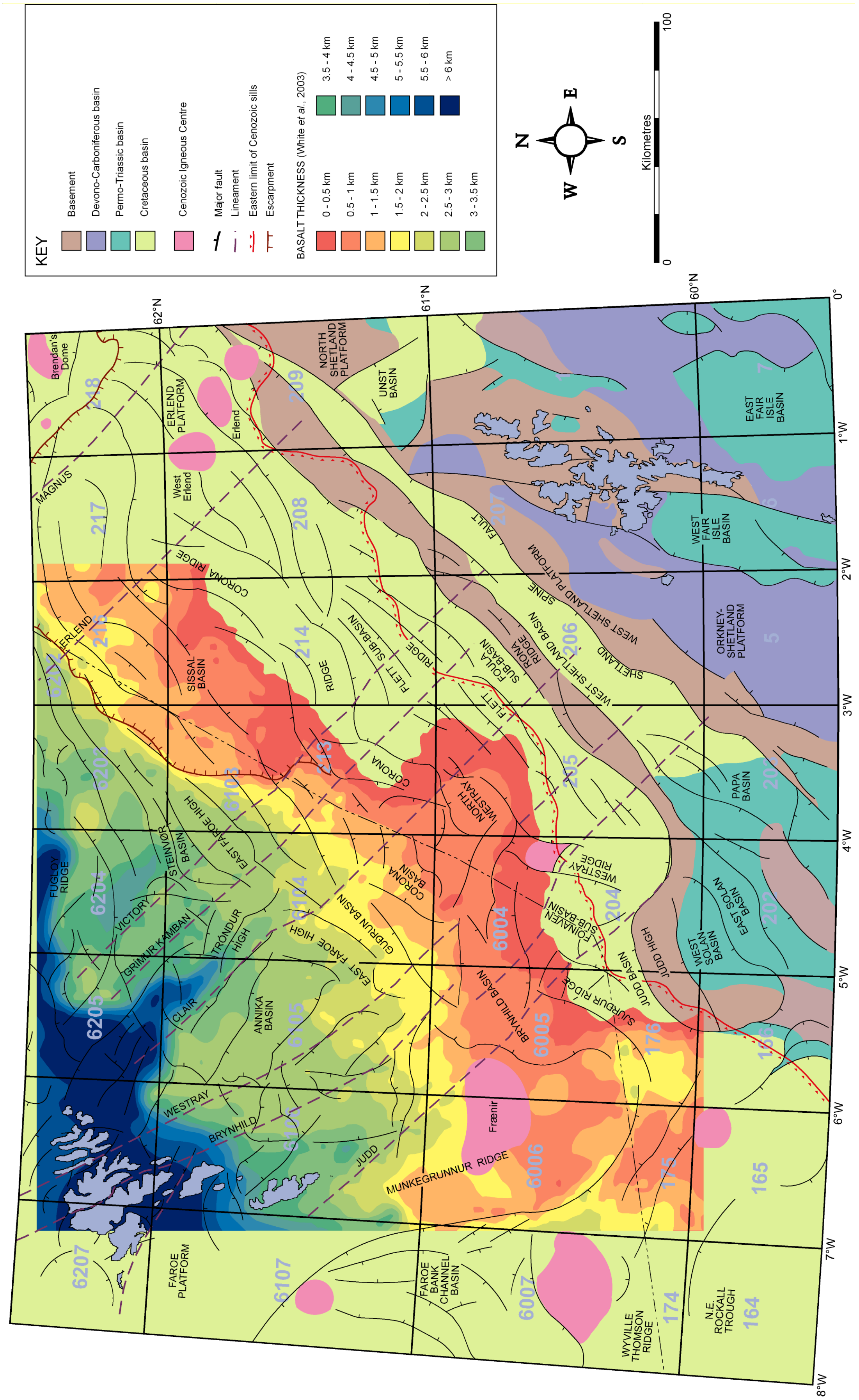

Figure 6.02: Paleocene-Eocene basalt thickness (after White *et al.* 2003).

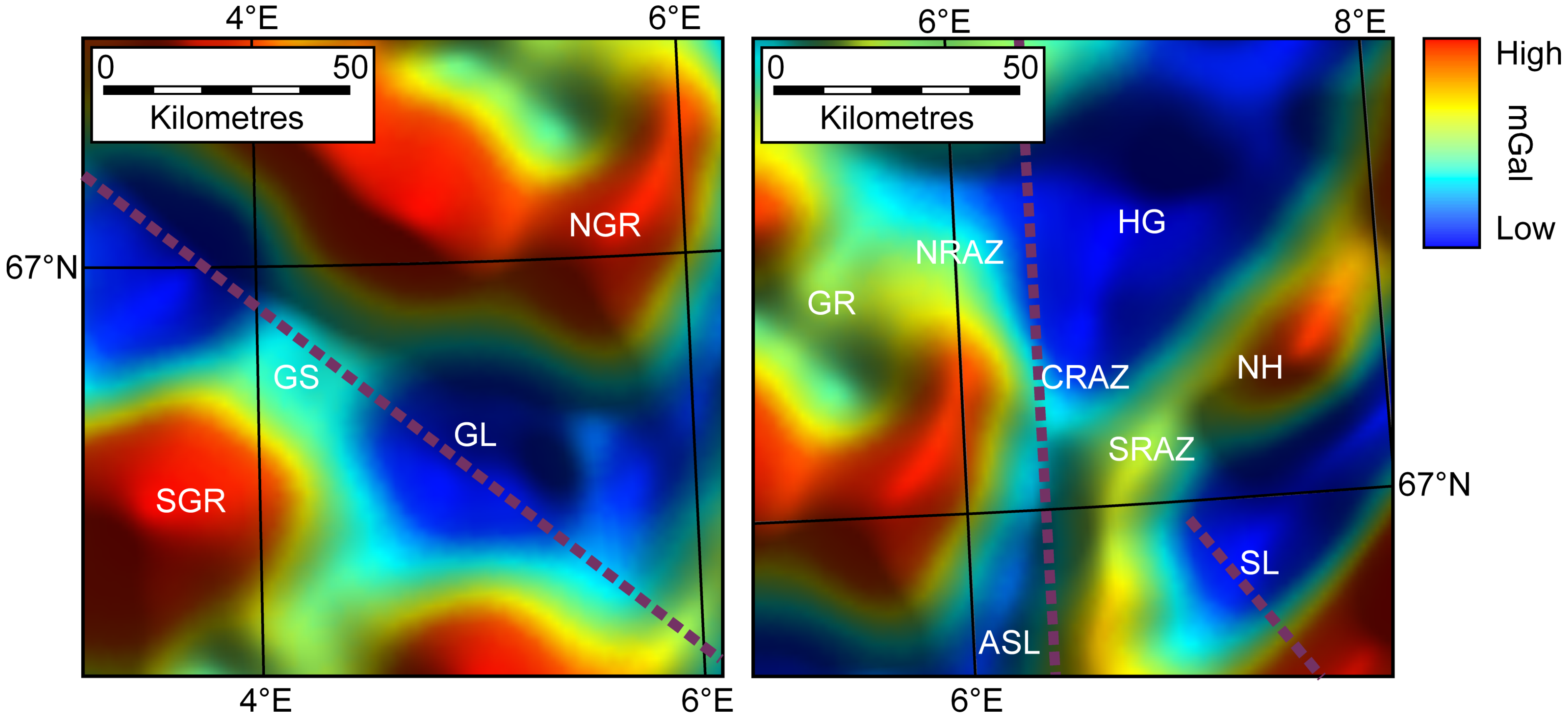

Figure 6.03: Bouguer gravity anomaly map of the Gleipne Lineament/Saddle (left) and the Rym Accommodation Zone (right). **SGR** – Southern Gjallar Ridge; **NGR** – Northern Gjallar Ridge; **GS** – Gleipne Saddle; **GL** – Gleipne Lineament; **GR** – Gjallar Ridge; **NH** – Nyk High; **HG** – Hel Graben; **N/C/SRAZ** – Northern/Central/Southern Rym Accommodation Zone; **SL** Surt Lineament; **ASL** Alternative Surt Lineament. Bouguer Gravity data provided by StatoilHydro under licence from Norges Geologiske Underøkelse (NGU).

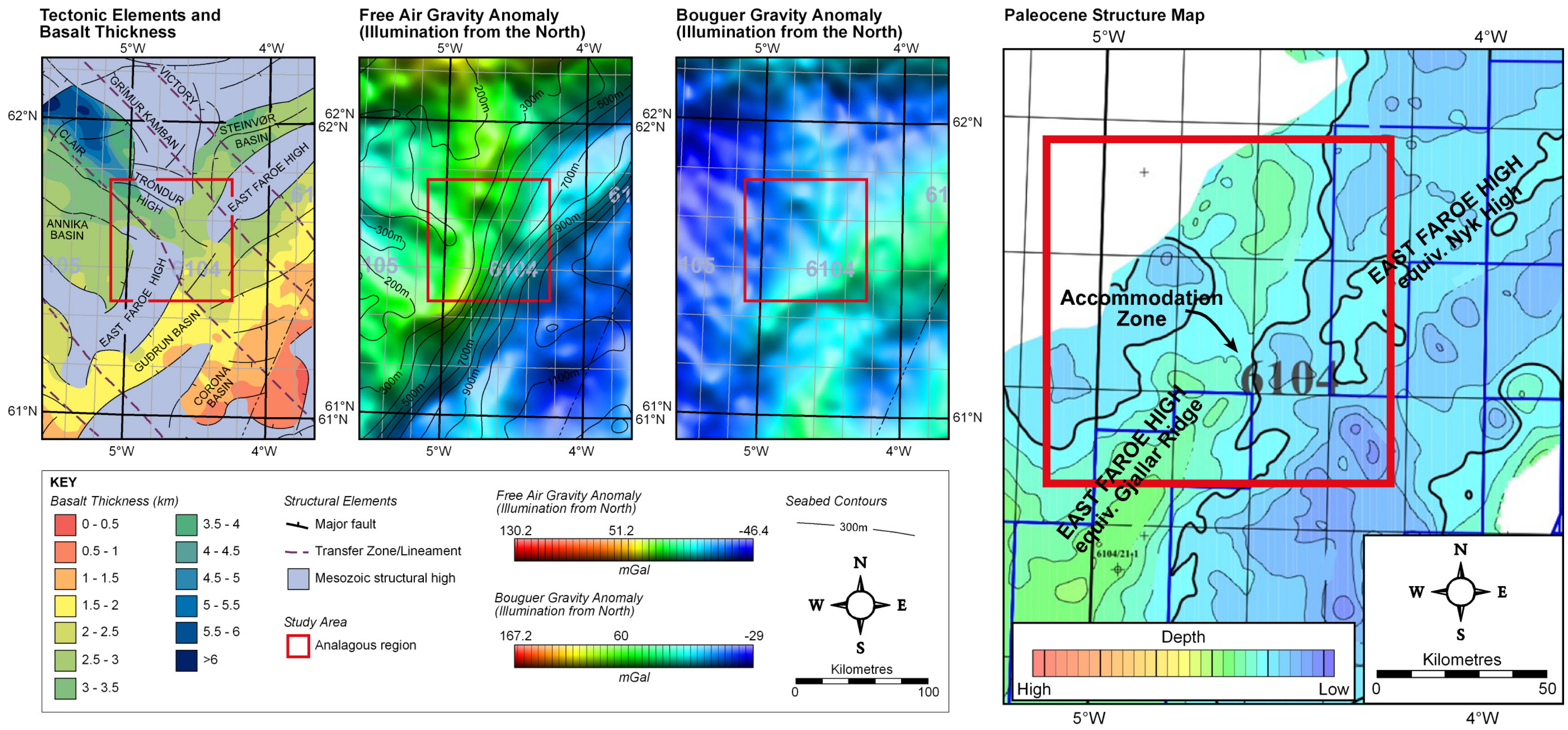

Figure 6.04: Proposed location of an accommodation with similar characteristics of the Rym Accommodation Zone in the northern Vøring Basin. Basalt thickness (after White *et al.* 2003; left), free air and Bouguer gravity anomaly data (Chacksfield & Kimbell 2005; centre) and Paleocene structure map (provided by Statoil U.K. Ltd; right). For the regional location of the segmenting structure see Figure 6.01.

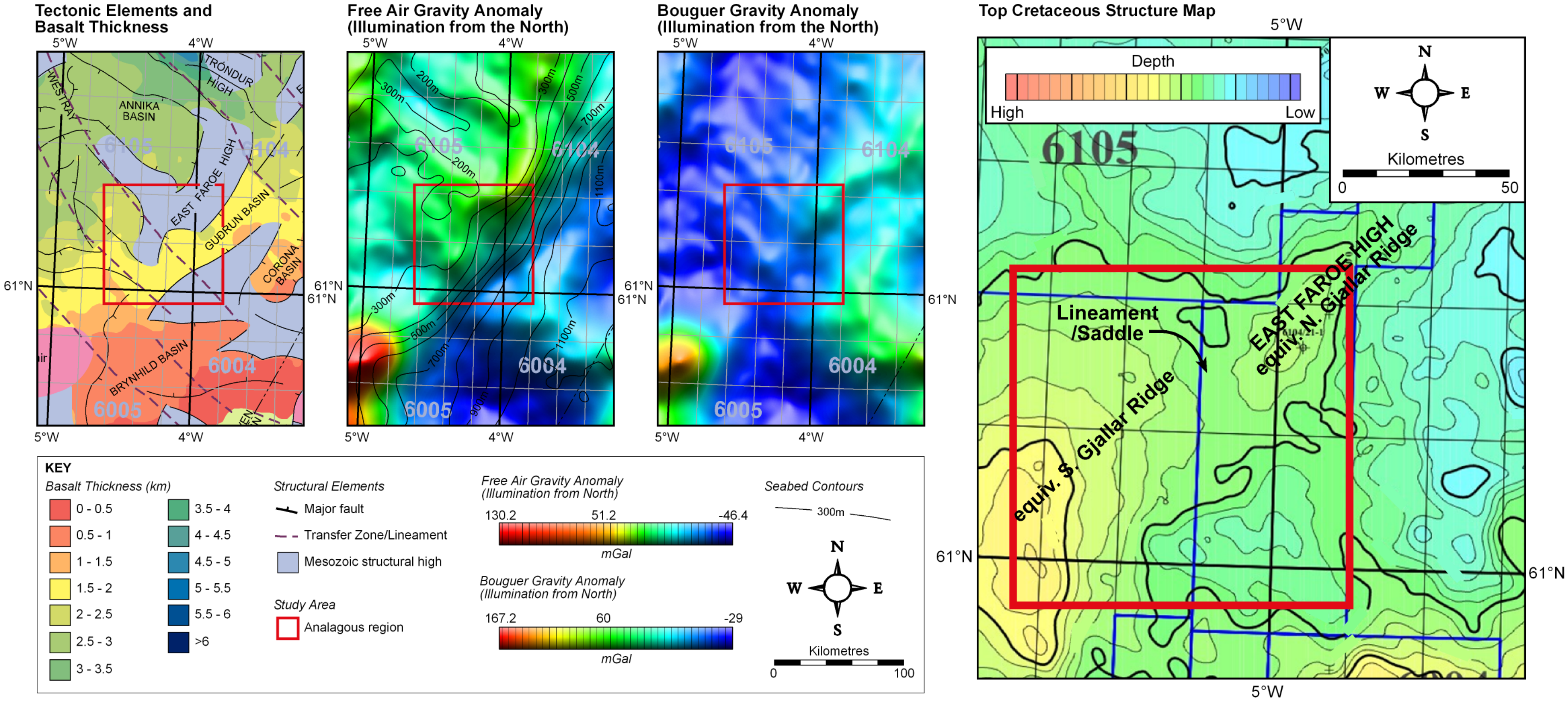

Figure 6.05: Proposed location of a low-relief ‘saddle’ structure with similar characteristics of the Gleipne Lineament/Saddle in the northern Vøring Basin. Basalt thickness (after White *et al.* 2003; left), free air and Bouguer gravity anomaly data (Chacksfield & Kimbell 2005; centre) and top Cretaceous structure map (provided by Statoil U.K. Ltd; right). For the regional location of the segmenting structure see Figure 6.01.

Appendix A

Supporting material for Chapter 2

Compilation of potential field data from the Faroese region

GRAVITY DATA PROCESSING

The gravity data processing employed the following steps:

1. The overlaps between different surveys were inspected in order to identify major differences in free-air gravity anomaly levels. Manual datum shifts were applied to selected surveys in order to provide approximate levelling in advance of more detailed adjustment.
2. More detailed levelling was undertaken using Geosoft routines. This involved the generation of a table identifying differences in free-air anomaly at line intersections and reducing these errors by applying shifts and tilts to the relevant lines (i.e. the correction applied to a particular line was allowed to vary linearly along the line). The disparate nature of the data sources means that all line segments are not well constrained by appropriately located intersections, but there were generally sufficient intersections to make the levelling process effective.
3. The levelled free-air gravity anomaly was imaged and inspected. The results were largely satisfactory, but some artefacts were still evident and were typically attributable to alongline noise, sampling problems (wide point spacing) or closely spaced subparallel lines with poor across-line control. Further editing was undertaken to remove these artefacts and the levelling process repeated.
4. A polygon mask was drawn around the trackline free-air gravity Compilation, defining the region within which it was considered the most appropriate data source and excluding areas with sparse coverage. This mask was used to merge the trackline data with nodes from the KMS free-air gravity anomaly grid. The overall gravity datum was adjusted to match that employed by KMS. Bouguer gravity anomaly values from the onshore surveys on the Faroe Islands were also incorporated at this stage (reduction density 2.67 Mg/m^3).
5. The complete compilation was gridded at 1 km intervals using a minimum tension algorithm.
6. The grid was smoothed by application of a low-pass 8th degree Butterworth filter with a central wavelength of 7.5 km. This filtered grid is illustrated in Figure 4 (the GIS also includes unfiltered versions for comparison).

Bouguer and isostatic gravity anomalies were derived by combining the gridded free-air gravity values with corrections derived using the topographic data compilation. The corrections were derived by 3D gravity modelling using the Gmod program (Dabek and Williamson, 1999). Bouguer anomalies were calculated assuming a reduction density of 2.20 Mg/m^3 in the offshore area. Isostatically corrected Bouguer gravity anomalies were calculated assuming an upper crustal density of 2.75 Mg/m^3, a density contrast across the Moho of 0.4 Mg/m^3 and a reference Moho depth of 30 km. The Bouguer component of the combined Bouguer and isostatic correction was calculated using a density characteristic of the crystalline upper crust (rather than the seabed sediments) following Lee (1996) who demonstrated why this is more appropriate in areas characterised by large water depth variations. The isostatic model was extended 200 km beyond the limits of the project area to avoid edge effects.

PGS UK

SUMMARY OF PROCESSING

WEST OF BRITAIN MEGA MERGE

3D SURVEY

PGS Job No. WOS-01

Prepared by:

PGS Data Processing

January 2002

PGS Data Processing
Bridge View,
1 North Esplanade West,
Aberdeen,
AB15 5QF.

Tel: +44 1224 24 7370
Fax: +44 1224 24 7380

Introduction

This report summarises the processing performed by PGS Data Processing for the merge of 4 final migrated 3D seismic surveys in the West of Shetland area. This merged survey is known as MC3D WOS-01.

Four 3D surveys were merged, these are known as MC3D Q213-99 (Tranche 6), MC3D Q214-96/97/98 (Tranche 4), MC3D WZ-T7/8 (Tranche 7 and 8) and MC3D WZ-96/97/98 (White Zone). It was decided from the outset that the MC3D Q213-99 survey would be the base to which all other merge surveys would be matched. A location map, indicating the position of MC3D WOS-01 relative to the other surveys in the area, can be found in PGS Appendix A.

Processing

3D Processing grids were designed from UTM information received. Each survey to be merged was reformatted from SEG-Y to internal format with the trace length extended to 8500ms, that of the Q213 survey, and binned onto the appropriately designed processing grid.

Each survey on input was QC'd by a series of inline, xline and time-slice paper plots, to visually check for missing or miss-positioned data. Log files were checked for any anomalies. PGS Appendix B details the individual grids used as well as the final merge grid.

Each survey was then re-binned to the final merge grid, which was based on the orientation and bin spacing of the grid for the Q213 survey. This took part in two stages. QC of this was again a series of paper plots, and log file QC. The plots initially were compared visually with those of the neighbouring surveys, now on the same grid, to check the tie of events from one survey to another, complete miss-ties indicating a problem with the re-binning, none were found.

A series of fold plots were made, which highlighted the overlap area between surveys enabling a more accurate design of the merge area. As the Q213 survey had a 10km merge pre-migration for aperture for its final processing, it was possible to ensure the merge during this project between the Q213, Q214 and WZ data was carried out over fully migrated data. The merge zone was a blend merge, over 100 traces.

Once the merge area was designed, a series of amplitude analyses were carried out over common data both in the inline and xline direction, for the Q213-Q214 data, Q213-WZ data and the WZ-TR7&8 data.

On comparing the amplitude decay curves for the Q213-Q214 data, it could be seen that the final Q213 data had a relatively flat amplitude decay, whereas the Q214 data had some decay. A robust AGC was chosen and applied to the Q214 data, which when analysed again provided a close match in amplitude. See PGS Appendix C Fig 1.

The Q213 and WZ data both had a similar AGC applied for their final scaling before the data was received. On reviewing the amplitude analysis a constant gain was chosen to match the two. See PGS Appendix C Fig 2.

Similarly with the WZ-TR7&8 amplitude analysis, carried out after the WZ was matched to the Q213 data, showed a constant gain best matched the two surveys. See PGS Appendix C Fig 3.

A table showing the amplitude corrections applied to each survey can be found in PGS Appendix C Table 1.

A series of inline and xline paper plots were used to QC the merge of the data, and to evaluate visually the application of the amplitude matching. These showed that in all cases the amplitude matching chosen was acceptable, and was approved by PGS Exploration UK.

The displays mentioned above were also used to evaluate any bulk static shifts required to tie the data at the waterbottom.

The west of Shetlands is renowned for water-column static shifts, caused by a combination of naturally occurring factors in the sea at the time of acquisition. Indeed every survey merged for this project has had a water column static solution applied to tie individual saillines during its production processing.

On careful QC using the deskSeis, areas where breaks in the water bottom are apparent are not extensive, and are less than 4ms, (1 sample), no breaks in these areas were apparent at deeper times in the data. The breaks occur over a portion of the merge between the WZ and the TR7&8 survey, see PGS Appendix D Fig 4. (deskSeis is a desktop version of PGS's proprietary 3D visualisation and interpretation system – holoSeis^{TM}).

Correcting these breaks, however, would generate a break over a larger portion and over different parts of the merge area. It was decided that no static adjustment was to be applied during this merge, see PGS Appendix D Fig 4.

Noise attenuation was considered for each survey, but as each survey to be merged had had post migration noise attenuation applied during their production processing, it was thought unnecessary. The level of noise was thought not to be a major factor inhibiting the continuation of events over the merge area from one survey to the other.

Post merge, a final robust AGC was applied to the entire merge survey. A waterbottom horizon was picked using the deskSeis and was used to apply a waterbottom clean-up mute, (PGS Appendix D Fig 4.). An example time-slice through the merged area can be found in PGS Appendix E.

This survey MC3D WOS-01 was then output to SEG-Y format, with an example EBCDIC header shown in Appendix F.

PGS Appendix A

Location Map:

MC3D WOS-01 merge survey area is outlined in red.

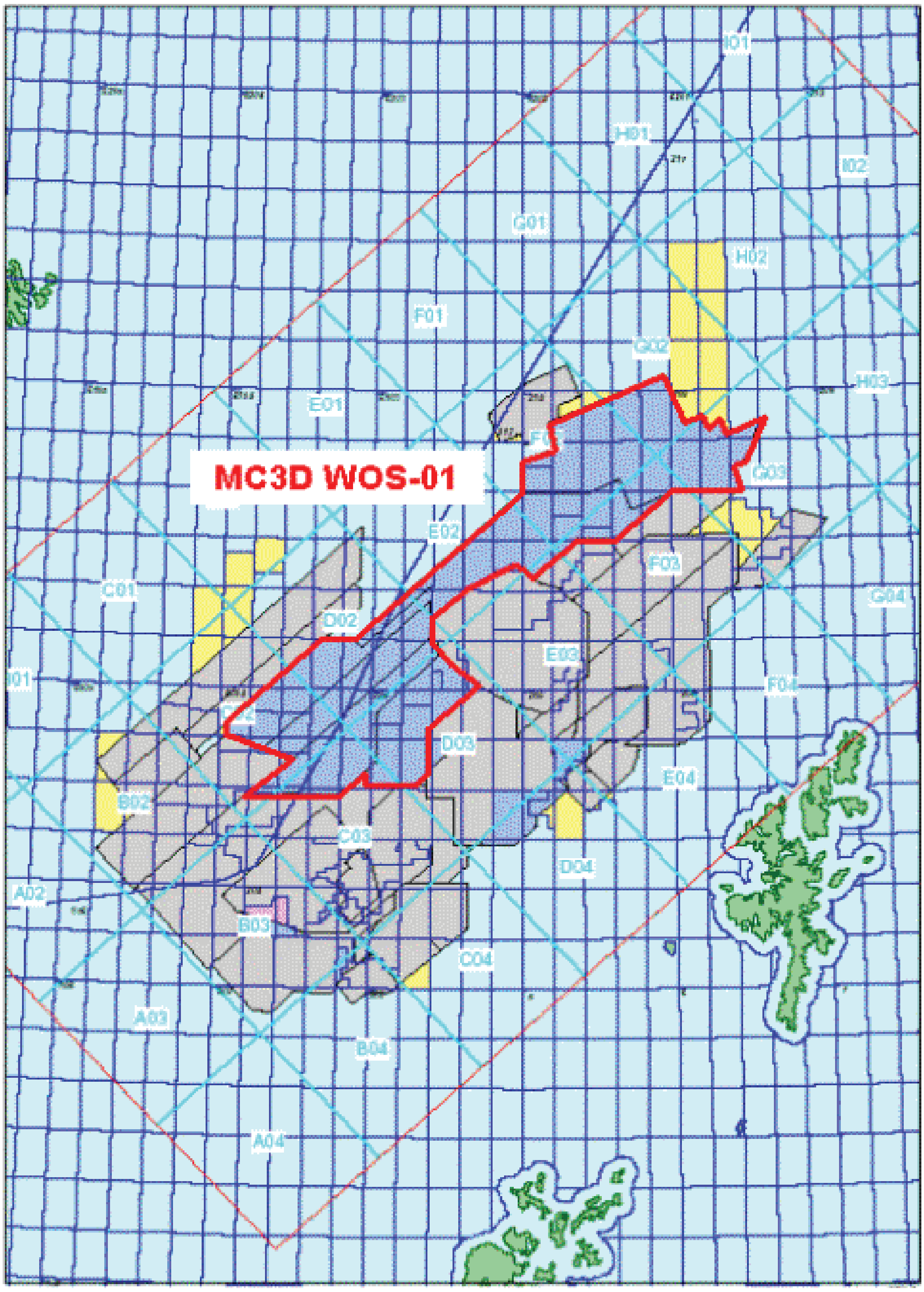

PGS Appendix B

Grid information:

All grids used:
Geodetic datum ED50. SPHEROID INT1924 : 6378388.00 297.00
Central Meridian 03 0 0.0W. Projection UTM Zone 30N.
All grids at 12.5m x 12.5m bin spacing.

Final Merge Grid				
Grid corners				
subline	xline	cdp	cdpx	cdpy
1	1	1	242341.09	6739081.50
1	36000	36000	573528.25	7043719.50
20000	36000	720000000	742767.81	6859730.50
20000	1	719964001	411580.625	6555092.50
Q213 grid:				
Grid corners				
subline	xline	cdp	cdpx	cdpy
3500	3000	1	449020.81	6776931.00
3500	10000	7001	513420.00	6836168.00
5000	10000	10508501	526113.56	6822368.00
5000	3000	10501501	461714.41	6763131.00
Q214 grid:				
Grid corners				
subline	xline	cdp	cdpx	cdpy
1242	6884	1	484275.19	6857290.50
1242	15360	8477	581298.56	6899856.50
6884	15360	47835711	609632.38	6835273.50
6884	6884	47827235	512609.03	6792707.50
WZ grid:				
Grid corners				
subline	xline	cdp	cdpx	cdpy
2300	2500	1	421836.00	6737987.50
2300	6500	4001	458635.56	6771837.00
3300	6500	4005001	450173.19	6781037.00
3300	2500	4001001	413373.63	6747187.50
TR7&8 grid:				
Grid corners				
subline	xline	cdp	cdpx	cdpy
20	131	1	455237.59	6711090.50
20	4952	4822	499595.03	6751882.50
3796	4952	18212694	467645.09	6786625.00
3796	131	18207873	423287.66	6745833.00

PGS Appendix C

Fig 1: Q213-Q214 Amplitude decay, post correction.

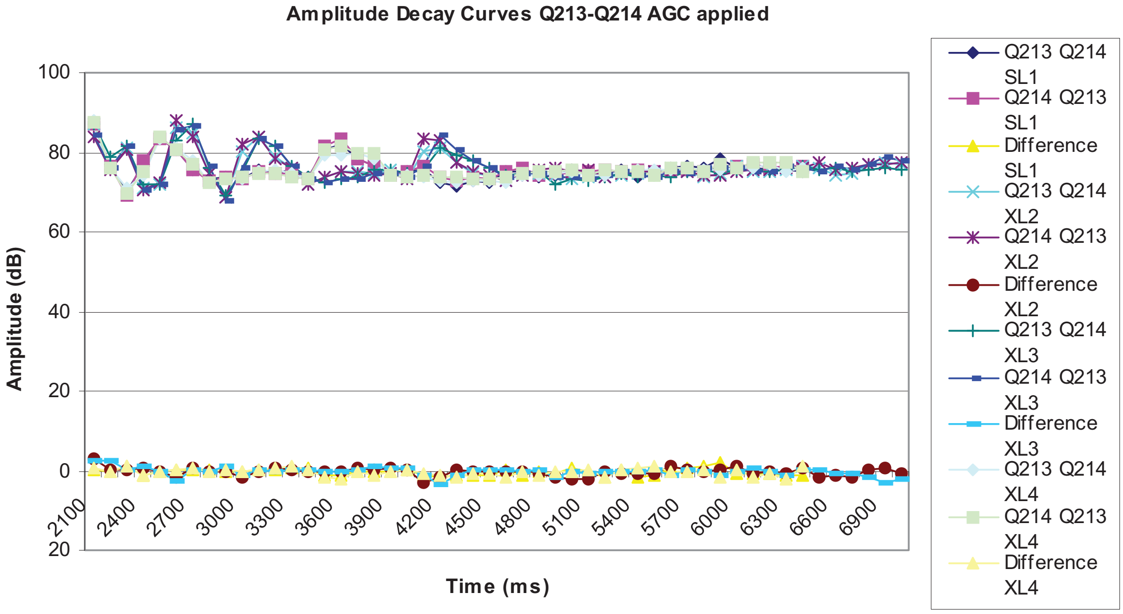

Merge AGC to Q214 data; Time Gate	Robust factor 2.0
0	500
1000	500
3000	1000
End	1000

Fig 2: Q213-WZ Amplitude decay, post correction.

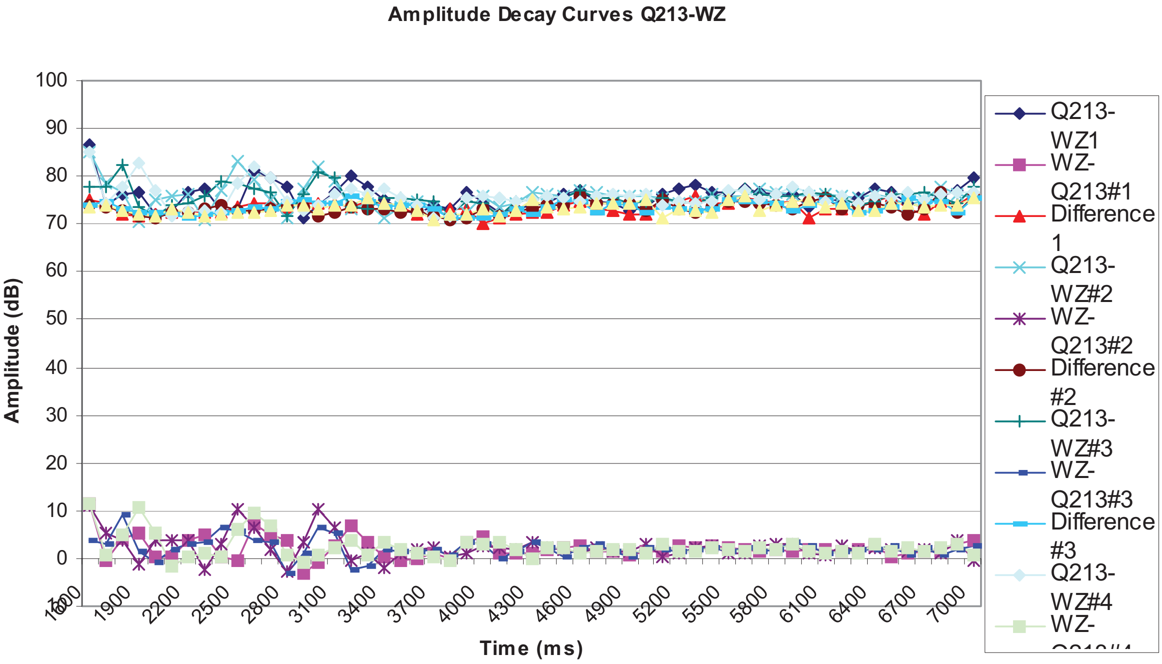

Amplitude Match applied to WZ to match Q213; +73db

Fig 3: WZ-TR7&8 Amplitude decay, post correction.

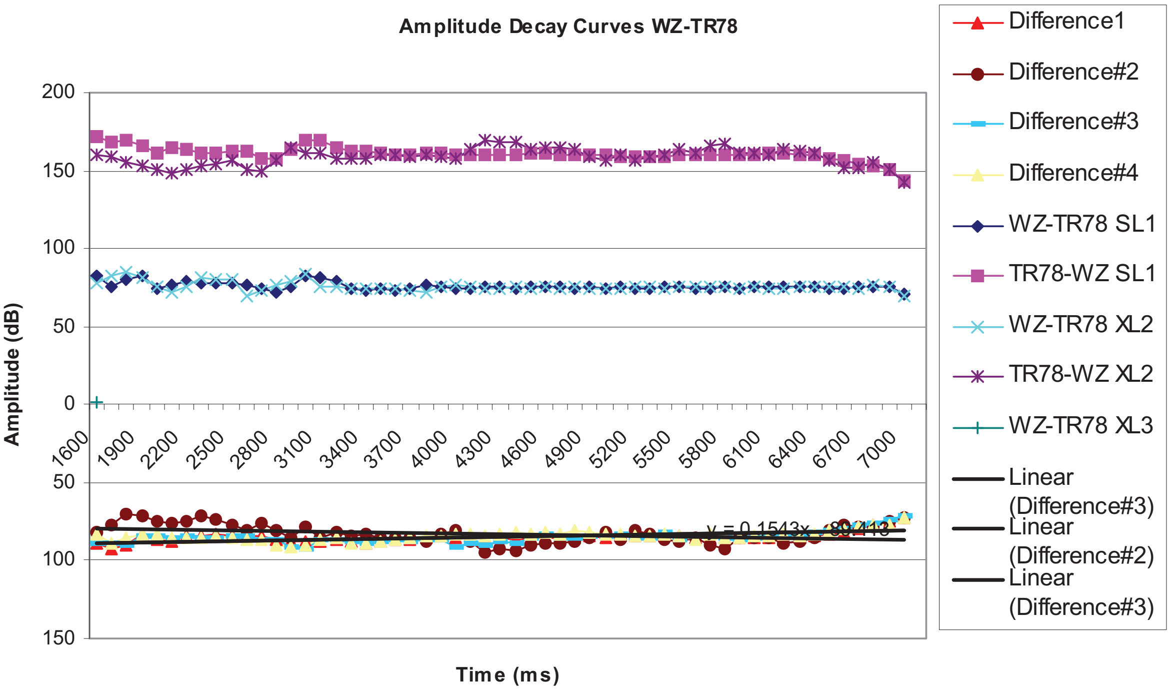

Amplitude Match applied to TR7&8 to match corrected WZ;   84db

Table 1: Summary of amplitude matching

Survey Name	Amplitude correction
Q213	None, (Base survey)
Q214	Robust AGC, Time/Gate: 0 500, 1000 500, 3000 1000, data end 1000, Robust 2.0
WZ	Constant +73db
Tr7&8	Constant 84db

PGS Appendix D

Fig 4: Post merge waterbottom horizon picked in deskSeis.

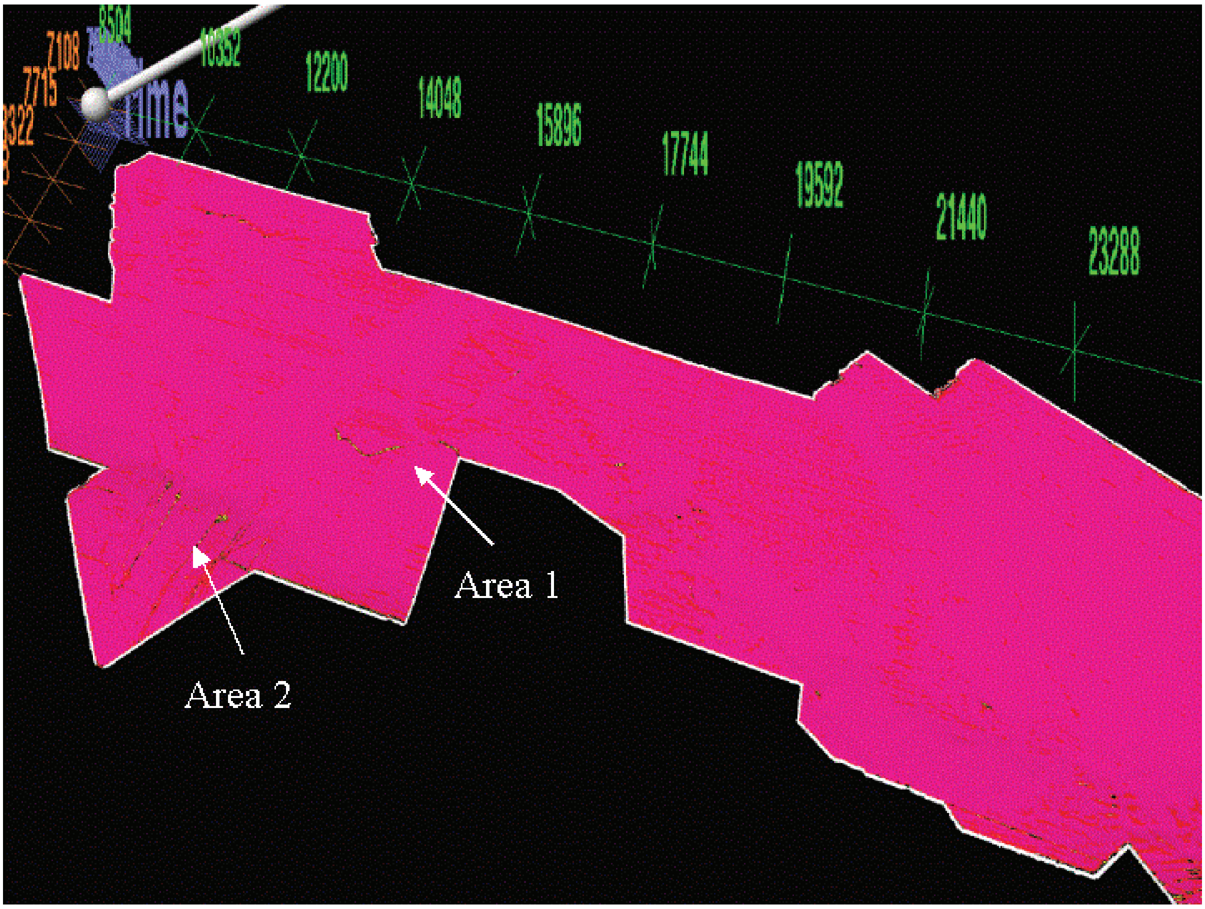

It can be seen from Figure 4 above that there is an area where the waterbottom does not tie exactly, marked as Area 1. Area 2 is entirely within the TR7&8 survey, and on review of the seismic data, shows apparent channels within the seabed.

PGS Appendix E

Example time-slice through merged data.

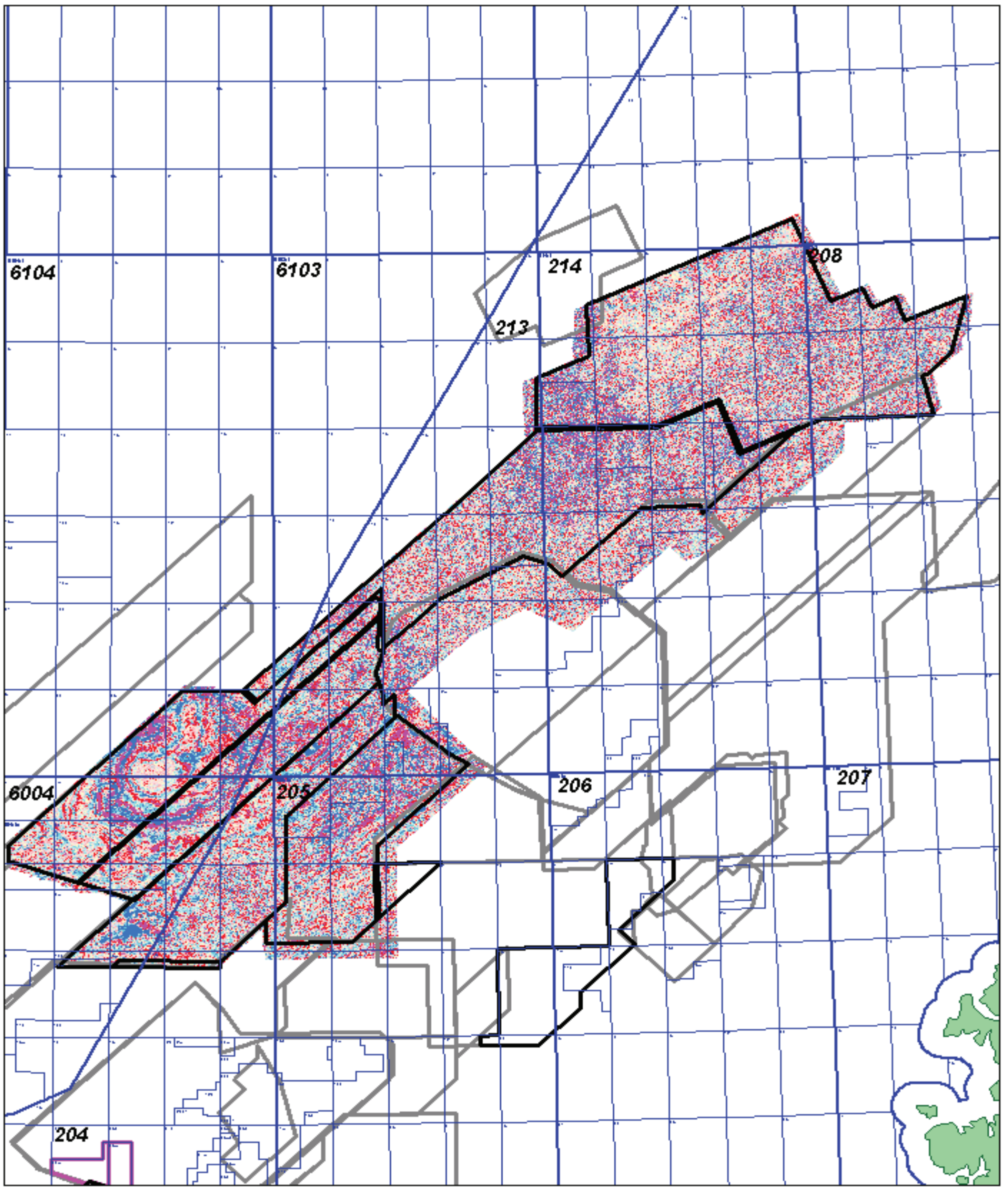

PGS Appendix F

Example EBCDIC header:

```
c1   CLIENT: PGS EXPLORATION UK LTD
c2   AREA: MC3D WOS 01
c3   PROJECT: MEGA SURVEY
c4
c5   MERGED 3D MIGRATION DATA
c6   INLINES : 7113 to 13170 EV 1 / XLINE RANGE 8500 27000 (MIN/MAX) /
c7   THIS SUBLINE
c8   SAMPLE RATE 4MS / TRACE LENGTH 8500MS / 32BIT IBM FLOATING POINT /
c9
c10   12.5m X 12.5m BINS /
c11
c12   MERGED BY PGS DATA PROCESSING  MAY 2001 TO JANUARY 2002
c13
c14
c15   PROCESSING:
c16   FINAL MIGRATION DATASETS AS SUPPLIED / REFORMAT TO INTERNAL
c17   FORMAT / REBIN ONTO MASTER GRID / AMPLITUDE MATCHING /
c18   STATIC CORRECTION AS REQUIRED / BLEND MERGE / SEG Y OUTPUT /
c19
c20
c21
c22
c23
c24
c25
c26
c27   GRID INFO:
c28   ORIGIN: SL 1 XL 1  X 242341.09  Y 6739081.50
c29   SL 1 XL 36000  X 573528.25  Y 7043719.50
c30   SL 20000 XL 36000  X 742767.81  Y 6859730.50
c31   SL 20000 XL1  X 411580.62  Y 6555092.50
c32
c33
c34   HEADER INFO : SL BYTES 9 12 & 189 192 / XL BYTES 13 16 & 193 196 /
c35   CDP X BYTES 73 76 & 81 84 / CDP Y BYTES 77 80 & 85 88 /
c36   CDP BYTES 21 24 & 201 204 /
c37
c38   GEODETIC DATUM ED50 / SPHEROID INT1924 6378388.00 297.00 /
c39   CENTRAL MERDIAN  03 0 0.0W / PROJECTION UTM ZONE 30N /
c40   END EBCDIC
```

PGS MegaSurveys - Processing

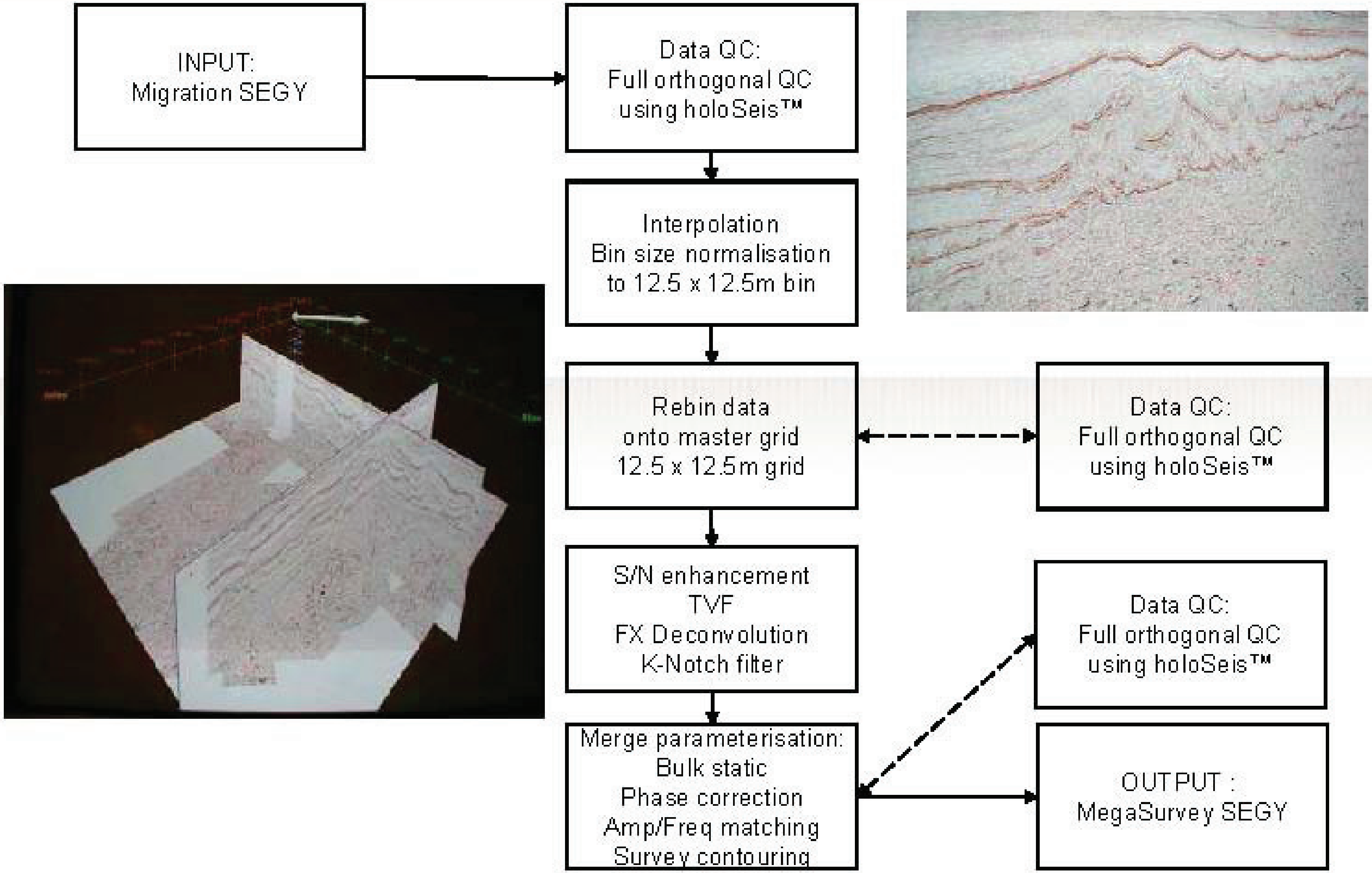

INPUT:
Migration SEGY

Data QC:
Full orthogonal QC
using holoSeis™

Interpolation
Bin size normalisation
to 12.5 x 12.5m bin

Rebin data
onto master grid
12.5 x 12.5m grid

Data QC:
Full orthogonal QC
using holoSeis™

S/N enhancement
TVF
FX Deconvolution
K-Notch filter

Merge parameterisation:
Bulk static
Phase correction
Amp/Freq matching
Survey contouring

Data QC:
Full orthogonal QC
using holoSeis™

OUTPUT :
MegaSurvey SEGY

1994 NPD Reprocessing
B85, VB87, 89, 90
Survey length: 5 943 km

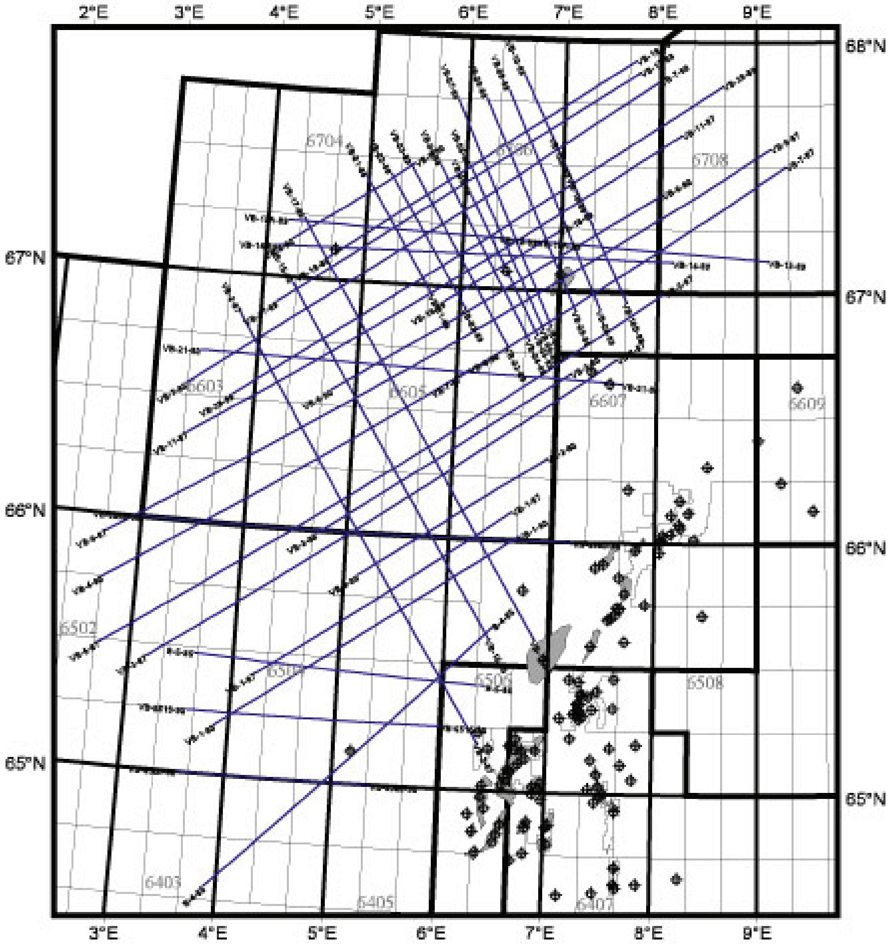

VØRING BASIN - B85, VB87, 89, 90

The reprocessing of NPD seismic data (B85, VB87, 89, 90) was sponsored by Saga Petroleum, Statoil and Norsk Hydro.

Vøring Basin-B85

The acquisition of the seismic data was originally carried out by Geco using the vessel, the *M/V Malene Ostervold* during the month of May 1985.

Source:		**Streamer:**	
Type	Sleeve Air Gun	Length	3000
Volume	4752 cu.in.	Group interval	50 m
SP interval	50 m	No. of groups	60
Depth	7.5 m	Depth	12 m
Recording:		**Navigation:**	
Record length	14 sec	Argo	
Sample interval	4 ms		
Fold of coverage	30		

The Vøring Basin (B85) data was reprocessed by Digital Exploration Ltd., September 1994.

Vøring Basin - VB87

The acquisition of the seismic data was originally carried out by Western Geophysical using the vessel, the *M/V Western Challenger* during the month of July 1997.

Source:		**Streamer:**	
Type	Sleeve Air Gun	Length	3200
Volume	4860 cu.in.	Group interval	26.67 m
SP interval	53.32 m	No. of groups	120
Depth	7 m	Depth	9 m

Recording:		**Navigation:**
Record length	15 sec	Argo
Sample interval	2 ms	
Fold of coverage	60	

The Vøring Basin (VB87) data was reprocessed by Digital Exploration Ltd.

Vøring Basin - VB89

The acquisition of the seismic data was originally carried out by Geco using the vessel, the *M/V Geco Gamma* during the month of July 1989.

Source:		**Streamer:**	
Type	Airgun array	Length	3600
Volume	8104 cu.in.	Group interval	12.5 m
SP interval	25 m	No. of groups	288
Depth	6 m	Depth	10 m

Recording:		**Navigation:**
Record length	8 sec	Geoloc / Syledis
Sample interval	2 ms	
Fold of coverage	72	

The Vøring Basin (VB89) data was reprocessed by Digital Exploration Ltd., September 1994.

Vøring Basin - VB90

The acquisition of the seismic data was originally carried out by Master Seismic using the vessel, the *M/V Skandi Pioneer* during the month of October 1990.

Source:		**Streamer:**	
Type	HGS Sleeve Guns	Length	3000
Volume	2660 cu.inch	Group interval	25 m

SP interval	37.5 m	No. of groups	120
Depth	7 m	Depth	10 m

Recording:		**Navigation:**
Record length	10 sec	Geoloc
Sample interval	2 ms	
Fold of coverage	40	

The Vøring Basin (VB90) data was reprocessed by Digital Exploration Ltd., October 1994.

Data available:

Navigation data	UKOOA format
Velocity data	ESSO V2 format
Field data	SEG-D or SEG-Y
Raw stack	SEG-Y format
Raw migration	SEG-Y format
Final migration	SEG-Y format

Contact information

Mid Norway Regional 2004-05-06-07-08

MNR

Survey length: 49,000 km

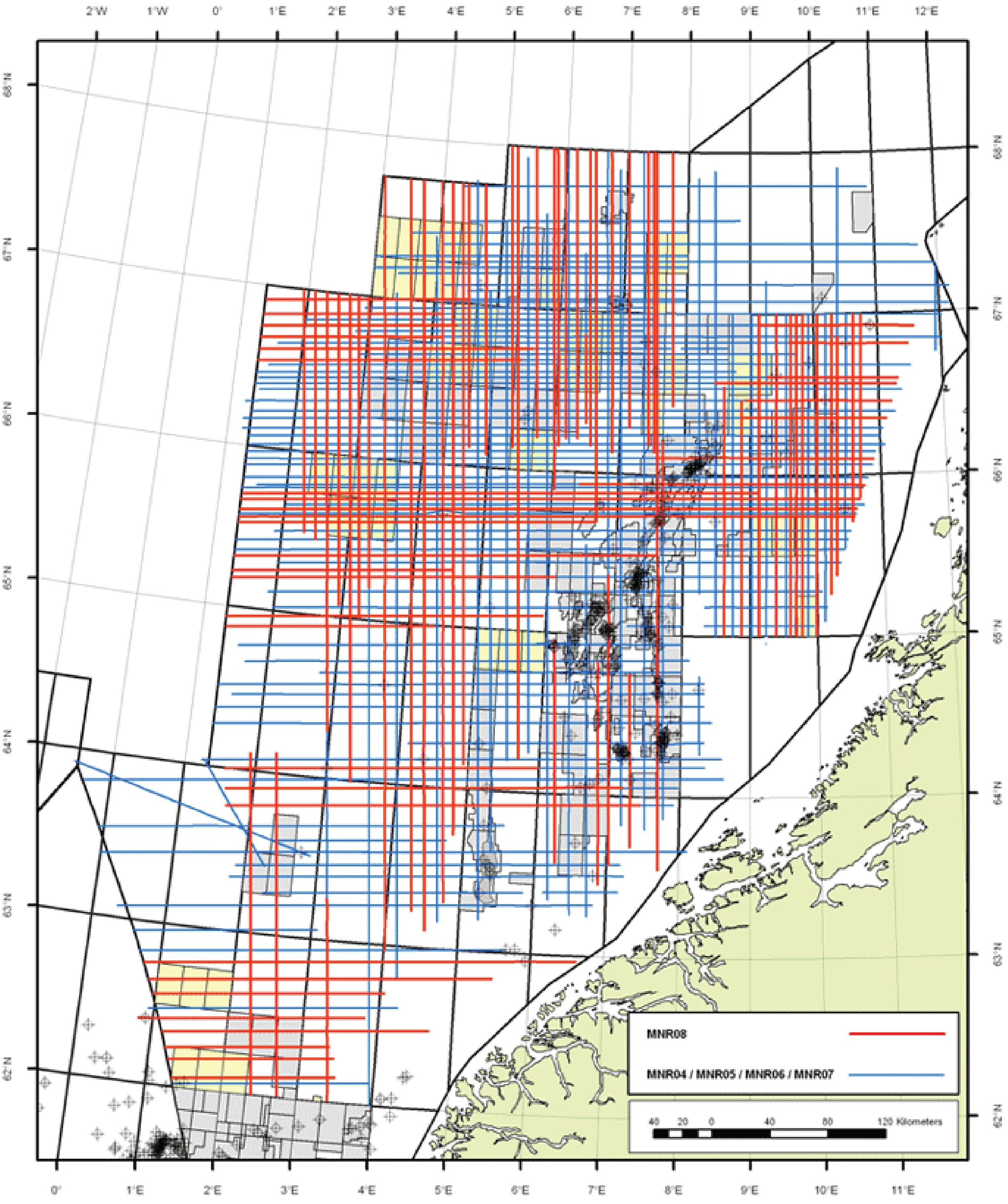

MNR

The MNR survey has been acquired by Fugro Multi Client Services in co-operation with TGS.

The acquisition of the seismic data was carried out by Fugro-Geoteam AS using the vessel *R/V Polar Princess* during June - August 2004, June-September 2005 and June-August 2006. The 2007 acquistion was carried out by M/V Akademik Shatskiy during May - October 2007. The 2008 acquisition was carried out by Hawk Explorer and Geo Arctic during April - October.

Source:

Type	Air gun
Volume	4640 cu.in.
SP interval	25 m
Depth	7.5 +/-1 m
Output	104 bar m (DFS 0-128 Hz)

Streamer:

Length	10 050 m
Group interval	12.5m
No. of groups	804
Depth	9 +/-1 m

Recording:

Record length	10.2 sec
Sample interval	2 ms
Fold of coverage	201

Navigation:

Starfix HP

The MNR04 data was processed by Geotrace. The data acquired in 2005, 2006 and 2007 has been processed by Western Geco. A fast track version of selected MNR08-lines is available now.

Data available:

Navigation data	UKOOA
Velocity data	ESSO V2
Field data	SEG-D
Raw migration	SEG-Y
Final migration	SEG-Y
4 Angle related offset stack volumes (raw mig with & without pre-stack de-noise, no global gain) (final mig with & without pre-stack de-noise, global gain:	SEG-Y
CMP gathers (with & without NMO-correction)	
Gravity data	

Contact information

2000 Gjallar Vema Fles Reprocessed 2008
GVF00RE08

Survey length: 3 035 km

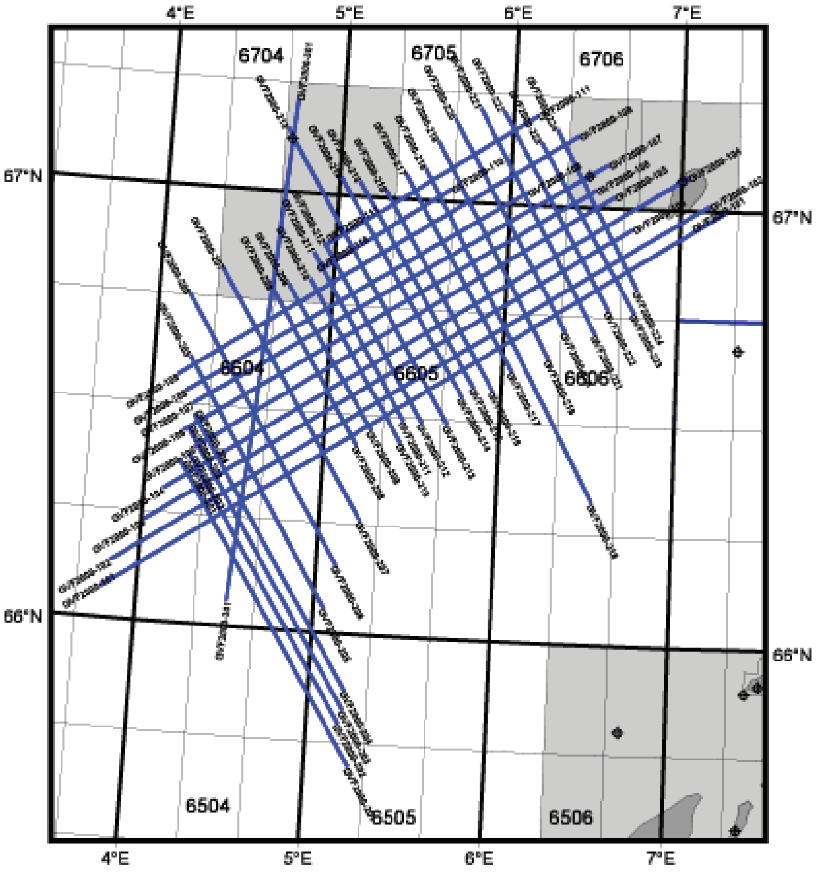

GVF00RE08

The GVF00RE08 survey was acquired by Fugro-Geoteam in co-operation with TGS.

The acquisition of the seismic data was carried out using Fugro-Geoteam's vessel, *R/V Geolog Dm. Nalivkin* during the months of July and August 2000.

Source:

Type	Sleeve Gun/ G-Gun
Volume	3410 cu.inch
SP interval	25 m
Depth	6 m
Output	99 bar m (DFS 0-128 Hz)

Streamer:

Length	6000 m
Group interval	12.5 m
No. of groups	480
Depth	8 m

Recording:

Record length	8 sec
Sample interval	2 ms
Fold of coverage	120

Navigation:

Starfix DGPS

The GVF00RE08 data was processed by Fugro-Geoteam AS. The data was reprocessed by Geokinetics Processing UK Limited in 2008.

Data available:

Navigation data

Velocity data

Field data
Angle stacks (6 volumes)
CDP sorted demultiple gathers
CDP sorted k-pstm Radon gathers
Raw migrated stacks
Final migrated stacks

Contact information

Ant Tracking Workflow

The patent pending Ant Tracking algorithm automatically extracts fault surfaces from fault attributes. The algorithm uses the principles from ant colony systems to extract surfaces appearing like trends in very noisy data. Intelligent software agents (“ants”) will try to extract features in the attribute corresponding to expectations about the faults. True fault information in the attribute should fulfill these expectations and be extracted by many ants, whereas noise and remains of reflectors should be extracted by no ants or by only single ants (in which case they will be deleted). The approach is fully 3D and is able to take advantage of surface information in the surrounding voxels. This makes it possible to derive detailed information from the attribute. By writing the extracted surfaces back to a volume, we get what is referred to as an enhanced attribute, or ant track cube. This cube contains only what is likely to be true fault information.

The process can be divided into four main activities: (1) seismic conditioning, (2) edge detection, (3) edge enhancement, and (4) interactive interpretation (surface extraction). A collection of surface segments, fault patches, can be extracted after the generation of the ant-track attribute. This is a volume of fault surface “pieces” having a high confidence of connectedness, which can be interactively merged into complete fault surfaces using the Automatic Fault Extraction process.

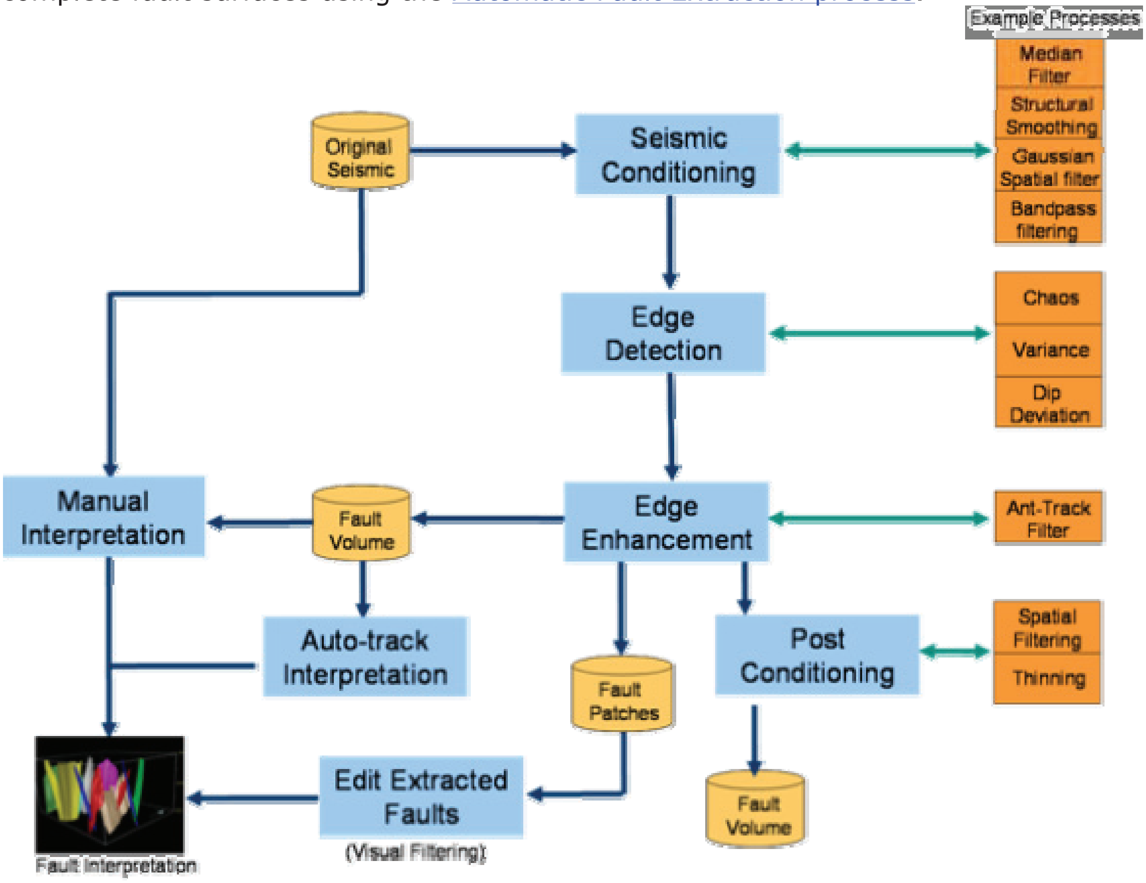

Ant Track workflow for creation of an ant-track attribute volume and for the generation of Fault Patches extracted after the Ant Tracking process.

With this new workflow, interpretation to create fault surfaces can occur in several ways. The traditional approach for interpreting on the seismic sections can be done at any time. In addition, manual interpretation can be performed on a processed seismic attribute volume, such as the ant-track enhanced edge volume. And interpretation of fault systems can be done based on spatial filtering of fault patches.

How to do the Ant Tracking Workflow

The main workflow can be seen in the illustration below.

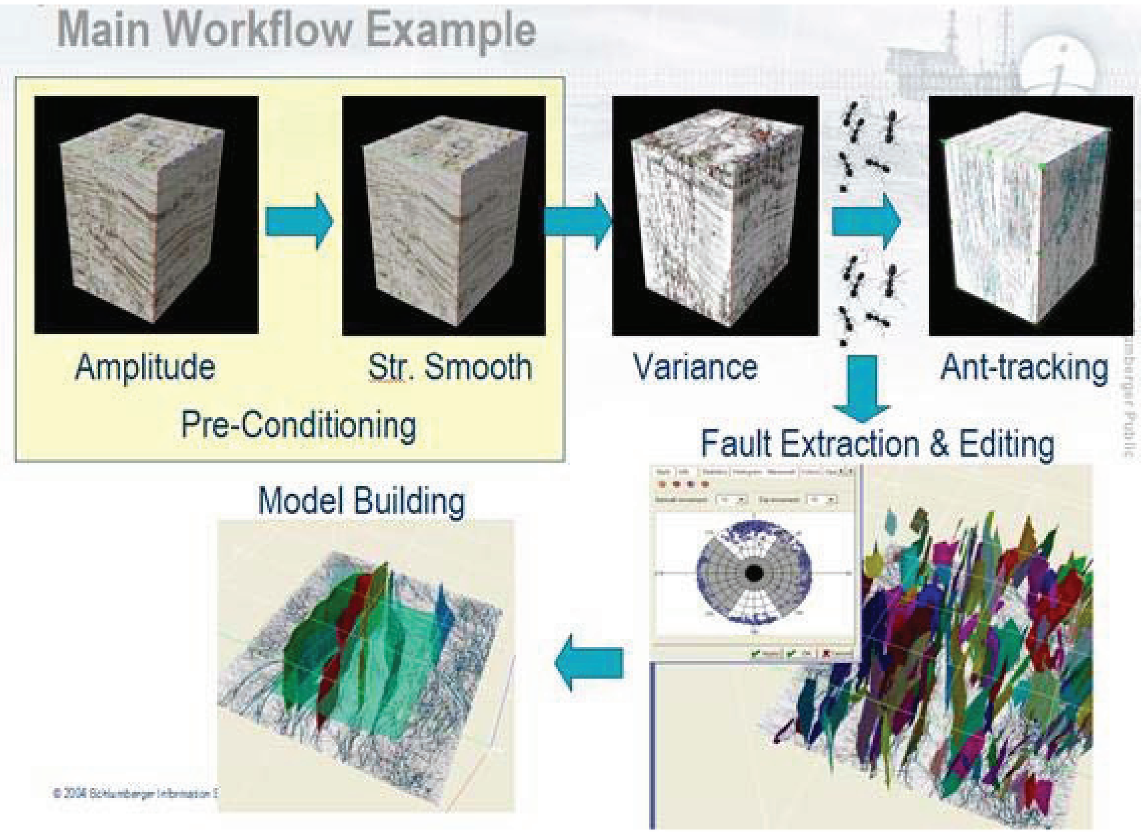

1. First the original seismic data can be processed or conditioned using the structural smoothing option with the fault edge preservation option.
2. Then a Variance cube needs to be generated that will contain all the discontinuities.
3. Alternatively, the Chaos attribute can be generated instead.
4. Either the Variance cube or the Chaos cube can be used as input for the Ant Tracking process.
5. You can also use any other input that enhances discontinuities. (like Coherency® for example). This volume needs to be loaded to Petrel first, either using the SEG-Y loader or the Open-Spirit connectivity.
6. Next, the Ant Tracking algorithm generates an enhanced Ant cube. This cube can be used for manual fault interpretation or, preferably, as input into the Automatic fault extraction process.
7. If the Automatic fault extraction process is used, based on the set parameters, extracted surfaces will be generated and saved under a separate folder.
8. The new workflow is a top-down approach, where the interpreter interacts with automatically extracted fault surfaces in a 3D canvas. Several properties are connected with the surfaces, which the interpreter can use for organizing the data. For example, the surfaces can be split into groups representing fault systems. The faults that make a system have common strike, meaning that the same stress field has created them in the same time period.

The new workflow offers:

1. **Increased objectivity**: Manual interpretation is highly subjective because it is difficult to map the discontinuities in the seismic data and understand their nature in 3D. In the new workflow, the surfaces are objectively extracted using automatic algorithms that work in true 3D.
2. **Increased level of detail**: The automatic extraction maps all discontinuities that have some extent in the data. When mapping surfaces manually, the interpreter typically does not have time to interpret details.
3. **Early understanding of fault systems**: With automatically extracted surfaces, the interpreter now starts out with a structural overview of the faults in the area. From the beginning, the interpreter will start thinking in terms of fault system and tectonic history.
4. **Faster interpretation**: Order of magnitude timesavings are obtained by automating the surface mapping, which traditionally is a very time-consuming manual task. The interpreter’s job is moved from low-level mapping of discontinuities on seismic slices, to high-level analysis of automatically extracted surfaces.

Appendix B

Supporting material for Chapter 3

Victory Lineament

Clair Lineament

Judd Lineament

01 Well 214/27-1 well to seismic tie and seismic stratigraphy

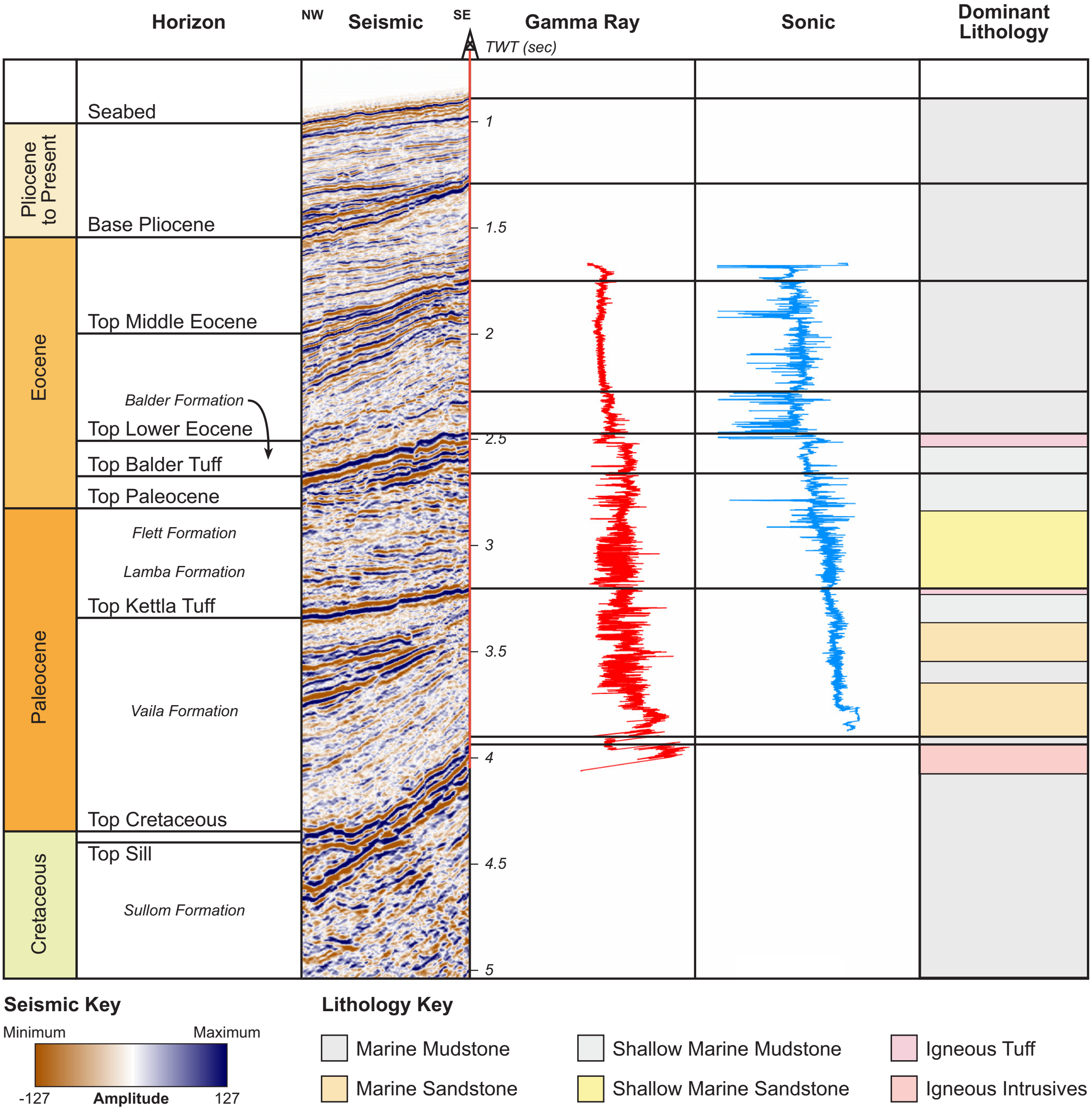

Top Kettla Tuff Time-Structure Map

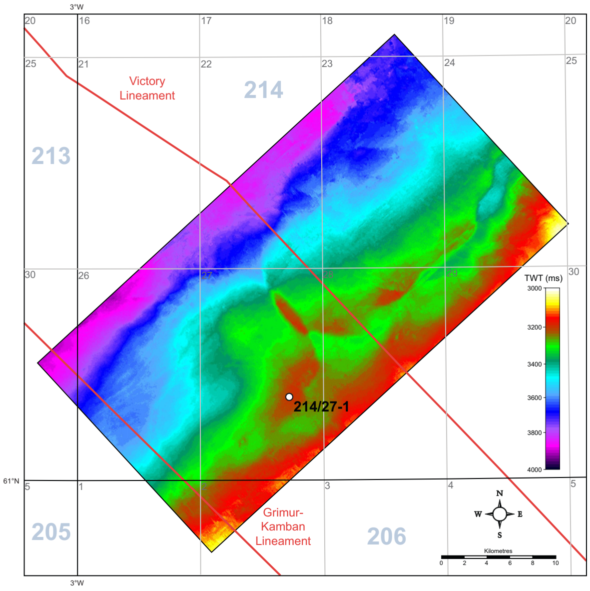

Figure 01

Well 214/27-1 penetrates the entire Paleocene-Eocene sequence recognised in the Faroe-Shetland Basin, reaching total depth in the Upper Cretaceous within which a dolerite sill and marine mudstones are encountered. The sill corresponds with a strong maximum relector which was selected due to an inferred large acoustic impedence contrast between the mudstone and dolerite lithologies.

The Cenozoic sequence is dominated by regressive marine to shallow marine sandstones and mudstones, with two regional igneous tuff horizons correlating with strong amplitude reflections.

02 Well 214/27-2 well to seismic tie and seismic stratigraphy

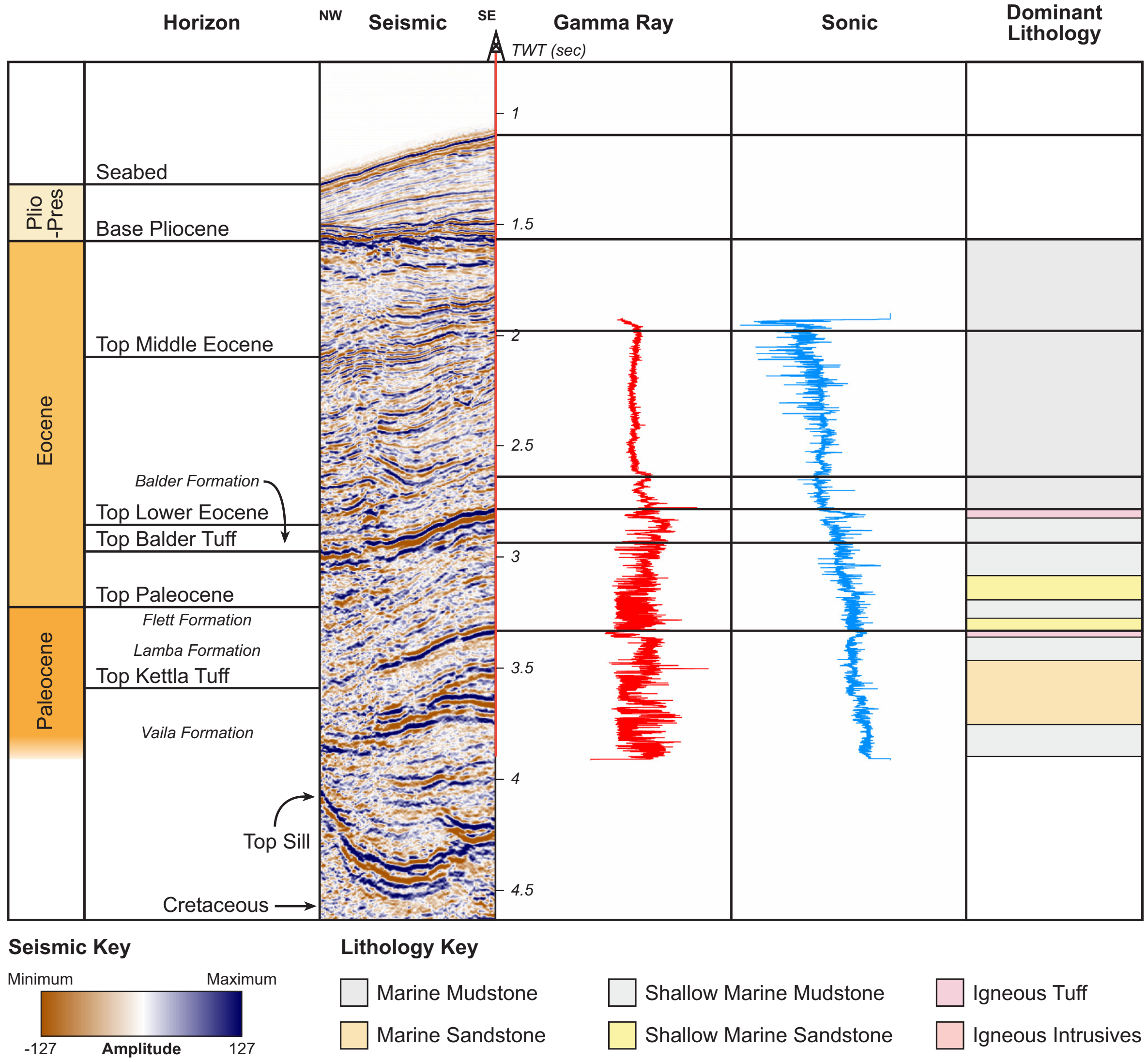

Top Kettla Tuff Time-Structure Map

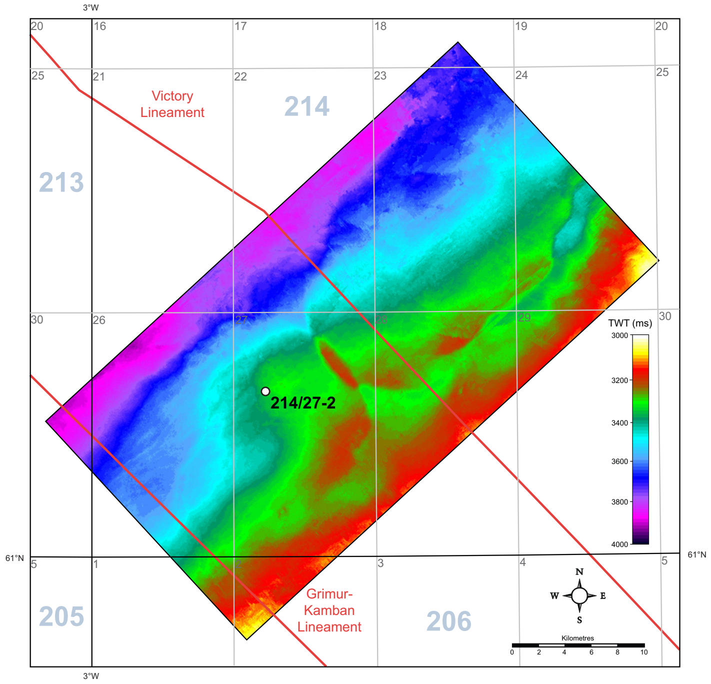

Figure 02

Well 214/27-2 is located down dip from well 214/27-1 and although is drilled to a similar depth, does not encounter Cretaceous age strata in the well. Reaching total depth in the Paleocene, it encounters a very similar early Cenozoic regressive sequence as recognised previously in well 214/27-1.

The Kettla and Balder Tuffs are similarly recognised in the well and correlate well with a strong positive amplitude reflector on the seismic data. After the deposition of the Balder Tuff the basin begins to subside again with a gradual return to marine mudstone deposition.

03 Well 214/28-1 well to seismic tie and seismic stratigraphy

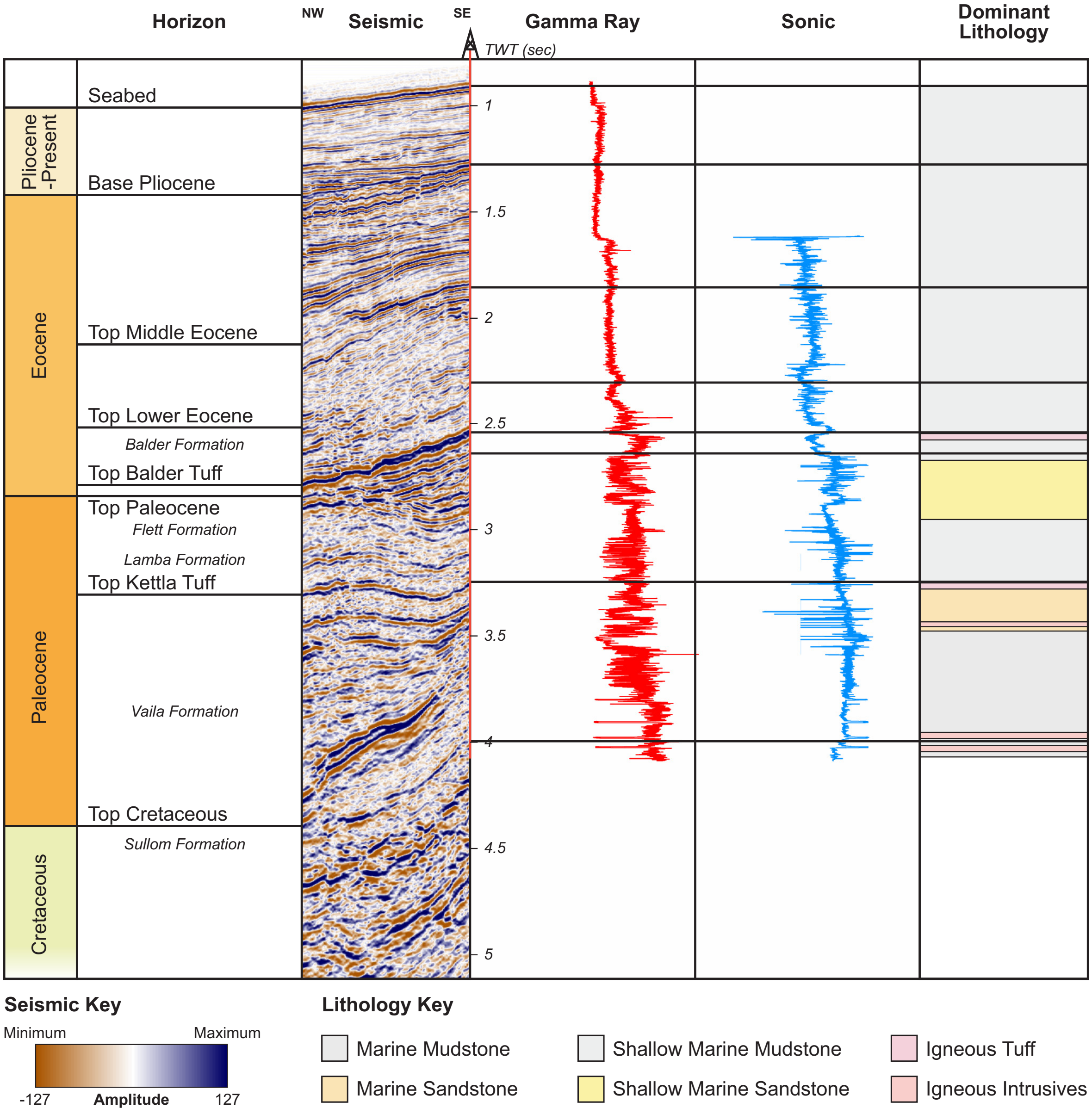

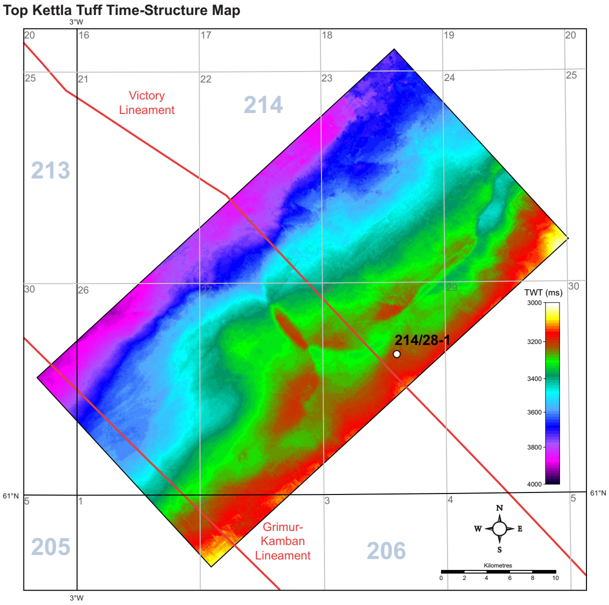

Figure 03

Well 214/28-1 reached a total depth in the Cretaceous and encounters both marine mudstones and a relatively small amount of intermediate igneous material which corresponds with thin discontinuous bright reflections on the seismic data. These may be associated with a high amplitude reflector located down dip.

The Tuff horizons correlate with a series of coherent strong amplitude reflections . The Cenozoic sandstones and mudstones give the succession a parallel layered appearance in contrast to the transparent relectivity post deposition of the Balder Tuff.

04 Paleocene sills time-structure map

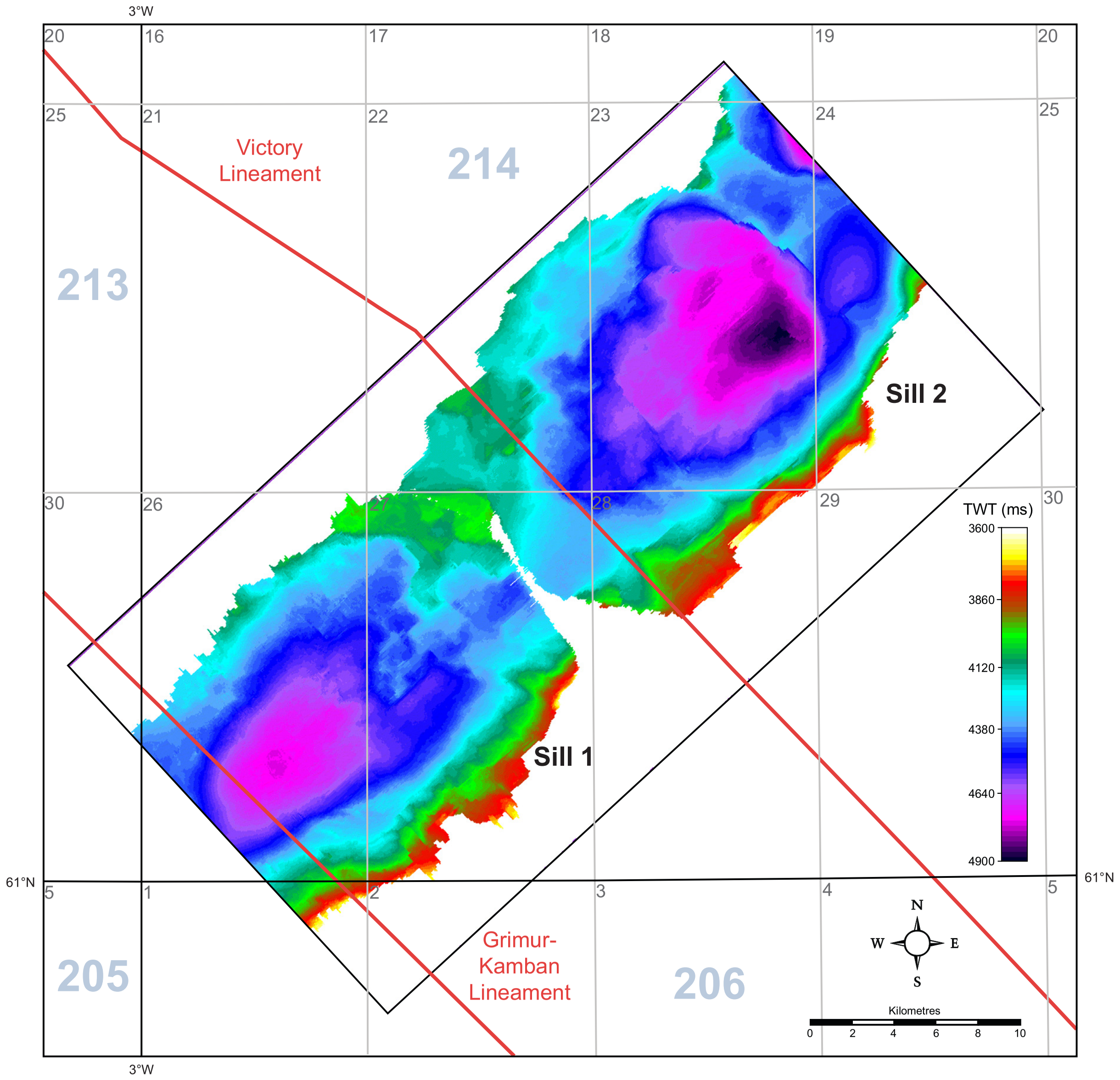

Figure 04
Sill 1 was sampled in Well 214/27-1. From this point, mapping of the sill based upon the strength of the amplitude response lead to the recognition that the sill has a ‘saucer-shaped’ geometry, and is preferentially elongated in a NE-SW orientation, extending outside the defined study area (~18km wide x >20km long). The south-eastern edge is structurally higher than elsewhere and is believed to be constrained to the south-east by the Flett Ridge.

Sill 2 was recognised from the seismic data due to the similar amplitude response exhibited on the seismic data. The interpreted structure of the sill is very similar to that of Sill 1 but is larger in extent (~19km wide x >25km long). The north-easterly limit of Sill 2 is difficult to ascertain as it merges with another sill complex in this area.

It is unclear whether the two sills merge in the region of blocks 214/22 and 214/27. It is likely the sills are located at a similar depth in this location, as they may be exploiting a similar zone of weakness.

05 Paleocene sill morphology (section view)

Sill penetrated by well 214/27-1 (Sill 1)

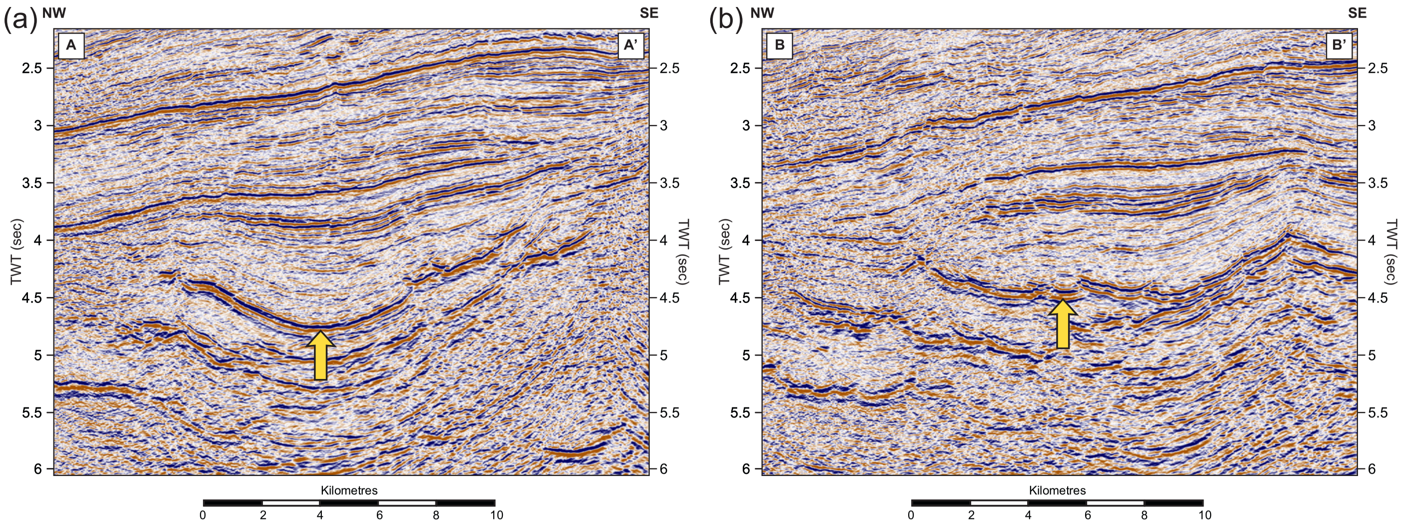

Sill to the north-east (Sill 2)

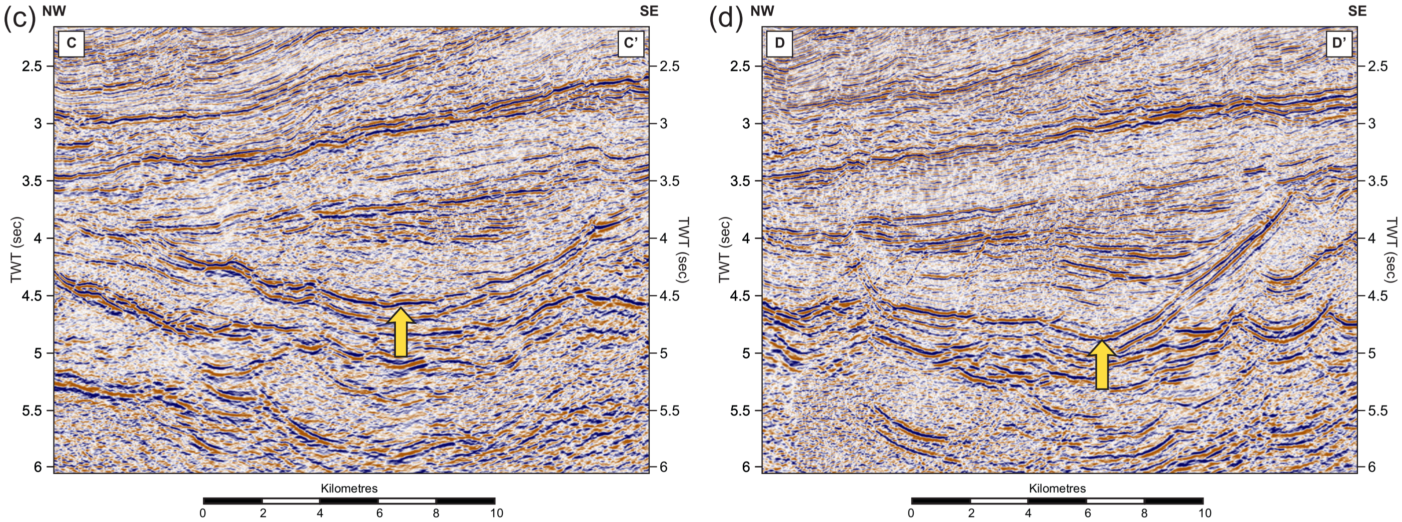

Top Sills Time-Structure Map

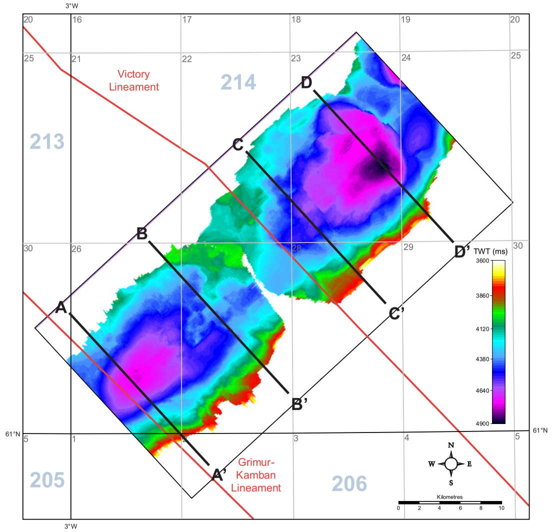

Figure 05
On each of the seismic lines the interpreted sills are highlighted, both associated with a strong amplitude response. Each display the assymetric concave up morphology as described by Bell and Butcher (2002) and largely conformable with the sedimentary fill of the basin. It is inferred that towards their northwest and southeast limits they cut up through the sedimentary overburden but the sill hampers seismic imaging of the sedimentary units below to confirm this. Evidence for this process is greatest in (d) where the overlying sediment is rotated into larger dips.

There is also evidence of other igneous intrusives exploiting the Cretaceous stratigraphy with multiple high amplitude reflections recognised in the deeper sequence.

06 Morphology of the sills along basin strike

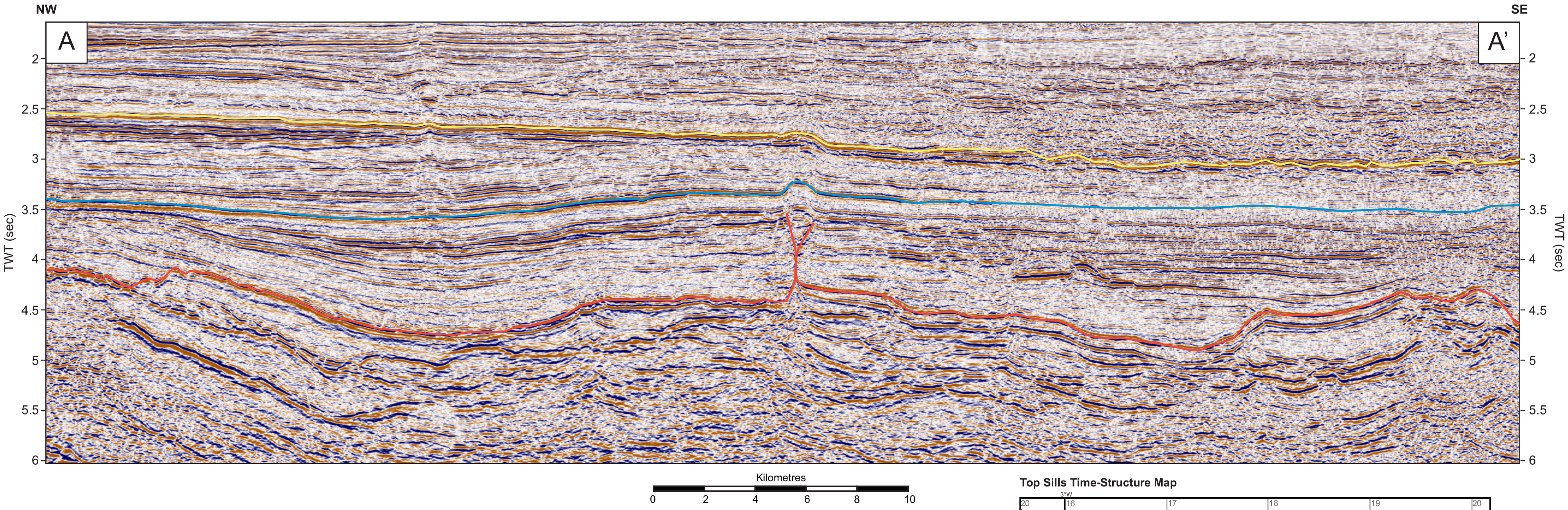

Figure 06

Horizons: Yellow = Top Balder Tuff   Blue = Top Kettla Tuff   Red = Top Sills

The sills display an undulating morphology along the strike of the basin which is interpreted to be caused by the sills taking intruding along weak Cretaceous horizons. These could also be caused by the sill cutting up through the stratigraphy, but lack of well control, poor imaging of the sub-sill stratal fill and other deeper igneous material makes it difficult to confirm whether this is the case.

To the north-east, Sill 2 can be seen to cut up through the lower Paleocene strata, the reason for this being unclear. One hypothesis is that an increase in high amplitudes down dip from the sill may be older igneous sills which have blocked the lateral propogation of Sill 2. Sill 2 would then exploit another weak horizon; potentially between a mudstone and sandstone package as identified in well 214/28-1.

It is unclear how and where the sills are sourced from, but with the inference of a major sill and dyke complex at depth within the Cretaceous sequence, this may be the original source. An alternative hypothesis is that the material is sourced from depth along and up the Victory Lineament but there is no evidence of an inferred structure associated with the lineament at depth.

Top Sills Time-Structure Map

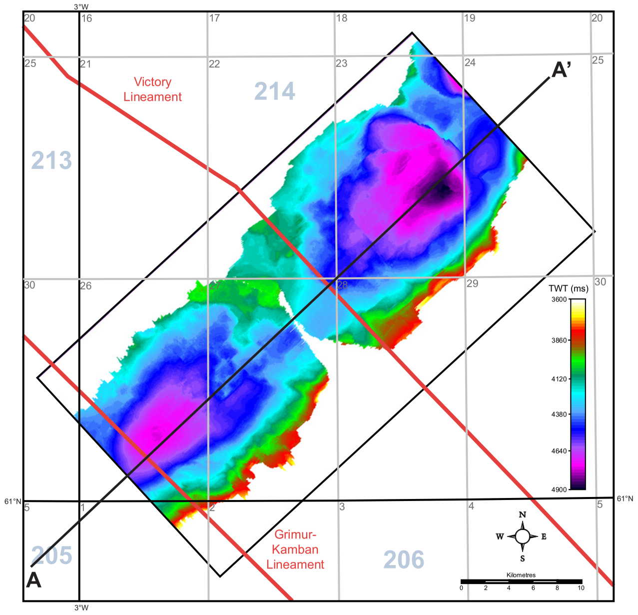

07 Paleocene Sill amplitude, dip, azimuth and dip-azimuth maps

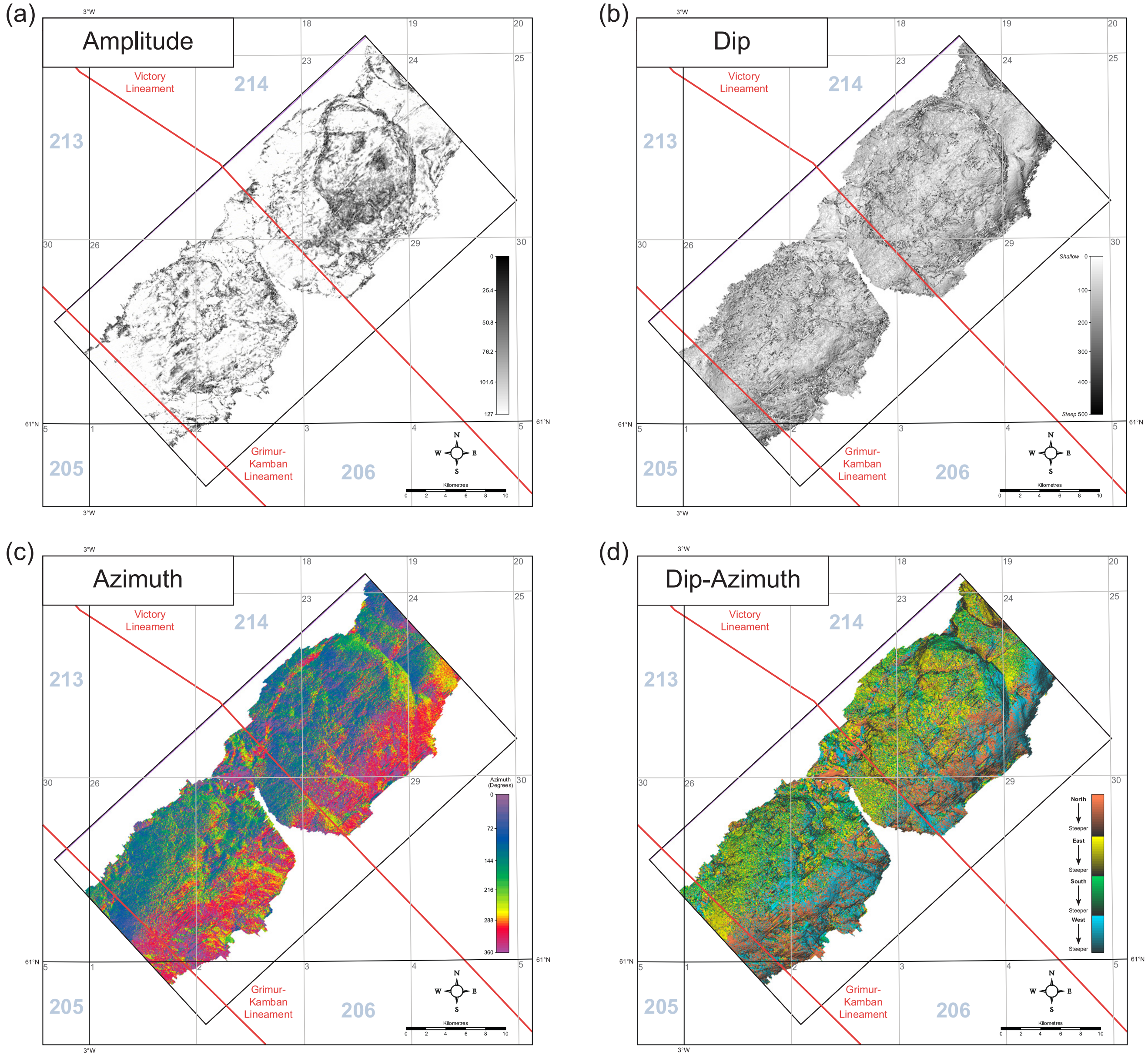

Figure 07
Map (a) of the two sills displays the strength of the extracted amplitude response from the sills which is very high. A lower amplitude response is associated with the deeper regions of the sills and also correlate with the areas of increased dip.

Map (b) displays that the sills are of relatively low dip and any variations are short and steep. Towards the edges of the sills, the relative dip of the sills increase and correspond with the sills cutting up through the overlying strata.

Map (c) displays a bimodal distribution with two dominant dip directions to the north-west and south-east. There are local variations of this theme which are probably attributed to small scale variations of the relief of the sills.

In map (d), it can be seen that the steeper dips within the sill correspond with a change in the azimuth, implying a limitation to the lateral propogation of the igneous material was encountered in these areas. This resulted in the upward flow of material before reintruding along a weaker horizon in the younger strata (Thomson 2007).

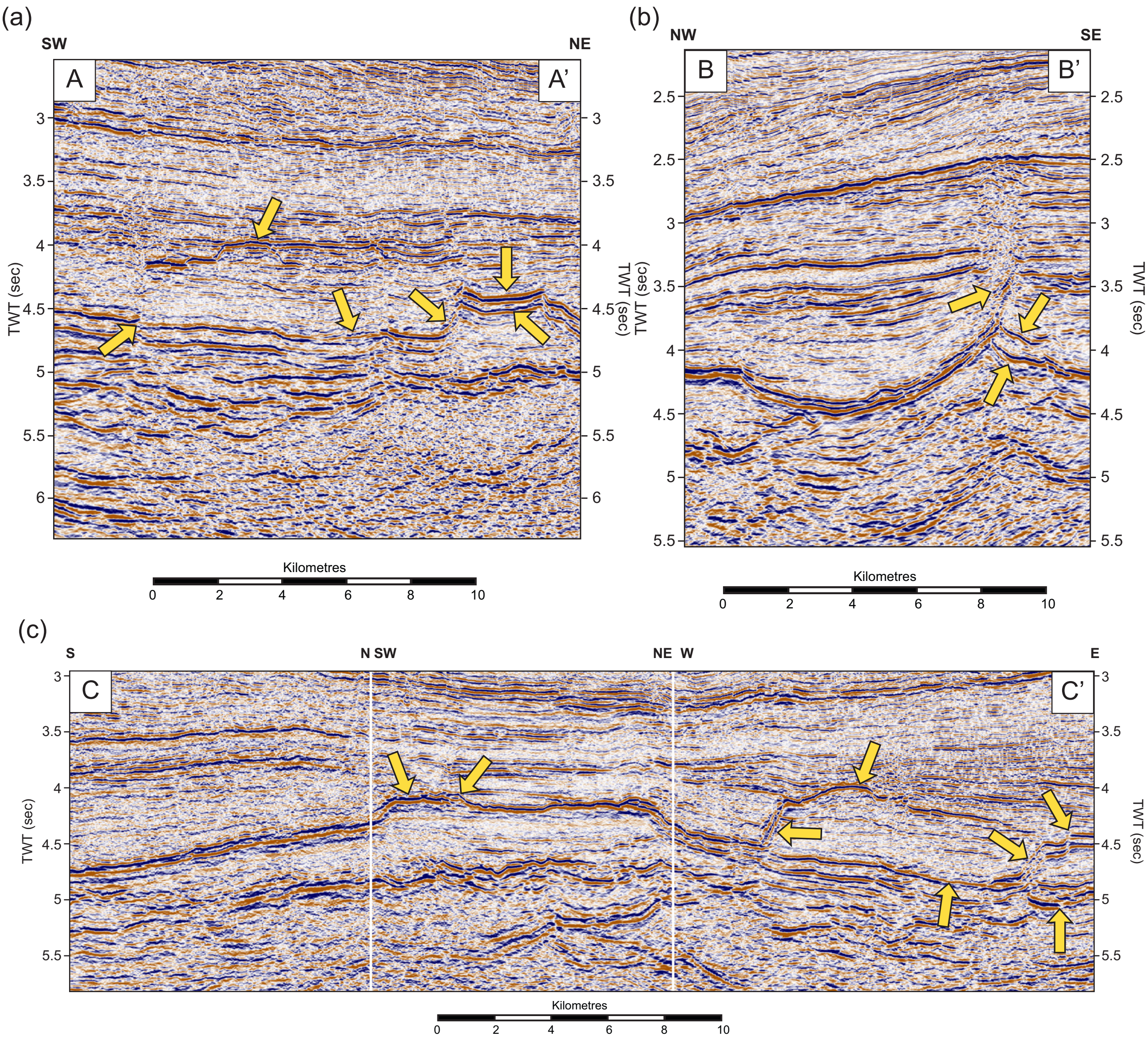

Top Sills Time-Structure Map

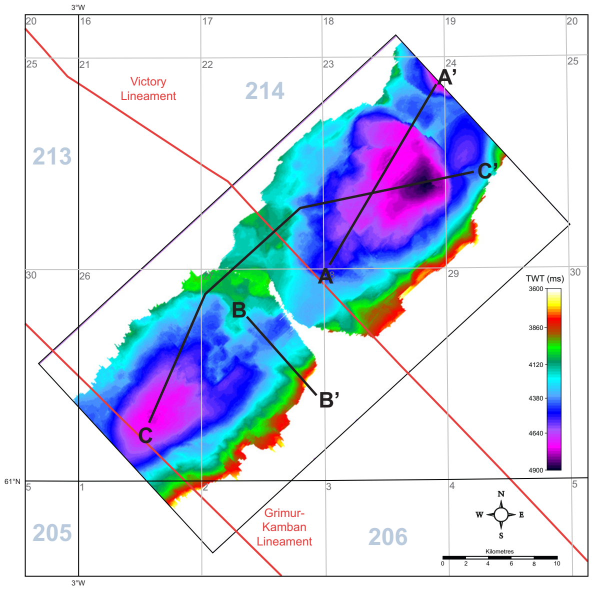

Figure 08

The two interpreted sills were occasionally difficult to map despite the strong amplitude of the relectors compared to the surrounding mudstone strata which is relatively transparent. An example where it proved difficult to interpret was across vertical offsets (a) which may be attributed to sub-vertical dykes, features which are difficult to image in seismic data. Notably, horizon amplitudes were not always coherent which may be a processing artefact. This meant it was sometimes difficult to identify which horizon was the top of the sills, especially if the sills were not continuous and appear to cut up through the stratigraphy (b). A further complication was the affect of deeper sills and dykes which also cut up through the interpreted sills and intrude the younger strata above (c). It is also unclear whether the two sills are linked where they apparently overlap.

09 Top Kettla Tuff time-structure map

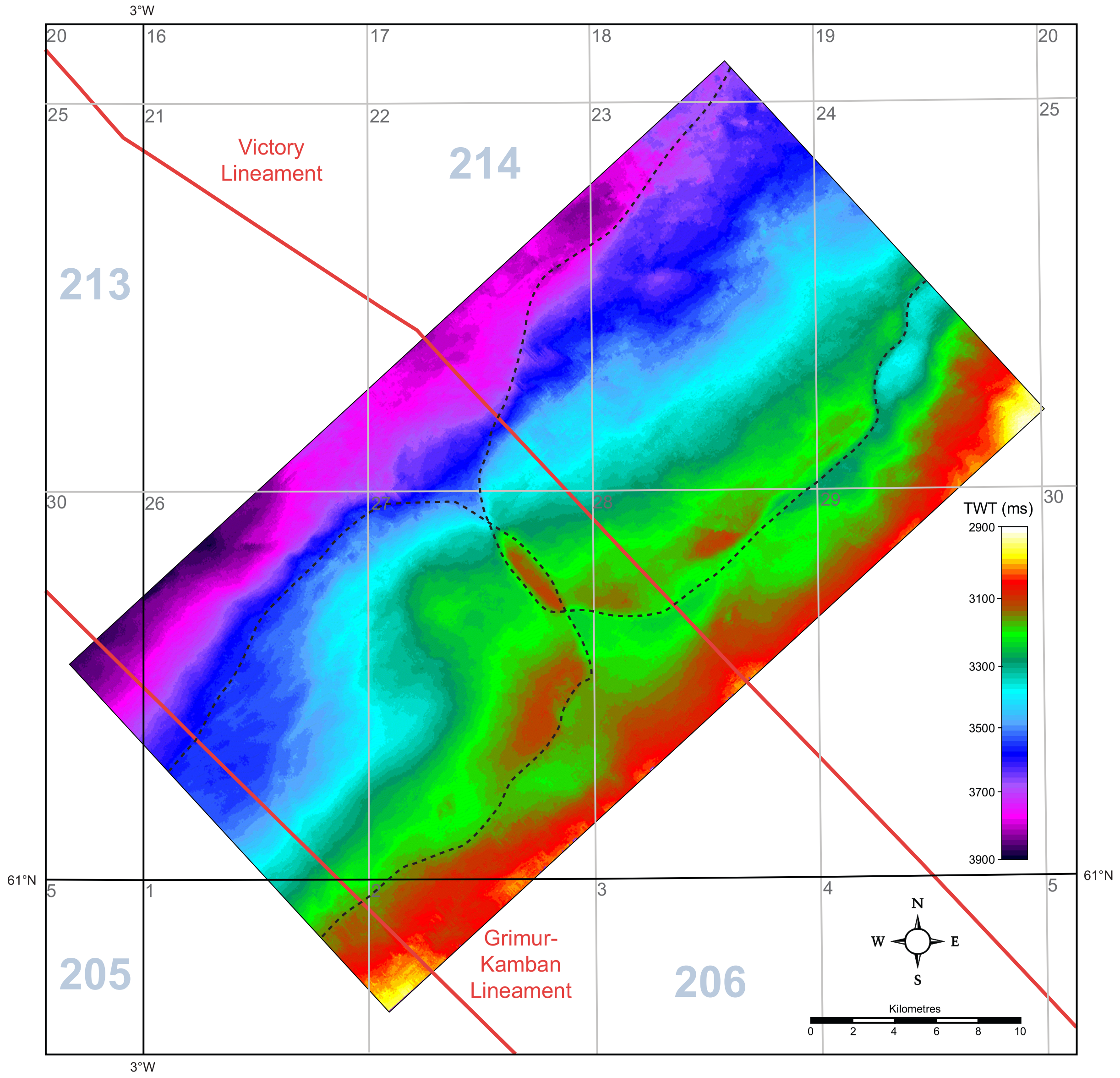

Figure 09
As described in the text, the Kettla Tuff displays two sub-circular but irregular structures. Between each of these, a NW-SE trending antiformal structure has formed.

10 Top Kettla Tuff edge, dip, azimuth and dip-azimuth maps

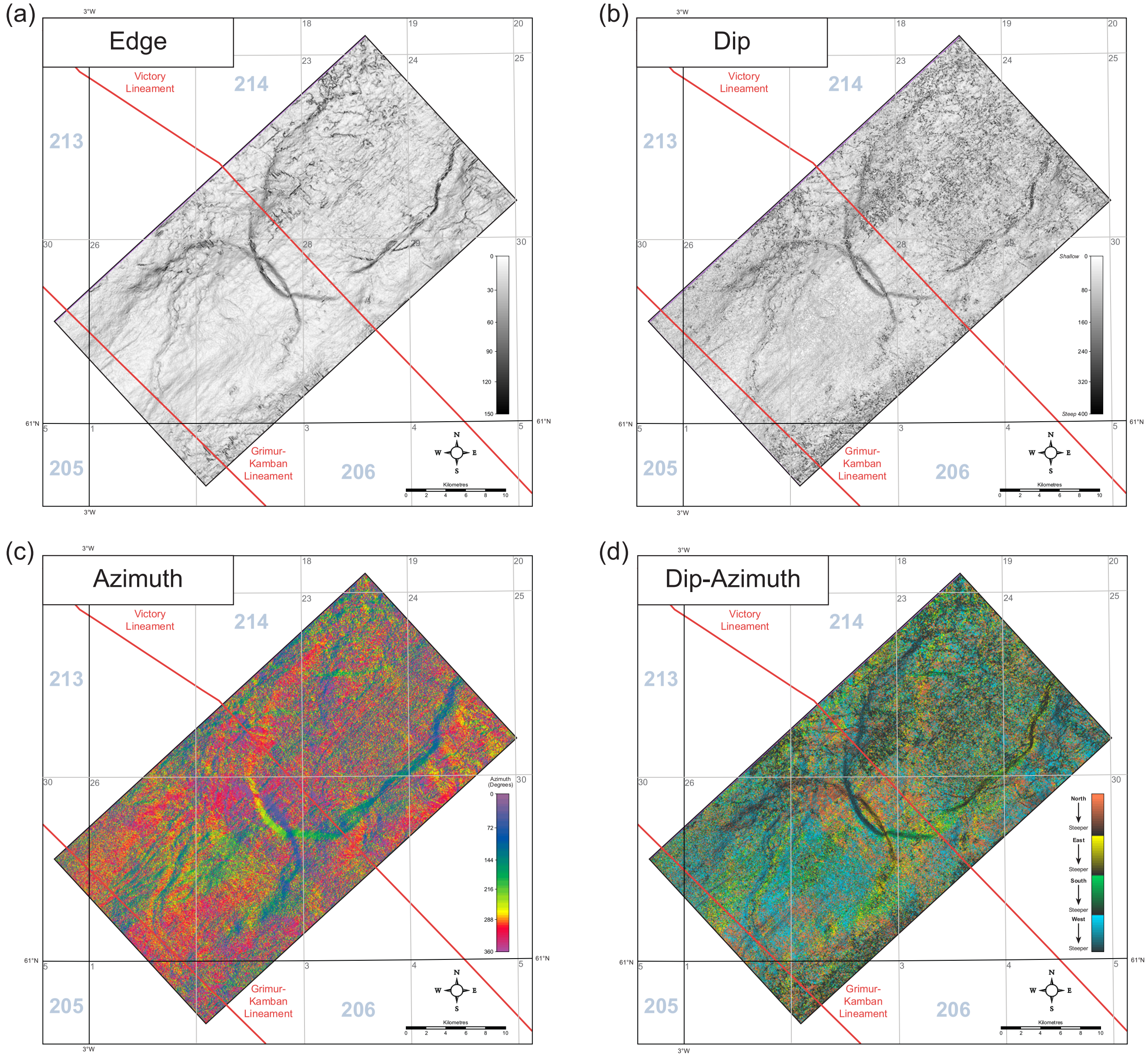

Figure 10
Map (a) identifies areas where the Kettla Tuff horizon varies in dip, darkest in the areas of highest dip. This, as well as map (b), clearly identify the edges of the aforementioned sub-circular structures and the NW-SE antiform.

The edge map also highlights some minor east-west trending features which correlate with small-scale normal faults. Subtle NE-SW trending lineaments are found on the edge map and are also recognised in map (c). It is difficult to ascertain exactly what these features are but as the Kettla Tuff was deposited in sand prone shallow marine conditions, they may be related to the depositional environment (e.g. offshore sand bars).

The dominant dip direction of the horizon is to the northwest but changes in the orientation around the sub-circular structures implies the Kettla Tuff has been uplifted in these areas. When combining this with the dip map (d) the higher dips correlate with the changes in the azimuth confirming the causes of the directional changes are linked.

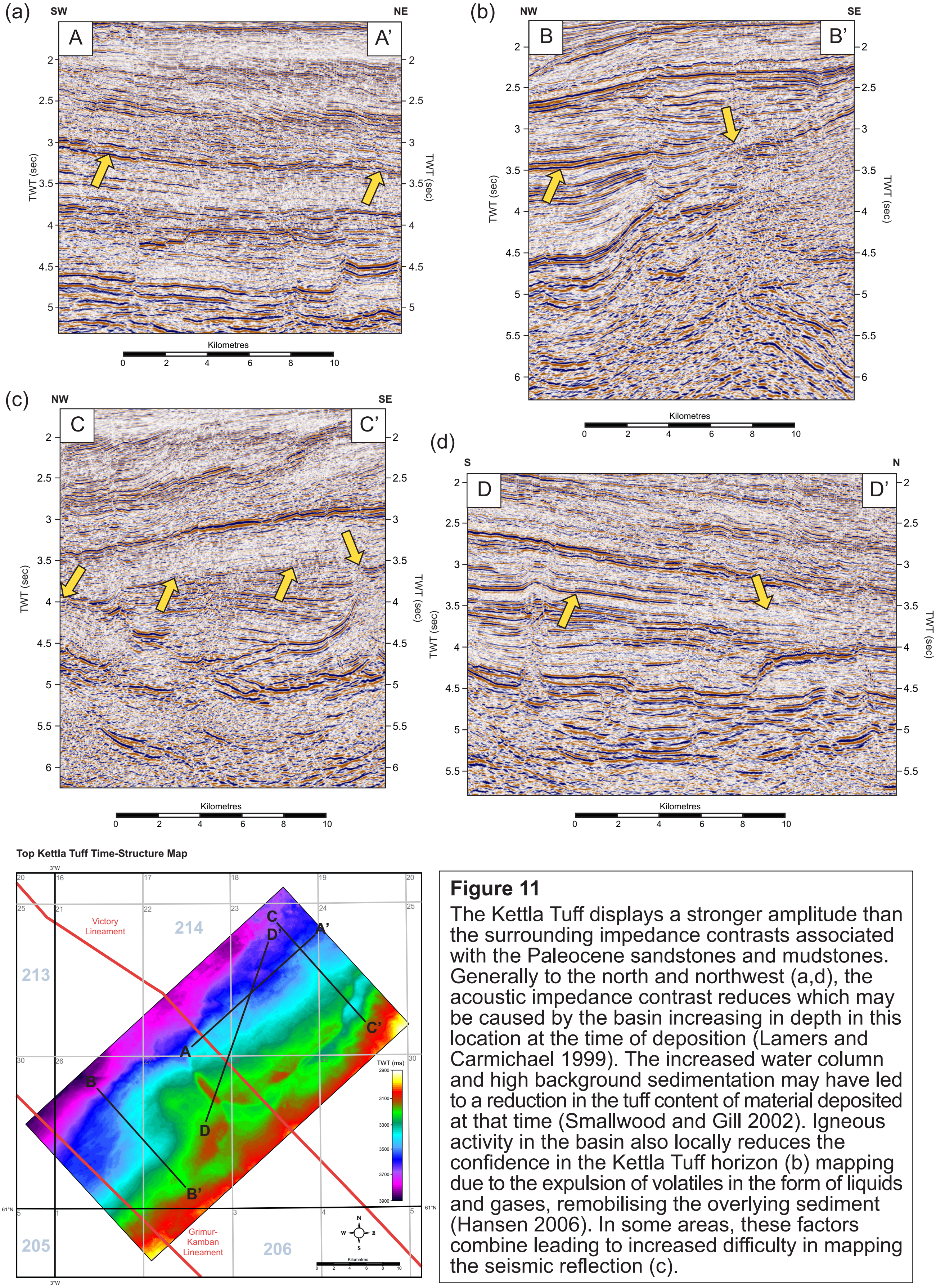

Figure 11
The Kettla Tuff displays a stronger amplitude than the surrounding impedance contrasts associated with the Paleocene sandstones and mudstones. Generally to the north and northwest (a,d), the acoustic impedance contrast reduces which may be caused by the basin increasing in depth in this location at the time of deposition (Lamers and Carmichael 1999). The increased water column and high background sedimentation may have led to a reduction in the tuff content of material deposited at that time (Smallwood and Gill 2002). Igneous activity in the basin also locally reduces the confidence in the Kettla Tuff horizon (b) mapping due to the expulsion of volatiles in the form of liquids and gases, remobilising the overlying sediment (Hansen 2006). In some areas, these factors combine leading to increased difficulty in mapping the seismic reflection (c).

12 Top Balder Tuff time-structure map

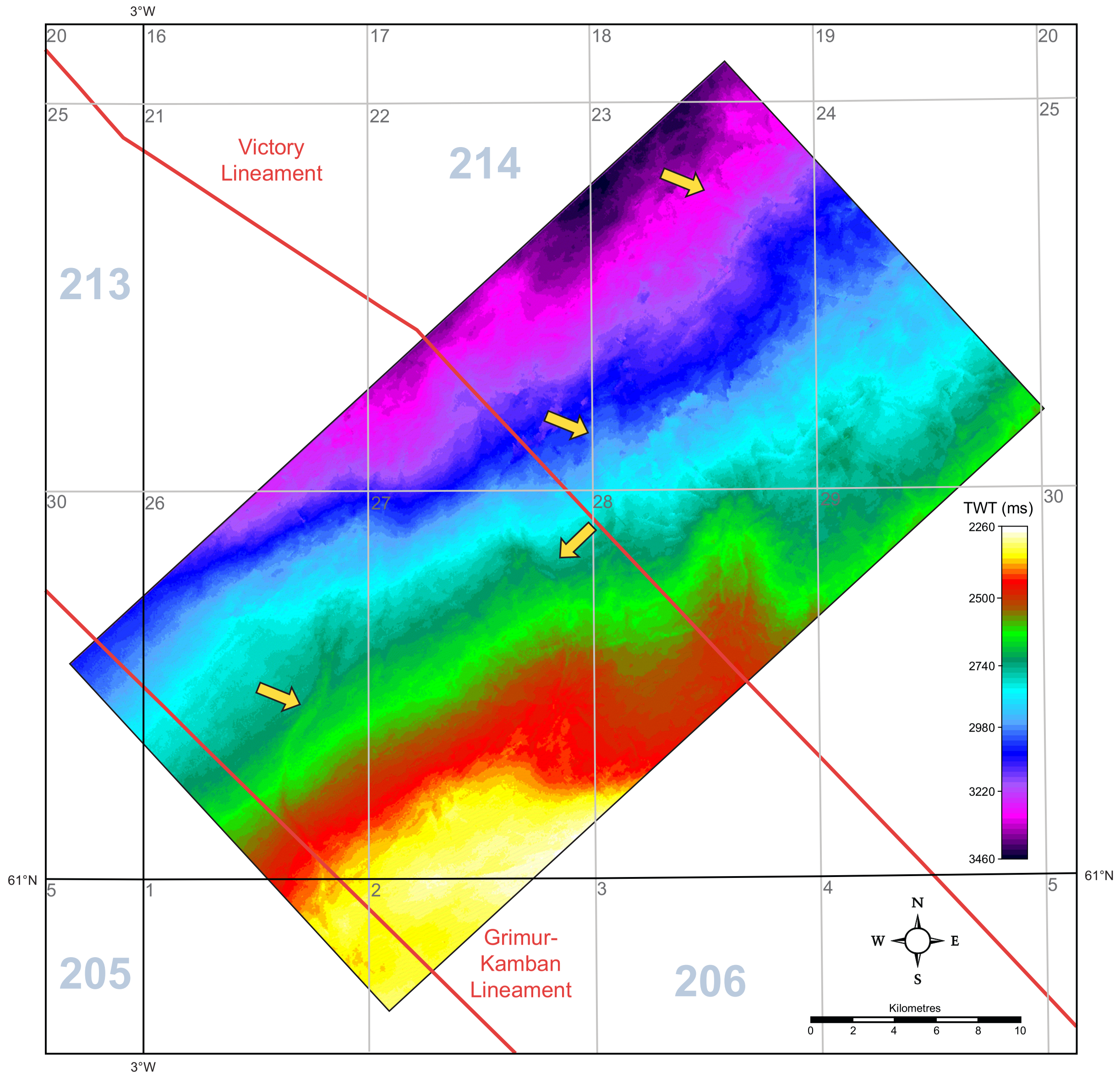

Figure 12
The Balder Tuff displays a gradual deepening of the basin towards the north. There are a number of localised irregularities which have exerted controls upon the horizon. These processes are discussed in the other Appendix B figures.

13 Top Balder Tuff amplitude, dip, azimuth and dip-azimuth maps

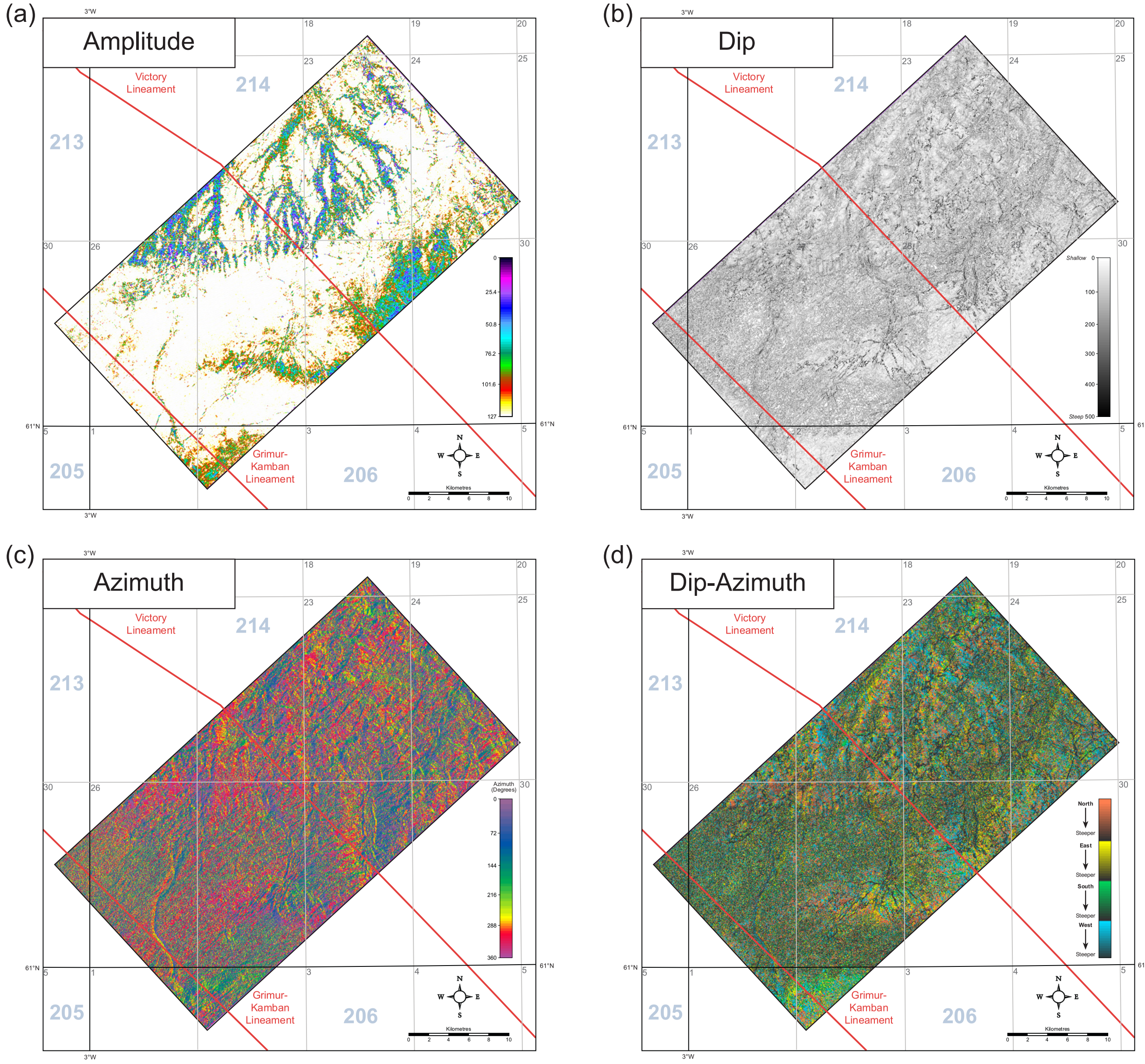

Figure 13
Map (a) of the Balder Tuff horizon displays a similar result to that of Lamers and Carmichael (1999) who interpreted the depositional environment to be shallow marine. A submarine drainage network is formed to the north upon the palaeoslope of the basin. Other weaker amplitude regions (compared to the amplitudes of the Balder Tuff) have been interpreted as shallow marine sand bars to the southeast.

Map (b) displays the low relief of the horizon but also highlights fault structures which extend out from a central point in a variety of orientations. Subtle ‘meandering’ features are found in a general N-S trend and are associated with increased dips. In the areas above the edges of the sub-circular features, recognised in the Kettla Tuff Horizon, there are subtle changes in the relief of the horizon implying the Balder Tuff has also been affected by the intruded sills.

Map (c) is dominantly dipping to the northwest but the ‘meandering’ N-S features dip from east to west. A similar set of features formed in a NE-SW trend as previously observed in the Kettla Tuff is recognised (d); the origin of which remains unclear. The density of the trend may be related to sub-seismic scale processes which could include faulting or soft-sediment deformation.

14 Areas of difficulty interpreting the Balder Tuff

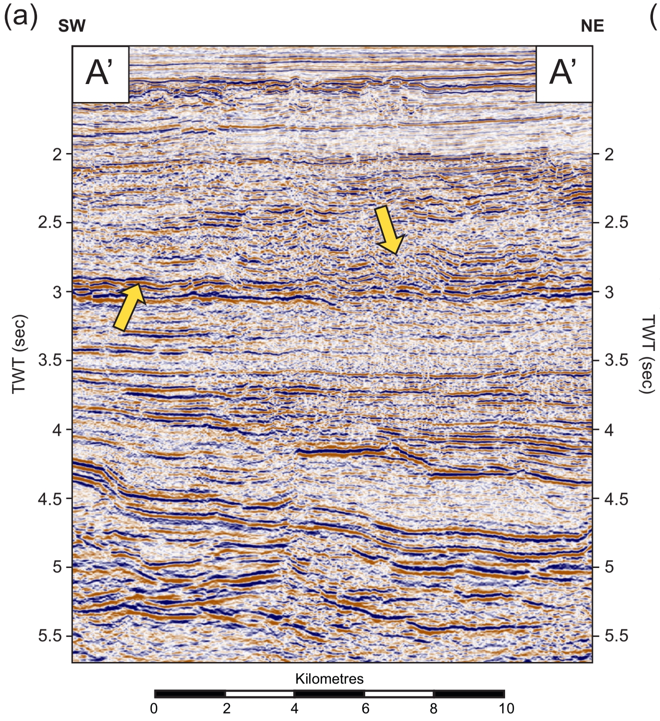

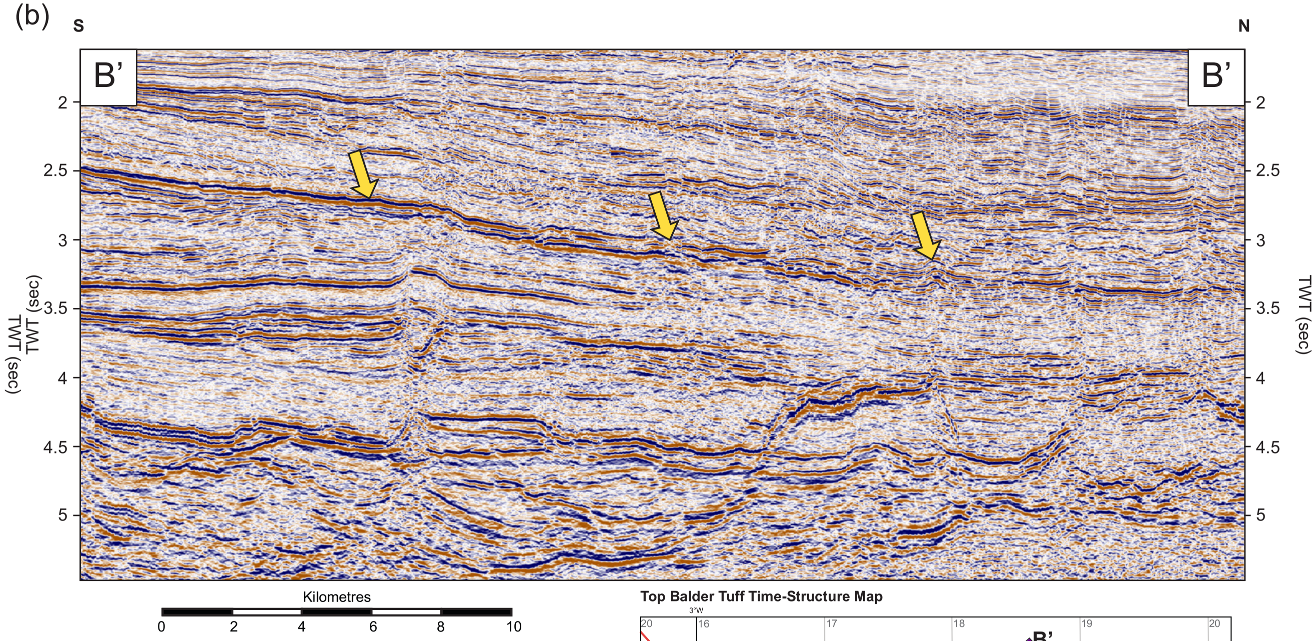

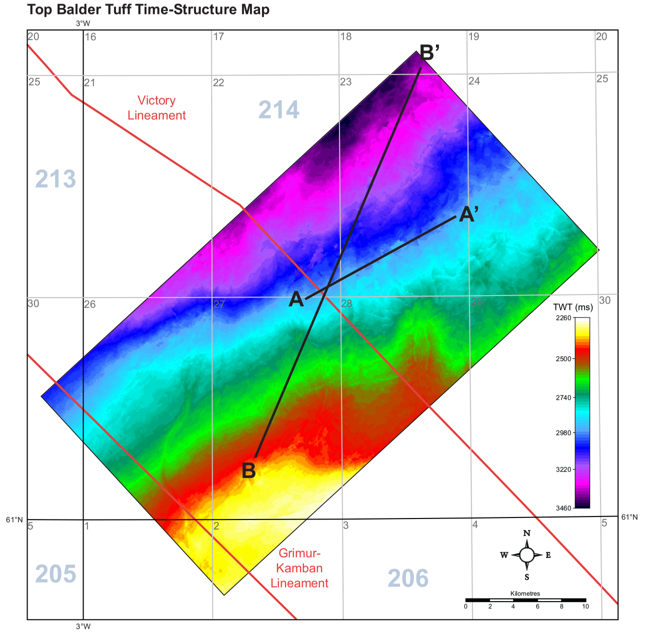

Figure 14
The Balder Tuff horizon displays a stronger amplitude response in comparison to the Kettla Tuff making it relatively simple to interpret in much of the study area. However, the Balder Formation is complex due to the environment of deposition at that time. The channel network imaged within the amplitude map of the horizon needed to be carefully interpreted as it is highly undulating and irregular (a) due to the erosional (and depositional) processes occurring and the associated amplitude changes of the horizon this causes.

This is further complicated by three other factors:

1) Zones which scatter the seismic signal; maybe caused by gas chimneys.
2) Uplift and thickening of sediments within the Balder Formation (b) caused by the formation of hydrothermal vent complexes or volcanic fissures.
3) Deepening of the basin to the north leads to the reduction of concentrated tuff deposits and the acoustic impedance contrast associated with the deposited material.

15 Top Kettla Tuff to top sills time-thickness map

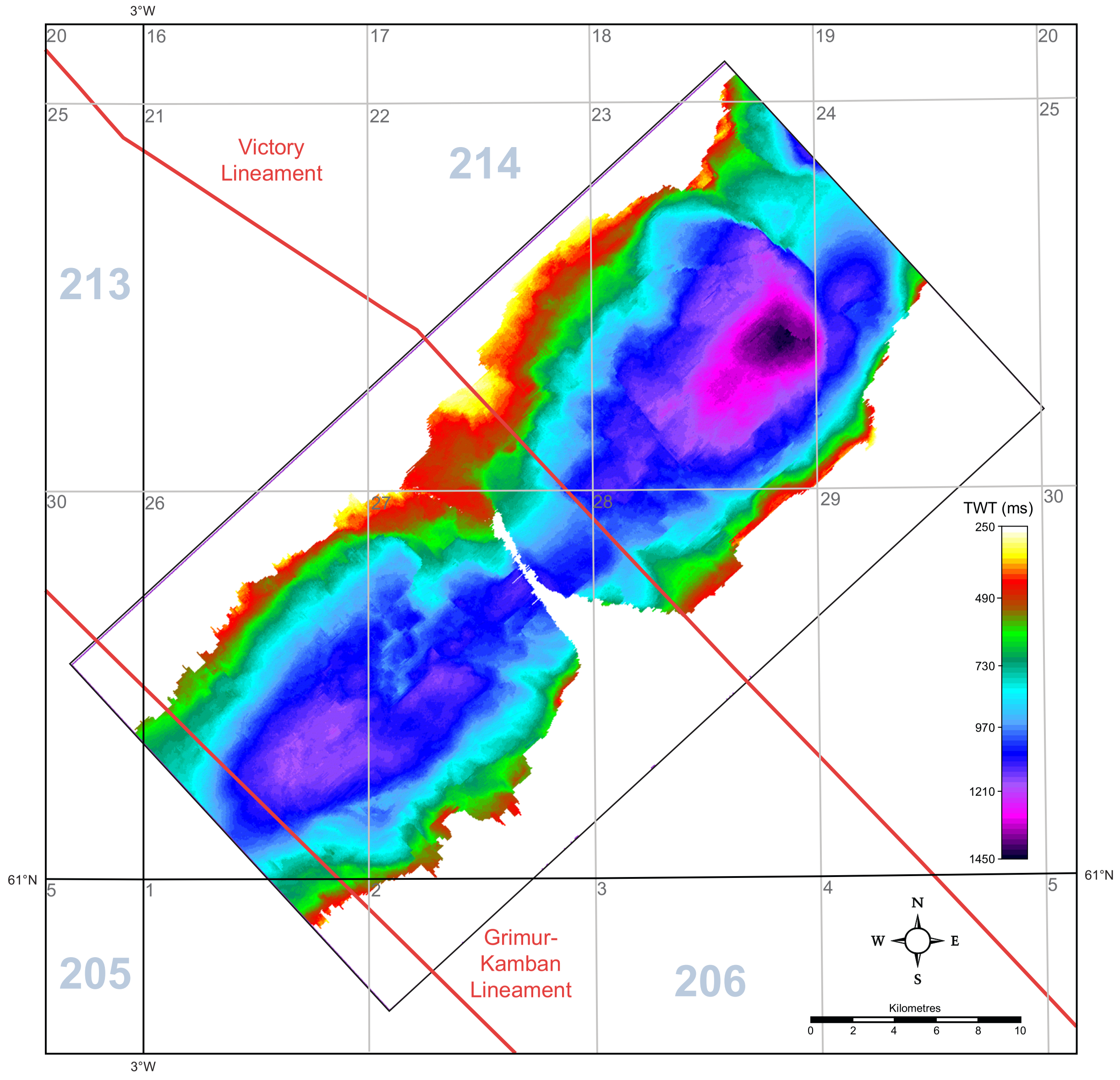

Figure 15
The time-thickness map displays that the greatest sediment thickness between the sills and the overlying Kettla Tuff is correlatable to areas where the sills are at their greatest depth. The thickness rapidly thins to the northwest and southeast implying the sills do cut up through the overlying sequence in these areas. The thickness mirrors the depth of the sills in a NE-SW orientation inferring the sill does not cut up through the stratigraphy in this orientation.

Equally, there is no apparent change in the stratigraphical thickness across the inferred Victory Lineament, nor the Grimur Kamban Lineament to the southwest as has been previously inferred (Mitchell *et al*. 1993).

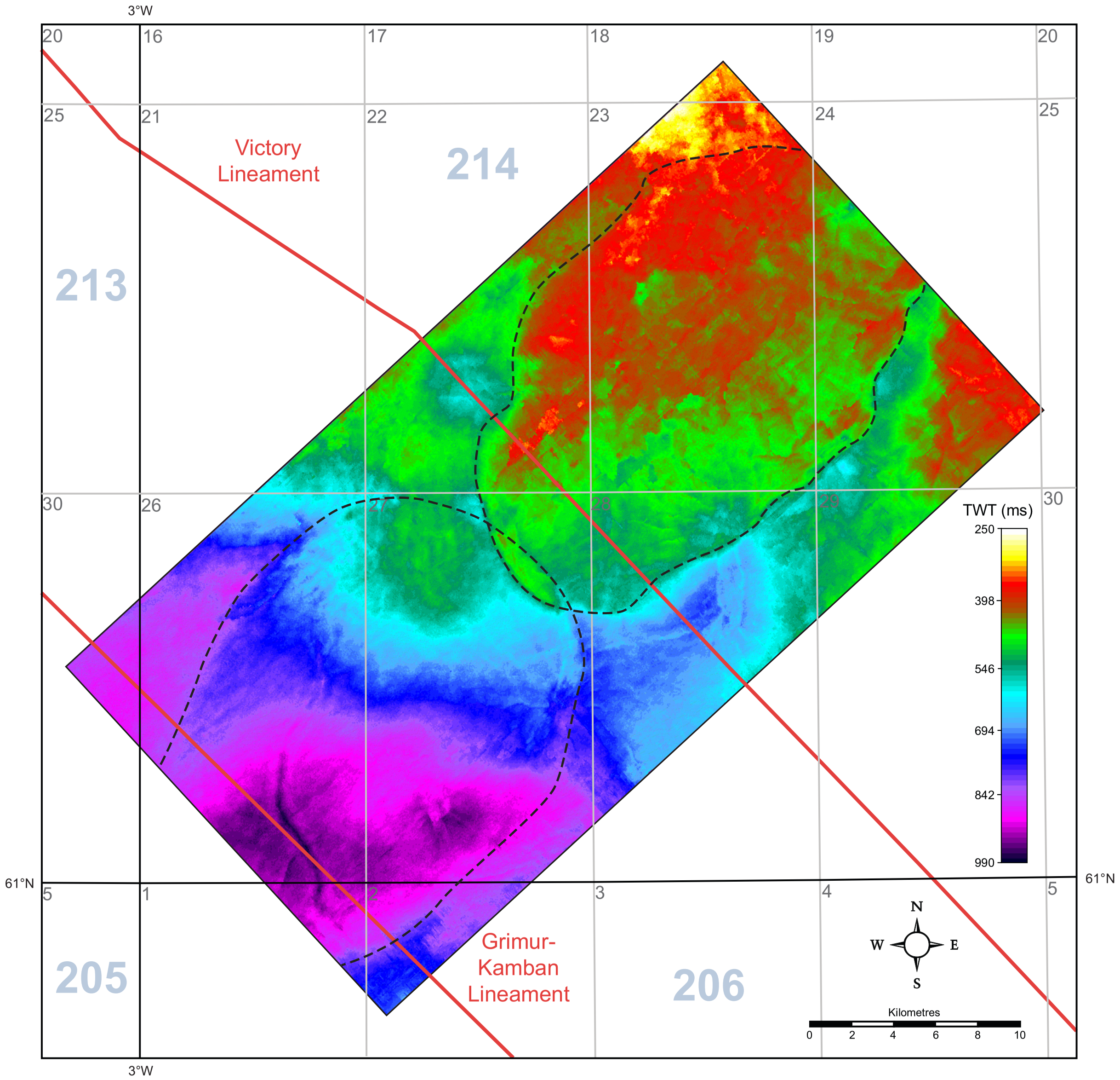

Figure 16
The greatest time-thickness of sediment between the Balder and Kettla Tuffs is to the southwest of the study area, thinning to the northeast, inferring sediment may be preferentially sourced into the south at this time. On top of this general trend there are many localised anomalies. The first is the uplift associated with the intrusion of the sills. It can be clearly seen that the intrusion of the sills has exerted a control on the late Paleocene to earliest Eocene sediment thickness. In the areas above the sills, ‘jacking up’ the sediment leading to the preferential deposition of sediment to the northwest and souheast of these two relative highs.

Sediment thickness is less above Sill 2 compared to Sill 1 because the sill has apparently intruded a stratigraphically younger horizon. There is also a notable thinning of sediment across the NW-SE trending antiform structure due to the increased uplift associated with the intruded laccolith at depth.

To the southwest of the study area the previously recognised N-S trending ‘meandering’ feature is associated with a thickening of the basin fill. In the north of the study area, an irregular thickness pattern is associated with the submarine channel network which had formed.

17 The antiformal junction between the two sills

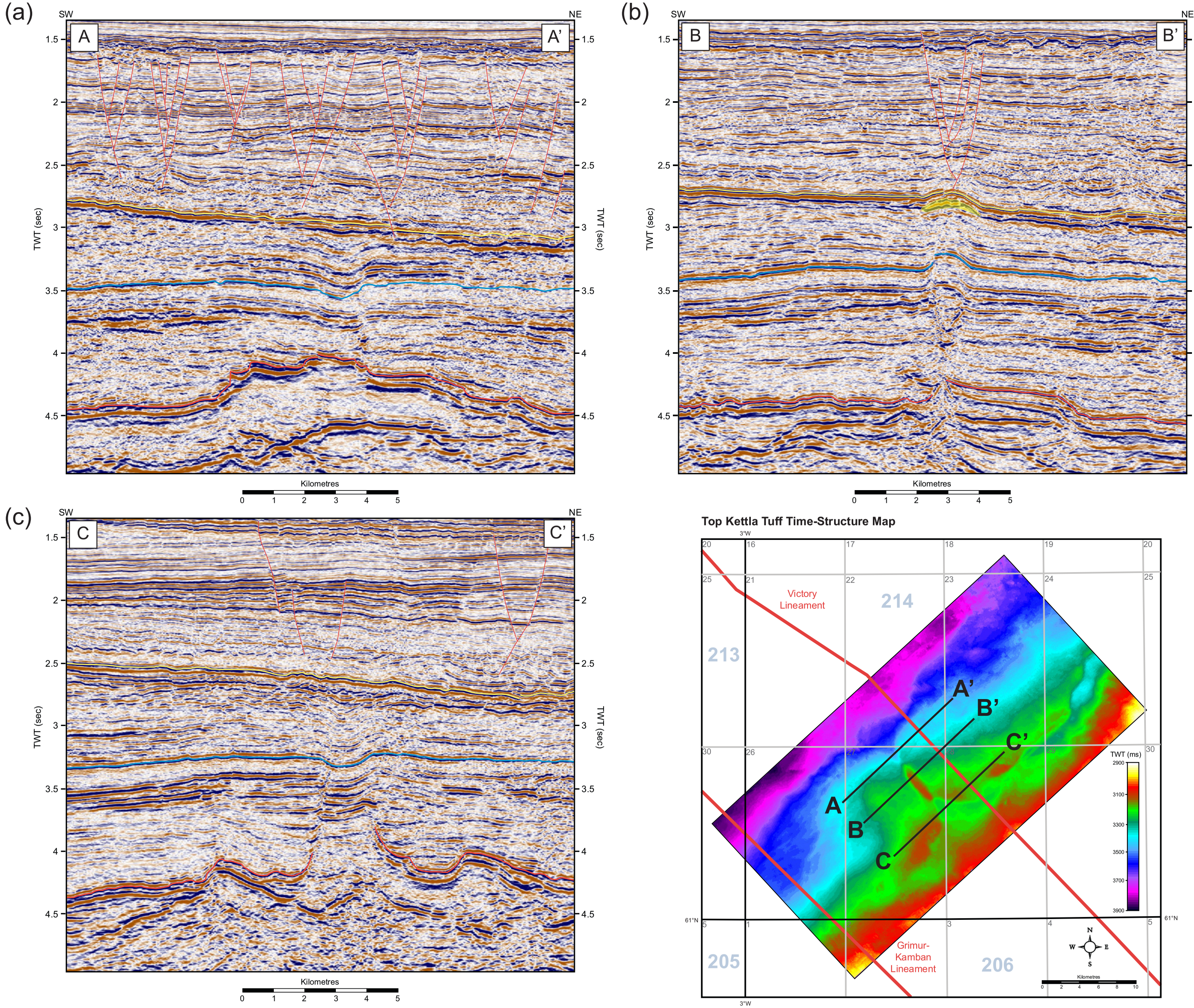

Figure 17
Horizons: Yellow = Balder Tuff, Blue = Kettla Tuff, Red = Sills.

Different views across the antiformal junction between the two sills can strongly suggest wrench faulting due to the rapid change in apparent structure along strike (Harding 1990). This change can be explained by the igneous activity.

The sills appear to coalesce in the north (a). If they do, they are inferred to be relatively thin located the feather edge of the sills. The Kettla Tuff horizon is structurally higher to the northeast and southwest as it has been subjected to a greater uplift because of an increased thickness of the sill at depth. A sedimentary thickening prior to the deposition of the Balder Tuff has occurred for this reason.

Across the antiformal junction (b) the Kettla and Balder Tuffs are uplifted due to the laccolith intrusion. Thickening caused by either a hydrothermal vent complex or volcanic fissure, exerts an influence on the post Balder faulting.

To the southwest (c), the sills can be imaged to cut up through the stratigraphy with sub-vertical dykes forming at the tips, feeding minor sills leading to a localised brightening of horizons.

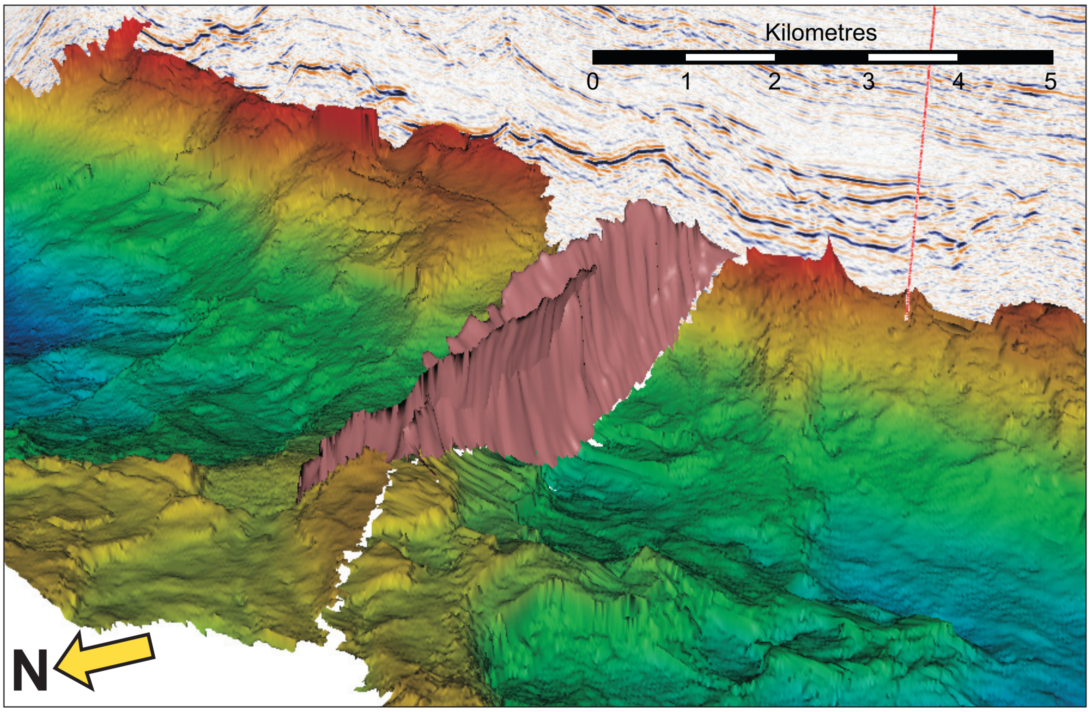

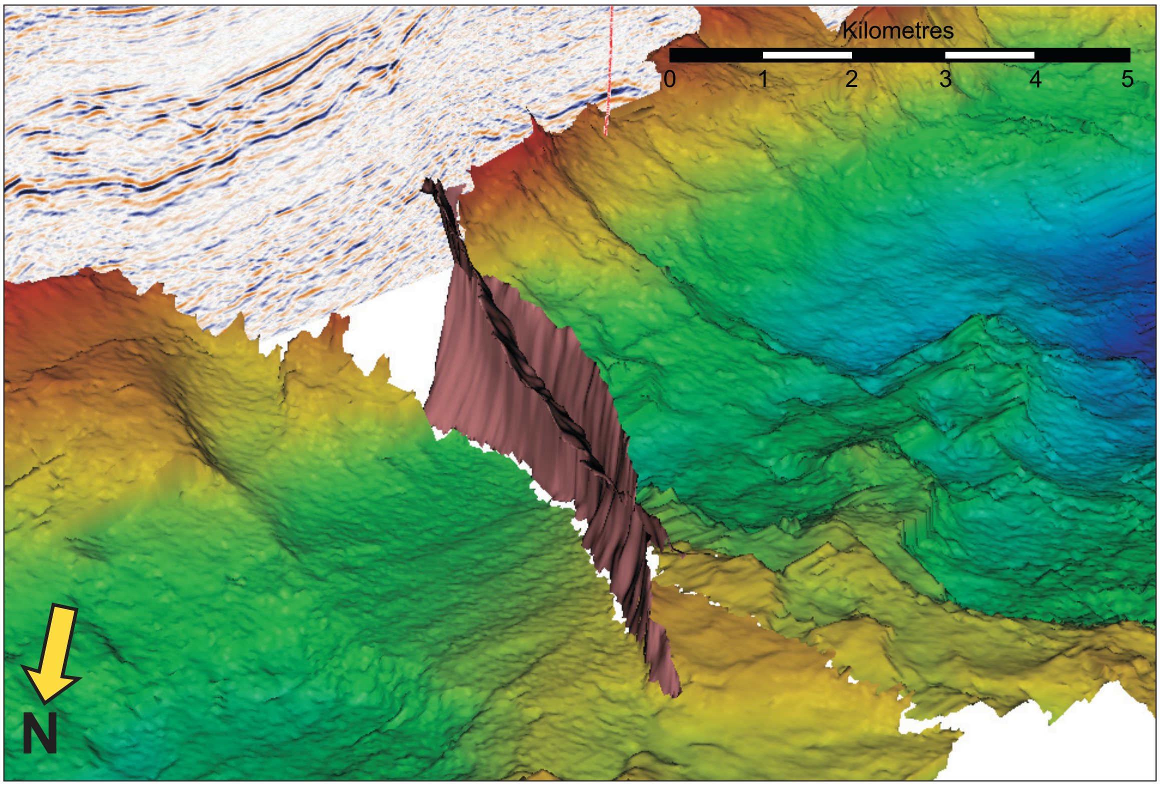

Figure 18
Sub-vertical dykes on seismic data are difficult to image, however distortions are recognised, where amplitude changes are evident (possible early stage sill formation; Thomson 2007). When mapping these distortions, a fault interpretation for their origin can be discarded as they are observed to link with the sills at depth, reversals in dip polarity occur along strike and despite cutting across each other, there is no offset associated with this. The only remaining hypothesis is that they are dykes sourced by the sills at depth which also feed the laccolith intrusion. Equally, they could be the source for any hydrothermal vent complexes or volcanic fissures at the seabed.

19 Semblance time slice (3620 ms) of the Paleocene sedimentary sequence

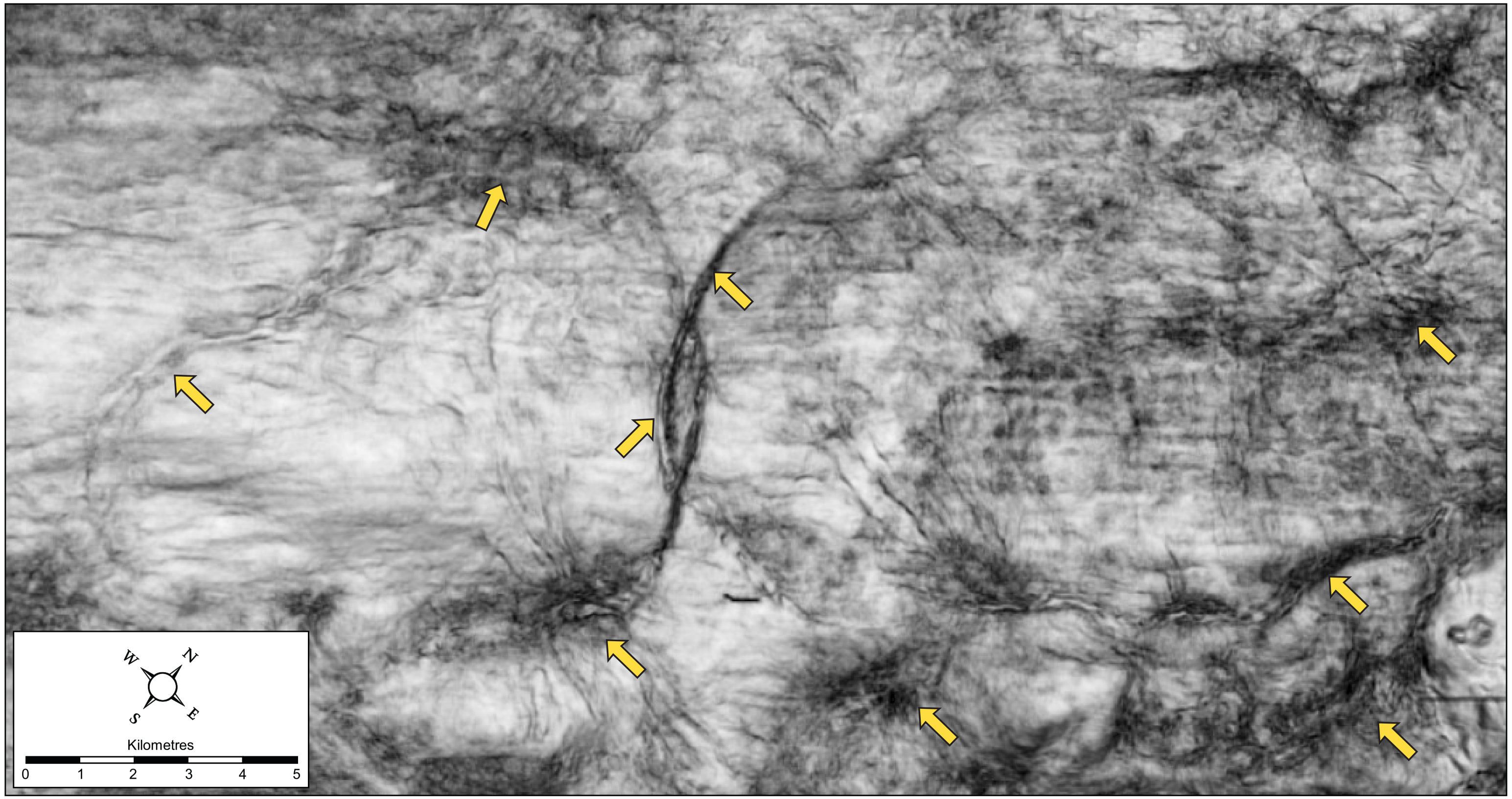

Figure 19
A semblance slice through the Paleocene strata reveals the impact of the igenous material on the basins early Cenozoic evolution (highlighted). Dykes are imaged above the sills and above the sill tips. The chimneys of hydrothermal vent complex can also be observed. These features could similarly be interpreted as volcanic fissures however these are broader features with internal reflectivity within the seismic data, implying these are not conduits for magma (Hansen and Cartwright 2007). Equally, other laccolith style intrusions can not be dismissed. Smaller scale dykes are also visible, sourced from within and below the sills, not only at the edge. There are also dykes which may not be sourced from these two sills, but instead from the sill and dyke complex which has invaded the deeper Cretaceous sequence in this region.

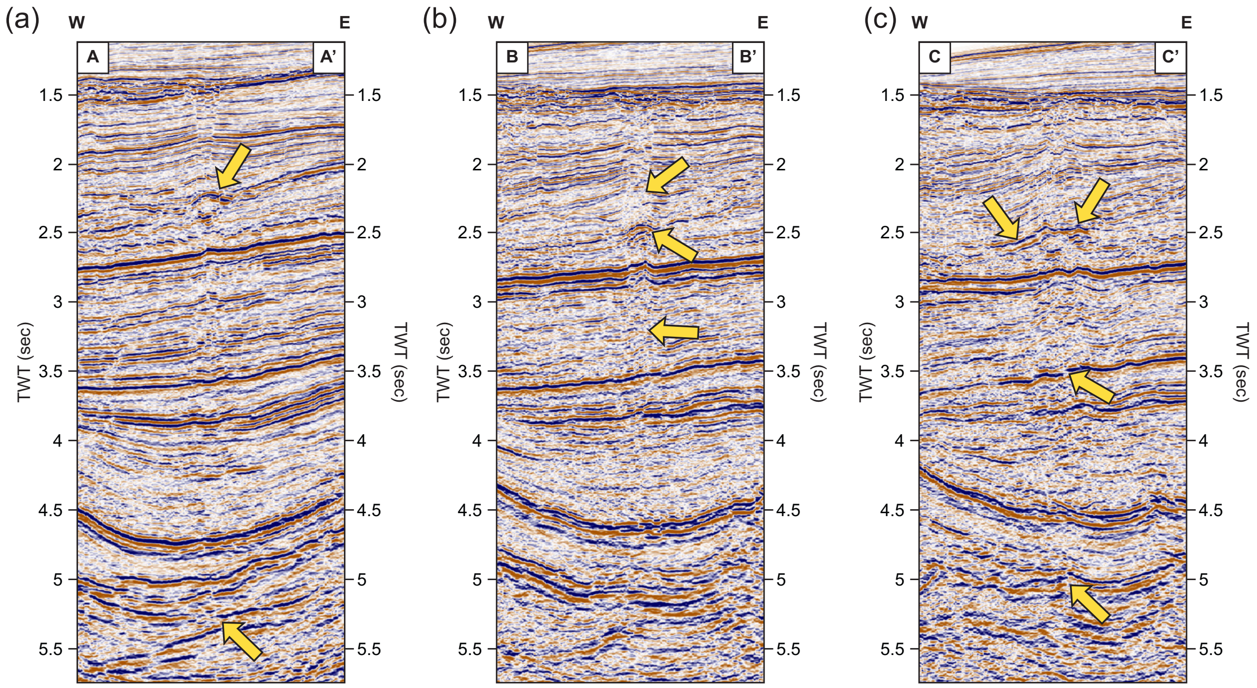

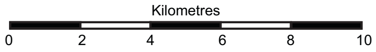

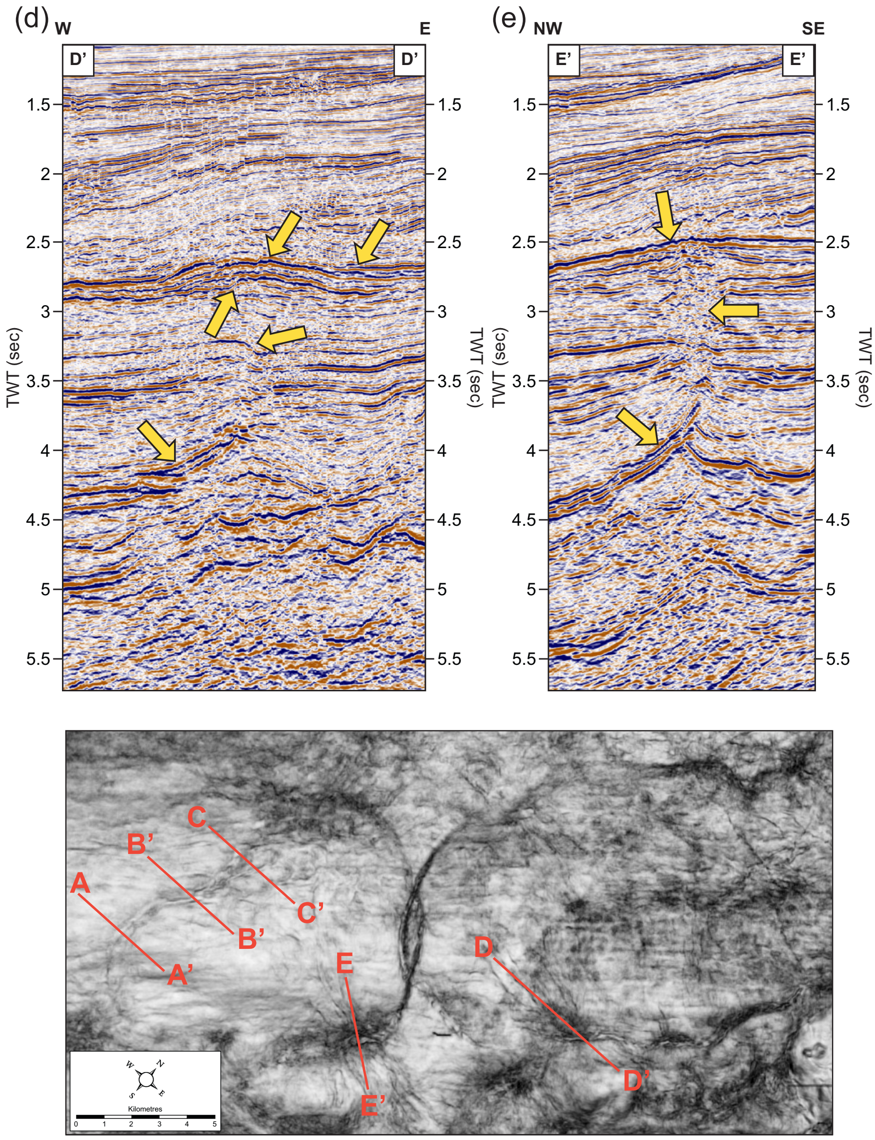

Figure 20
The N-S 'meandering' features are interpreted as dykes sourced from deeper igneous material. A minor sub-vertical distortion is recognised (a) with apparent offset of horizons across it. This dyke is interpreted to have sourced a volcanic fissure at the seabed within the middle Eocene strata which gives a time constraint for its activity. The morphology of this fissure varies along the length of the dyke (b,c) but is believed to consist of basic-intermediate igneous material as a series of pillow lavas (Davies *et al*. 2002).

In contrast to this are the hydrothermal vent complexes which have formedabove sill tips (d,e) creating a broader zone of deformation in the subsurface (chimney) and a larger mounding of remobilised sediment on the seabed. Equally, this provides a control on the timing of igneous activity in the basin (Hansen 2006).

21 Well 205/10-2b well to seismic tie and seismic stratigraphy

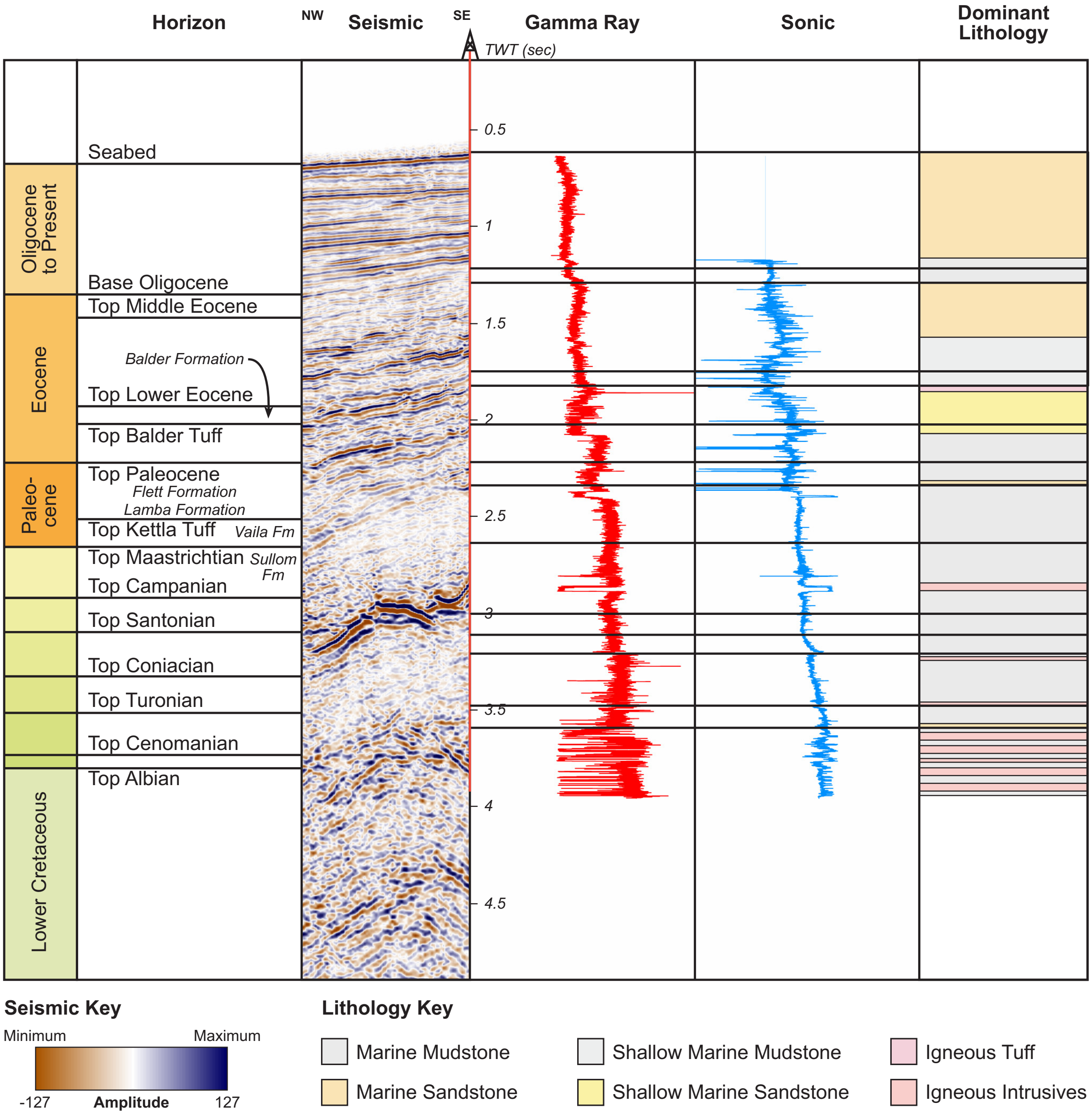

Top Cretaceous Time-Structure Map

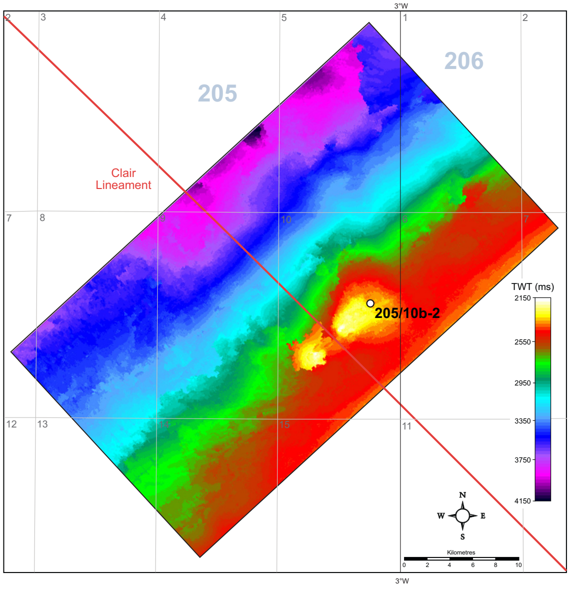

Figure 21

Well 205/10-2b reaches total depth in the lower Cretaceous strata and encounters both marine mudstones and a suite of igneous intrusives, giving rise to parallel, discontinuous, strong amplitude facies on the seismic data. Mudstones give rise to transparent seismic facies which gradates into weak amplitude parallel continuous reflectors reflecting interbedded sandstones and mudstones in a regressive early Cenozoic system. Tuff horizons are visible on the seismic data but of weak amplitude response, in particular the Kettla Tuff which is very difficult to interpret accurately.

22 Well 205/8-1 well to seismic tie and seismic stratigraphy

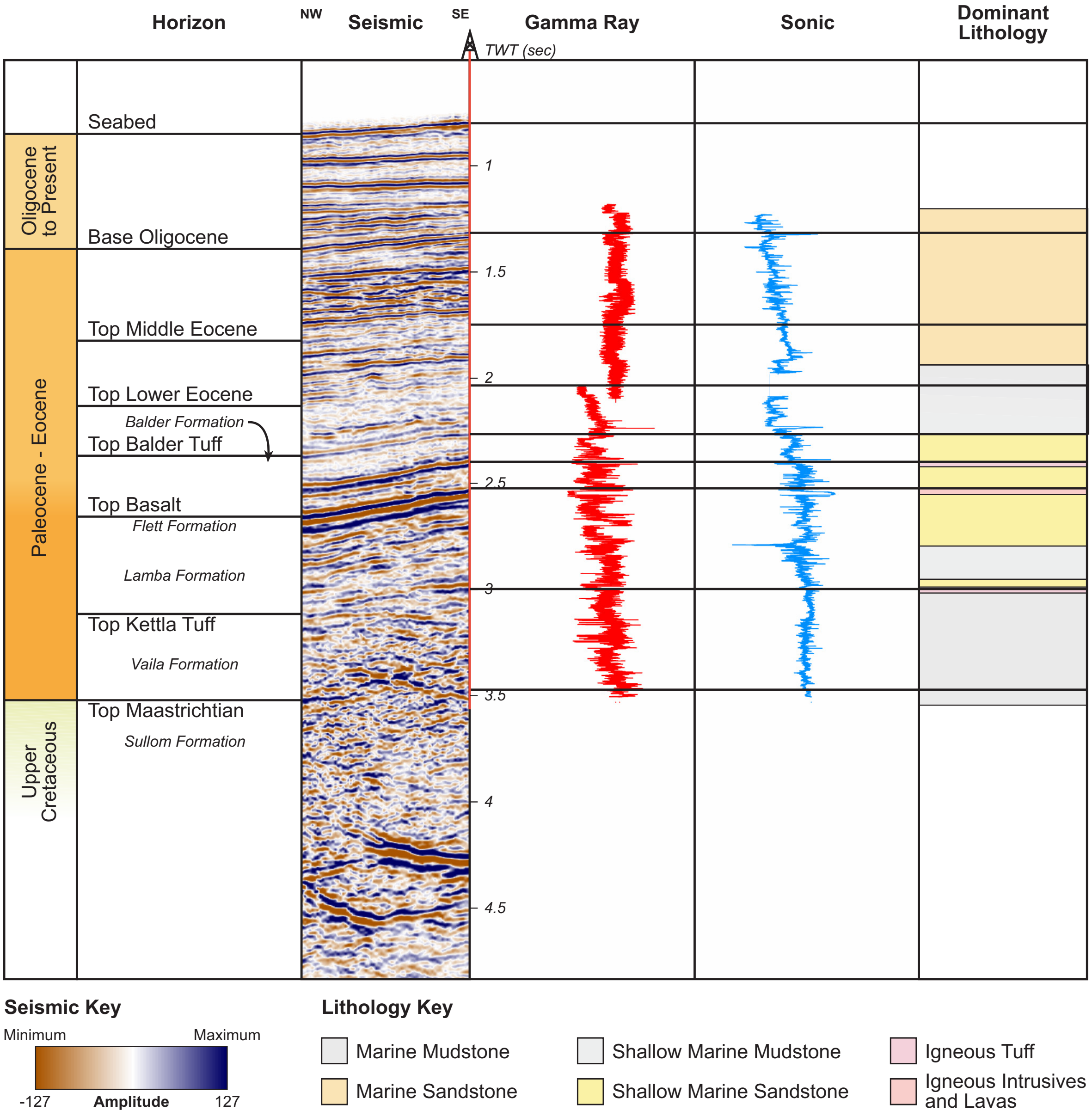

Top Cretaceous Time-Structure Map

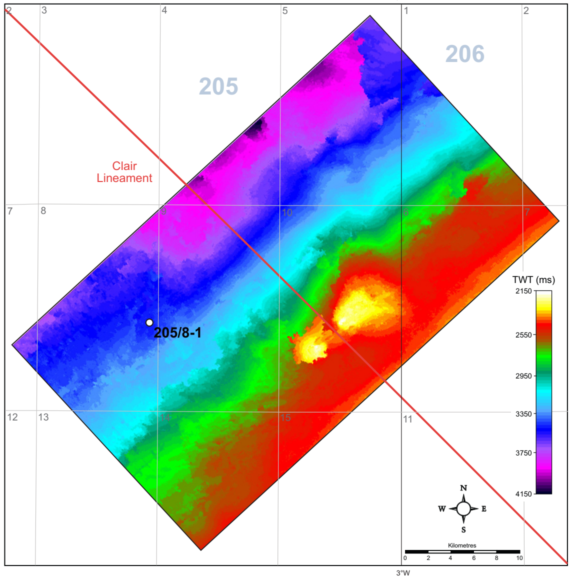

Figure 22

Well 205/8-1 reaches total depth in the upper Cretaceous, with a strong amplitude positive reflector at the top. Mudstones interbedded with minor sandstone units lead to parallel discordant reflections within the Paleocene strata before grading into concordant parallel shallow marine sandstone units. A bright positive reflector marks a large acoustic impedance contrast between the sandstones and a Paleocene basalt lava flow. The Kettla Tuff is difficult to identify on the seismic data but the Balder Tuff is recognised. Marine sandstone units are dominant during the middle Eocene following continental breakup.

23 Top Cretaceous time-structure map

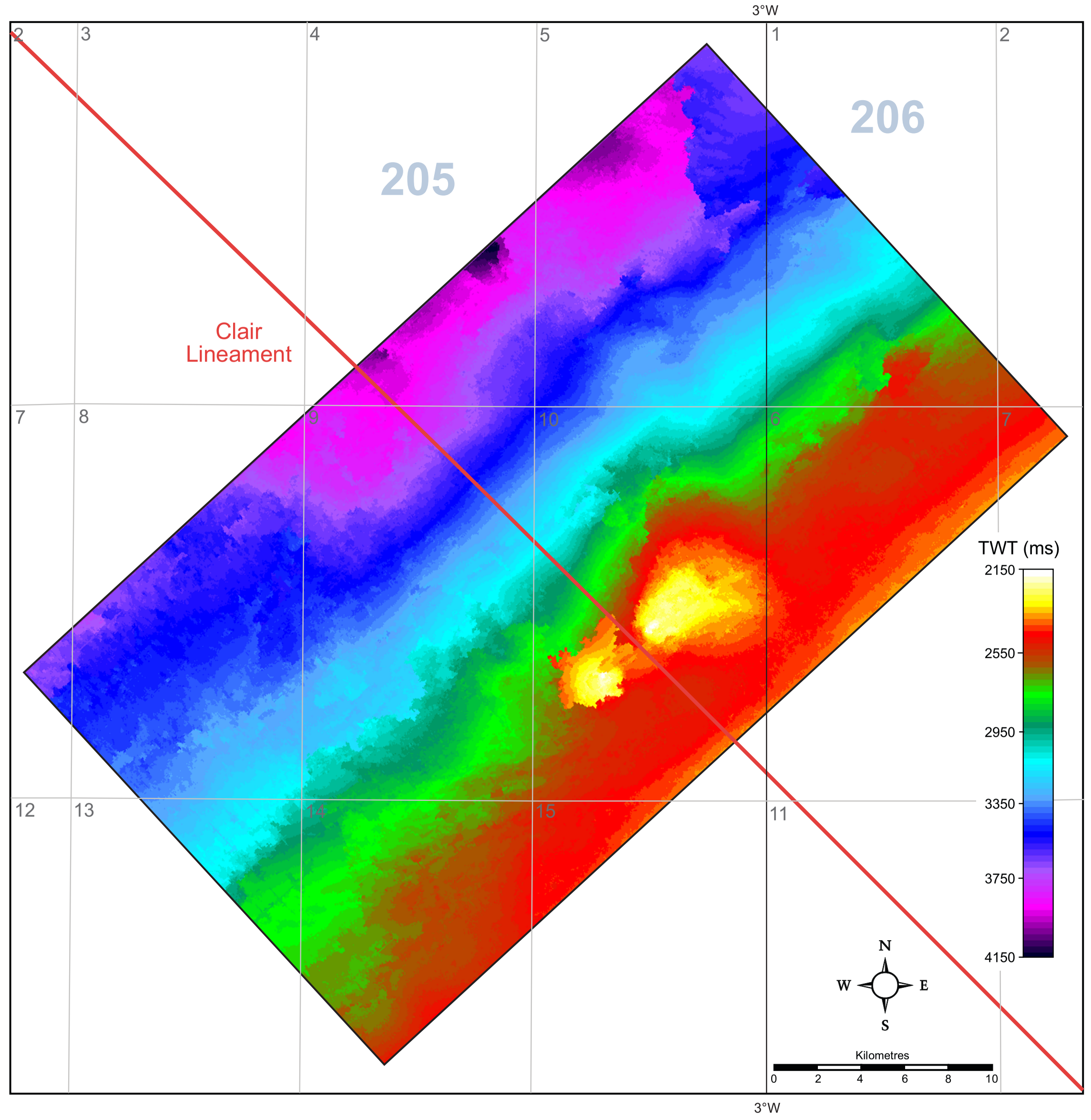

Figure 23
The top Cretaceous map displays a gradual deepening of the horizon to the northwest.There is little or no apparent influence of the underlying Flett Ridge on the horizon except for two highs in the region of the Clair Lineament which are sub-circular in map view and have diameters of up to 10km.

24 Top Cretaceous amplitude map

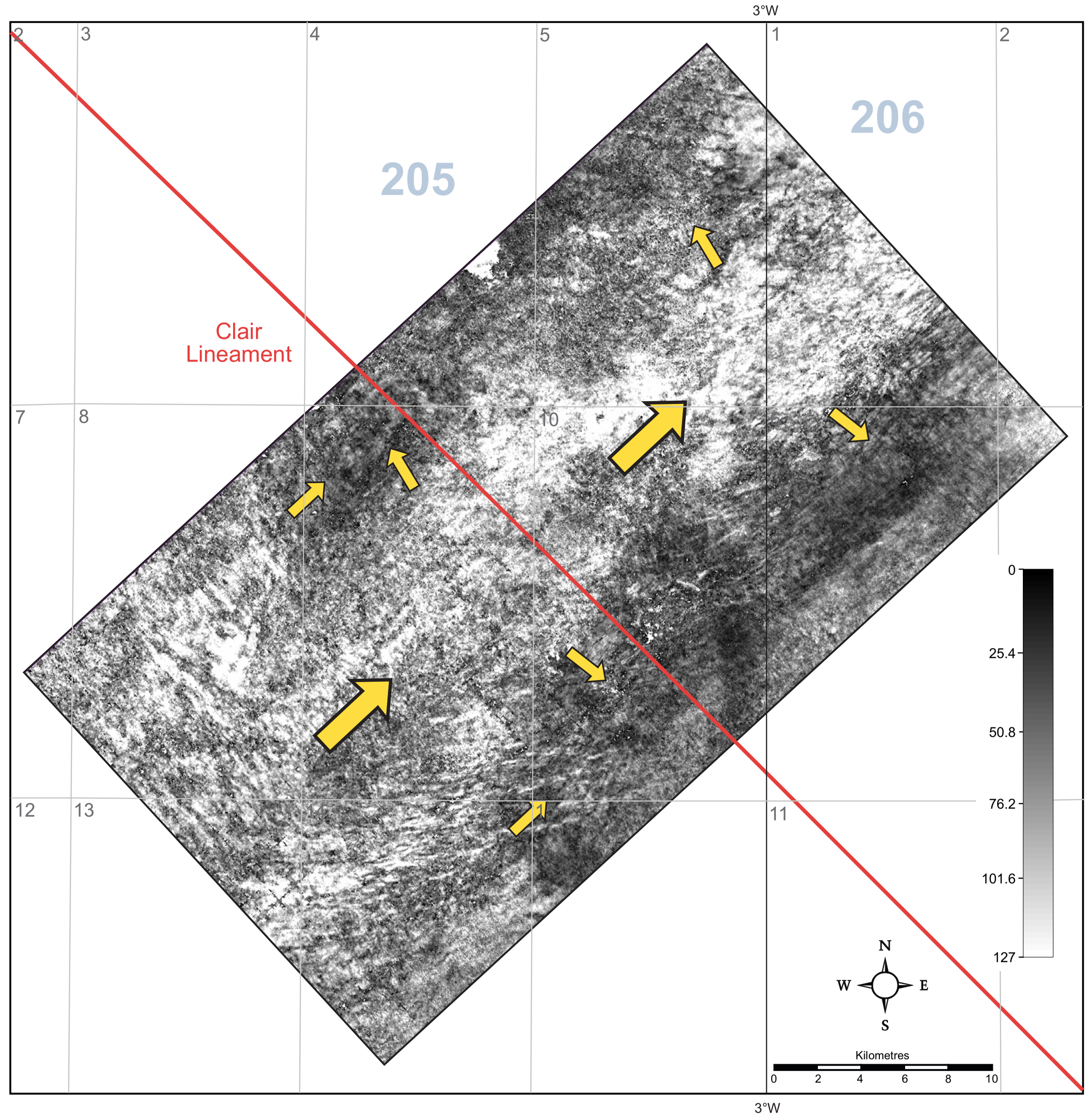

Figure 24
An amplitude extraction of the top Cretaceous horizon suggests there may be an influence on the stratigraphical fill by the Flett Ridge located at depth. The brighter amplitude regions are interpreted to represent sandier facies in comparison to the darker areas which are likely to be mud prone. An interpretation as to the cause of this is that the region above the Flett Ridge is structurally higher compared to the sub-basins to the northwest and southeast with more sand prone deposition in shallower regions to the more basinal depocentres (Reading and Richards 1994).

A source for the sand may be from the southeast. It appears this area may be more sand prone and could be an area into which sand enters from the rift flanks. Notably, there is no similar influence associated with the Clair Lineament on the interpreted facies pattern in this region during the late Mesozoic.

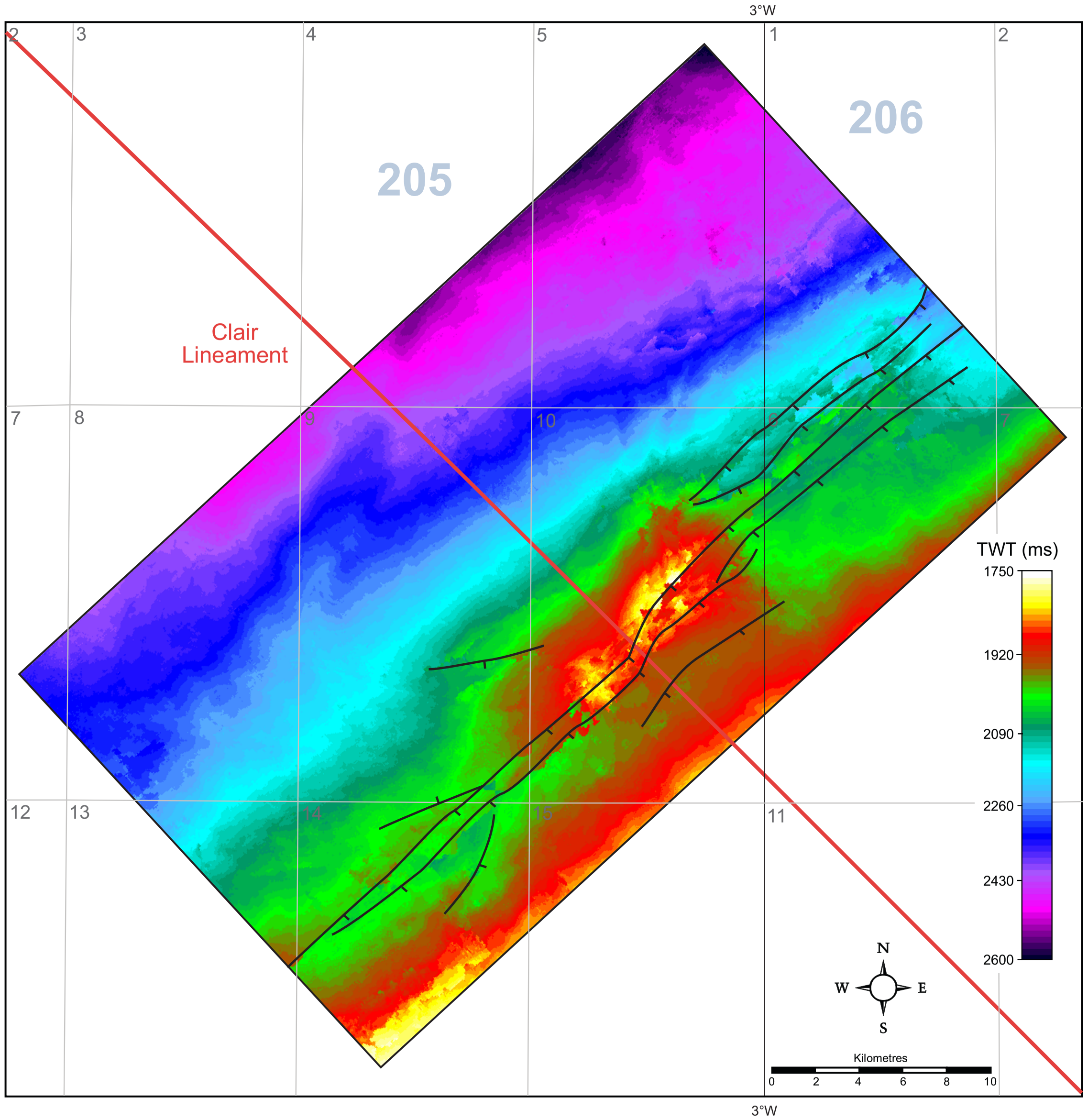

Figure 25

The top Balder Tuff map displays a gradual deepening of the horizon to the north and northwest. There is a NE-SW trending structural high located along the Clair Lineament in Block 205/10. Absent from the top Cretaceous map, a series of NE-SW trending normal faults which predominantly dip to the southeast are observed to offset the horizon but only display minor offsets. The location of the faults lie above the south-easterly edge of the Flett Ridge and may be tectonically related to the high. Equally, another hypothesised origin is for the faults is to have formed due to differential compaction across the high (Færsth and Lien 2002).

There is an apparent left lateral offset of the faults across the Clair Lineament in the same region as the aforementioned structural high. In this area some faults link through across the high but some tip out along strike. These features suggest an accommodation zone (c.f. Faulds and Varga 1998) interpretation may be more suitable to the defined Clair Lineament rather than a transfer zone or wrench fault interpretation in this region. However, this is a Cenozoic aged feature rather than Mesozoic age and as the faults do not appear to offset the top Cretaceous unconformity, detaching within the Paleocene sequence itself these features may not be rift related.

26 Top Balder Tuff amplitude, dip, azimuth and dip-azimuth maps

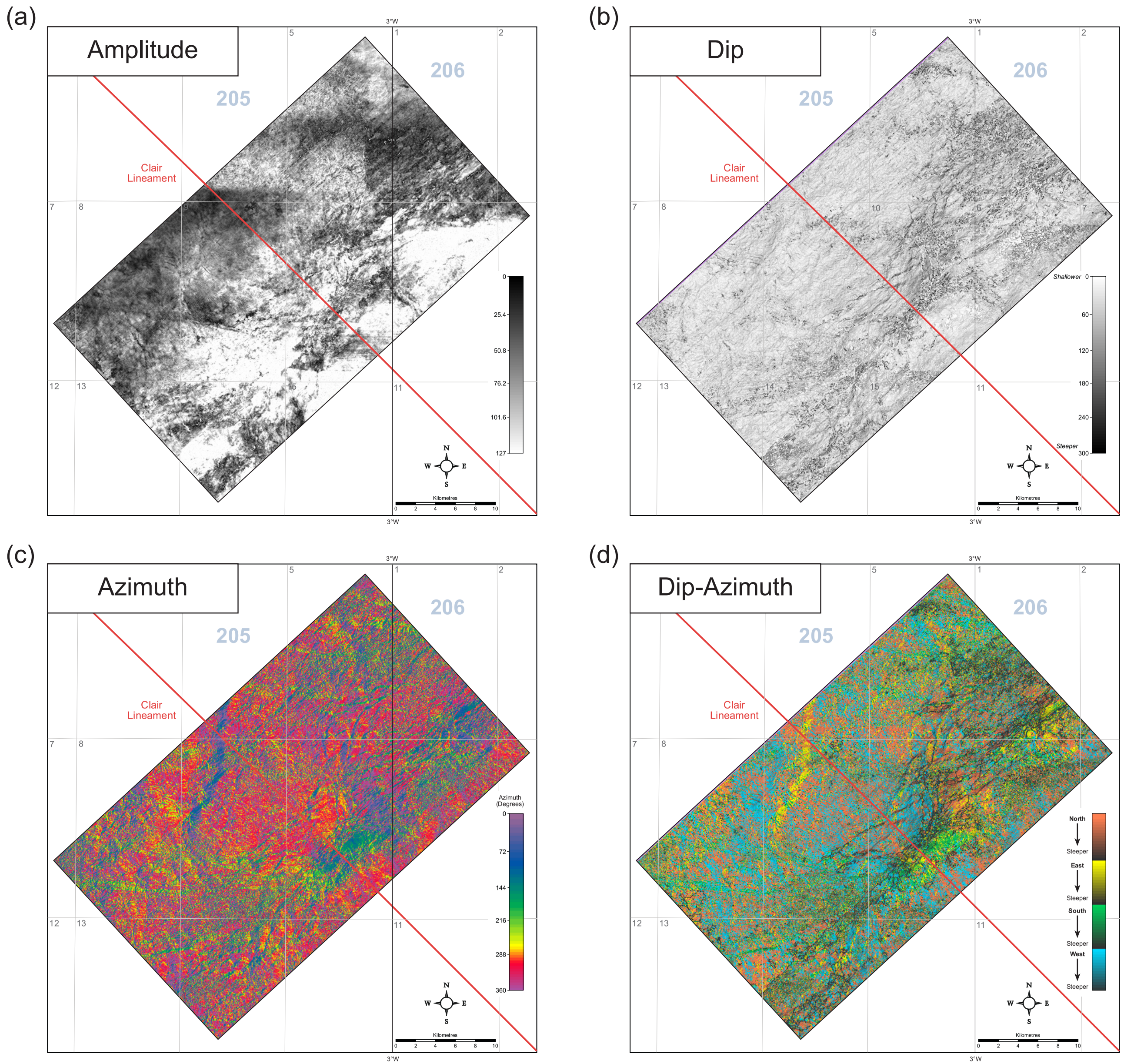

Figure 26
Map (a) displays a notable strong amplitude to the southeast in the Foula Sub-Basin which is interpreted to represent relatively thick (<10m) Tuff horizons which display a strong acoustic impedance contrast. The darker areas are located to the NW and are found in the deeper areas of the basin suggesting a more mud prone facies. However, interspersed are white/grey amplitudes within the mudstone sequence which are interpreted to be shallow marine sandstone deposits.

Map (b) highlights the areas affected by NE-SW oriented Paleocene faulting which is offset along the Clair Lineament against a background of relatively gentle dips.

Map (c) displays a general dip direction of the horizon predominantly dipping to the northwest but highlights the dip of NE-SW faults to the southeast. It also highlights subtle changes in the dips of the sedimentary horizons which could be associated with sub-seismic scale faulting. A north-south trending feature dipping to the east is found in blocks 205/4 and 205/9 which may be a dyke similar to what is recognised in the Victory Study Area. Map (d) highlights all the above features but also some variation in dip direction which may be caused by sedimentary processes occurring at the time of deposition (e.g. NW-SE submarine shelf channels).

27 Top Balder Tuff to top Cretaceous time-thickness map

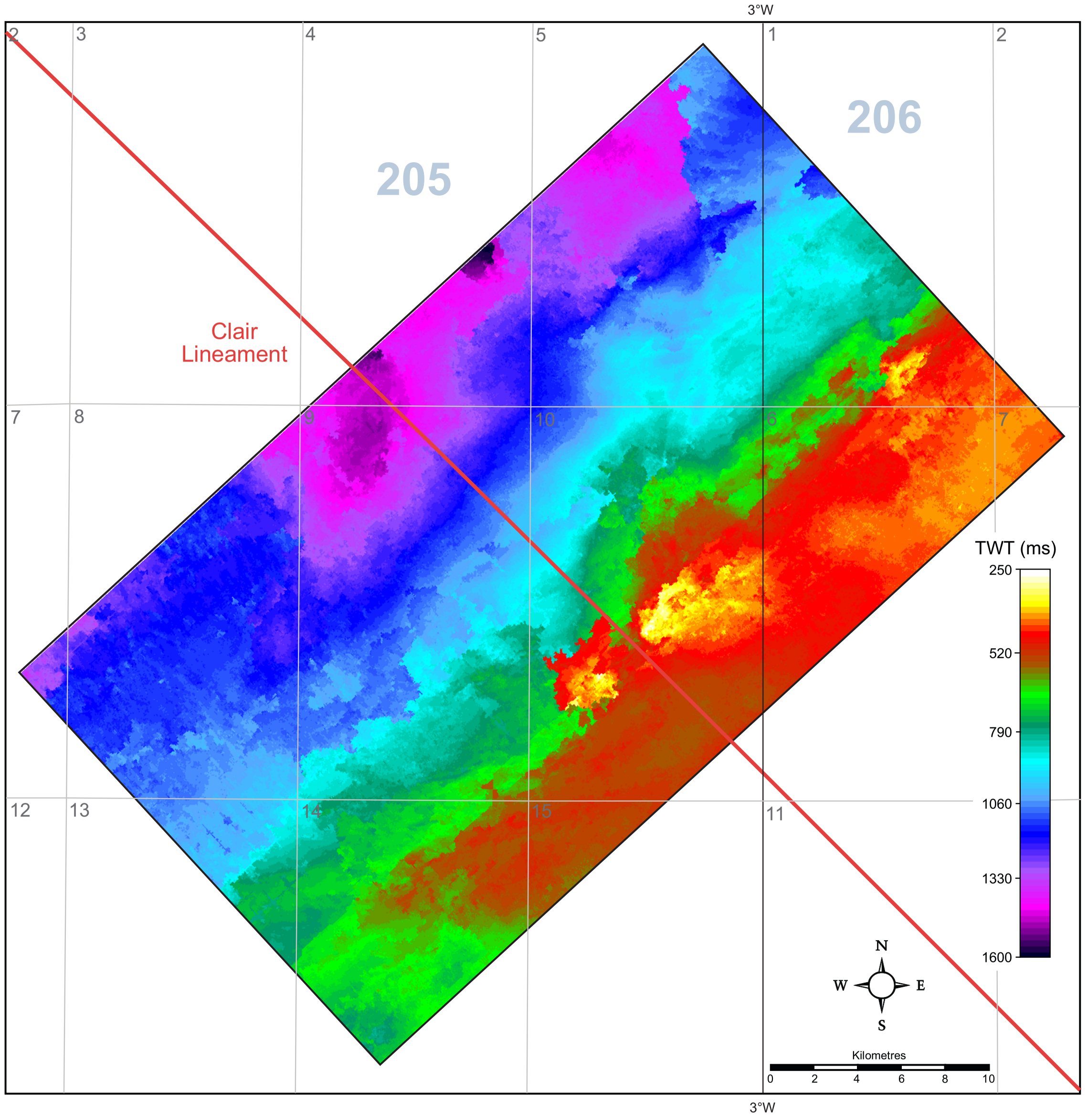

Figure 27
The time-thickness map of the Paleocene strata gradually thickens from the southeast to the northwest. Increases in the Paleocene thickness are visible across the Paleocene faults implying they were active during this time. Above the structural highs located along the strike of the Clair Lineament reductions in sediment thickness are observed. With the results displayed in this map, the original single structural high is revealed as being formed of two separate highs which have different origins. The ~ 3 km wide high to the southwest is associated with volcanic activity in the area, however the main high (~8km wide) is part of a larger high; this being the Flett Ridges highest point.

28 The structure of the Flett Ridge in the vicinity of the Clair Lineament

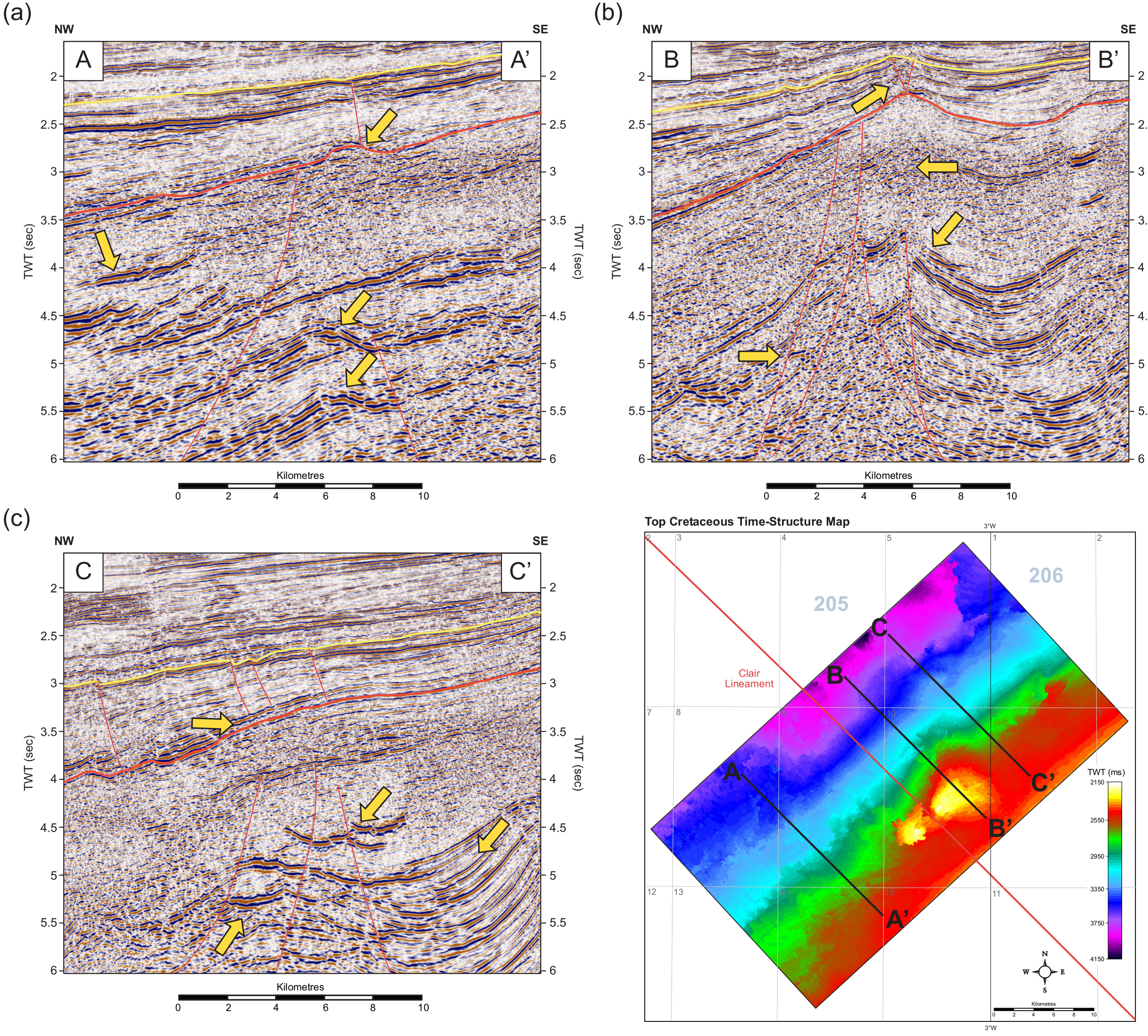

Figure 28

Horizons: Yellow = Top Paleocene, Red = Top Cretaceous

The Flett Ridge is very difficult to recognise on the seismic data, obscured by multiple sills which are clearly imaged in the Mesozoic sequence (a). High amplitude igneous material may lead to interpretational bias but a coherent structural interpretation of the high is illustrated (b,c). The faults create a horst structure with normal planar faults to the NW and SE dipping away from the ridge. Ages of the faulting are very difficult to ascertain due to the lack of well data which has penetrated this succession, but is believed to be early Cretaceous in age with reactivations in the late Cretaceous. There is no evidence of fault reactivation during Paleocene rifting (Dean *et al*. 1999) suggesting the inferred event did not affect the upper crustal regions of the basin.

Paleocene faulting appears to detach within the Cenozoic sequence and does not couple to the faults at depth, possibly due to a thick mudstone sequence deposited in the Upper Cretaceous. The cause for the faulting is not clear but may be related to minor reactivation of the faults during the post-rift thermal subsidence stage of basin formation (c). Alternatively the Flett Ridge may exert a control on the location of the faulting (b) which does not have a tectonic origin.

29 Velocity pull up by igneous sills

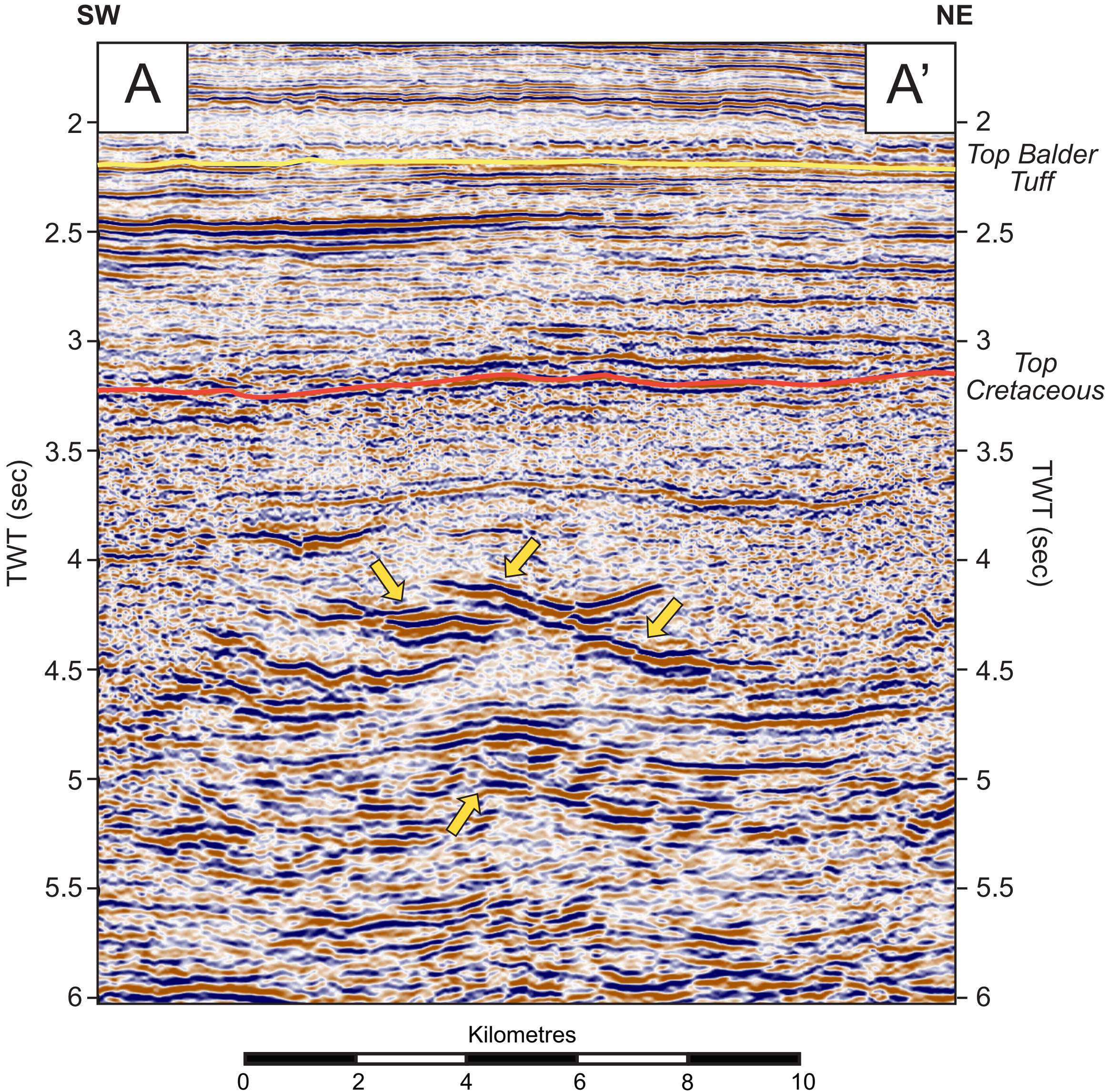

Top Cretaceous Time-Structure Map

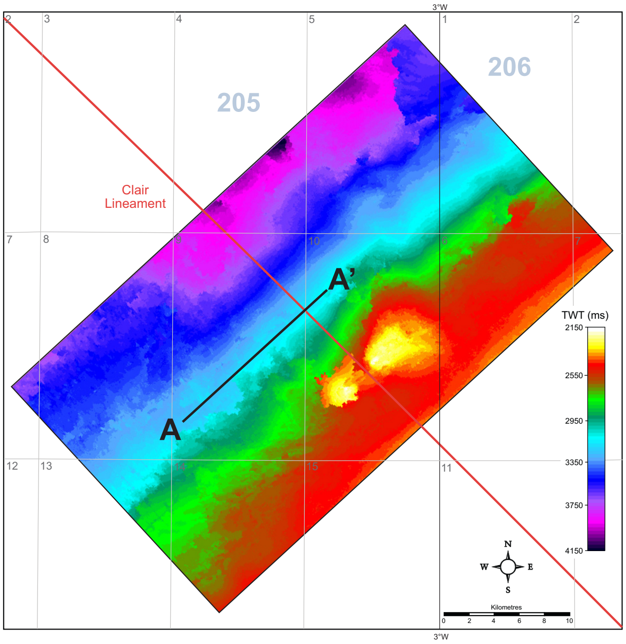

Figure 29

The sills cause a problem with time migrated seismic data as they are of a higher velocity in comparison to the surrounding sedimentary fill of the basin. This leads to artificial structural highs which, when migrated in depth, (taking into account the velocities of the rock) are not recognised. Above is an example of sills within the Mesozoic succession which have led to velocity pull up of the underlying sequence at depth, creating an apparent structural high which is may not exist.

30 Velocity push down by hydrocarbon gas chimneys

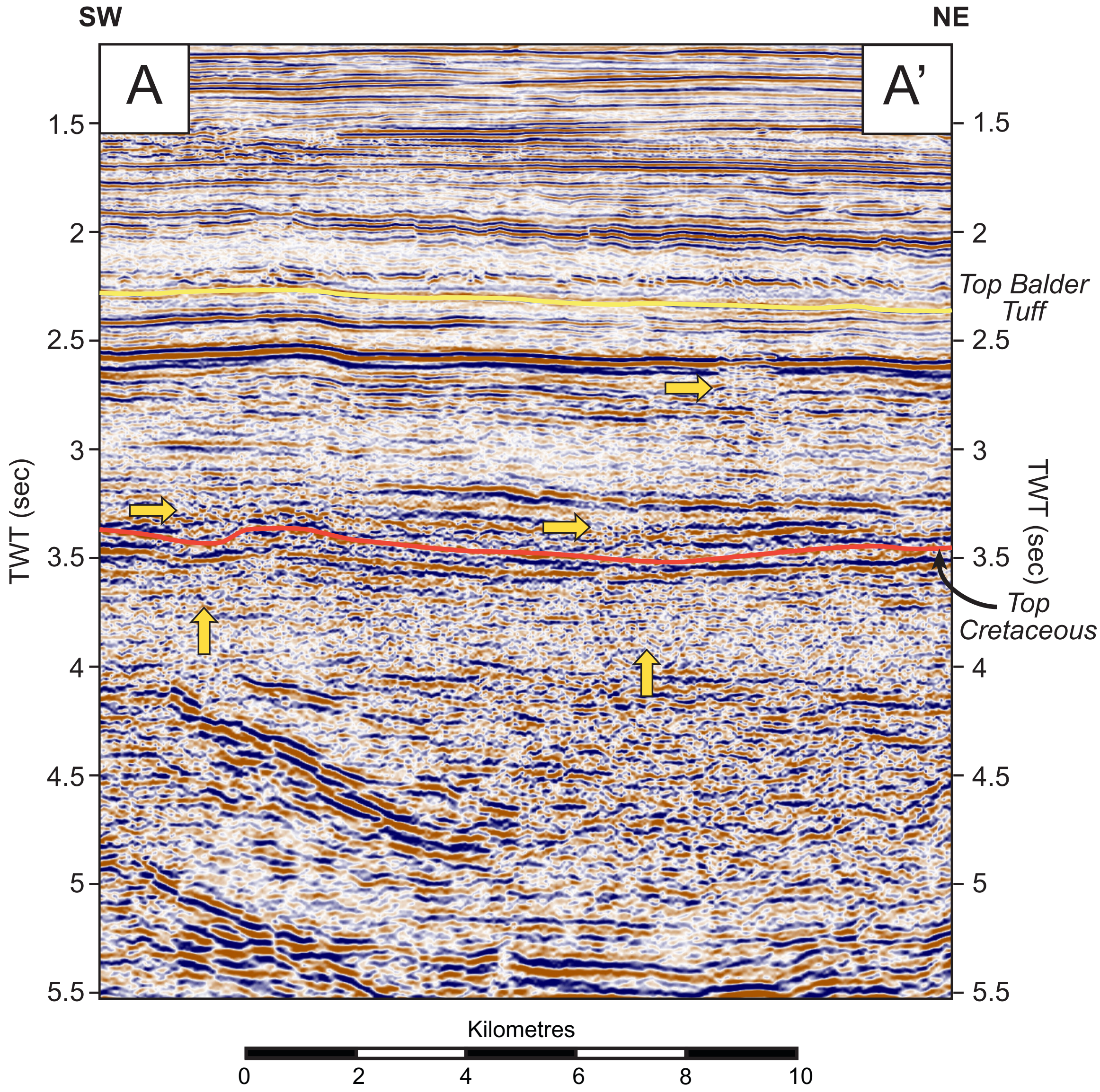

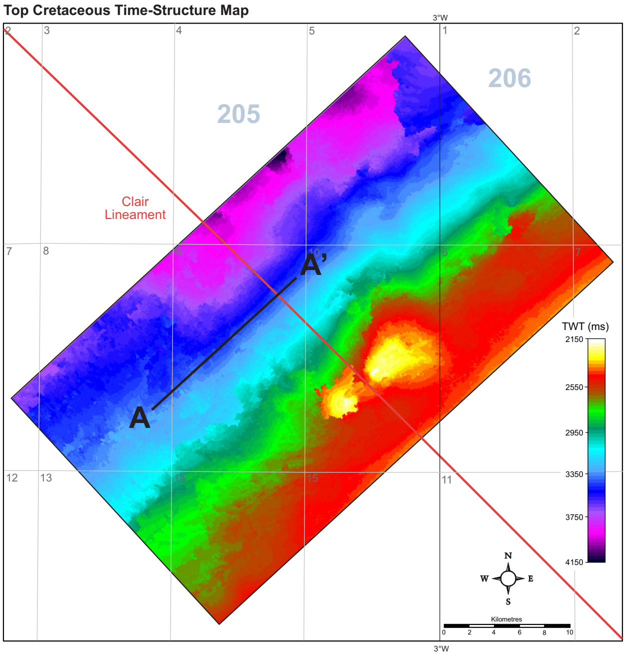

Figure 30
Hydrocarbon chimneys, containing natural gas (CH_4), infiltrate the pore space of sedimentary rocks resulting in the lowering of the velocity of the rock. This leads to the ‘pushing down’ of time-migrated seismic data beneath the chimneys and the formation of apparent low areas of relief. This is particularly evident within the Paleocene sequence as the migrating gas has filled the porosity of sandstone units (and with no seal rock above), has been able to migrate vertically creating gas chimneys. These zones affect the amplitude and lead to chaotic zones in the seismic data. Beneath these, artificial lows are imaged, leading to depressions along the top Cretaceous unconformity.

31 A major hydrothermal vent complex forming a prominent structural high

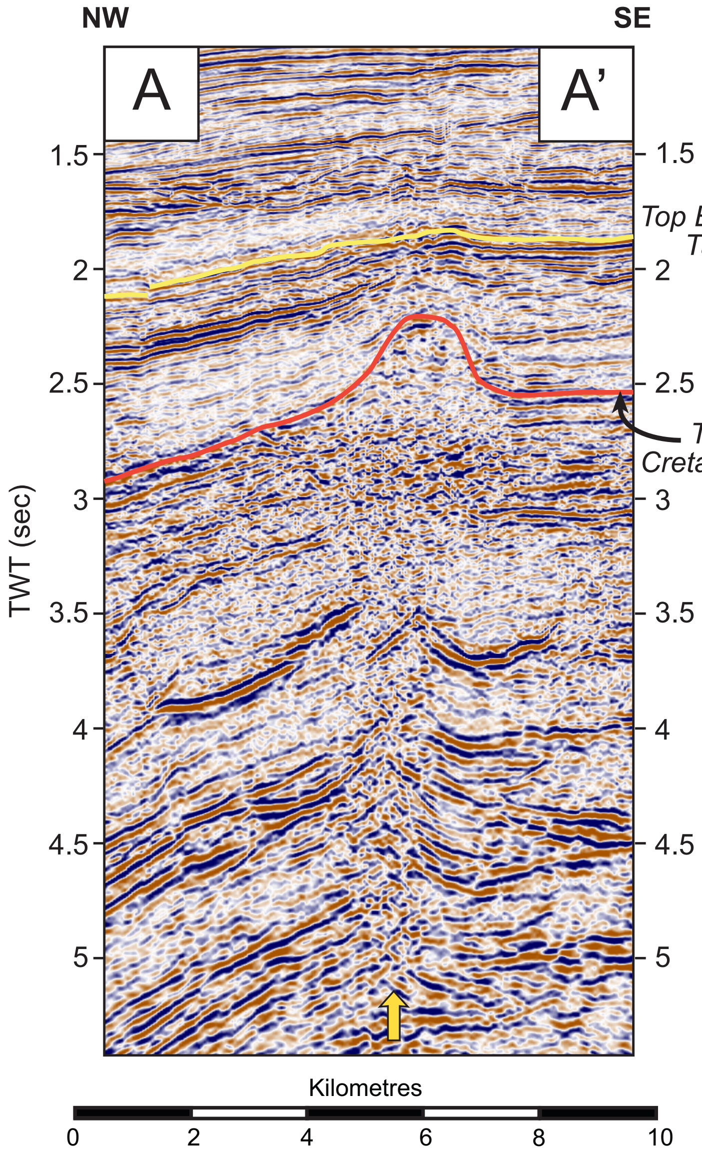

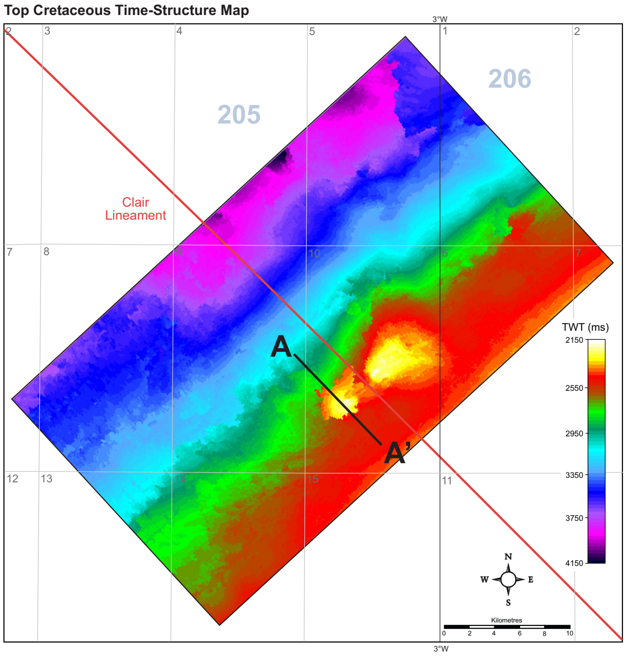

Figure 31

Strong amplitude reflectors interpreted to be igneous sills are the source for volatile gases and liquids erupted from their tips, rising under hydrostatic pressure and remobilising the overlying sediment. This is then erupted on the overlying seabed, from which an age for the process can be ascertained. The major 3km wide feature on the top Cretaceous map is associated with this activity, creating a wide zone of positive relief on the seabed during the Paleocene. Later sedimentation is also observed to onlap the erupted material. The Clair Lineament may influence the location of the inferred hydrothermal vent complex (e.g. advancing up a major sub-vertical fault zone) but this can not be proven.

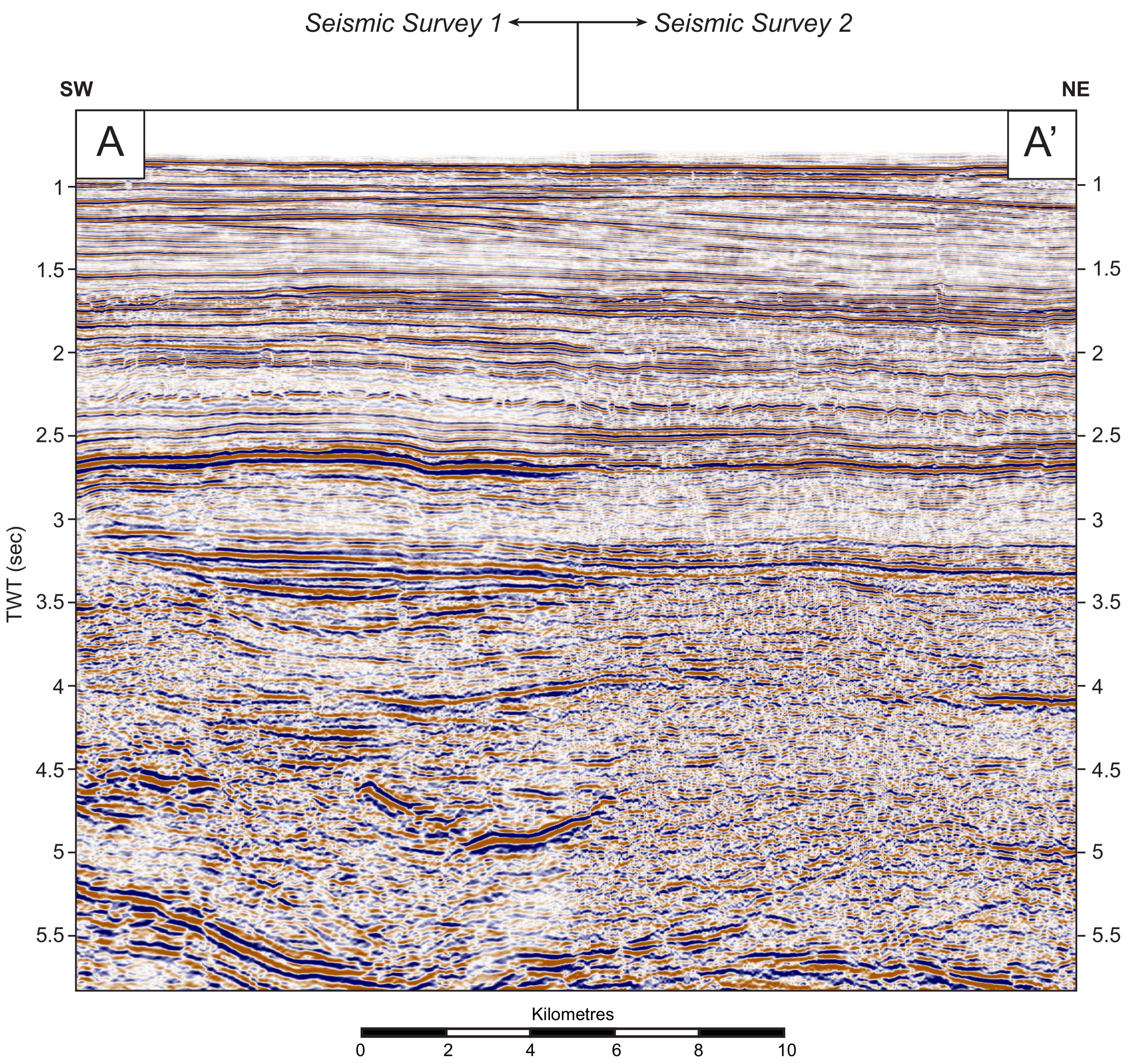

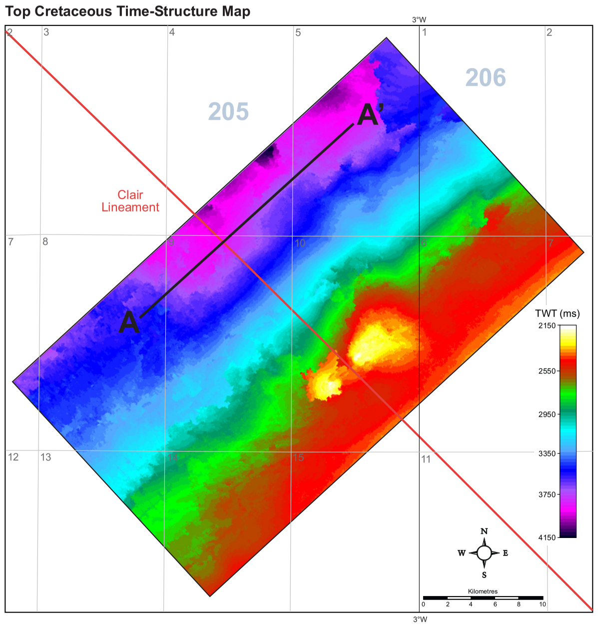

Figure 32
An artefact associated with the merging of multiple 3D seismic datasets is how the original datasets have processed using different parameters. The edges of these datasets are reprocessed to match and produce a coherent 3D MegaSurvey. However, there is a difference between conjugate datasets which greatly impacts the level of interpretation possible. In this study area, this problem is visible as a merge occurs close to the inferred strike of the Clair Lineament, meaning identification of any features associated with the lineament is difficult.

33 Well 204/23-1 well to seismic tie and seismic stratigraphy

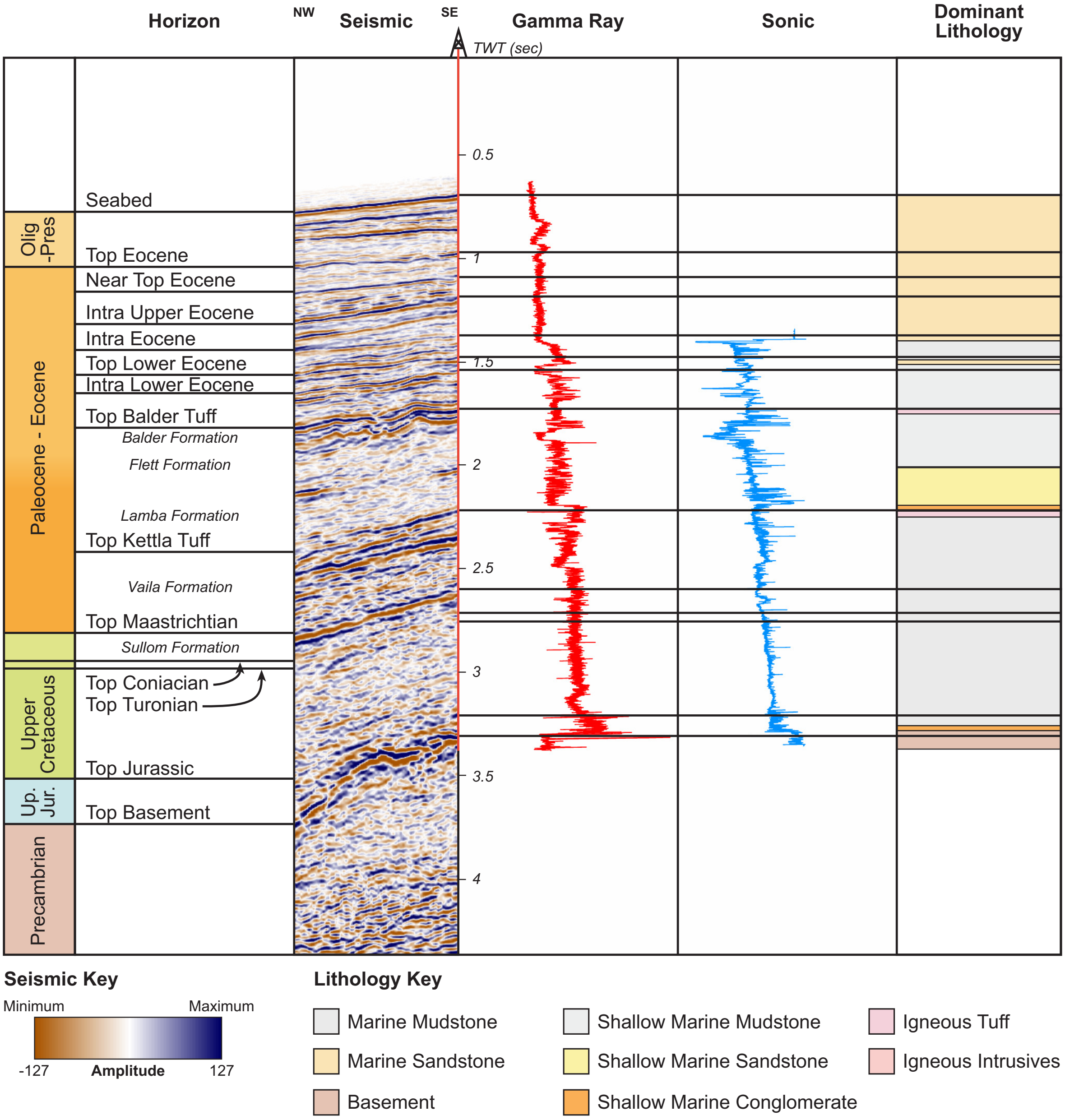

Top Precambrian Basement Time-Structure Map

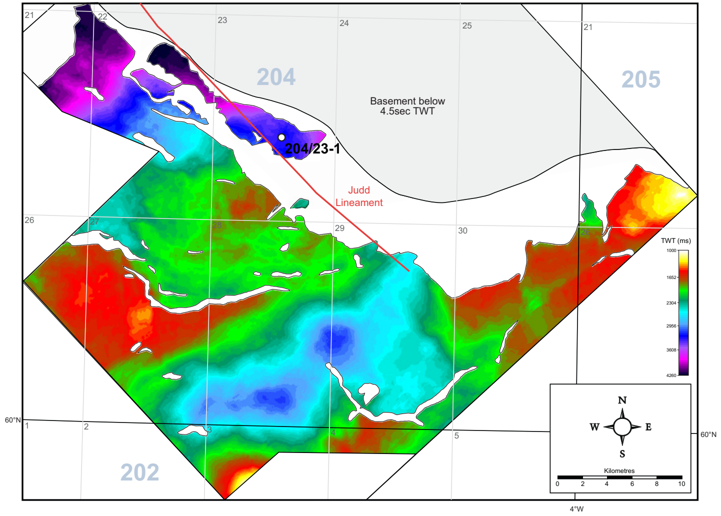

Figure 33

Well 204/23-1 reaches total depth in Precambrain crystalline basement after penetrating upper Jurassic - lower Paleocene marine mudstone facies; which are discordant reflections on the seismic data. A bright, positive, coherent reflector marks the top Cretaceous unconformity, but a dominantly mud prone Paleocene succession is transparent within the seismic data. The Balder Tuff is also a bright positive reflector with interbedded sandstones and mudstones dominant from the Eocene until the present day.

34 Well 202/3a-3 well to seismic tie and seismic stratigraphy

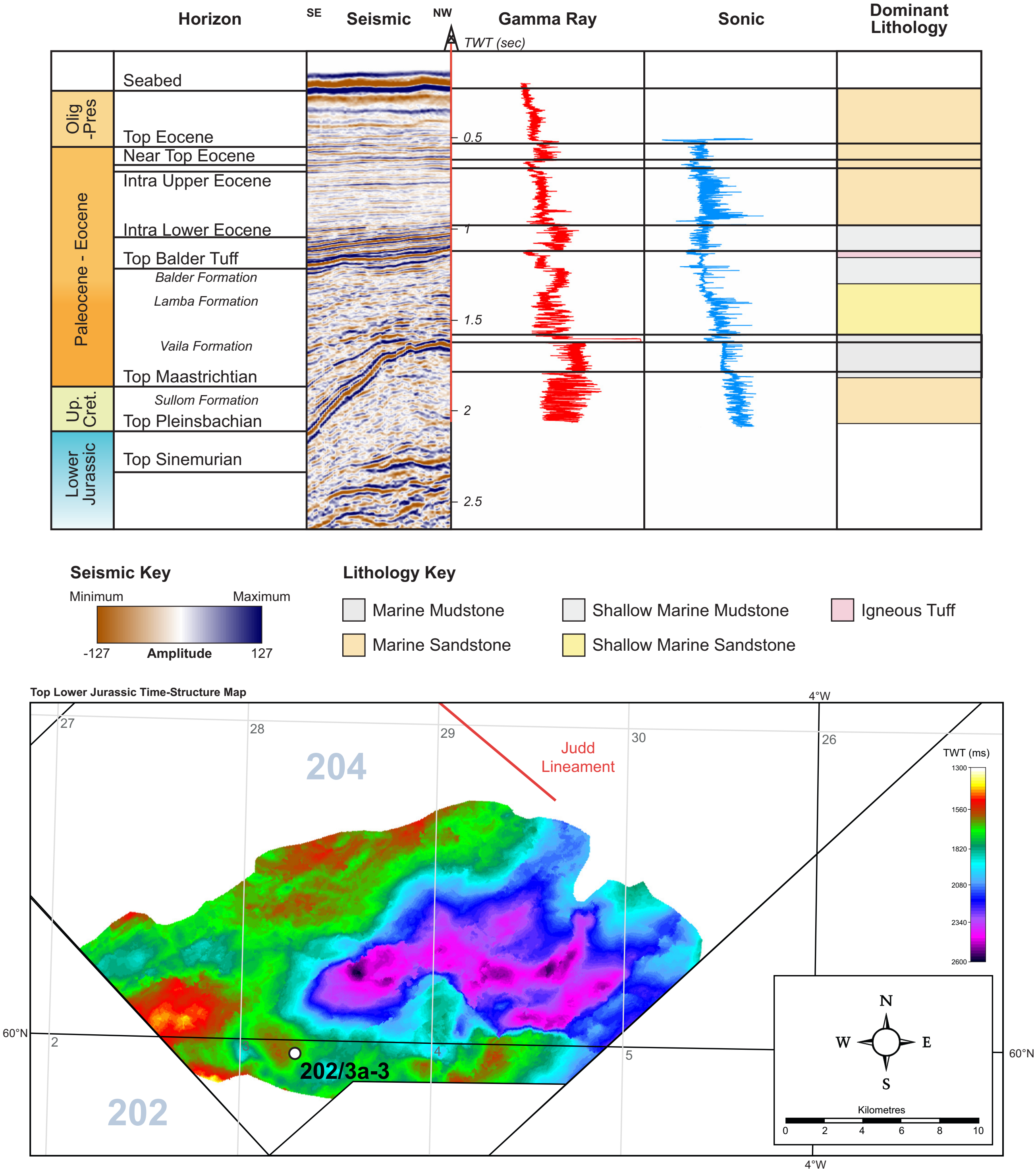

Figure 34

Well 202/3a-3 reaches total depth in the lower Jurassic sequence, but despite having a transparent appearance on the seismic data, a marine sandstone was encountered capped by a marine mudstone. The Maastrichtian is very thin in the well represented by a single mudstone unit; its upper limit related to a relatively bright but discordant reflector. The Paleocene strata is dominated by a shallow marine sandstone package followed by dominant mud-prone deposition. The Kettla Tuff is not recorded in the well but the Balder Tuff is represented by a strong positive amplitude response in comparison to the weaker shallow marine mudstone sequence, prior to middle Eocene to present day deposition of marine sandstones.

35 Well 204/19-1 well to seismic tie and seismic stratigraphy

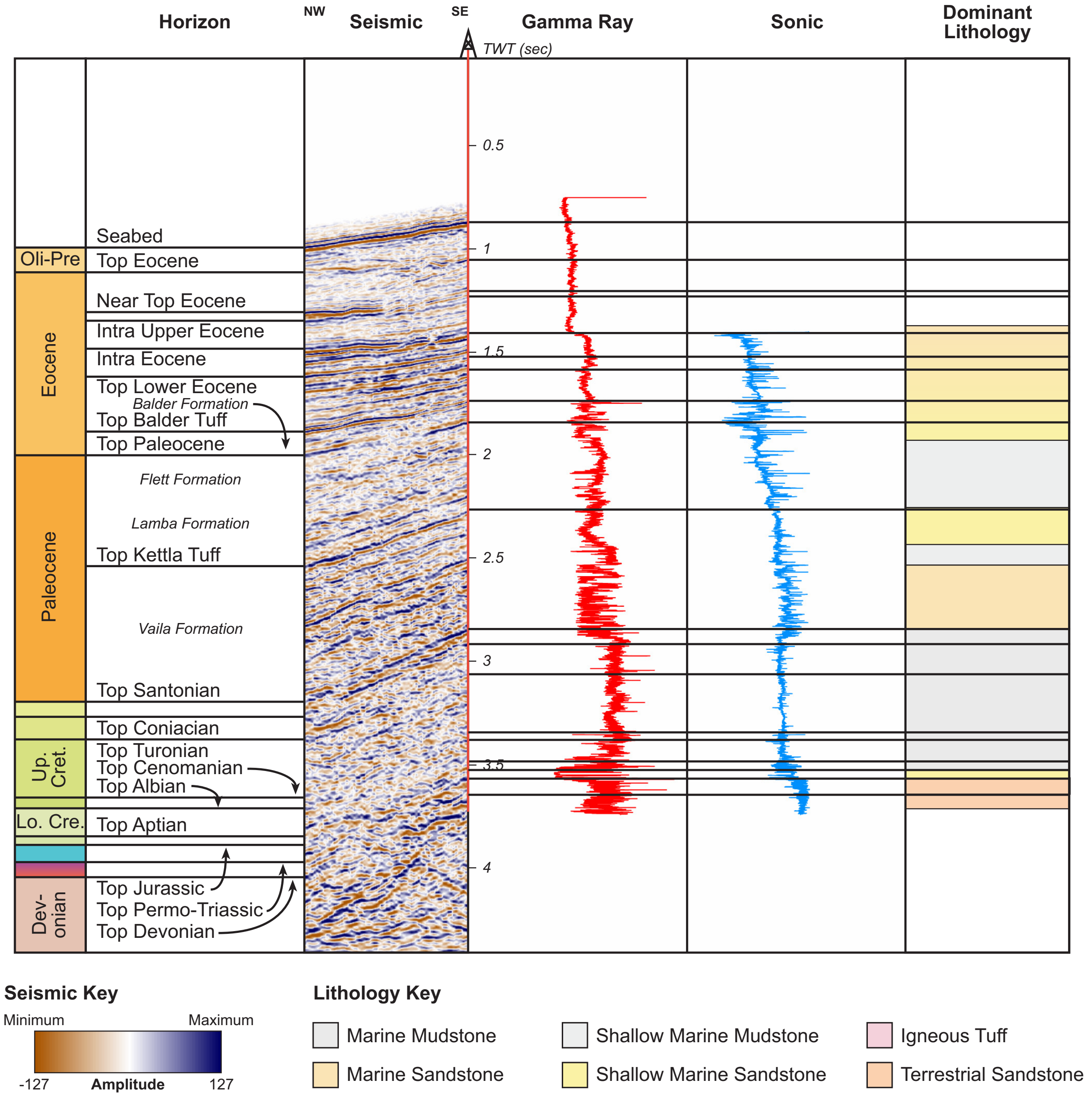

Top Cretaceous Time-Structure Map

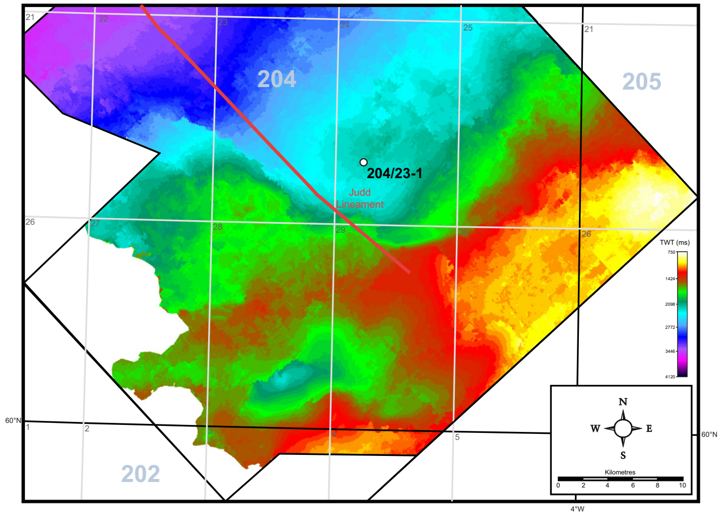

Figure 35

Well 204/19-1 drilled terrestrial sandstones of Devonian and Permo-Triassic age which are difficult to identify on the seismic data. A thin Jurassic sandstone is recognised, but despite a substantial portion of Cretaceous aged stratigraphy penetrated, only a relatively thin sequence of marine mudstones is encountered. The seismic data is chaotic in nature making it is difficult to map horizons within this sequence. Paleocene sandstones and mudstones lead to enhanced seismic imaging of the early Cenozoic sequence.

36 Top Precambrian basement amplitude map

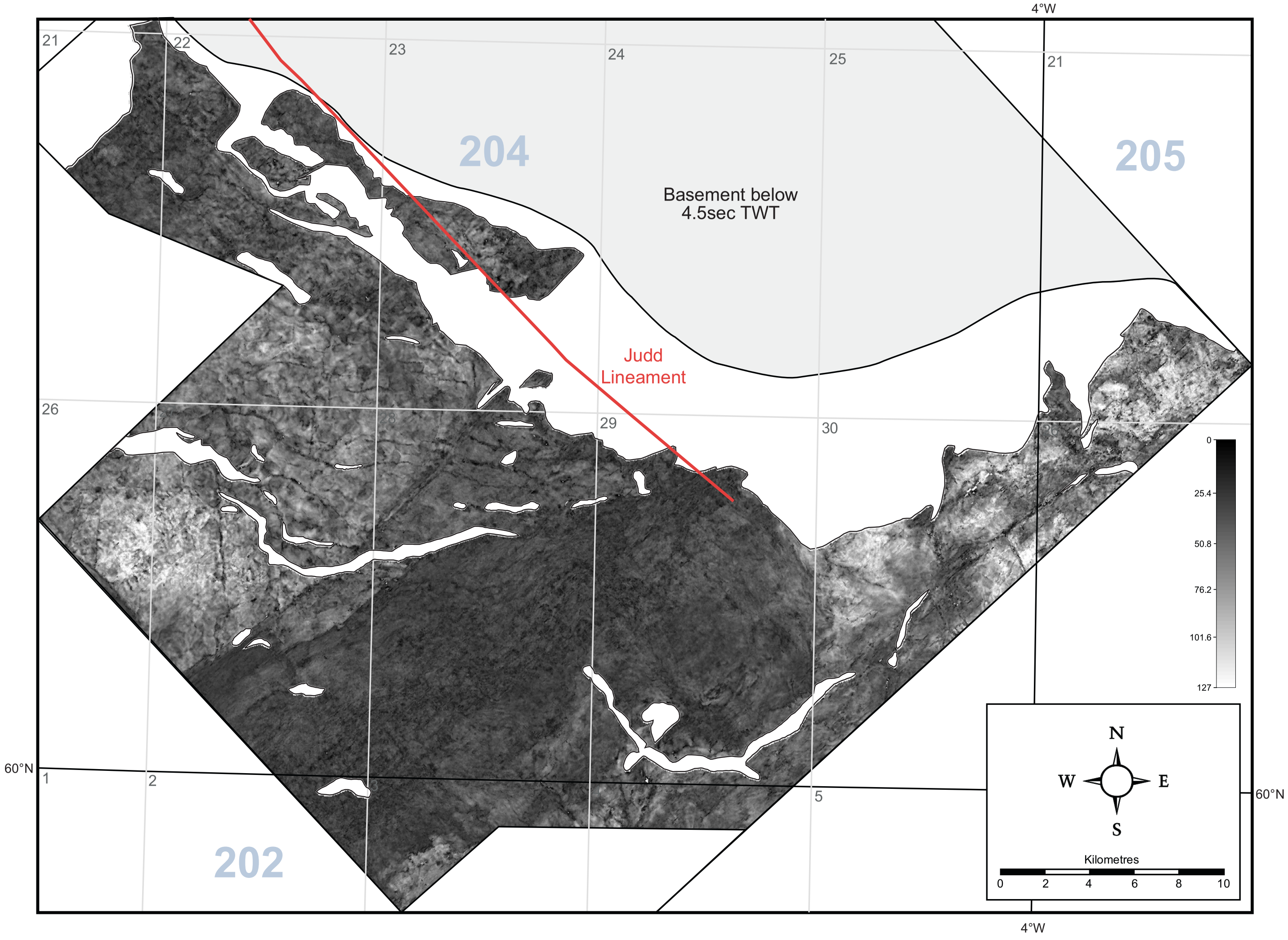

Figure 36
The amplitude extraction of the top Precambrian basement horizon is interpreted to reveal areas which have been exposed to erosion, which has been the case for the Rona Ridge and Judd High. Within the West Solan Basin the amplitude response is weaker which may be attributed to the increased depth at which the Precambrian basement horizon is located. In this area it is also more difficult to interpret the basement because of a very weak amplitude response and therefore may not have been subaerially exposed (and eroded) since at least the Carboniferous.

The amplitude map also picks up fault patterns within the basement structure which are generally NW-SE and E-W trending; probably relating to the later Mesozoic rift events. However, it has been reported that NW-SE trending Precambrian shear zones have been recognised in the basement structure elsewhere in the Faroe-Shetland Basin (S. Clarke, Keele University, pers. comm.). In this area, it is very difficult to recognise these complex structural zones, but the notable NW-SE fault structures may have successfully reactivated these features during the later rift events.

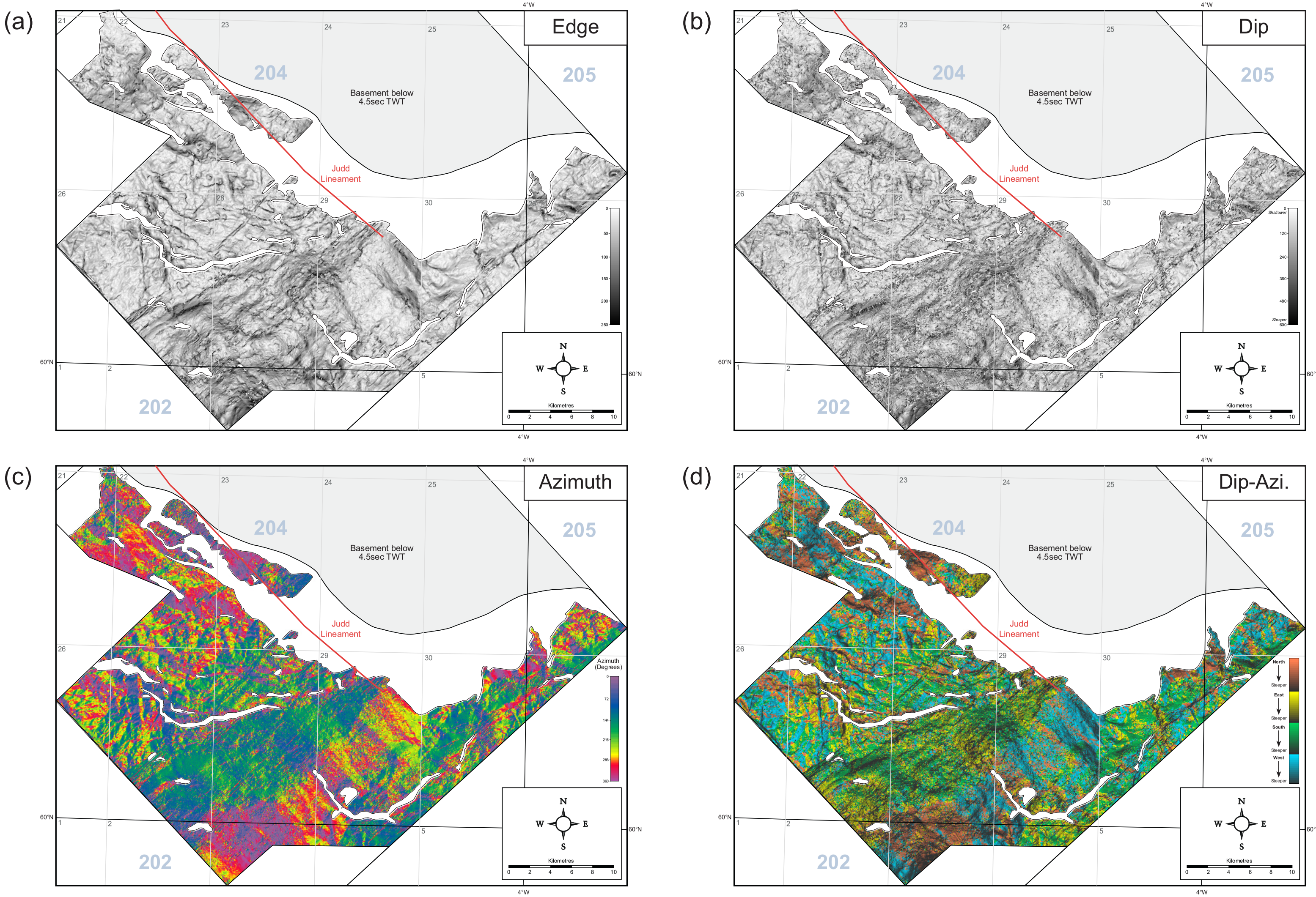

Figure 37
The edge map (a) highlights changes in the dip of the Precambrian basement and broadly recognises the faults reported previously, but the dip map (b) recognises some contrasting NW-SE trending features. The azimuth map (c) also highlights these trends, particularly in the West Solan Basin and upon the Judd High. These correlate with the areas highlighted on the dip and edge maps (d) which may be Precambrian features.

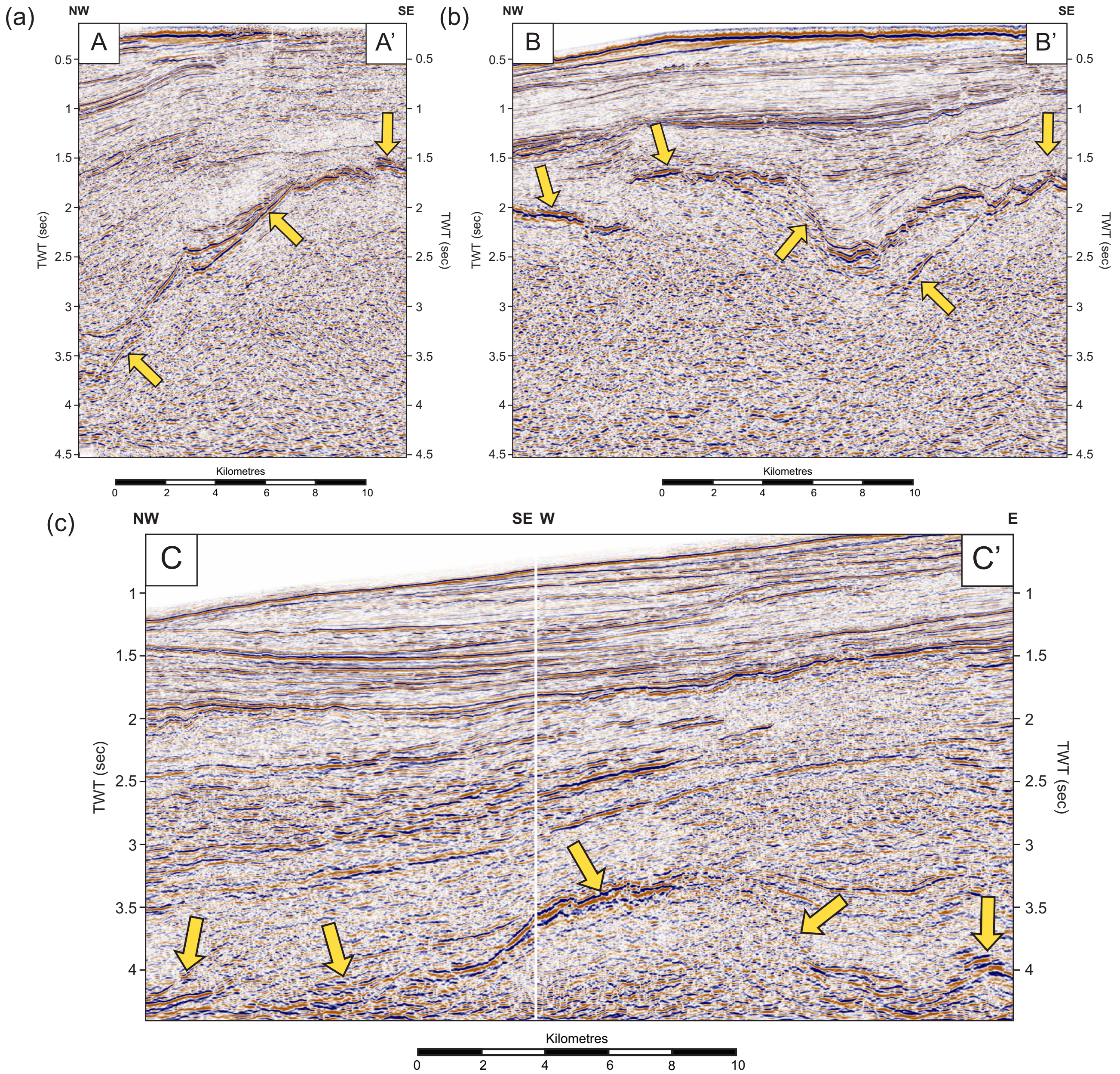

Top Precambrian Basement Time-Structure Map

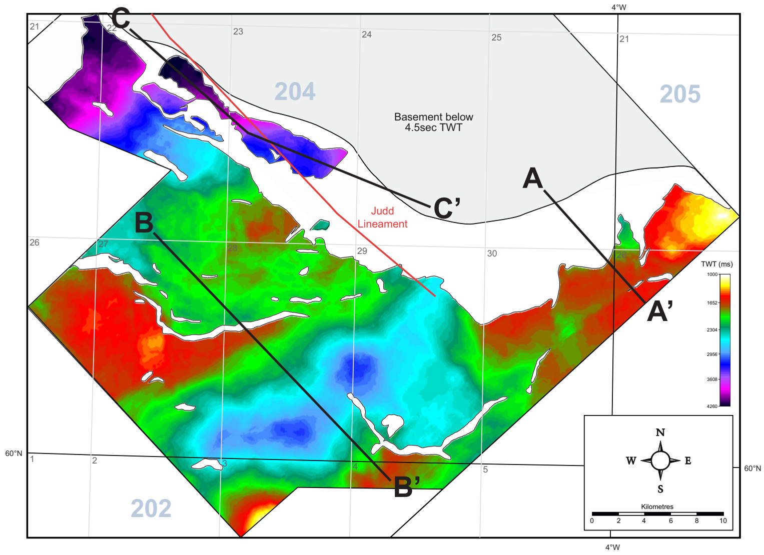

Figure 38

The Precambrian basement is a bright reflector and relatively simple to map except in some locations. On the Rona Ridge (a) it is difficult to seperate faulted and non-faulted Precambrian basement. With increasing depth the amplitude response also weakens making fault interpretation difficult in this area. Similarly, within the West Solan Basin (b) top Precambrian basement exhibits a weak amplitude response and it is unclear whether the horizon is a set of over rotated low-angle Permo-Triassic normal faults. The extent of the breached relay ramp of the Judd Transfer Zone (c) is difficult to map for very similar reasons.

39 Top lower Jurassic time-structure map

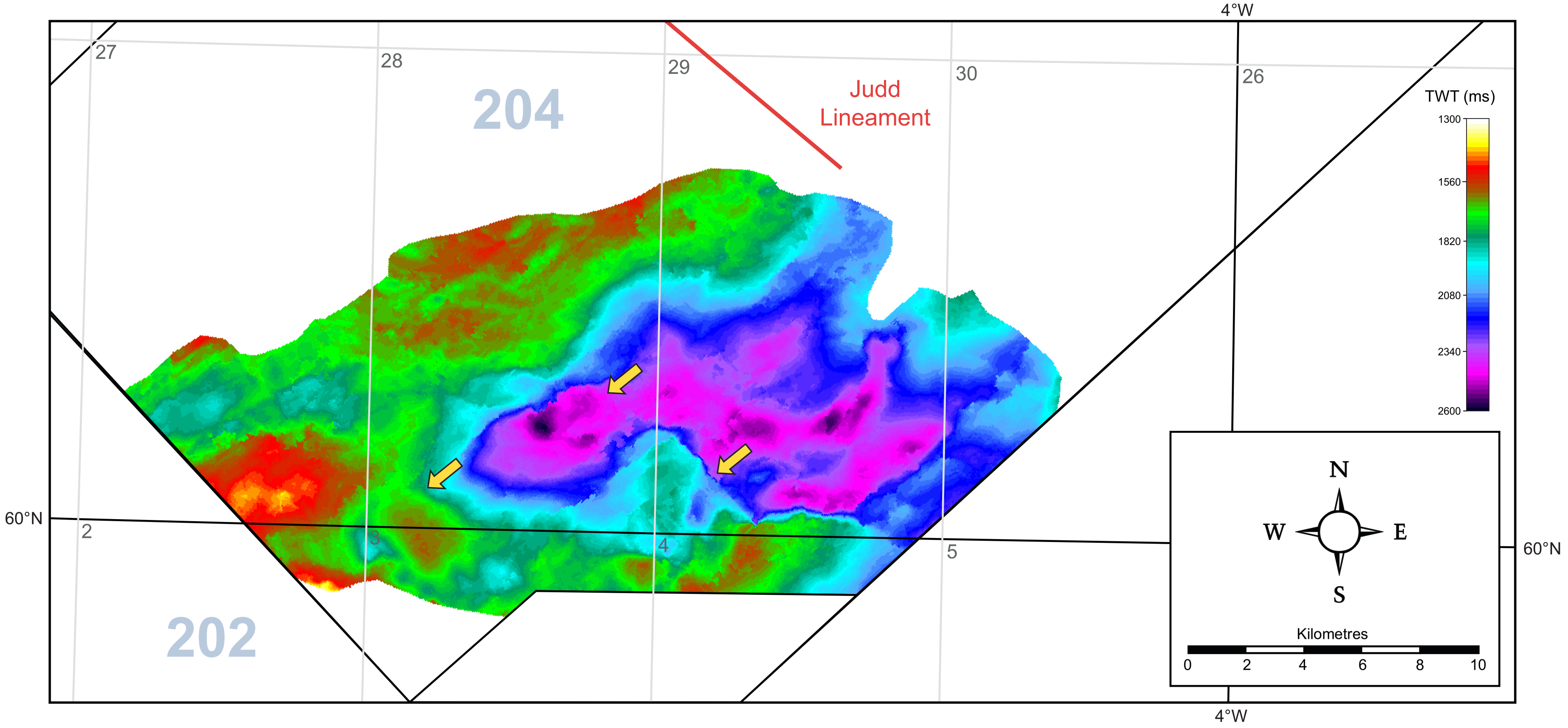

Figure 39
The lower Jurassic is mappable only in the West Solan Basin as elsewhere in the study area it is either thin or absent. The horizon is deepest towards the centre and northeast of the West Solan Basin but there are notable depth changes across faults in these locations implying they were active during later rift events (e.g. Cretaceous). The main basin bounding faults (NE-SW and E-W oriented) are recognised but the map also highlights the importance of some NW-SE trending fault structures which appear syn-kinematic.

40 Top lower Jurassic amplitude, dip, azimuth and dip-azimuth maps

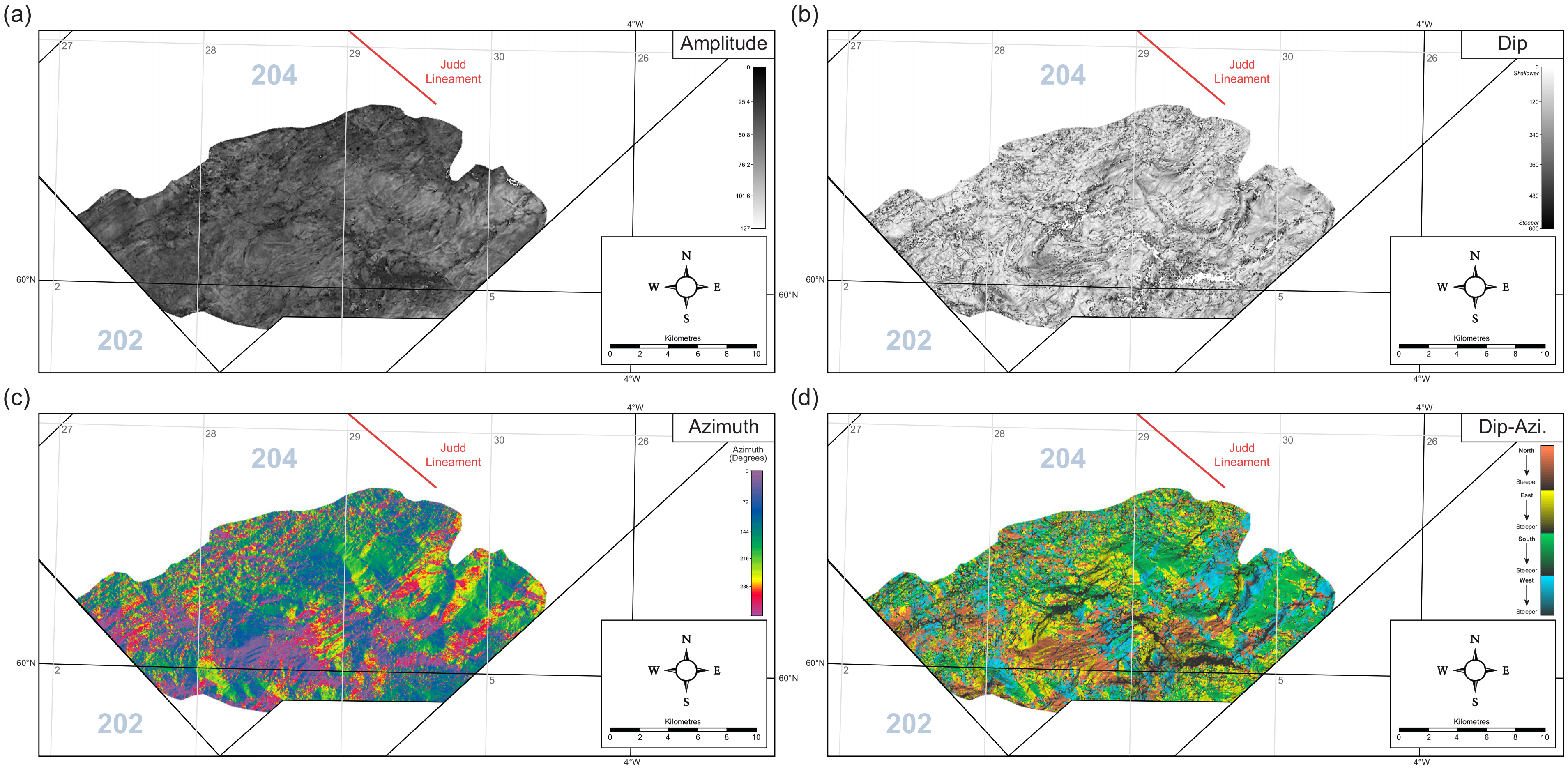

Figure 40

Map (a) highlights the main NE-SW, NW-SE and E-W fault orientations in the basin, as well as map (b) which also highlights the arcuate nature of the Permo-Triassic-Jurassic faulting in the basin. Map (c) also picks up these trends with the NW-SE and NE-SW trends dominating. When combining the dip and azimuth maps (d) the main basin bounding faults are highlighted as well as the complex structure of the West Solan Basin. It also highlights a possible segmentation of the basin across NW-SE trending features which appear to correlate with the NW-SE trending features recognised in the Precambrian basement.

41 Top Cretaceous time-structure map

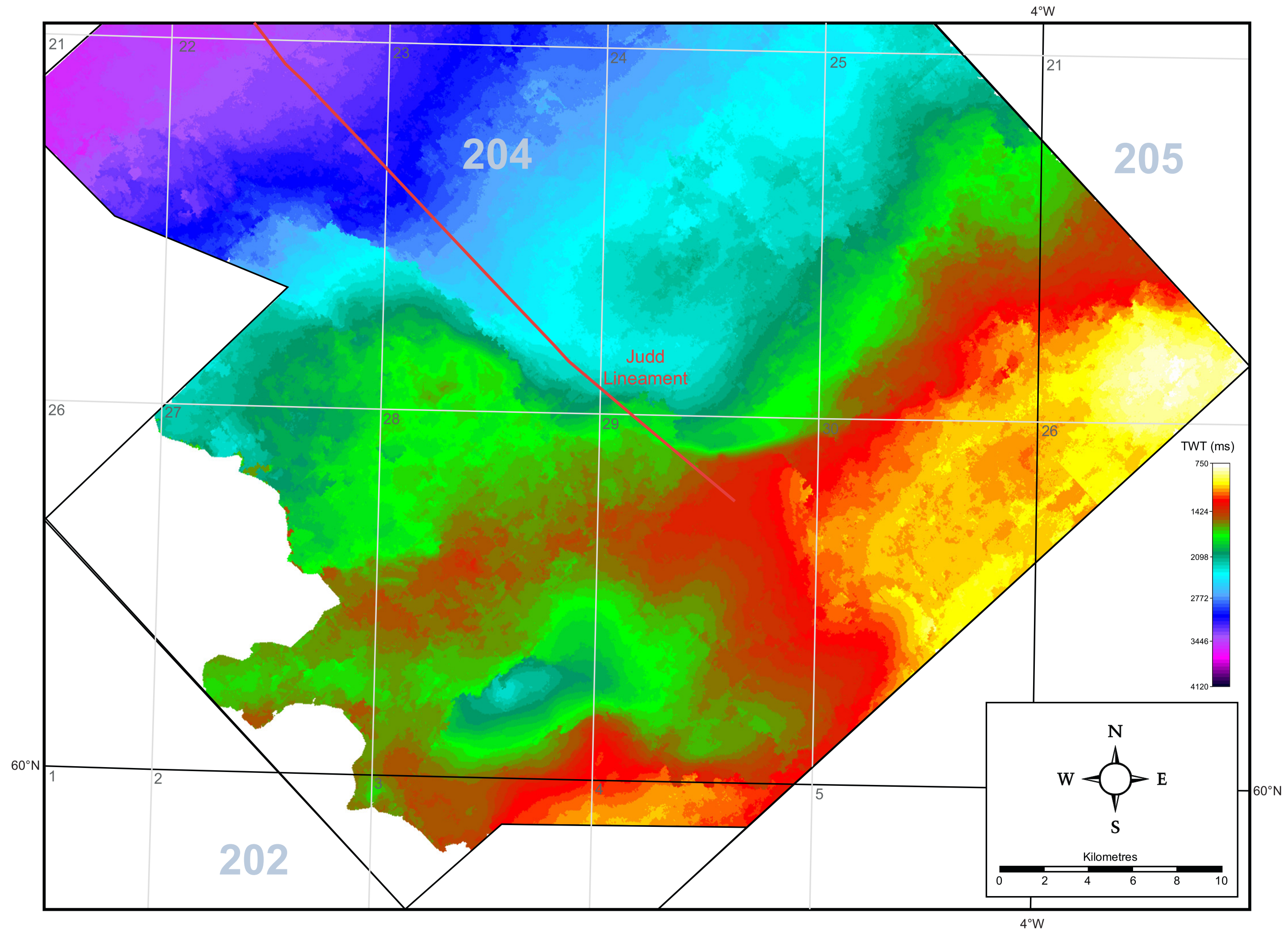

Figure 41
The top Cretaceous unconformity is structurally highest upon the Rona Ridge and to the south and north of the West Solan Basin. The horizon is deepest to the north in the Faroe-Shetland Basin where an offset from the Judd High along the Judd Transfer Zone is evident. A deepening of the horizon to the northwest of the Rona Ridge implies the bounding fault system was active during the late Mesozoic, forming accommodation space into which Cretaceous sediment was deposited.

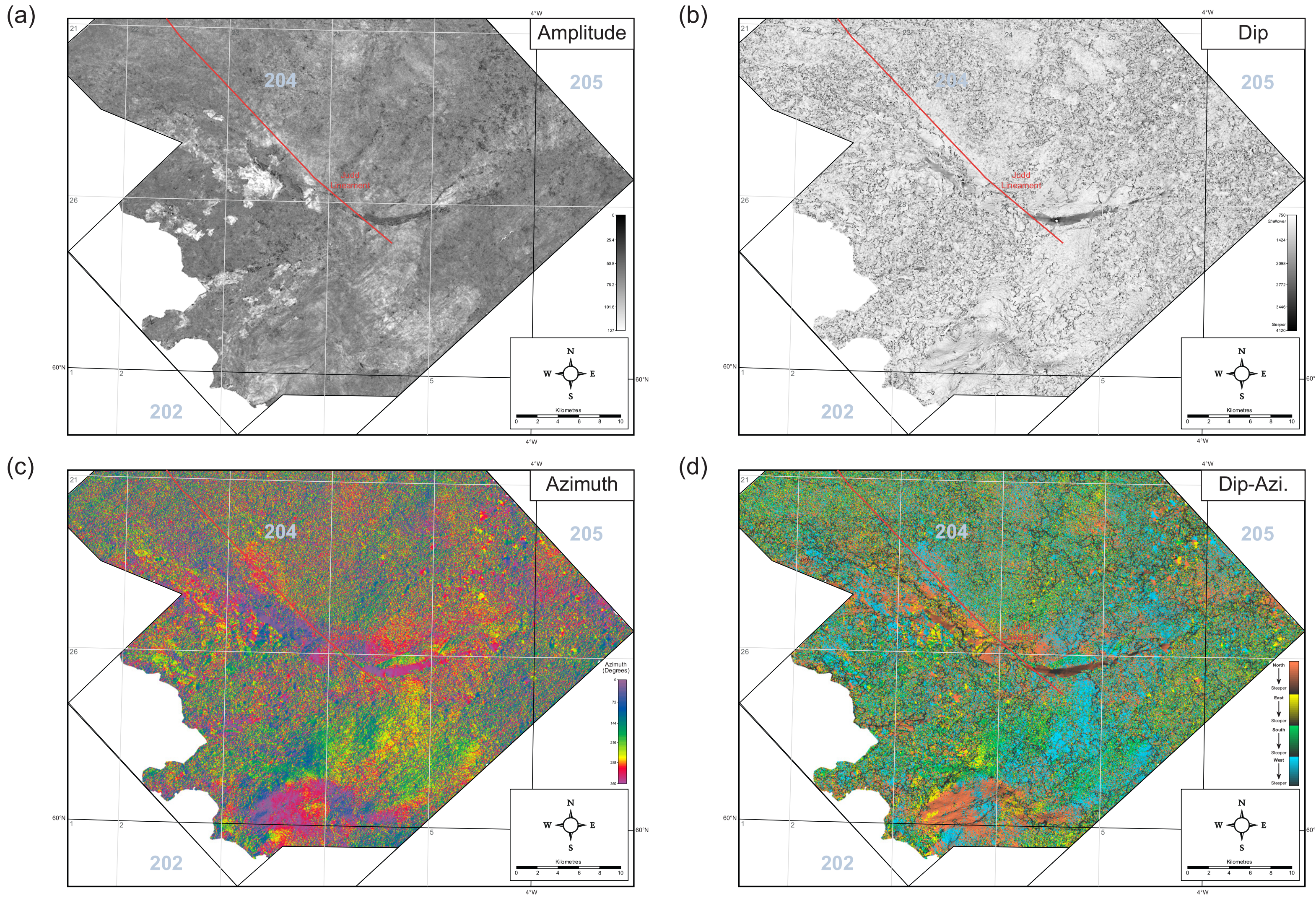

Figure 42
The edge and dip maps of the horizon (a,b) clearly identify how the bounding fault system of the Rona Ridge rotates round into the Judd Transfer Zone. Map (c) highlights this fault trend with dip on the fault planes to the north. This is evidence for an inferred northward movement of the hangingwall fault block in this area. A similar pattern is identified on the Cretaceous faults of the West Solan Basin.

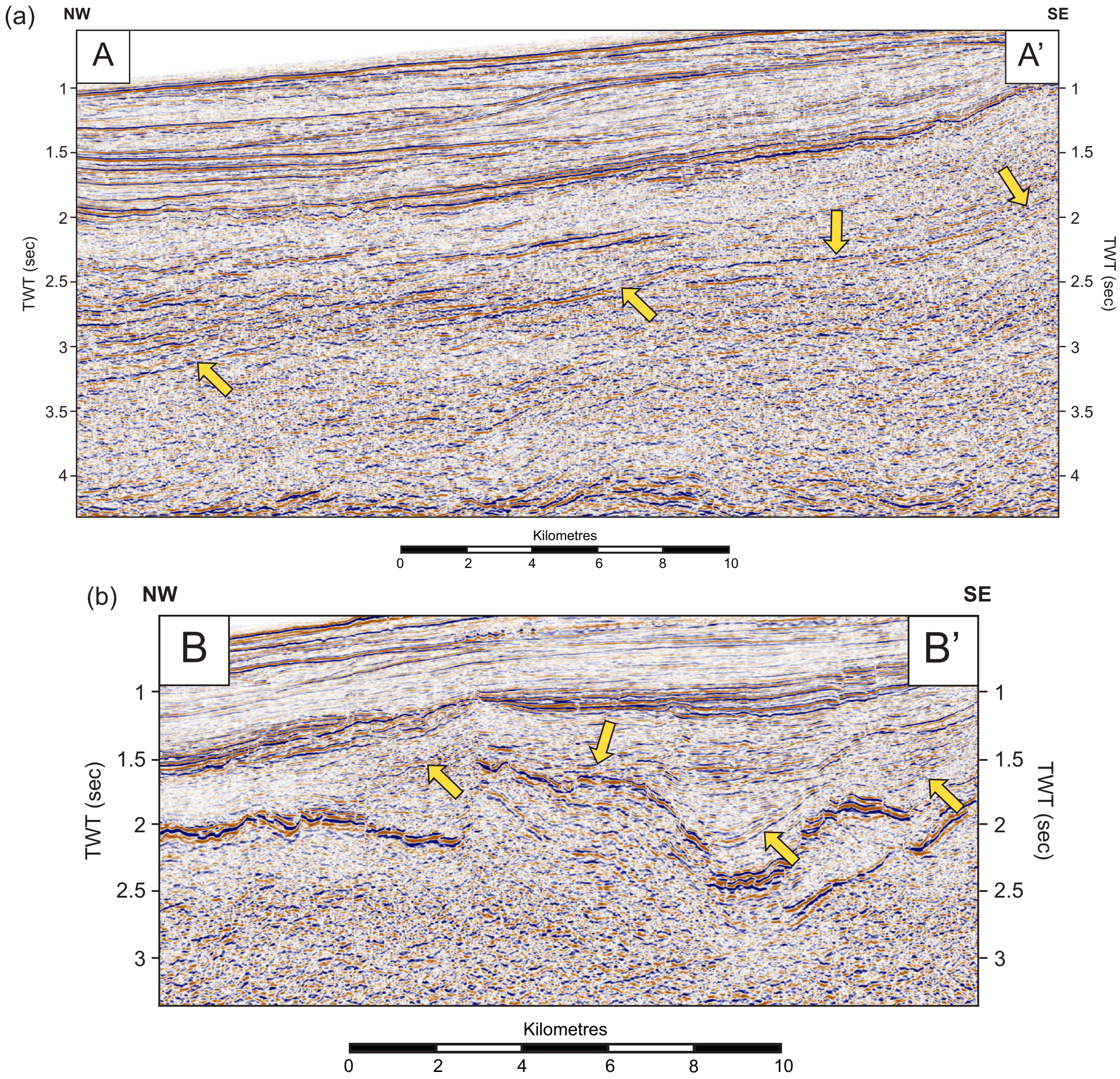

Top Cretaceous Time-Structure Map

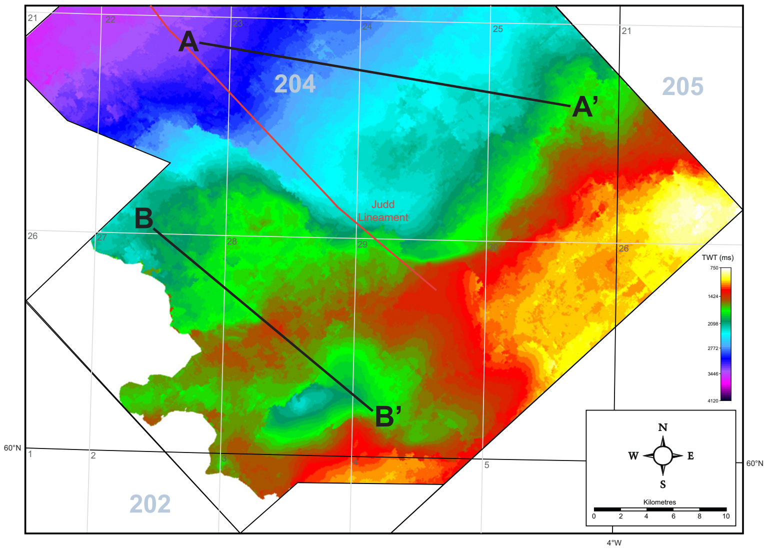

Figure 43

The top Cretaceous unconformity is very difficult to interpret within this region of the Faroe-Shetland Basin, even though it is a recognised unconformity. This is due to Paleocene mudstones deposited upon Cretaceous mudstones resulting in a weak acoustic impedance contrast. The reflector is of low amplitude, non-coherent (a) and is often difficult to identify from several other similar horizons. The difficulty mapping the horizon increases in areas of faulting (b) and the need for increased well data is required to confidently correlate across faults.

44 Top Balder Tuff time-structure map

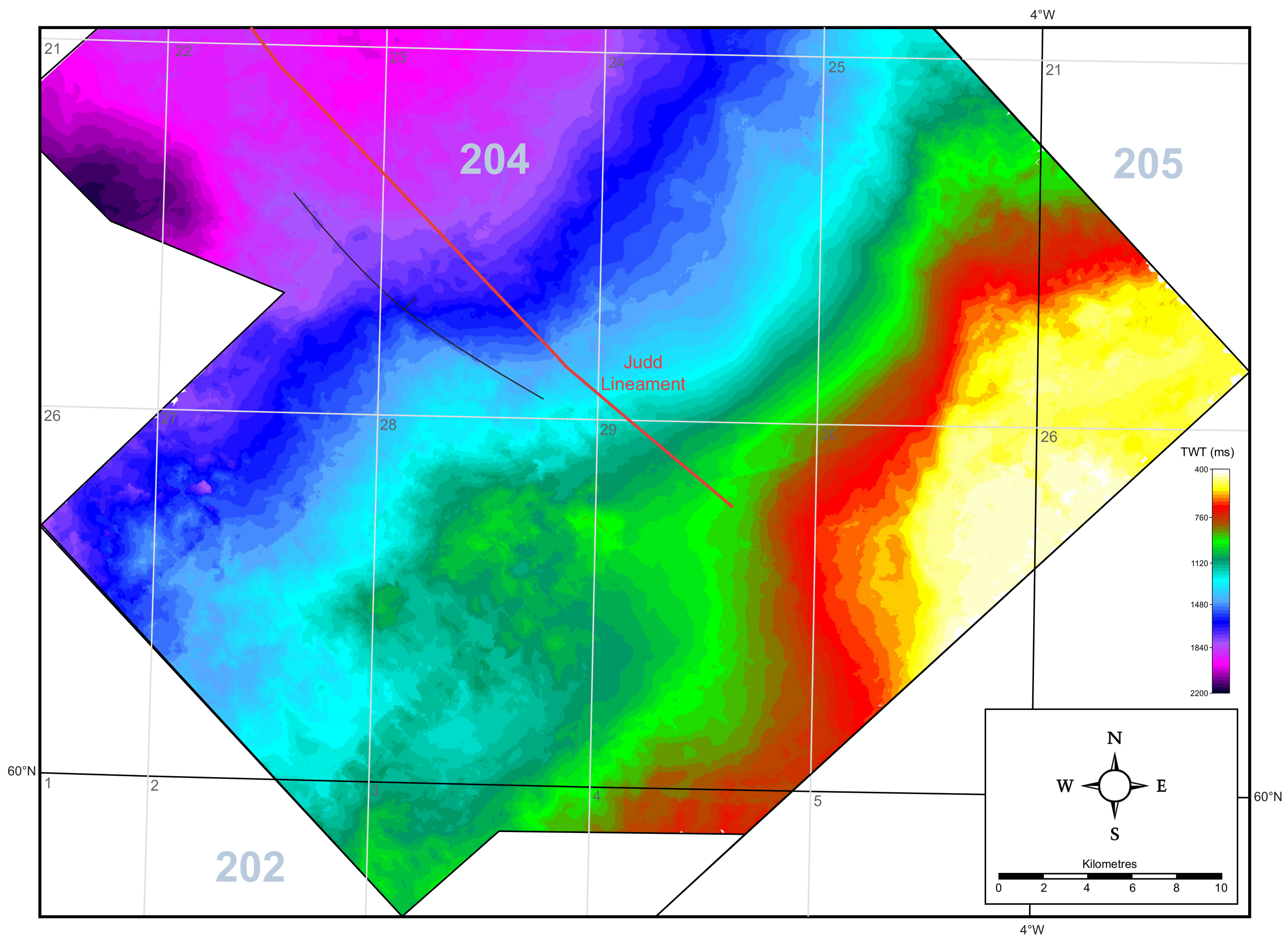

Figure 44
The top Balder Tuff horizon displays a gradual deepening to the northwest. It is shallowest upon the Rona Ridge and deepens above the West Solan Basin along strike, possibly controlled by post-rift thermal subsidence in this area. There is a minor offset across the Judd Transfer Zone but the horizon depth is not strongly influenced by this feature. The Paleocene displays the greatest depth in the area to the northwest of the Judd High within the Judd Sub-Basin. This enhanced deepening of the horizon implies the presence of faulting between these two regions akin to the faulting between the Rona Ridge and the Faroe-Shetland Basin.

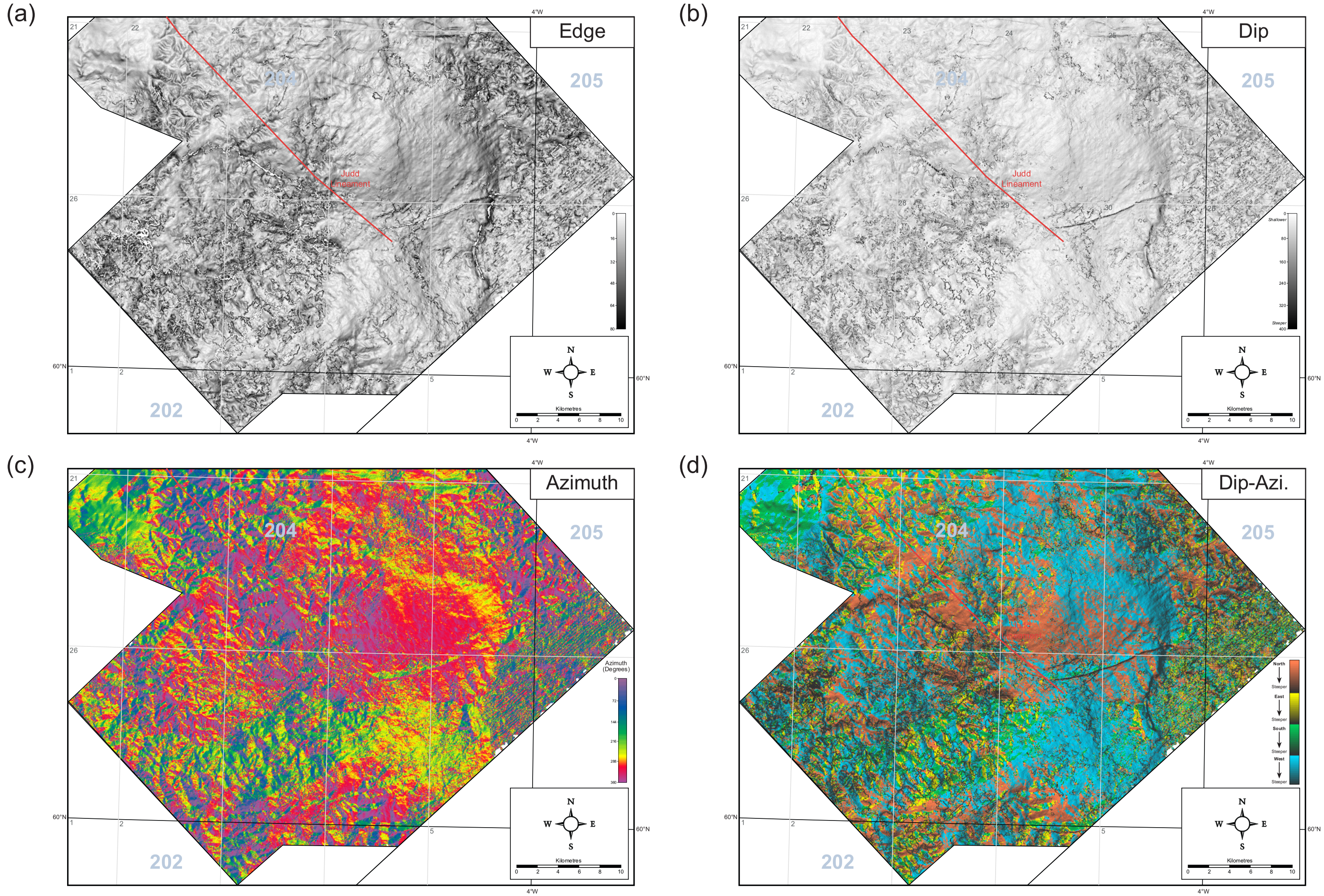

Figure 45

Map (a) displays a change in dip along some N-S meandering features may be channels which compliment the interpretation of dendritic drainage networks in block 204/22. These channels flow across normally reactivated Rona Ridge faults clearly identifiable in map (b). Maps (c) and (d) also pick up these features which contrast with the NW dip of the horizon, yet it is not clear if these features are submarine or subaerial.

46 Areas of difficulty interpreting the Balder Tuff

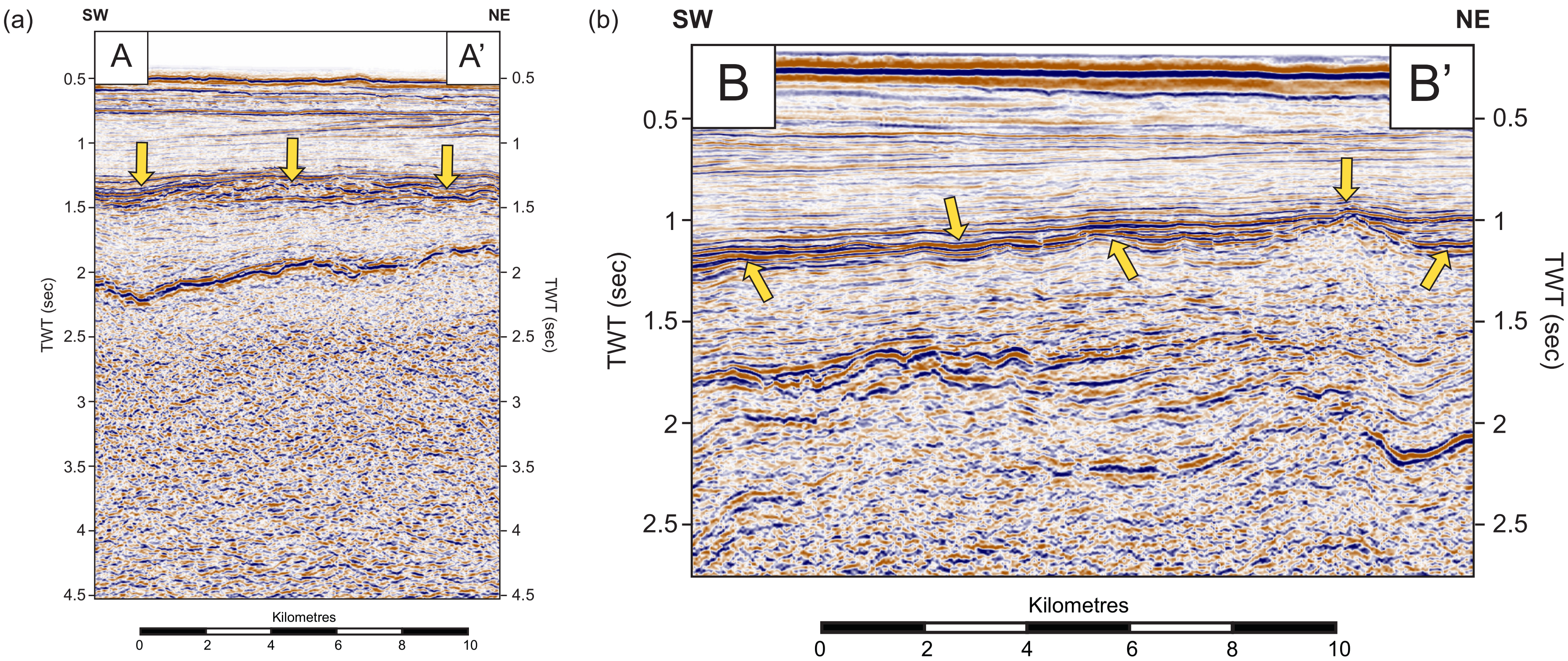

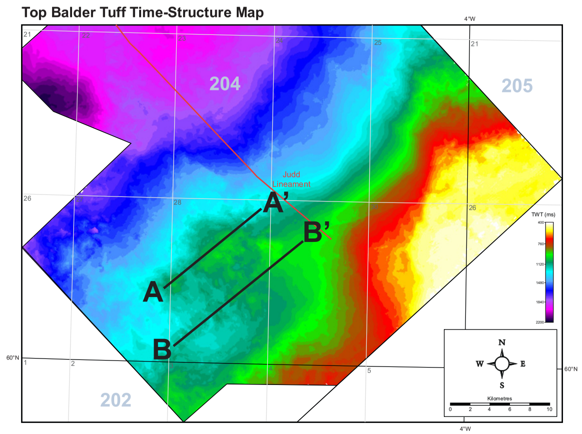

Figure 46
The Balder Tuff is a relatively strong amplitude reflector set amongst a series of strong reflections which appear truncated and eroded in many locations, meaning care is required to map the horizon accurately. Two examples are provided where it is very difficult to clearly identify the Balder Tuff from horizons above or below. This selection is also more difficult due to changes in the amplitude of the horizon which may be associated with variations in the ash and clay content of the horizon. This would be controlled by the environment of deposition at the time, and strong evidence of channelised erosion suggest a subaerial environment (Smallwood and Gill 2002). Amplitude maps made of the horizon failed to clearly confirm this interpretation and therefore a submarine channel system can not be fully ruled out as a hypothesis for the sedimentary environment.

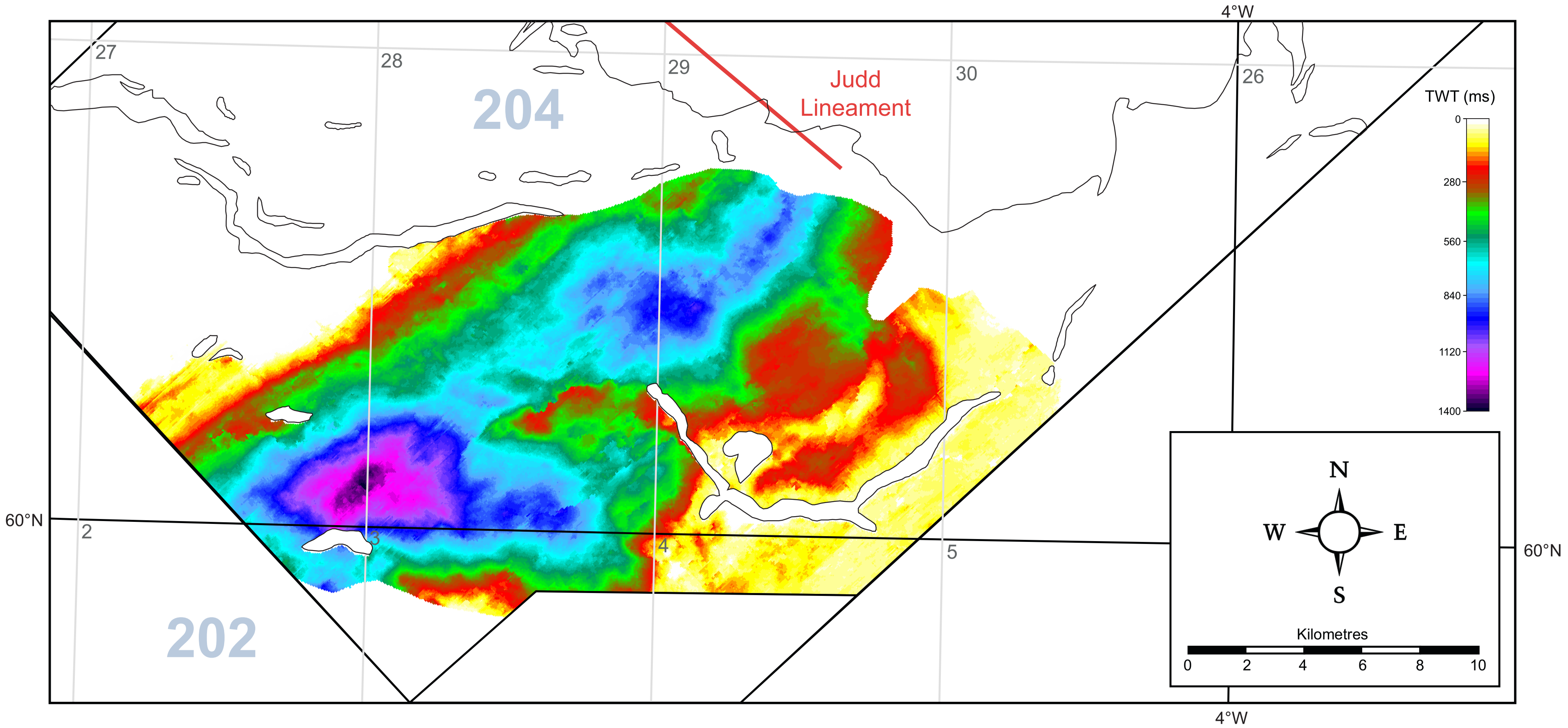

Figure 47
The time-thickness map includes the basinal fill of West Solan Basin (Carboniferous-Devonian pre-rift through to the Permian-Lower Jurassic syn-rift). Sedimentation is thin to absent on the flanks of the basin with the main depocentres located towards the centre, aligned in a NE-SW orientation. The sedimentation appears to be in two broad depocentres which are seperated by a thinner area of sedimentation in a NW-SE orientation (southern half of block 204/28) implying either sedimentation was focussed in these two regions or there is a structural barrier impeding the flow of sediment between each of these. Sedimentation patterns may be controlled by both these processes depending on the sedimentary processes at the time, but unfortunately there has been little characterisation of the Permo-Triassic-Lower Jurassic sequences in this basin due to a lack of well data. A hypothesis for the structural NW-SE high is that it was a high-relief accommodation zone (McClay *et al.* 2002) splitting the basin in two or alternatively the West Solan Basin may actually be two separate basins. The high is expected to be a source for sand in the basin due to active erosion under Permo-Triassic subaerial conditions which would be deposited within with the depocentre which may also outcrop beneath the Cretaceous Faroe-Shetland Basin to the north.

48 Cretaceous time-thickness map

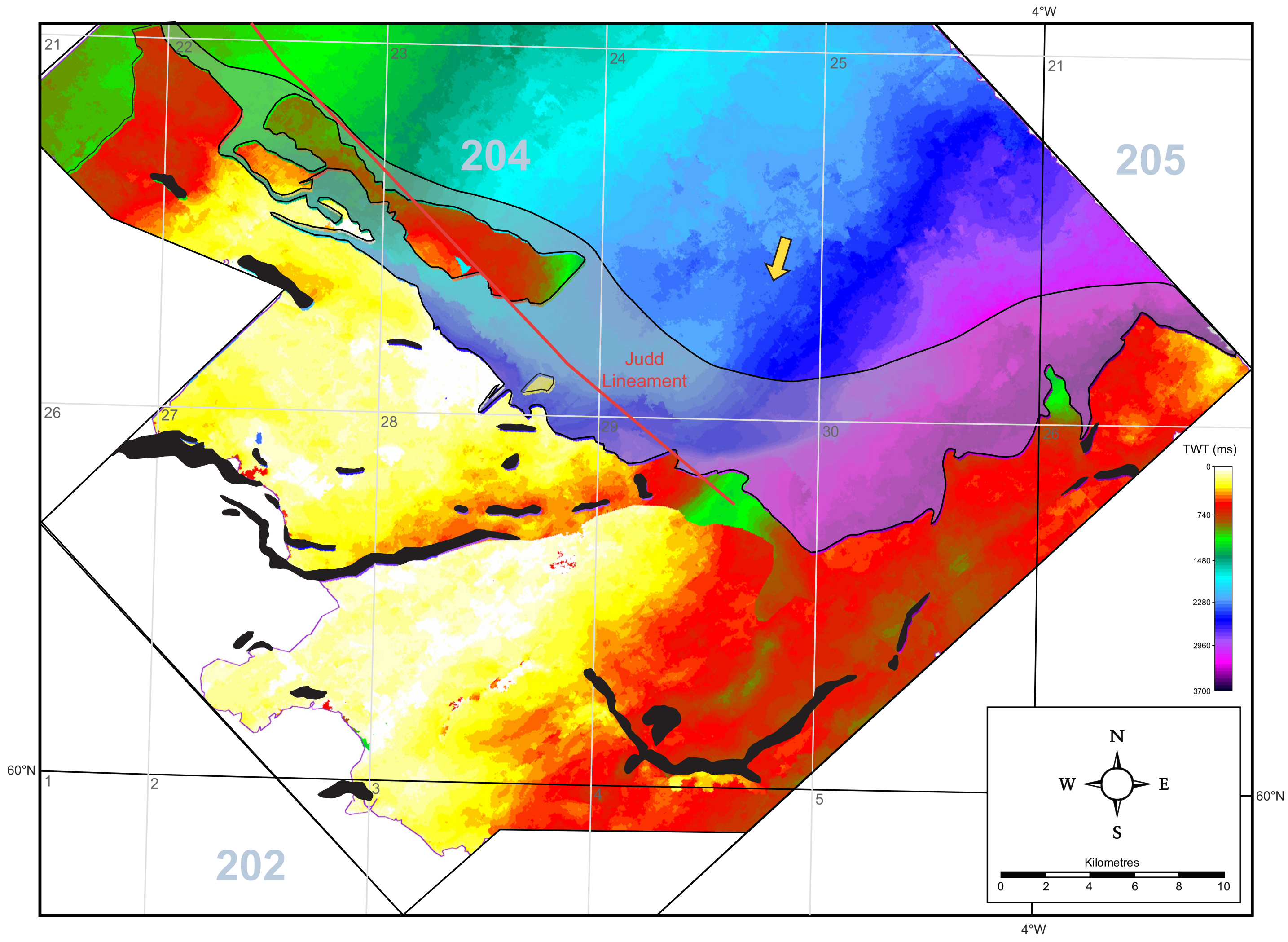

Figure 48
This map displays the areas with the thickest TWT Cretaceous succession within the study area. The sequence is thinnest upon the Judd High and within the West Solan Basin, but thickens to the southeast of the basin. This is due to the preferential reactivation of the bounding faults in this region during the deposition of the sequence.

The sequence is relatively thin upon the Rona Ridge but a thin subcrop implies the structural high was submerged at the time. The thickness of the sequence increases considerably into the Faroe-Shetland Basin however the base of the succession is very difficult to locate upon the seismic data. Also, the base of the succession to the north is limited by the vertical 4.5 sec TWT resolution of the seismic dataset. As the horizon deepens to the northwest, the calculated thickness decreases accordingly because of this. However, ithe observed thickness variation is believed to be representative of the Cretaceous succession as it is expected to thicken into the Rona Ridge Fault System. Similarly, there is evidence of thickening into the Judd Transfer Zone, particularly in the area of linkage between the fault systems and implying they were active at the same time.

To the northwest of the Judd High, an abrupt increase in the sediment thickness implies active Cretaceous faulting in this region.

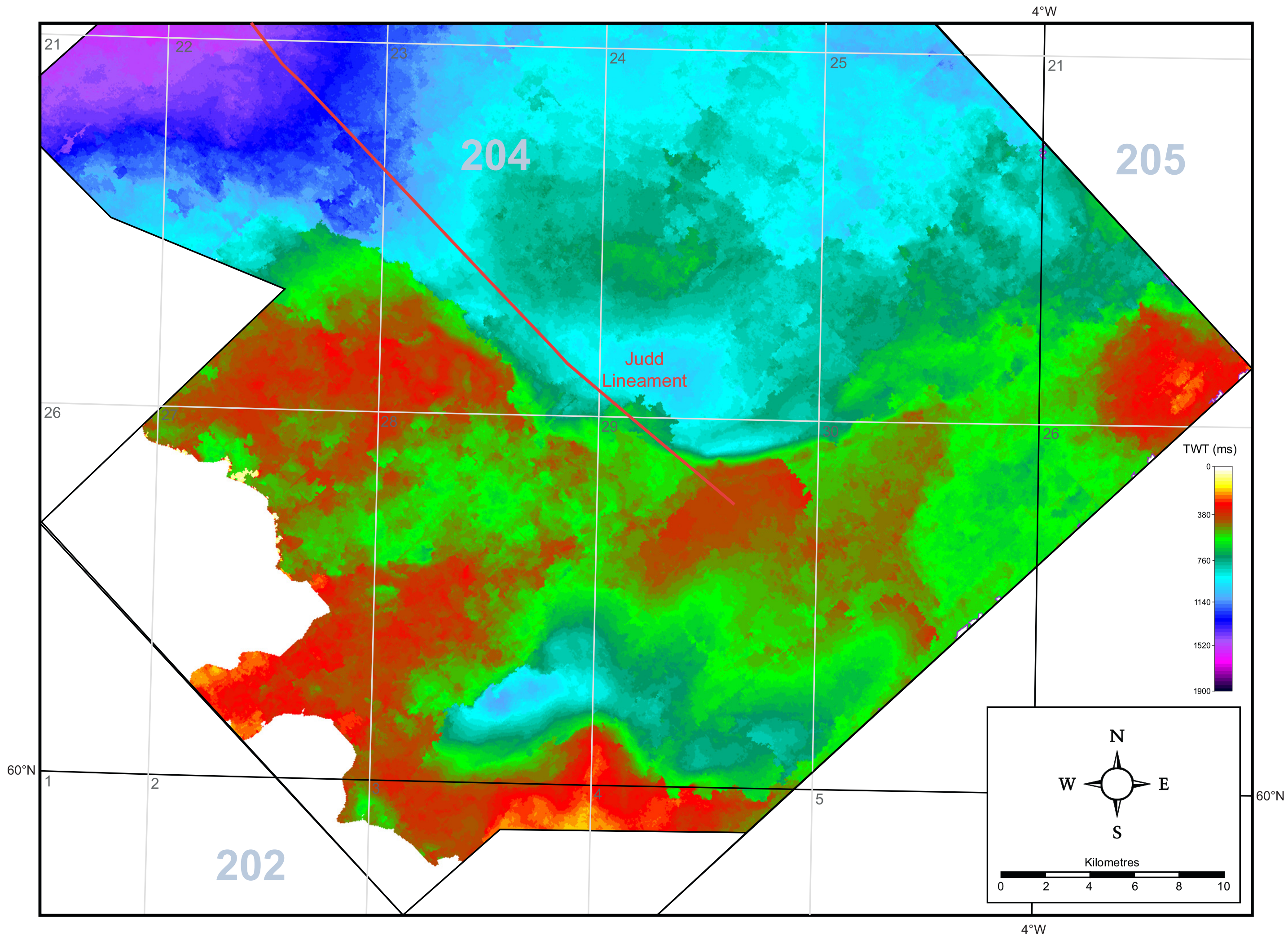

Figure 49
The Paleocene time-thickness map varies greatly across the study area however there is a lack of major faulting in the area to control the location of these thickness changes. In some areas there is a sharp transition, for example from the Rona Ridge and Judd High to the Faroe-Shetland Basin in blocks 204/23 and 204/29, which can be correlated with faults. However, there are areas along strike from these regions where the rate of thickness change is more gradual, implying sedimentation is simply filling the accommodation space created during Cretaceous rifting.

This pattern is similarly recognised in the West Solan Basin but there is little evidence supporting major faulting in the basin during this time. The thickness change displayed may be caused by an underfilling of the accommodation space during Cretaceous rift conditions and was subsequently filled by Paleocene sediment. Sedimentation rates in the Faroe-Shetland Basin increased greatly during this time (Smallwood and Gill 2002).

Variations in the thickness of Paleocene strata on the Judd High and Rona Ridge can also be linked to rifted areas on the high, but may also have been influenced by erosional processes in these areas during the early Eocene.

50 Post Paleocene time-thickness map

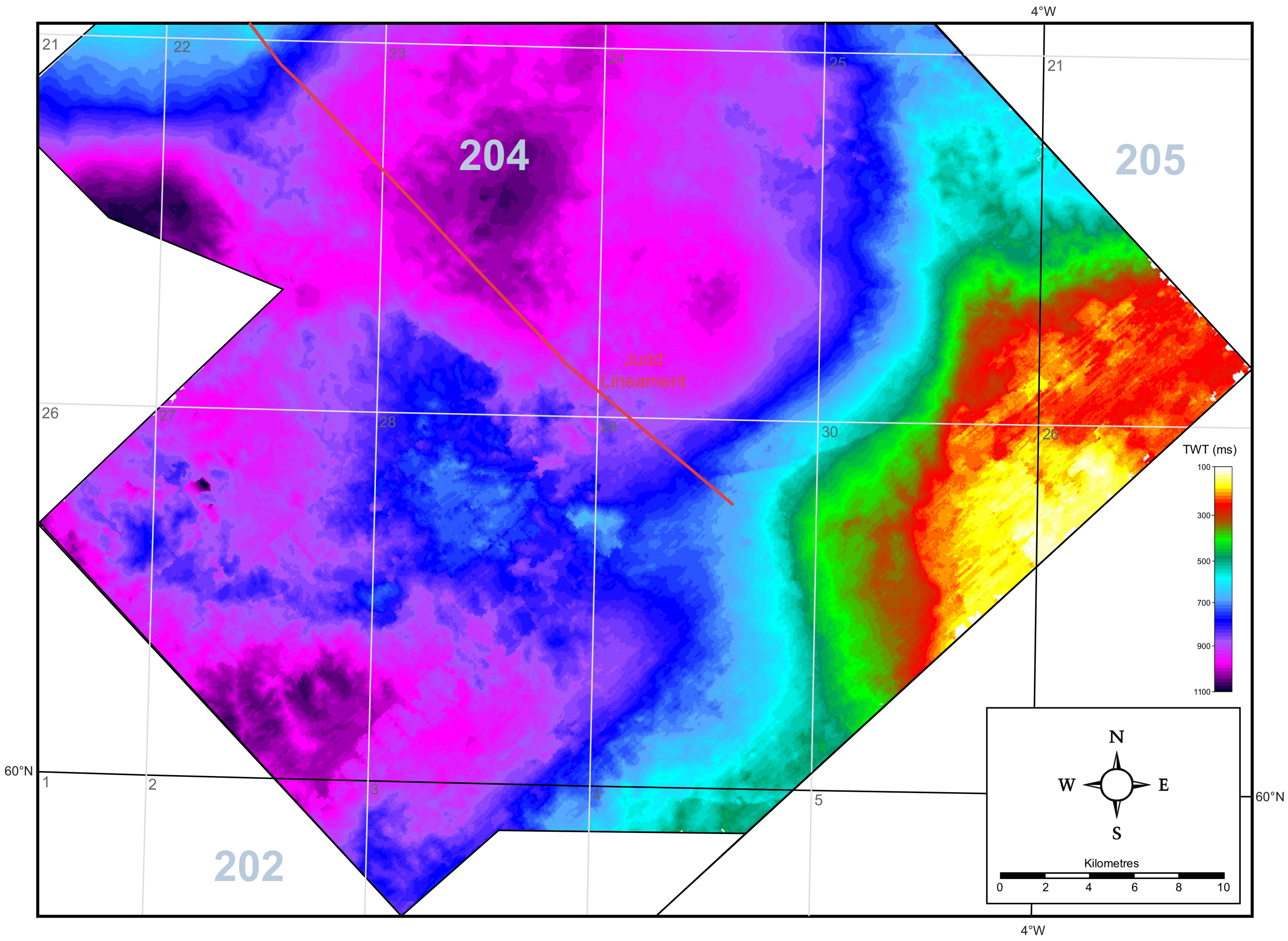

Figure 50
Post break-up sedimentation is greatest over the West Solan Basin, Judd High and Faroe-Shetland Basin. This is associated with the thermal subsidence of the Faroe-Shetland Basin in the areas directly above those which have been rifted. The Rona Ridge displays little subsidence following continental breakup as it is external to Cretaceous zone of rifting. The sediment thickness is not constant along the basins strike and although there are no longer active rift depocentres, the depcentres formed can be linked to the structural heterogeneity at depth.

The three depocentres are:

1) Above the West Solan Basin which was affected by Permo-Triassic-Lower Jurassic rifting with subsequent reactivation during the Cretaceous.
2) To the northwest of the Judd High in the Judd Sub-Basin, the transition between marked by Cretaceous faulting.
3) Above the Faroe-Shetland Basin near to the Judd Transfer Zone.

This complex post-rift pattern of sedimentation may infer the existence of rift oblique lineaments but can also be attributed to the complex rift topography at depth affecting the post-rift subsidence patterns.

51 Transition from the Rona Ridge to the Faroe-Shetland Basin

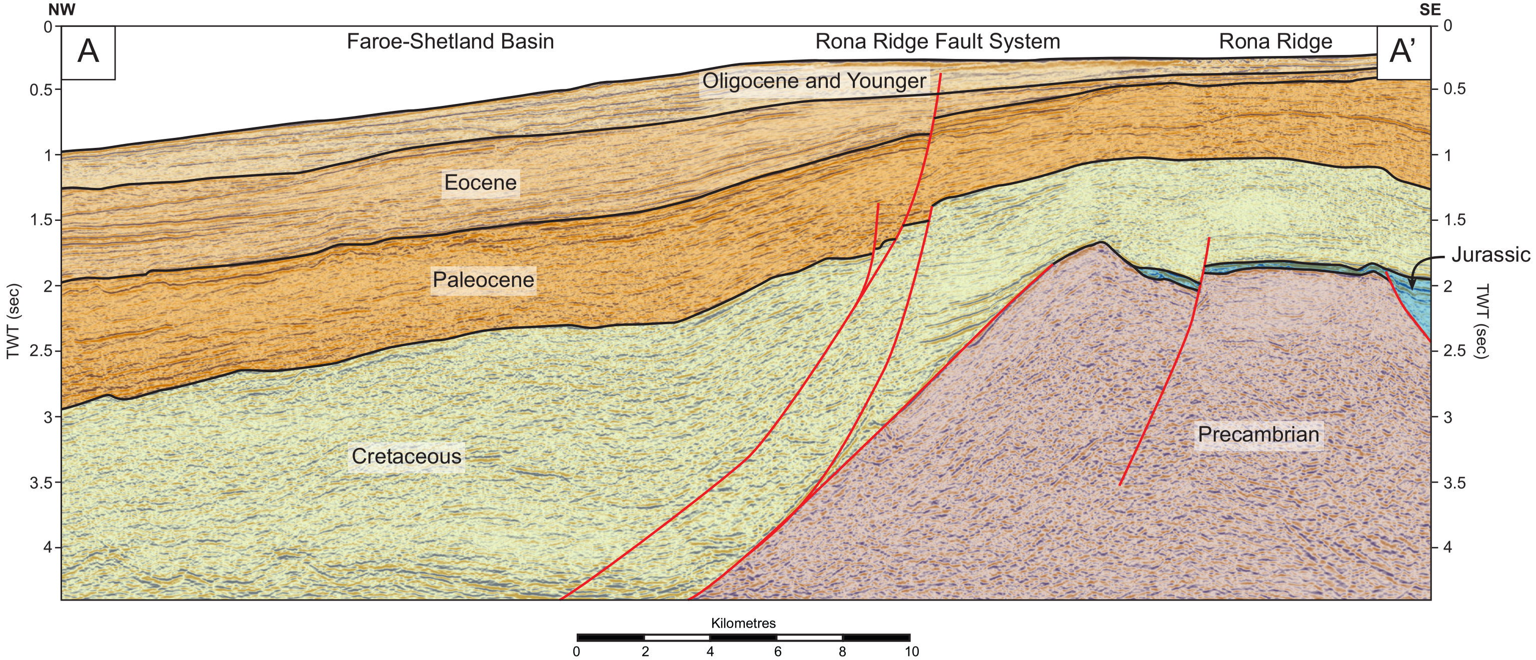

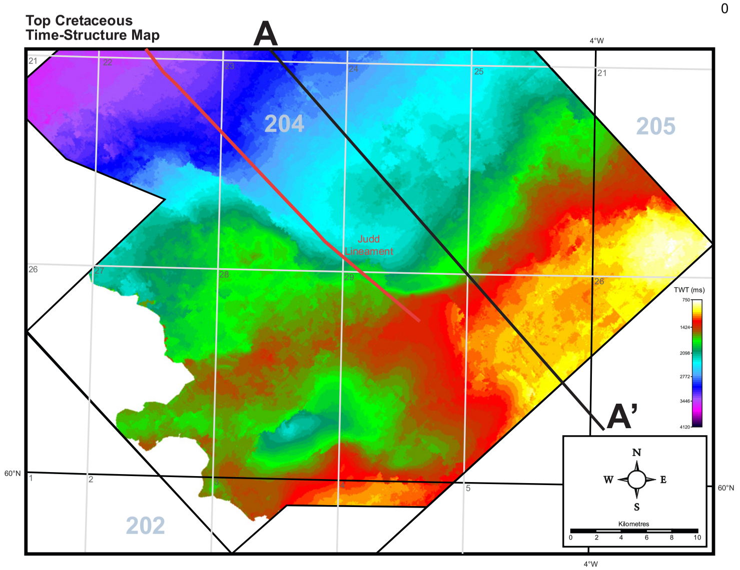

Figure 51
The Rona Ridge is cored by Precambrian basement with a thin Jurassic cover in this region. To the southeast, it bounds the Jurassic aged West Shetland Basin and to the northwest bounds the Cretaceous aged Faroe-Shetland Basin. Major Cretaceous faulting leads to a significant thickening of the sediment across the Rona Ridge but a lack of internal reflectivity within the sequence does not allow the exact timing to be clarified. Offsets of the top Cretaceous unconformity imply rifting continued into the Paleocene, but the small offsets and localised thickening of sediment may suggest an infilling of Cretaceous rift bathymetry by early Paleocene marine fans during tectonically quiescent conditions. Some faults extends close to the seabed, active during the Paleocene, Eocene and into the Neogene, but this may be related to the thermal subsidence of the basin and/or differential compaction of the sediment.

52 Transition from the Judd High to the Faroe-Shetland Basin

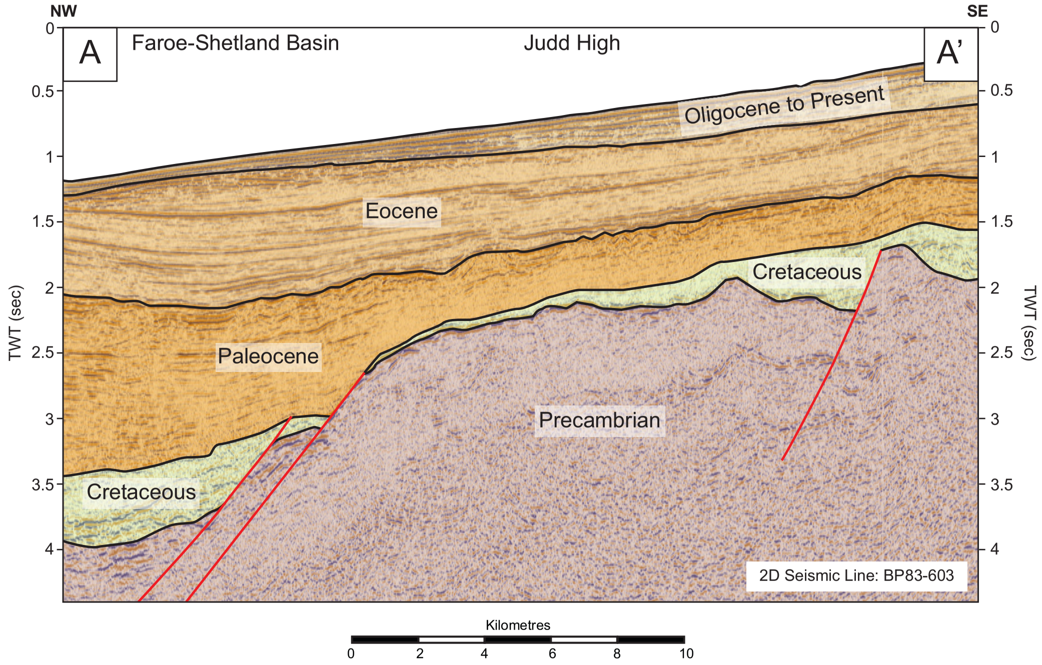

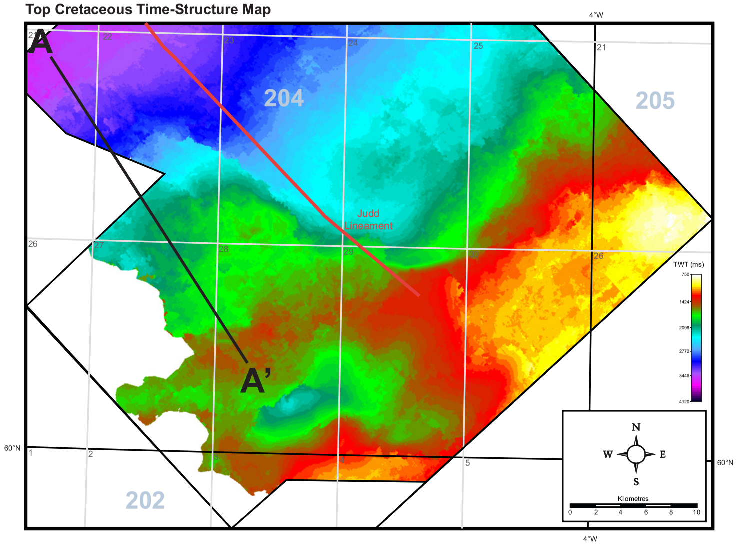

Figure 52

The Judd High is faulted down to the northwest, by inferred Cretaceous age faults. Thinning of the Cretaceous sequence across the high to the northwest and a lack of major thickening of the Cretaceous strata in the Judd Sub-Basin (despite major offsets across normal faults), suggests this area of the Faroe-Shetland Basin was underfilled during this time. There is little evidence for thickening of the Paleocene sequence into the fault offsetting the high from the sub-basin which compliments other interpretations that the Paleocene stratigraphy infills the pre-existing rift bathymetry. However this interpretation may be a limitation due to the lower resolution of the 2D seismic data. An additional problem associated with the Faroe-Shetland Basin is the increase in igneous intrusives within the Cretaceous succession to the northwest which can lead to errors in mapping of the sequences in that area.

53 Alternative examples of NW-SE oriented fault structures

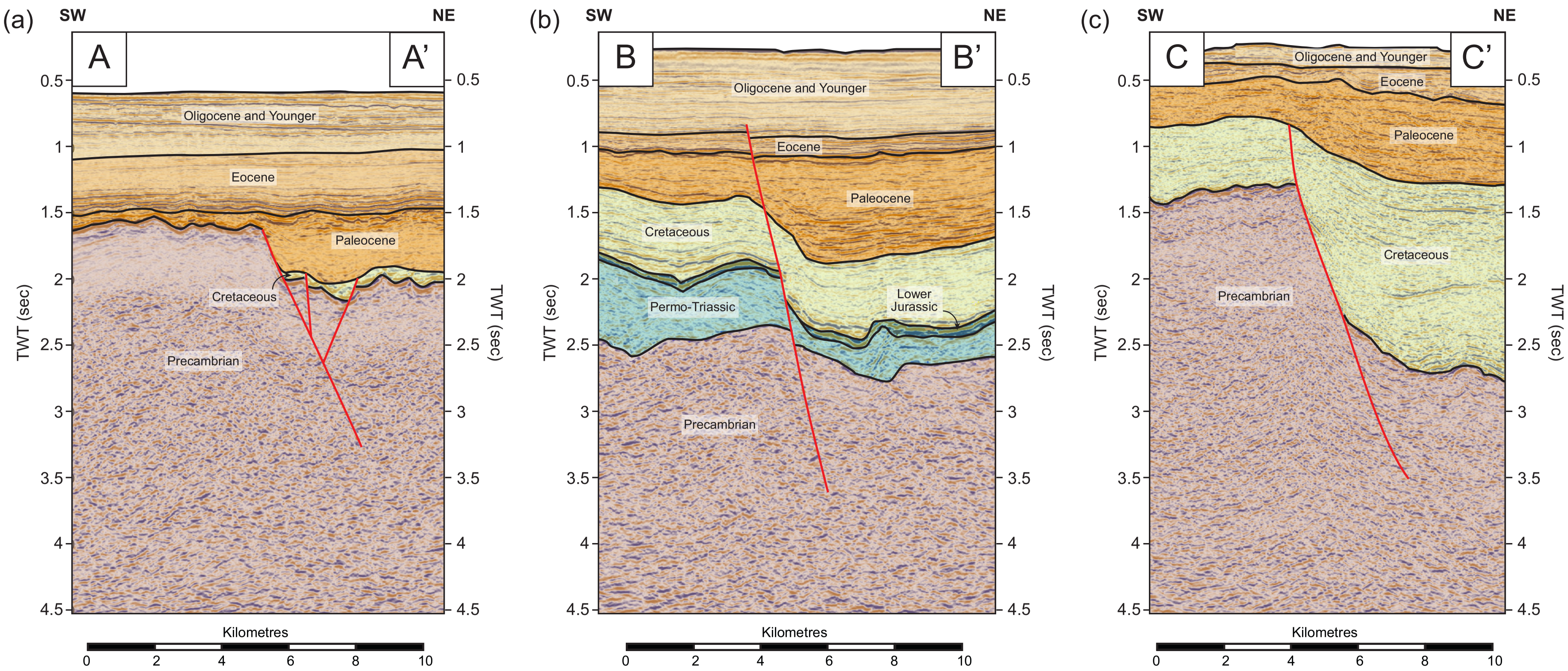

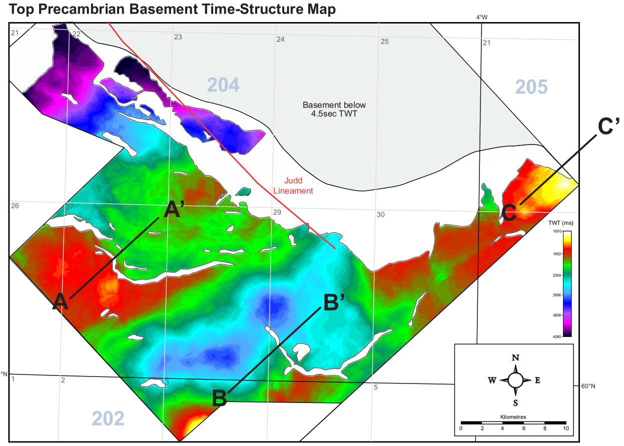

Figure 53
The Judd Transfer Zone is not the only NW-SE trending fault systems in the study area. Upon the Judd High (a) planar faulting normally offsets the Precambrian basement and is believed to be of Cretaceous age despite a thickening of Paleocene strata across the fault. It is believed that upon this high there was a large underfilling of the Cretaceous rift with sedimentation focussed down-dip in the Faroe-Shetland Basin. With increased sedimentation rates during a regressive systems tract in the Paleocene, the bathymetry was filled and then bypassed by marine mudstones and sandstones. Paleocene faulting can not be discounted but a transparent reflectivity of the sequence fails to clarify this. Cretaceous faulting is also evident along a NW-SE fault in the West Solan Basin (b) with minor reactivation in the Oligocene. Similarly, the Rona Ridge is segmented by Cretaceous faulting (c) to the east of the study area. A hypothesis as to why these faults form under Cretaceous rifting is that they are transfer zones on a smaller scale to the Judd Transfer Zone and may be successfully reactivating weak zones in the Precambrian basement.

54 Judd ant tracking fault interpretation results

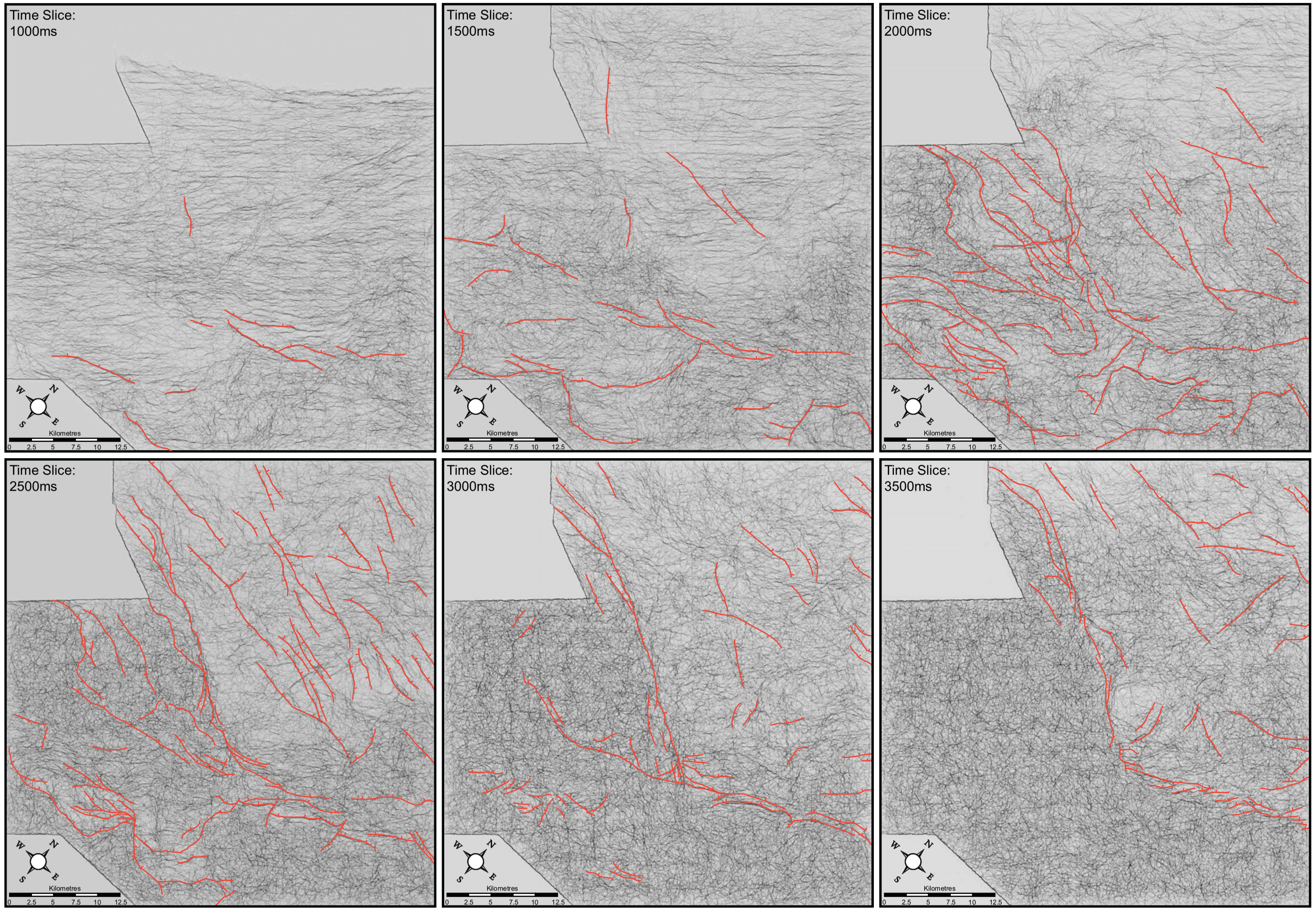

Methodology

A segy seismic volume was exported from the PGS MegaSurvey in Landmark to Schlumberger Petrel 2005 software.

Different variables were tested during the processing of the volume and those which gave the most favourable results are listed below:

Structural Smoothing:

Inline: 1.3
Crossline: 1.3
Vertical: 1.3

Variance:

Inline Range: 3
Crossline Range: 3
Vertical Smooth: 32

Ant Tracking (Passive Ants):

Initial Ant Boundary: 11
Ant Track Deviation: 3
Ant Step Size: 3
Illegal Steps: 2
Legal Steps: 2
Stop Criteria (%): 10

The volume was then re-imported to Landmark in order to correlate faults along strike interpreted in section views.

Figure 54

Due to the difficulty of interpreting Cretaceous faults within the Faroe-Shetland Basin an automated workflow (above) was attempted to interpret faults based upon the discontinuity of the seismic data. The resulting seismic volume contained increased amounts of noise making fault interpretation difficult in this area. However, the volume was used to map faults, initially recognised in cross section along various time slices; the results of which correlate well with the fault patterns identified from a variety of horizon maps. For example, the fault trends of the West Solan Basin, Rona Ridge, Judd High and Judd Transfer Zone as well as the east-west faulting of the Faroe-Shetland Basin are recognised. Unfortunately from this analysis, only strikes of the faults can be measured and not dip or dip direction.

55 Judd ant tracking fault orientations

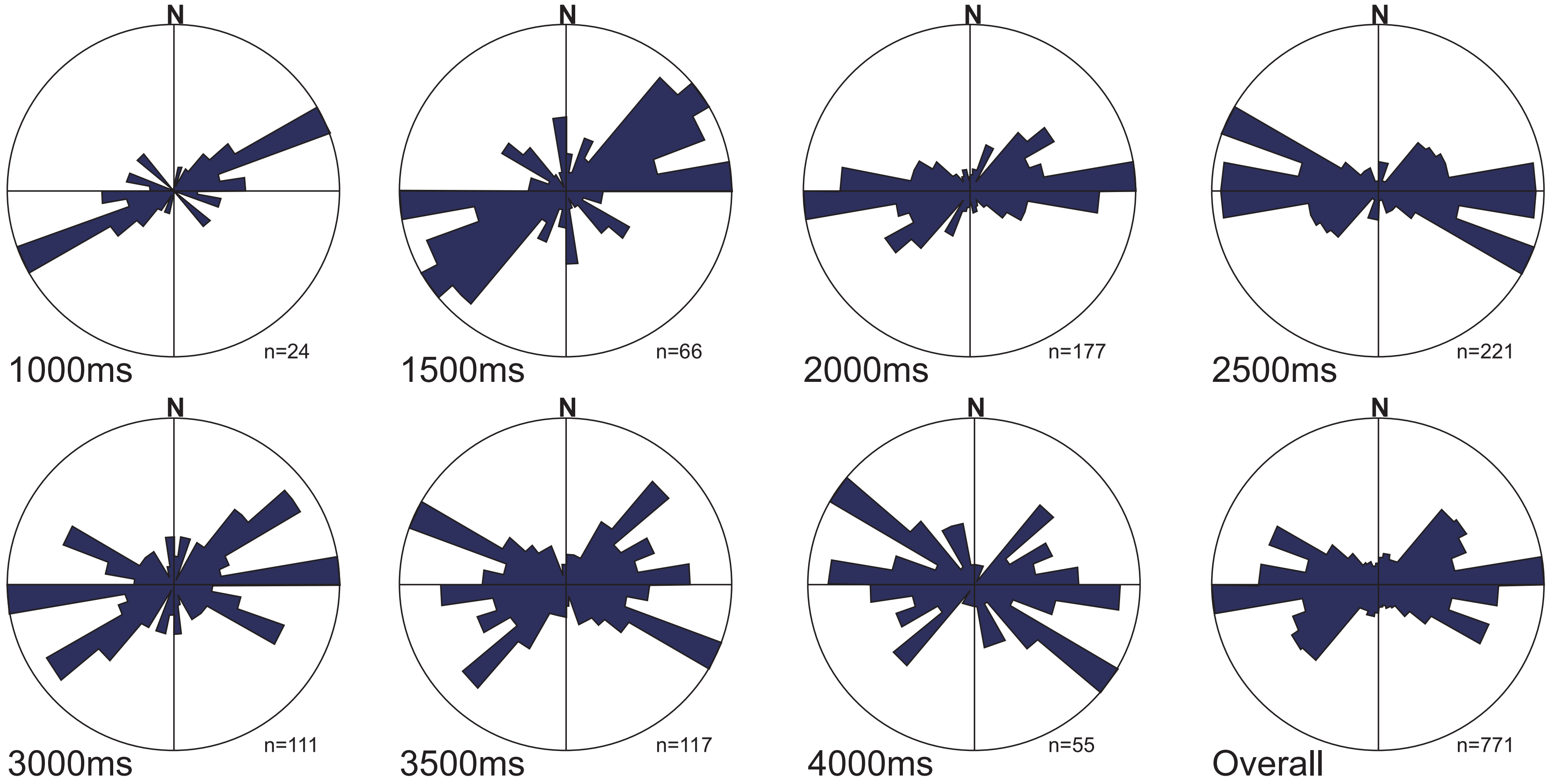

Figure 55

Fault orientation analyses of each time slice were made but as each of these slices dissect faults of different ages, the orientations change dramatically. The three main fault orientations are observed in the dataset are:

1) **E-W** - Permo-Triassic-Jurassic faulting in the West Solan Basin and Cretaceous faulting in the Faroe-Shetland Basin and upon the Judd High.
2) **NE-SW** - Faulting related to major Cretaceous rifting in the Faroe-Shetland Basin.
3) **NW-SE** - Dominantly associated with the Cretaceous Judd Transfer Zone but also smaller scale NW-SE faults upon the Judd High, Rona Ridge and West Solan Basin.

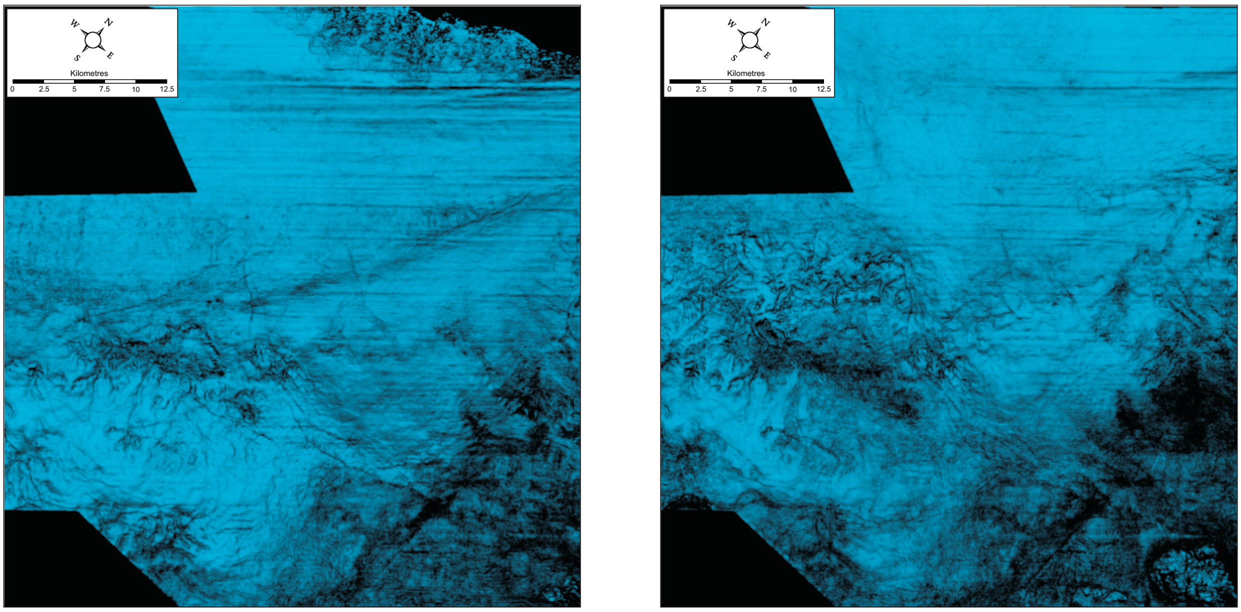

(a) 1500ms

(b) 1800ms

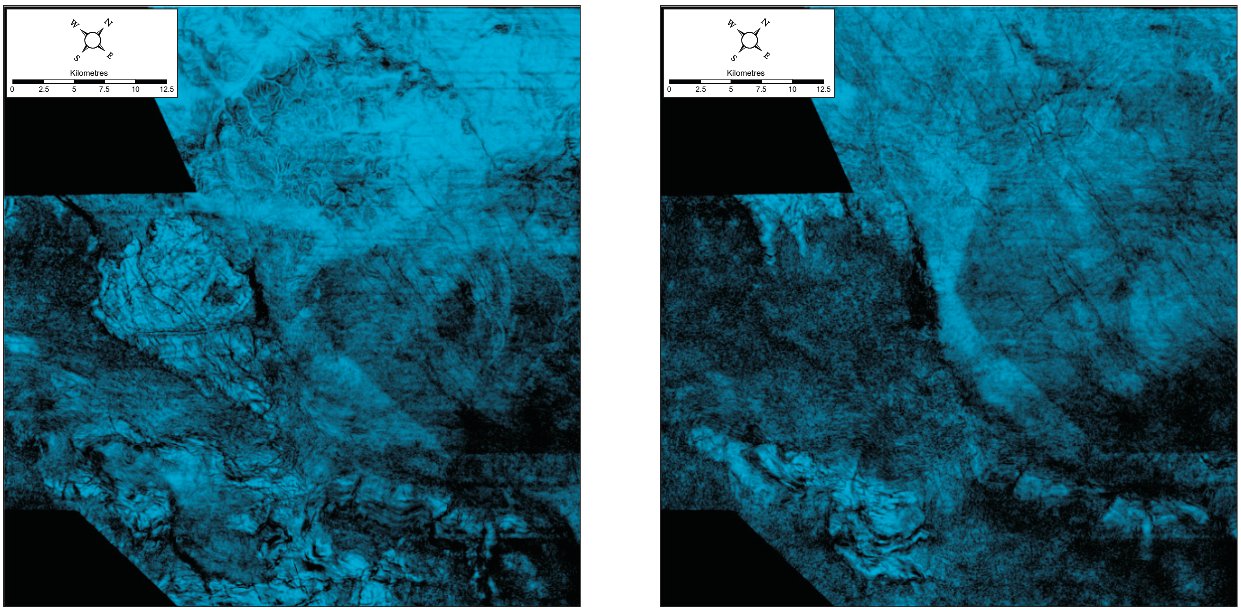

(c) 2452ms

(d) 2900ms

Figure 56

A semblance volume was created in Landmark Geoprobe software to compare the results with the Schlumberger Ant Tracking algorithm. The ant tracking volume was processed to identify faults but the semblance volume identifies any discontinuities which may be related to stratigraphical changes. Fault identification compares positively between the two processes (a) as well as the identification of processing artefacts associated with the acquisition and merging of 3D seismic datasets. Early Eocene fluvial networks are identified on the Judd High (b) and in the Faroe-Shetland Basin (c) but the semblance analysis improves the identification of the east-west faulting in the Faroe-Shetland Basin. The orientation of faults on the Judd High is clear within the semblance volume and also in the West Solan Basin (d). Analysis of the Precambrian fails to recognise any coherent NW-SE structures within the basement but still manages to identify east-west oriented faulting within the late Cretaceous of the Faroe-Shetland Basin at this depth. Below 3 sec TWT the resolution of the seismic data is reduced leading to increased noise in contrast to the Ant Tracking, where tentative fault interpretation can occur.

57 3D View of the Phanerozoic fault system in the Judd study area

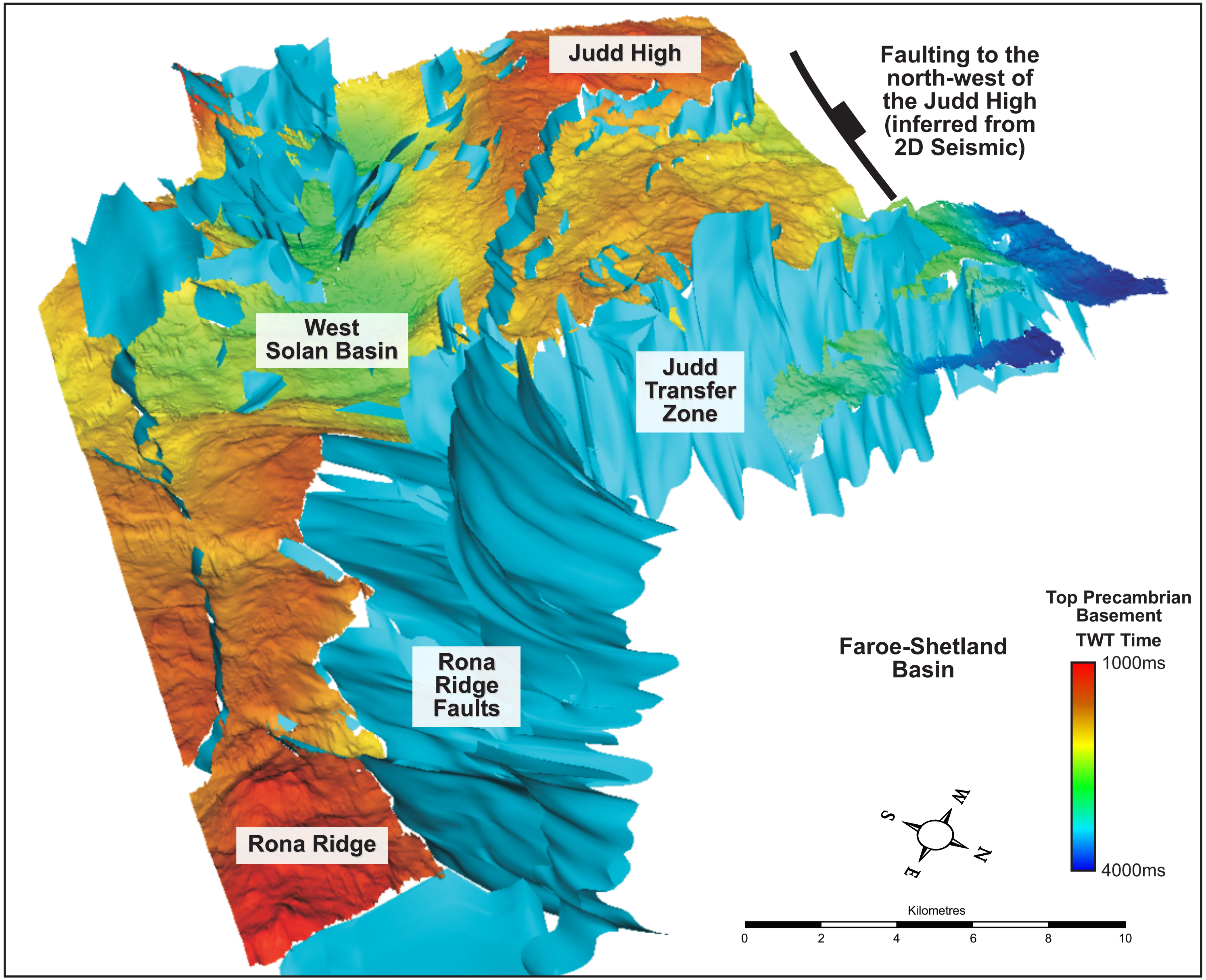

Figure 57
The West Solan Basin was formed under Permo-Triassic-lower Jurassic extension but the main phase of rifting that formed the Faroe-Shetland Basin was Cretaceous in age. The main orientation of the faults is NE-SW typified by the Rona Ridge Fault System, with similar normal faulting found to the northwest of the Judd High. Reactivations of the early rift faults occurred in the West Solan Basin and other Cretaceous faulting is observed upon the Judd High, however the majority of strain is transferred outboard of these regions by the Judd Transfer Zone.

Faults of the Rona Ridge rotate round into the Judd Transfer Zone and an area of hard linkage between the fault systems is observed. The Judd Transfer Zone is believed to have formed by reactivating zones of weakness in the Precambrian basement instead of rifting through an area of stronger lithosphere beneath the with West Solan Basin. Similar NW-SE trending faults are found in other areas of the dataset (West Solan Basin, Rona Ridge and Judd High) which may have formed for similar reasons.

Appendix C

Supporting material for Chapter 4

The fault data extracted from the structural models formed of the Gjallar Ridge and Nyk High are included upon the appended CD to the PhD thesis. This includes the raw fault data as extracted from Badleys TrapTester software and formulae used for the calculation of strain variation through time as displayed in Figures 4.14 and 4.20.

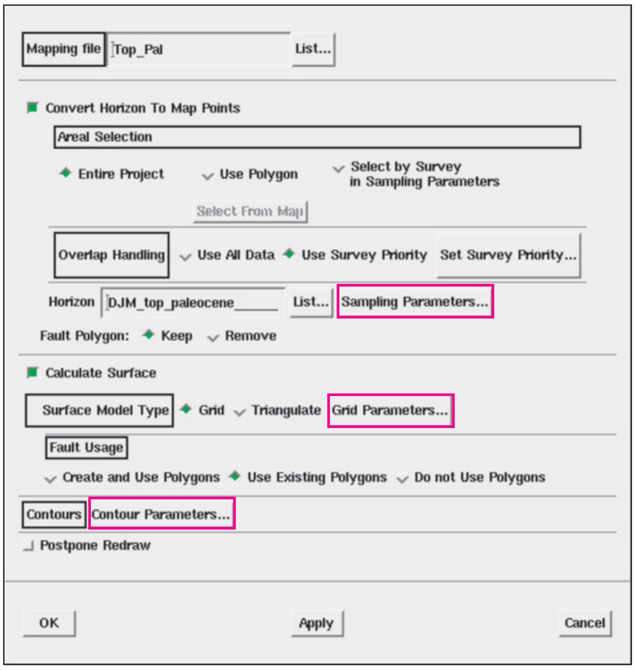

Mapping file: Top_Pal

☑ Convert Horizon To Map Points

Areal Selection: ● Entire Project ○ Use Polygon ○ Select by Survey in Sampling Parameters

Overlap Handling: ○ Use All Data ● Use Survey Priority

Horizon: DJM_top_paleocene

Fault Polygon: ● Keep ○ Remove

☑ Calculate Surface

Surface Model Type: ● Grid ○ Triangulate

Fault Usage: ○ Create and Use Polygons ● Use Existing Polygons ○ Do not Use Polygons

☐ Postpone Redraw

Sampling Parameters

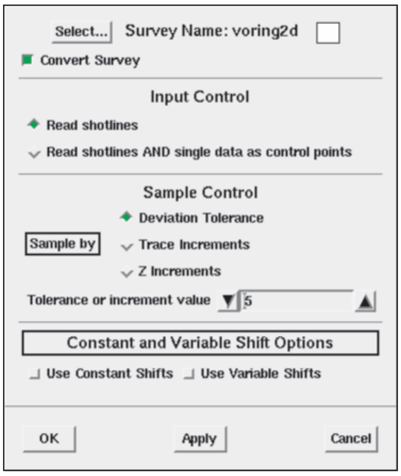

Survey Name: voring2d

☑ Convert Survey

Input Control: ● Read shotlines ○ Read shotlines AND single data as control points

Sample Control: Sample by ● Deviation Tolerance ○ Trace Increments ○ Z Increments

Tolerance or increment value: 5

Constant and Variable Shift Options: ☐ Use Constant Shifts ☐ Use Variable Shifts

Grid Parameters

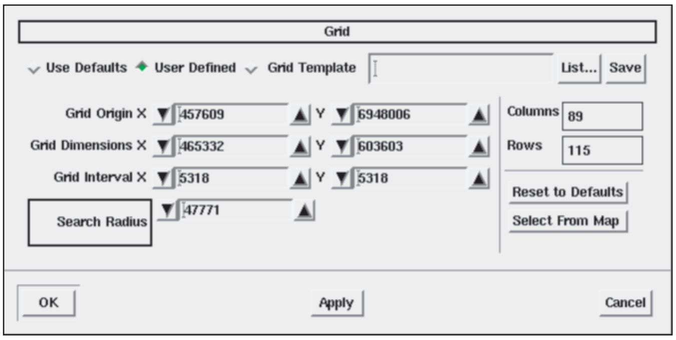

Grid: ○ Use Defaults ● User Defined ○ Grid Template

Grid Origin X 457609 Y 6948006

Grid Dimensions X 465332 Y 603603

Grid Interval X 5318 Y 5318

Search Radius 47771

Columns 89

Rows 115

Contour Parameters

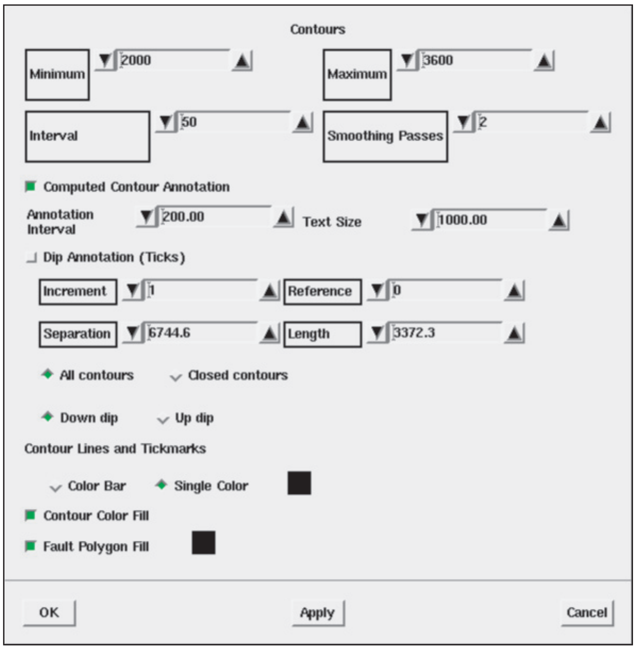

Contours

Minimum 2000 Maximum 3600

Interval 50 Smoothing Passes 2

☑ Computed Contour Annotation

Annotation Interval 200.00 Text Size 1000.00

☐ Dip Annotation (Ticks)

Increment 1 Reference 0

Separation 6744.6 Length 3372.3

● All contours ○ Closed contours

● Down dip ○ Up dip

Contour Lines and Tickmarks: ○ Color Bar ● Single Color ■

☑ Contour Color Fill

☑ Fault Polygon Fill ■

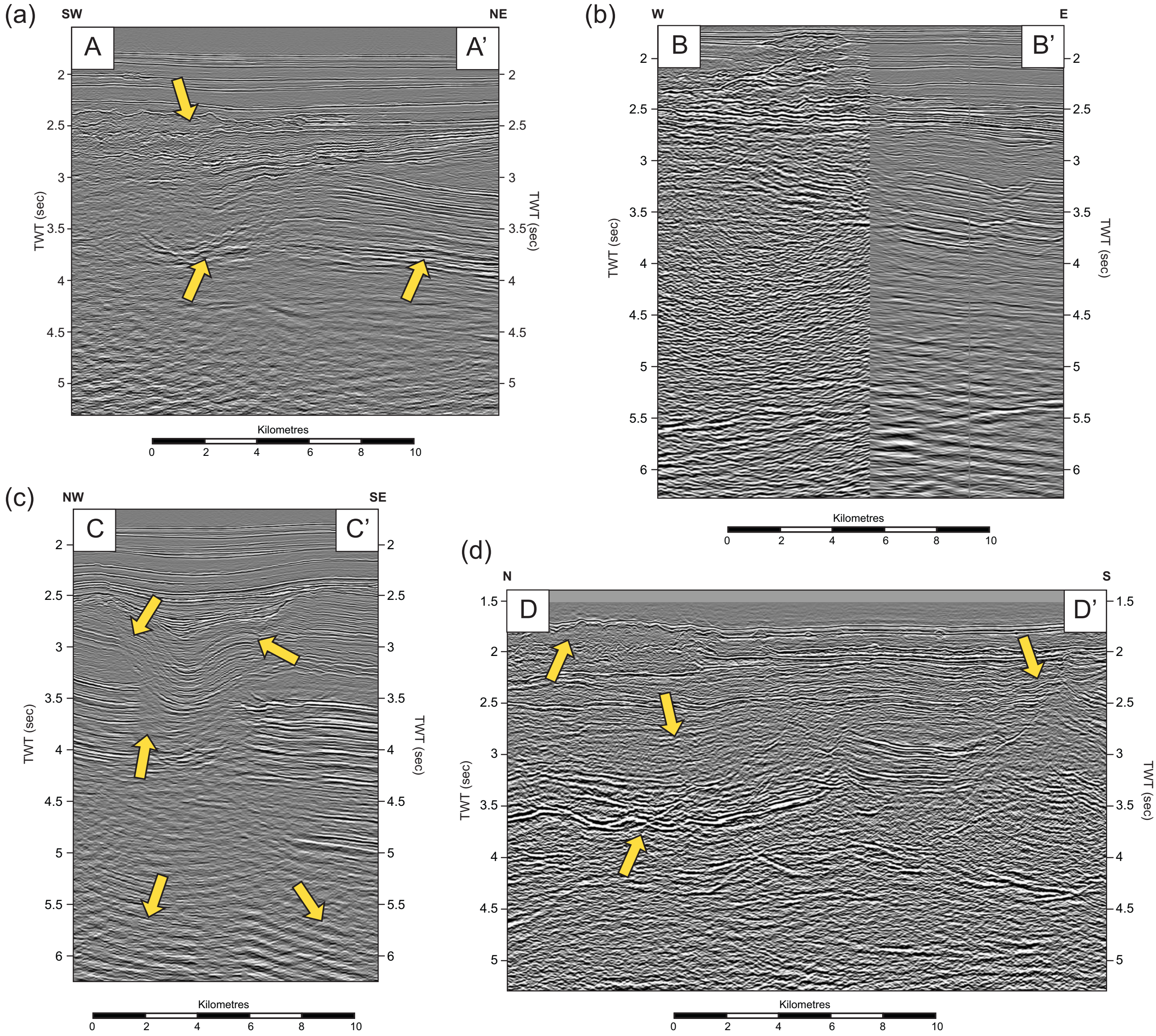

Figure 02
The Nyk High seismic dataset has a lower resolution to the Gjallar Ridge seismic data for multiple reasons. Firstly, remobilised siliceous ooze (a) attenuates the seismic signal resulting in poor definition of the deeper horizons. Secondly, the dataset is composed of two very differently processed datasets (b) which gives rise to a reduction of interpretation accuracy between the eastern and western surveys. Thirdly, the seismic dataset appears to have been over migrated in sections with poor definition of fault planes (c) with multiple migration smiles forming at depth. Fourthly, fault shadowing impacts upon the relectivity of the deeper sequences (c) and lastly Cenozoic igneous sill intrusions (d) reduce the resolution of the seismic data, making fault and horizon interpretation hazardous where present.

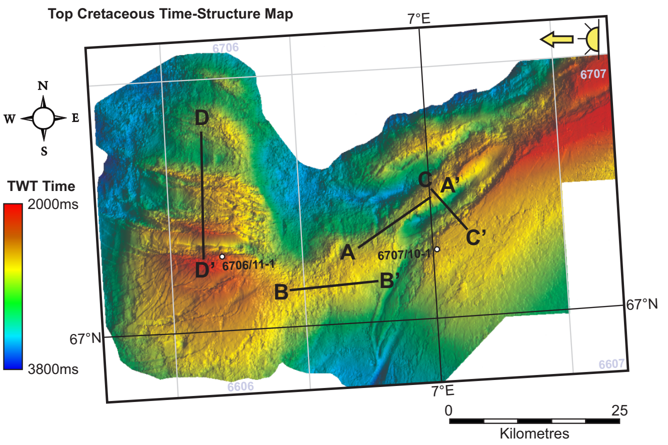

03 Well 6704/12-1 well to seismic tie and seismic stratigraphy

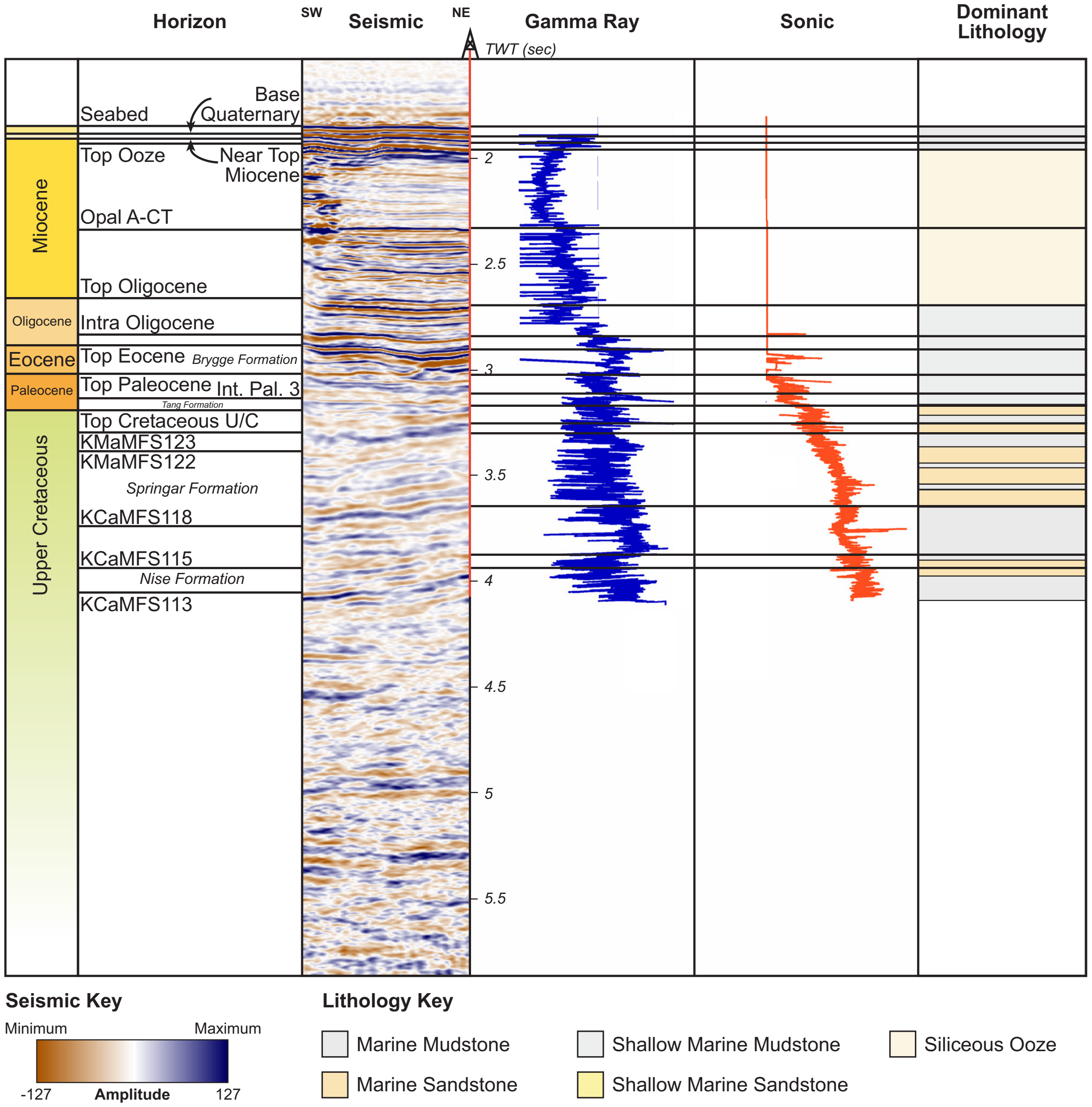

Lithology Key

- ▢ Marine Mudstone
- ▢ Marine Sandstone
- ▢ Shallow Marine Mudstone
- ▢ Shallow Marine Sandstone
- ▢ Siliceous Ooze

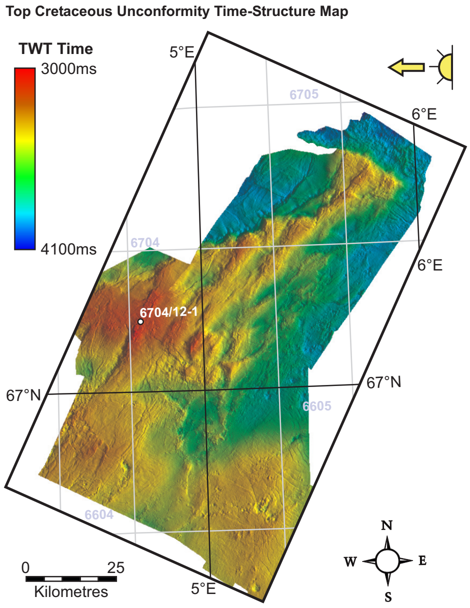

Figure 03

Well 6704/12-1 reached total depth in the Santonian, penetrating the upper Cretaceous strata which is dominantly mud prone. Due to this, low reflectivity on the seismic data makes it difficult to identify the maximum flooding surfaces. This leads to dating problems when correlating reflectors away from the well. Increasing amounts of marine fan sandstones in the Maastrichtian fail to display high reflectivity upon the seismic dataset. Equally, the late Cretaceous unconformity displays a weak, positive response.

Thin Paleocene and Eocene deposits give way to mudstone and siliceous ooze which are of increased reflectivity beneath the Opal A-CT transition.

04 Well 6706/11-1 well to seismic tie and seismic stratigraphy

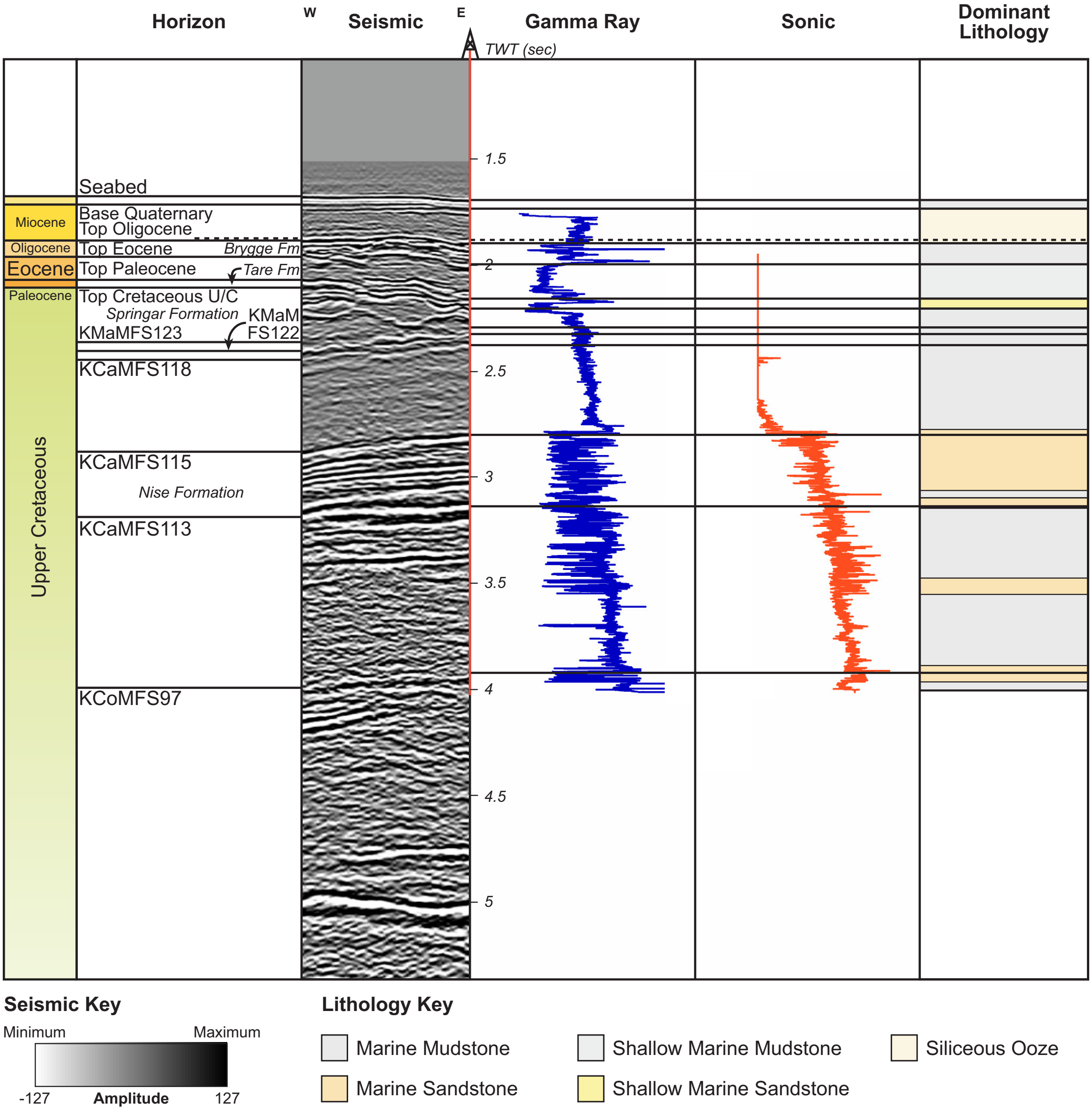

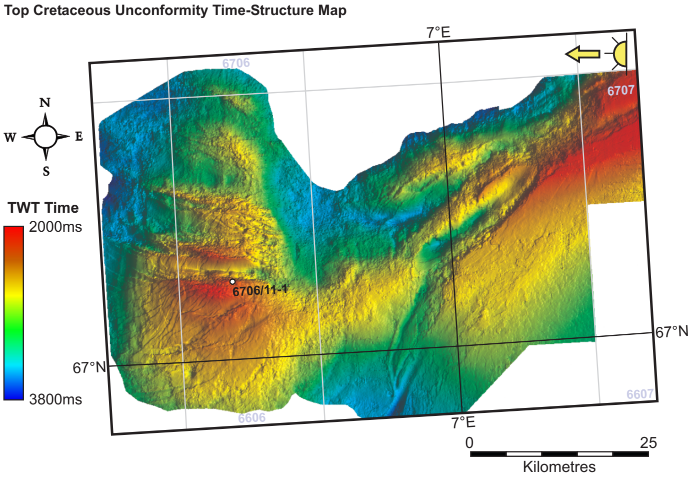

Figure 04

Well 6706/11-1 reached total depth in the upper Turonian, with the overlying Lysing Sandstone Member creating a prominent high amplitude response on the seismic data. The Campanian Nise Formation is displayed by a series of high amplitude, concordant reflections formed due to the varying quality of the marine fan sandstones (Kittilsen *et al.* 1999). The late Campanian sequence displays little internal reflectivity due to the dominant mudstone deposits, with the Maastrichtian and early Cenozoic horizons displaying a complex array of discordant strong and weak amplitude reflections.

05 Well 6707/10-1 well to seismic tie and seismic stratigraphy

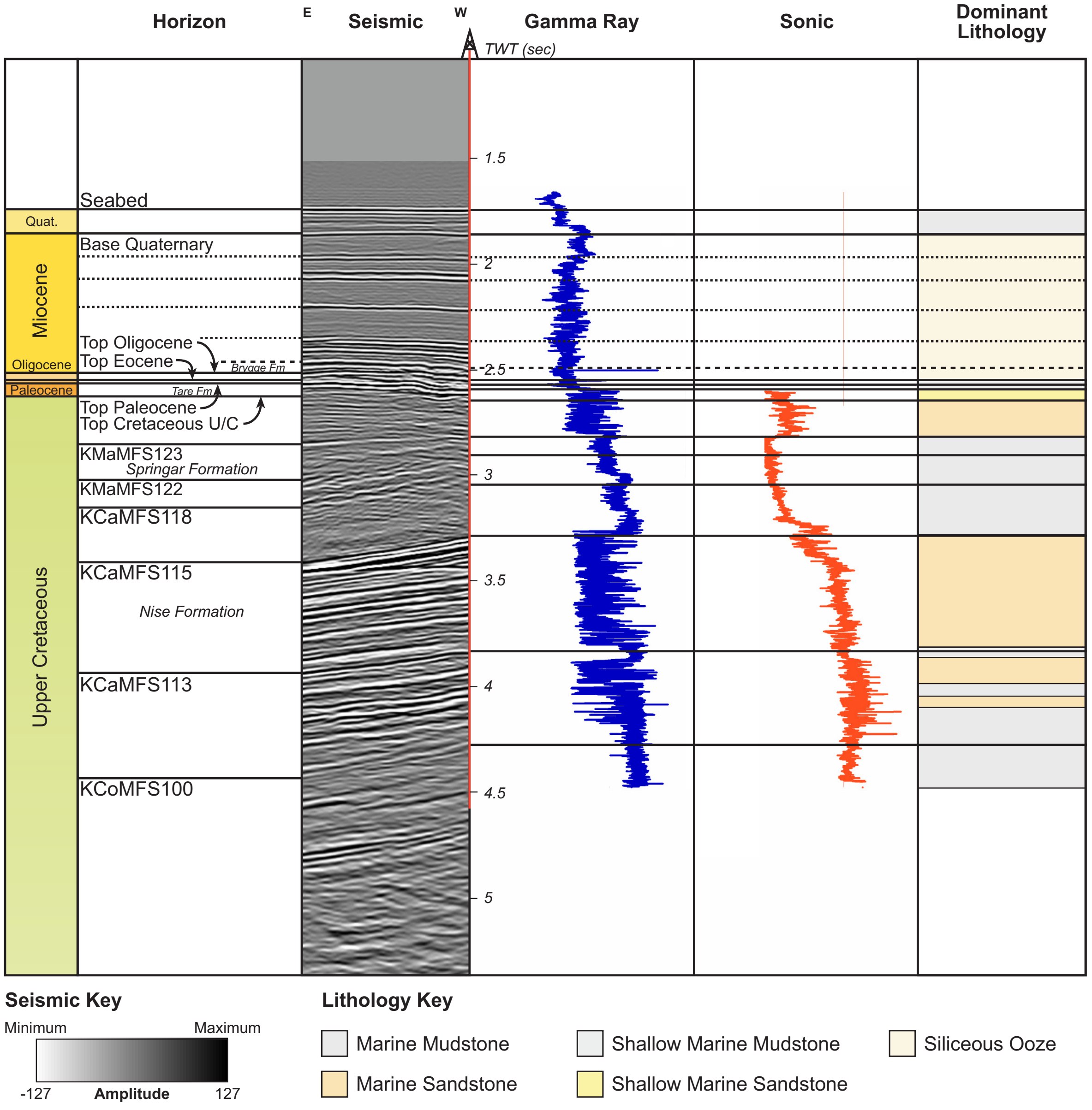

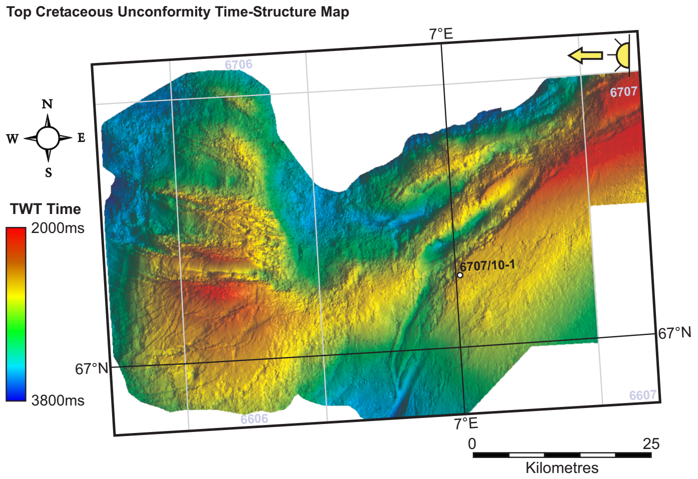

Figure 05

Well 6707/10-1 ties relatively well with the seismic data. Penetrating a thick Campanian sandstone sequence, the seismic data displays a concordant set of reflectors overlain by upper Campanian mudstones displaying a relatively transparent reflectivity. The overlying Maastrichtian successions displays somewhat increased internal reflectivity within a regressive sequence of marine deposits which is overlain by a series of lower Cenozoic shallow marine sandstones which display both strong and weak amplitude responses. The Miocene siliceous ooze is displayed as a series of concordant reflections.

Well 6704/12-1 (Gjallar Ridge)

Horizon	*TWT (ms)*	*Depth (m)*	*Difference - TWT (ms)*	*Difference - Depth (m)*	*Interval Velocity (m/s)*
Top Cretaceous	3155	2558			
Top Campanian	3620	3250	465	692	2976
Top Santonian	3941	3814	321	564	3514

Well 6706/11-1 (Southern Rym Accommodation Zone)

Horizon	*TWT (ms)*	*Depth (m)*	*Difference - TWT (ms)*	*Difference - Depth (m)*	*Interval Velocity (m/s)*
Top Cretaceous	2206	1723			
Top Campanian	2456	1931	250	208	1664
Top Santonian	3350	3154	894	1223	2736

Well 6707/10-1 (Nyk High)

Horizon	*TWT (ms)*	*Depth (m)*	*Difference - TWT (ms)*	*Difference - Depth (m)*	*Interval Velocity (m/s)*
Top Cretaceous	2636	2208			
Top Campanian	3032	2660	396	452	2282
Top Santonian	3890	3905	858	1245	2902

Therefore for the purposes of this study, the assumption for the ratio between TWT and depth (average interval velocity / 2) in the vicinity of:

the Gjallar Ridge;	1 sec TWT ~ 1600 m
the Southern Rym Accommodation Zone;	1 sec TWT ~ 1100 m
the Nyk High;	1 sec TWT ~ 1300 m

The lateral variation in the velocity of Cretaceous basin fill is relatively large, and is expected to increase where sills are present. Sills are assumed to be of basic composition as drilled elsewhere in the Vøring Basin and Faroe-Shetland Basin. Therefore a depth conversion of 1 sec TWT ~ 1500 m is considered accurate for all other areas of the region including the Hel Graben and Någrind and Vigrid Synclines.

07 Values for the distance vs. cumulative heave plot (Figure 4.14)

Gjallar Total Line Length (km) 26.84782609 **Line: Fig 4.13a**
Based on offset of Top Santonian KCaMFS113

Fault No.	Distance (km)	Cum. Heave (km)	Cum. Heave (km)
1	4.782608696	0.9	1.956521739
2	6.260869565	1	2.173913043
3	9.782608696	2.4	5.217391304
4	14.7826087	2.46	5.347826087
5	15.97826087	3.96	8.608695652
6	23.26086957	6.06	13.17391304
	26.84782609		

Note: Hangingwall intersection with Fault 6 not located on interpreted section

Nyk Total Line Length (km) 22.82608696 **Line: Fig 4.18b**
Based on offset of Top Santonian KCaMFS113

Fault No.	Distance (km)	Cum. Heave (km)	Cum. Heave (km)
1	8.804347826	0.05	0.108695652
2	9.782608696	0.12	0.260869565
3	10.54347826	0.16	0.347826087
4	14.23913043	0.66	1.434782609
5	16.73913043	0.69	1.5
6	21.41304348	1.34	2.913043478
	22.82608696		

Note: Hangingwall intersection with Fault 6 not located on interpreted section

S. RAZ Total Line Length (km) 30.90909091 **Line: Fig 4.19b**
Based on offset of Top Campanian KCaMFS118

Fault No.	Distance (km)	Cum. Heave (km)	Cum. Heave (km)
1	1.931818182	0.05	0.113636364
2	4.886363636	0.16	0.363636364
3	8.636363636	0.56	1.272727273
4	12.04545455	1.16	2.636363636
5	16.81818182	1.46	3.318181818
6	18.06818182	2.11	4.795454545
7	22.5	2.41	5.477272727
8	27.38636364	2.61	5.931818182
	30.90909091		

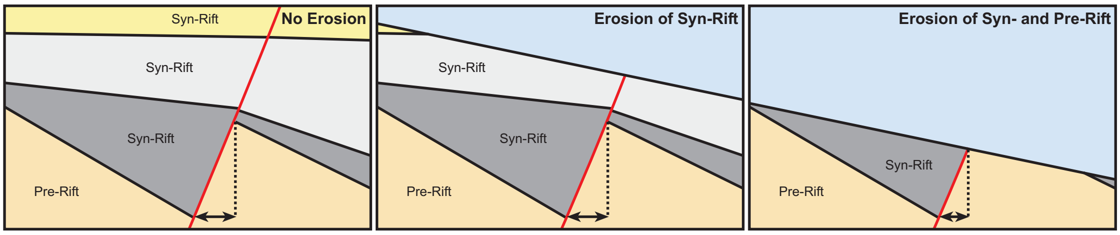

Figure 07
Heaves for individual faults were calculated from the top of the pre-rift succession in the footwall to the top of the pre-rift succession in the hangingwall. The heaves were calculated from offsets of the pre-rift sequence as this would account for the total extension along the fault in each of the late Cretaceous - Paleocene rift periods. This therefore excludes any associated effects caused by erosion of the syn-rift sequence, except where completely removed in close proximity to the faults leading to erosion of the pre-rift sequence. This effect is minimised in these calculations as the lines selected for the cumulative heave analysis have experienced little, if any erosion of the pre-rift succession.

The assumed pre-rift succession tops are as follows:

Gjallar Ridge	Top Coniacian (KCoMFS100)
Nyk High	Top Santonian (KCaMFS113)
Southern RAZ	Top Campanian (KCaMFS118)

Despite a variation in the pre-rift succession horizon used for the analysis in each area, it is believed that each of the selected horizons will account for all of the observed faulting. Varying the selected horizon will also reduce the associated error in the interpretation due to the improved seismic resolution gained at shallower depths, rather than selecting an uncertain constant horizon in the Nyk High and Vema Dome (e.g. Top Coniacian). It is also particularly poignant, as timing for initial rifting across the region varies.

08 Dip maps of the KCaMFS115, KCaMFS118, top Cretaceous and top Paleocene of the Nyk High and southern RAZ

(a) KCaMFS115

(b) KCaMFS118

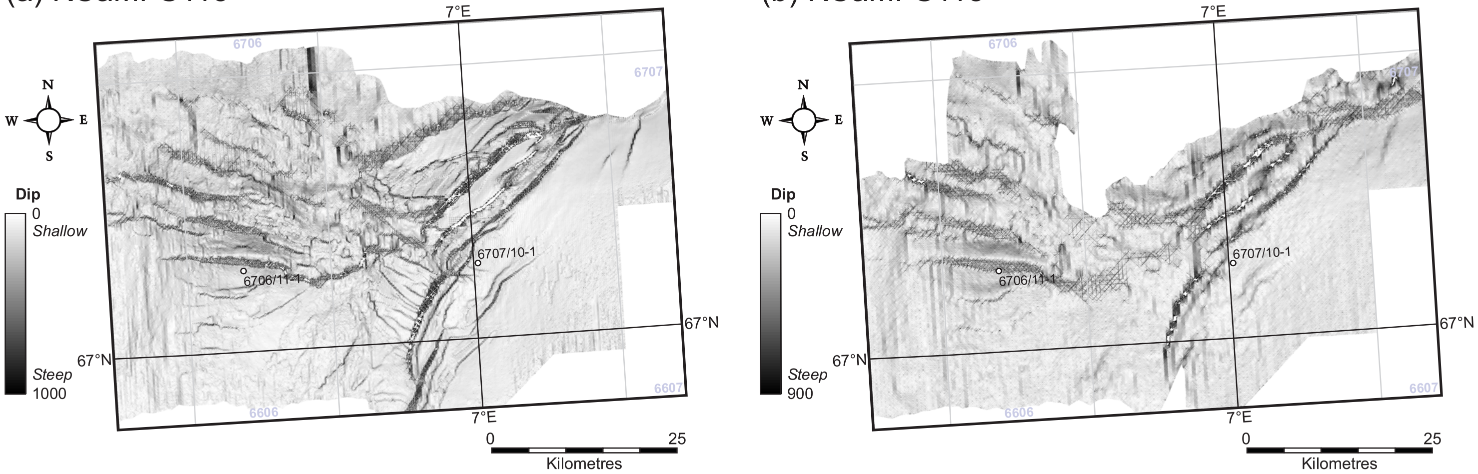

(c) Top Cretaceous

(d) Top Paleocene

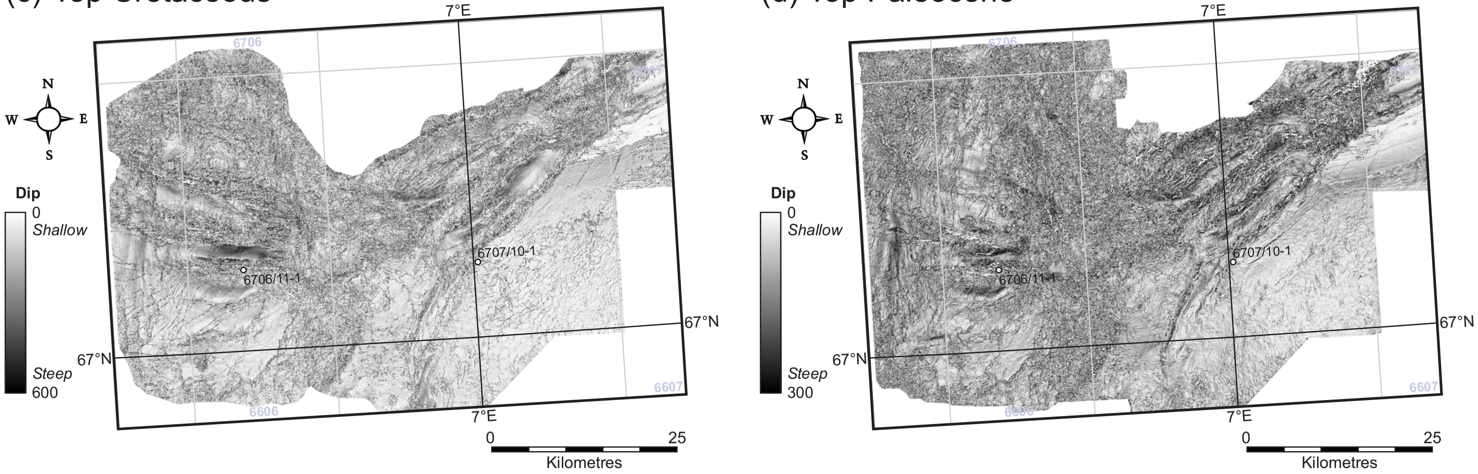

Figure 08

Dip maps of the horizons highlight the dominant fault trends within the Nyk High and the adjacent Rym Accommodation Zone. These dip maps aided in the correlation of fault sticks interpreted on 2D seismic sections within the 3D fault model produced in Badleys TrapTester software. The top Cretaceous and top Paleocene horizons highlight the complexity of faulting within the seismic dataset. Small scale faults are often poorly imaged by the seismic dataset and were often only recognised through analysis of the mapped horizons.

09 Fault Models used for strain analyses of the Gjallar Ridge and northern RAZ

KCaMFS115

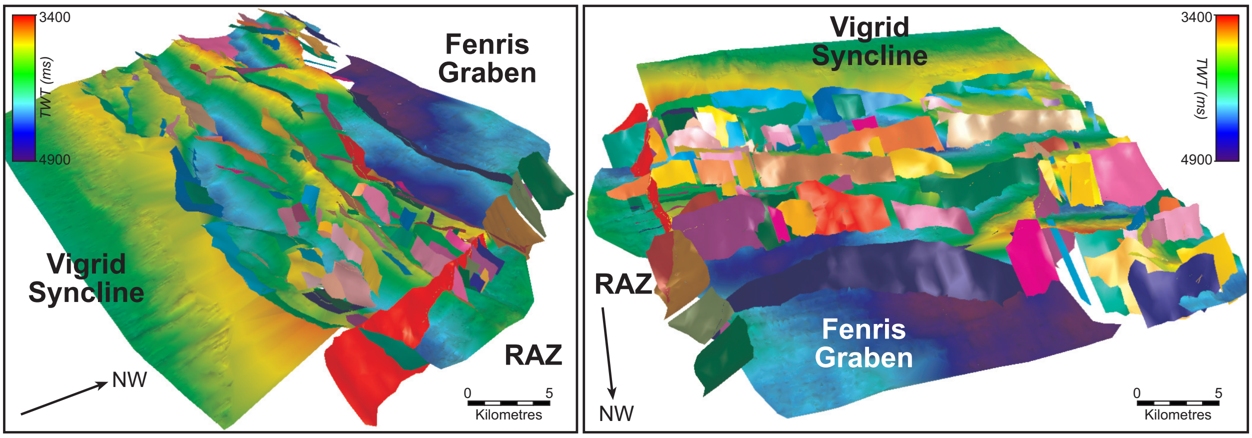

KCaMFS118

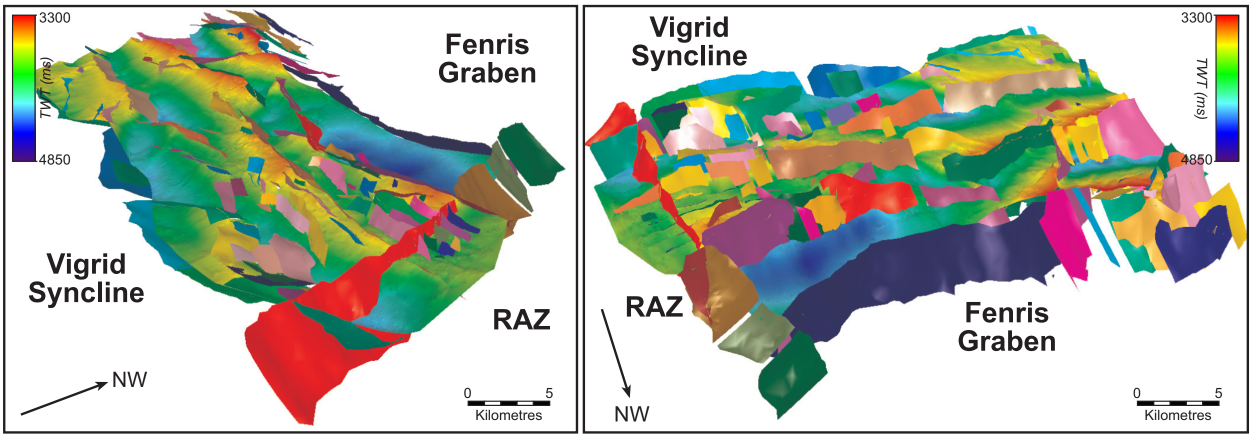

Top Cretaceous

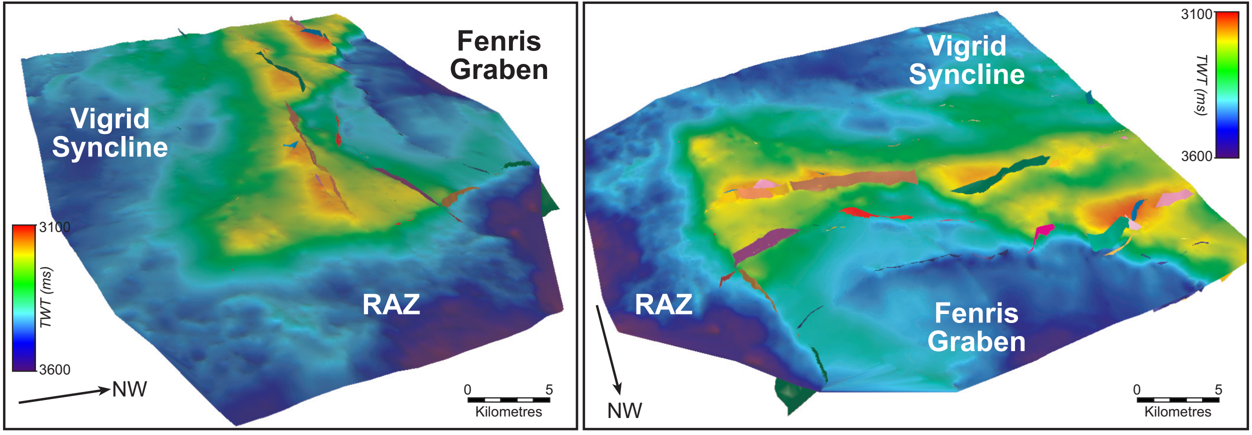

Figure 09

The Gjallar Ridge displays a complex anastomosing set of faults which are broadly NE-SW oriented. Dominantly dipping to the northwest, the majority of faults terminate along strike when intersected by a NW-SE oriented fault. Fault activity had ceased by the late Paleocene with only minor fault reactivations occurring at the north-western limit of the structurally highest areas.

10 KCaMFS115 and KCaMFS118 fault models used for strain analysis of the Nyk High and southern RAZ

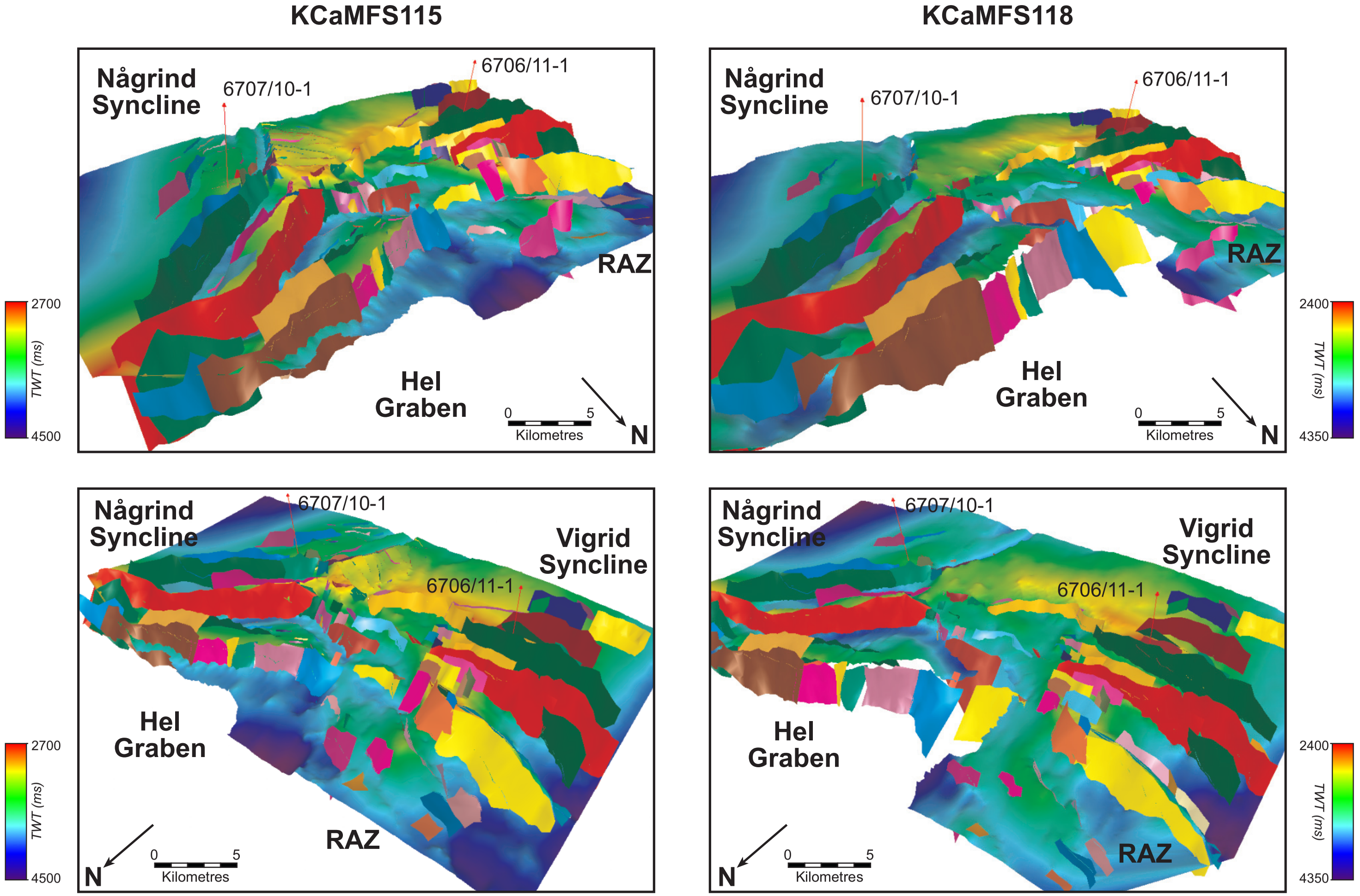

Figure 10
Faults of the Nyk High are dominantly oriented NE-SW, but upon entering the southern Rym Accommodation Zone, rotate round into more E-W and NW-SE orientations. A set of horsts and grabens are displayed within the Nyk High with a similar, but broader trend of fault blocks within the Rym Accommodation Zone.

11 Top Cretaceous and top Paleocene fault models used for strain analyses of the Nyk High and southern RAZ

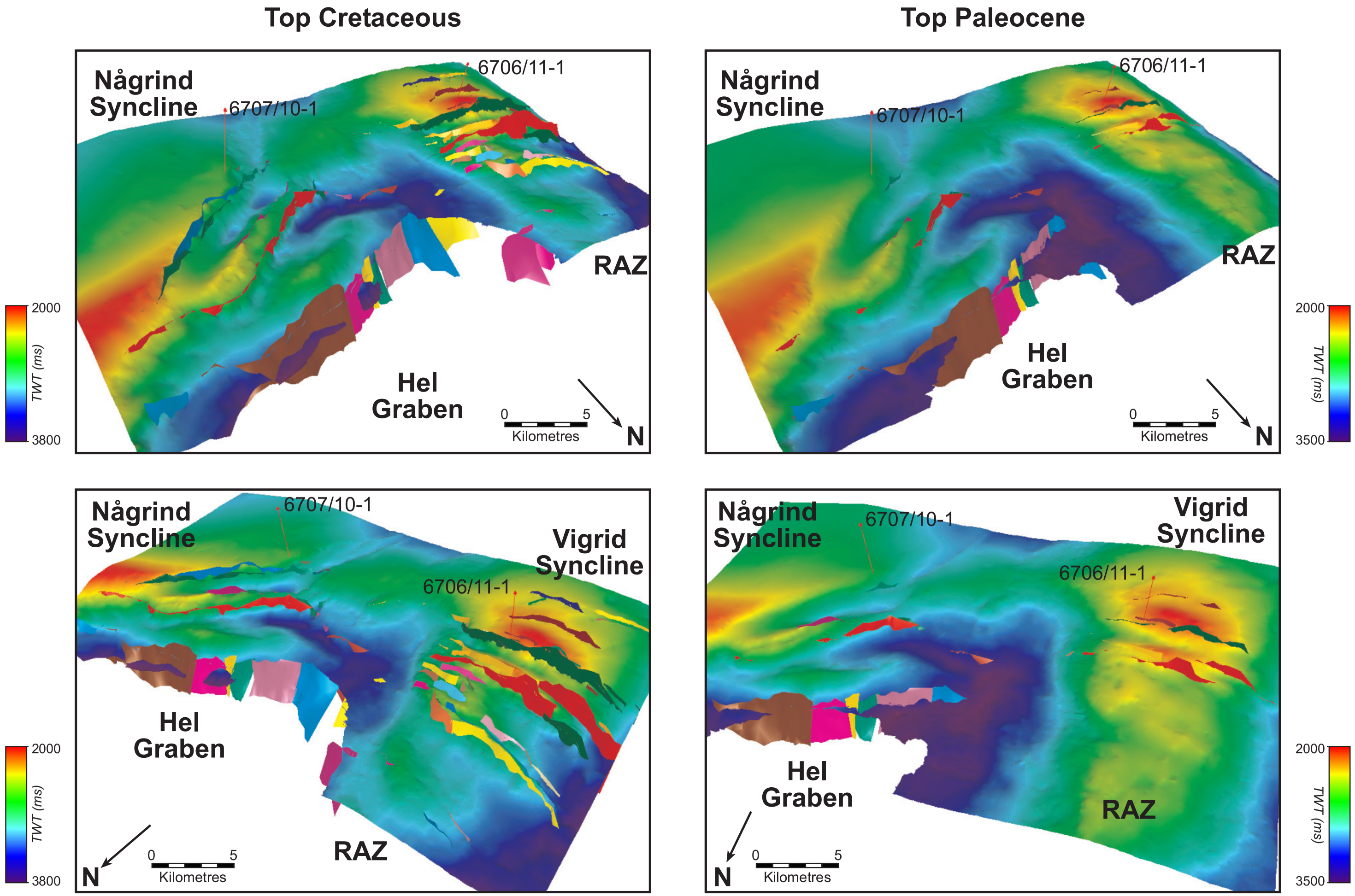

Figure 11
Paleocene fault activity represented by offsets of the top Cretaceous unconformity is relatively minor in the Nyk High when compared to the major offsets within the Rym Accommodation Zone along strike. These faults are preferentially reactivated later in the Cenozoic; believed to have been caused by thermal subidence and differential compaction across the fault blocks, rather than due to major rifting following continental breakup.

12 Process for strain calculation of the adjacent rift segments (see spreadsheets for formulae)

Fault heaves were preferred to throws for the strain analysis as they are of greater accuracy to the conversion of time-migrated seismic data to depth

Horizons recording rift periods: KCaMFS115 = *Campanian*, KCaMFS118 = *Maastrichtian*, Top Cretaceous = *Paleocene*, Top Paleocene = *Younger*

Sampling Parameters

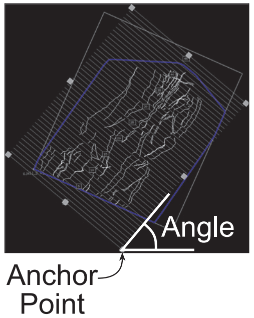

Data Exported from Badleys TrapTester

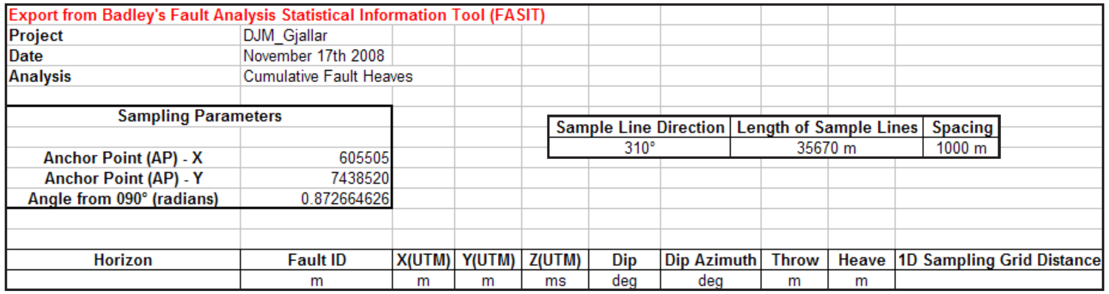

Export from Badley's Fault Analysis Statistical Information Tool (FASIT)

Project	DJM_Gjallar
Date	November 17th 2008
Analysis	Cumulative Fault Heaves

Sampling Parameters	
Anchor Point (AP) - X	605505
Anchor Point (AP) - Y	7438520
Angle from 090° (radians)	0.872664626

Sample Line Direction	Length of Sample Lines	Spacing
310°	35670 m	1000 m

Horizon	Fault ID	X(UTM)	Y(UTM)	Z(UTM)	Dip	Dip Azimuth	Throw	Heave	1D Sampling Grid Distance
	m	m	m	ms	deg	deg	m	m	

Calculation of Cum. Heave

1. Calculation of UTM start point for each sample line (southernmost point).
2. Calculation of distance along sample lines at which each fault intersects.
3. Cumulative heave along each sample line is calculated by summation of the fault heaves. The point at which the cumulative heave increases is located in respect to the distance along the sample line.

Absolute Heave

Fault heaves calculated from younger periods of rifting were subtracted from the older fault heaves, due to reactivation of the faults.

If this resulted in a negative fault heave (probably due to interpreting error), heaves were considered zero upon the individual fault for the defined rift period.

Absolute Cumulative Heave

This resulted in new calculations of cumulative heave for each defined rift period.

Strain Calculations within defined Study Zones

Due to fault and horizon interpretation differing in spatial extent, zones along the length of the sample lines were defined for strain calculations based upon the relative location of the fault arrays. As strain calculations rely greatly upon the original line length, the zone in which fault and horizon interpretation was present would best represent the true upper crustal extension.

Strain Calculation Zones: Distance along Sample Line

Gjallar Ridge

KCaMFS115: 6000 - 22500 m
KCaMFS118: 9000 - 19000 m
Top Cretaceous: 14000 - 25000 m

Nyk High

KCaMFS115: 9000 - 29500 m
KCaMFS118: 9000 - 22500 m
Top Cretaceous: 13500 - 26000 m
Top Paleocene: 13500 - 27000 m

Nyk High - RAZ

KCaMFS115: 8000 - 24000 m
KCaMFS118: 7500 - 19000 m
Top Cretaceous: 2000 - 21000 m
Top Paleocene: 7000 - 14500 m

Calculation of Beta Factor for each Sample Line

Beta Factor = Width of Study Zone / (Width of Study Zone - Cumulative Heave)

13 Fault polygons and sample lines for the Rym Accommodation Zone strain analysis

Gjallar Ridge

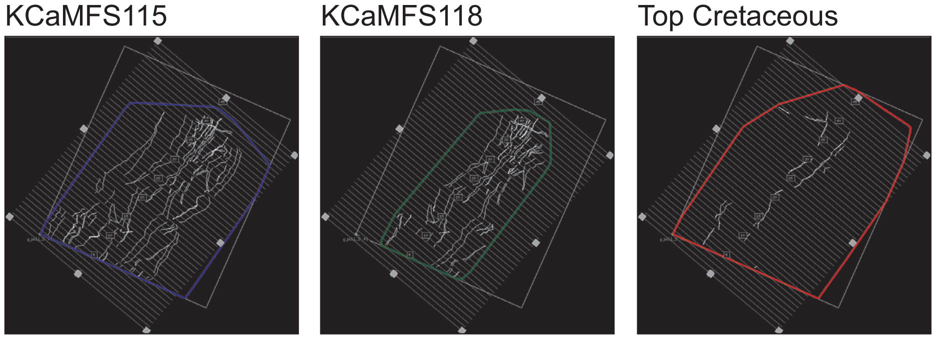
KCaMFS115 KCaMFS118 Top Cretaceous

Sample Line Settings

	Gjallar Ridge	*RAZ*	*Nyk High*
Sample Line Direction:	310°	010°	330°
Length of Sample Line (m):	35670	35235	48517
Sample Line Spacing (m):	1000	1000	1000

Southern Rym Accommodation Zone

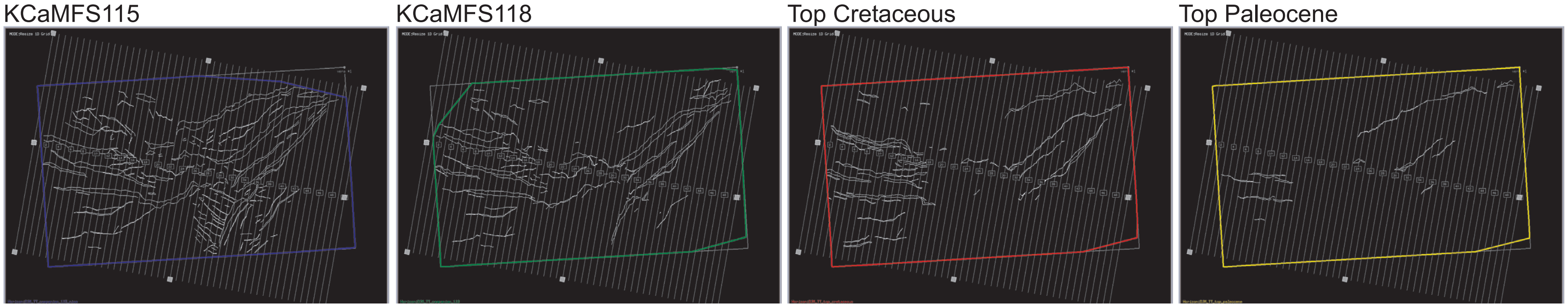
KCaMFS115 KCaMFS118 Top Cretaceous Top Paleocene

Nyk High

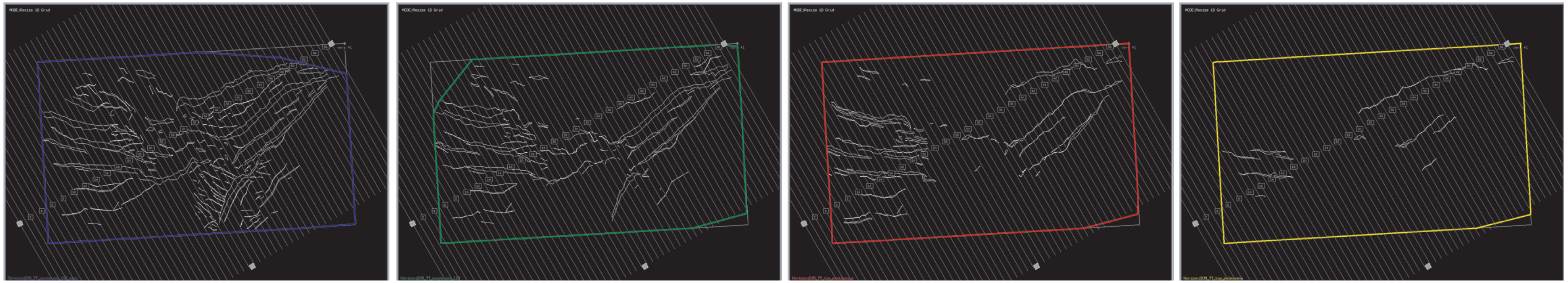

14 Oligo-Miocene time-thickness map above the Nyk High and southern Rym Accommodation Zone

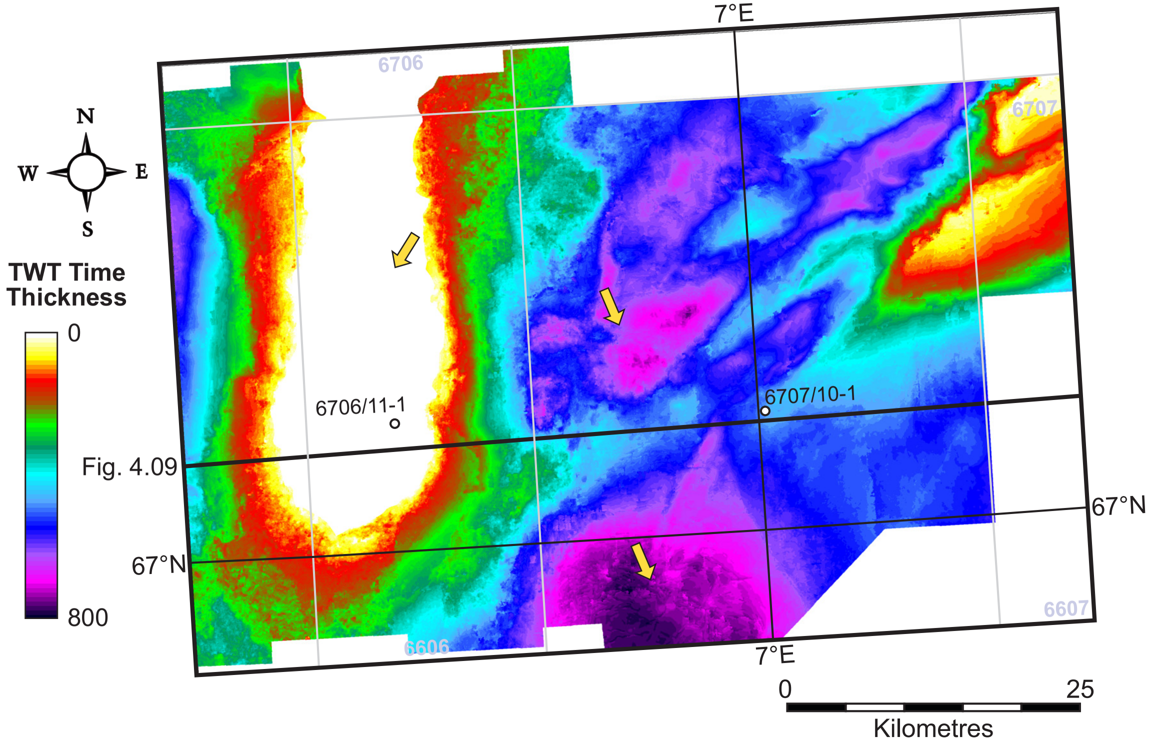

Intra-Miocene Time-Structure Map

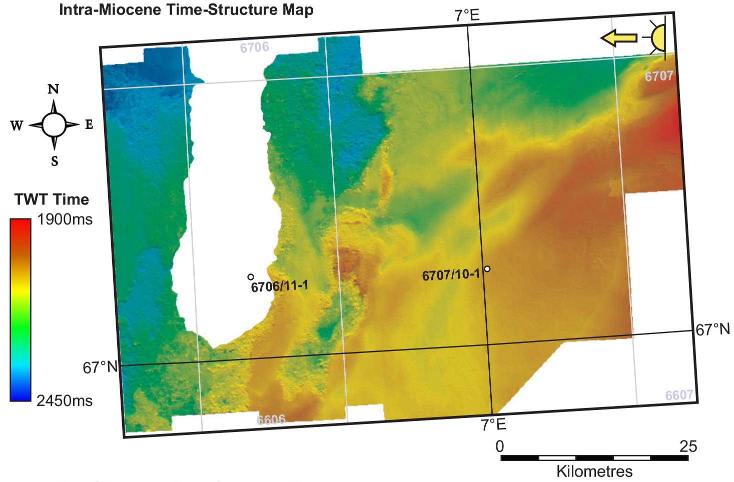

Top Oligocene Time-Structure Map

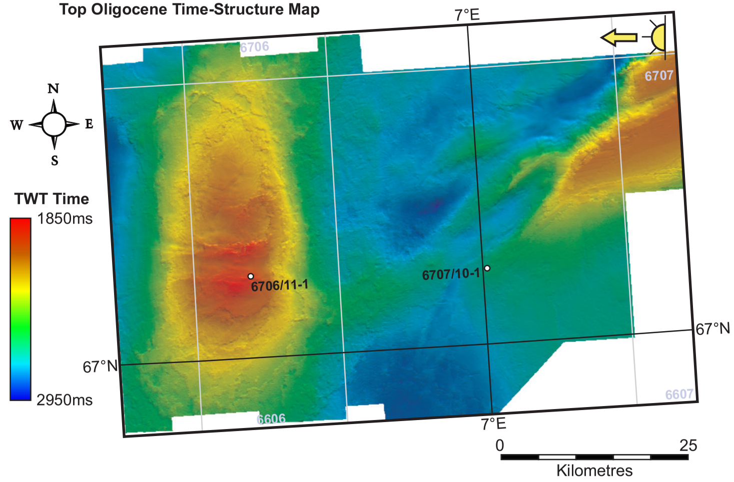

Figure 14

The above map displays the time-thickness of a sequence deposited between an intra-Miocene horizon of which the precise age is unknown and the top Oligocene horizon (right). The structural growth of the Vema Dome is clearly observed with marked thinning of the sequence and onlap of the intra-Miocene horizon onto the Vema Dome from the east, west and south. In the region directly above the harpoon structure to the east (Fig. 4.09) the thickest early Miocene sequence is found which suggests this was the primary depocentre at the time. If buttressing at depth had occurred along the N-S oriented Jurassic rift fault during this time, a similar thinning of the early Miocene sediment would be expected due to the uplift of the overlying stratigraphy, but this is not observed.

Appendix D

Supporting material for Chapter 5

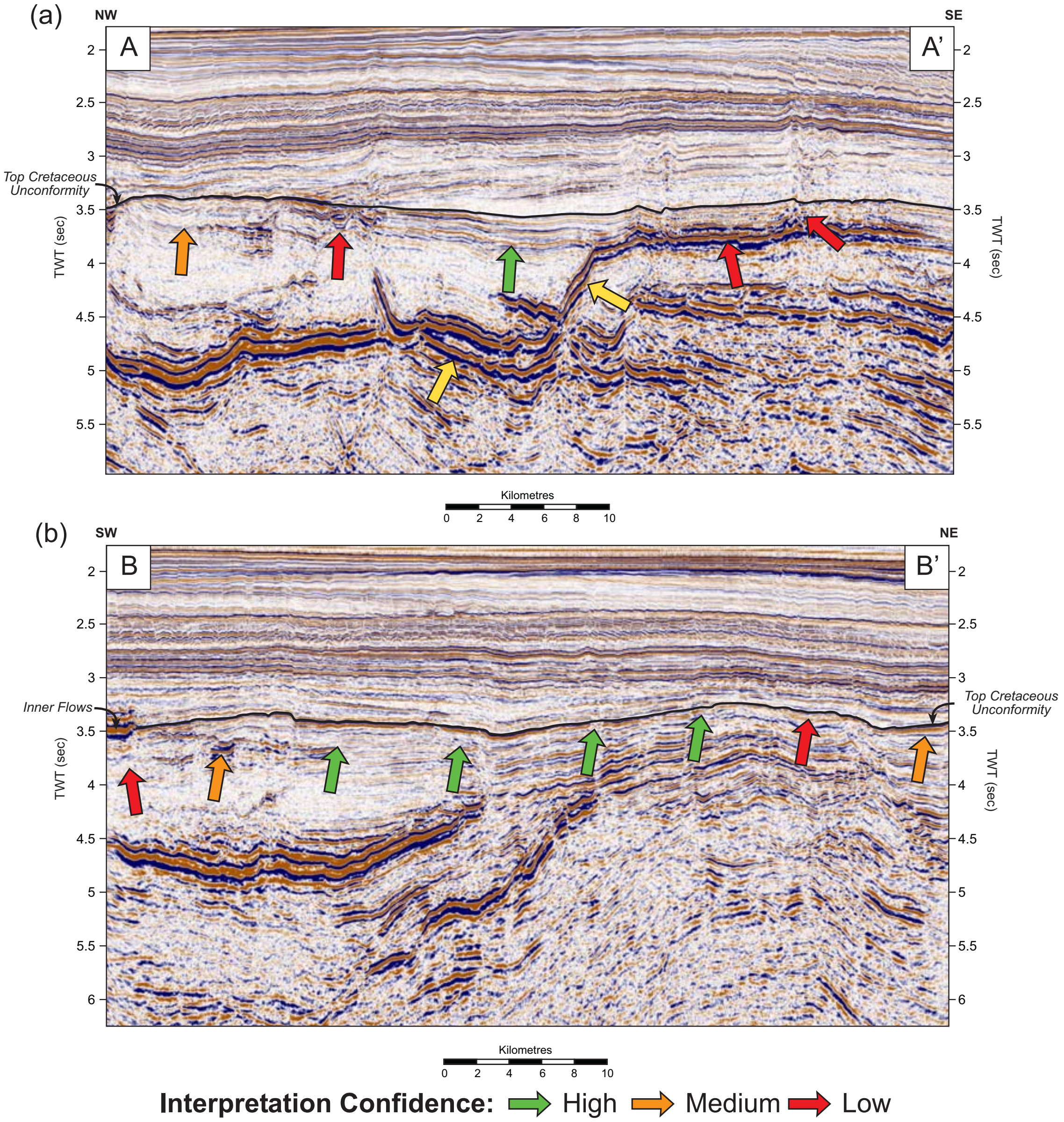

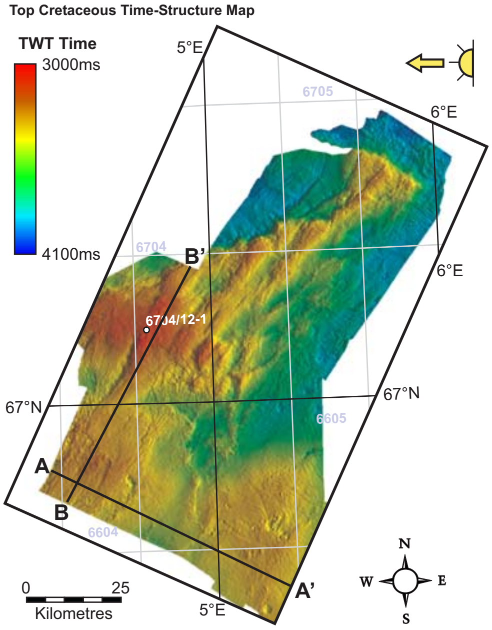

Figure 01
The late Maastrichtian marine fan sequences were particularly difficult to interpret in a variety of areas. Cenozoic igneous intrusions were emplaced within the sequences, imaged as high amplitude reflections within the sedimentary units (a). This reduced confidence in the interpretation and also affected amplitude extractions of the mapped horizons when present.

The inner flows, although minor in extent within the seismic survey, mapping below this Cenozoic horizon was not possible (b). Lack of well control also made it difficult to assess the spatial extent of the sequences along strike from the Gjallar Ridge, particularly in areas where normal faulting and erosional truncation is present.

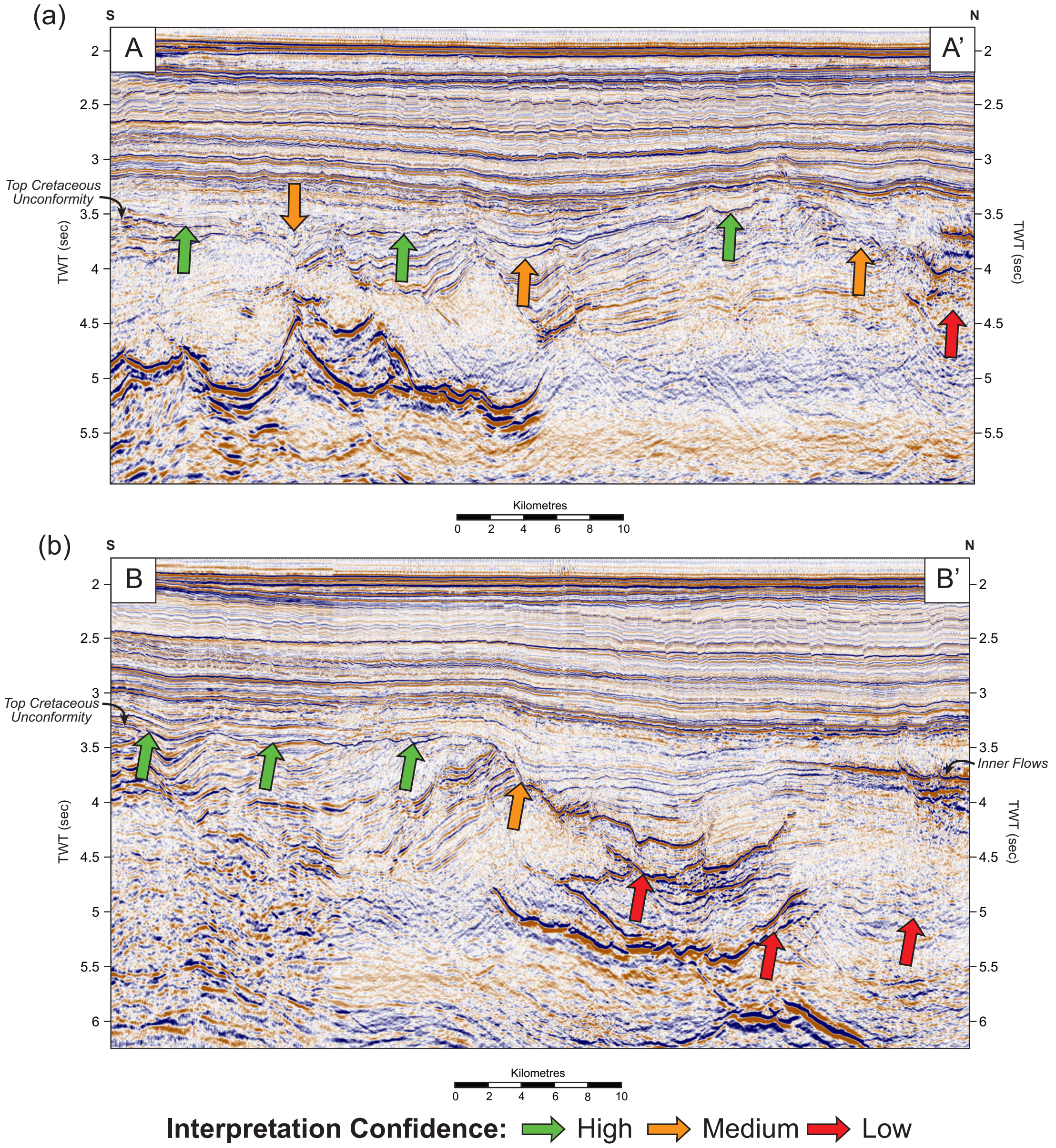

Figure 02

The top Cretaceous unconformity (which has a strong positive amplitude response) is relatively simple to map. Further identification of the horizon is possible by the recognition of stratigraphical onlap onto the unconformity and truncation of the underlying sequences.

Hydrothermal vent complexes above sill tips have disrupted the coherency of the unconformity in areas as displayed in (a). Reactivated faults at the boundary of the Gjallar Ridge and Fenris Graben (a), has also reduced confidence of identifying the top Cretaceous unconformity due to a lack of well control. Similarly, across the sharp transition into the Rym Accommodation Zone (b), igneous intrusive and extrusive bodies lead to possible erroros in the horizon interpretation.

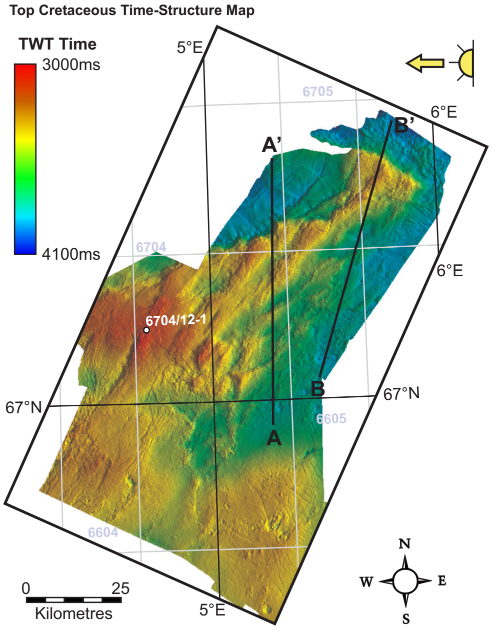

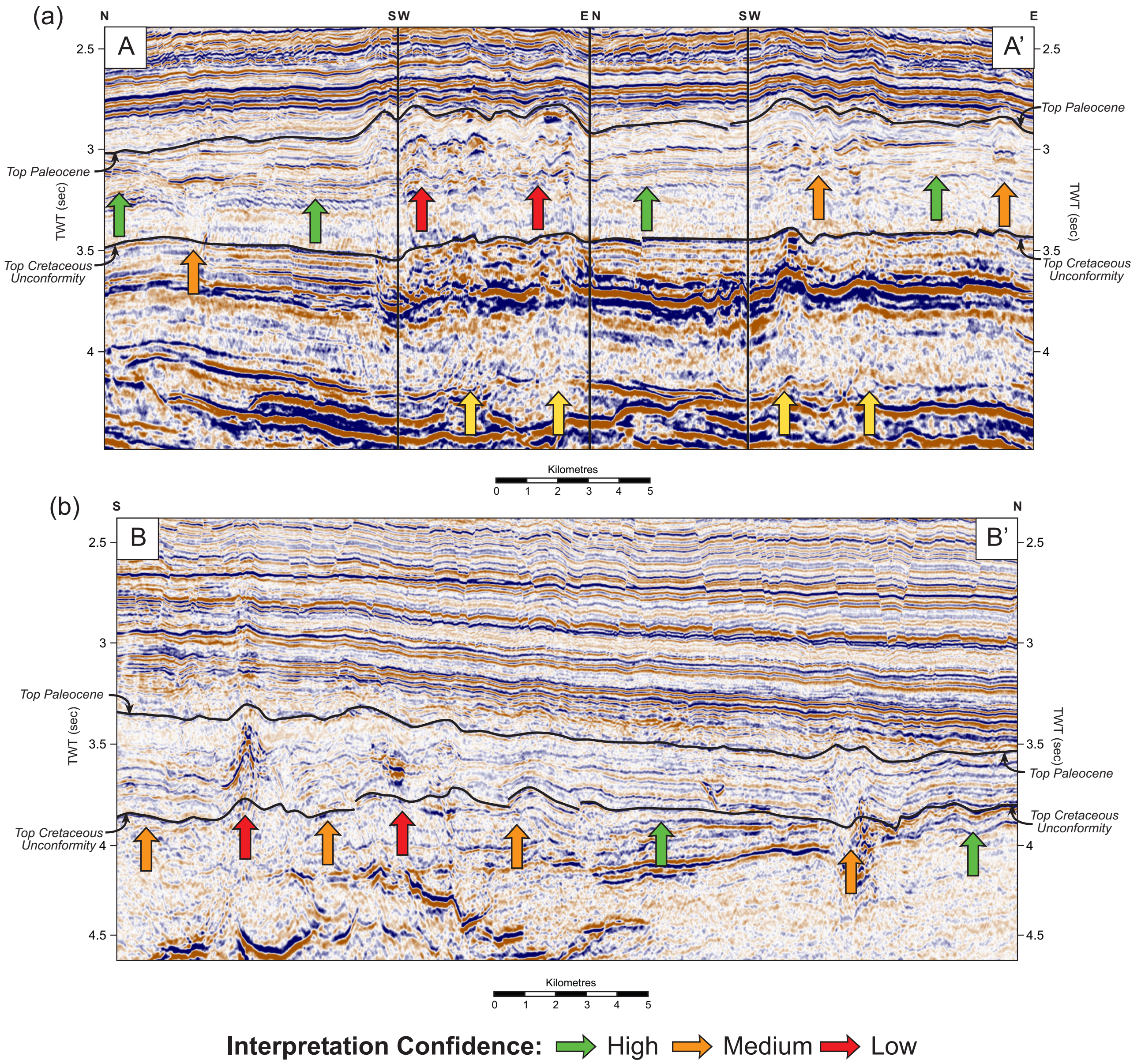

Figure 03
The intra Paleocene horizons are dominantly affected by the remobilisation of sediments caused by the intrusion of sills leading to the release of gases and liquids (a; Hansen 2006). This has severely modifed the Paleocene sequence in which multiple hydrothermal vent complexes are recognised, leading to a large reduction in the confidence of mapping horizons in these areas. Fortunately, many of the complexes appear to be point sourced and mapping accuracy is only reduced directly within the remobilised sediment. Further soft sediment deformation in the form of a compressional duplex of small scale thrust features (b), associated with slumping from the flanks of the Gjallar Ridge (App. D.11), also caused interpretation problems in the survey.

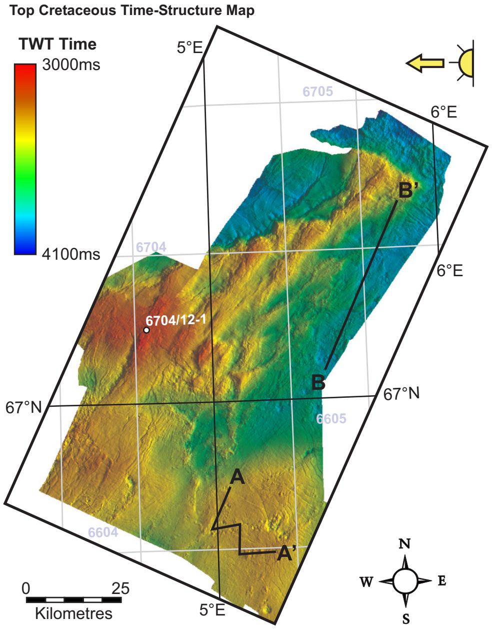

04 Areas of difficulty interpreting in the Rym Accommodation Zone

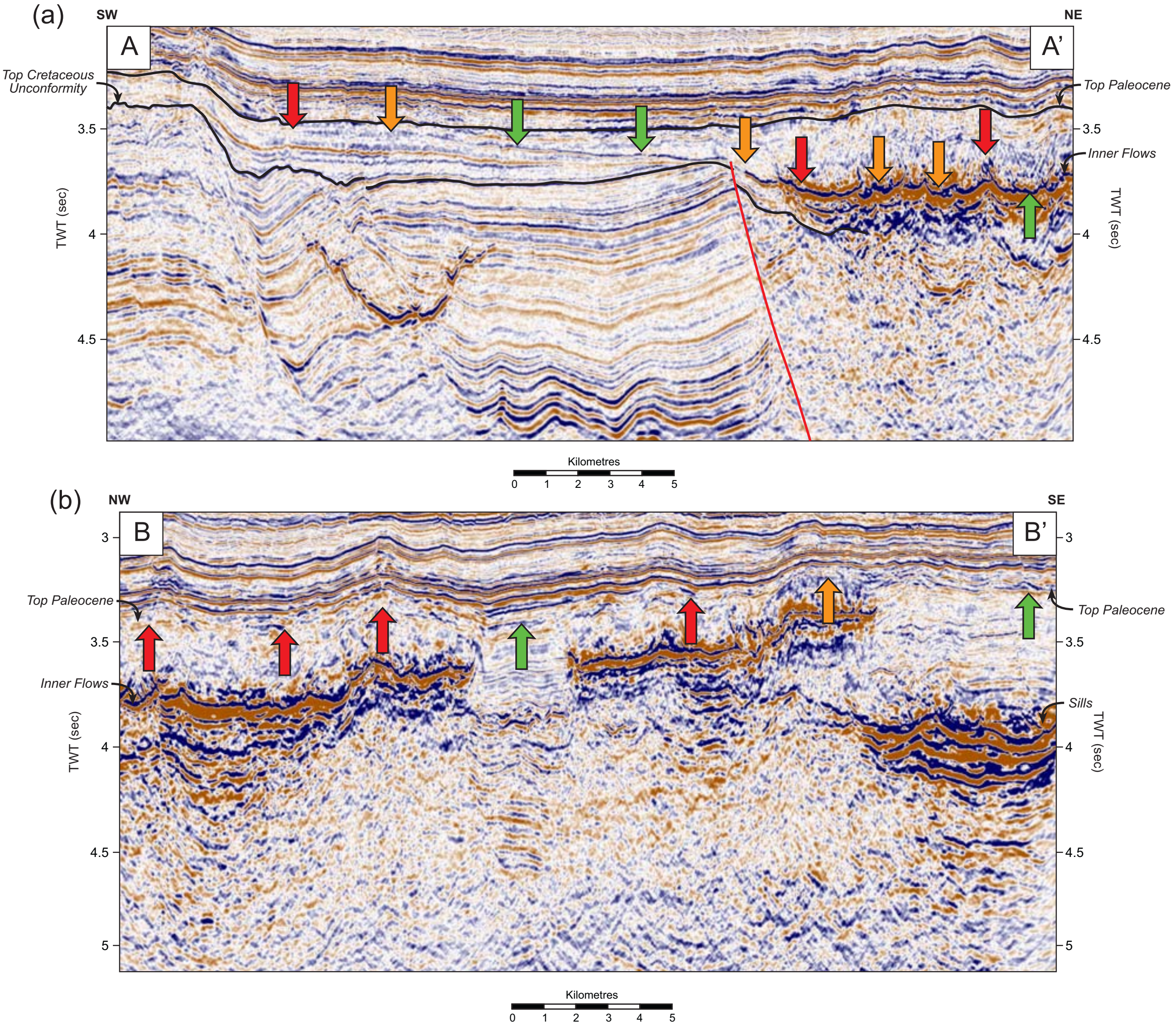

Interpretation Confidence: 🟩 High 🟧 Medium 🟥 Low

Figure 04

Intra Paleocene 4 and the top Paleocene horizons are particularly difficult to interpret in the Rym Accommodation Zone due to the igneous activity in the area. Intra Paleocene 4 appears to have formed synchronously with the deposition of the inner flows (a). The point at which the unconformity ends and the inner flows are deposited is often difficult to identify. The top of the inner flows is also difficult to identify due to the variety of cross cutting relationships and high relative dips observed (b). The mapping of the inner flows was focussed on the uppermost positive amplitude reflector. The top Paleocene horizon is also very difficult to map in the Rym Accommodation Zone as the late Paleocene inner flows appear to distort the overlying sedimentary sequence.

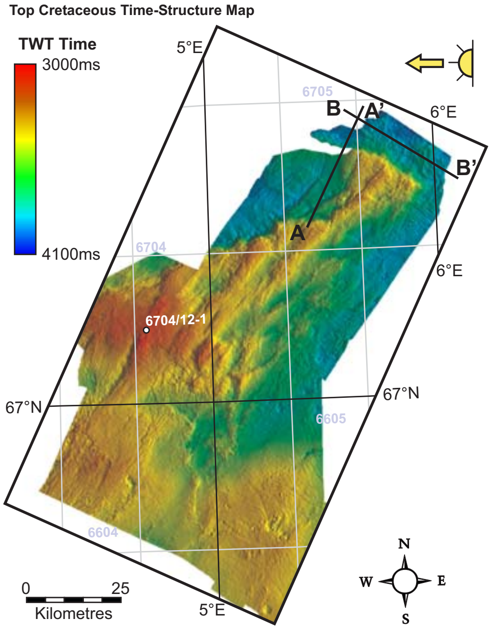

05 Paleocene faulting at the boundary between the Gjallar Ridge and Fenris Graben

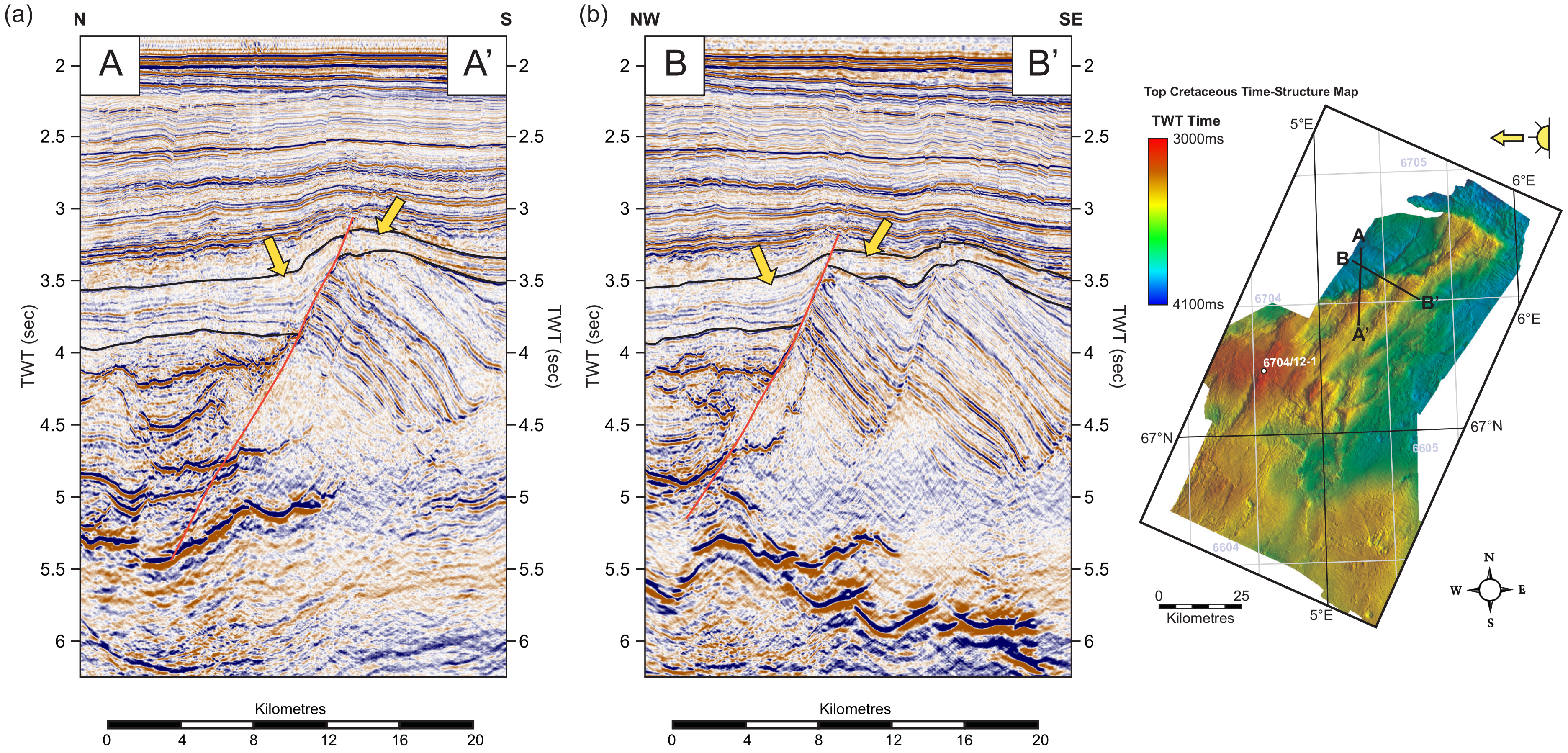

Figure 05

The Paleocene sequence is recognised to thicken from upon the Gjallar Ridge in south-east into the Fenris Graben to the north-west. Despite the identification of the top Cretaceous unconformity being uncertain, clear hangingwall thickening of the sequence in the north-west dipping bounding fault is evident. This implies that at least for some period during the Paleocene this fault was active; this is not recorded elsewhere upon other faults of the Gjallar Ridge. Even though not recognised, evidence of an early Paleocene rift event upon the Gjallar Ridge may have been subsequently eroded. The hypothesised eroded remains would potentially be deposited into the Fenris Graben which remained a structural low.

06 Oligo-Miocene sequence time-thickness maps above the Gjallar Ridge

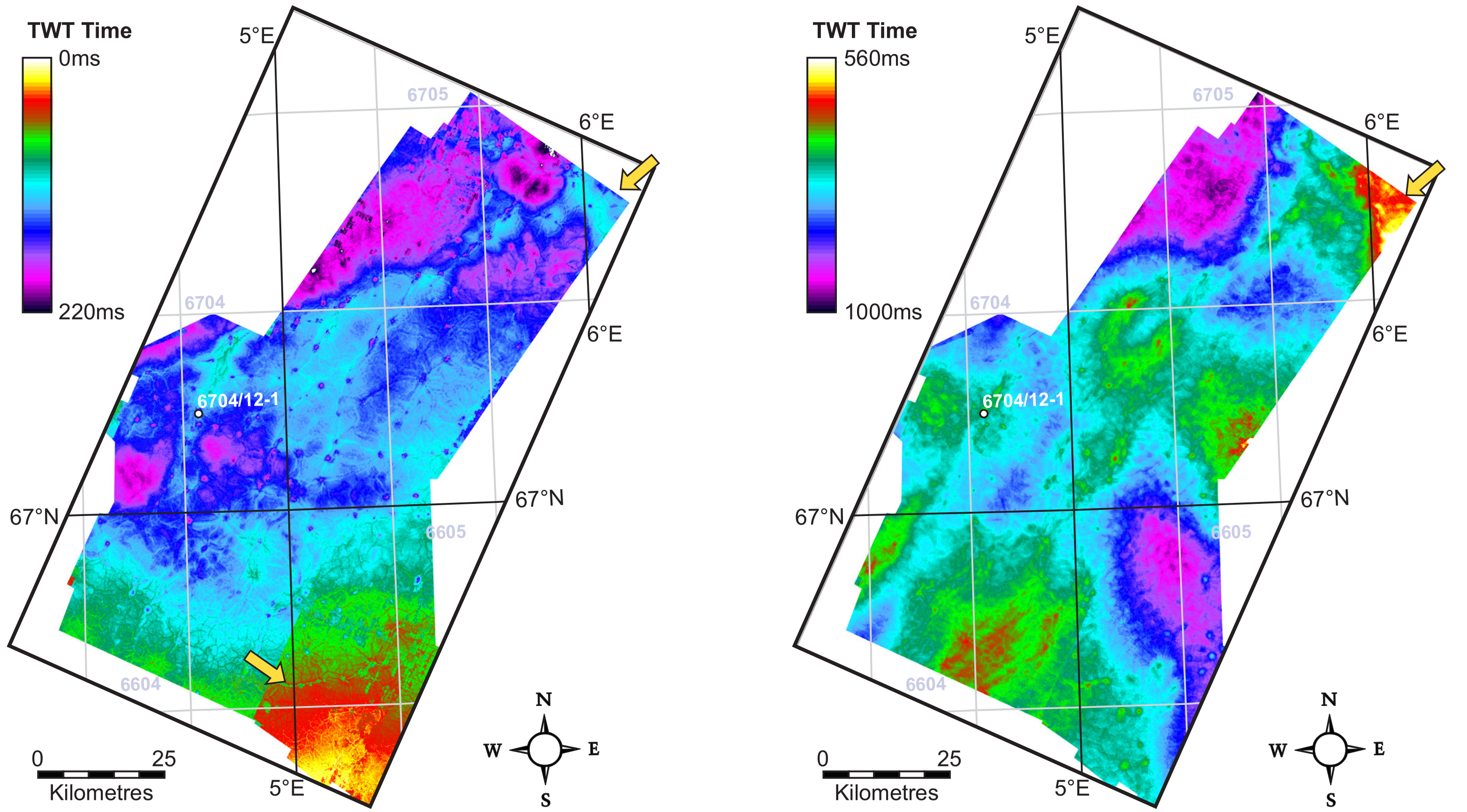

(a) Base Ooze to Intra Oligocene Sedimentary Tiime-Thickness

(b) Top Ooze to Base Ooze Sedimentary Time-Thickness

Figure 06
The sedimentary time-thickness maps relate to the late Oligocene (a) and Miocene (b) series during which a number of dome structures were formed along the Norwegian continental margin (Doré *et al.* 2008). This is no different in the northern Vøring Basin in which the Vema and Naglfar Domes are located. Evidence for Oligo-Miocene growth of these domes is evident within the Gjallar Ridge survey, particularly in the Rym Accommodation Zone to the north-west where significant thinning of the sedimentary succession is observed. This may be a northern continuation of the Vema Dome structural trend which was argued to have formed due to buttressing against a Jurassic rift fault at depth (Chapter 4). Thinning of the upper Oligocene strata also occurs to the south of the survey in the Vigrid Syncline which is interpreted to be caused by differential compaction above a major sill complex located in this area.

07 Paleocene submarine erosion and deposition in the Nyk High

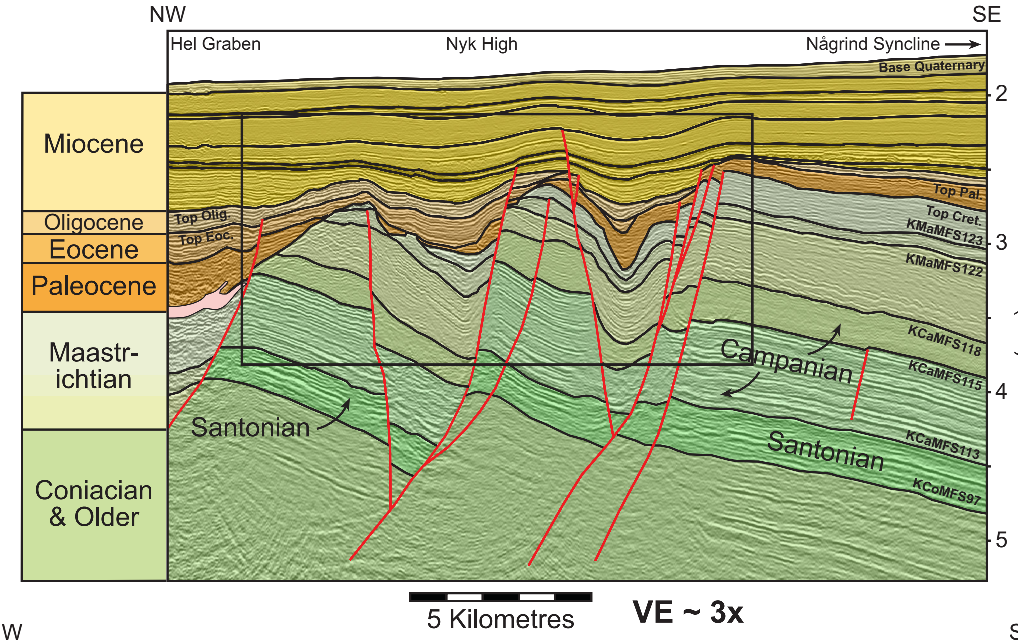

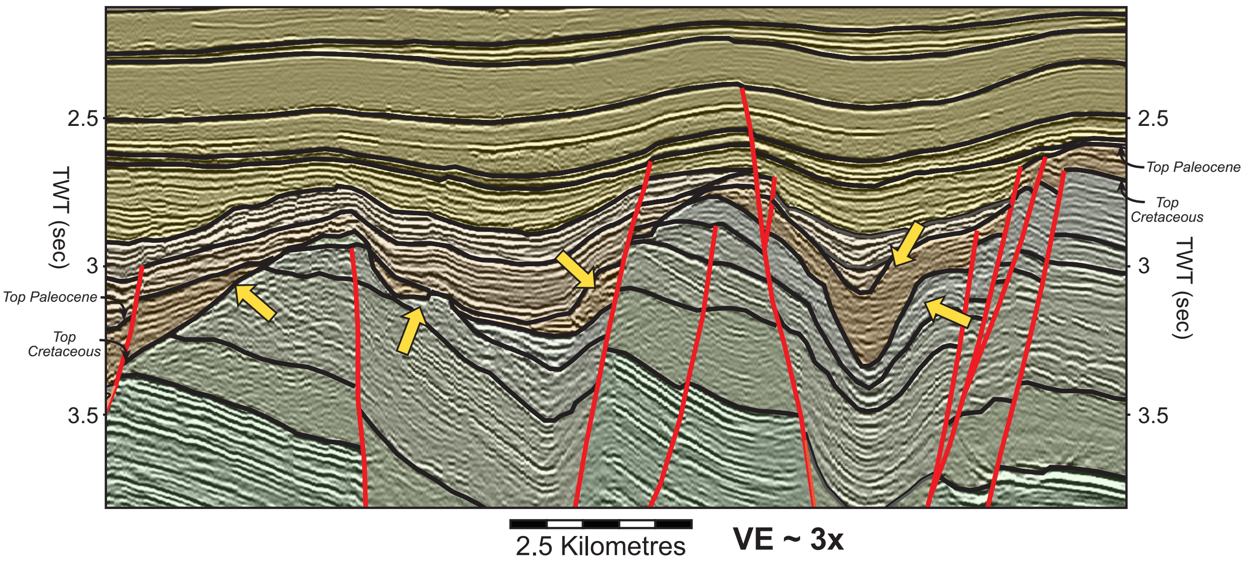

Figure 07
A variety of erosional styles and products are evident upon the Nyk High, particularly in the grabens which are structurally lower than the non-eroded horst blocks. An explanation for this is a process of submarine erosion by bottom water currents in the early Cenozoic. Evidence for this includes truncation of the late Cretaceous strata within localised pockets upon the grabens, implying focussed marine bottom-water currents in these locations. Lateral erosion of the horsts is also recognised at the boundary between the Nyk High and Hel Graben, with evidence of the erosional products deposited upon the flanks of the grabens. The cause for this erosion may be due to the relative uplift of the Nyk High and growth of the Vøring Marginal High which may have forced the modification of oceanic currents at the time.

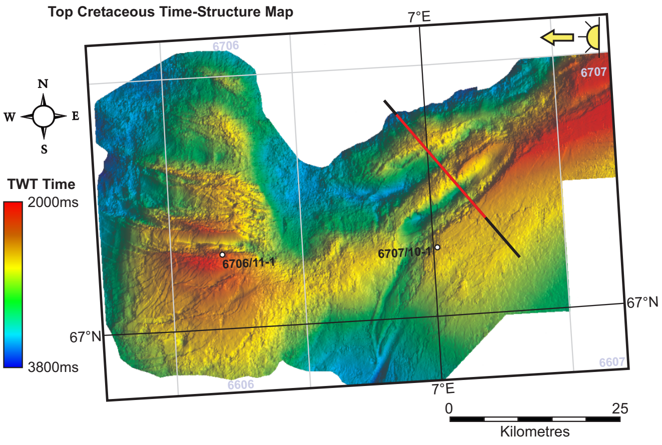

08 Top Cretaceous and top Paleocene amplitude maps of the Nyk High

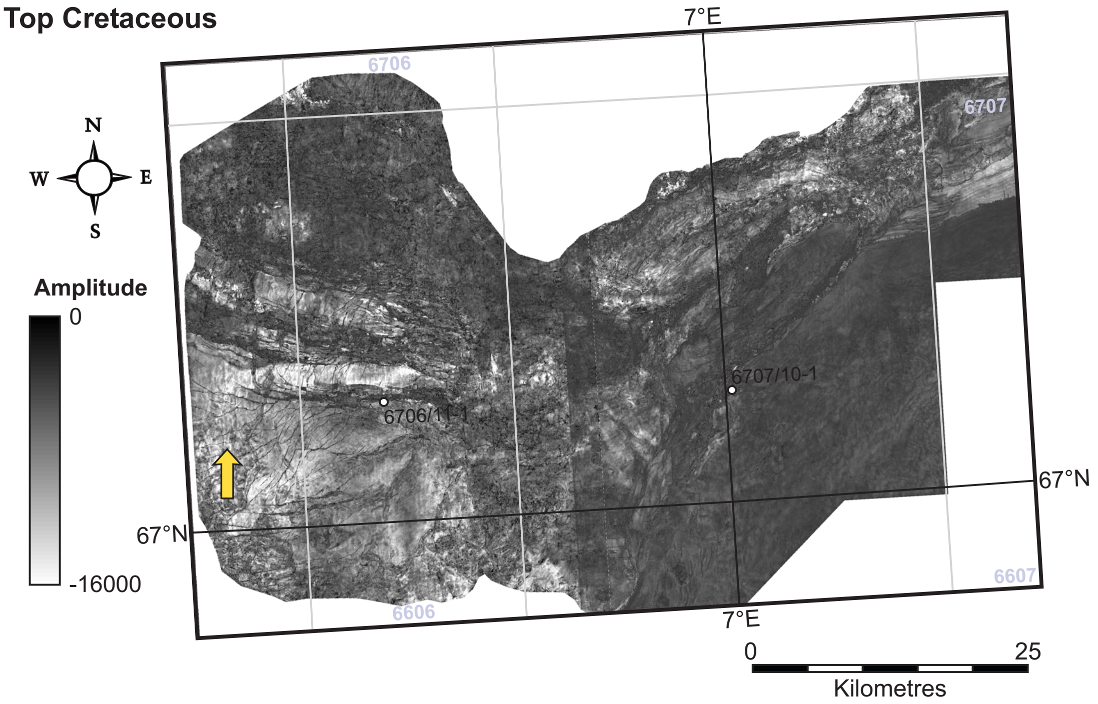

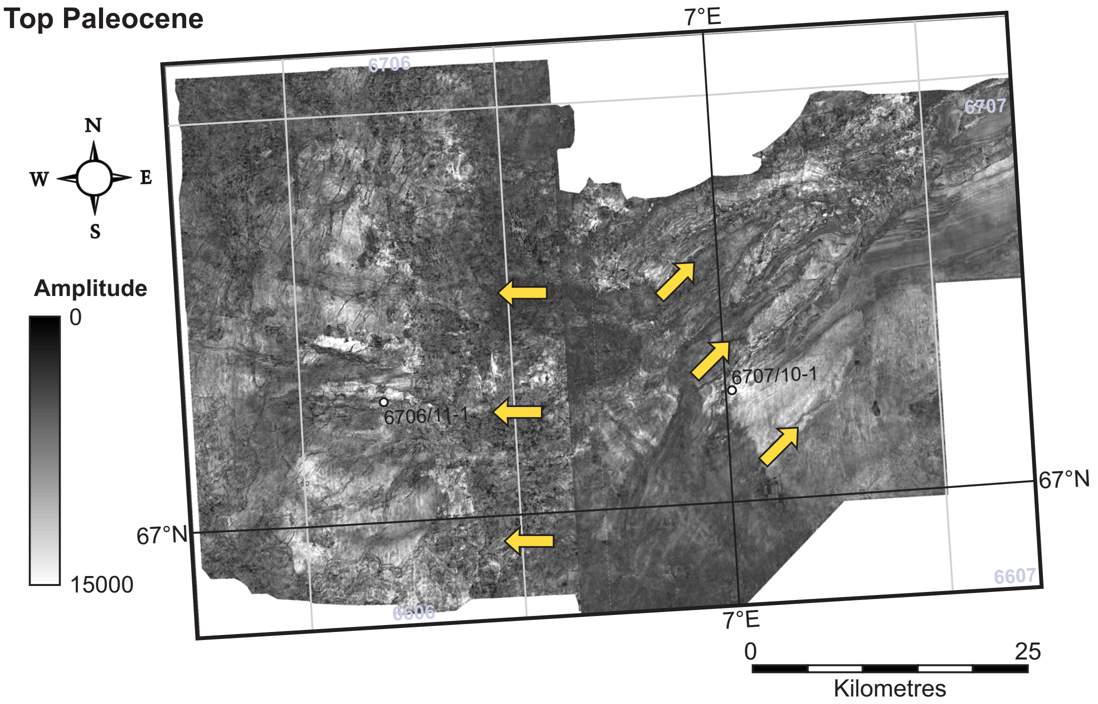

Figure 08

The top Cretaceous amplitude map highlights areas which are likely to be sand and mud prone, however as the horizon is a distinct unconformity in the vicinity of the Nyk High, the amplitude response of the horizon varies due to the changes in acoustic impedance contrast between the eroded sequences beneath and above the unconformity. A series of minor faults are highlighted by the amplitude extraction in the Rym Accommodation Zone, the origins of which remain unexplained. The top Paleocene horizon highlights distinct sand and mud prone regions to either side of the area that experienced Paleocene uplift and erosion (Chapter 4). This implies that the north-south oriented uplift may have been a local sediment source material deposited within the Nyk High and the southern Rym Accommodation Zone to the east and west respectively.

09 Origin of uplift in the Vigrid Syncline in the vicinity of the Gleipne Lineament

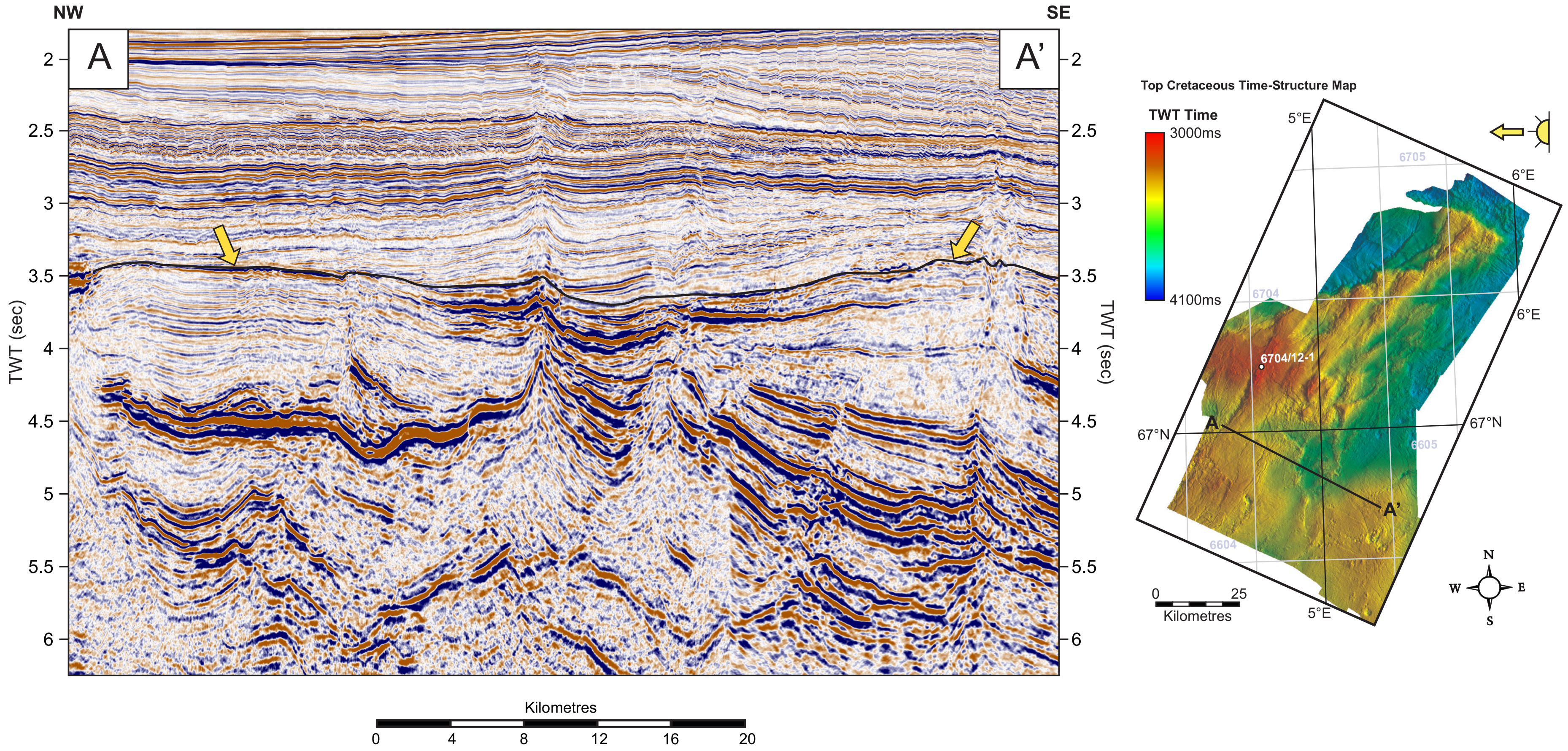

Figure 09
The origin of the Paleocene aged uplift in the Vigrid Syncline close to the Gleipne Lineament appears to have been controlled by the intrusion of igneous material into the upper crust. The top Cretaceous unconformity (shown) is of greater relief in the Vigrid Syncline than above the Gjallar Ridge; the reason for this can be clearly illustrated by the above seismic line. High amplitude reflections on the seismic data are interpreted to be intruded igneous material in the form of sills and dykes. The volume of material emplaced varies in space, with increased amounts within the Vigrid Syncline in the southeast than to the Gjallar Ridge in the northwest. This volume change of the basin fill led to structural uplift as previously recognised within the Vøring Basin (Hansen and Cartwright 2006) and elsewhere upon the NE Atlantic Margin (Moy and Imber 2009).

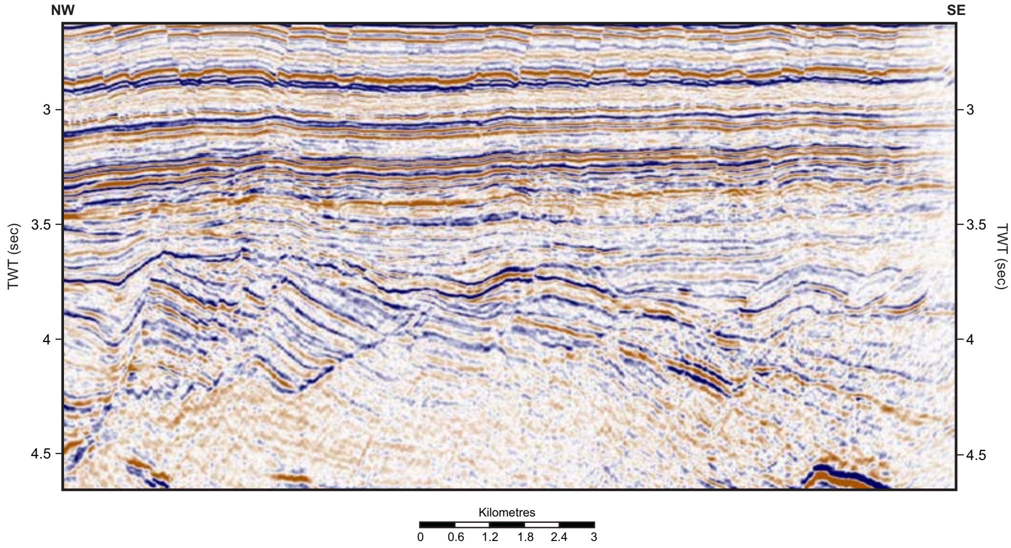

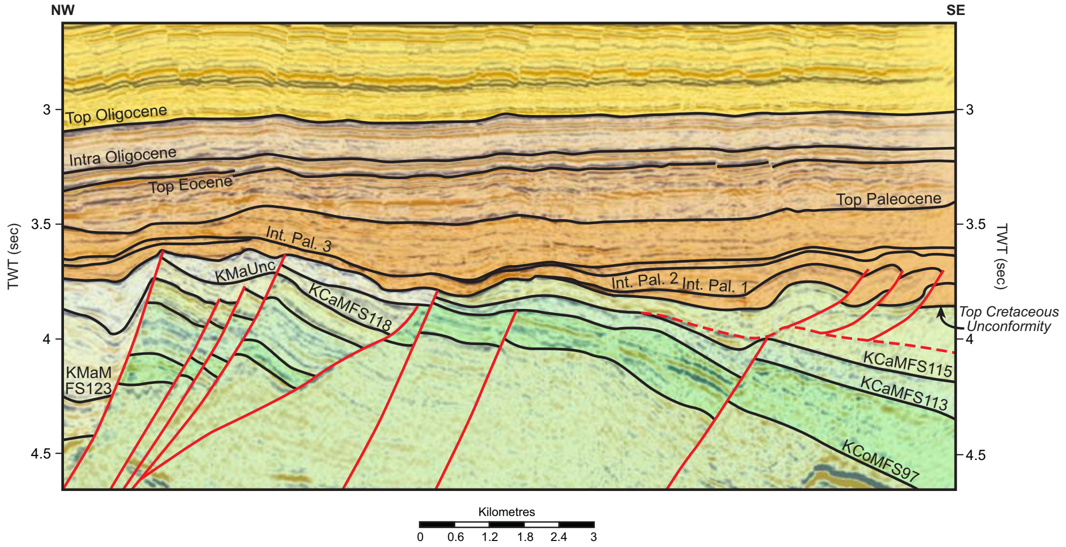

Figure 10

Upon the south-eastern flank of the Gjallar Ridge, a series of thrusts have developed within the Paleocene sequence. Timing for the slumping which formed the thrust duplex is estimated as being late Paleocene (Thanetian), with the intra Paleocene 3 horizon infilling the thrust relief. A normal fault within the late Cretaceous sequence may have instigated the formation of the thrust duplex which can be mapped out in three dimensions (right). The foreland for the system is to the southwest (the Vigrid Syncline) with the hinterland to the north. The detachment (dashed) for the compressional system is within the mud prone KCaMFS118 sequence which acted as a décollement. Enhanced relative uplift of the Gjallar Ridge and/or subsidence in the Vigrid Syncline may have created the necessary conditions for the sediment to pass the angle of repose and fail.

Top Cretaceous Time-Structure Map

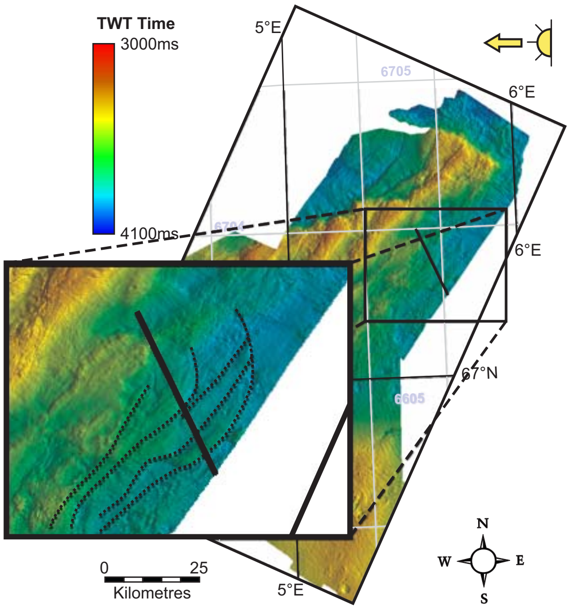

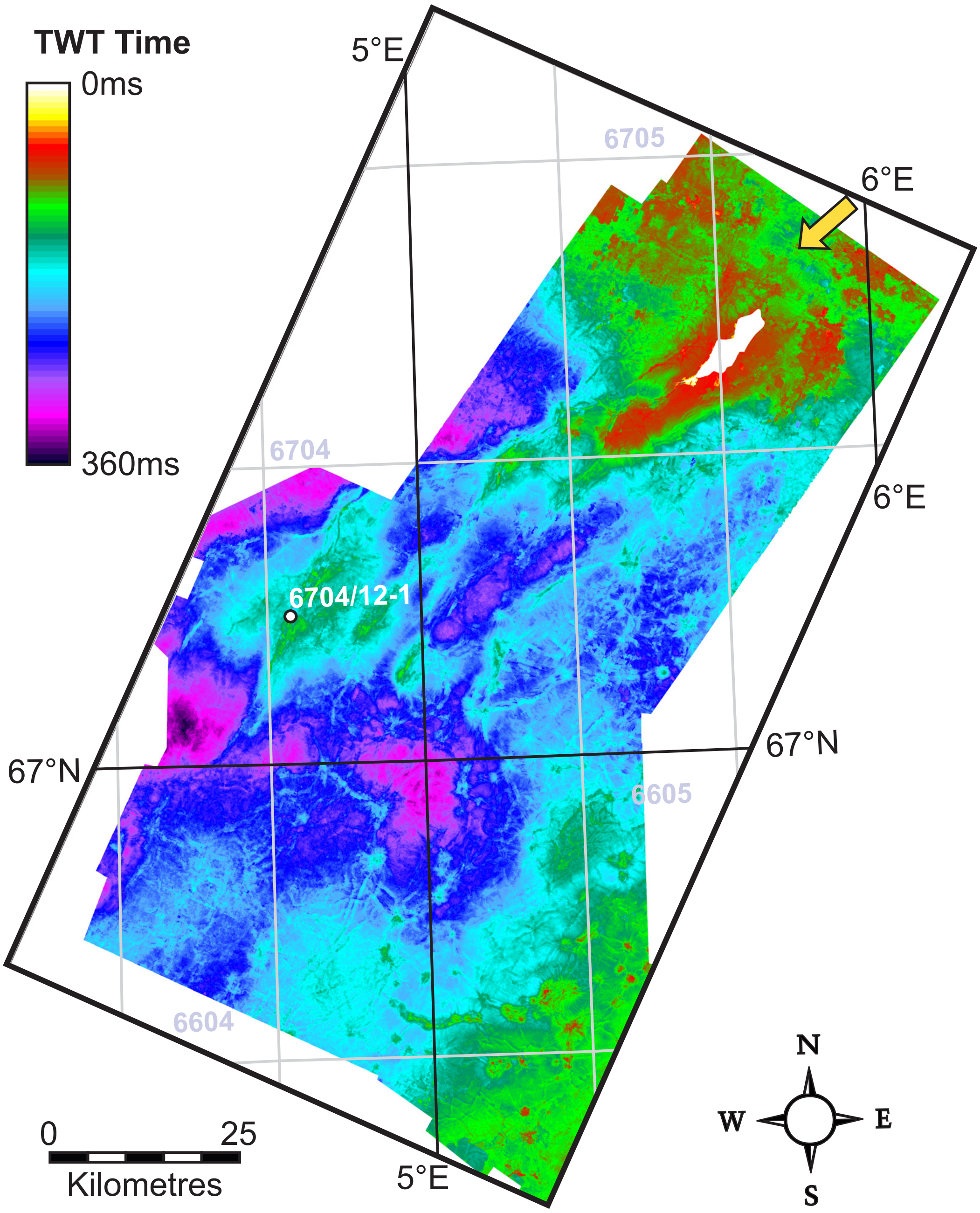

Figure 11
The Eocene depositional sequence is unfaulted except in areas where minor normal fault reactivation has occurred. The variation in the thickness of the depositional sequence is therefore expected to be predominantly controlled by the pre-existing relief of the basin. This is particularly well displayed as the Eocene strata are thinner above the crests of rotated fault blocks in the Gjallar Ridge than in the fault hangingwalls. Unusually, sediments are also thinner in the Rym Accommodation Zone despite forming a major depocentre during the Paleocene. Ren *et al.* (2003) recognised that the Rym Accommodation Zone formed a topographical high at this time. This is interpreted to be caused by the differential compaction of sediment in the area. The late Paleocene dense volcanic inner flow units are expected to compact much less than the adjacent porous sediments which would lead to increasing structural prominence of the Rym Accommodation Zone under post-rift conditions.

Appendix E

Paper Reprints

Journal of the Geological Society, *London*, Vol. **166**, 2009, pp. 831 844. doi: 10.1144/0016-76492009-010.

A critical analysis of the structure and tectonic significance of rift-oblique lineaments ('transfer zones') in the Mesozoic–Cenozoic succession of the Faroe–Shetland Basin, NE Atlantic margin

D. J. MOY* & J. IMBER
Reactivation Research Group, Department of Earth Sciences, University of Durham, Science Site, South Road, Durham DH1 3LE, UK
**Corresponding author (e-mail: d.j.moy@durham.ac.uk)*

Abstract: NW SE-trending rift-oblique lineaments ('transfer zones') occur along the length of the NE Atlantic margin. Previous workers have suggested that these lineaments played an important role in providing conduits and/or barriers to sedimentation during the Cretaceous and Palaeocene; it has also been suggested that they were active as discrete, basin-wide strike-slip faults. This study uses a well-calibrated 3D seismic survey of regional extent to critically assess the structural and stratigraphic evidence for three rift-oblique lineaments in the UK sector of the Faroe Shetland Basin (Victory, Clair and Judd Lineaments). Structures previously attributed to basin-wide strike-slip deformation can be more simply explained as igneous intrusions, hydrothermal vent complexes, gas chimneys and/or faults that transfer extensional strain between en echelon rift segments. There is little evidence to suggest that activity along discrete, basin-wide lineaments controlled Palaeocene sedimentation within the Faroe Shetland Basin. Rather, sediment transport and deposition at this time are likely to have been controlled by along- and across-strike variations in the magnitude of thermal subsidence, which in turn reflect the 3D nature of the underlying Mesozoic rift architecture.

Rift basins and passive margins are commonly inferred to be segmented by lineaments that are oriented sub perpendicular to the basin trend. In onshore extensional provinces, such as the East African Rift, Gulf of Suez and the Basin and Range (Morley *et al*. 1990; Stewart 1998; Younes & McClay 2002), field mapping and analysis of satellite and aerial images have been used to identify and ground truth these rift oblique trends. Here, these lineaments are often associated with marked changes in structural geometry along the strike of the basin. Such changes include alternations in the polarity of half graben asymmetry and/or apparent lateral offsets of rift bounding structures or intrabasinal highs (e.g. Morley *et al*. 1990). In many cases, these lineaments appear to compartmentalize the basin on a variety of scales, which in turn influences the stratigraphic evolution of the rift zone (e.g. Younes & McClay 2002).

Potential field data have been widely used to identify rift oblique trends in offshore basins such as the NE Atlantic volcanic passive margin and the NW shelf of Australia (e.g. Doré *et al*. 1997; Keep & Harrowfield 2005). These lineaments are commonly inferred to be associated with abrupt changes in crustal structure (e.g. Mjelde *et al*. 2003) and/or have controlled sediment transport and deposition within the basin (e.g. Jolley & Morton 2007). Thus, better understanding of these rift oblique trends is important both in terms of assessing their apparently fundamental control on rift architectures and because of their implications for hydrocarbon exploration in extensional basins. Nevertheless, there is surprisingly little published information available on the structural expression of such lineaments in offshore regions, primarily because of the low resolution of regional potential field datasets and/or the limited availability of well calibrated seismic reflection datasets. In many cases, these lineaments are simply represented on regional maps as straight lines crossing the continental margin (e.g. Jolley & Morton 2007, p. 554, fig. 1).

The NE Atlantic volcanic passive margin is an important target for hydrocarbon exploration and therefore benefits from extensive coverage by a range of geological and geophysical datasets, including wells and gravity, magnetic and seismic reflection surveys. The dominant trend of the major rift basins ranges from NE SW to north south, but highly oblique NW SE trending lineaments have long been recognized from analysis of potential field data (Rumph *et al*. 1993; Doré *et al*. 1997; Kimbell *et al*. 2005). These lineaments appear to extend across the continental shelf, but rarely align with the oceanic fracture zones that developed following continental break up *c*. 54 Ma. The origin of these proposed margin scale lineaments remains unclear and a variety of hypotheses have been proposed: reactivation of Precambrian shear zones, such as those exposed in NW Scotland and Norway (e.g. Watson 1984; Knott *et al*. 1993; Fichler *et al*. 1999); structural inheritance from compressional fault systems that originated during the Caledonian orogeny (Doré *et al*. 1997); or the result of Mesozoic rift processes accommodating oblique extension (Rumph *et al*. 1993; Ren *et al*. 2003).

The 3D structure and kinematic significance of these lineaments also remain poorly understood. This aim of this study is to critically assess the structural and stratigraphic evidence for three regional scale lineaments that have been inferred within a major rift basin on the NE Atlantic margin: the Faroe Shetland Basin (Fig. 1). Previous studies have attempted to address this problem through analysis of regional potential field data and correlation of structures and stratigraphic markers using 2D seismic datasets of variable resolution. In contrast, this study will use well calibrated 2D and 3D seismic data to constrain the geometry, growth and tectonic significance of these enigmatic lineaments.

Rift oblique lineaments within the Faroe Shetland Basin, and other similar features elsewhere on the NE Atlantic margin, have previously been referred to as 'transfer zones' (e.g. Doré *et al*.

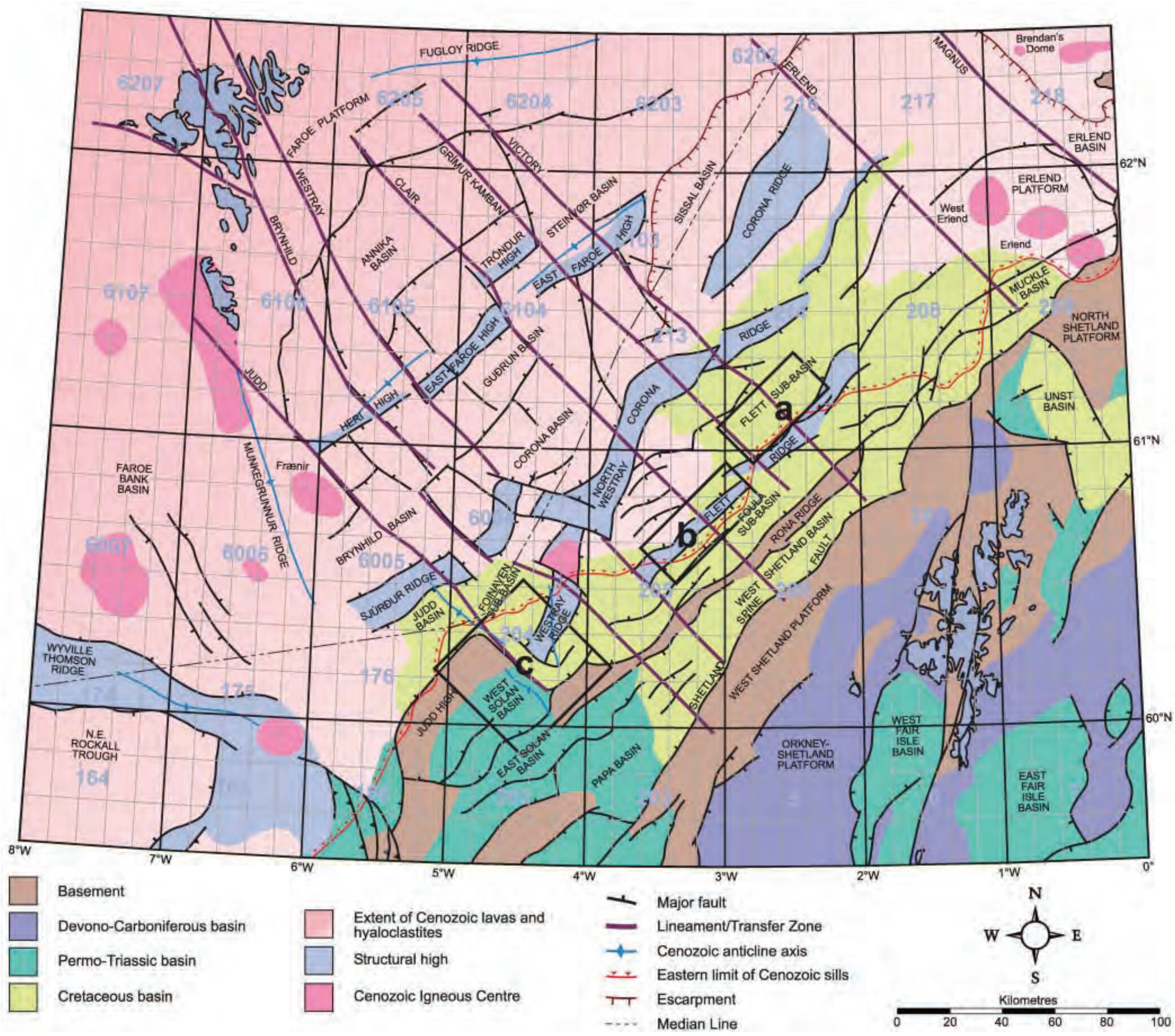

Fig. 1. Structural elements of the Faroe–Shetland Basin with the location of the three lineament case studies described in this paper: a, Victory Lineament; b, Clair Lineament; c, Judd Lineament (after Ellis *et al.* 2009). Map projection is WGS84, UTM 30N.

1997; Ellis *et al.* 2009). However, to avoid confusion, we use the term 'lineament' (or 'rift-oblique lineament') to distinguish structural trends that have been identified primarily using potential field datasets from specific geological features identified through analysis of well-calibrated 2D and 3D seismic reflection data (see below).

Tectonic framework of the Faroe–Shetland Basin

The Faroe–Shetland Basin comprises a series of NE–SW trending sub-basins (Fig. 1) that formed during a sequence of Devono-Carboniferous, Permo-Triassic, Cretaceous and Palaeocene rift events following the end of the Caledonian orogeny (*c.* 390 Ma; Coward 1990). The sub-basins are separated by horst blocks (locally referred to as 'highs' or 'ridges') that are cored by metamorphic basement rocks. This basement can be correlated with the Precambrian gneisses of the Lewisian Complex exposed onshore in NW Scotland (Ritchie & Darbyshire 1984; Hitchen & Ritchie 1987). Many workers (e.g. Duindam & van Hoorn 1987; Mudge & Rashid 1987; Earle *et al.* 1989; Dean *et al.* 1999; Sørensen 2003) have given full accounts of the basin evolution, so only a summary is given here.

Collapse of the Caledonian orogen in the Devonian led to the formation of several 'Old Red Sandstone' basins in the proto-North Atlantic region (Roberts *et al.* 1999). Renewed rifting during the Permo-Triassic was associated with the development of strongly asymmetrical half-graben basins in a semi-arid environment (Herries *et al.* 1999). Fluvial and alluvial environments gave way to marine conditions in the early Jurassic, with a regional unconformity removing much of the middle Jurassic succession (Booth *et al.* 1993). Jurassic extension in NW Europe (Doré *et al.* 1999) was characterized by the formation of mainly north–south trending rifts, including the North Sea and Porcupine Basins and parts of the Halten Terrace. However, the distinct lack of north–south trending structures within the Faroe–Shetland Basin implies that late Jurassic rifting probably did not occur here.

Early Cretaceous rifting has been inferred from the observation that packages of coarse-grained, Early Cretaceous clastic sediments thicken towards the hanging walls of mainly NE–SW trending normal faults within the Faroe–Shetland Basin (Booth *et al*. 1993). Minor rifting in the Middle Cretaceous (Dean *et al*. 1999) continued into the Late Cretaceous against a backdrop of rising eustatic sea levels, leading to dominantly marine conditions and the deposition of a regressive, highly mud-prone sequence (Mudge & Rashid 1987; Turner & Scrutton 1993). The dominant NE–SW trend of the Faroe–Shetland Basin had been established by the end of the Cretaceous, by which time rifting had ceased and basin flank uplift gave rise to deposition of a regressive Palaeocene succession (Smallwood & Gill 2002).

Palaeocene rifting in the SW part of the Faroe–Shetland Basin has been inferred by Dean *et al*. (1999) on the basis that some Cretaceous normal faults appear to have been reactivated during the Palaeocene. Nevertheless, Dean *et al*. (1999) acknowledged that these 'rift' faults could be attributed to minor deformation during post-rift thermal subsidence (Duindam & van Hoorn 1987). Alternatively, fault initiation and/or reactivation at this time may have been associated with differential compaction of sediments over structural highs (e.g. Færseth & Lien 2002). Current models for the development of the NE Atlantic margin imply a progressive northwestward migration in the locus of active rifting, towards the eventual zone of continental break-up (Lundin & Doré 1997). Thus, evidence for a Palaeocene rift event may exist beneath, and be largely obscured by, the thick Palaeogene lava pile in the NW part of the present-day Faroe–Shetland Basin (Fig. 1).

Continental break-up (Eldholm & Grue 1994) was associated with widespread basin uplift and magmatism across the NE Atlantic region, in the form of continental flood basalts, sill and dyke complexes, igneous centres, magmatic underplating and the deposition of regional tuff horizons (White & McKenzie 1989; Naylor *et al*. 1999; Lundin & Doré 2005). Following continental break-up in the early Eocene (*c*. 54 Ma) the tectonic evolution of the Faroe–Shetland Basin has been dominated by thermal subsidence and the growth of large-scale Cenozoic anticlines (Davies *et al*. 2004; Stoker *et al*. 2005; Ritchie *et al*. 2008). These folds have been attributed to a variety of mechanisms including ridge push, sedimentary draping and reactivation of basement structures (Doré *et al*. 2008, and references therein).

Despite the uncertainties surrounding the precise nature and timing of deformation events, the consensus is that the Faroe–Shetland Basin developed as a result of multiple rift episodes prior to continental break-up. Nevertheless, several previous workers have proposed that NW–SE trending rift-oblique lineaments played an important role during basin evolution, and may have influenced the quality and distribution of reservoir sands. The following section summarizes previous work on these lineaments and proposes a number of testable hypotheses to explain their origin and development.

Rift-oblique lineaments ('transfer zones') within the Faroe–Shetland Basin

Rift-oblique lineaments were initially recognized within the Faroe–Shetland Basin by Duindam & van Hoorn (1987) and further discussed by Rumph *et al*. (1993), who inferred 15 orthogonal-to-basin-strike lineaments from interpretations of regional gravity and magnetic datasets. Today, up to seven lineaments are generally recognized, although the reason for this reduction in number has not been clearly explained in the subsequent literature. Nevertheless, these remaining seven lineaments appear to form a key component of the tectonic architecture of the Faroe–Shetland Basin (Fig 1; see Jolley & Morton 2007; Ellis *et al*. 2009).

Various workers have argued that the distribution of Palaeocene age sediments in the southeastern part of the basin was strongly influenced by rift-oblique lineaments (Mitchell *et al*. 1993; Grant *et al*. 1999; Lamers & Carmichael 1999; Naylor *et al*. 1999), implying that the lineaments had significant structural and geomorphological expressions at the Earth's surface during and after rifting (see Gawthorpe & Leeder 2000). More recently, with hydrocarbon exploration interest turning towards the Faroese sector in the NW part of the basin, it has been proposed that rift-oblique lineaments played an important role in the transport of sediments sourced in the Kangerlussuaq region of Greenland (Larsen *et al*. 1999; Larsen & Whitham 2005), through the Faroe Islands (Passey & Bell 2007; Ellis *et al*. 2009), and into the Faroe–Shetland Basin (Whitham *et al*. 2004; Frei *et al*. 2005; Jolley & Morton 2007). They are believed to have exerted a control upon the Palaeocene sediment distribution within this part of the basin, as well as on the distribution and thickness of subaerial basalt flows, shallow marine hyaloclastites (White *et al*. 2003; Ellis *et al*. 2009), the locations of dyke swarms (Naylor *et al*. 1999) and igneous centres (Rumph *et al*. 1993; Ritchie *et al*. 1999).

Several previous workers have inferred large-scale (basin-wide) strike-slip or transpressional deformation along NW–SE trending lineaments within the Faroe–Shetland Basin and elsewhere on the NE Atlantic margin (e.g. Dean *et al*. 1999; Ellis *et al*. 2009). Other workers (e.g. Doré *et al*. 1997) have suggested that some of these apparent discontinuities (e.g. the Jan Mayen Lineament, offshore Norway) may have originated as shear zones in the basement, and in some instances have accommodated minor strike-slip movements in the Cenozoic. These interpretations were based primarily on the lateral offsets in the continental margin, the presence of en echelon Cenozoic anticlines within strata that overlie the inferred position of these lineaments, and on the apparent offsets of structural highs within the Atlantic margin basins (e.g. Fig. 1; Dean *et al*. 1999; Brekke 2000; Ritchie *et al*. 2003). The hypothesis that these lineaments accommodated strike-slip movements implies they are likely to be associated with the classic indications of strike-slip faulting, such as the presence of positive and negative flower structures within the Cenozoic overburden (e.g. Harding 1990). These features should be clearly visible and capable of being mapped along strike using up-to-date high-resolution 3D seismic datasets.

Alternatively, segmentation of rift basins by rift-oblique lineaments may be controlled by the development of transfer zones or accommodation zones (*sensu* Faulds & Varga 1998). Transfer zones are defined as discrete zones of subvertical strike-slip and oblique-slip faulting that trend near-parallel to the extension direction, facilitating the transfer of strain between two en echelon rift domains (Faulds & Varga 1998). Accommodation zones are defined as regions of overlapping fault terminations where strain is transferred between fault tips through a series of relay structures (i.e. 'soft linkage'; e.g. Morley *et al*. 1990; Acocella *et al*. 1999; Moustafa 2002). The key criteria defining transfer and accommodation zones are that extensional strain is conserved along the length of the segmented rift basin (Gibbs 1984; Morley *et al*. 1990), and that transfer and accommodation zones do not extend beyond the region of active rifting (Faulds & Varga 1998, p. 8, fig. 4). Thus, transfer and accommodation zones are second order features that are inherently related to the rift architecture. They are distinct from the regional scale strike slip fault interpretations previously proposed to explain the NW SE trending lineaments on the NE Atlantic margin. An alternative hypothesis, therefore, is that the rift oblique lineaments observed within the Faroe Shetland Basin may have originated as transfer or accommodation zones during periods of rifting prior to continental break up.

It is also important to consider other hypotheses that are not directly related to tectonic or structural processes. These include the influence of intrusive igneous rocks on seismic and regional magnetic field data, or the misinterpretation of other geological phenomena (e.g. hydrothermal vent complexes) that may be difficult to identify using sparse 2D seismic data. Equally, the apparent NW SE fabric may result from the subjective interpretation of coincidentally aligned, but geologically unrelated structural elements within the rift basin. The following sections will test each of these hypotheses against new interpretations of structures that appear to be associated with three previously inferred rift oblique lineaments in the Faroe Shetland Basin: the Victory, Clair and Judd lineaments. Notably, the study areas encompass regions where the lineaments are inferred to cut both sub basins (Flett, Foula, Foinaven and West Solan Sub Basins) and structural highs (Judd High and Flett Ridge) within the Faroe Shetland Basin (Fig. 1).

Methods

PGS Geophysical's time migrated Faroe Shetland Basin 3D seismic MegaSurvey (in effect, a 3D seismic survey of regional extent) was used to analyse structures within the UK sector (i.e. southeastern part) of the Faroe Shetland Basin that appear to be associated with these previously inferred lineaments. Well data provided by Statoil U.K. Ltd were used to date, correlate and understand the stratigraphic significance of seismic reflections mapped within the MegaSurvey dataset. Importantly, the locations of the three case studies lie beyond the southern extent of the Palaeogene flood basalts (Fig. 1), which are known to cause a drop in resolution of seismic data as a result of the attenuation of high frequency waves at the sediment igneous interface (Gallagher & Dromgoole 2008).

The reliance on mainly 3D, as opposed to 2D seismic data is critical to this study because exploration 2D seismic lines are most commonly acquired perpendicular to basin strike, making it difficult to recognize structures that are oblique to the basin trend. Additionally, 3D seismic data allow features to be traced and mapped along strike, providing greater confidence in any subsequent geological interpretations. Importantly, the PGS MegaSurvey covers a substantial portion of the UK sector of the Faroe Shetland Basin. Analysis of the entire dataset revealed little direct structural evidence for most of the previously inferred rift oblique lineaments (Fig. 1), with only three of the aforementioned lineaments having any expression within the Mesozoic Cenozoic succession.

Victory Lineament

The Victory Lineament study area is located within the Cretaceous Flett Sub Basin to the NW of the Flett Ridge. The area is intruded by igneous bodies, which affect seismic imaging at depth (>4000 ms two way travel time (TWT)), particularly within the Cretaceous section.

Dean *et al.* (1999) interpreted the Victory Lineament to be a Palaeocene transpressional pop up structure, which they incorrectly associated with the Clair Lineament, some 50 km to the SW. This subvertical pop up structure appears to be characterized by a vertical offset (throw) of >100 ms at the level of the base Tertiary unconformity, a marked antiformal structure within the intra Palaeocene (Kettla Tuff) interval, and a low amplitude monocline within early Eocene strata (at around Balder Tuff level). Thus, movement along the pop up was inferred to have continued until early Eocene times, synchronous with deposition of the Balder Tuff (Fig. 2a). Various Palaeocene seismic reflectors display notable changes in amplitude across the trace of this structure, consistent with distinct across fault changes in seismic facies. These observations are all characteristic of strike slip (or

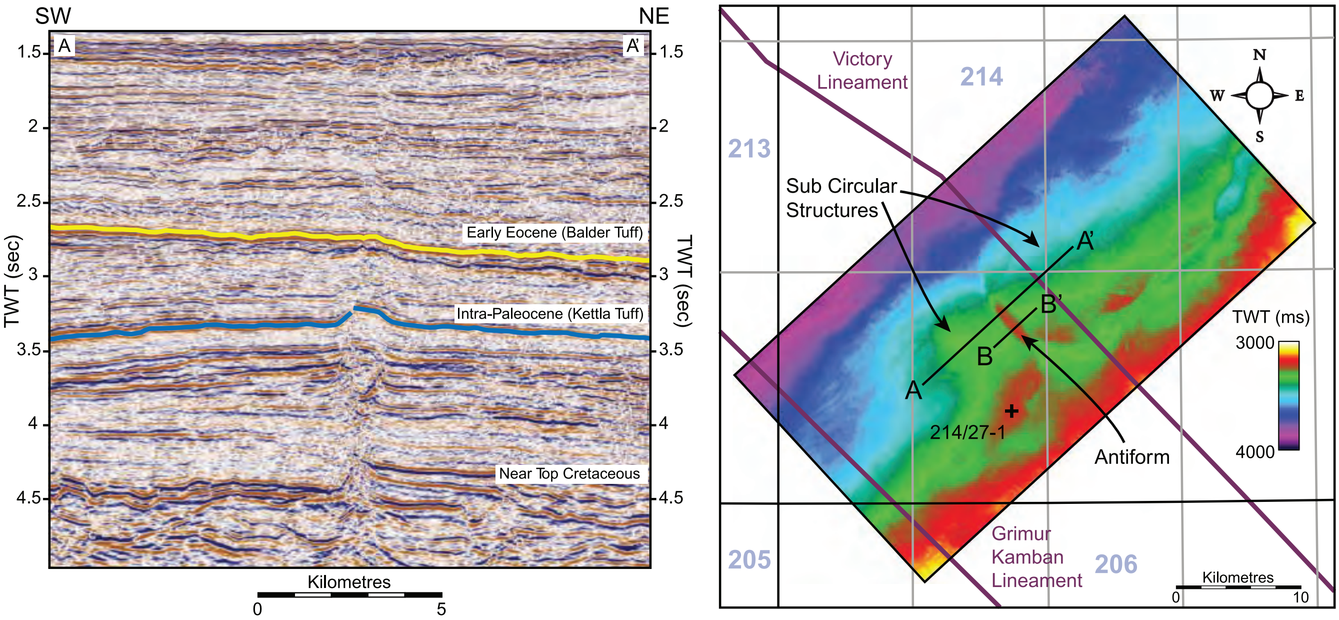

Fig. 2. The transpressional pop-up structure associated with the Victory Lineament interpreted by Dean *et al.* (1999) (left) and a time structure map of the top Kettla Tuff horizon (right). MegaSurvey seismic data courtesy of PGS Geophysical.

transpressional) faulting as inferred from seismic data (Harding 1990). However, not all seismic reflections are offset across the structure and there is little direct evidence of faults splaying upwards from the inferred principal displacement zone at depth.

New 3D seismic mapping of the intra Palaeocene Kettla Tuff reflector reveals a NW SE trending antiform oriented parallel to the inferred trace of the Victory Lineament. However, the antiform lies 5 km to the SW of the lineament and is clearly not laterally continuous across the basin, being only *c.* 5 km in length. Two raised, sub circular structures immediately to the NE and SW of the antiform are also recognized at this level, and appear to be continuous with this structure (Fig. 2b).

The apparent absence of seismically imaged faults along the length of the antiform and the small lateral extent of this structure are not consistent with a wrench or transpressional faulting hypothesis. An alternative hypothesis is that the antiform may have originated as a sediment or fluid injectite, because of its potentially diapiric character (Fig. 2a) and structural relief in map view (Fig. 2b). Such features have been recognized from 3D seismic datasets in other parts of the Faroe Shetland Basin (Davies *et al.* 2006) and in the North Sea (Hurst *et al.* 2003). The timing of sediment or fluid migration would appear to have been during the Palaeocene. However, this hypothesis fails to explain the sub circular structures on either side of the central antiform.

Well 214/27 1 (Figs 2b and 3) penetrates the complete Palaeocene sequence, encountering a series of alternating marine mudstones and sandstones, which shallow upwards into shelf facies deposits (Smallwood & Gill 2002). It also penetrates two regionally important seismic marker horizons, the Kettla Tuff (*c.* 58.5 Ma) and Balder Tuff (*c.* 55.0 Ma; ages estimated from model 1 of Jolley *et al.* (2002)). A *c.* 200 m thick dolerite sill was encountered within the Maastrichtian succession just beneath the late Cretaceous unconformity near the bottom of the well. Unspecified radiometric age dating by Chevron Exploration North Sea Ltd in 1985 of a sample of spotted hornfels from below the sill yielded an age of 55.0 ± 0.6 Ma, implying that deposition of the Balder Tuff and intrusion of the sill were near contemporaneous.

This sill can be correlated with the high amplitude 'Near Top Cretaceous' reflection (Fig. 2a), which lies close to the position of the base Tertiary unconformity. Three dimensional seismic mapping of this and adjacent reflections reveals the presence of a second sill, with similar seismic characteristics, immediately to the NE of the antiformal structure. Both sills have sub circular outlines in map view (slightly elongated in a NE SW direction; Fig. 1) and display concave up, 'saucer shape' geometries (Fig. 4a), which are characteristic of igneous sills mapped elsewhere on the NE Atlantic margin (e.g. Bell & Butcher 2002). Thus, the two raised circular structures observed at the level of the Kettla Tuff horizon (Fig. 4b) can be explained by 'jacking up' (Trude *et al.* 2003) of the Palaeocene strata by *c.* 150 m, leading to the development of forced folds with four way dip closure (Hansen & Cartwright 2006) during the emplacement of two sills within the underlying Upper Cretaceous succession.

The intervening NW SE trending antiform (Figs 1a and 4b) is located immediately above the sill tips. Viewed in seismic sections displayed at near 1:1 scale (i.e. no vertical exaggeration), the region between the sill tips and the crest of the Palaeocene antiform is characterized by high amplitude reflections that dip at *c.* 60° and cross cut surrounding subhorizontal reflectors (Fig. 5). These observations suggest that the cross cutting reflectors represent the edge of an intrusive igneous body with a laccolithic style emplacement. We propose that the laccolith was fed by subvertical dykes, which in turn were sourced from the tips of the two mapped sills (Fig. 6; compare the 'antiformal junction' described by Thomson & Hutton (2004)). The NW SE trending antiformal structure is therefore interpreted to have formed as a consequence of the localized volume increase during igneous intrusion within the Palaeogene section above the steeply dipping sill tips.

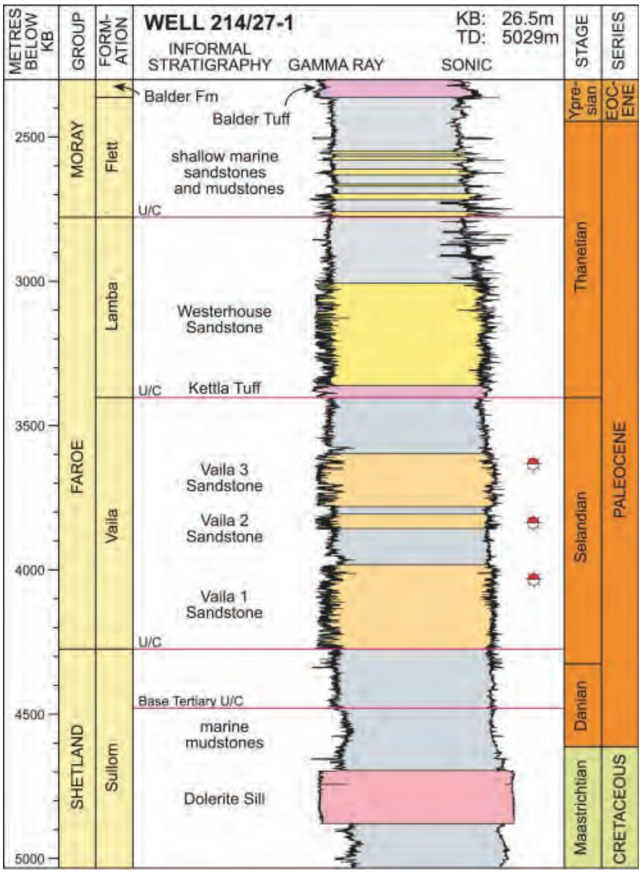

Fig. 3. Well 214/27-1 displaying the Lower Cenozoic to Maastrichtian stratigraphy and the Eocence-aged dolerite sill (after Mudge & Bujak 2001; Gallagher & Dromgoole 2007). U/C, unconformity; TD, total depth; KB, kelly bushing.

The reflections overlying the crest of the antiform and immediately beneath the Balder Tuff marker are characterized by an apparent thickening and a distinct increase in seismic amplitude, across an area of *c.* 2 km × 3 km (Fig. 5). These observations are consistent with the hydrothermal vent complexes described elsewhere on the NE Atlantic margin by Hansen (2006, and references therein). These complexes are associated with sediment remobilization towards the surface as a result of the expulsion of liquids and gases from underlying igneous intrusions. Alternatively, Thomson (2007) has hypothesized that such features may in fact be volcanic fissures, generating local accumulations of pillow lavas or hyaloclastites at the sea floor, which originate from a series of feeder dykes. Nevertheless, both interpretations imply that hydrothermal circulation or igneous extrusion took place immediately prior to deposition of the Balder Tuff. The timing and location of this enhanced hydrothermal and/or extrusive activity are therefore consistent with our preferred explanation for the antiformal structure, and are consistent with the radiometric age date obtained from thermally metamorphosed sediments beneath the dolerite sill encountered in well 214/27 1.

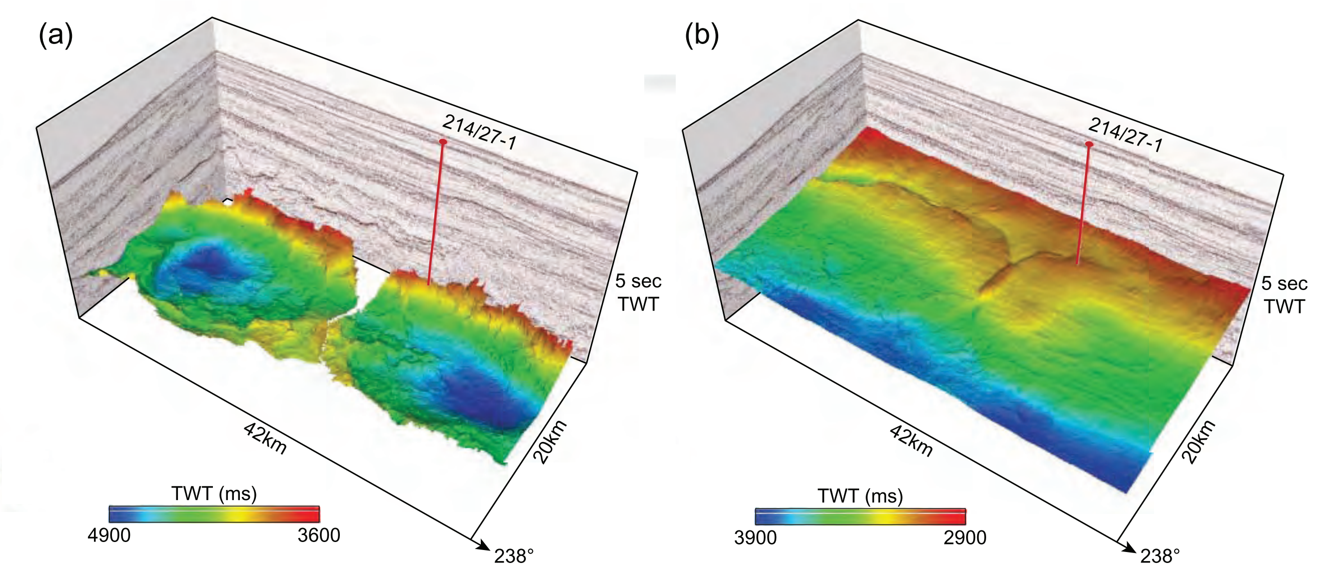

Fig. 4. (**a**) The two Eocene sills with concave-up 'saucer shape' characteristics and (**b**) the associated uplift of the sedimentary overburden displayed by the Kettla Tuff horizon producing two large low-relief forced folds.

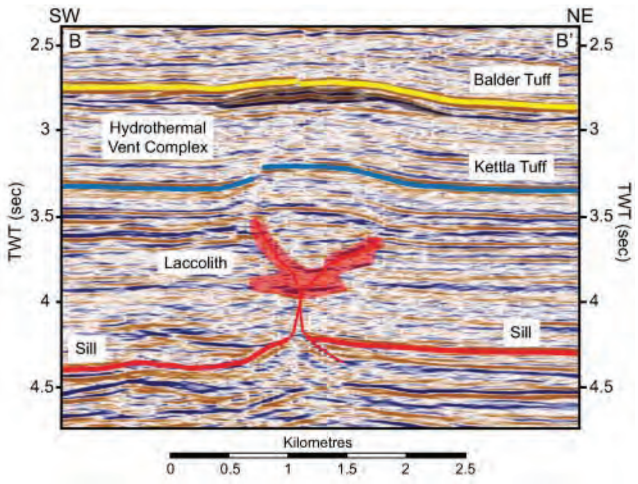

Fig. 5. Near 1:1 scale display of a laccolithic intrusion within the Palaeocene strata (highlighted by red shading). The intrusion is fed by two subvertical dykes extending from the sill tips. Timing of emplacement of the igneous material can be ascertained from the age at which a hydrothermal vent complex (highlighted by dark shading) formed prior to the deposition of the Balder Tuff in the Early Eocene. Line location is shown in Figure 2. MegaSurvey seismic data courtesy of PGS Geophysical.

In summary, a previously interpreted Palaeocene transpressional pop up structure associated with the Victory Lineament is more likely to have originated as a result of local igneous and/or hydrothermal activity just prior to continental break up. There is no conclusive evidence from the seismic data to support the idea that the Victory Lineament had a significant regional structural expression at any time during the Cenozoic, apart from localized uplift above the igneous intrusions. Nevertheless, the high density of sills within the underlying Cretaceous section makes it impossible to test the hypothesis that a through going strike slip (or transpressional) fault exists at depth within the basin, at least using existing 3D seismic datasets.

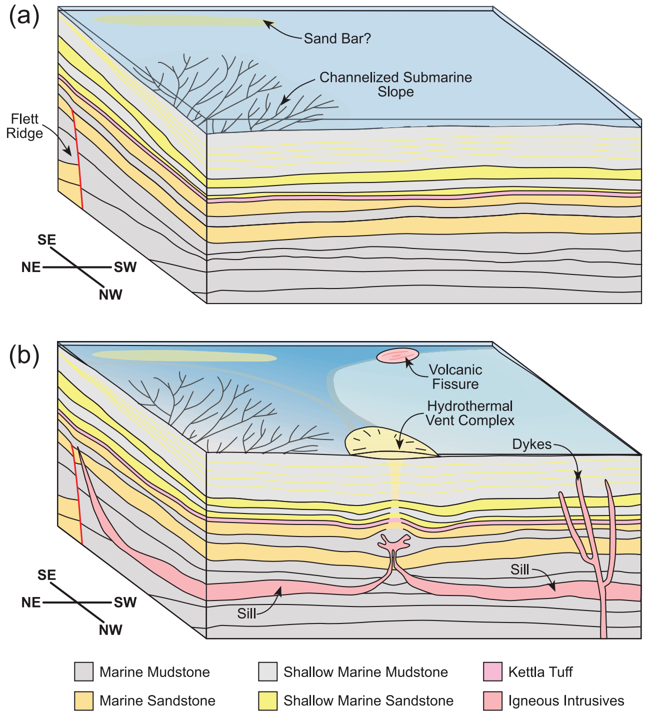

Fig. 6. Block model summary of the inferred Victory Lineament example of Dean *et al*. (1999) (**a**) prior to sill emplacement and (**b**) after sill emplacement. Interpreted hydrothermal vent complexes could be volcanic fissures and vice versa (see Hansen (2006) and Thomson (2007) for discussion). Palaeogeographical interpretation from Lamers & Carmichael (1999).

Clair Lineament

The Clair Lineament is located to the SW of the Victory Lineament, with the study area encompassing part of the NE SW trending Flett Ridge and Flett and Foula Sub Basins (Figs 1 and 7a). This area was selected to clarify the possible structural

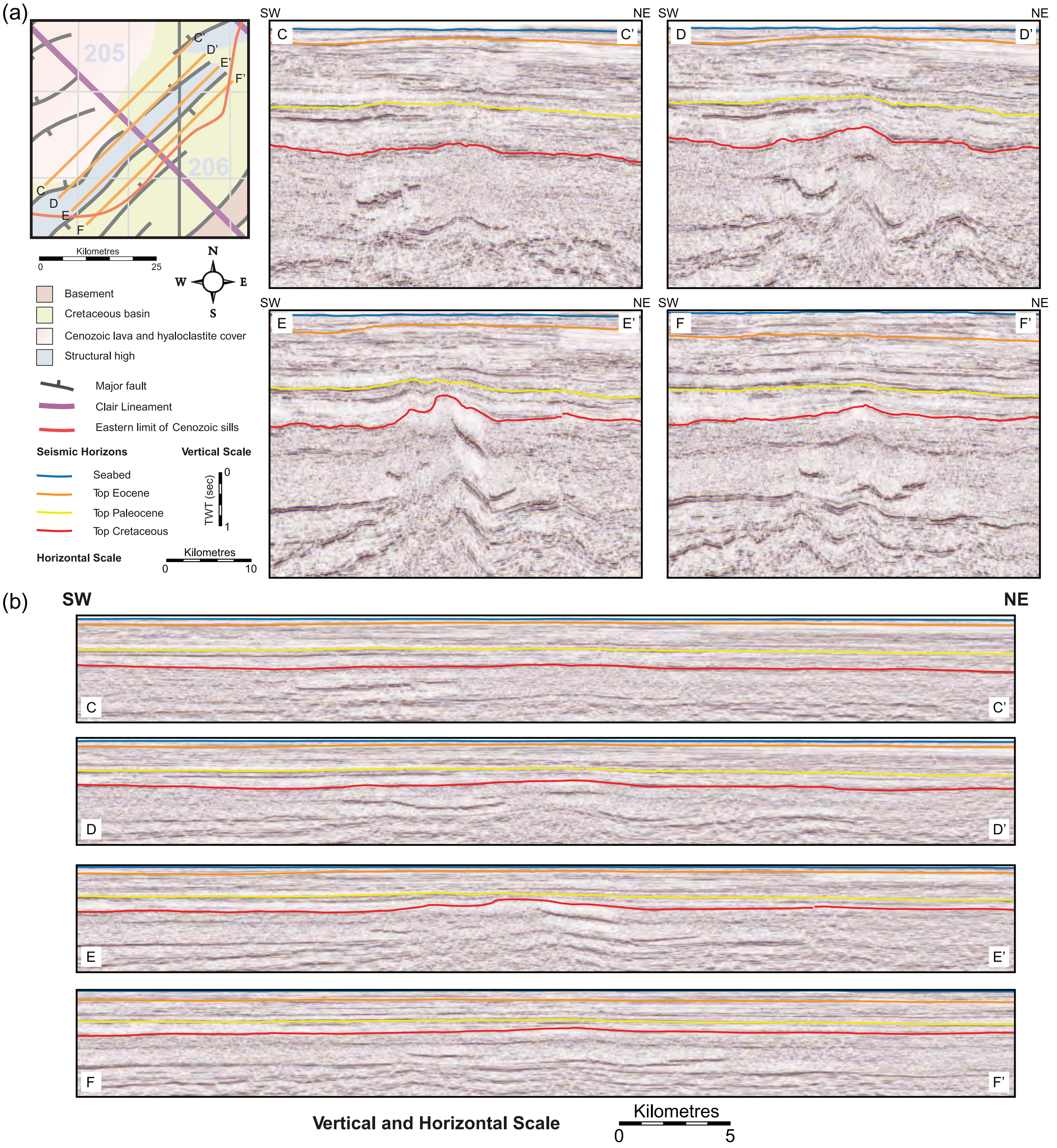

Fig. 7. (**a**) Four seismic lines at 5 km spacing across the inferred Clair Lineament, displaying a rapid change in structure along strike as a result of the compressed display of the data. (**b**) When displayed at near equal horizontal and vertical scale, the apparent effect of the Clair Lineament is negligible, with uplift of strata probably caused by the emplacement of sills into the Cretaceous succession. The Clair Lineament is inferred to intersect near the centre of each seismic line. MegaSurvey seismic data courtesy of PGS Geophysical.

and stratigraphic interaction between the hypothesized Clair Lineament and the two regional depocentres and structural high. Furthermore, Grant *et al*. (1999) have previously recognized a plunging anticline associated with the Clair Lineament in the study area that in a regional sense compartmentalizes the Faroe Shetland Basin along its strike but notably was not formed by 'discrete transfer faults'.

Four NE SW trending seismic sections spaced every 5 km across the inferred position of the Clair Lineament are displayed in Figure 7a. The sections clearly show a rapid change in structural style along the strike of the lineament. This observation, and the development of antiformal structures at the level of the Top Cretaceous marker are consistent with the presence of a NW SE trending strike slip fault in this area (Harding 1990).

However, accurate fault and horizon interpretation is difficult because of the poor quality of the seismic imaging. This problem is caused by four factors. First, NE SW trending Mesozoic normal faults bound the Flett Ridge (Fig. 1), making highly oblique intersections with the seismic lines. Second, there is a high density of sills (high amplitude, concave upward reflections in Fig. 7; compare Figs 2 and 4) within the pre Cenozoic section in the vicinity of the Clair Lineament. Third, a significant (*c*. 3 km wide, up to 500 m thick) late Palaeocene aged hydrothermal vent complex has led to an area of increased structural relief at the Top Cretaceous horizon along a section of the inferred Clair Lineament. Fourth, there are a number of gas discoveries in the area; gas chimneys give rise to local velocity push down effects and can lead to identification of spurious structural features in normal time migrated seismic data.

Analysis of the data at near 1:1 scale (no vertical exaggeration; Fig. 7b) shows that the marked Cretaceous antiform visible in Figure 7a can be considered an artefact of the condensed display. Moreover, there is little evidence of major faulting within the Cenozoic section. It is therefore difficult to demonstrate conclusively that the Clair Lineament had a significant structural and/or geomorphological expression during the Palaeogene, apart from possible localized uplift above igneous intrusions in this region. This conclusion is similar for the Victory Lineament described previously, and also for the intervening Grimur Kamban Lineament shown in Figure 1.

Judd Lineament

The Judd Lineament, originally known as the Faroe Transfer Zone (Mudge & Rashid 1987), is located in the SW of the Faroe Shetland Basin (Fig. 1). In the UK sector, the lineament has a well defined structural expression as a NW SE oriented fault system, which is believed to mark the southwestern limit to the basin in this area (Duindam & van Hoorn 1987). The Judd Lineament has been inferred to extend northwestward across the Judd Basin, into the Faroese sector of the Faroe Shetland Basin (Fig. 1). However, its structural expression is not well defined in this region, which lies outside the area of continuous 3D seismic data coverage. In the UK sector, the NW SE trending faults that make up the Judd Lineament (informally referred to here as the 'Judd fault system') juxtapose the basement cored Judd High in the footwall to the SW against the Cretaceous Foinaven Sub Basin in the hanging wall to the NE. The Judd fault system appears to terminate against, or link with the NE SW trending faults that define the northern margin of the Rona Ridge, a major basement cored horst block that separates the Foula Sub Basin from the West Shetland Basin (Fig. 1). The NW SE trending faults of the Judd fault system have previously been inferred to have either a sinistral (Kirton & Hitchen 1987) or dextral (Hitchen & Ritchie 1987) sense of displacement, a conclusion that is discussed further below.

A time structure map of the top Precambrian basement seismic marker (Fig. 8) displays the gross structure of the study area highlighted in Figure 1. The dominant fault trends in this area are NE SW (040 070°; as exemplified by the faults bounding the Rona Ridge) and NW SE (120 130°; as exemplified by the faults associated with the Judd Lineament), with a subordinate, approximately east west (080 100°) trending fault set (Fig. 8). The Permo Triassic West Solan Basin, an asymmetric half graben system with an alluvial and fluvial sedimentary fill (Booth *et al*. 1993), is located on the southeastern part of the Judd High, adjacent to the Rona Ridge. Previous workers have proposed that this rift detaches onto Caledonian thrust planes, which are believed to have been reactivated as low angle normal faults within the Precambrian basement (Coward & Enfield 1987; Nelson & Lamy 1987).

The NW SE trending fault system associated with the Judd Lineament has been reinterpreted using the 3D seismic dataset and is seen to comprise three major en echelon faults and associated splays, which show large apparent normal offsets with a downthrow (a minimum of *c*. 1000 ms TWT) towards the NE. This new mapping also reveals that the Judd fault system does not continue inboard across, nor does it terminate against the Rona Ridge. Rather, the faults appear to swing round towards a NE SW trend and merge with the faults on the northern margin of the Rona Ridge, apparently without significant change in displacement (Fig. 8). The northwestern extent of the Judd fault

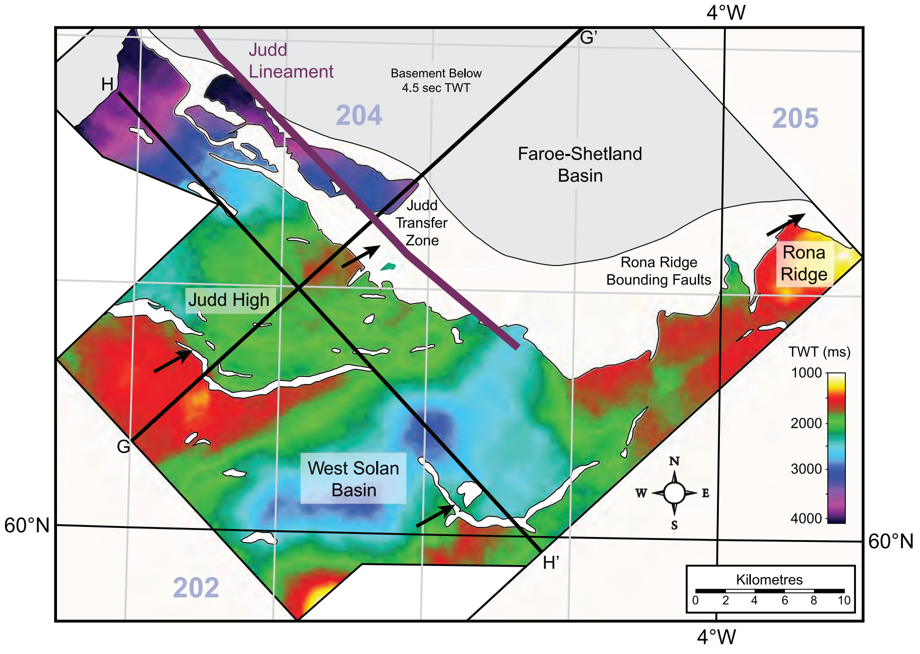

Fig. 8. Time structure map of the top Precambrian basement displaying the West Solan and Faroe Shetland Basins. Fault polygons are displayed in white with black outline and show the dominant fault orientations within the basin (NE SW, NW SE and east west). Arrows highlight the areas of NW SE faulting referred to in the text. Areas shaded in grey are beyond the resolution limits of the seismic data.

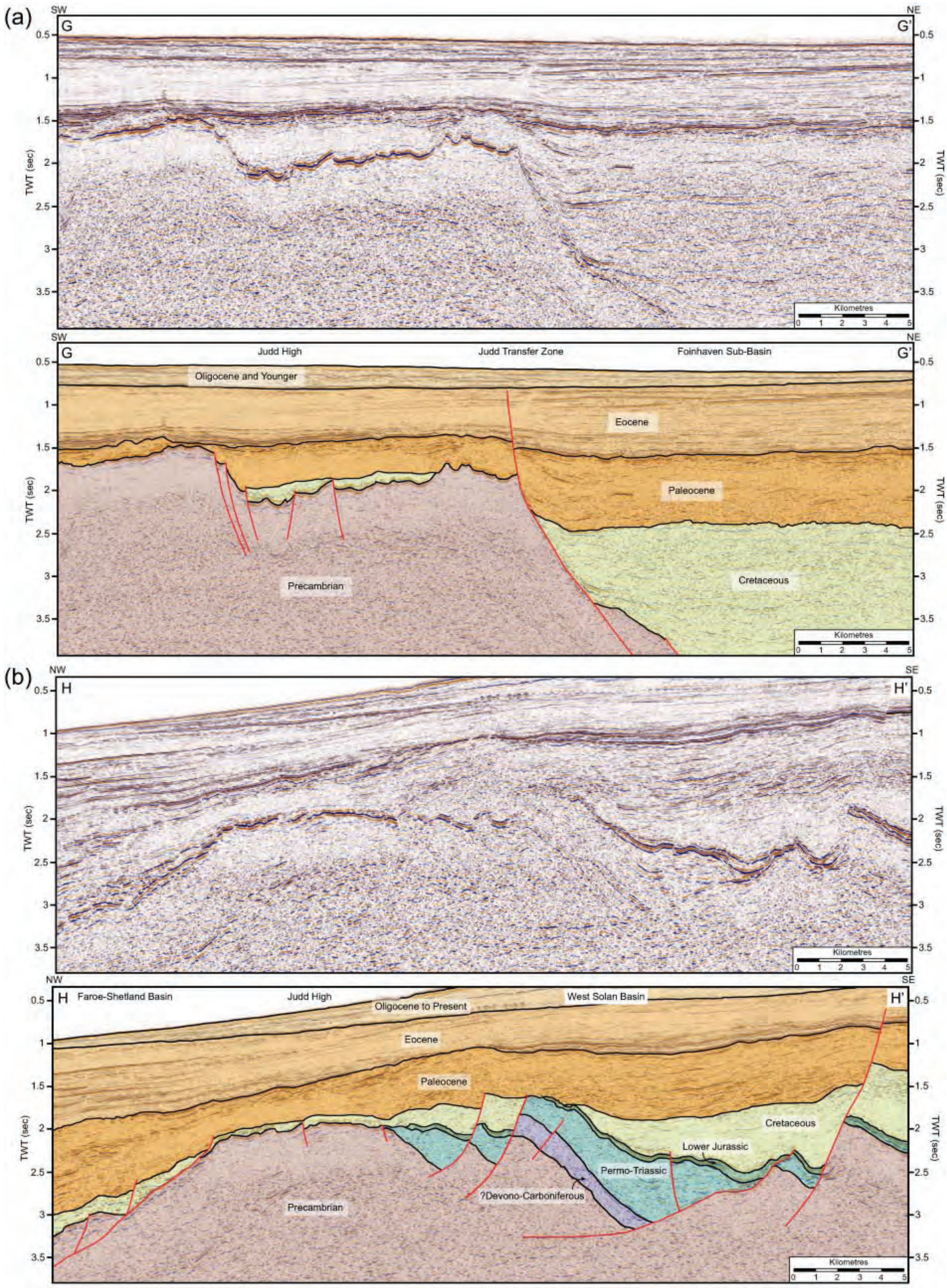

Fig. 9. Seismic lines displaying the tectonic style across (**a**) the Judd Transfer Zone and (**b**) the West Solan Basin. Line location is shown in Figure 8. MegaSurvey seismic data courtesy of PGS Geophysical.

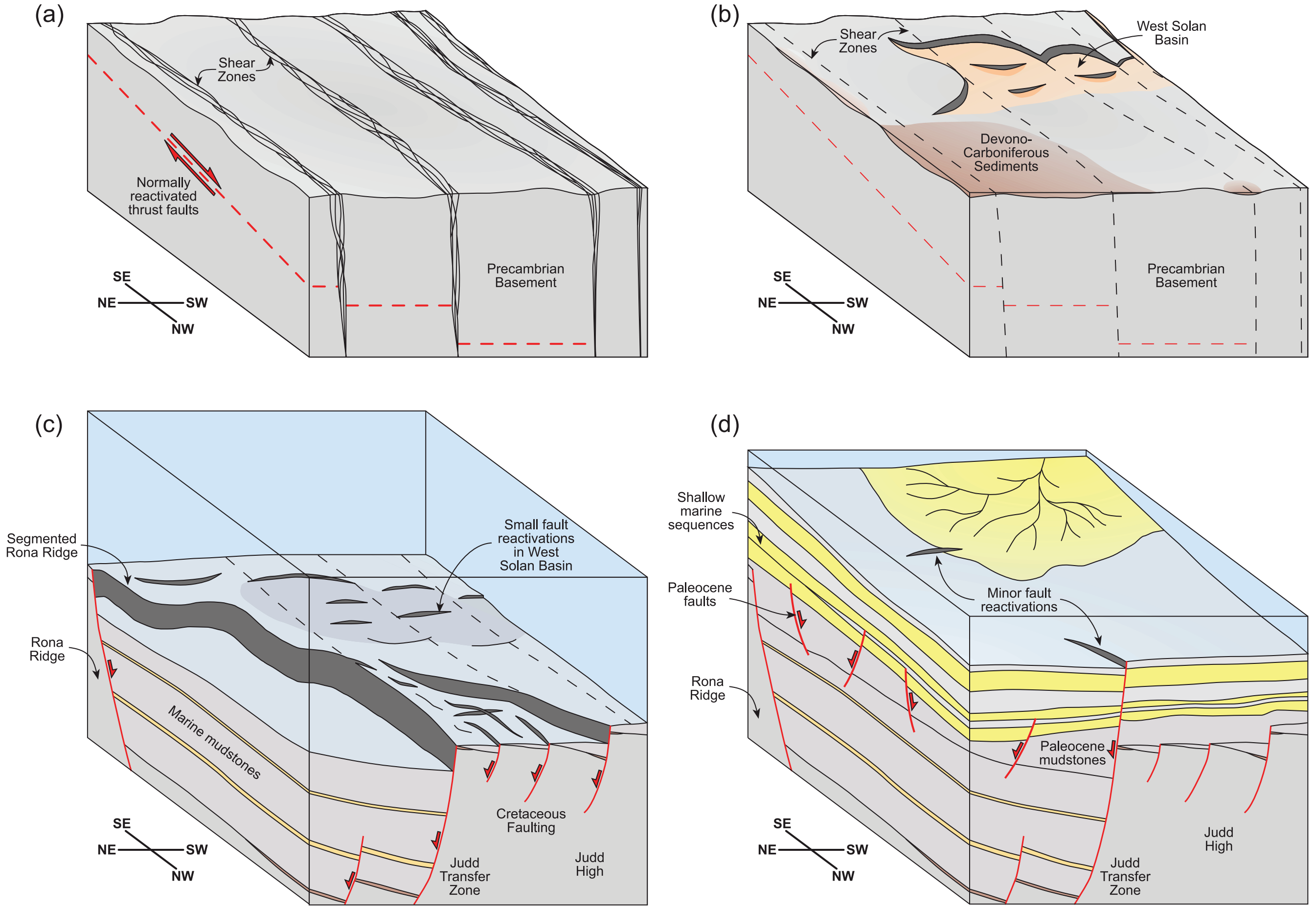

Fig. 10. Block model summaries at various stages of the evolution of the present-day SW Faroe Shetland Basin. (**a**) Proterozoic and Archaean shear zones are reactivated during the Caledonian orogeny with thrust faults normally reactivated during orogenic collapse. (**b**) The Permo-Triassic rift of the West Solan Basin is apparently segmented by NW SE faulting, potentially reactivating inferred NW SE zones of weakness. (**c**) Major late Cretaceous rifting leads to the formation of the Rona Ridge and Judd fault systems. (**d**) Following the cessation of rifting and continental break-up, the Eocene is a period of tectonic quiescence with only minor fault reactivations.

system lies beyond the limit of the 3D seismic MegaSurvey, but analysis of regional 2D lines suggests that this fault system may link with NE SW trending faults that define the northwestern margin of the Judd High (Fig. 1).

Figure 9a shows a NE SW seismic section across the Judd High into the Foinaven Sub Basin. A thin, discontinuous Cretaceous sequence on the Judd High (i.e. in the footwall of the Judd fault system) is seen to expand to more than 1500 ms thickness within the Foinaven Sub Basin. This Upper Cretaceous marine sequence has been dated in a number of wells in the basin. However, because of the poor imaging within the Cretaceous section (which is common throughout the Faroe Shetland Basin because of the dominant mudstone lithology), it is difficult to ascertain whether internal fanning of stratal fills occurs against the Judd fault system (Fig. 9a). Nevertheless, the most plausible explanation for some, if not all, the observed across fault thickening is that the Judd fault system (and associated NE SW trending faults at the northern margin of the Rona Ridge (not shown)) was active and accommodated large basinward throws during deposition of the Upper Cretaceous sequence. The base of this synrift package has not been drilled and can only be inferred from regional 2D seismic data that image the deeper structure.

Figure 9b shows a NW SE oriented seismic section across the Judd High and West Solan Basin. Here, there is clear thickening of Permo Triassic, Lower Jurassic and Upper Cretaceous strata towards the mainly NW dipping faults. The Upper Cretaceous sequence appears to be thinner within the West Solan Basin than it is in the Foinaven Sub Basin, implying that the magnitude of Late Cretaceous rifting was greater in the Faroe Shetland Basin than in the West Solan Basin (Fig. 9a and b). Some faults shown on these sections appear to have been continuously active (or reactivated) into the Palaeocene and/or Eocene (Fig. 9a and b), but along strike mapping shows that such activity was discontinuous along the length of both the NW SE Judd and NE SW Rona Ridge fault systems. Thus, the main phase of rifting in both the West Solan Basin and the southwestern part of the Faroe Shetland Basin is inferred to have ceased by the Palaeocene.

To summarize, the Judd and Rona Ridge fault systems both show large apparent normal displacements and (within the limitations of the available data) appear to link rather than cross cut. These observations suggest that both NE SW (Rona Ridge) and NW SE (Judd) fault systems, together with relatively minor faults within the West Solan Basin, were active synchronously during Late Cretaceous rifting. Taken with the generally accepted view that the Faroe Shetland Basin is an extensional rift basin, the simplest explanation is that the Judd fault system represents a transfer zone (*sensu* Gibbs 1984; Faulds & Varga 1998) that transfers some of the displacement (extensional strain) from the

Rona Ridge fault system outboard by *c*. 30 km to the NE–SW trending faults on the northern margin of the Judd High (Fig. 8). Thus, the Judd Lineament does not represent a through-going basin-scale strike-slip fault (Ellis *et al*. 2009); rather, it is a second-order structure that was active during Late Cretaceous rifting within the Faroe–Shetland Basin (Fig. 10). In this model, the bounding faults of Rona Ridge are inferred to have accommodated predominantly normal displacements, whereas the Judd fault system is expected to have accommodated sinistral oblique movements with a downthrow towards the NE (Fig. 10; see Gibbs 1984, p. 616, fig. 14). Although this hypothesis is, in our view, the most parsimonious explanation of the available data, more rigorous testing will not be possible until there is an improvement in seismic resolution below the Palaeogene flood basalts and an extension of the 3D seismic coverage into the Faroese sector.

An outstanding issue is to explain why a transfer fault system developed adjacent to the Judd High. One possibility is that this ‘stepping’ of the rift towards the proto-Atlantic margin may have been caused by strengthening of the lithosphere beneath the West Solan Basin following Late Palaeozoic and Mesozoic rifting (see Steckler & Tenbrink 1986). Lundin & Doré (1997) used a similar argument to explain the progressive northwestward migration in the locus of active rifting prior to continental break-up in the Norwegian Sea region. Alternatively, Hitchen & Ritchie (1987) have inferred a lateral offset of the Moine Thrust plane along strike from the Judd fault system, which they attributed to activity along a Palaeozoic shear zone. We speculate that the location of the Judd fault system may also have been influenced by a pre-existing zone of weakness in the crystalline basement if this, or an older structure comparable with the similarly oriented NW–SE trending Precambrian shear zones exposed within the Lewisian basement of NW Scotland (e.g. Beacom *et al*. 2001), were to extend northwestwards beneath the Faroe–Shetland Basin. A similar hypothesis has been proposed for the origin of the NW–SE lineaments in the Møre and Vøring Basins offshore Norway by Doré *et al*. (1997).

Discussion

Analysis of three previously inferred rift-oblique lineaments (‘transfer zones’) in the Faroe–Shetland Basin using a well-calibrated regional 3D seismic survey has not found any conclusive evidence to support the hypothesis that the Victory, Clair and Judd Lineaments acted as basin-wide strike-slip faults with significant structural or geomorphological expression during the Cenozoic. Rather, structures associated with these lineaments appear to be local features that developed as a result of igneous processes (e.g. sill emplacement and associated hydrothermal activity) or transfer of extensional strain between one rift segment to another. This reinterpretation is partly the result of an improved understanding of the processes that occur on volcanic margins (e.g. Bell & Butcher 2002; Hansen 2006; Hansen & Cartwright 2006) and partly the result of a more data-driven approach using better quality seismic reflection datasets than have hitherto been available (e.g. Gallagher & Dromgoole 2007). Nevertheless, two important questions remain. The first is to address whether the previously hypothesized control of rift-oblique lineaments (‘transfer zones’) on sediment transport and deposition within the Faroe–Shetland Basin is compatible with our findings. The second is to consider whether our results are compatible with observations that rift-oblique lineaments are associated with abrupt changes in crustal structure.

Control on sediment transport and deposition within the Faroe–Shetland Basin

Jolley & Morton (2007) have used palynological and heavy mineral analyses of rock samples from boreholes to investigate along-strike variations in sediment source and distribution within the UK sector of the Faroe–Shetland Basin. They identified four distinct geographical populations of flora, which varied along the basin trend. Jolley & Morton (2007) suggested that NW–SE trending ‘transfer zones’ may have acted as both barriers and long-range conduits to sediment transport at different times throughout the Palaeocene. Our findings suggest that active rifting had largely ceased within the southeastern (UK) part of the Faroe–Shetland Basin at this time, and that there is little evidence to suggest that the basin was compartmentalized by major, through-going NW–SE structures. We speculate that sediment pathways across and depocentres within the southeastern Faroe–Shetland Basin during the Palaeocene were mainly controlled by the topographic relief associated with post-rift thermal subsidence following Late Cretaceous rifting. It is clear that the Late Cretaceous rift was segmented; for example, by the Judd fault system and probably elsewhere, too, such as at the en echelon segments observed along the Flett and Corona Ridges (Fig. 1). Thus, the spatial distribution of thermal subsidence is likely to have been variable along the strike of the basin and cannot be modelled adequately using a 2D ‘steer’s head’ representation. Along-strike changes (e.g. Mitchell *et al*. 1993; Lamers & Carmichael 1999) in patterns of sediment transport and deposition may largely reflect the along-strike variations in thermal subsidence (i.e. accommodation space), which in turn was controlled by the complex, segmented geometry of the underlying Mesozoic rift. Uplift caused by ‘jacking up’ of strata above igneous intrusions during the Late Palaeocene may have locally modified the geometry of these thermally subsiding sediment depocentres, and sediment transport from further afield (e.g. Greenland; Larsen & Whitham 2005; Jolley & Morton 2007) may also have been controlled by the evolving Palaeocene rift system within the northwestern (Faroese) part of the Faroe–Shetland Basin (see Gawthorpe & Leeder 2000). Thus, we see little requirement to invoke activity along discrete, basin-wide NW–SE ‘transfer zones’ during the Palaeocene. A critical test of our revised model would be to map regional changes in thickness and seismic facies within the post-rift Palaeocene succession using well-calibrated 3D seismic data. These observations should be integrated with sediment provenance data and a comprehensive study of the underlying Late Cretaceous rift architecture within the southeastern part of the Faroe–Shetland Basin.

Deep crustal structure

Mjelde *et al*. (1998, 2003) have mapped five NW–SE- to north–south-trending lineaments on the Vøring margin, offshore Norway, using wide-angle seismic and gravity data. These lineaments are defined by abrupt changes in the thickness of the crystalline basement, variations in Moho depth and by apparent lateral offsets in the locations of high-velocity, lower crustal bodies, which may have originated as igneous material underplated at the base of the crust during continental break-up and/or as eclogitic roots formed during the Caledonian orogeny. There is some uncertainty in the precise location and orientation of these lineaments, but structures in the basement and lower crust appear to be critical in defining these features. Upper crustal structures are less significant in this respect (Mjelde *et al*. 2003). These findings from the Vøring margin are compatible with our results from the Faroe Shetland Basin. We have found no basin scale expressions of the Victory, Clair or Judd Lineaments within the post rift Cenozoic sequence. However, these observations in no way rule out the possibility that these lineaments, originally identified using potential field data, may be associated with changes in deep crustal structure along the strike of the Faroe Shetland Basin (e.g. England *et al*. 2005). Such changes would be consistent with the distinct crustal terranes that have been inferred to exist within the Lewisian Complex of NW Scotland (Friend & Kinny 2001) and which are bounded by mainly NW SE trending shear zones. In addition, variations in deep crustal structure could explain the possible increase in the number of igneous intrusions in the vicinity of the Clair Lineament (Fig. 7). A heterogeneous deep crustal structure could even provide a rationale for the observed segmentation of the Late Cretaceous rift along NW SE transfer zones (*sensu* Faulds & Varga 1998). Nevertheless, such models remain speculative until future studies precisely resolve the deep crustal structure beneath the Faroe Shetland Basin.

Conclusions

Structural and stratigraphic interpretations of a well calibrated 3D seismic survey from the UK sector of the Faroe Shetland Basin suggest that three previously inferred NW SE trending rift oblique lineaments ('transfer zones') did not have regional structural or geomorphological expression during the Cenozoic. There is no evidence to suggest that the Victory, Clair, Judd, or any other previously inferred rift oblique lineaments were active as discrete, basin wide strike slip faults at that time. New results show the following.

(1) Structures within the Flett Sub Basin that are associated with the Victory Lineament (Dean *et al*. 1999) can be related to the effects of igneous intrusion at depth below the Cenozoic strata. Emplacement of two concave up sills (*c*. 200 m thick) below the base Tertiary unconformity led to uplift of the sedimentary overburden, with laccolithic style emplacement at the junction between two sills. The timing of hydrothermal vent and/or extrusive igneous activity above the sill tips agrees with unpublished radiometric dates of one of the sills.

(2) Structures within the Flett and Foula Sub Basins that are associated with the Clair Lineament (Grant *et al*. 1999) can be attributed to the compressed display of poor quality seismic data, and the oblique intersection with NE SW trending normal faults that bound the Flett Ridge, a NE SW trending structural high. Imaging problems are exacerbated by velocity pull up effects from a gas chimney and the large number of igneous sills in the vicinity of the Clair Lineament.

(3) The Judd Lineament (Kirton & Hitchen 1987) is defined by a NW SE trending normal fault system, which we infer to have developed during Cretaceous rifting. This 'Judd fault system' probably transferred extensional strain between two en echelon, NE SW trending rift segments, the Rona Ridge and the Judd High.

The complex architecture of the underlying Late Cretaceous rift system may have given rise to along strike variations in thermal subsidence (accommodation space), which was the principal control on sediment transport pathways and depocentres during the Palaeocene.

This work forms part of an NERC CASE Studentship with Statoil U.K. Ltd (NER/S/C/2006/14276). PGS Geophysical is gratefully acknowledged for permission to publish images from the Faroe Shetland Basin Seismic MegaSurvey. Landmark Graphics Corporation through the Strategic University Alliance Agreement (2006-COM-032168) is acknowledged for providing seismic processing and interpretation software and technical support. D. Stevenson and G. Wilkinson provided continuing technical support within the Department of Earth Sciences. The authors would also like to thank R. England and A. Doré for their constructive reviews of the manuscript. Funding of the colour reproduction costs by Statoil UK Ltd is appreciated.

References

Acocella, V., Faccenna, C., Funiciello, R. & Rossetti, F. 1999. Sand-box modelling of basement-controlled transfer zones in extensional domains. *Terra Nova*, **11**, 149 156.

Beacom, L.E., Holdsworth, R.E., McCaffrey, K.J.W. & Anderson, T.B. 2001. A quantitative study of the influence of pre-existing compositional and fabric heterogeneities upon fracture-zone development during basement reactivation. *In:* Holdsworth, R.E., Strachan, R.A., Magloughlin, J.F. & Knipe, R.J. (eds) *The Nature and Tectonic Significance of Fault Zone Weakening*. Geological Society, London, Special Publications, **186**, 195 211.

Bell, B.R. & Butcher, H. 2002. On the emplacement of sill complexes: evidence from the Faroe Shetland Basin. *In:* Jolley, D.W. & Bell, B.R. (eds) *The North Atlantic Igneous Province: Stratigraphy, Tectonic, Volcanic and Magmatic Processes*. Geological Society, London, Special Publications, **197**, 307 329.

Booth, J., Swiecicki, T. & Wilcockson, P. 1993. The tectono-stratigraphy of the Solan Basin, West of Shetland. *In:* Parker, J.R. (ed.) *Petroleum Geology of Northwest Europe: Proceedings of the 4th Conference*. Geological Society, London, 987 998.

Brekke, H. 2000. The tectonic evolution of the Norwegian Sea continental margin, with emphasis on the Vøring and Møre basins. *In:* Nøttvedt, A. (ed.) *Dynamics of the Norwegian Margin*. Geological Society, London, Special Publications, **167**, 327 378.

Coward, M.P. 1990. The Precambrian, Caledonian and Variscan framework to NW Europe. *In:* Hardman, R.F.P. & Brooks, J. (eds) *Tectonic Events Responsible for Britain's Oil and Gas Reserves*. Geological Society, London, Special Publications, **55**, 1 34.

Coward, M.P. & Enfield, M.A. 1987. The structure of the West Orkney and adjacent basins. *In:* Brooks, J. & Glennie, K. (eds) *Petroleum Geology of North West Europe*. Graham and Trotman, London, 687 696.

Davies, R., Cloke, I., Cartwright, J., Robinson, A. & Ferrero, C. 2004. Post-breakup compression of a passive margin and its impact on hydrocarbon prospectivity: An example from the Tertiary of the Faeroe-Shetland Basin, United Kingdom. *AAPG Bulletin*, **88**, 1 20.

Davies, R.J., Huuse, M., Hirst, P., Cartwright, J. & Yang, Y.S. 2006. Giant clastic intrusions primed by silica diagenesis. *Geology*, **34**, 917 920.

Dean, K., McLachlan, K. & Chambers, A. 1999. Rifting and the development of the Faeroe Shetland Basin. *In:* Fleet, A.J. & Boldy, S.A.R. (eds) *Petroleum Geology of Northwest Europe: Proceedings of the 5th Conference*. Geological Society, London, 533 544.

Doré, A.G., Lundin, E.R., Fichler, C. & Olesen, O. 1997. Patterns of basement structure and reactivation along the NE Atlantic margin. *Journal of the Geological Society, London*, **154**, 85 92.

Doré, A.G., Lundin, E.R., Jensen, L.N., Birkeland, Ø., Eliassen, P.E. & Fichler, C. 1999. Principal tectonic events in the evolution of the northwest European Atlantic margin. *In:* Fleet, A.J. & Boldy, S.A.R. (eds) *Petroleum Geology of Northwest Europe: Proceedings of the 5th Conference*. Geological Society, London, 41 61.

Doré, A.G., Lundin, E.R., Kusznir, N.J. & Pascal, C. 2008. Potential mechanisms for the genesis of Cenozoic domal structures on the NE Atlantic margin: pros, cons and some new ideas. *In:* Johnson, H., Doré, A.G., Gatliff, R.W., Holdsworth, R.E., Lundin, E.R. & Ritchie, J.D. (eds) *The Nature and Origin of Compression in Passive Margins*. Geological Society, London, Special Publications, **306**, 1 26.

Duindam, P. & van Hoorn, B. 1987. Structural evolution of the West Shetland continental margin. *In:* Brooks, J. & Glennie, K. (eds) *Petroleum Geology of North West Europe*. Graham and Trotman, London, 765 773.

Earle, M.M., Jankowski, E.J. & Vann, I.R. 1989. Structural and stratigraphic evolution of the Faeroe Shetland Channel and northern Rockall Trough. *In:* Tankard, A.J. & Balkwill, H.R. (eds) *Extensional Tectonics and Stratigraphy of the North Atlantic Margins*. AAPG Memoirs, **46**, 461 469.

Eldholm, O. & Grue, K. 1994. North Atlantic volcanic margins: dimensions and production rates. *Journal of Geophysical Research Solid Earth*, **99**, 2955 2968.

Ellis, D., Jolley, D.W., Passey, S.R. & Bell, B.R. 2009. Transfer zones: The application of new geological information from the Faroe Islands applied to the offshore exploration of intra basalt and sub-basalt strata. *In:* Ziska, H. & Varming, T. (eds) *Faroe Islands Exploration Conference: Proceedings of the*

2nd Conference. Annales Societatis Scientarum Faroensis Supplement **50**, 205 226.

England, R.W., McBride, J.H. & Hobbs, R.W. 2005. The role of Mesozoic rifting in the opening of the NE Atlantic: evidence from deep seismic profiling across the Faroe Shetland Trough. *Journal of the Geological Society, London*, **162**, 661 673.

Færseth, R.B. & Lien, T. 2002. Cretaceous evolution in the Norwegian Sea a period characterized by tectonic quiescence. *Marine and Petroleum Geology*, **19**, 1005 1027.

Faulds, J.E. & Varga, R.J. 1998. The role of accommodation zones and transfer zones in the regional segmentation of extended terranes. *In:* Faulds, J.E. & Stewart, J.H. (eds) *Accommodation Zones and Transfer Zones: The Regional Segmentation of the Basin and Range Province*. Geological Society of America, Special Papers, **323**, 1 45.

Fichler, C., Rundhovde, E., Olesen, O., Saether, B.M., Rueslatten, H., Lundin, E. & Doré, A.G. 1999. Regional tectonic interpretation of image enhanced gravity and magnetic data covering the mid-Norwegian shelf and adjacent mainland. *Tectonophysics*, **306**, 183 197.

Frei, D., Frei, M. & Knudsen, C. 2005. *Linking the Faroese area and Greenland: an innovative, integrated provenance study.* Danmarks og Grønlands Geologiske Undersøgelse Rapport, **2005/54**.

Friend, C.R.L. & Kinny, P.D. 2001. A reappraisal of the Lewisian Gneiss Complex: geochronological evidence for its tectonic assembly from disparate terranes in the Proterozoic. *Contributions to Mineralogy and Petrology*, **142**, 198 218.

Gallagher, J.W. & Dromgoole, P.W. 2007. Exploring below the basalt, offshore Faroes: a case history of sub-basalt imaging. *Petroleum Geoscience*, **13**, 213 225.

Gallagher, J.W. & Dromgoole, P.W. 2008. Seeing below the basalt offshore Faroes. *Geophysical Prospecting*, **56**, 33 45.

Gawthorpe, R.L. & Leeder, M.R. 2000. Tectono-sedimentary evolution of active extensional basins. *Basin Research*, **12**, 195 218.

Gibbs, A.D. 1984. Structural evolution of extensional basin margins. *Journal of the Geological Society, London*, **141**, 609 620.

Grant, N., Bouma, A. & McIntyre, A. 1999. The Turonian play in the Faeroe Shetland Basin. *In:* Fleet, A.J. & Boldy, S.A.R. (eds) *Petroleum Geology of Northwest Europe: Proceedings of the 5th Conference*. Geological Society, London, 661 673.

Hansen, D.M. 2006. The morphology of intrusion-related vent structures and their implications for constraining the timing of intrusive events along the NE Atlantic margin. *Journal of the Geological Society, London*, **163**, 789 800.

Hansen, D.M. & Cartwright, J. 2006. The three-dimensional geometry and growth of forced folds above saucer-shaped igneous sills. *Journal of Structural Geology*, **28**, 1520 1535.

Harding, T.P. 1990. Identification of wrench faults using subsurface structural data criteria and pitfalls. *AAPG Bulletin*, **74**, 1590 1609.

Herries, R., Poddubiuk, R. & Wilcockson, P. 1999. Solan, Strathmore and the back basin play, West of Shetland. *In:* Fleet, A.J. & Boldy, S.A.R. (eds) *Petroleum Geology of Northwest Europe: Proceedings of the 5th Conference*. Geological Society, London, 693 712.

Hitchen, K. & Ritchie, J.D. 1987. Geological review of the West Shetland area. *In:* Brooks, J. & Glennie, K. (eds) *Petroleum Geology of North West Europe*. Graham and Trotman, London, 737 749.

Hurst, A., Cartwright, J., Huuse, M., Jonk, R., Schwab, A., Duranti, D. & Cronin, B. 2003. Significance of large-scale sand injectites as long-term fluid conduits: evidence from seismic data. *Geofluids*, **3**, 263 274.

Jolley, D.W. & Morton, A.C. 2007. Understanding basin sedimentary provenance: evidence from allied phytogeographic and heavy mineral analysis of the Palaeocene of the NE Atlantic. *Journal of the Geological Society, London*, **164**, 553 563.

Jolley, D.W., Clarke, B. & Kelley, S. 2002. Paleogene time scale miscalibration: Evidence from the dating of the North Atlantic igneous province. *Geology*, **30**, 7 10.

Keep, M. & Harrowfield, M. 2005. Basement reactivation and inversion mechanisms in the Timor and Norwegian seas. *In:* Doré, A.G. & Vining, B.A. (eds) *Petroleum Geology: North-West Europe and Global Perspectives Proceedings of the 6th Petroleum Geology Conference*. Geological Society, London, 861 871.

Kimbell, G.S., Ritchie, J.D., Johnson, H. & Gatliff, R.W. 2005. Controls on the structure and evolution of the NE Atlantic margin revealed by regional potential field imaging and 3D modelling. *In:* Doré, A.G. & Vining, B.A. (eds) *Petroleum Geology: North-West Europe and Global Perspectives Proceedings of the 6th Petroleum Geology Conference*. Geological Society, London, 933 945.

Kirton, S.R. & Hitchen, K. 1987. Timing and style of crustal extension north of the Scottish mainland. *In:* Coward, M.P., Dewey, J. & Hancock, P.L. (eds) *Continental Extensional Tectonics*. Geological Society, London, Special Publications, **28**, 501 510.

Knott, S.D., Burchell, M.T., Jolley, E.J. & Fraser, A.J. 1993. Mesozoic to Cenozoic plate reconstructions of the North Atlantic and hydrocarbon plays of the Atlantic margins. *In:* Parker, J.R. (ed.) *Petroleum Geology of Northwest Europe: Proceedings of the 4th Conference*. Geological Society, London, 953 974.

Lamers, E. & Carmichael, S.M. M. 1999. The Paleocene deepwater sandstone play West of Shetland. *In:* Fleet, A.J. & Boldy, S.A.R. (eds) *Petroleum Geology of Northwest Europe: Proceedings of the 5th Conference*. Geological Society, London, 645 659.

Larsen, M. & Whitham, A.G. 2005. Evidence for a major sediment input point into the Faroe Shetland Basin from the Kangerlussuaq region of southern East Greenland. *In:* Doré, A.G. & Vining, B.A. (eds) *Petroleum Geology: North-West Europe and Global Perspectives Proceedings of the 6th Petroleum Geology Conference*. Geological Society, London, 913 922.

Larsen, M., Hamberg, L., Olaussen, S., Norgaard-Pedersen, N. & Stemmerik, L. 1999. Basin evolution in southern East Greenland: An outcrop analog for Cretaceous Paleogene basins on the North Atlantic volcanic margins. *AAPG Bulletin*, **83**, 1236 1261.

Lundin, E.R. & Doré, A.G. 1997. A tectonic model for the Norwegian passive margin with implications for the NE Atlantic: Early Cretaceous to break-up. *Journal of the Geological Society, London*, **154**, 545 550.

Lundin, E.R. & Doré, A.G. 2005. NE Atlantic break-up: a re-examination of the Iceland mantle plume model and the Atlantic Arctic linkage. *In:* Doré, A.G. & Vining, B.A. (eds) *Petroleum Geology: North-West Europe and Global Perspectives Proceedings of the 6th Petroleum Geology Conference*. Geological Society, London, 739 754.

Mitchell, S.M., Beamish, G.W.J., Wood, M.V., Malacek, S.J., Armentrout, J.A., Damuth, J.E. & Olson, H.C. 1993. Paleogene sequence stratigraphic framework for the Faeroe Basin. *In:* Parker, J.R. (ed.) *Petroleum Geology of Northwest Europe: Proceedings of the 4th Conference*. Geological Society, London, 1011 1023.

Mjelde, R., Digranes, P., Shimamura, H., et al. 1998. Crustal structure of the northern part of the Vøring Basin, mid-Norway margin, from wide-angle seismic and gravity data. *Tectonophysics*, **293**, 175 205.

Mjelde, R., Shimamura, H., Kanazawa, T., Kodaira, S., Raum, T. & Shiobara, H. 2003. Crustal lineaments, distribution of lower crustal intrusives and structural evolution of the Vøring Margin, NE Atlantic; new insight from wide-angle seismic models. *Tectonophysics*, **369**, 199 218.

Morley, C.K., Nelson, R.A., Patton, T.L. & Munn, S.G. 1990. Transfer zones in the East African Rift System and their relevance to hydrocarbon exploration in rifts. *AAPG Bulletin*, **74**, 1234 1253.

Moustafa, A.R. 2002. Controls on the geometry of transfer zones in the Suez rift and northwest Red Sea: Implications for the structural geometry of rift systems. *AAPG Bulletin*, **86**, 979 1002.

Mudge, D.C. & Bujak, J.P. 2001. Biostratigraphic evidence for evolving palaeoenvironments in the Lower Paleogene of the Faeroe Shetland Basin. *Marine and Petroleum Geology*, **18**, 577 590.

Mudge, D.C. & Rashid, B. 1987. The geology of the Faeroe Basin area. *In:* Brooks, J. & Glennie, K. (eds) *Petroleum Geology of North West Europe*. Graham and Trotman, London, 751 763.

Naylor, P.H., Bell, B.R., Jolley, D.W., Durnall, P. & Fredsted, R. 1999. Palaeogene magmatism in the Faeroe Shetland Basin: influences on uplift history and sedimentation. *In:* Fleet, A.J. & Boldy, S.A.R. (eds) *Petroleum Geology of Northwest Europe: Proceedings of the 5th Conference*. Geological Society, London, 545 558.

Nelson, P.H. H. & Lamy, J.M. 1987. The Møre/West Shetlands area: a review. *In:* Brooks, J. & Glennie, K. (eds) *Petroleum Geology of North West Europe*. Graham and Trotman, London, 775 784.

Passey, S.R. & Bell, B.R. 2007. Morphologies and emplacement mechanisms of the lava flows of the Faroe Islands Basalt Group, Faroe Islands, NE Atlantic Ocean. *Bulletin of Volcanology*, **70**, 139 156.

Ren, S.C., Faleide, J.I., Eldholm, O., Skogseid, J. & Gradstein, F. 2003. Late Cretaceous Paleocene tectonic development of the NW Vøring Basin. *Marine and Petroleum Geology*, **20**, 177 206.

Ritchie, J.D. & Darbyshire, D.P.F. 1984. Rb Sr dates on Precambrian rocks from marine exploration wells in and around the West Shetland Basin. *Scottish Journal of Geology*, **20**, 31 36.

Ritchie, J.D., Gatliff, R.W. & Richards, P.C. 1999. Early Tertiary magmatism in the offshore NW UK margin and surrounds. *In:* Fleet, A.J. & Boldy, S.A.R. (eds) *Petroleum Geology of Northwest Europe: Proceedings of the 5th Conference*. Geological Society, London, 573 584.

Ritchie, J.D., Johnson, H. & Kimbell, G.S. 2003. The nature and age of Cenozoic contractional deformation within the NE Faroe Shetland Basin. *Marine and Petroleum Geology*, **20**, 399 409.

Ritchie, J.D., Johnson, H., Quinn, M.F. & Gatliff, R.W. 2008. The effects of Cenozoic compression within the Faroe Shetland Basin and adjacent areas. *In:* Johnson, H., Doré, A.G., Gatliff, R.W., Holdsworth, R.E., Lundin, E.R. & Ritchie, J.D. (eds) *The Nature and Origin of Compression in Passive*

Margins. Geological Society, London, Special Publications, **306**, 121–136.

Roberts, D.G., Thompson, M., Mitchener, B., Hossack, J., Carmichael, S.M.M. & Bjørnseth, H.M. 1999. Palaeozoic to Tertiary rift and basin dynamics: mid-Norway to the Bay of Biscay – a new context for hydrocarbon prospectivity in the deep water frontier. *In:* Fleet, A.J. & Boldy, S.A.R. (eds) *Petroleum Geology of Northwest Europe: Proceedings of the 5th Conference*. Geological Society, London, 7–40.

Rumph, B., Reaves, C.M., Orange, V.G. & Robinson, D.L. 1993. Structuring and transfer zones in the Faeroe Basin in a regional tectonic context. *In:* Parker, J.R. (ed.) *Petroleum Geology of Northwest Europe: Proceedings of the 4th Conference*. Geological Society, London, 999–1009.

Smallwood, J.R. & Gill, C.E. 2002. The rise and fall of the Faroe–Shetland Basin: evidence from seismic mapping of the Balder Formation. *Journal of the Geological Society, London*, **159**, 627–630.

Sørensen, A.B. 2003. Cenozoic basin development and stratigraphy of the Faroes area. *Petroleum Geoscience*, **9**, 189–207.

Steckler, M.S. & Tenbrink, U.S. 1986. Lithospheric strength variations as a control on new plate boundaries – examples from the northern Red Sea region. *Earth and Planetary Science Letters*, **79**, 120–132.

Stewart, J.H. 1998. The role of accommodation zones and transfer zones in the regional segmentation of extended terranes. *In:* Faulds, J.E. & Stewart, J.H. (eds) *Regional Characteristics, Tilt Domains, and Extensional History of the Late Cenozoic Basin and Range Province, Western North America*. Geological Society of America, Special Papers, **323**, 47–74.

Stoker, M.S., Praeg, D., Shannon, P.M., et al. 2005. Neogene evolution of the Atlantic continental margin of NW Europe (Lofoten Islands to SW Ireland): anything but passive. *In:* Doré, A.G. & Vining, B.A. (eds) *Petroleum Geology: North-West Europe and Global Perspectives – Proceedings of the 6th Petroleum Geology Conference*. Geological Society, London, 1057–1076.

Thomson, K. 2007. Determining magma flow in sills, dykes and laccoliths and their implications for sill emplacement mechanisms. *Bulletin of Volcanology*, **70**, 183–201.

Thomson, K. & Hutton, D. 2004. Geometry and growth of sill complexes: insights using 3D seismic from the North Rockall Trough. *Bulletin of Volcanology*, **66**, 364–375.

Trude, J., Cartwright, J., Davies, R.J. & Smallwood, J. 2003. New technique for dating igneous sills. *Geology*, **31**, 813–816.

Turner, J.D. & Scrutton, R.A. 1993. Subsidence patterns in western margin basins: evidence from the Faeroe–Shetland Basin. *In:* Parker, J.R. (ed.) *Petroleum Geology of Northwest Europe: Proceedings of the 4th Conference*. Geological Society, London, 975–983.

Watson, J. 1984. The ending of the Caledonian Orogeny in Scotland – President's anniversary address 1983. *Journal of the Geological Society, London*, **141**, 193–214.

White, R. & McKenzie, D. 1989. Magmatism at rift zones: the generation of volcanic continental margins and flood basalts. *Journal of Geophysical Research – Solid Earth and Planets*, **94**, 7685–7729.

White, R.S., Smallwood, J.R., Fliedner, M.M., Boslaugh, B., Maresh, J. & Fruehn, J. 2003. Imaging and regional distribution of basalt flows in the Faeroe–Shetland Basin. *Geophysical Prospecting*, **51**, 215–231.

Whitham, A.G., Morton, A.C. & Fanning, C.M. 2004. Insights into Cretaceous–Palaeogene sediment transport paths and basin evolution in the North Atlantic from a heavy mineral study of sandstones from southern East Greenland. *Petroleum Geoscience*, **10**, 61–72.

Younes, A.I. & McClay, K. 2002. Development of accommodation zones in the Gulf of Suez–Red Sea rift, Egypt. *AAPG Bulletin*, **86**, 1003–1026.

Received 21 January 2009; revised typescript accepted 28 April 2009.
Scientific editing by Ian Alsop.

Appendix F

CD Contents

The files located upon the included CD were created using an HP dv9088ea notebook PC. The operating system used was Microsoft Windows XP Media Center Edition, Version 2002, Service Pack 3.

The following file types are located upon the CD:

.pdf **.xls** **.txt** **.png** **.ppt**

The software used to create the file types are:

.pdf	Adobe Acrobat 9 Pro – Version 9.2.0
.xls	Microsoft Office Excel 2003 (11.8307.8221) SP3 – Part of Microsoft Office Professional Edition 2003
.txt	Badley's Fault Analysis Statistical Information Tool (FASIT)
.png	Portable network graphics formed within standard graphic manipulation software
.ppt	Microsoft Office PowerPoint 2003 (11.8307.8221) SP3 – Part of Microsoft Office Professional Edition 2003

The file structure and listing of included files upon the CD is detailed below:

\Chapter 4 – Fault Statistics\Figure 4.14\Cumulative Heaves.xls
\Chapter 4 – Fault Statistics\Figure 4.20\Gjallar\Campanian_115_gjallar.txt
\Chapter 4 – Fault Statistics\Figure 4.20\Gjallar\Campanian_118_gjallar.txt
\Chapter 4 – Fault Statistics\Figure 4.20\Gjallar\Gjallar Strain.xls
\Chapter 4 – Fault Statistics\Figure 4.20\Gjallar\Gjallar_map_camp_115.png
\Chapter 4 – Fault Statistics\Figure 4.20\Gjallar\Gjallar_map_camp_118.png
\Chapter 4 – Fault Statistics\Figure 4.20\Gjallar\Gjallar_map_top_cret.png
\Chapter 4 – Fault Statistics\Figure 4.20\Gjallar\Top_Cretaceous_gjallar.txt
\Chapter 4 – Fault Statistics\Figure 4.20\Nyk\Nyk Strain.xls
\Chapter 4 – Fault Statistics\Figure 4.20\Nyk\Nyk_camp_115_data.txt
\Chapter 4 – Fault Statistics\Figure 4.20\Nyk\Nyk_camp_118_data.txt
\Chapter 4 – Fault Statistics\Figure 4.20\Nyk\Nyk_map_camp_115.png
\Chapter 4 – Fault Statistics\Figure 4.20\Nyk\Nyk_map_camp_118.png
\Chapter 4 – Fault Statistics\Figure 4.20\Nyk\Nyk_map_top_cret.png
\Chapter 4 – Fault Statistics\Figure 4.20\Nyk\Nyk_map_top_pal.png
\Chapter 4 – Fault Statistics\Figure 4.20\Nyk\Nyk_top_cret_data.txt
\Chapter 4 – Fault Statistics\Figure 4.20\Nyk\Nyk_top_pal_data.txt
\Chapter 4 – Fault Statistics\Figure 4.20\Southern RAZ\Vema Strain.xls
\Chapter 4 – Fault Statistics\Figure 4.20\Southern RAZ\Vema_camp_115_data.txt
\Chapter 4 – Fault Statistics\Figure 4.20\Southern RAZ\Vema_camp_118_data.txt
\Chapter 4 – Fault Statistics\Figure 4.20\Southern RAZ\Vema_map_camp_115.png
\Chapter 4 – Fault Statistics\Figure 4.20\Southern RAZ\Vema_map_camp_118.png
\Chapter 4 – Fault Statistics\Figure 4.20\Southern RAZ\Vema_map_top_cret.png
\Chapter 4 – Fault Statistics\Figure 4.20\Southern RAZ\Vema_map_top_pal.png
\Chapter 4 – Fault Statistics\Figure 4.20\Southern RAZ\Vema_top_cret_data.txt
\Chapter 4 – Fault Statistics\Figure 4.20\Southern RAZ\Vema_top_pal_data.txt
\Chapter 4 – Fault Statistics\Figure 4.20\Sample Line Settings.xls

\Conference Presentations\01 Faroes Exploration Conference (Torshavn, Faroe Islands) September 2006\Faroe Islands Exploration Conference 2006.pdf
\Conference Presentations\02 Petroleum Geoscience Collaboration Conference (London, UK) November 2006\Information.txt
\Conference Presentations\03 TSG Annual Meeting (La Roche en Ardenne, Belgium) January 2008\Abstract - David Moy.pdf
\Conference Presentations\03 TSG Annual Meeting (La Roche en Ardenne, Belgium) January 2008\TSG 2008 - David Moy.ppt
\Conference Presentations\04 Rifts Renaissance, Petroleum Group, Geological Society (Houston, Texas, USA) August 2008\Abstract - David Moy.pdf
\Conference Presentations\04 Rifts Renaissance, Petroleum Group, Geological Society (Houston, Texas, USA) August 2008\Rifts Renaissance - David Moy.ppt
\Conference Presentations\05 Petroleum Geoscience Forum (Aberdeen, UK), November 2008\Abstract - David Moy.pdf
\Conference Presentations\05 Petroleum Geoscience Forum (Aberdeen, UK), November 2008\Petroleum Geoscience Research Forum - David Moy.pdf
\Conference Presentations\05 Petroleum Geoscience Forum (Aberdeen, UK), November 2008\Petroleum Geoscience Research Forum - David Moy.ppt
\Conference Presentations\06 AGU Fall Meeting (San Francisco, California, USA), December 2008\Abstract - David Moy.pdf
\Conference Presentations\06 AGU Fall Meeting (San Francisco, California, USA), December 2008\AGU 2008 - David Moy.pdf
\Conference Presentations\07 TSG Annual Meeting (Keele University, UK), January 2009\Abstract - David Moy.pdf
\Conference Presentations\07 TSG Annual Meeting (Keele University, UK), January 2009\TSG 2009 - David Moy.pdf
\Conference Presentations\08 7th Petroleum Geology Conference (London, UK), March-April 2009\7th PGC - David Moy.pdf
\Conference Presentations\08 7th Petroleum Geology Conference (London, UK), March-April 2009\Abstract - David Moy.pdf
\Conference Presentations\09 AAPG Annual Convention (Denver, Colorado, USA), June 2009\AAPG 2009 - David Moy.pdf
\Conference Presentations\09 AAPG Annual Convention (Denver, Colorado, USA), June 2009\Abstract - David Moy.pdf
\Conference Presentations\10 3rd Faroese Exploration Conference (Torshavn, Faroe Islands) September 2009\3rd FIEC - David Moy.ppt
\Conference Presentations\10 3rd Faroese Exploration Conference (Torshavn, Faroe Islands) September 2009\3rd FIEC Poster - David Moy.pdf
\Conference Presentations\10 3rd Faroese Exploration Conference (Torshavn, Faroe Islands) September 2009\Poster Abstract - David Moy.pdf
\Conference Presentations\10 3rd Faroese Exploration Conference (Torshavn, Faroe Islands) September 2009\Talk Abstract - David Moy.pdf

\Paper Reprints\Moy and Imber, 2009.pdf

\PhD Thesis\Rift-Oblique Lineaments on the NE Atlantic Margin – David J. Moy.pdf

\Well Time-Depth Tables\202-3a-3\2023a3.pdf
\Well Time-Depth Tables\202-3a-3\2023a3.txt
\Well Time-Depth Tables\202-3a-3\2023a3.xls

\Well Time-Depth Tables\204-19-1\204191.pdf
\Well Time-Depth Tables\204-19-1\204191.txt
\Well Time-Depth Tables\204-19-1\204191.xls
\Well Time-Depth Tables\204-23-1\204231.pdf
\Well Time-Depth Tables\204-23-1\204231.txt
\Well Time-Depth Tables\204-23-1\204231.xls
\Well Time-Depth Tables\205-8-1\20581.pdf
\Well Time-Depth Tables\205-8-1\20581.txt
\Well Time-Depth Tables\205-8-1\20581.xls
\Well Time-Depth Tables\205-10-2b\205102b.pdf
\Well Time-Depth Tables\205-10-2b\205102b.txt
\Well Time-Depth Tables\205-10-2b\205102b.xls
\Well Time-Depth Tables\214-27-1\214271.pdf
\Well Time-Depth Tables\214-27-1\214271.txt
\Well Time-Depth Tables\214-27-1\214271.xls
\Well Time-Depth Tables\214-27-2\214272.pdf
\Well Time-Depth Tables\214-27-2\214272.txt
\Well Time-Depth Tables\214-27-2\214272.xls
\Well Time-Depth Tables\214-28-1\214281.pdf
\Well Time-Depth Tables\214-28-1\214281.txt
\Well Time-Depth Tables\214-28-1\214281.xls
\Well Time-Depth Tables\6704-12-1\6704121.pdf
\Well Time-Depth Tables\6704-12-1\6704121.txt
\Well Time-Depth Tables\6704-12-1\6704121.xls
\Well Time-Depth Tables\6706-11-1\6706111.pdf
\Well Time-Depth Tables\6706-11-1\6706111.txt
\Well Time-Depth Tables\6706-11-1\6706111.xls
\Well Time-Depth Tables\6707-10-1\6707101.pdf
\Well Time-Depth Tables\6707-10-1\6707101.txt
\Well Time-Depth Tables\6707-10-1\6707101.xls

References

ABEBE, B., ACOCELLA, V., KORME, T. and AYALEW, D. 2007. Quaternary faulting and volcanism in the main Ethiopian Rift. *Journal of African Earth Sciences*, **48**, 115-124.

ACOCELLA, V., FACCENNA, C., FUNICIELLO, R. and ROSSETTI, F. 1999a. Sand-box modelling of basement-controlled transfer zones in extensional domains. *Terra Nova*, **11**, 149-156.

ACOCELLA, V., MORVILLO, P. and FUNICIELLO, R. 2005. What controls relay ramps and transfer faults within rift zones? Insights from analogue models. *Journal of Structural Geology*, **27**, 397-408.

ACOCELLA, V., SALVINI, F., FUNICIELLO, R. and FACCENNA, C. 1999b. The role of transfer structures on volcanic activity at Campi Flegrei (Southern Italy). *Journal of Volcanology and Geothermal Research*, **91**, 123-139.

ALLEN, M. B., MACDONALD, D. I. M., XUN, Z., VINCENT, S. J. and BROUET-MENZIES, C. 1997. Early Cenozoic two-phase extension and late Cenozoic thermal subsidence and inversion of the Bohai basin, northern China. *Marine and Petroleum Geology*, **14**, 951-972.

ALLEN, P. A. and ALLEN, J. R. 1990. *Basin analysis: principles and applications*. Blackwell Publishing, Padstow, Cornwall, United Kingdom, 451pp.

ANDERSEN, M. S. and BOLDREEL, L. O. 1995. Tertiary compression structures in the Faroe–Rockall area. *In:* SCRUTTON, R. A., STOKER, M. S., SHIMMIELD, G. B. and TUDHOPE, A. W. (eds) *The Tectonics, Sedimentation and Palaeooceanography of the North Atlantic Region*. Geological Society, London, Special Publications, **90**, 215-216.

ANDERSEN, M. S., SØRENSEN, A. B., BOLDREEL, L. O. and NIELSEN, T. 2002. Cenozoic evolution of the Faroe Platform, comparing denudation and deposition. *In:* DORÉ, A. G., CARTWRIGHT, J. A., STOKER, M. S., TURNER, J. P. and WHITE, N. J. (eds) *Exhumation of the North Atlantic Margin: Timing, Mechanisms and Implications for Petroleum Exploration*. Geological Society, London, Special Publications, **196**, 291-312.

ANDERSEN, T. B. 1998. Extensional tectonics in the caledonides of southern Norway, an overview. *Tectonophysics*, **285**, 333-351.

ANDERSON, D. L. 2000. The thermal state of the upper mantle; no role for mantle plumes. *Geophysical Research Letters*, **27**, 3623-3626.

AXEN, G. J. 1998. The Caliente-Enterprise zone, southeastern Nevada and southwestern Utah. *In:* FAULDS, J. E. and STEWART, J. H. (eds) *Accommodation Zones and Transfer Zones: The Regional Segmentation of the Basin and Range Province*. Geological Society of America Special Paper, **323**, 181-194.

BADLEY, M. E., EGEBERG, T. and NIPEN, O. 1984. Development of rift basins illustrated by the structural evolution of the Oseberg feature, Block 30/6, offshore Norway. *Journal of the Geological Society*, **141**, 639-649.

BEACOM, L. E., HOLDSWORTH, R. E., MCCAFFREY, K. J. W. and ANDERSON, T. B. 2001. A quantitative study of the influence of pre-existing compositional and fabric heterogeneities upon fracture-zone development during basement reactivation. *In:* HOLDSWORTH, R. E., STRACHAN, R. A., MAGLOUGHLIN, J. F. and KNIPE, R. J. (eds) *The nature and tectonic significance of fault zone weakening*. Geological Society, London, Special Publications, **186**, 195-211.

BEHN, M. D. and LIN, J. 2000. Segmentation in gravity and magnetic anomalies along the US East Coast passive margin: Implications for incipient structure of the oceanic lithosphere. *Journal of Geophysical Research-Solid Earth*, **105**, 25769-25790.

BELL, B. R. and BUTCHER, H. 2002. On the emplacement of sill complexes: evidence from the Faroe-Shetland Basin. *In:* JOLLEY, D. W. and BELL, B. R. (eds) *The North Atlantic Igneous Province: Stratigraphy, Tectonic, Volcanic and Magmatic Processes*. Geological Society, London, Special Publications, **197**, 307-329.

BERATAN, K. K. 1998. Structural control of rock-avalanche deposition in the Colorado River extensional corridor, southeastern California–western Arizona. *In:* FAULDS, J. E. and STEWART, J. H. (eds) *Accommodation Zones and Transfer Zones: The Regional Segmentation of the Basin and Range Province*. Geological Society of America Special Paper, **323**, 115-125.

BERNDT, C., MJELDE, R., PLANKE, S., SHIMAMURA, H. and FALEIDE, J. I. 2001. Controls on the tectono-magmatic evolution of a volcanic transform margin: the Vøring Transform Margin, NE Atlantic. *Marine Geophysical Researches*, **22**, 133-152.

BERNDT, C., SKOGLY, O. P., PLANKE, S., ELDHOLM, O. and MJELDE, R. 2000. High-velocity breakup-related sills in the Vøring Basin, off Norway. *Journal of Geophysical Research-Solid Earth*, **105**, 28443-28454.

BJØRNSETH, H. M., GRANT, S. M., HANSEN, E. K., HOSSACK, J. R., ROBERTS, D. G. and THOMPSON, M. 1997. Structural evolution of the Vøring Basin, Norway, during the Late Cretaceous and Palaeogene. *Journal of the Geological Society*, **154**, 559-563.

BLYSTAD, P., BREKKE, H., FAERSETH, R. B., LARSEN, B. T., SKOGSEID, J. and TØRUDBAKKEN, B. 1995. *Structural elements of the Norwegian continental shelf. Part II. The Norwegian Sea region*. Norwegian Petroleum Directorate, 45pp.

BOILLOT, G., FERAUD, G., RECQ, M. and GIRARDEAU, J. 1989. Undercrusting by serpentinite beneath rifted margins. *Nature*, **341**, 523-525.

BOLDREEL, L. O. and ANDERSEN, M. S. 1993. Late Paleocene to Miocene compression in the Faeroe-Rockall area. *In:* PARKER, J. R. (eds) *Petroleum Geology of Northwest Europe: Proceedings of the 4th Conference*. Geological Society, London, 1025-1034.

BOLDREEL, L. O. and ANDERSEN, M. S. 1998. Tertiary compressional structures on the Faroe-Rockall Plateau in relation to northeast Atlantic ridge-push and Alpine foreland stresses. *Tectonophysics*, **300**, 13-28.

BOLDREEL, L. O., ANDERSEN, M. S. and KUIJPERS, A. 1998. Neogene seismic facies and deep-water gateways in the Faeroe Bank area, NE Atlantic. *Marine Geology*, **152**, 129-140.

BOOTH, J., SWIECICKI, T. and WILCOCKSON, P. 1993. The tectono-stratigraphy of the Solan Basin, West of Shetland. *In:* PARKER, J. R. (eds) *Petroleum Geology of Northwest Europe: Proceedings of the 4th Conference*. Geological Society, London, 987-998.

BOSWORTH, W. 1994. A model for the 3-dimensional evolution of continental rift basins, northeast Africa. *Geologische Rundschau*, **83**, 671-688.

BREKKE, H. 2000. The tectonic evolution of the Norwegian Sea continental margin, with emphasis on the Vøring and Møre basins. *In:* NØTTVEDT, A. (eds) *Dynamics of the Norwegian Margin*. Geological Society, London, Special Publications, **167**, 327-378.

BREKKE, H., DAHLGREN, S., NYLAND, B. and MAGNUS, C. 1999. The prospectivity of the Vøring and Møre basins on the Norwegian Sea continental margin. *In:* FLEET, A. J. and BOLDY, S. A. R. (eds) *Petroleum Geology of Northwest Europe: Proceedings of the 5th Conference*. Geological Society, London, 261-274.

BRODIE, J. and WHITE, N. 1994. Sedimentary basin inversion caused by igneous underplating: Northwest European continental shelf. *Geology*, **22**, 147-150.

BUKOVICS, C. and ZIEGLER, P. A. 1985. Tectonic development of the Mid-Norway continental margin. *Marine and Petroleum Geology*, **2**, 2-22.

CARTWRIGHT, J. and HANSEN, D. M. 2006. Magma transport through the crust via interconnected sill complexes. *Geology*, **34**, 929-932.

CARTWRIGHT, J. and HUUSE, M. 2005. 3D seismic technology: the geological 'Hubble'. *Basin Research*, **17**, 1-20.

CERAMICOLA, S., STOKER, M. S., PRAEG, D., SHANNON, P. M., DE SANTIS, L., HOULT, R., HJELSTUEN, B. O., LABERG, J. S. and MATHIESEN, A. 2005. Anomalous Cenozoic subsidence along the 'passive' continental margin from Ireland to mid-Norway. *Marine and Petroleum Geology*, **22**, 1045-1067.

CHACKSFIELD, B. C. and KIMBELL, G. S. 2005. Compilation of potential field data from the Faroese region. *British Geological Survey Commisioned Report*, **CR/05/179**.

CHAMPION, M. E. S., WHITE, N. J., JONES, S. M. and LOVELL, J. P. B. 2008. Quantifying transient mantle convective uplift: An example from the Faroe-Shetland basin. *Tectonics*, **27**, 1-18.

CHRISTIE, P. A. F., GOLLIFER, I. and COWPER, D. 2006. Borehole seismic studies of the volcanic succession from the Lopra-1/1A borehole in the Faroe Islands, northern North Atlantic. *In:* CHALMERS, J. A. and WAAGSTEIN, R. (eds) *Scientific results from the deepened Lopra-1 borehole, Faroe Islands*. Geological Survey of Denmark and Greenland Bulletin, **9**, 23-40.

CHRISTIE-BLICK, N. and BIDDLE, K. T. 1985. Deformation and basin formation along strike-slip faults. *In:* BIDDLE, K. T. and CHRISTIE-BLICK, N. (eds) *Strike slip deformation, basin formation, and sedimentation*. SEPM Special Publication, **37**, 1–34.

CLIFT, P. D. 1999. The thermal impact of Paleocene magmatic underplating in the Faeroe-Shetland-Rockall region. *In:* FLEET, A. J. and BOLDY, S. A. R. (eds) *Petroleum Geology of Northwest Europe: Proceedings of the 5th Conference*. Geological Society, London, 585-593.

CLIFT, P. D. and TURNER, J. 1998. Paleogene igneous underplating and subsidence anomalies in the Rockall-Faeroe-Shetland area. *Marine and Petroleum Geology*, **15**, 223-243.

CLIFT, P. D., CARTER, A. and HURFORD, A. J. 1998. The erosional and uplift history of NE Atlantic passive margins: constraints on a passing plume. *Journal of the Geological Society*, **155**, 787-800.

COFFIELD, D. Q. and SCHAMEL, S. 1989. Surface expression of an accommodation zone within the Gulf of Suez Rift, Egypt. *Geology*, **17**, 76-79.

COFFIN, M. F. and ELDHOLM, O. 1994. Large igneous provinces - crustal structure, dimensions, and external consequences. *Reviews of Geophysics*, **32**, 1-36.

CORDELL, L. 1978. Regional geophysical setting of the Rio-Grande rift. *Geological Society of America Bulletin*, **89**, 1073-1090.

CORFIELD, S. M., WHEELER, W., KARPUZ, R., WILSON, M. and HELLAND, R. 2004. Exploration 3D Seismic over the Gjallar Ridge, Mid-Norway: Visualization of Structures on the Norwegian Volcanic Margin from Moho to Seafloor. *Geological Society, London, Memoirs*, **29**, 177-186.

CORTI, G., BONINI, M., CONTICELLI, S., INNOCENTI, F., MANETTI, P. and SOKOUTIS, D. 2003. Analogue modelling of continental extension: a review focused on the relations between the patterns of deformation and the presence of magma. *Earth-Science Reviews*, **63**, 169-247.

COWARD, M. P. 1990. The Precambrian, Caledonian and Variscan framework to NW Europe. *In:* HARDMAN, R. F. P. and BROOKS, J. (eds) *Tectonic Events Responsible for Britains Oil and Gas Reserves*. Geological Society Publishing House, Bath, **55**, 1-34.

COWARD, M. P. and ENFIELD, M. A. 1987. The structure of the West Orkney and adjacent basins. *In:* BROOKS, J. and GLENNIE, K. (eds) *Petroleum Geology of North West Europe*. Graham and Trotman, London, 687-696.

CRIDER, J. G. and PEACOCK, D. C. P. 2004. Initiation of brittle faults in the upper crust: a review of field observations. *Journal of Structural Geology*, **26**, 691-707.

DAVIES, R. and CARTWRIGHT, J. 2002. A fossilized Opal A to Opal C/T transformation on the northeast Atlantic margin: support for a significantly elevated Palaeogeothermal gradient during the Neogene? *Basin Research*, **14**, 467-486.

DAVIES, R. J., HUUSE, M., HIRST, P., CARTWRIGHT, J. and YANG, Y. S. 2006. Giant clastic intrusions primed by silica diagenesis. *Geology*, **34**, 917-920.

DAVIES, R., BELL, B. R., CARTWRIGHT, J. A. and SHOULDERS, S. 2002. Three-dimensional seismic imaging of Paleogene dike-fed submarine volcanoes from the northeast Atlantic margin. *Geology*, **30**, 223-226.

DAVIES, R., CLOKE, I., CARTWRIGHT, J., ROBINSON, A. and FERRERO, C. 2004. Post-breakup compression of a passive margin and its impact on hydrocarbon prospectivity: An example from the Tertiary of the Faeroe-Shetland Basin, United Kingdom. *Aapg Bulletin*, **88**, 1-20.

DE PAOLA, N., HOLDSWORTH, R. E., MCCAFFREY, K. J. W. and BARCHI, M. R. 2005. Partitioned transtension: an alternative to basin inversion models. *Journal of Structural Geology*, **27**, 607-625.

DEAN, K., MCLACHLAN, K. and CHAMBERS, A. 1999. Rifting and the development of the Faeroe-Shetland Basin. *In:* FLEET, A. J. and BOLDY, S. A. R. (eds) *Petroleum Geology of Northwest Europe: Proceedings of the 5th Conference*. Geological Society, London, 533-544.

DEWEY, J. F. 1982. Plate-tectonics and the evolution of the British-Isles. *Journal of the Geological Society*, **139**, 371-412.

DORÉ, A. G. 1991. The structural foundation and evolution of Mesozoic seaways between Europe and the Arctic. *Palaeogeography Palaeoclimatology Palaeoecology*, **87**, 441-492.

DORÉ, A. G. and GAGE, M. S. 1987. Crustal alignments and sedimentary domains in the evolution of the North Sea, North-east Atlantic Margin and Barents Shelf. *In:* BROOKS, J.

and GLENNIE, K. (eds) *Petroleum Geology of North West Europe*. Graham and Trotman, London, 1131-1148.

DORÉ, A. G. and LUNDIN, E. R. 1996. Cenozoic compressional structures on the NE Atlantic margin: Nature, origin and potential significance for hydrocarbon exploration. *Petroleum Geoscience*, **2**, 299-311.

DORÉ, A. G., CARTWRIGHT, J. A., STOKER, M. S., TURNER, J. P. and WHITE, N. J. 2002. Exhumation of the North Atlantic margin: introduction and background. *In:* DORÉ, A. G., CARTWRIGHT, J. A., STOKER, M. S., TURNER, J. P. and WHITE, N. J. (eds) *Exhumation of the North Atlantic Margin: Timing, Mechanisms and Implications for Petroleum Exploration*. Geological Society, London, Special Publications, **196**, 1-12.

DORÉ, A. G., LUNDIN, E. R., BIRKELAND, O., ELIASSEN, P. E. and JENSEN, L. N. 1997a. The NE Atlantic Margin: implications of late Mesozoic and Cenozoic events for hydrocarbon prospectivity. *Petroleum Geoscience*, **3**, 117-131.

DORÉ, A. G., LUNDIN, E. R., FICHLER, C. and OLESEN, O. 1997b. Patterns of basement structure and reactivation along the NE Atlantic margin. *Journal of the Geological Society*, **154**, 85-92.

DORÉ, A. G., LUNDIN, E. R., JENSEN, L. N., BIRKELAND, Ø., ELIASSEN, P. E. and FICHLER, C. 1999. Principal tectonic events in the evolution of the northwest European Atlantic margin. *In:* FLEET, A. J. and BOLDY, S. A. R. (eds) *Petroleum Geology of Northwest Europe: Proceedings of the 5th Conference*. Geological Society, London, 41-61.

DORÉ, A. G., LUNDIN, E. R., KUSZNIR, N. J. and PASCAL, C. 2008. Potential mechanisms for the genesis of Cenozoic domal structures on the NE Atlantic margin: pros, cons and some new ideas. *In:* JOHNSON, H., DORÉ, A. G., GATLIFF, R. W., HOLDSWORTH, R. E., LUNDIN, E. R. and RITCHIE, J. D. (eds) *The Nature and Origin of Compression in Passive Margins*. Geological Society, London, Special Publications, **306**, 1-26.

DUEBENDORFER, E. M., BEARD, L. S. and SMITH, E. I. 1998. Restoration of Tertiary deformation in the Lake Mead region, southern Nevada: The role of strike-slip transfer faults. *In:* FAULDS, J. E. and STEWART, J. H. (eds) *Accommodation Zones and Transfer Zones: The Regional Segmentation of the Basin and Range Province*. Geological Society of America Special Paper, **323**, 127-148.

DUINDAM, P. and VAN HOORN, B. 1987. Structural evolution of the West Shetland continental margin. *In:* BROOKS, J. and GLENNIE, K. (eds) *Petroleum Geology of North West Europe*. Graham and Trotman, London, 765-773.

EARLE, M. M., JANKOWSKI, E. J. and VANN, I. R. 1989. Structural and stratigraphic evolution of the Faeroe-Shetland Channel and northern Rockall Trough. *In:* TANKARD, A. J. and BALKWILL, H. R. (eds) *Extensional Tectonics and Stratigraphy of the North Atlantic Margins*. AAPG Memoir, **46**, 461-469.

EBBING, J., LUNDIN, E., OLESEN, O. and HANSEN, E. K. 2006. The mid-Norwegian margin: a discussion of crustal lineaments, mafic intrusions, and remnants of the Caledonian root by 3D density modelling and structural interpretation. *Journal of the Geological Society*, **163**, 47-59.

EBINGER, C. J. 1989a. Geometric and kinematic development of border faults and accommodation zones, Kivu-Rusizi rift, Africa. *Tectonics*, **8**, 117-133.

EBINGER, C. J. 1989b. Tectonic development of the western branch of the East-African rift system. *Geological Society of America Bulletin*, **101**, 885-903.

EBINGER, C. J. and CASEY, M. 2001. Continental breakup in magmatic provinces: An Ethiopian example. *Geology*, **29**, 527-530.

EBINGER, C. J., DEINO, A. L., DRAKE, R. E. and TESHA, A. L. 1989. Chronononology of volcanism and rift basin propagation - Rungwe Volcanic Province, East-Africa. *Journal of Geophysical Research-Solid Earth and Planets*, **94**, 15785-15803.

EBINGER, C. J., YEMANE, T., HARDING, D. J., TESFAYE, S., KELLEY, S. and REX, D. C. 2000. Rift deflection, migration, and propagation: Linkage of the Ethiopian and Eastern rifts, Africa. *Geological Society of America Bulletin*, **112**, 163-176.

EBINGER, C. J., YEMANE, T., WOLDEGABRIEL, G., ARONSON, J. L. and WALTER, R. C. 1993. Late Eocene - recent volcanism and faulting in the southern main Ethipian rift. *Journal of the Geological Society*, **150**, 99-108.

ELDHOLM, A. 1989. Structural and stratigraphic evolution of the Faeroe-Shetland Channel and northern Rockall Trough. *In:* TANKARD, A. J. and BALKWILL, H. R. (eds) *Extensional Tectonics and Stratigraphy of the North Atlantic Margins*. AAPG Memoir, **46**, 461-469.

ELDHOLM, O. 1990. Paleogene North Atlantic magmatic-tectonic events: environmental implications. *Memorie Societa Geologica Italiana*, **44**, 13-28.

ELDHOLM, O. and GRUE, K. 1994. North Atlantic volcanic margins: dimensions and production rates. *Journal of Geophysical Research-Solid Earth*, **99**, 2955-2968.

ELDHOLM, O., TSIKALAS, F. and FALEIDE, J. I. 2002. Continental margin off Norway 62-75°N: Palaeogene tectono-magmatic segmentation and sedimentation. *In:* JOLLEY, D. W. and BELL, B. R. (eds) *The North Atlantic Igneous Province: Stratigraphy, Tectonic, Volcanic and Magmatic Processes*. Geological Society, London, Special Publications, **197**, 39-68.

ELLIS, D., BELL, B. R., JOLLEY, D. W. and O'CALLAGHAM, M. 2002. The stratigraphy, environment of eruption and age of the Faroes Lava Group, NE Atlantic Ocean. *In:* JOLLEY, D. W. and BELL, B. R. (eds) *The North Atlantic Igneous Province: Stratigraphy, Tectonic, Volcanic and Magmatic Processes*. Geological Society, London, Special Publications, **197**, 253-270.

ELLIS, D., JOLLEY, D. W., PASSEY, S. R. and BELL, B. R. 2009. Transfer Zones: The application of new geological information from the Faroe Islands applied to the offshore exploration of intra basalt and sub-basalt strata. *In:* ZISKA, H. and VARMING, T. (eds) *Faroe Islands Exploration Conference: Proceedings of the 2nd Conference*. Annales Societatis Scientarium Faeroensis Supplementum, **50**, 205-226.

ENGLAND, R. W., MCBRIDE, J. H. and HOBBS, R. W. 2005. The role of Mesozoic rifting in the opening of the NE Atlantic: evidence from deep seismic profiling across the Faroe-Shetland Trough. *Journal of the Geological Society*, **162**, 661-673.

EVANS, D., MCGIVERON, S., HARRISON, Z., BRYN, P. and BERG, K. 2002. Alongslope variation in the late Neogene evolution of the mid-Norwegian margin in response to uplift and tectonism. *In:* DORÉ, A. G., CARTWRIGHT, J. A., STOKER, M. S., TURNER, J. P. and WHITE, N. J. (eds) *Exhumation of the North Atlantic Margin: Timing, Mechanisms and Implications for Petroleum Exploration*. Geological Society, London, Special Publications, **196**, 139-151.

FÆRSETH, R. B. and LIEN, T. 2002. Cretaceous evolution in the Norwegian Sea - a period characterized by tectonic quiescence. *Marine and Petroleum Geology*, **19**, 1005-1027.

FAULDS, J. E. and VARGA, R. J. 1998. The role of accommodation zones and transfer zones in the regional segmentation of extended terranes. *In:* FAULDS, J. E. and STEWART, J. H. (eds) *Accommodation Zones and Transfer Zones: The Regional Segmentation of the Basin and Range Province*. Geological Society of America Special Paper, **323**, 1-45.

FAULDS, J. E., OLSON, E. L., HARLAN, S. S. and MCINTOSH, W. C. 2002. Miocene extension and fault related folding in the Highland Range, southern Nevada: a three-dimensional perspective. *Journal of Structural Geology*, **24**, 861-886.

FERNANDEZ, M., TORNE, M., GARCIA-CASTELLANOS, D., VERGES, J., WHEELER, W. and KARPUZ, R. 2004. Deep structure of the Vøring Margin: the transition from a continental shield to a young oceanic lithosphere. *Earth and Planetary Science Letters*, **221**, 131-144.

FICHLER, C., RUNDHOVDE, E., OLESEN, O., SAETHER, B. M., RUESLATTEN, H., LUNDIN, E. and DORÉ, A. G. 1999. Regional tectonic interpretation of image enhanced gravity and magnetic data covering the mid-Norwegian shelf and adjacent mainland. *Tectonophysics*, **306**, 183-197.

FITZGERALD, D. M., BUYNEVICH, I. V., FENSTER, M. S. and MCKINLAY, P. A. 2000. Sand dynamics at the mouth of a rock-bound, tide-dominated estuary. *Sedimentary Geology*, **131**, 25-49.

FJELDSKAAR, W., GRUNNALEITE, I., ZWEIGEL, J., MJELDE, R., FALEIDE, J. I. and WILSON, J. 2009. Modelled palaeo temperature on Vøring, offshore mid Norway - the effect of the Lower Crustal Body. *Tectonophysics*, **474**, 544-558.

FJELLANGER, E., SURLYK, F., WAMSTEEKER, L. C. and MIDTUN, T. 2005. Upper Cretaceous basin-floor fans in the Vøring Basin. *In:* WANDÅS, B. T. G., NYSTUEN, J. P., EIDE, E. A. and GRADSTEIN, F. M. (eds) *Onshore-Offshore Relationships on the North Atlantic Margin*. NPF Special Publication, **12**, 135-164.

FLIEDNER, M. M. and WHITE, R. S. 2001. Sub-basalt imaging in the Faroe-Shetland Basin with large-offset data. *First Break*, 247-252.

FOULGER, G. 2002. Plumes, or plate tectonic processes? *Astronomy & Geophysics*, **43**, 19-23.

FOULGER, G. R., PRITCHARD, M. J., JULIAN, B. R., EVANS, J. R., ALLEN, R. M., NOLET, G., MORGAN, W. J., BERGSSON, B. H., ERLENDSSON, P., JAKOBSDOTTIR, S., RAGNARSSON, S., STEFANSSON, R. and VOGFJORD, K. 2001. Seismic tomography shows that upwelling beneath Iceland is confined to the upper mantle. *Geophysical Journal International*, **146**, 504-530.

FOURNIER, M., HUCHON, P., KHANBARI, K. and LEROY, S. 2007. Segmentation and along-strike asymmetry of the passive margin in Socotra, eastern Gulf of Aden: Are they controlled by detachment faults? *Geochemistry Geophysics Geosystems*, **8**, 1-17.

FRANKE, D., NEBEN, S., LADAGE, S., SCHRECKENBERGER, B. and HINZ, K. 2007. Margin segmentation and volcano-tectonic architecture along the volcanic margin off Argentina/Uruguay, South Atlantic. *Marine Geology*, **244**, 46-67.

FREI, D., FREI, M. and KNUDSEN, C. 2005. Linking the Faroese area and Greenland: an innovative, integrated provenance study. *Danmarks og Grønlands Geologiske Undersøgelse Rapport*, **2005/54**.

FRIEND, C. R. L. and KINNY, P. D. 2001. A reappraisal of the Lewisian Gneiss Complex: geochronological evidence for its tectonic assembly from disparate terranes in the Proterozoic. *Contributions to Mineralogy and Petrology*, **142**, 198-218.

FRIEND, P. F., WILLIAMS, B. P. J., FORD, M. and WILLIAMS, E. A. 2000. Kinematics and dynamics of Old Red Sandstone basins. *In:* FRIEND, P. F. and WILLIAMS, B. P. J. (eds) *New Perspectives on the Old Red Sandstone*. Geological Society, London, Special Publications, **180**, 29-60.

FUGELLI, E. M. G. and OLSEN, T. R. 2005. Screening for deep-marine reservoirs in frontier basins: Part 1 - Examples from offshore mid-Norway. *Aapg Bulletin*, **89**, 853-882.

GABRIELSEN, R. H., BRAATHEN, A., OLESEN, O., FALEIDE, J. I., KYRKJEBØ, R. and REDFIELD, T. F. 2005. Vertical movements in south-western Fennoscandia: a discussion of regions and processes from the Present to the Devonian. *In:* WANDÅS, B. T. G., NYSTUEN, J. P., EIDE, E. A. and GRADSTEIN, F. M. (eds) *Onshore-Offshore Relationships on the North Atlantic Margin*. NPF Special Publication, **12**, 1-28.

GABRIELSEN, R. H., ODINSEN, T. and GRUNNALEITE, I. 1999. Structuring of the Northern Viking Graben and the Møre Basin; the influence of basement structural grain, and the particular role of the Møre-Trondelag Fault Complex. *Marine and Petroleum Geology*, **16**, 443-465.

GAINA, C., GERNIGON, L. and BALL, P. 2009. Palaeocene-Recent plate boundaries in the NE Atlantic and the formation of the Jan Mayen microcontinent. *Journal of the Geological Society*, **166**, 601-616.

GALLAGHER, J. W. and DROMGOOLE, P. W. 2007. Exploring below the basalt, offshore Faroes: a case history of sub-basalt imaging. *Petroleum Geoscience*, **13**, 213-225.

GALLAGHER, J. W. and DROMGOOLE, P. W. 2008. Seeing below the basalt - offshore Faroes. *Geophysical Prospecting*, **56**, 33-45.

GALLOWAY, W. E. 1989. Genetic stratigraphic sequences in basin analysis. 1. Architecture and genesis of flooding-surface bounded depositional units. *Aapg Bulletin*, **73**, 125-142.

GAWTHORPE, R. L. and HURST, J. M. 1993. Transfer zones in extensional basins - their structural style and influence on drainage development and stratigraphy. *Journal of the Geological Society*, **150**, 1137-1152.

GAWTHORPE, R. L. and LEEDER, M. R. 2000. Tectono-sedimentary evolution of active extensional basins. *Basin Research*, **12**, 195-218.

GAWTHORPE, R. L., FRASER, A. J. and COLLIER, R. E. L. 1994. Sequence stratigraphy in active extensional basins - implications for the interpretation of ancient basin-fills. *Marine and Petroleum Geology*, **11**, 642-658.

GERNIGON, L., LUCAZEAU, F., BRIGAUD, F., RINGENBACH, J. C., PLANKE, S. and LE GALL, B. 2006. A moderate melting model for the Vøring margin (Norway) based on structural observations and a thermo-kinematical modelling: Implication for the meaning of the lower crustal bodies. *Tectonophysics*, **412**, 255-278.

GERNIGON, L., RINGENBACH, J. C., PLANKE, S. and LE GALL, B. 2004. Deep structures and breakup along volcanic rifted margins: insights from integrated studies along the outer Vøring Basin (Norway). *Marine and Petroleum Geology*, **21**, 363-372.

GERNIGON, L., RINGENBACH, J. C., PLANKE, S., LE GALL, B. and JONQUET-KOLSTO, H. 2003. Extension, crustal structure and magmatism at the outer Vøring Basin, Norwegian margin. *Journal of the Geological Society*, **160**, 197-208.

GIBB, F. G. F. and KANARIS-SOTIRIOU, R. 1988. The geochemistry and origin of the Faeroe–Shetland sill complex. *In:* MORTON, A. C. and PARSONS, L. M. (eds) *Early Tertiary volcanism and the opening of the NE Atlantic*. Geological Society, London, Special Publications, **39**, 241-252.

GIBBS, A. D. 1984. Structural evolution of extensional basin margins. *Journal of the Geological Society*, **141**, 609-620.

GJELBERG, J. G., MARTINSEN, O. J., CHARNOCK, M. A., MØLLER, N. and ANTONSEN, P. 2005. The reservoir development of the Late Maastrichtian–Early Paleocene Ormen Lange gas field, Møre Basin, Mid-Norwegian Shelf. *In:* DORÉ, A. G. and VINING, B. A. (eds) *Petroleum Geology: North-West Europe and Global Perspectives - Proceedings of the 6th Petroleum Geology Conference*. Geological Society, London, 1165-1184.

GOMEZ, M., VERGES, J., FERNANDEZ, M., TORNE, M., AYALA, C., WHEELER, W. and KARPUZ, R. 2004. Extensional geometry of the mid Norwegian Margin before Early Tertiary continental breakup. *Marine and Petroleum Geology*, **21**, 177-194.

GRANT, N., BOUMA, A. and MCINTYRE, A. 1999. The Turonian play in the Faeroe-Shetland Basin. *In:* FLEET, A. J. and BOLDY, S. A. R. (eds) *Petroleum Geology of Northwest Europe: Proceedings of the 5th Conference*. Geological Society, London, 661-673.

GRØNLIE, A. and ROBERTS, D. 1989. Resurgent strike-slip duplex development along the Hitre-Snåsa and Verran Faults, Møre–Trøndelag Fault Zone, Central Norway. *Journal of Structural Geology*, **11**, 295-305.

GRUNNALEITE, I. and GABRIELSEN, R. H. 1995. Structure of the Møre Basin, mid-Norway continental margin. *Tectonophysics*, **252**, 221-251.

HAALAND, H. J., FURNES, H. and MARTINSEN, O. J. 2000. Paleogene tuffaceous intervals, Grane Field (Block 25/11), Norwegian North Sea: their depositional, petrographical, geochemical character and regional implications. *Marine and Petroleum Geology*, **17**, 101-118.

HAFLIDASON, H., SEJRUP, H. P., NYGARD, A., MIENERT, J., BRYN, P., LIEN, R., FORSBERG, C. F., BERG, K. and MASSON, D. 2004. The Storegga Slide: architecture, geometry and slide development. *Marine Geology*, **213**, 201-234.

HALL, B. D. and WHITE, N. 1994. Origin of anomalous Tertiary subsidence adjacent to North Atlantic continental margins. *Marine and Petroleum Geology*, **11**, 702-714.

HANSEN, D. M. 2006. The morphology of intrusion-related vent structures and their implications for constraining the timing of intrusive events along the NE Atlantic margin. *Journal of the Geological Society*, **163**, 789-800.

HANSEN, D. M. and CARTWRIGHT, J. 2006. The three-dimensional geometry and growth of forced folds above saucer-shaped igneous sills. *Journal of Structural Geology*, **28**, 1520-1535.

HAQ, B. U., HARDENBOL, J. and VAIL, P. R. 1988. Mesozoic and Cenozoic chronostratigraphy and cycles of sea level changes. *In:* WILGUS, C. K., HASTINGS, B. S.,

KENDALL, C. G. S. C., POSAMENTIER, H. W., ROSS, C. A. and VAN WAGONER, J. C. (eds) *Sea-level changes – an integrated approach*. SEPM Special Publication, **42**, 1121-1132.

HARDING, T. P. 1974. Petroleum traps associated with wrench faults. *Aapg Bulletin*, **58**, 1290-1304.

HARDING, T. P. 1990. Identification of wrench faults using subsurface structural data - criteria and pitfalls. *Aapg Bulletin*, **74**, 1590-1609.

HARROWFIELD, M. and KEEP, M. 2005. Tectonic modification of the Australian North-West Shelf: episodic rejuvenation of long-lived basin divisions. *Basin Research*, **17**, 225-239.

HENRIKSEN, S., FICHLER, C., GRØNLIE, A., HENNINGSEN, T., LAURSEN, I., LØSETH, H., OTTESEN, D. and PRINCE, I. 2005. The Norwegian Sea during the Cenozoic. *In:* WANDÅS, B. T. G., NYSTUEN, J. P., EIDE, E. A. and GRADSTEIN, F. M. (eds) *Onshore-Offshore Relationships on the North Atlantic Margin*. NPF Special Publication, **12**, 111-134.

HENRY, C. D. 1998. Basement-controlled transfer zones in an area of low-magnitude extension, eastern Basin and Range province, Trans-Pecos Texas. *In:* FAULDS, J. E. and STEWART, J. H. (eds) *Accommodation Zones and Transfer Zones: The Regional Segmentation of the Basin and Range Province*. Geological Society of America Special Paper, **323**, 75-88.

HERRIES, R., PODDUBIUK, R. and WILCOCKSON, P. 1999. Solan, Strathmore and the back basin play, West of Shetland. *In:* FLEET, A. J. and BOLDY, S. A. R. (eds) *Petroleum Geology of Northwest Europe: Proceedings of the 5th Conference*. Geological Society, London, 693-712.

HITCHEN, K. and RITCHIE, J. D. 1987. Geological review of the West Shetland area. *In:* BROOKS, J. and GLENNIE, K. (eds) *Petroleum Geology of North West Europe*. Graham and Trotman, London, 737-749.

HJELSTUEN, B. O., ELDHOLM, O. and SKOGSEID, J. 1997. Vøring Plateau diapir fields and their structural and depositional settings. *Marine Geology*, **144**, 33-57.

HJELSTUEN, B. O., ELDHOLM, O. and SKOGSEID, J. 1999. Cenozoic evolution of the northern Vøring margin. *Geological Society of America Bulletin*, **111**, 1792-1807.

HOPPER, J. R., MUTTER, J. C., LARSON, R. L., MUTTER, C. Z., BUHL, P., DIEBOLD, J. B., ALSOP, J., FALVEY, D., WILLIAMSON, P., BRASSIL, F. and LORENZO, J. M. 1992. Magmatism and rift margin evolution - evidence from northwest Australia. *Geology*, **20**, 853-857.

HOVLAND, M., NYGAARD, E. and THORBJORNSEN, S. 1998. Piercement shale diapirism in the deep-water Vema Dome area, Vøring basin offshore Norway. *Marine and Petroleum Geology*, **15**, 191-201.

HUDSON, M. R., ROSENBAUM, J. G., GROMMÉ, C. S., SCOTT, R. B. and ROWLEY, P. D. 1998. Paleomagnetic evidence for counterclockwise rotation in a broad sinistral shear zone, Basin and Range province, southeastern Nevada and southwestern Utah. *In:* FAULDS, J. E. and STEWART, J. H. (eds) *Accommodation Zones and Transfer Zones: The Regional Segmentation of the Basin and Range Province*. Geological Society of America Special Paper, **323**, 149-180.

Hurst, A., Cartwright, J., Huuse, M., Jonk, R., Schwab, A., Duranti, D. and Cronin, B. 2003. Significance of large-scale sand injectites as long-term fluid conduits: evidence from seismic data. *Geofluids*, **3**, 263-274.

Imber, J., Holdsworth, R. E., McCaffrey, K. J. W., Wilson, R. W., Jones, R. R., England, R. W. and Gjeldvik, G. 2005. Early Tertiary sinistral transpression and fault reactivation in the western Vøring Basin, Norwegian Sea: Implications for hydrocarbon exploration and pre-breakup deformation in ocean margin basins. *Aapg Bulletin*, **89**, 1043-1069.

Imber, J., Holdsworth, R. E., McCaffrey, K. J. W., Wilson, R. W., Jones, R. R., England, R. W. and Gjeldvik, G. 2005. Early Tertiary sinistral transpression and fault reactivation in the western Vøring Basin, Norwegian Sea: Implications for hydrocarbon exploration and pre-breakup deformation in ocean margin basins. *Aapg Bulletin*, **89**, 1043-1069.

Johnson, H., Ritchie, J. D., Hitchen, K., McInroy, D. B. and Kimbell, G. S. 2005. Aspects of the Cenozoic deformational history of the northeast Faroe–Shetland Basin, Wyville–Thomson Ridge and Hatton Bank areas. *In:* Doré, A. G. and Vining, B. A. (eds) *Petroleum Geology: North-West Europe and Global Perspectives - Proceedings of the 6th Petroleum Geology Conference*. Geological Society, London, 993-1007.

Jolley, D. W. and Bell, B. R. 2002a. The evolution of the North Atlantic Igneous Province and the opening of the NE Atlantic rift. *In:* Jolley, D. W. and Bell, B. R. (eds) *The North Atlantic Igneous Province: Stratigraphy, Tectonic, Volcanic and Magmatic Processes*. Geological Society, London, Special Publications, **197**, 1-13.

Jolley, D. W. and Bell, B. R. 2002b. Genesis and age of the Erlend Volcano, NE Atlantic Margin. *In:* Jolley, D. W. and Bell, B. R. (eds) *The North Atlantic Igneous Province: Stratigraphy, Tectonic, Volcanic and Magmatic Processes*. Geological Society, London, Special Publications, **197**, 95-110.

Jolley, D. W. and Morton, A. C. 2007. Understanding basin sedimentary provenance: evidence from allied phytogeographic and heavy mineral analysis of the Palaeocene of the NE Atlantic. *Journal of the Geological Society*, **164**, 553-563.

Jolley, D. W. and Whitham, A. G. 2004. A stratigraphical and palaeoenvironmental analysis of the sub-basaltic Palaeogene sediments of East Greenland. *Petroleum Geoscience*, **10**, 53-60.

Jolley, D. W., Clarke, B. and Kelley, S. 2002. Paleogene time scale miscalibration: Evidence from the dating of the North Atlantic igneous province. *Geology*, **30**, 7-10.

Jolley, D. W., Morton, A. and Prince, I. 2005. Volcanogenic impact on phytogeography and sediment dispersal patterns in the NE Atlantic. *In:* Doré, A. G. and Vining, B. A. (eds) *Petroleum Geology: North-West Europe and Global Perspectives - Proceedings of the 6th Petroleum Geology Conference*. Geological Society, London, 969-975.

Jones, E. J. W., Mitchell, J. G. and Perry, R. G. 1986. Early tertiary igneous activity west of the Outer Hebrides, Scotland: evidence from magnetic-anomalies and dredged basaltic rocks. *Marine Geology*, **73**, 47-59.

Karson, J. A. and Brooks, C. K. 1999. Structural and magmatic segmentation of the Tertiary East Greenland Volcanic Rifted Margin. *Geological Society, London, Special Publications*, **164**, 313-338.

KEEP, M. and HARROWFIELD, M. 2005. Basement reactivation and inversion mechanisms in the Timor and Norwegian seas. *In:* DORÉ, A. G. and VINING, B. A. (eds) *Petroleum Geology: North-West Europe and Global Perspectives - Proceedings of the 6th Petroleum Geology Conference*. Geological Society, London, 861-871.

KELLY, S. R. A., WHITHAM, A. G., KORAINI, A. M. and PRICE, S. P. 1998. Lithostratigraphy of the Cretaceous (Barremian-Santonian) Hold with Hope Group, NE Greenland. *Journal of the Geological Society*, **155**, 993-1008.

KESER NEISH, J. and ZISKA, H. 2005. Structure of the Faroe Bank Channel Basin, offshore Faroe Islands. *In:* DORÉ, A. G. and VINING, B. A. (eds) *Petroleum Geology: North-West Europe and Global Perspectives - Proceedings of the 6th Petroleum Geology Conference*. Geological Society, London, 873-885.

KHALIL, S. M. and MCCLAY, K. R. 2009. Structural control on syn-rift sedimentation, northwestern Red Sea margin, Egypt. *Marine and Petroleum Geology*, **26**, 1018-1034.

KIMBELL, G. S., RITCHIE, J. D., JOHNSON, H. and GATLIFF, R. W. 2005. Controls on the structure and evolution of the NE Atlantic margin revealed by regional potential field imaging and 3D modelling. *In:* DORÉ, A. G. and VINING, B. A. (eds) *Petroleum Geology: North-West Europe and Global Perspectives - Proceedings of the 6th Petroleum Geology Conference*. Geological Society, London, 933-945.

KIØRBOE, L. 1999. Stratigraphic relationships of the Lower Tertiary of the Faeroe Basalt Plateau and the Faeroe-Shetland Basin. *In:* FLEET, A. J. and BOLDY, S. A. R. (eds) *Petroleum Geology of Northwest Europe: Proceedings of the 5th Conference*. Geological Society, London, 559-572.

KIRTON, S. R. and HITCHEN, K. 1987. Timing and style of crustal extension north of the Scottish mainland. *In:* COWARD, M. P., DEWEY, J. and HANCOCK, P. L. (eds) *Continental Extensional Tectonics*. Geological Society, London, Special Publications, **28**, 501-510.

KITTILSEN, J. E., OLSEN, R. R., MARTEN, R. F. and HANSEN, E. K. 1999. The first deepwater well in Norway and its implications for the Upper Cretaceous Play, Vøring Basin. *In:* FLEET, A. J. and BOLDY, S. A. R. (eds) *Petroleum Geology of Northwest Europe: Proceedings of the 5th Conference*. Geological Society, London, 275-280.

KJENNERUD, T. and VERGARA, L. 2005. Cretaceous to Palaeogene 3D palaeobathymetry and sedimentation in the Vøring Basin, Norwegian Sea. *In:* DORÉ, A. G. and VINING, B. A. (eds) *Petroleum Geology: North-West Europe and Global Perspectives - Proceedings of the 6th Petroleum Geology Conference*. Geological Society, London, 815-831.

KNOTT, S. D., BURCHELL, M. T., JOLLEY, E. J. and FRASER, A. J. 1993. Mesozoic to Cenozoic plate reconstructions of the North Atlantic and hydrocarbon plays of the Atlantic margins. *In:* PARKER, J. R. (eds) *Petroleum Geology of Northwest Europe: Proceedings of the 4th Conference*. Geological Society, London, 953-974.

KNOX, R. W. O. B. and MORTON, A. C. 1988. The record of early Tertiary N Atlantic volcanism in sediments of the North Sea Basin. *Geological Society, London, Special Publications*, **39**, 407-419.

KORNSAWAN, A. and MORLEY, C. K. 2002. The origin and evolution of complex transfer zones (graben shifts) in conjugate fault systems around the Funan Field, Pattani Basin, Gulf of Thailand. *Journal of Structural Geology*, **24**, 435-449.

KUSZNIR, N. J., HUNSDALE, R., ROBERTS, A. M. and ISIMM TEAM. 2005. Timing and magnitude of depth-dependent lithosphere stretching on the southern Lofoten and northern

Vøring continental margins offshore mid-Norway: implications for subsidence and hydrocarbon maturation at volcanic rifted margins. *In:* DORÉ, A. G. and VINING, B. A. (eds) *Petroleum Geology: North-West Europe and Global Perspectives - Proceedings of the 6th Petroleum Geology Conference*. Geological Society, London, 767-784.

LABERG, J. S., STOKER, M. S., DAHLGREN, K. I. T., DE HAAS, H., HAFLIDASON, H., HJELSTUEN, B. O., NIELSEN, T., SHANNON, P. M., VORREN, T. O., VAN WEERING, T. C. E. and CERAMICOLA, S. 2005. Cenozoic alongslope processes and sedimentation on the NW European Atlantic margin. *Marine and Petroleum Geology*, **22**, 1069-1088.

LAMERS, E. and CARMICHAEL, S. M. M. 1999. The Paleocene deepwater sandstone play West of Shetland. *In:* FLEET, A. J. and BOLDY, S. A. R. (eds) *Petroleum Geology of Northwest Europe: Proceedings of the 5th Conference*. Geological Society, London, 645-659.

LANGROCK, U. and STEIN, R. 2004. Origin of marine petroleum source rocks from the Late Jurassic to Early Cretaceous Norwegian Greenland Seaway - evidence for stagnation and upwelling. *Marine and Petroleum Geology*, **21**, 157-176.

LARSEN, M. and WHITHAM, A. G. 2005. Evidence for a major sediment input point into the Faroe–Shetland Basin from the Kangerlussuaq region of southern East Greenland. *In:* DORÉ, A. G. and VINING, B. A. (eds) *Petroleum Geology: North-West Europe and Global Perspectives - Proceedings of the 6th Petroleum Geology Conference*. Geological Society, London, 913-922.

LARSEN, M., HAMBERG, L., OLAUSSEN, S. and STEMMERIK, L. 1996. Cretaceous-Tertiary pre-drift sediments of the Kangerlussuaq area, southern East Greenland. *Bulletin Grønlands Geologiske Undersøgelse*, **172**, 37-41.

LARSEN, M., HAMBERG, L., OLAUSSEN, S., NORGAARD-PEDERSEN, N. and STEMMERIK, L. 1999. Basin evolution in southern East Greenland: An outcrop analog for Cretaceous-Paleogene basins on the North Atlantic volcanic margins. *Aapg Bulletin*, **83**, 1236-1261.

LEZZAR, K. E., TIERCELIN, J. J., LE TURDU, C., COHEN, A. S., REYNOLDS, D. J., LE GALL, B. and SCHOLZ, C. A. 2002. Control of normal fault interaction on the distribution of major Neogene sedimentary depocenters, Lake Tanganyika, East African rift. *Aapg Bulletin*, **86**, 1027-1059.

LIEN, T. 2005. From rifting to drifting: effects on the development of deep-water hydrocarbon reservoirs in a passive margin setting, Norwegian Sea. *Norwegian Journal of Geology*, **85**, 319-332.

LIEN, T., ELIN MIDTBØ, R. and MARTINSEN, O. J. 2006. Depositional facies and reservoir quality of deep-marine sandstones in the Norwegian Sea. *Norwegian Journal of Geology*, **86**, 71-92.

LISTER, G. S., ETHERIDGE, M. A. and SYMONDS, P. A. 1986. Detachment faulting and the evolution of passive continental margins. *Geology*, **14**, 246-250.

LØSETH, H. and HENRIKSEN, S. 2005. A Middle to Late Miocene compression phase along the Norwegian passive margin. *In:* DORÉ, A. G. and VINING, B. A. (eds) *Petroleum Geology: North-West Europe and Global Perspectives - Proceedings of the 6th Petroleum Geology Conference*. Geological Society, London, 845-860.

LUNDIN, E. and DORÉ, A. G. 2002. Mid-Cenozoic post-breakup deformation in the 'passive' margins bordering the Norwegian-Greenland Sea. *Marine and Petroleum Geology*, **19**, 79-93.

LUNDIN, E. R. and DORÉ, A. G. 1997. A tectonic model for the Norwegian passive margin with implications for the NE Atlantic: Early Cretaceous to break-up. *Journal of the Geological Society*, **154**, 545-550.

LUNDIN, E. R. and DORÉ, A. G. 2005. NE Atlantic break-up: a re-examination of the Iceland mantle plume model and the Atlantic–Arctic linkage. *In:* DORÉ, A. G. and VINING, B. A. (eds) *Petroleum Geology: North-West Europe and Global Perspectives - Proceedings of the 6th Petroleum Geology Conference*. Geological Society, London, 739-754.

MACK, G. H. and SEAGER, W. R. 1995. Transfer zones in the southern Rio-Grande rift. *Journal of the Geological Society*, **152**, 551-560.

MACLENNAN, J. and LOVELL, B. 2002. Control of regional sea level by surface uplift and subsidence caused by magmatic underplating of Earth's crust. *Geology*, **30**, 675-678.

MARFURT, K. J., KIRLIN, R. L., FARMER, S. L. and BAHORICH, M. S. 1998. 3-D seismic attributes using a semblance-based coherency algorithm. *Geophysics*, **63**, 1150-1165.

MARTINSEN, O. J., BOEN, F., CHARNOCK, M. A., MANGERUD, G. and NOTTVEDT, A. 1999. Cenozoic development of the Norwegian margin 60-64°N: sequences and sedimentary response to variable basin physiography and tectonic setting. *In:* FLEET, A. J. and BOLDY, S. A. R. (eds) *Petroleum Geology of Northwest Europe: Proceedings of the 5th Conference*. Geological Society, London, 293-304.

MARTINSEN, O. J., LIEN, T. and JACKSON, C. 2005. Turbidite systems offshore Norway. *In:* DORÉ, A. G. and VINING, B. A. (eds) *Petroleum Geology: North-West Europe and Global Perspectives - Proceedings of the 6th Petroleum Geology Conference*. Geological Society, London, 1147-1164.

MAY, S. R., EHMAN, K. D., GRAY, G. G. and CROWELL, J. C. 1993. A new angle on the tectonic evolution of the Ridge Basin, a strike-slip basin in southern California. *Geological Society of America Bulletin*, **105**, 1357-1372.

MCCLAY, K. and KHALIL, S. 1998. Extensional hard linkages, eastern Gulf of Suez, Egypt. *Geology*, **26**, 563-566.

MCCLAY, K. R. and WHITE, M. J. 1995. Analog modeling of orthogonal and oblique rifting. *Marine and Petroleum Geology*, **12**, 137-151.

MCCLAY, K. R., DOOLEY, T., WHITEHOUSE, P. and MILLS, M. 2002. 4-D evolution of rift systems: Insights from scaled physical models. *Aapg Bulletin*, **86**, 935-959.

MCCLAY, K. R., DOOLEY, T., WHITEHOUSE, P., FULLARTON, L. and CHANTRAPRASERT, S. 2004. 3D Analogue Models of Rift Systems: Templates for 3D Seismic Interpretation. *Geological Society, London, Memoirs*, **29**, 101-115.

MCCLAY, K. R., NORTON, M. G., CONEY, P. and DAVIS, G. H. 1986. Collapse of the Caledonian Orogen and the Old Red Sandstone. *Nature*, **323**, 147-149.

MCGRANE, K., READMAN, P. W. and O'REILLY, B. M. 2001. Interpretation of transverse gravity lineaments in the Rockall Basin. *In:* SHANNON, P. M., HAUGHTON, P. D. W. and CORCORAN, D. V. (eds) *The Petroleum Exploration of Ireland's Offshore Basins*. Geological Society, London, Special Publications, **188**, 393-399.

MCKENZIE, D. 1978. Some remarks on the development of sedimentary basins. *Earth and Planetary Science Letters*, **40**, 25-32.

McKinley, J. M., Worden, R. H. and Ruffell, A. H. 2001. Contact diagenesis: The effect of an intrusion on reservoir quality in the Triassic Sherwood Sandstone Group, Northern Ireland. *Journal of Sedimentary Research*, **71**, 484-495.

Meadows, N. S., Macchi, L., Cubitt, J. M. and Johnson, B. 1987. Sedimentology and reservoir potential in the West of Shetland, UK, exploration area. *In:* Brooks, J. and Glennie, K. (eds) *Petroleum Geology of North West Europe*. Graham and Trotman, London, 723-736.

Milani, E. J. and Davison, I. 1988. Basement control and transfer tectonics in the Reconcavo Tucano Jatoba Rift, northeast Brazil. *Tectonophysics*, **154**, 41-70.

Mitchell, S. M., Beamish, G. W. J., Wood, M. V., Malacek, S. J., Armentrout, J. A., Damuth, J. E. and Olson, H. C. 1993. Paleogene sequence stratigraphic framework for the Faeroe Basin. *In:* Parker, J. R. (eds) *Petroleum Geology of Northwest Europe: Proceedings of the 4th Conference*. Geological Society, London, 1011-1023.

Mitchum, R. M., Vail, P. R. and Sangree, J. B. 1977b. Stratigraphic interpretation of seismic reflection patterns in depositional sequences. *In:* Payton, C. E. (eds) *American Association of Petroleum Geologists Memoirs*. American Association of Petroleum Geologists, **26**, 117-134.

Mitchum, R. M., Vail, P. R. and Thompson, I., S. 1977a. The depositional sequence as a basic unit for stratigraphic analysis. *In:* Payton, C. E. (eds) *Seismic stratigraphy: applications to hydrocarbon exploration - American Association of Petroleum Geologists Memoirs*. American Association of Petroleum Geologists, **26**, 53-62.

Mjelde, R., Digranes, P., Shimamura, H., Shiobara, H., Kodaira, S., Brekke, H., Egebjerg, T., Sorenes, N. and Thorbjornsen, S. 1998. Crustal structure of the northern part of the Vøring Basin, mid-Norway margin, from wide-angle seismic and gravity data. *Tectonophysics*, **293**, 175-205.

Mjelde, R., Digranes, P., Van Schaack, M., Shimamura, H., Shiobara, H., Kodaira, S., Naess, O., Sorenes, N. and Vagnes, E. 2001. Crustal structure of the outer Vøring Plateau, offshore Norway, from ocean bottom seismic and gravity data. *Journal of Geophysical Research-Solid Earth*, **106**, 6769-6791.

Mjelde, R., Iwasaki, T., Shimamura, H., Kanazawa, T., Kodaira, S., Raum, T. and Shiobara, H. 2003a. Spatial relationship between recent compressional structures and older high-velocity crustal structures; examples from the Vøring Margin, NE Atlantic, and Northern Honshu, Japan. *Journal of Geodynamics*, **36**, 537-562.

Mjelde, R., Kasahara, J., Shimamura, H., Kamimura, A., Kanazawa, T., Kodaira, S., Raum, T. and Shiobara, H. 2002. Lower crustal seismic velocity-anomalies; magmatic underplating or serpentinized peridotite? Evidence from the Vøring Margin, NE Atlantic. *Marine Geophysical Researches*, **23**, 169-183.

Mjelde, R., Kodaira, S., Shimamura, H., Kanazawa, T., Shiobara, H., Berg, E. W. and Riise, O. 1997. Crustal structure of the central part of the Vøring Basin, mid-Norway margin, from ocean bottom seismographs. *Tectonophysics*, **277**, 235-257.

Mjelde, R., Raum, T., Breivik, A., Shimamura, H., Murai, Y., Takanami, T. and Faleide, J. I. 2005. Crustal structure of the Vøring Margin, NE Atlantic: a review of geological implications based on recent OBS data. *In:* Doré, A. G. and Vining, B. A. (eds) *Petroleum Geology: North-West Europe and Global Perspectives - Proceedings of the 6th Petroleum Geology Conference*. Geological Society, London, 803-813.

MJELDE, R., RAUM, T., MURAI, Y. and TAKANAMI, T. 2007. Continent-ocean-transitions: Review, and a new tectono-magmatic model of the Vøring Plateau, NE Atlantic. *Journal of Geodynamics*, **43**, 374-392.

MJELDE, R., SHIMAMURA, H., KANAZAWA, T., KODAIRA, S., RAUM, T. and SHIOBARA, H. 2003b. Crustal lineaments, distribution of lower crustal intrusives and structural evolution of the Vøring Margin, NE Atlantic; new insight from wide-angle seismic models. *Tectonophysics*, **369**, 199-218.

MOGENSEN, T. E., NYBY, R., KARPUZ, R. and HAREMO, P. 2000. Late Cretaceous and Tertiary structural evolution of the northeastern part of the Vøring Basin, Norwegian Sea. *In:* NØTTVEDT, A. (eds) *Dynamics of the Norwegian Margin*. Geological Society, London, Special Publications, **167**, 379-396.

MOKHTARI, M. and PEGRUM, R. M. 1992. Structure and evolution of the Lofoten continental margin, offshore Norway. *Norsk Geologisk Tidsskrift*, **72**, 339-355.

MOLLER, N. K., GJELBERG, J. G., MARTINSEN, O., CHARNOCK, M. A., FAERSETH, R. B., SPERREVIK, S. and CARTWRIGHT, J. A. 2004. A geological model for the Ormen Lange hydrocarbon reservoir. *Norwegian Journal of Geology*, **84**, 169-190.

MOREWOOD, N. C., MACKENZIE, G. D., SHANNON, P. M., O'REILLY, B. M., READMAN, P. W. and MAKRIS, J. 2005. The crustal structure and regional development of the Irish Atlantic margin region. *In:* DORÉ, A. G. and VINING, B. A. (eds) *Petroleum Geology: North-West Europe and Global Perspectives - Proceedings of the 6th Petroleum Geology Conference*. Geological Society, London, 1023-1033.

MORLEY, C. K. 1999. How successful are analogue models in addressing the influence of pre-existing fabrics on rift structure? *Journal of Structural Geology*, **21**, 1267-1274.

MORLEY, C. K., NELSON, R. A., PATTON, T. L. and MUNN, S. G. 1990. Transfer zones in the East African Rift System and their relevance to hydrocarbon exploration in rifts. *Aapg Bulletin*, **74**, 1234-1253.

MORTON, A. C. and GRANT, S. 1998. Cretaceous depositional systems in the Norwegian Sea: Heavy mineral constraints. *Aapg Bulletin*, **82**, 274-290.

MORTON, A. C., WHITHAM, A. G., FANNING, C. M. and CLAOUÉ-LONG, J. 2005. The role of East Greenland as a source of sediment to the Vøring Basin during the late Cretaceous. *In:* WANDÅS, B. T. G., NYSTUEN, J. P., EIDE, E. A. and GRADSTEIN, F. M. (eds) *Onshore-Offshore Relationships on the North Atlantic Margin*. NPF Special Publication, **12**, 83-110.

MORTON, N., SMITH, R. M., GOLDEN, M. and JAMES, A. V. 1987. Comparative stratigraphic study of Triassic-Jurassic sedimentation and basin evolution in the northern North Sea and north-west of the British Isles. *In:* BROOKS, J. and GLENNIE, K. (eds) *Petroleum Geology of North West Europe*. Graham and Trotman, London, 697-709.

MOSAR, J. 2000. Depth of the extensional faulting on the Mid-Norway Atlantic passive margin. *Norges Geologiske Undersøkelse Bulletin*, **437**, 33-43.

MOSAR, J., LEWIS, G. and TORSVIK, T. H. 2002. North Atlantic sea-floor spreading rates: implications for the Tertiary development of inversion structures of the Norwegian-Greenland Sea. *Journal of the Geological Society*, **159**, 503-515.

MOUSTAFA, A. R. 1996. Internal structure and deformation of an accommodation zone in the northern part of the Suez rift. *Journal of Structural Geology*, **18**, 93-107.

MOUSTAFA, A. R. 1997. Controls on the development and evolution of transfer zones: The influence of basement structure and sedimentary thickness in the Suez rift and Red Sea. *Journal of Structural Geology*, **19**, 755-768.

MOUSTAFA, A. R. 2002. Controls on the geometry of transfer zones in the Suez rift and northwest Red Sea: Implications for the structural geometry of rift systems. *Aapg Bulletin*, **86**, 979-1002.

MOY, D. J. and IMBER, J. 2009. A critical analysis of the structure and tectonic significance of rift-oblique lineaments ('transfer zones') in the Mesozoic-Cenozoic succession of the Faroe-Shetland Basin, NE Atlantic margin. *Journal of the Geological Society*, **166**, 831-844.

MUDGE, D. C. and BUJAK, J. P. 2001. Biostratigraphic evidence for evolving palaeoenvironments in the Lower Paleogene of the Faeroe-Shetland Basin. *Marine and Petroleum Geology*, **18**, 577-590.

MUDGE, D. C. and RASHID, B. 1987. The geology of the Faeroe Basin area. *In:* BROOKS, J. and GLENNIE, K. (eds) *Petroleum Geology of North West Europe*. Graham and Trotman, London, 751-763.

NAYLOR, D. and SHANNON, P. M. 2005. The structural framework of the Irish Atlantic Margin. *In:* DORÉ, A. G. and VINING, B. A. (eds) *Petroleum Geology: North-West Europe and Global Perspectives - Proceedings of the 6th Petroleum Geology Conference*. Geological Society, London, 1009-1021.

NAYLOR, P. H., BELL, B. R., JOLLEY, D. W., DURNALL, P. and FREDSTED, R. 1999. Palaeogene magmatism in the Faeroe-Shetland Basin: influences on uplift history and sedimentation. *In:* FLEET, A. J. and BOLDY, S. A. R. (eds) *Petroleum Geology of Northwest Europe: Proceedings of the 5th Conference*. Geological Society, London, 545-558.

NEEDHAM, D. T., YIELDING, G. and FREEMAN, B. 1996. Analysis of fault geometry and displacement patterns. *Geological Society, London, Special Publications*, **99**, 189-199.

NELSON, P. H. H. and LAMY, J. M. 1987. The Møre/West Shetlands area: a review. *In:* BROOKS, J. and GLENNIE, K. (eds) *Petroleum Geology of North West Europe*. Graham and Trotman, London, 775-784.

NELSON, R. A., PATTON, T. L. and MORLEY, C. K. 1992. Rift-segment interaction and its relation to hydrocarbon exploration in continental rift systems. *Aapg Bulletin*, **76**, 1153-1169.

NICHOLS, G. J. 2005. Sedimentary evolution of the Lower Clair Group, Devonian, west of Shetland: climate and sediment supply controls on fluvial, aeolian and lacustrine deposition. *In:* DORÉ, A. G. and VINING, B. A. (eds) *Petroleum Geology: North-West Europe and Global Perspectives - Proceedings of the 6th Petroleum Geology Conference*. Geological Society, London, 957-967.

OLESEN, O., EBBING, J., LUNDIN, E., MAURING, E., SKILBREI, J. R., TORSVIK, T. H., HANSEN, E. K., HENNINGSEN, T., MIDBOE, P. and SAND, M. 2007. An improved tectonic model for the Eocene opening of the Norwegian-Greenland Sea: Use of modern magnetic data. *Marine and Petroleum Geology*, **24**, 53-66.

OLESEN, O., LUNDIN, E., NORDGULEN, O., OSMUNDSEN, P. T., SKILBREI, J. R., SMETHURST, M. A., SOLLI, A., BUGGE, T. and FICHLER, C. 2002. Bridging the gap between the onshore and offshore geology in Nordland, northern Norway. *Norwegian Journal of Geology*, **82**, 243-262.

OSMUNDSEN, P. T. and EBBING, J. 2008. Styles of extension offshore mid-Norway and implications for mechanisms of crustal thinning at passive margins. *Tectonics*, **27**, 1-25.

OSMUNDSEN, P. T., SOMMARUGA, A., SKILBREI, J. R. and OLESEN, O. 2002. Deep structure of the Mid Norway rifted margin. *Norwegian Journal of Geology*, **82**, 205-224.

PASSEY, S. R. and BELL, B. R. 2007. Morphologies and emplacement mechanisms of the lava flows of the Faroe Islands Basalt Group, Faroe Islands, NE Atlantic Ocean. *Bulletin of Volcanology*, **70**, 139-156.

PAYTON, C. E. 1977. *Seismic stratigraphy: applications to hydrocarbon exploration*. American Association of Petroleum Geologists, 516pp.

PEACOCK, D. C. P. and SANDERSON, D. J. 1994. Geometry and development of relay ramps in normal-fault systems. *Aapg Bulletin*, **78**, 147-165.

PEACOCK, D. C. P., PRICE, S. P., WHITHAM, A. G. and PICKLES, C. S. 2000. The World's biggest relay ramp: Hold With Hope, NE Greenland. *Journal of Structural Geology*, **22**, 843-850.

PICKERING, G., BULL, J. M. and SANDERSON, D. J. 1995. Sampling power-law distributions. *Tectonophysics*, **248**, 1-20.

PLANKE, S. and ELDHOLM, O. 1994. Seismic response and construction of seaward dipping wedges of flood basalts - Vøring volcanic margin. *Journal of Geophysical Research-Solid Earth*, **99**, 9263-9278.

PLANKE, S., RASMUSSEN, T., REY, S. S. and MYKLEBUST, R. 2005. Seismic characteristics and distribution of volcanic intrusions and hydrothermal vent complexes in the Vøring and Møre basins. *In:* DORÉ, A. G. and VINING, B. A. (eds) *Petroleum Geology: North-West Europe and Global Perspectives - Proceedings of the 6th Petroleum Geology Conference*. Geological Society, London, 833-844.

PLANKE, S., SYMONDS, P. A., ALVESTAD, E. and SKOGSEID, J. 2000. Seismic volcanostratigraphy of large-volume basaltic extrusive complexes on rifted margins. *Journal of Geophysical Research-Solid Earth*, **105**, 19335-19351.

POSAMENTIER, H. W. and KOLLA, V. 2003. Seismic geomorphology and stratigraphy of depositional elements in deep-water settings. *Journal of Sedimentary Research*, **73**, 367-388.

POSAMENTIER, H. W., DAVIES, R. J., CARTWRIGHT, J. A. and WOOD, L. 2007. Seismic geomorphology - an overview. *Geological Society, London, Special Publications*, **277**, 1-14.

PRAEG, D., STOKER, M. S., SHANNON, P. M., CERAMICOLA, S., HJELSTUEN, B., LABERG, J. S. and MATHIESEN, A. 2005. Episodic Cenozoic tectonism and the development of the NW European 'passive' continental margin. *Marine and Petroleum Geology*, **22**, 1007-1030.

RAUM, T., MJELDE, R., BERGE, A. M., PAULSEN, J. T., DIGRANES, P., SHIMAMURA, H., SHIOBARA, H., KODAIRA, S., LARSEN, V. B., FREDSTED, R., HARRISON, D. J. and JOHNSON, M. 2005. Sub-basalt structures east of the Faroe Islands revealed from wide-angle seismic and gravity data. *Petroleum Geoscience*, **11**, 291-308.

RAUM, T., MJELDE, R., DIGRANES, P., SHIMAMURA, H., SHIOBARA, H., KODAIRA, S., HAATVEDT, G., SORENES, N. and THORBJORNSEN, T. 2002. Crustal structure of the southern part of the Vøring Basin, mid-Norway margin, from wide-angle seismic and gravity data. *Tectonophysics*, **355**, 99-126.

Raum, T., Mjelde, R., Shimamura, H., Mural, Y., Brastein, E., Karpuz, R. M., Kravlk, K. and Kolsto, H. J. 2006. Crustal structure and evolution of the southern Vøring basin and Vøring transform margin, NE Atlantic. *Tectonophysics*, **415**, 167-202.

Reading, H. G. and Richards, M. 1994. Turbidite systems in deep-water basin margins classified by grain-size and feeder system. *Aapg Bulletin*, **78**, 792-822.

Readman, P. W., O'Reilly, B. M., Shannon, P. M. and Naylor, D. 2005. The deep structure of the Porcupine Basin, offshore Ireland, from gravity and magnetic studies. *In:* Doré, A. G. and Vining, B. A. (eds) *Petroleum Geology: North-West Europe and Global Perspectives - Proceedings of the 6th Petroleum Geology Conference*. Geological Society, London, 1047-1056.

Reemst, P. and Cloetingh, S. 2000. Polyphase rift evolution of the Vøring margin (mid-Norway): Constraints from forward tectonostratigraphic modeling. *Tectonics*, **19**, 225-240.

Ren, S. C., Faleide, J. I., Eldholm, O., Skogseid, J. and Gradstein, F. 2003. Late Cretaceous-Paleocene tectonic development of the NW Vøring Basin. *Marine and Petroleum Geology*, **20**, 177-206.

Ren, S. C., Faleide, J. I., Eldholm, O., Skogseid, J. and Gradstein, F. 2003. Late Cretaceous-Paleocene tectonic development of the NW Vøring Basin. *Marine and Petroleum Geology*, **20**, 177-206.

Ren, S. C., Skogseid, J. and Eldholm, O. 1998. Late Cretaceous-Paleocene extension on the Vøring Volcanic Margin. *Marine Geophysical Researches*, **20**, 343-369.

Reston, T. J., Pennell, J., Stubenrauch, A., Walker, I. and Perez-Gussinye, M. 2001. Detachment faulting, mantle serpentinization, and serpentinite-mud volcanism beneath the Porcupine Basin, southwest of Ireland. *Geology*, **29**, 587-590.

Reynolds, J. M. 1997. *An introduction to applied and environmental geophysics*. John Wiley & Sons Ltd, Chichester, 796pp.

Rider, M. H. 1991. *The geological interpretation of well logs - revised edition*. Whittles Publishing, Caithness, Scotland, 175pp.

Ritchie, J. D. and Darbyshire, D. P. F. 1984. RB-SR dates on Precambrian rocks from marine exploration wells in and around the West Shetland Basin. *Scottish Journal of Geology*, **20**, 31-36.

Ritchie, J. D., Gatliff, R. W. and Richards, P. C. 1999. Early Tertiary magmatism in the offshore NW UK margin and surrounds. *In:* Fleet, A. J. and Boldy, S. A. R. (eds) *Petroleum Geology of Northwest Europe: Proceedings of the 5th Conference*. Geological Society, London, 573-584.

Ritchie, J. D., Johnson, H. and Kimbell, G. S. 2003. The nature and age of Cenozoic contractional deformation within the NE Faroe-Shetland Basin. *Marine and Petroleum Geology*, **20**, 399-409.

Ritchie, J. D., Johnson, H., Quinn, M. F. and Gatliff, R. W. 2008. The effects of Cenozoic compression within the Faroe-Shetland Basin and adjacent areas. *In:* Johnson, H., Doré, A. G., Gatliff, R. W., Holdsworth, R. E., Lundin, E. R. and Ritchie, J. D. (eds) *The Nature and Origin of Compression in Passive Margins*. Geological Society, London, Special Publications, **306**, 121-136.

ROBERTS, A. M., CORFIELD, R. I., KUSZNIR, N. J., MATTHEWS, S. J., HANSEN, E.-K. and HOOPER, R. J. 2009. Mapping palaeostructure and palaeobathymetry along the Norwegian Atlantic continental margin: Møre and Vøring basins. *Petroleum Geoscience*, **15**, 27-43.

ROBERTS, A. M., LUNDIN, E. R. and KUSZNIR, N. J. 1997. Subsidence of the Vøring Basin and the influence of the Atlantic continental margin. *Journal of the Geological Society*, **154**, 551-557.

ROBERTS, D. G., THOMPSON, M., MITCHENER, B., HOSSACK, J., CARMICHAEL, S. M. M. and BJØRNSETH, H. M. 1999. Palaeozoic to Tertiary rift and basin dynamics: mid-Norway to the Bay of Biscay - a new context for hydrocarbon prospectivity in the deep water frontier. *In:* FLEET, A. J. and BOLDY, S. A. R. (eds) *Petroleum Geology of Northwest Europe: Proceedings of the 5th Conference*. Geological Society, London, 7-40.

ROCCHI, S., STORTI, F., DI VINCENZO, G. and ROSSETTI, F. 2003. Intraplate strike-slip tectonics as an alternative to mantle plume activity for the Cenozoic rift magmatism in the Ross Sea region, Antarctica. *Intraplate Strike-Slip Deformation Belts*, 145-158.

ROMER, R. L. and BAX, G. 1992. The rhombohedral framework of the Scandinavian Caledonides and their foreland. *Geologische Rundschau*, **81**, 391-401.

ROSENDAHL, B. R. 1987. Architecture of continental rifts with special reference to east-Africa. *Annual Review of Earth and Planetary Sciences*, **15**, 445-503.

ROWLEY, P. D. 1998. Cenozoic transverse zones and igneous belts in the Great Basin, western United States: Their tectonic and economic implications. *In:* FAULDS, J. E. and STEWART, J. H. (eds) *Accommodation Zones and Transfer Zones: The Regional Segmentation of the Basin and Range Province*. Geological Society of America Special Paper, **323**, 195-228.

RUMPH, B., REAVES, C. M., ORANGE, V. G. and ROBINSON, D. L. 1993. Structuring and transfer zones in the Faeroe Basin in a regional tectonic context. *In:* PARKER, J. R. (eds) *Petroleum Geology of Northwest Europe: Proceedings of the 4th Conference*. Geological Society, London, 999-1009.

SCHALTEGGER, U. and BRACK, P. 2007. Crustal-scale magmatic systems during intracontinental strike-slip tectonics: U, Pb and Hf isotopic constraints from Permian magmatic rocks of the Southern Alps. *International Journal of Earth Sciences*, **96**, 1131-1151.

SCHLISCHE, R. W. and WITHJACK, M. O. 2009. Origin of fault domains and fault-domain boundaries (transfer zones and accommodation zones) in extensional provinces: Result of random nucleation and self-organized fault growth. *Journal of Structural Geology*, **31**, 910-925.

SCHOLZ, C. A. and HUTCHINSON, D. R. 2000. Stratigraphic and structural evolution of the Selenga Delta Accommodation Zone, Lake Baikal Rift, Siberia. *International Journal of Earth Sciences*, **89**, 212-228.

SCOTCHMAN, I. C., GRIFFITH, C. E., HOLMES, A. J. and JONES, D. M. 1998. The Jurassic petroleum system north and west of Britain: a geochemical oil-source correlation study. *Organic Geochemistry*, **29**, 671-700.

SÉRANNE, M. 1992. Late Palaeozoic kinematics of the Møre–Trøndelag Fault Zone and adjacent areas, central Norway. *Norsk Geologisk Tidsskrift*, **72**, 141-158.

SHANNON, P. M. 1991. The development of Irish offshore sedimentary basins. *Journal of the Geological Society*, **148**, 181-189.

SHANNON, P. M. and SPENCER, A. M. 1999. Atlantic Margin: offshore Norway to offshore Ireland. *In:* FLEET, A. J. and BOLDY, S. A. R. (eds) *Petroleum Geology of Northwest Europe: Proceedings of the 5th Conference*. Geological Society, London, 229-230.

SHOULDERS, S. J. and CARTWRIGHT, J. 2004. Constraining the depth and timing of large-scale conical sandstone intrusions. *Geology*, **32**, 661-664.

SHOULDERS, S. J., CARTWRIGHT, J. and HUUSE, M. 2007. Large-scale conical sandstone intrusions and polygonal fault systems in Tranche 6, Faroe-Shetland Basin. *Marine and Petroleum Geology*, **24**, 173-188.

SKILBREI, J. R. and OLESEN, O. 2005. Deep structure of the Mid-Norwegian shelf and onshore-offshore correlations: Insight from potential field data. *In:* WANDÅS, B. T. G., NYSTUEN, J. P., EIDE, E. A. and GRADSTEIN, F. (eds) *Onshore-Offshore Relationships on the North Atlantic Margin*. NPF Special Publication, **12**, 43-68.

SKOGSEID, J. 1994. Dimensions of the late Cretaceous Paleocene Northeast Atlantic rift derived from Cenozoic Subsidence. *Tectonophysics*, **240**, 225-247.

SKOGSEID, J., PEDERSEN, T., ELDHOLM, A. and LARSEN, B. T. 1992. Tectonism and magmatism during NE Atlantic continental break-up: the Vøring Margin. *In:* STOREY, B. C., ALABASTER, T. and PANKHURST, R. J. (eds) *Magmatism and the causes of Continental Break-up*. Geological Society, London, Special Publications, **68**, 305-320.

SKOGSEID, J., PLANKE, S., FALEIDE, J. I., PEDERSEN, T., ELDHOLM, O. and NEVERDAL, F. 2000. NE Atlantic continental rifting and volcanic margin formation. *In:* NØTTVEDT, A. (eds) *Dynamics of the Norwegian Margin*. Geological Society, London, Special Publications, **167**, 295-326.

SMALLWOOD, J. R. and GILL, C. E. 2002. The rise and fall of the Faroe-Shetland Basin: evidence from seismic mapping of the Balder Formation. *Journal of the Geological Society*, **159**, 627-630.

SMALLWOOD, J. R. and MARESH, J. 2002. The properties, morphology and distribution of igneous sills: modelling, borehole and 3D seismic from the Faroe-Shetland area. *In:* JOLLEY, D. W. and BELL, B. R. (eds) *The North Atlantic Igneous Province: Stratigraphy, Tectonic, Volcanic and Magmatic Processes*. Geological Society, London, Special Publications, **197**, 271-306.

SMALLWOOD, J. R., STAPLES, R. K., RICHARDSON, K. R. and WHITE, R. S. 1999. Crust generated above the Iceland mantle plume: From continental rift to oceanic spreading center. *Journal of Geophysical Research-Solid Earth*, **104**, 22885-22902.

SMALLWOOD, J. R., TOWNS, M. J. and WHITE, R. S. 2001. The structure of the Faeroe-Shetland Trough from integrated deep seismic and potential field modelling. *Journal of the Geological Society*, **158**, 409-412.

SØRENSEN, A. B. 2003. Cenozoic basin development and stratigraphy of the Faroes area. *Petroleum Geoscience*, **9**, 189-207.

SPENCER, A. M., BIRKELAND, Ø., KNAG, G. Ø. and FREDSTED, R. 1999. Petroleum systems of the Atlantic margin of northwest Europe. *In:* FLEET, A. J. and BOLDY, S. A. R. (eds) *Petroleum Geology of Northwest Europe: Proceedings of the 5th Conference*. Geological Society, London, 231-246.

STECKLER, M. S. and TENBRINK, U. S. 1986. Lithospheric strength variations as a control on new plate boundaries - examples from the northern Red Sea region. *Earth and Planetary Science Letters*, **79**, 120-132.

STEWART, J. H. 1998. The role of accommodation zones and transfer zones in the regional segmentation of extended terranes. *In:* FAULDS, J. E. and STEWART, J. H. (eds) *Regional characteristics, tilt domains, and extensional history of the late Cenozoic Basin and Range province, western North America*. Geological Society of America Special Paper 323, 47-74.

STOKER, M. S., HOULT, R. J., NIELSEN, T., HJELSTUEN, B. O., LABERG, J. S., SHANNON, P. M., PRAEG, D., MATHIESEN, A., VAN WEERING, T. C. E. and MCDONNELL, A. 2005a. Sedimentary and oceanographic responses to early Neogene compression on the NW European margin. *Marine and Petroleum Geology*, **22**, 1031-1044.

STOKER, M. S., PRAEG, D., HJELSTUEN, B. O., LABERG, J. S., NIELSEN, T. and SHANNON, P. M. 2005b. Neogene stratigraphy and the sedimentary and oceanographic development of the NW European Atlantic margin. *Marine and Petroleum Geology*, **22**, 977-1005.

STOKER, M. S., PRAEG, D., SHANNON, P. M., HJELSTUEN, B. O., LABERG, J. S., NIELSEN, T., VAN WEERING, T. C. E., SEJRUP, H. P. and EVANS, D. 2005c. Neogene evolution of the Atlantic continental margin of NW Europe (Lofoten Islands to SW Ireland): anything but passive. *In:* DORÉ, A. G. and VINING, B. A. (eds) *Petroleum Geology: North-West Europe and Global Perspectives - Proceedings of the 6th Petroleum Geology Conference*. Geological Society, London, 1057-1076.

SURLYK, F. 1990. Timing, style and sedimentary evolution of Late Paleozoic–Mesozoic extensional basins of East Greenland. *In:* HARDMAN, R. F. P. and BROOKS, C. K. (eds) *Tectonic Events Responsible for Britain's Oil and Gas Reserves*. Geological Society, London, Special Publications, **55**, 107-125.

SURLYK, F. 1991. Sequence stratigraphy of the Jurassic lowermost Cretaceous of east Greenland. *Aapg Bulletin*, **75**, 1468-1488.

SWIECICKI, T., GIBBS, P. B., FARROW, G. E. and COWARD, M. P. 1998. A tectonostratigraphic framework for the Mid-Norway region. *Marine and Petroleum Geology*, **15**, 245-276.

TATE, M. P. 1993. Structural framework and tectono-stratigraphic evolution of the Porcupine Seabight Basin offshore western Ireland. *Marine and Petroleum Geology*, **10**, 95-123.

TATE, M., WHITE, N. and CONROY, J. J. 1993. Lithospheric extension and magmatism in the Porcupine Basin west of Ireland. *Journal of Geophysical Research-Solid Earth*, **98**, 13905-13923.

TELFORD, W. M., GELDART, L. P., SHERIFF, R. E. and KEYS, D. A. 1990. *Applied geophysics second edition*. Cambridge University Press, Cambridge, 770pp.

THOMSON, K. 2005a. Extrusive and intrusive magmatism in the North Rockall Trough. *In:* DORÉ, A. G. and VINING, B. A. (eds) *Petroleum Geology: North-West Europe and Global Perspectives - Proceedings of the 6th Petroleum Geology Conference*. Geological Society, London, 785-802.

THOMSON, K. 2005b. Volcanic features of the North Rockall Trough: application of visualisation techniques on 3D seismic reflection data. *Bulletin of Volcanology*, **67**, 116-128.

THOMSON, K. 2007. Determining magma flow in sills, dykes and laccoliths and their implications for sill emplacement mechanisms. *Bulletin of Volcanology*, **70**, 183-201.

THOMSON, K. and HUTTON, D. 2004. Geometry and growth of sill complexes: insights using 3D seismic from the North Rockall Trough. *Bulletin of Volcanology*, **66**, 364-375.

TORNE, M., FERNANDEZ, M., WHEELER, W. and KARPUZ, R. 2003. Three-dimensional crustal structure of the Vøring Margin (NE Atlantic): A combined seismic and gravity image. *Journal of Geophysical Research-Solid Earth*, **108**, 1-11.

TRUDE, J., CARTWRIGHT, J., DAVIES, R. J. and SMALLWOOD, J. 2003. New technique for dating igneous sills. *Geology*, **31**, 813-816.

TRUDGILL, B. and CARTWRIGHT, J. 1994. Relay-ramp forms and normal-fault linkages, Canyonlands National Park, Utah. *Geological Society of America Bulletin*, **106**, 1143-1157.

TSIKALAS, F., ELDHOLM, O. and FALEIDE, J. I. 2002. Early Eocene sea floor spreading and continent-ocean boundary between Jan Mayen and Senja fracture zones in the Norwegian-Greenland Sea. *Marine Geophysical Researches*, **23**, 247-270.

TSIKALAS, F., ELDHOLM, O. and FALEIDE, J. I. 2005a. Crustal structure of the Lofoten-Vesterdlen continental margin, off Norway. *Tectonophysics*, **404**, 151-174.

TSIKALAS, F., FALEIDE, J. I. and ELDHOLM, A. 2001. Lateral variations in tectono-magmatic style along the Lofoten-Vesterahen volcanic margin off Norway. *Marine and Petroleum Geology*, **18**, 807-832.

TSIKALAS, F., FALEIDE, J. I. and KUSZNIR, N. J. 2008. Along-strike variations in rifted margin crustal architecture and lithosphere thinning between northern Vøring and Lofoten margin segments off mid-Norway. *Tectonophysics*, **458**, 68-81.

TSIKALAS, F., FALEIDE, J. I., ELDHOLM, O. and WILSON, J. 2005b. Late Mesozoic–Cenozoic structural and stratigraphic correlations between the conjugate mid-Norway and NE Greenland continental margins. *In:* DORÉ, A. G. and VINING, B. A. (eds) *Petroleum Geology: North-West Europe and Global Perspectives - Proceedings of the 6th Petroleum Geology Conference*. Geological Society, London, 785-802.

TURNER, J. D. and SCRUTTON, R. A. 1993. Subsidence patterns in western margin basins: evidence from the Faeroe-Shetland Basin. *In:* PARKER, J. R. (eds) *Petroleum Geology of Northwest Europe: Proceedings of the 4th Conference*. Geological Society, London, 975-983.

VAGNES, E., GABRIELSEN, R. H. and HAREMO, P. 1998. Late Cretaceous-Cenozoic intraplate contractional deformation at the Norwegian continental shelf: timing, magnitude and regional implications. *Tectonophysics*, **300**, 29-46.

VAIL, P. R., MITCHUM, R. M., TODD, R. G., WIDMIER, J. M., THOMPSON, I., S., SANGREE, J. B., BUBB, J. N. and HATLELID, W. G. 1977. Seismic stratigraphy: applications to hydrocarbon exploration. *In:* PAYTON, C. E. (eds) *American Association of Petroleum Geologists Memoirs*. American Association of Petroleum Geologists, **26**, 49-212.

VAN WIJK, J. W. and CLOETINGH, S. 2002. Basin migration caused by slow lithospheric extension. *Earth and Planetary Science Letters*, **198**, 275-288.

VAN WIJK, J. W., HUISMANS, R. S., TER VOORDE, M. and CLOETINGH, S. 2001. Melt generation at volcanic continental margins: no need for a mantle plume? *Geophysical Research Letters*, **28**, 3995-3998.

VAN WIJK, J. W., VAN DER MEER, R. and CLOETINGH, S. 2004. Crustal thickening in an extensional regime: application to the mid-Norwegian Vøring margin. *Tectonophysics*, **387**, 217-228.

WALKER, I. M., BERRY, K. A., BRUCE, J. R., BYSTOL, L. and SNOW, J. H. 1997. Structural modelling of regional depth profiles in the Vøring Basin: Implications for the structural and stratigraphic development of the Norwegian passive margin. *Journal of the Geological Society*, **154**, 537-544.

WALSH, J. J. and WATTERSON, J. 1991. Geometric and kinematic coherence and scale effects in normal fault systems. *Geological Society, London, Special Publications*, **56**, 193-203.

WATSON, J. 1984. The ending of the Caledonian Orogeny in Scotland - Presidents anniversary address 1983. *Journal of the Geological Society*, **141**, 193-214.

WERNICKE, B. 1985. Uniform-sense normal simple shear of the continental lithosphere. *Canadian Journal of Earth Sciences*, **22**, 108-125.

WHITE, N. and LOVELL, B. 1997. Measuring the pulse of a plume with the sedimentary record. *Nature*, **387**, 888-891.

WHITE, R. and MCKENZIE, D. 1989. Magmatism at rift zones: the generation of volcanic continental margins and flood basalts. *Journal of Geophysical Research-Solid Earth and Planets*, **94**, 7685-7729.

WHITE, R. S., SMALLWOOD, J. R., FLIEDNER, M. M., BOSLAUGH, B., MARESH, J. and FRUEHN, J. 2003. Imaging and regional distribution of basalt flows in the Faeroe-Shetland Basin. *Geophysical Prospecting*, **51**, 215-231.

WHITE, R. S., SMITH, L. K., ROBERTS, A. W., CHRISTIE, P. A. F. and KUSZNIR, N. J. 2008. Lower-crustal intrusion on the North Atlantic continental margin. *Nature*, **452**, 460-465.

WHITHAM, A. G., MORTON, A. C. and FANNING, C. M. 2004. Insights into Cretaceous-Palaeogene sediment transport paths and basin evolution in the North Atlantic from a heavy mineral study of sandstones from southern East Greenland. *Petroleum Geoscience*, **10**, 61-72.

WHITHAM, A. G., PRICE, S. P., KORAINI, A. M. and KELLY, S. R. A. 1999. Cretaceous (post-Valanginian) sedimentation and rift events in the NE Greenland (71°–77°N). *In:* FLEET, A. J. and BOLDY, S. A. R. (eds) *Petroleum Geology of NW Europe: Proceedings of the 5th Conference*. Geological Society, London, 325-336.

WILSON, C. K., LONG, D. and BULAT, J. 2004. The morphology, setting and processes of the Afen slide. *Marine Geology*, **213**, 149-167.

WILSON, R. W., MCCAFFREY, K. J. W., HOLDSWORTH, R. E., IMBER, J., JONES, R. R., WELBON, A. I. F. and ROBERTS, D. 2006. Complex fault patterns, transtension and structural segmentation of the Lofoten Ridge, Norwegian margin: Using digital mapping to link onshore and offshore geology. *Tectonics*, **25**, 1-28.

WOODCOCK, N. H. and FISCHER, M. 1986. Strike-slip duplexes. *Journal of Structural Geology*, **8**, 725-735.

YOUNES, A. I. and MCCLAY, K. 2002. Development of accommodation zones in the Gulf of Suez-Red Sea rift, Egypt. *Aapg Bulletin*, **86**, 1003-1026.

YOUNG, M. J., GAWTHORPE, R. L. and SHARP, I. R. 2000. Sedimentology and sequence stratigraphy of a transfer zone coarse-grained delta, Miocene Suez Rift, Egypt. *Sedimentology*, **47**, 1081-1104.

ZIEGLER, P. A. 1988. *Evolution of the Arctic–North Atlantic and western Tethys*. AAPG, 198pp.

ZIEGLER, P. A., CLOETINGH, S. and VANWEES, J. D. 1995. Dynamics of intra-plate compressional deformation: The Alpine foreland and other examples. *Tectonophysics*, **252**, 7-59.